INTERNATIONAL JOURNAL OF PHARMA AND BIO SCIENCES

Internationally indexed journal

Indexed in Chemical Abstract Services (USA), Index coppernicus, Ulrichs Directory of Peroidicals, Google scholar, PSOAR, EBSCO, Open J gate, Proquest, EMBASE, etc.

Rapid and Easy Publishing

The "International Journal of Pharma and Bio Sciences" (IJPBS) is an international journal in English published quartely. The aim of IJPBS is to publish peer reviewed research and review articles rapidly without delay in the developing field of pharmaceutical and biological sciences.

Indexed in Elsevier Bibliographic Database (EMBASE)
SCImago Journal Rank 0.329
Impact factor 7.291* (SJIF)

Pharmaceutical Sciences

- Pharmaceutics
- Novel drug delivery system
- Nanaotechnology
- Pharmacology
- Pharmacognosy
- Analytical chemistry
- Pharmacy practice
- Pharmacogenomics
- Polymer sciences
- Biomaterial sciences
- Medicinal chemistry
- Natural chemistry
- Biotechnology
- Pharmacoinformatics
- Biopharmaceutics

Biological Sciences

- Biochemistry
- Biotechnology
- Bioinformatics
- Cell biology
- Microbiology
- Molecular biology
- Neurobiology
- Cytology
- Pathology
- Immunobiology

ELSEVIER INDEXED JOURNAL

SNIP VALUE - 0.538
SJR - 0.274
CITESCORE - 0.35
SNIP - Source Normalised Impact per Paper
SJR - SCImago Journal rank
Source - www.journalmetrics.com
(powered by scopus (ELSEVIER)

ELSEVIER EMBASE

ISSN 0975-6299 CODEN IJPBJ2

INDEX COPERNICUS INTERNATIONAL

Crossref

DOI: https://doi.org/10.22376/ijpbs

IARA
Research Delights Innovation
INDIAN ACADEMIC RESEARCHERS ASSOCIATION

Google Scholar BETA

CrossMark
click for updates

ISI INTERNATIONAL Scientific Indexing

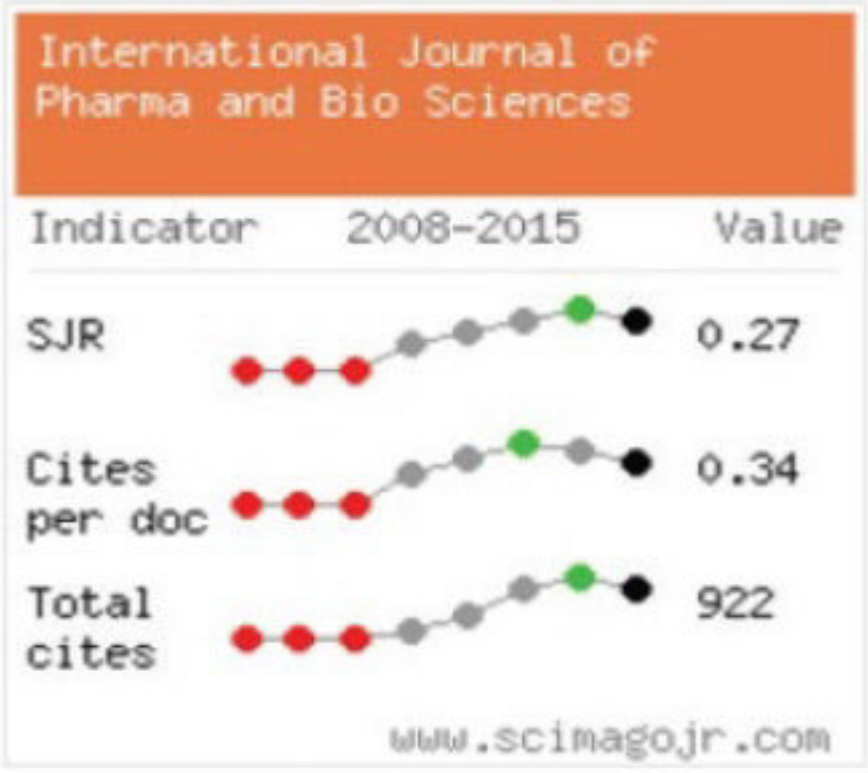

OCLC WorldCat

ProQuest

CAS
A division of the American Chemical Society

CiteFactor
Academic Scientific Journals

:::plagium™
The Plagiarism Checker

doi®

CASSI℠
A CAS SOLUTION
CAS Source Index (CASSI) Search Tool

AGF
Arbeitsgemeinschaft der deutschen Familienorganisationen e.V.

ICMJE
INTERNATIONAL COMMITTEE of MEDICAL JOURNAL EDITORS
Site designed and hosted by Annals of Internal Medicine / American College of Physicians.

WZB
Berlin Social Science Center

ResearchGATE
scientific network

International Journal of Pharma and Bio Sciences is also cataloged in the following universities libraries

United States Universities

UC Berkeley Libraries,
California, United States

University of Washington Libraries,
Seattle, Washington, United States

Branford Price Millar Library,
Oregon, United States

Colombus, Ohio, United States

Tucson, Arizona, United States

Houston Cole Library
Alabama, United States

Miami, Florida, United States

Ralph Brown Draughon Library,
Auburn, United States

Oklahoma, United States

United Kingdom Universities

**Birmingham University Library,
Birmingham , United Kingdom**

New Britain, Connecticut

**Bodleian Libraries,
Oxford, United Kingdom**

Lancaster, England

Bristol, England

Other Universities

**James Cook University Library,
Singapore**

**The university of Manchester Library,
Singapore**

A Special issue of:

5th Biotechnology Symposium

"Biotechnology for Sustainable Development to Meet Global Challenges"

Kota Kinabalu, 15-16 November 2017

Volume 9, SP – 01/Dec/2018

DOI: http://dx.doi.org/10.22376/ijpbs/9.SP01/Dec/2018.1-273

In conjuction with

CONTENT

FP-01

PHENOTYPIC AND MOLECULAR CHARACTERIZATION OF EXTENDED-SPECTRUM BETA-LACTAMASES (ESBL) *Escherichia coli* IN RAW CHICKEN MEAT AND BEAN SPROUTS (*Viga radiata)* IN KOTA BHARU, KELANTAN

ERKIHUN AKLILU[1*], KAUSALYA RAMAN[1], MOHD MOKHTAR BIN ARSHAD[1]

[1]Faculty of Veterinary Medicine, Universiti Malaysia Kelantan, Locked Bag36, 16100 Pengkalan Chepa, Kota Bharu, Kelantan, Malaysia

[*]Corresponding author: erkihun@umk.edu.my

ABSTRACT

Antimicrobial resistance (AMR) in food-borne pathogens especially *Escherichia coli*, is of a serious concern in recent years. Extended beta-lactamase resistant (ESBL) resistant E.coli species have recently emerged and have been the source of concern in both human and animal health. This study was conducted to detect the presence of ESBL resistant *E.coli* in raw chicken meat and bean sprouts in Kota Bharu, Kelantan by using Kirby-Bauer methods for antibiotic sensitivity test (AST) and molecular detection of the ESBL resistance encoding genes by using polymerase chain reaction (PCR). A total of 100 samples comprised of 50 raw chicken meat and 50 bean sprouts were collected and processed microbiologically. Out of 100 food samples that were collected and processed through routine microbiological isolation, 31% (31/100) of *E. coli* were identified phenotypically. However, based on PCR results, 93.5% (29/31) of the phenotypically detected isolates were confirmed as *E.coli.* Raw chicken meat yielded 46% (23/50) *E.coli* isolates while 12% (6/50) *E. coli* was isolated from bean sprouts samples. Based on the results of AST, raw chicken meat showed highest percentage of antimicrobial resistance, 95.7% (22/23) against Amoxycillin/Clavulanic Acid, followed by Enrofloxacin 60.9% (14/23), Colistin 39.1% (9/23) and Gentamicin 30.4% (7/23). Whereas for bean sprouts, highest percentage of antimicrobial resistance was observed towards Amoxycillin/Clavulanic Acid with the percentage of 33.3% (2/6), followed by Colistin 16.7% (1/6). ESBL gene resistance detection against family of ^{bla}TEM and ^{bla}CTX genes showed that 62.1% (18/29) of *E.coli* isolates from both food samples were positive for ^{bla}TEM gene and all the isolates were negative for blaCTX. Out of 18 samples positive resistance towards ^{bla}TEM gene, 94.4% (17/18) were from raw chicken meat and 5.6% (1/18) were from bean sprouts. In conclusion, ESBL resistant *E.coli* was detected in the food samples collected from local markets. These findings imply that ESBL resistant E.coli can easily contaminate raw food items such as chickens and vegetables and may pose public health risks. Hence, rational usage of antibiotics and strict practicing of hygienic handling of food items, especially chicken meat and vegetables are recommended.

KEYWORDS:
Antimicrobial resistance, Molecular detection, PCR, Extended Spectrum-Beta Lactamases (ESBL), Multidrug-resistant, Bean sprouts

INTRODUCTION:

Antimicrobial resistance (AMR) in food-borne pathogens such as *E.coli* has been of a serious public health concern in recent years. In the past few decades and since its emergence in the 1980s, the occurrence and prevalence of extended spectrum lactamases (ESBL) producing *Enterobacteriaceae* in humans and different animal species and food samples have been reported from different countries (Schmid *et al*., 2013).

One of the driving factors that have been known to contribute to the emergence and spread of antimicrobial resistant bacteria is the misuse and overuse of antibiotics in animal production to boost food animal productivity and promote animal health. The demand for chicken meat as a cheaper and readily available

source of protein and its consumption has been increasing globally. However, with this increased global poultry production driven by the rise in global demand has come the emergence and spread of several antimicrobial resistant bacteria such as ESBL producing *E.coli* species. Antibiotics are used for both therapeutic purposes and prophylaxis. In addition, there has been increased use of antibiotics as growth promoters in food animal production, mainly in poultry production (Akond *et al.,* 2009). Chicken meat may get contaminated with bacteria during the slaughtering, processing, transport and handling at any stage from farm to table (Mead, 1989). Poultry meat has high chance of getting contaminated with potentially pathogenic microorganisms due to the common exposures to unhygienic sources that come in contact with it. The commonly identified bacteria that are known to be common contaminants of chicken meat include *E. coli, Salmonella, Campylobacter, Staphylococcus aureus and Listeria* (Adeyanju and Ishola, 2014; Cohen *et al*., 2007; Gorman *et al*., 2002). Contamination of poultry meat with *E. coli* is well documented and numerous food-borne diseases outbreaks have commonly been reported. Generally, *E. coli* is a commensal of the intestinal tract of humans and animals. Besides, it's presence in raw food products is usually indicative of direct or indirect fecal contamination. Hence, this has been used an indicator organism to possibly look out for the presence of other enteric pathogens in food and water (Simmons *et al.,* 2003). Apart from that, some strains of *E. coli* strains are pathogenic in humans and animals due to virulence characteristics. In relation to that, those pathogenic strains are usually responsible for enteric and diarrheal diseases, urinary tract infections, sepsis and meningitis. With all these characteristics, *E. coli* is recognized as the most important cause of foodborne diseases and outbreaks all over the world (Kaper *et al*., 2004; Kalchayanand *et al*., 2013; Majowicz *et al*., 2014). Antimicrobial resistances in bacteria that are commensally present in animals have been in rise and *E. coli* among such bacteria. Commonly, *E. coli* in food animals are resistant to 3rd and 4th generation of cephalosporins and fluoroquinolones. Meanwhile, the usage of antibiotics in food animals has been known to select for transferable resistance genes in different bacterial species that affect humans and animals alike. Hence, this raises the chance of resistance genes possibly transferred from animals to humans via non-pathogenic bacteria in food products and finally transmission to bacterial pathogens in the human gastrointestinal tract. In Malaysia there are few reports on the prevalence and detection of ESBL *E.coli* and other Enterobacteriacae, particularly, *Klebseilla pneumonae*. However, these reports are mostly from health care facilities and few are from other sources such as urban surface water. However, there is no report on the phenotypic and molecular characterization of ESBL producing *E.coli* from food samples, i.e chicken meat and vegetables such as bean sprouts. Therefore, this study was conducted to determine the molecular and phenotypic characterization of ESBL producing *E.coli* from raw chicken meat and bean sprouts from different local markets in Kota Bharu, Kelantan.

MATERIALS AND METHODS:

Sample Collection and Preparation

One hundred (n=100) raw food samples comprised of fifty (n=50) raw chicken meat samples and fifty (n=50) bean sprouts, were collected from supermarkets, markets and road side stalls of different locations in Kota Bharu. Each sample was placed into sterile ziplock-bags and 10 mL normal saline water was added into each sample collection bag. Then, the samples were brought to Bacteriology Laboratory, Faculty of Veterinary Medicine, Universiti Malaysia Kelantan. Buffer Peptone Water (BPW) was used as the primary pre-enrichment broth to permit recovery of bacteria after sublethal injury caused by heat, preservatives, or other processing techniques. Mac-Conkey (OXOID, UK) agar was used to isolate Enterobacteriacea family. Eosin Methylene Blue (EMB) agar was used as a differential and selective medium to observe for the growth of *E. coli.* After the collection, all samples were homogenised using a stomacher and 1 mL of suspension was transferred into 10 mL buffered peptone water using disposable pipette and the homogenates were incubated at 37 °C for 16-18h.

Isolation and identification of *E. coli*

After an overnight incubation in the pre-enrichment broth, a small amount of inoculum from BPW was transferred into Mac-Conkey agar using a disposable pipette and streaked using a sterile wire loop. The inoculated plates samples were then incubated at 37°C for 24 h. After inoculation and isolating colonies from Mac-Conkey agar, Eosin Methylene Blue agar (EMB), a selective media for *E. coli* was further used

for screening. Only the lactose fermenting colonies from Mac-Conkey were chosen and streaked on EMB and incubated at 37°C for further 24 h. Greenish metallic sheen colonies on EMB were transferred to Nutrient Agar to nourish and maintain the colonies before conducting biochemical test for *E. coli*. Other routine bacteriological characterizations such as Gram staining and biochemical tests were also conduct to identify *E.coli*.

Antimicrobial Susceptibility Test

All the confirmed *E. coli* isolates were subjected to antimicrobial susceptibility testing towards selected antibiotics, Colistin, Amoxycillin, Gentamycin and Enrofloxacin using Kirby Bauer methods. The Clinical and Laboratory Standard Institute (CLSI) were used as a reference for determination of susceptibility (CLSI, 2013). Mueller-Hinton Agar (MHA) was used for antimicrobial sensitivity test. A swab of single colony from nutrient agar plate was transferred into test tube with 10 mL containing 0.9% normal saline. Subsequently, the turbidity of the samples was compared with 0.5% of McFarland standard and the suspension was uniformly streaked on MHA. After placing the antibiotic discs aseptically, the plates were incubated at 37°C for 24 h and the zone of inhibition were measured and interpreted according to CLSI guidelines (CLSI, 2013).

Detection of *E. coli* by Polymerase Chain Reaction (PCR)

The genomic DNA was extracted using GF-1 Bacterial DNA Extraction Kit (Vivantis) following the manufacturer's recommendations. The extracted bacterial DNA was then stored in freezer at -20°C until used.

The primers used in this study for PCR identification of *E. coli* species and their resistance genes for Beta Lactamase genes were selected based on previous studies (Table 1). The PCR analyses were conducted for *E. coli* genes of family (Pho) and ESBL genes (CTX and TEM). Primers were obtained from Singapore (Integrated DNA Technologies).

Table 1
Primer sequences used for detection of *E. coli* and extended spectrum beta-lactamases (ESBL) genes

Primers	(°C)	Nucleotide Sequences (5'-3') References	Amplicon size (bp)	Reference
blaCTX-F	54	CCCATGGTTAAAAAACACTGC	950	Horton *et al.,* 2011
blaCTX-R	54	CAGCGCTTTTGCCGTCTAAG		
Pho-F	56	GTGACAAAAGCCCGGACACCATAAA TGC	903	Kong *et al.,* 1999
Pho-R	56	TACACTGTCATTACGTTGCGGATTTG GCG		
blaTEM-F	54	ATAAAATTCTTGAAGACGAAA	1080	Weill *et al.,* 2004
blaTEM-R	54	GACAGTTACCAATGCTTAATC		

DNA Amplification

Amplification of E. coli genes

As for the amplification procedure, the PCR mixtures was done for all samples that yield positive *E. coli* genus with respective primer pairs to obtain gene resistance results. Firstly, 2µL of bacterial DNA was amplified in 12.5µL of 2× Taq Mastermix (Vivantis) which connsist of Taq DNA Polymerase (0.05µ/µL), 2× Vibuffer A, 0.4Mm dNTPs and 3.0Mm MgCl2., 8.5µL of Nuclease Water and 1µL of each primers respectively. Furthermore, PCR protocols were specifically set for each reaction. As for PCR reaction for *E. coli* genus using Pho-F/Pho-R, inital denaturation at 94°C for 2 minutes, final denaturation at 94°C for 1 minute, annealing at 56°C for 1 minute, extension at 72°C for 1 minute, cycle repeated at step 2 (94°C for 1 minute), followed by final extension at 72°C for 10 minutes and kept at hold at temperature 12°C.

Amplification of ESBL genes

As for ESBL genes, multiplex PCR was conducted following the PCR protocols whereby, 2µL of bacterial DNA was amplified in 12.5µL of 2× Taq Mastermix (Vivantis) which connsist of Taq DNA Polymerase (0.05µ/µL), 2× Vibuffer A, 0.4Mm dNTPs and 3.0Mm MgCl2., 6.5µL of Nuclease Water and 1µL of each primers respectively. Thus, PCR protocol condition for blaCTX-F/ blaCTX-R and blaTEM-F/ blaTEM primer pair genes was conducted with initial denaturation of DNA at 94°C for 4 m, followed by final denaturation at 94°C for 1 m, annealing at 54°C for 1 m, extension at 72°C for 2 m, then the cycle was repeated for 30 times at step 2 (94°C for 1 m), subsequently to final extension at 72°C for 4 m and finally, keep it hold at 4°C (Lalzampuia *et al.,* 2013). After obtaining the PCR products analyses were conducted on 1.0% agarose gel (Agarose Vivantis) prepared in 60 mL of 1×TBE Buffer added with 1.2µL of Midori Green Then, electrophoresis was conducted at 100V, 400A for 40 minutes for *E. coli, mcr-2* and ESBL. The gel was captured and analyzed using Gel Doc™ EZ Imager BIO-RAD.

RESULTS:

Isolation and identification of *E. coli*

Based on the routine phenotypic isolation and identification, presumptive *E. coli* isolates were detected in 54% (27/50) of raw chicken meat and 20% (10/50) of the bean sprouts. Out of 31 presumptive *E. coli* isolates, 29 samples were positive for the presence of *E. coli* species specific gene Pho-F/Pho-R at 903 bp. Out of these 29 samples, 23 were from raw chicken meat and 6 were from bean sprouts.

PCR results for detection of ESBL resistance genes

As for the detection of ESBL resistance genes, all the confirmed isolates of *E. coli* species through PCR were screened for ESBL resistance genes blaCTX and blaTEM. The results show that 17 samples of raw chicken meat and one sample of bean sprout showed positive for resistance genes against blaTEM with the presence of bands at 1080bp (Figure 1). However, none of the *E. coli* isolates from both food samples showed positive resistance genes for blaCTX.

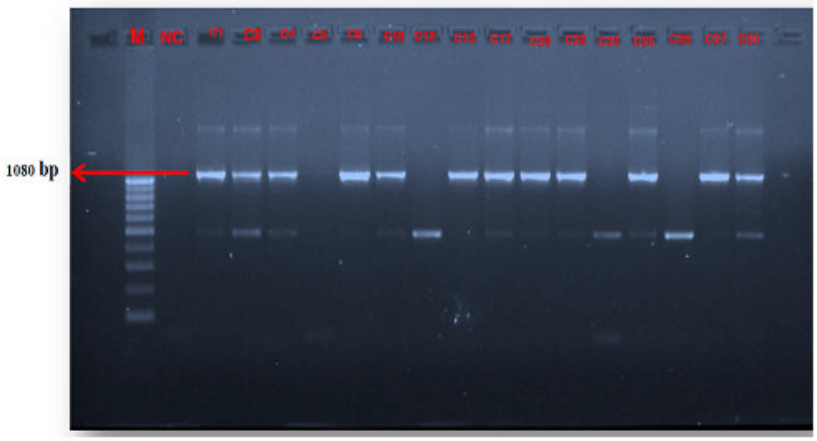

Figure 1
***E. coli* isolates that is positive for ESBL resistance genes. NC- Negative control, M- DNA ladder 100 bp (Marker), C- E.coli isolates from raw chicken meat samples**

Antimicrobial Sensitivity Test

As for AST results, four antibiotics (Amoxycillin/Clavulanic Acid, Colistin, Enrofloxacin, Gentamicin) were used and based on sensitivity of *E. coli* isolates from raw chicken meat, highest number of samples showed resistance towards Amoxycillin, followed with Enrofloxacin, Colistin and Gentamicin. Meanwhile, as for the bean sprouts, most of the resistance detected against Amoxycillin and Colistin, however, no resistance towards Enrofloxacin and Gentamicin. Moreover, MDR *E. coli* were also detected with resistance ranging from two to all antibiotics tested. The outcome of the determination of MDR isolates

observed mostly in raw chicken meat as compared to bean sprouts with none of the isolates showed MDR. The overall AST results of samples with *E. coli* isolates tabulated below (Table 8). Meanwhile, Table 9 shows the tabulation of result for determination of MDR isolates of *E. coli* from both food samples.

Table 2
Antimicrobial susceptibility patterns of *E. coli* (n = 29) isolates from raw chicken meat and bean sprouts

	Types of Samples					
	Raw Chicken Meat (n=23)			Bean Sprouts (n=6)		
Antibiotic Disc (Concentration- µg)	R No.(%)	I No.(%)	S No.(%)	R No.(%)	I No. (%)	S No. (%)
AML (10µg)	22 (95.7)	0 (0)	1 (4.3)	2 (33.3)	3 (50.0)	1 (16.7)
CT (10µg)	9 (39.1)	-	14 (60.9)	1 (16.7)	-	5 (83.3)
ENR (5µg)	14 (60.9)	7 (30.4)	2 (8.7)	0	0 (0)	6 (100)
CN (10µg)	7 (30.4)	1 (4.3)	15 (65.2)	0 (0)	0 (0)	6 (100)

R: Resistant, I: Intermediate, S: Susceptible

Table 3
Multidrug-Resistant (MDR) isolates of *E. coli* from raw chicken meat and bean sprouts

Antibiotic drugs as MDR	Source of MDR isolates	
	Raw chicken meat No. (%)	Bean sprouts No. (%)
AML, ENR	14 (26.4)	0 (0)
AML, CT	9 (17.0)	0 (0)
AML, CN	8 (15.1)	0 (0)
AML, ENR, CT	7 (13.2)	0 (0)
AML, ENR, CN	6 (11.3)	0 (0)
AML, CT, CN	5 (9.4)	0 (0)
AML, ENR, CT, CN	4 (7.5)	0 (0)
TOTAL	**53**	**0**

DISCUSSIONS:

Based on the results from routine bacterial culture and biochemical results, a total of 46% (23/50) and 12% (6/50) of raw chicken meat and bean sprouts were identified as *E. coli* respectively. This could be well supported by the fact that *E. coli* is commensally present in all warm-blooded animals at the enteric regions, hence, high percentage of *E. coli* isolates to be obtained in raw chicken meat due to contaminants as compared to bean sprouts. According to Chang *et al*. (2013), handling of meat and animal carcasses, cross contamination from soil, cutting instruments and the use of contaminated water for washing purpose can be a prominent source of contamination. In this research other members of the *Enterobacteriaceae* family including *Enterobacter aerogenes* and *Klebsiella pneumoniae* were also identified. The presence of *E. coli* in food materials are considered to be an indicator for the presence of other pathogenic bacteria in the respective food items. Meanwhile, as for isolation of *E. coli* in bean sprouts with percentage of 24% is considered high in vegetables as *E. coli* is normally not expected to be isolated from vegetables. Hence, this

is very indicative of high occurrence of contaminations of bean sprouts possibly through untreated sewage water that could possibly be mixed with manure of animals (Rasheed *et al.,* 2014). This reasoning is well supported by many research and studies in recent years when food-borne pathogens is isolated from vegetables and trigger food poisoning outbreak. Monitoring of foodborne pathogens in food products are the only means to cope with the problem promptly.

As to the AST results for raw chicken meat, the highest resistance were observed against Amoxycillin, example of Beta-lactam group of antibiotics with 95.7%, followed by Enrofloxacin, fluoroquionolone group of anitbiotic with 60.9%, Colistin which belongs to Polymyxin group with 39.1% and lastly, Gentamicin of Aminoglycoside group with 30.4%. These results clearly show that poultry meat sold in Kota Bharu harbour antibiotic resistant *E. coli*. The emergence of resistance towards drugs can be associated with the transmission through genetically from one bacterium to another by transmissible elements like plasmids (Neu, 1992). Furthermore, commonly, the resistant bacteria able to pass their resistance genes to their offspring by replication or to related bacteria through conjugation (Courvalin, 1994). As for *E. coli*, it exchanges the resistance genes with the help of conjugation (Madden, 2009). Based on the findings in this research, MDR of *E. coli* isolates were detected through AST. As reported earlier multiple antibiotic resistances may be acquired through mobile genetic elements such as plasmids, transposons, and class 1 integrons (Rasheed *et al*., 2014). Moreover, number of studies has documented on the prevalence of ESBL-producing *Enterobacteriaceae* has increased rapidly around the world. ESBLs are often encoded by genes located on large plasmids, and these also carry genes for resistance to other antimicrobial agents. In recent study from India reported that a substantial number of tap water samples were contaminated with carbapenemase $bla_{\text{NDM-1}}$ producing organisms. Most of the studies on this subject have been conducted in developed countries, but the major epicenters of ESBL-expressing bacteria are located in Asia, Africa, and the Middle East (Ahamed *et al.,* 2014). Hence, antimicrobial resistance has been a growing global threat. The findings from this research may suggest that the disemmination of resistance genes in *E. coli* is spreading at fast pace. Meanwhile, as for AST results in bean sprouts, multi-drug resistance patterns were not observed.

Meanwhile, as for the PCR detection results of the 31 persumptive *E. coli* isolates, 2 samples showed negative result. This shows that molecular method of detection is superior to phenotypical detection for the identifcation of ESBL producing *E.coli*. In this research, ESBL resistance genes of the family of ^{bla}TEM were detected. Out of 29 samples, 17 samples of *E. coli* isolates from raw chicken meat and one sample from bean sprouts showed resistance towards ^{bla}TEM at base pair of 1080bp. This indicates that 62.1% (18/29) of the *E. coli* were resistant to ESBL. Meanwhile, as for ^{bla}CTX family genes, all the isolates were found to be negative. However, CTX gene is said to occur in a higher percentage in most areas around the world (Mohamed *et al*., 2016). In addition, to further support the previous statement, based on a study conducted by Vaida *et al*. (2016), about 96% of most of the ESBL gene found in *E. coli* isolates are common of CTX type. However, in contrast to the current result in this study, there are several reports from Europe and Asia that CTX gene is now slowly replacing TEM and SHV (other ESBL gene) as the upcoming most prevalent type of ESBL gene globally (Mohamed *et al*., 2016). Thus, the possible explanation for the absence of detection of CTX gene in the current study is perhaps, due to the possibility that the changing pattern of CTX gene is yet to be observed in *E. coli* isolates in the study area. In conclusion, based on the findings of AMR in this study, it is very concerning and an alarming issue that ESBL resistant *E. coli* are prevalent in chicken meat intended for human consumption. These findings underscore the importance and urgency to encounter the emergence and spread of these resistant bacteria. Left to themselves, multidrug resistant bacteria continue to spread while posing serious public health risks.

ACKNOWLEDGEMENTS:

The authors would like to acknowledge the laboratory technicians in Bacteriology and Molecular Biology laboratories at Faculty of Veterinary Medicine, Universiti Malaysia Kelantan for their assistance and supports.

REFERENCES:

1. Adeyanju, G. T. and Ishola, O. (2014). Salmonella and Escherichia coli contamination of poultry meat from a processing plant and retail markets in Ibandan, Oyo state, Nigeria. Springer plus; 3; 139.
2. Ahmed, S. H., Daef, E. A., Badary, M. S., Mahmoud, M. A., and Abd-Elsayed, A. A. (2009). Nosocomial blood stream infection in intensive care units at Assiut University Hospitals (Upper Egypt) with special reference to extended spectrum β-lactamase producing organisms.BMC Research Notes;2(1), 76.
3. Akond, M. A., Alam, S., Hasan, S., Mubassara, S., Uddin, S. N., & Shirin, M. (2009). Bacterial contaminants in carbonated soft drinks sold in Bangladesh markets. *International Journal of Food Microbiology, 130*(2), 156-158.
4. Chang WS, Afsah-Hejri L, Rukayadi Y, Khatib A, Lye YL, Loo, YY. (2013). Quantification of Escherichia coli O157:H7 in organic vegetables and chickens. IFRJ. 20: 1023-29.
5. Clinical and Laboratory Standards Institute (CLSI) (2013).Performance Standards for Antimicrobial Susceptibility Testing; Twenty-Third Informational Supplement. M100-S23.
6. Cohen N, Ennaji H, Bouchrif B, Hassar M, Karib H. (2007). Comparitive study of microbiological quality of raw poultry meat at various seasons and fordifferent slaughtering processes in Casablanca (Moracco). J Appl Poult Res. 16; 502-508.
7. Courvalin, P. (1994). Transfer of antibiotic resistance genes between gram-positive and gram-negative bacteria. Antimicrob. Agents Chemother. 38: 1447–1451.
8. Gorman R, Bloomfield S, Adley C. C. (2002). A study of cross-contamination of food born e pathogens in the domestic kitchen in the republic of Ireland. Int J Food Microbiol.76; 143-150.
9. Horton RA, Randall LP, Snary EL, Cockrem H, Lotz S, Wearing H, Duncan D, Rabie A, McLaren I, Watson E, La Ragione RM, Coldham NG: Fecal carriage and shedding density of CTX-M extended-spectrum ß-lactamase-producing Escherichia coli in cattle, chickens, and pigs: Implications for environmental contamination and food production. Appl Environ Microbiol 2011, 77 :3715-3719.
10. Kalchayanand, N., T.M. Arthur, J.M. Bosilevac, J.E. Wells, and T.L. Wheeler. 2013. Chromogenic agar medium for detection and isolation of *Escherichia coli* serogroups O26, O45, O103, O111, O121, and O145 from fresh beef and cattle feces. J. Food Prot. 76:192–199.
11. Kaper, J.B., J.P. Nataro, and H.L.T. Mobley. 2004. Pathogenic *Escherichia coli*.Nat. Rev. Microbiol. 2:123–140.
12. Kong, R. Y. C., So, C. L., Law, W. F., Wu, R. S. S. (1999). A sensitive and versatile multiplex PCR system for the rapid detection of enterotoxigenic (ETEC), enterohaemorrhagic (EHEC) and enteropathogenic (EPEC) strains of *Escherichia coli.* Mar. Pollut. Bull.38:1207–1215.
13. Madden, D. 2009. Antibiotic resistance in E. coli. A practical investigation of bacterial conjugation. The Wellcome trust, national centre for biotechnology education university of Reading UK, pp.1-12.
14. Majowicz, S. E., Scallan, E., Jones-Bitton, A., Sargeant, J. M., Stapleton, J., Angulo, F. J., Yeung DH, Kirk MD. (2014). Global incidence of human Shiga toxin-producing Escherichia coli infections and deaths: a systematic review and knowledge synthesis. Foodborne Pathogens and Disease, 11, 447e455.
15. Mead, C. (1989). Hygiene Problems and Control of Process Contamination. In: Processing of poultry, Mead G. C., Ed. Elsevier Science Publishers Ltd., pp. 183-220.
16. Mohammed, Y., Galadima, G.B., Zailani, S.B., Aboderin, A. O. (2016). Characterization of Extended Spectrum Beta-lactamase from Escherichia coli and Klebsiella speciesfrom north-eastern, Nigeria. Journal of Clinical and Diagnostic Research. 10(2):7-10.
17. Neu, H.C. (1992). The crisis in antibiotic resistance. Sci. 257:1064-73.
18. Rasheed, M.U., Thajuddin, N., Ahamed, P., Teklemariam, Z., Jamil, K. (2014). Antimicrobial drug resistance in strains of Escherichia coli isolated from food sources. Rev Inst Med Trop Sao Paulo. 56: 341-46.
19. Schmid A, Hormansdorfer S, Messelhausser U, Kasbohrer A, Sauter-Louis C, Mansfeld R. (2013). Prevalence of extended-spectrum beta-Lactamase-producing Escherichia coli on bavarian dairy and beef cattle farms. Applied and Environmental Microbiology, 79(9):3027-3032.

20. Simmons M, Fletcher DL, Cason, J.A. Berrang, M.E. (2003). Recovery of Salmonella from retail broilers by a whole-carcass enrichment procedure. Journal of Food Protection 66:446-450.
21. Weill, F. X., M. Demartin, D. Tande´, E. Espie´, I. Rakotoarivony, and P. A. D Grimont. (2004). Extended-spectrum-lactamase (SHV-12 like)-producing strains of Salmonella enterica serotypes Babelsberg and Enteritidis isolated in France among infants adopted from Mali. J. Clin. Microbiol.42: 2432–2437.

FP-02

CYTOTOXICITY EFFECTS OF SELECTED TERPENOIDS ON BREAST CANCER CELL LINE, MCF-7

ALEX WALZICO ROBERT[1], TEOH PEIK LIN[1]*

[1]Biotechnology Research Institute, Universiti Malaysia Sabah, Jalan UMS, 88400 Kota Kinabalu, Sabah, Malaysia

*Corresponding author: peiklin@ums.edu.my

ABSTRACT

Recent attempts in discovering anti-cancer drugs derived from natural products has become a trend among researchers worldwide. Terpenoids, one of the largest classes of natural products appear promising to act as potential chemopreventive and therapy agent. This paper reported the cytotoxicity effects of selected terpenoids (squalene, betulin and lupeol) on breast cancer cell line, MCF-7. The results showed that squalene has no significant effect on cell proliferation; meanwhile betulin and lupeol inversely act as potent inhibitors on cancer cell proliferation. Besides that, the morphology of squalene treated cells showed no difference from untreated cells. However, the other two terpenoids potentially cause the induction of apoptosis as the condensed chromatin was observed in the treated cells. Further investigations are needed to examine how betulin and lupeol provoke the programmed cell death.

KEYWORDS:
Terpenoids, Squalene, Betulin, Lupeol, Breast cancer, Cytotoxicity

INTRODUCTION:

Breast cancer has been known as the second leading cause of cancer related death in women. It continues to affect the lives of millions of women worldwide. There are several risk factors of breast cancer but the strongest risk factor is age.[1] Based on the breast cancer statistics, the cases increased rapidly with increasing age among pre-menopausal women, which aged below 50 years. The increment of the cases occurred at a slower rate among post-menopausal women that aged over 50 years.[1]

There are various methods used for cancer prevention and treatment, including the usage of chemotherapeutic agents. But it still does not meet the satisfactory expectation; the demand to develop effective and affordable anticancer medicines is still on-going.[2] The interest in natural products as anticancer agent has grown due to their biological activities and rich source of compounds. Generally, terpenoids are the largest family of natural compounds which consists of over 40 000 different molecules.[3] It can be extracted mainly from higher plants and also lower invertebrates including marine organisms, for examples sea cucumbers, marine-derived fungi, marine algae and sponges.[4,5] One of the selected terpenoids, squalene can be specifically found in sharks and olives[6]; while betulin is found in birch bark[7], and lupeol in fruits, vegetables and medicinal plants.[8] Although these compounds are among the natural products that have been known to possess beneficial effects for human, their underlying mechanisms towards programmed cell death are largely unknown.

Due to controversy findings reported by previous studies, we have re-examined the cytotoxicity effects of squalene, betulin and lupeol on MCF-7 cells. The results obtained showed that squalene possess insignificant effects towards MCF-7 while both betulin and lupeol exhibited anti-proliferative effects on this cell line. This was also supported by the morphological changes that found in the treated cells. These findings will serve as a stepping stone for further investigating their roles in programmed cell death such as apoptosis.

MATERIALS AND METHODS:

Chemicals

Squalene, betulin, and lupeol were purchased from Sigma (St Louis, MO). The stock and working solution of the selected terpenoids were prepared using dimethyl sulfoxide (Fisher Scientific, UK) .

Cell culture and treatments

Breast cancer cell line, MCF-7 was cultured in RPMI1640 medium (Nacalai Tesque, Japan) supplemented with 10% fetal bovine serum (Gibco, Life Technologies, USA) and 1% antibiotic-antimycotic (Gibco, Life Technologies, USA). The cultured cells were incubated at 37°C in a humidified incubator supplied with 5% CO_2. Cells were regularly monitored and subcultured using 1x trypsin-EDTA (Gibco, Life Technologies, USA).

MCF-7 cells were treated with various ranges of concentrations: squalene (0-10 µg/ml), betulin (0-20 µg/ml) and lupeol (0-50 µg/ml). Cells were seeded and treated as mentioned. The effect of terpernoids on cell morphology was observed by using an inverted microscope after 24, 48 and 72 h treatments.

Proliferation assay

The cytotoxicity effects of squalene, betulin and lupeol on the proliferation of MCF-7 cells were determined by using Cell Proliferation kit (Sigma, St Louis, MO). The experiment was carried out according to the manufacturer's protocol. Briefly, cells were plated in 96-well plate and incubated for 24 h. Cells were treated with the selected terpernoids for 72 h. After this, 10 µl of MTT (3-[4,5-dimethylthiazol-2-yl]-2,5-diphenyl tetrazoliumbromide) was added into each well followed by further 4 h incubation. Finally, 100 µl of solubilization buffer was added into each well and incubated overnight to dissolve the purple formazan salt crystals. Each experiment was done in triplicates and the average absorbance values were obtained. In order to determine the 50% inhibition concentration (IC_{50}), a graph (cell proliferation vs concentration) was plotted.

RESULTS AND DISCUSSION:

The assessment of the cytotoxicity effects of squalene, betulin and lupeol on MCF-7 was studied by treating the cells with various concentrations of terpernoids. The principal of this experiment was to study the ability of active MCF-7 cells to cleave the yellow tetrazolium salt of MTT to purple formazan after treatment.

Previous epidemiological studies in Greece suggested that high consumption of olive oil was correlated with lower cancer cases.[9] Rao et al. (1998) hypothesized that the anticancer properties observed in olive oil intake inversely related to lower incidence of breast cancer. This could be due to squalene, which is abundantly present in olive oil.[10] However, our results suggested that squalene (Fig. 1a) exerted insignificant effects on this cancer cell proliferation. To further confirm the cytotoxicity effect of squalene, the concentration of squalene had been increased up to 50 µg/ml but no much changes was observed after treatment (data not shown). Similar to the study done by Warleta et al. (2010), squalene was found to not killing cancer cells. Nonetheless, it might contribute to the preventive effects of olive oil in carcinogenesis by inhibiting oxidative stress.[11]

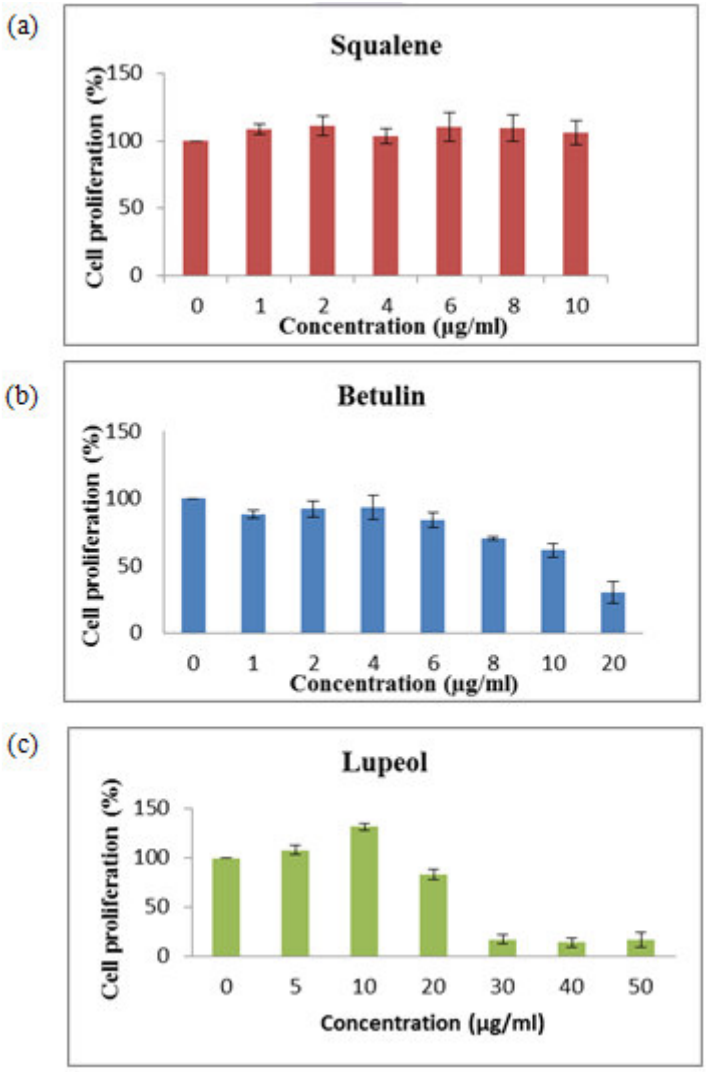

Figure 1
The anti-proliferative effect of terpenoids on MCF-7 cells. Cells were treated with (a) squalene, (b) betulin and (c) lupeol at the indicated concentrations for 72 hours.

Table 1
IC_{50} values of betulin and lupeol for MCF-7 cells after treated for 72 h.

Cell line	Treatment (µg/ml)	
	Betulin	Lupeol
MCF-7	13.97 ± 3.02	24.67 ± 1.15

Betulin and lupeol exhibited profound inhibitory effect on the growth of MCF-7 cells. A minimal inhibition of cell growth was observed at the concentration up to 6 µg/ml and 20 µg/ml for betulin and lupeol, respectively. For betulin, anti-proliferative effect was gradually increased to about 40% when the concentration reached 20 µg/ml (Fig. 1b). On the other hand, the lupeol treatment caused a drastic decrease after 20 µg/ml (Fig. 1c). The IC_{50} values obtained for betulin and lupeol are depicted in Table 1. This suggested that MCF-7 cells are more suspectible to betulin compared to lupeol.

The morphology of MCF-7 treated with 10 µg/ml squalene for 24 h, 48 h, and 72 h (Fig. 2) also showed no obvious differences between squalene-treated and untreated cells. For cells treated with betulin and lupeol, an obvious reduction of cell population was found (Fig. 2b & 2c). A close-up morphology of MCF-7 cells showing morphological alteration such chromatin condensation and circle-like shrinkage shape (red arrows)

after 72 h treatment with betulin and lupeol (Fig. 2c). Moreover, more betulin-treated cells showed these characteristics than cells treated with lupeol. This morphological observation indicates the occurence of apoptosis-related programmed cell death in MCF-7 after treatment.

Compare to the study done by Pitchai et al.[12], lupeol extracted from *Elephantopus scaber* L. inhibited the cell proliferation of MCF-7 with the IC_{50} of 80 µM (~30 µg/ml). This value is slightly higher than the IC_{50} value we obtained. The discrepancy of IC_{50} values could be due to the inpurities present in the isolated lupeol thus affecting suspectibility of cancer cells towards the compound. The cytotoxicity effects of betulin have been studied in other cancer cell lines such as RCCA (kidney cancer cells) and SGC7901 (gastric cancer cells).[7,13] The IC_{50} obtained in our study is comparable to the value (13 µg/ml) reported in gastric cancer cells.[10] In addition, it has also been demonstrated that betulin induces apoptosis via intrinsic pathway as evidenced by the accumulation of BAX and BAK proteins.[10] Therefore, this could be happened in MCF-7 cells also but further investigation is required.

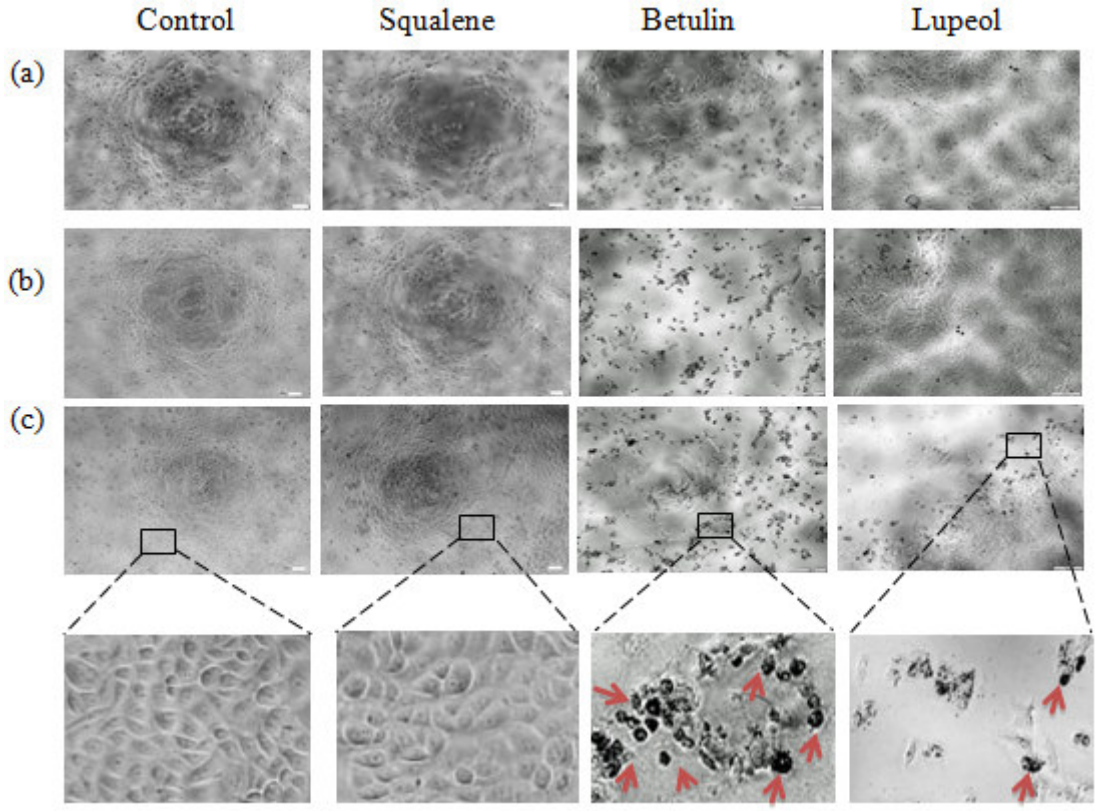

Figure 2

The morphological changes of MCF-7 cells after treatment. Cells were treated with squalene, betulin and lupeol using their respectively IC_{50} value for (a) 24 h, (b) 48 h and (c) 72 h. Close-up morphological changes of MCF-7 cells (in rectangular boxes) treated for 72 h were enlarged. Red arrows indicate cells with condensed nucleus.

CONCLUSION:

Overall, our preliminary results based on growth inhibition and morphological studies suggest that betulin and lupeol on MCF-7 suppressed the cell proliferation in a dose-dependent manner potentially through the apotosis pathways.

ACKNOWLEDMENTS:

The authors thank Universiti Malaysia Sabah for providing funding (GUG0051-SG2/2016) and Sabah Government for sponsoring AWR.

REFERENCES:

1. Ma J, Jemal A. Breast cancer statistics. In: Ahmad A, editor. Breast cancer metastasis and drug resistance. New York: Springer; 2013. p. 18.
2. Solowey E, Lichtenstein M, Sallon S, Paavilainen H, Solowey E, Lorberboum-Galski H. Evaluating medicinal plants for anticancer activity. Sci World J. 2014;2014:1–12.
3. Aharoni A, Jongsma MA, Bouwmeester HJ. Volatile science? Metabolic engineering of terpenoids in plants. Trends Plant Sci. 2005;10(12):594–602.
4. Li Y-X, Himaya SW, Kim S-K. Triterpenoids of marine origin as anti-cancer agents. molecules. 2013;18:7886–7909.
5. González Y, Torres-Mendoza D, Jones GE, Fernandez PL. Marine diterpenoids as potential anti-inflammatory agents. Mediators Inflamm. 2015;2015:1–14.
6. Desai KN, Wei H, Lamartiniere CA. The preventive and therapeutic potential of the squalene-containing compound, Roidex, on tumor promotion and regression. Cancer Lett. 1996;101(1):93–96.
7. Li Y, Liu X, Jiang D, Lin Y. Betulin induces reactive oxygen species-dependent apoptosis in human gastric cancer SGC7901 cells. Arch Pharm Res. 2016;39(9):1257–1265.
8. Saleem M. Lupeol, a novel anti-inflammatory and anti-cancer dietary triterpene. Cancer Lett. 2009;285(2):109–115.
9. Katsouyanni K, Trichopoulou A, Stuver S, Garas Y, Kritselis A, Kyriakou G, et al. The association of fat and other macronutrients with breast cancer: A case-control study from Greece. Br J Cancer. 1994;70(3):537–541.
10. Rao CV, Newmark HL, Reddy BS. Chemopreventive effect of squalene on colon cancer. Carcinogenesis. 1998;19(2):287–90.
11. Warleta F, Campos M, Allouche Y, Sanchez-Quesada C, Ruiz-Mora J, Beltran G, et al. Squalene protects against oxidative DNA damage in MCF10A human mammary epithelial cells but not in MCF7 and MDA-MB-231 human breast cancer cells. Food Chem Toxicol. 2010;48:1092–1100.
12. Pitchai D, Roy A, Ignatius, C. *In vitro* evaluation of anticancer potentials of lupeol isolated from *Elephantopus scaber* L. on MCF-7 cell line. J Adv Pharm Technol Res. 2014;5(4): 179–184.
13. Rzeski W, Stepulak A, Szymanski M, Juszczak M, Grabarska A, Sifringer M, et al. Betulin elicits anti-cancer effects in tumour primary cultures and cell line in vitro. J Compil. 2009;105:425–432.

FP-03

ACTIVATING EFFECT OF AROMATHERAPY INHALATION WITH *Citrus hystrix* (KAFFIR LIME) LEAVES OIL ON HUMAN

ALISA STEPHANIE RASION[1] AND HOW SIEW ENG[1*]

[1]Faculty of Science and Natural Resources, Universiti Malaysia Sabah, Jalan UMS, 88400, Kota Kinabalu, Sabah, Malaysia

[*]Corresponding author: sehow@ums.edu.my

ABSTRACT

Citrus hystrix leaves oil is rich in citronellal which offers soothing effects and has the potential to be used as aromatherapy. Although the applications of *C. hystrix* are expanding in several industries, there is little-published research on *C. hystrix* leaves oil and its efficacy as aromatherapy. The effects of *C. hystrix* leaves oil on human behavioural parameters after inhalation were investigated in this study. *C. hystrix* essential oil was extracted from fresh leaves by steam distillation. Forty healthy volunteers participated in this study who was randomly assigned to two groups, control group (treated with virgin coconut oil) and the *C. hystrix* oil group in which each group consisted of twenty respondents. The behavioural parameters were assessed by means of visual analogue scales (VAS) where the subjects had to rate their emotional condition in order to assess subjective behavioural arousal in terms of relaxation, vigour, calmness, attentiveness, mood and alertness after inhalation. Mann-Whitney-U-Test, Wilcoxon Signed Rank Test, and Spearman's Rho Correlation were used in this study. The Mann-Whitney U Test showed that subjects in the *C. hystrix* oil group rated themselves as more relaxed ($U= 43.50$, $z= –4.52$, $p= 0.00$, $r= 1.00$), more vigorous ($U= 52.00$, $z= –4.28$, $p= 0.00$, $r= 0.96$) and more attentive ($U= 111.00$, $z= –2.66$, $p= 0.01$, $r= 0.59$) than subjects in the control group. Wilcoxon signed rank test for beginning and ending time supported the data obtained from Mann-Whitney U Test which showed significantly different in the score of effects at the beginning and ending observation data for relaxation, vigorous and attentiveness rated by subjects. The strength of these data were supported by the Spearman's Rho Correlation test where relaxation had positive medium correlation with variable vigorous, $r = 0.47$, $n = 20$, $p < 0.05$, and variable vigorous had positive strong correlation with variable attentiveness, $r = 0.74$, $n = 20$, $p < 0.05$. These results demonstrate the activating effect of *C. hystrix* oil and provide evidence for its use in aromatherapy for the relief of depression and uplifting mood in humans.

KEY WORDS:

Behavioural parameters, Visual analogue scale (VAS), Behavioural arousal, Mann-Whitney-U-Test, Wilcoxon Signed Rank Test, Spearman's Rho Correlation

INTRODUCTION:

Modern aromatherapy makes use of both essential oils and their aromas for balancing, harmonizing and promoting the health of body, mind and spirit. A mixture of fat-soluble chemicals is an odour that gives effect to the brain via skin absorption, inhalation or directly through the nose[1]. Generally, the respiratory tract is the most instant way of entry followed by the dermal pathway[2]. The inhalation of essential oils has given rise to olfactory aromatherapy, where simple inhalation has resulted in emotional wellness, calmness, relaxation or rejuvenation arousal of the human body while the release of stress is welded with pleasurable scents which unlock odour memories[3]. The inhalation of essential oils may provide a cost-effective, safe, and appropriate therapy for some mental disorders[4]. The essential oil *Citrus hystrix* is increasingly used as a fragrance in the food, perfumery and cosmetic industries. Active compounds such as phenolic acids,

flavonoids, limonoids, coumarins, glycerolipids and α-tocopherol in *C. hystrix* leaves possess various pharmaceutical effects including anti-tumour, antimicrobial, anti-inflammation and antioxidant activities[5]. It reported that *C. hystrix* fractional extract may have potential as anti-cancer compounds as well as can be a promising natural alternative to chemotherapy for leukaemia as it is shown to decrease the viability of leukemic cell lines[6]. The result shows *C. hystrix* essential oil gives a good repellency properties against the *S. litura* larvae and excellent activity against many respiratory bacteria at the various activity levels and this repellency might be due to β-citronellal[7-8]. In medicine, interest in the usage of citrus oils as therapeutically active agents has grown considerably. The previous conducted double-blinded, randomized controlled clinical trial study on aromatherapy shows that citrus oil is good in relieving the first stage labour pain and it is effective in controlling nausea and vomiting along with its mood elevating property[3]. Bergamot essential oil which is a fragrant citrus fruit when inhaled together with water vapour via the nose into the alveoli, inducing mental and physical effects by inhalation alone and therefore it can be used as a relatively simple form of stress reduction, which might be useful to treat the chronic stress[9]. Patients who are exposed to orange odour had a lower level of state anxiety, a more positive mood, and a higher level of calmness compared to the patients in the control condition and the patients that exposed to a music has an intermediate effect[10]. This study indicates that the essential oil inhalation can produce objective effects on cognitive performance as well as subjective effects on mood but until now there are still a few studies of the efficacy of *C. hystrix* leaves oil as aromatherapy. Therefore, the main objectives of the present study were to evaluate the effects of *C. hystrix* leaves oil on human behavioural parameters after inhalation.

MATERIALS AND METHODS:

Fresh Kaffir lime leaves (*C. hystrix*) were obtained from Kaffir lime orchard in Kg Gansing, Kimanis, Papar and before extraction by steam distillation apparatus, the Kaffir lime leaves were weighted at 1.00 Kg. After extraction, the oil was dried with 4.00 g anhydrous sodium sulphate and by centrifugation at 2000 to 3000 rpm[11].

Subjects

Forty healthy volunteers took part in the study. Subjects were randomly assigned to two groups, the virgin coconut oil (VCO) as a control and the *C. hystrix* oil group. Each group consisted of 20 subjects. Visual analogue scale (VAS) was used for self-evaluation of smells performance. The VAS questionnaires from the previous study were followed with some modification[12]. This scale consisted of six items questionnaires designed to differentiate subjective responses to the experiment room, including "totally relaxed-extremely tense", "totally energized- extremely weak", "totally calm-extremely anxious", "totally attentive-extremely dreamy", "totally positive-extremely negative", and "totally alert-extremely sleepy". Subjects were asked to mark their assessment between each of the two end-points.

Statistical analysis

Data were analysed using SPSS. Mann-Whitney-U-Test, Wilcoxon Signed Rank Test, and Spearman's Rho Correlation analysis of variances were used in this study.

RESULTS:

Subjects

Of 35% male and 65% female with different race and age range from 25 to 50 year were taking this survey. There were 18% of respondents with age range from 25 to 30 years old, 35% of respondents age range from 31 to 35 years old, 33% of respondents with age range from 36 to 40 years old, 10% respondents with age range from 41 to 50 years old and 5% respondents with age range more than 50 years old while for race, there were 15% of Malay respondents, 3% represent Chinese, 70% of Dusun, 10% Indians and 3% Sungai. This experiment took 15 days for each person to rate themselves in response to odours for both control category and *C. hystrix* oil category to get the sufficient data.

Comparison of Control and Treatment Related to Six Variables

Table 1 shows there were no significant differences of response for respondents in control and *C. hystrix* oil category in the effects of calmness, mood and alertness. Nonetheless, the Mann-Whitney U Test revealed significant differences between effects of relaxation, vigorous and attentiveness for control and *C. hystrix* oil category.

Comparison Beginning and Ending

The Wilcoxon Signed Rank Test was used to compare two related variables which were the beginning and ending observation time for both control group and *C. hystrix* oil group. Participants who are in the control group showed significant differences in the effects of relaxation, vigorous, calmness, attentiveness, mood and alertness for beginning and ending observation time (Table 2) while participants who are exposed to *C. hystrix* showed only significant differences in the effects of relaxation, vigorous, attentiveness, mood and alertness for beginning and ending observation time (Table 3).

Correlational Analyses

The Spearman's Rho Correlation test was used to analyze the strength of association between these six variables for the effects of *C. hystrix* which is presented in Table 4. This result showed that Relaxation had positive medium correlation with variable Vigorous, $r = 0.47$, $n = 20$, $p < 0.05$, and Variable Vigorous had positive strong correlation with variable Attentiveness, $r = 0.74$, $n = 20$, $p < 0.05$ which showed that *C. hystrix* oil gave positive arousal effects in relaxation, vigorous and attentiveness.

Table 1

Comparison of mean rank and sum of rank between Control and C. hystrix leaves oil category for the effects of relaxation, vigorous, calmness, attentiveness, mood and alertness

	Control (VCO) (n=20)		*C. hystrix* oil (n=20)		P-value
	Mean rank	Sum of Rank	Mean rank	Sum of Rank	
Relaxation	28.33	566.50	12.68	253.50	0.00*
Vigorous	27.90	558.00	13.10	262.00	0.00*
Calmness	20.38	407.50	20.63	412.50	0.94
Attentiveness	24.95	499.00	16.05	321.00	0.01*
Mood	22.15	443.00	18.85	377.00	0.33
Alertness	19.38	387.50	21.63	432.50	0.52

*Significant at the 0.05 level (2-tailed)

Table 2

Rating mean (±standard deviation) and comparison of rating at the beginning and ending observation time of six variables rated by 20 respondents for the effects of Virgin Coconut Oil (VCO) (Control)

	Relaxation		Vigorous		Calmness		Attentiveness		Mood		Alertness	
	Beginning	Ending	Beginning	Ending	Beginning	Ending	Beginning	Ending	Beginning	Ending	Beginning	Ending
Control (n=20)	4.40±1.50	6.10±1.33	3.95±1.28	5.60±1.05	3.40±1.64	4.80±1.40	3.45±1.28	4.95±0.45	3.10±1.37	4.25±1.41	2.90±1.33	3.75±1.45
Z	-3.45*		-3.33*		-3.46*		-3.68*		-3.37*		-3.21*	
Asymp. Sig. (2-tailed)	0.00		0.00		0.00		0.00		0.00		0.00	

Significant at the 0.05 level (2-tailed)

Table 3

Rating mean (±standard deviation) and comparison of rating at the beginning and ending observation time of six variables rated by 20 respondents for the effects of Citrus hystrix leaves oil

	Relaxation		Vigorous		Calmness		Attentiveness		Mood		Alertness	
	Beginning	Ending	Beginning	Ending	Beginning	Ending	Beginning	Ending	Beginning	Ending	Beginning	Ending
Treatment (n=20)	5.80±0.95	4.00±0.56	5.85±0.49	4.20±0.62	5.05±0.89	5.10±0.55	5.80±0.70	4.25±0.85	5.80±0.95	3.95±0.65	5.65±0.99	3.95±0.83
Z	-3.79*		-4.02*		0.00		-3.37*		-3.79*		-3.80*	
Asymp. Sig (2-tailed)	0.00		0.00		1.00		0.00		0.00		0.00	

*Significant at the 0.05 level (2-tailed)

Table 4
Spearman's Rho Correlation between six variables rated by 20 respondents for the effects of Citrus hystrix leaves oil

Scale	1	2	3	4	5	6
1. Relaxation	-	0.47*	0.37	0.36	0.86*	0.47*
2. Vigorous		-	0.42	0.74*	0.44	0.57
3. Calmness			-	0.33	0.33	0.30
4. Attentiveness				-	0.34	-0.16
5. Mood					-	0.37
6. Alertness						-

*Correlation is significant at the 0.05 level (2-tailed

DISCUSSION:

The pale yellow essential oil yielded from *C. hystrix* leaves by steam distillation technique was 0.3% which was lower than a reported yield of 0.43% [13] possibly due to various factors such as weather conditions, soil, elevation, and harvest time[14]. In this study, the *C. hystrix* oil and the control oil (virgin coconut oil) were analysed whether there were rated differently and thus, the mean rating scores given by the subjects of the *C. hystrix* group with the mean scores of the control group were compared using Mann-Whitney U Test (Table 1) while the effect of oil before and after treatment perception was tested using Wilcoxon matched-pairs tests which are presented in Table 2 and Table 3 respectively. The Mann-Whitney U Test revealed that there were significant different in the effect of relaxation (U= 43.50, z= –4.52, p= 0.00, r= 1.00), vigorous (U= 52.00, z= –4.28, p= 0.00, r= 0.96) and attentiveness (U= 111.00, z= –2.66, p= 0.01, r= 0.59) in comparisons of the control group with the *C. hystrix* oil group (Table 1). This result is supported by the beginning and ending observation time data of *C. hystrix* oil group which showed significantly different in the score of effects at the beginning and ending observation data for relaxation, vigorous and attentiveness rated by the respondents (Table 3). Most of the respondents showed positive feedback where they could feel the distinctive arousal effect of relaxation, vigorous and attentiveness after treated with *C. hystrix* oil. Meanwhile for the arousal effects of calmness, mood and alertness, the Mann-Whitney U Test result revealed that there were no significant differences in variables of calmness (U= 197.50, z= –0.07, p= .94, r= 0.02), mood (U= 167.00, z= –0.97, p= 0.33, r= 0.22) and alertness (U= 177.5, z= –0.64, p= 0.52, r= 0.14) in comparisons of the control group and the *C. hystrix* oil group which indicated that the arousal effects of calmness, mood and alertness in *C. hystrix* oil and control groups were merely equal. On the other hand,

there were significant differences of effects in the beginning and ending observation time for relaxation, vigorous, attentiveness, mood and alertness effects, as the arousal effects were felt by the respondents at the end of observation time after being treated with *C. hystrix* oil (Table 3). The effects of mood and alertness in *C. hystrix* oil were merely equal with virgin coconut oil among respondents, although there were significantly different effects of mood and alertness for *C. hystrix* oil and indicated positive effects in comparison with beginning respond. There are no calmness effects to the respondents in *C. hystrix* oil group as there was no significant difference in calmness effects comparison in control (Md= 5.00, n=20) and treatment (Md= 5.00, n = 20), U= 197.50, z= –0.07, p= .94, r= 0.02, based on Mann-Whitney U Test and no significant different in calmness effects at beginning and ending observation time for *C. hystrix* oil category (Table 3). The Spearman's Rho Correlation between six variables rated by 20 respondents for the effects of *C. hystrix* oil leaves group is presented in Table 4 which was used to measure the strength of association between these six variables for the effects of *C. hystrix* oil.

This finding shows those five effects, relaxation, vigorous, attentiveness, mood and alertness shared medium to a strong correlation. There were arousal effects in relaxation, vigorous and attentiveness after treated with *C. hystrix* oil and these were supported by The Spearman's Rho Correlation test where Relaxation had positive medium correlation with variable Vigorous, $r = 0.47$, $n = 20$, $p < 0.05$, and Variable Vigorous had positive strong correlation with variable Attentiveness, $r = 0.74$, $n = 20$, $p < 0.05$. The exposure to *C. hystrix* leaves oil caused arousal effects in relaxation, vigorous and attentiveness. It was described that the characteristic aroma of *C. hystrix* leaves a blend of citronella oil and lime oil, can be classified as aldehydic, citrus like and slightly warm with floral odour[15] and when mental illness has to be treated, citronella can be clarifying and balancing and to bring even more of a brightening effect to the mind, combining the citronellal oil with lemon oil is the best option[16]. The *C. hystrix* leaves oil yielded a high number of oxygenated monoterpenes and it was approximately 86.15% of the total oil where the major component characterized from the *C. hystrix* leaves oil was β-citronellal and it is the active component that has a sedative activity and has a relaxant effect[7-1]. The inhalation of lemon odour is reported to improve concentration, reduced exhaustion and maintained vigour, without affecting subjects work efficacy[17] and this might be due to the high content of monoterpenes (d-limonene) in the essential oil[18]. Our results are not much different compared to a reported research where the *C. hystrix* essential oil obtained from the fresh peels of *C. hystrix* by hydrodistillation caused a significant increase in alertness, attentiveness, mood and vigorous than subjects in the control group after massage treatment[19]. Conclusively, the results of this study indicate that *C. hystrix* leaves oil inhalation also can increase the level of arousal in relaxation, vigorous and attentiveness as assessed through test subjects self-evaluation.

CONCLUSION:

This finding reveals that *C. hystrix* oil gave arousal effects in relaxation, vigorous and attentiveness as compared with the control group and thus provides an evidence for the essential oil industry that the inhalation of *C. hystrix* leaves oil increases behavioural arousal and can be uplifting, help to increase attentiveness as well as safe to use. This research is likely to represent the activating effects of *C. hystrix* leaves oil as aromatherapy via inhalation. Future research on the effect of soothing smells of *C. hystrix* leaves oil on heart rate, diastolic and systolic blood pressure and memory could be studied for a better understanding of the effective mechanism of *C. hystrix* leaves oil inhalation.

REFERENCES:

1. Baser CHK, Buchbauer G, editors. Handbook of Essential Oils: Science, Technology, and Applications. CRC Press; 2009 Dec 28.
2. Bouayed J, Bohn T, editors. Nutrition, Well-Being and Health. Intech Publication; 2012 Feb 23.
3. Ali B, Al-Wabel AN, Shams S, Ahamad A, Khan AS, Anwar F. Essential oils used in aromatherapy: A systemic review. Asian Pacific Journal of Tropical Biomedical. 2015;5(8):601–611.
4. Han X, Gibson J, Eggett DL, Parker TL. Bergamot (Citrus bergamia) essential oil inhalation improves positive feelings in the waiting room of a mental health treatment centre: a pilot study.

Phytother Res. 2017;31(5):812–816.

5. Abirami A, Nagarani G, Siddhuraju P. The medicinal and nutritional role of underutilized citrus fruit- *citrus hystrix* (kaffir lime): A review. Drug Invention Today. 2014;6(1):1-5.
6. Chueahongthong F, Ampasavate C, Okonogi S, Tima S, Anuchapreeda S. Cytotoxic effects of crude kaffir lime (*Citrus hystrix*, dc.) leaf fractional extracts on leukemic cell lines. J Med Plant. Res. 2011;5(14):3097-3105.
7. Loh SF, Awang MR, Omar D, Rahmani M. Insecticidal properties of *Citrus hystrix* dc leaves essential oil against *Spodoptera litura* Fabricius. J Med Plant. Res. 2011;5(16):3739-3744.
8. Srisukh V, Tribuddharat C, Nukoolkarn V, Bunyapraphatsara N, Chokephaibulkit K, Phoomniyom S, Chuanphung S, Srifuengfung S. Antibacterial activity of essential oils from *Citrus hystrix* (makrut lime) against respiratory tract pathogens. Science Asia. 2012;38:212-217.
9. Watanabe E, Kuchta K, Kimura M, Rauwald WH, Kamei T, Imanishi J. Effects of bergamot (Citrus bergamia (Risso) wright & Arn.) essential oil aromatherapy on mood states, parasympathetic nervous system activity, and salivary cortisol levels in 41 healthy females. Forsch Komplementmed. 2015;22:43–49.
10. Lehrner J, Marwinski G, Lehr S, Johren P, Deecke L. Ambient odours of orange and lavender reduce anxiety and improve mood in a dental office. Physiol Behav. 2005;86:92 – 95.
11. Hussein MM, Essential oils treated to remove harsh notes therefrom. Patent.1991 April 9.
12. Matsubara E, Tsunetsugu Y, Ohira T, and Sugiyama M. Essential oil of Japanase cedar (*Cryptomeria japonica*) wood increases salivary dehydroepiandrosterone sulfate levels after monotonous work. Int J Environ Res Public Health. 2017;4(1): 97.
13. Kasuan N, Yunus M, Rahiman MHF, Aris SRS, Taib MN. Essential oil composition of kaffir lime: comparative analysis between controlled steam distillation and hydrodistillation extraction process. Proceedings of 2009 Student Conference on Research and Development (SCOReD 2009). 2009 Nov 16-18.
14. Department of Agriculture, Forestry and Fisheries, editor. Essential oil crops production guidelines for lavender. **A**gricultural Information Services. 2009 Nov.
15. Muhammad Nor, O. Volatile aroma compounds in Citrus hystrix oil. J Trop Agric and Fd Sc. 1999;27(2): 225–229.
16. Wany A, Jha S, Nigam KV, and Pandey MD. Chemical analysis and therapeutic uses of citronella oil from *Cymbopogon winterianus*: a short review. International Journal of Advanced Research. 2013;1(6): 504-521.
17. Kawamoto R, Murase C, Ishida I, Nakatani J, Haraga M, Shimizu J. The effect of lemon fragrance on simple mental performance and psychophysiological parameters during task performance. J UOEH. 2005;27:305–13.
18. Keniston-Pond K. Essential oils 101: your guide to understanding and using essential oils. F+W Media, Inc. 2017 Mar 1.
19. Hongratanaworakit T, Buchbauer G. Chemical composition and stimulating effect of *Citrus hystrix* oil on humans. Flavour and Fragr J. 2007;22:443–449.

FP-04

POLYMORPHISM AT THE ANGIOTENSINOGEN GENE (AGT) AS A RISK FACTOR FOR DIABETIC NEPHROPATHY IN PATIENTS WITH TYPE II DIABETES MELLITUS

KURNIAWATY E[1], SADEWA H[2], SYUKUR S[3], WIRASTI Y[3], YERIZEL E[3]

[1]Medical Faculty Lampung University, Lampung, Indonesia, [2]Medical faculty Jogjakarta University, Jogjakarta, Indonesia, [3]Medical Faculty Andalas University, Padang, Indonesia

[*]Corresponding author: evikurniawati800@gmail.com

ABSTRACT

There are many works reported that angiotensin II type 1 receptor (AGT) gene polymorphisms associated with diabetic nephropathy and has variable expression in different ethnic groups. However, the distribution data of AGT gene polymorphism in patients with diabetic nephropathy in Indonesia is still lacking. This study aimed to determine the polymorphism of AGT gene M235T in patients with Type 2 diabetes mellitus in Yogyakarta, Indonesia. The subjects of the research were 60 patients with Type 2 diabetes, 30 diabetic nephropathy and 30 without nephropathy respectively. Gene polymorphisms were determined by PCR-RFLP method and the PCR products were digested with PsyI restriction enzyme. The results showed the frequency distribution of genotypes of AGT gene in patients with diabetic nephropathy were 23.3% for MM, 26.7% for MT, and 50% for TT respectively and the frequency distribution of genotypes of AGT gene in patients with non diabetic nephropathy were 10% for MM, 53.3% for MT, and 36.7% for TT respectively Genotype TT is more prevalent in the DN group while in the non DN group genotype MT is more prevalent.

KEYWORDS:

AGTgene, M235T, Diabetes mellitus, Type 2 diabetes, Diabetic nephropathy

INTRODUCTION:

Diabetes mellitus (DM) is a metabolic disorder which causes chronic complications such as atherosclerosis, diabetic nephropathy, blindness and terminal kidney failure or end stage renal disease (ESRD). There are several types of DM, which are DM type 1, type 2 and gestational DM1[1]. DM type 2 covers up to 80-90% of all DM type diseases. At this point and time Diabetes Mellitus remains the most occurring disease among people worldwide with a prevalence rate of 4%. Its prevalence rate continues to increase and it is estimated it will reach 5.4% by 2025.Most of its patients are above 40 and has diabetic symptoms[2]. 15 million people suffer from DM in the United States, of which 10% suffer from DM type 1 and 90% suffer from DM type 2[3]. Even though DM type 1 dan type 2 could cause ESRD DM type 2 remains the biggest contributor to ESRD. Only DM type 2 could develop to overt nephropathy. Abot 40% of DM develops to diabetic nephropathy4. Research shows that in DM type 1 and 2, genetic factors could increase the risk of contracting DN5.

RAS (*Renin Angiotensin System)* has an important role in patophysiologic diabetic nephropathy (DN)6. One of the hormones involved in RAS (*Renin Angiotensin System)* is angiotensin II. Angiotensin II is a strong vasoconstrictor and acts as an intermediary in cellular profileration to extracelular protein synthesis. Research shows that angiotensin II is an active metabolic hormone which initiates insulin resistance, an increase in the number of free radicals, a decrease in leptin and adiponectin production as well as an increase in oxidative stress8. Angiotensin II acts as a pro-mitosis, pro-proliferative and has an angiogenic effect. Angiotensin II intermediates a complex physiological effect by the bonding of 2 different receptors, AGTR1 dan AGTR26.

M235T Polymorphism (metionin digantikan treonin pada kodon 235) has been intensively researched in cardiovascular diseases and in kidneys. There is a correlation between M235T gene AGT polymorphism and progressive kidney failure in primary kidney disease patients. This polymorphism has a high risk of penyakit gagal ginjal konis9. Several researchers report the relation between the T allele in this polymorphism with the development of kidney disease

MATERIALS AND METHODS:

Following informed consent the demographic and laboratory variables of the patients including age, gender, BMI, diagnostic period, systolic and diastolic (hypertension/ non hypertension), total colesterol, HDL and triglyceride were noted. Furthermore, peripheral blood lymphocytes were isolated by the standard phenol extraction method and used as DNA samples in genotype analysis in this study. The M235T variant of the AGT gene was detected using primers: 5' CCGTTTGTGCAGGGCCTGGCTCTCT-3' as the forward and 5'-CAGGGTGCTGTCCACACTGGACCCC-3'' as the reverse primers. The PCR product was digested with the *PsyI* restriction enzyme (Thermo Fisher Scientific Inc.). The data were statistically analyzed using chi square, t-test, odds ratio test.

RESULTS:

There were 60 patients with Type 2 diabetes mellitus, 30 subjects with nephropathy and 30 subjects without diabetic nephropathy, were included in this research. The demographic and laboratory variables of patients participated in this are presented in Table 1. The results of RFLP analysis with *PsyI 1*of PCR on AGT gene are shown in Fig 1. Genotypes MM, MT and TT were found in case and control subjects.

Table 1
Demographic and laboratory characteristics of the studied patients

Variables	DN (n=30)	Non-DN (n=30)	p<0.05
Age (yr)	59.63 ± 8.15	58.17 ± 7.96	ns
Gender (F/M)	14/16	13/17	ns
Total Cholesterol (mg/dl)	199.41 ± 39.94	191.40 ± 53.49	ns
Triglyceride (mg/dl)	159.85 ± 69.45	145.21 ± 74.96	ns
HDL (mg/dl)	42.64 ± 14.37	45.48 ± 13.87	ns
BMI (kg/m²)	24.62 ± 4.46	23.79 ± 2.94	ns
Systolic (mmHg)	134.67 ± 22.70	122.83 ± 14.00	S
Diastolic (mmHg)	84.67 ± 13.06	79.83 ± 7.71	ns

DN: Type 2 diabetes patients with nephropathy; Non-ND: Type 2 diabetes patients without nephropathy

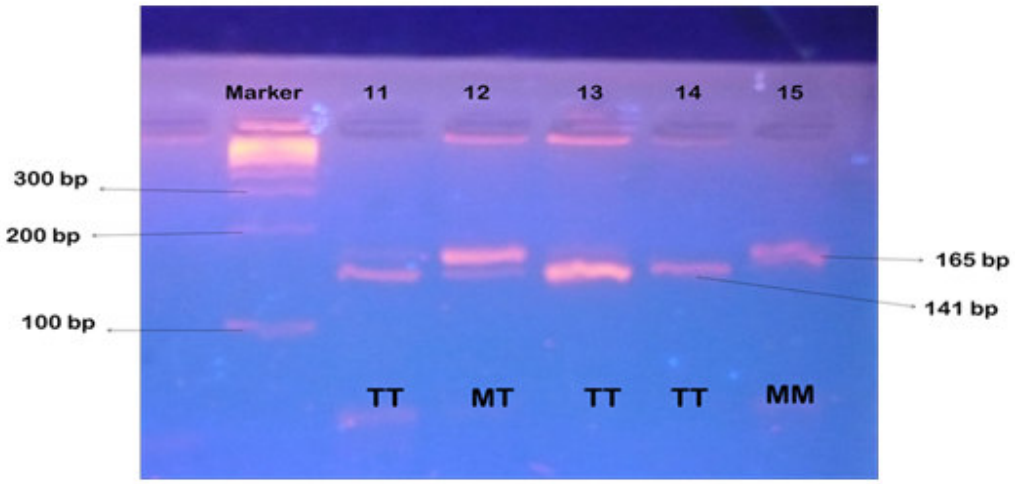

Figure 1
Polymorphism of AGT gene: pysldigestion of the PCR product. The wild type gene was 165 bp and the mutant was 141 bp.

The frequency distribution of AGT genotypes in Type 2 diabetes mellitus patients with and without nephropathy are presented in Tabel 2.

Table 2
Distribution of AGT M235T genotypes in Type 2 diabetes mellitus patients with and without nephropathy

	DN patients	Non-DN patients	P < 0.05
Genotype	(n = 30)	(n = 30)	
MM	7 (23.3%)	3 (10%)	ns
MT	8(26.7%)	16 (53.3%)	S
TT	15 (50%)	11(36.7%)	S
M allele	22(36.7%)	22 (36.7%)	ns
T allele	38 (63.3%)	38(63.3%)	ns

DN: Type 2 diabetes patients with nephropathy; Non-ND: Type 2 diabetes patients without nephropathy

Frequency distribution of AGT genotypes in the DN group are as follows, 23.3% (n=7) of the subjects with MM genotype, 26.7% (n=8) with MT genotype, and 50% (n=15) with TT genotype. Whereas in Non-DN group there were 10% (n=3) subjects with MM genotype, 53.3% (n=16) with with AC genotype and 36.7% (n=11) with MT genotype. The frequency distribution of AGT allele M and allele T in DN group are 36.7% (n=22) and 63.3% (n=38) respectively. Whereas in non-DN group the frequency of allele M and allele T consecutively are 36.7% (n= 22) and 63.3% (n=38). However, between the two groups there is no statistical difference in the both gene and allele frequency distribution at *P*=0.05

DISCUSSIONS:

Current findings suggest that among Indonesian patients, AGT gene M235T genotype TT is more prevalent in the DN group while in the non DN group genotype MT is more prevalent. When these results are compared to the data from other countries, referred to Zhang et al. as shown in **Table 3**, it seems that M235T genotype polymorphism of AGT gene in Indonesian patients are similar to that of Chinese.

Table 3

Population of AGT Gene M235T Genotype among Different Countries

Year	Population	MM	MT	TT
2009	Indonesian	16.7%	40%	43.3%
2007	Taiwan	0.5%	24.5%	75%
2003	Japan	3.8%	30.7%	65.5%
2005	Germany	34%	62.4%	3.65%
2007	Mexico	16%	58.5%	25.5%

The data showed that in Asian ethnicity (Indonesia, Taiwan and Japan), the frequency of TT genotypes have the greatest number . However in (Germany and Mexico) the number of MT genotypes is the most. The effect of intra renal RAS is kidney hemodynamic change such as the increase in intra glomeruler pressure, stimulation from mesangial cell proliferation and matrix production . The function of angiotensin II is to increase efferren arteriol pressure and afferren or preglomeruler strand that causes autoregulation response in systemic blood pressure increase causing the increase in glomerulus capillar pressure. Beside, angiotensin II also plays a role in growth stimulation, fibrogenesis induction and regulates endotel function .

CONCLUSIONS:

Frequency genotype TT polymorphism of AG2 M235T gene is more common in DN than non DN. T allele frequency of M235T AGT polymorphism in DN is as much as non-DN.

REFERENCES:

1. American Diabetes Association, 2004, Diagnosis and Classification of Diabetes mellitus. *Diabetes Care*, 27 [Suppl 1], S5 – S10.
2. Gardner, D.G., Shoback, D., 2004, Pancreatic Hormone & Diabetes Mellitus. *Greenspan's Basic & Clinical Endocrinology*. 8 : 661 – 744.
3. Grissom, F.E., 2008, The Endocrin Pancreas ppt. Howard University.
4. Zychma, 2000, Angiotensinogen M235T and Chymase Gene CMA/B Polimorphysms are not associated with Nephropathy in Type II Diabetes. *Nephrology Dialysis Transplantation*, 15 : 1965 – 1970.
5. Hansen, T., 2007, Microvascular Complications. *STAR Research Course Epidemiology.*
6. Wiecek, A., Chudek, J., and Kokot, F., 2003, Role of Angiotensin II in the Progression of Diabetic Nephropathy-Therapeutic Implications. *Nephrol Dial Transplant,* 18 [Suppl 5]: v16–v20
7. Buraczynska, M., Ksiazek, P., Drop, A., Zaluska, W., Spasiewicz, D., 2005. Genetic Polymorphism of the Renin – Angiotensin System in End Stage Renal Disease. Nephrology Dialysis Transplantation (NDT) ., 21 : 979 – 983.
8. Ferder, L., Inserra, F., Martinez, 2006, Inflammation and the metabolic Syndrome : Role of Angiotensin II and Oxidative Stress. *Curr Hypertens Rep,* 8 : 191 – 198.
9. Rong, C., Cheng, C.H., Shu, K.H., Chen, C.H., Lian, J.D., Wu, M.Y., 2003, Study of th Polymorphism of Angiotensinogen, Anigiotensin-Converting Enzyme and Angiotensin Receptor in Type II Diabetes with End-Stage Rena Disease in Taiwan. *Journal of the Chinese Medical Association*, 66 ; 51 – 56

10. Kanwar, Y., Wada, J., Sun, L., Xie, P., Wallner, E., Chen, S., Chugh, S., Danesh, F., 2008. Diabetic Nephropathy : Mechanisms of Renal Disease Progression. Society for Experimental Biology and Medicine. 233 : 4 – 11.
11. Yulianti, E., Asj'ari, S,R., dan Sadewa, A.H., 2009, Polimorfisme Gena *Transforming Growth Factor β 1* (TGF β 1) sebagai Faktor Risiko Terjadinya Nefropati Diabetika pada Penderita Diabetes Mellitus Tipe 2. Tesis Program Studi IKD dan Biomedis UGM. Jogjakarta.
12. Setyono, J., Asj'ari, S,R., dan Sadewa, A.H., 2009, Polimorfisme Gena Reseptor MCP-1 (CCR2) dan RANTES (CCR5) sebagai Faktor Risiko Nefropati Diabetika pada Penderita DM tipe 2. Tesis Program Studi IKD dan Biomedis UGM. Jogjakarta.
13. Furuichi, K., Wada, T., Iwata, Y., Kitagawa, K., Kobayashi, K., Hashimoto, H., Ishiwata, Y., Asano, M., Wang, H., Matsushima, K., Takeya, M., Kuziel, W. A., Mukaida, N., and Yokohama, H., 2003. CCR2 Signaling Contributes to Ischemia – Reperfusion in Kidney. *J Am Soc Nephrol*, 14 : 2503 – 2515.

FP-05

COSMECEUTICAL POTENTIALS AND BIOACTIVE COMPONENTS OF FERMENTED RICE BY-PRODUCTS

DANG LELAMURNI ABD RAZAK*, ANISAH JAMALUDDIN, NUR YUHASLIZA ABD RASHID, AMSAL ABD GHANI, AZLINA MANSOR AND MUSAALBAKRI ABDUL MANAN

Biotechnology and Nanotechnology Research Centre, Malaysian Agricultural Research and Development Institute (MARDI), P.O Box 12301, General Post Office, 50774 Kuala Lumpur, Malaysia.

*Corresponding author: danglela@mardi.gov.my

ABSTRACT

The rice milling industry in Malaysia creates many types of by-products of which are mainly under-utilized and have low value. Using biotechnology, these by-products can be converted into a high-value material. In this study, rice by-products namely broken rice and rice bran were each subjected to solid-state fermentation with the fungi *Aspergillus oryzae* and *Rhizopus oligosporus*. The extracts of these fermented rice by-products were evaluated for their cosmeceutical potentials by the analysis of tyrosinase and elastase enzyme inhibition as well as antioxidant activities. The results showed that the extracts of rice by-products fermented with *R. oligosporus* exhibited higher elastase inhibition activity than extracts of substrates fermented with *A. oryzae*. On the other hand, fermentation with *A. oryzae* resulted in higher tyrosinase inhibition activity of both broken rice and rice bran extracts, compared to fermentation with *R. oligosporus*. It was also observed that antioxidant activities of rice bran fermented with *A. oryzae* were higher than with *R. oligosporus* and vice versa for broken rice. Analysis of bioactive compounds using High-Performance Liquid Chromatography (HPLC) revealed that phenolic acids such as gallic, caffeic, ferulic and coumaric, as well as organic acids such as oxalic, citric, kojic and ascorbic were detected in the fermented extracts. Based on these results, both broken rice and rice bran have the necessary potential to be developed as cosmeceutical ingredients through the use of fungal solid-state fermentation.

KEYWORDS:
Broken rice, Rice bran, Antioxidant, Cosmeceuticals, Solid-state fermentation

INTRODUCTION:

Rice (*Oryza sativa)* is a staple food for most of the world's population especially in Asian countries.[1] The process of rice milling produces several rice by-products including broken rice and rice bran, which are mainly used as animal feed. Due to their high nutritional value, especially rice bran, it would be beneficial and interesting for these by-products to be converted into value-added products in food, nutraceutical or cosmeceutical industries.

Cosmeceuticals products are applied topically as cosmetics but contain ingredients that influence the skin's biological function.[2] The cosmeceutical sector has become one of the fastest-growing product categories globally, where cosmetic companies are heavily investing in research and development.[3] Interest in natural ingredients is on the rise as more consumers are looking for products that are effective, gentle and safe. Extracts from fermented plants or plant products such as soy, rice and papaya, are making their way into cosmeceutical products as active ingredient due to their multifunctional properties and lesser side effects compared to synthetic ingredients.

Solid state fermentation (SSF) is a promising technology for by-products or waste valorisation by using microorganisms to convert them into high value-added products.[4] The simplicity of SSF has made this process becoming an increasing trend in the biotechnology field in recent years; in addition it has high productivity, low energy consumption and minimal waste water generation.[5] Many species of bacteria, yeasts and fungi are used in SSF, but filamentous fungi, as described in a report by Raimbault[6] are considered to be the most important group of microorganisms used in SSF. This is due to their physiological, enzymological as well as their biochemical properties. *Aspergillus* spp. and *Rhizopus* spp. have long been utilized industrially; *A. niger* for the production of citric acid through large-scale fermentation vats and *R. oryzae* for the production of enzymes and various fermented food.

The present study aims to investigate the influence of SSF on rice by-products using fungi, specifically on the cosmeceutical-related activities such as antioxidant activity, as well as the content of bioactive compounds.

MATERIALS AND METHODS:

Culture preparation, fermentation process and extraction procedure

Fungal cultures of *A. oryzae* and *R. oligosporus* from MARDI's Collection of Functional Food Cultures (CFFC) were used in this study. Thirty grams of broken rice (BR) and rice bran (RB) were added to separate Erlenmeyer flasks and autoclaved at 121 °C for 15 min. Thirty-five mL of sterilized distilled water and 1% fungal spores (10^6 spores/mL) were mixed into each flask and incubated at 32 °C. After 18 days, the fermented samples were harvested and oven dried at 50 °C for 24 h. All samples were subjected to hot water extraction by mixing 1 g of sample with 5 mL distilled water and boiled for 15 min in a water bath. The samples were then centrifuged for 15 min at 10,000 rpm and the supernatant was collected and filtered using filter paper (Whatman No.1). The filtrates were then stored at -20 °C for further analysis. Experiments were performed in triplicate.

Determination of total phenolic content, total flavonoid content and antioxidant activities

Total phenolic content (TPC)

The Folin-Ciocalteu method was used to determine the phenolic content in each extract. An aliquot (1 mL) of each extract was added to the Folin-Ciocalteu reagent (5 mL) and 7.5% sodium carbonate solution (4 mL). The mixture was allowed to react for 2 h in the dark. The absorbance at 765 nm was measured using a spectrophotometer. Gallic acid was used as the reference standard.

Total flavonoid content (TFC)

The total flavonoid content of extracts was determined by the aluminium chloride colorimetric method.[7] In brief, 1 mL of extract was mixed with 4 mL of distilled water and then with 0.3 mL of 5% $NaNO_2$ solution. After 5 min of incubation, 0.3 mL of 10% $AlCl_3$ solution was added and the mixture was allowed to stand for 6 min. Then, 2 mL of 1 M NaOH solution was added, and the final volume of the mixture was made up to 10 mL with double-distilled water. The mixture was allowed to react for 15 min, and the absorbance at 430 nm was then measured. Quercetin was used as the reference standard.

Ferric reducing antioxidant power (FRAP) assay

The FRAP assay was performed as previously described.[8] An aliquot of extract (150 µL) was allowed to react with the freshly prepared FRAP working solution (2850 µL) for 30 min in the dark. The absorbance at 593 nm was measured using a spectrophotometer. Ferrous sulphate was used as the reference standard.

DPPH (2,2-diphenyl-1-picrylhydrazyl) assay

The radical scavenging activity of the samples was determined as described previously.[9] An aliquot of extract (150 µL) was mixed with a fresh DPPH working solution (2850 µL). The mixture was allowed to

react in the dark for 30 min. Then, absorbance of each mixture was read at 517nm using a spectrophotometer. The following equation was used to determine the percentage of scavenging activity:

$$\text{DPPH radical scavenging activity (\%)} = [(A_{blank} - A_{sample})/A_{blank}] \times 100$$

Determination of cosmeceutical-related enzymatic inhibition activities

Tyrosinase inhibition activity

Skin lightening or anti-pigmentation potential of extracts was determined by evaluating their tyrosinase inhibition activity. For this purpose, the dopachrome method[10] with some modifications was performed using L-DOPA as the substrate. The experiment was conducted using the 96-well plates. A mixture containing 40 µL of extract, 80 µL of 0.1 M phosphate buffer (pH 6.8) and 40 µL of mushroom tyrosinase (31 U/mL) was prepared. Sample and blank solutions with and without enzyme were also prepared. Forty µL of 10 mM L-DOPA solution (as the reaction substrate) was added into all wells containing extract and blank. The final mixtures were allowed to react at 25°C in the dark for 5 min. A microplate reader was used to determine the quantity of dopachrome produced in the reaction mixture. The measurement was taken at 475 nm. Kojic acid was used as a reference inhibitor.

Elastase inhibition activity

Anti-wrinkle potential of extracts was evaluated by measuring their elastase inhibition activity using Elastase Assay Kit (EnzChek, USA). The assay was performed by adding 50 µL of extract or positive control to 100 µL of porcine pancreatic elastase (0.5 U/mL). The mixture was then incubated in the dark at room temperature. After 15 min, 50 µL of DQ™ elastin working solution (25 µg/mL) was added into the mixture and allowed to react for 30 min in the dark at room temperature. Absorbance at 505/515 nm (Ex/Em) was measured using a fluorescent microplate reader. N-methoxy (N-methoxysuccinyl-Ala-Ala-Pro-Val-chloromethyl ketone) was used as a reference inhibitor. Inhibition of tyrosinase and elastase activities was calculated using the following equation:

$$\text{\% elastase/tyrosinase inhibition} = \{[(A - B) - (C - D)] / (A - B)\} \times 100$$

Note:
A = absorbance of blank solution with enzyme
B = absorbance of blank solution without enzyme
C = absorbance of sample solution with enzyme
D = absorbance of sample solution without enzyme

Determination of bioactive compounds composition of fermented RB extracts by high performance liquid chromatography (HPLC)

Phenolic acids

An Alliance Separation Module (Waters 2695) equipped with a photo-diode array detector (Waters 2996) with a reversed-phase analytical column (150 mm x 4.6 mm x Bridge C18, 3.5 µm, Waters) was used in the determination of phenolic acid composition.[11] To separate the compounds, the mobile phase used was 0.1% formic acid (A) and methanol (B) with the flow rate set at 0.7 mL/min. Peak identification was performed by comparing the retention times and the spectral data at 270 nm and 325 nm to the standard compounds. Quantification of phenolic acids was performed using the calibration curves obtained by injecting known amounts of standard compounds.

Organic acids

The organic acids in the sample were separated on a 250 mm x 4.6 mm, Extrasil ODS 5µm column.[12] The determination of organic acids was conducted in isocratic conditions at 30°C, using 50 mM phosphate solution (pH 2.8) as the mobile phase with the flow rate of 0.7 mL/min. α-tocopherol and γ-oryzanol were determined using a reversed phase (4.6 x 100 mm, 3.5 µm) column. The detector was set at λ = 325 nm.

Statistical analysis

Mean values and standard deviations were calculated from the data obtained from triplicate experiments. In determining the significance of the data, one-way analysis of variance (ANOVA) was conducted using Minitab Statistical Software (Version 14). Differences between means with a *p*-value of <0.05 were considered statistically significant.

RESULTS AND DISCUSSION:

Biological components and antioxidant activities of fermented BR and RB extracts

Polyphenols mainly exist in rice bran.[13] Rice bran is richer in nutrients including phenolics and flavonoid compounds compared to broken rice which are polished grains.[14] Our results (Table 1) indicate that major changes in the content of phenolics and flavonoids occurred with fermentation. As explained in a previous report[15], enhanced content of phenolics during rice bran fermentation is mainly caused by the cleavage of compounds complexed with lignin.

Table 1
Total phenolic (TPC) and total flavonoid (TFC) content of unfermented and fermented BR and RB extracts

Substrate	Treatment	TPC (mg GAE / g sample)*	TFC (mg QE / g sample)[1]
Broken Rice	UF	0.03±0.00^{e}	0.04±0.00^{d}
	A. oryzae	2.79±0.12^{d}	0.39±0.01^{c}
	R. oligosporus	3.87±0.30^{c}	0.65±0.02^{c}
Rice Bran	UF	3.61±0.03^{c}	2.74±0.01^{b}
	A. oryzae	11.05±0.89^{a}	4.75±0.14^{a}
	R. oligosporus	8.06±1.11^{b}	5.60±0.89^{a}

*Each value is expressed as mean ± SD. The values in the column with different letter are significantly different (p<0.05). UF= unfermented.

Ingredients with antioxidant properties are essential in any cosmeceutical and cosmetic formulation because of their function in protecting skin from free radical damage, as well as in protecting the formulation itself from auto-oxidation. In this study, extracts were subjected to radical scavenging (DPPH) and reducing antioxidant (FRAP) assays. As depicted in Figure 1(A), ferric reducing antioxidant activity of broken rice and rice bran was increased upon fermentation with both types of fungi. The highest activity (143.6 mM FE / g sample) was detected in *A. oryzae*-fermented rice bran extract with a 3-fold increment compared to its unfermented counterpart. Interestingly, DPPH radical scavenging activity of rice bran was marginally decreased upon fermentation with both fungi, as displayed in Figure 1(B). In contrast, almost a 10-fold increment was discovered in fermented broken rice extracts, compared to its unfermented counterpart. However, it is important to note that radical scavenging activity of rice bran prior to the fermentation process was high (94%).

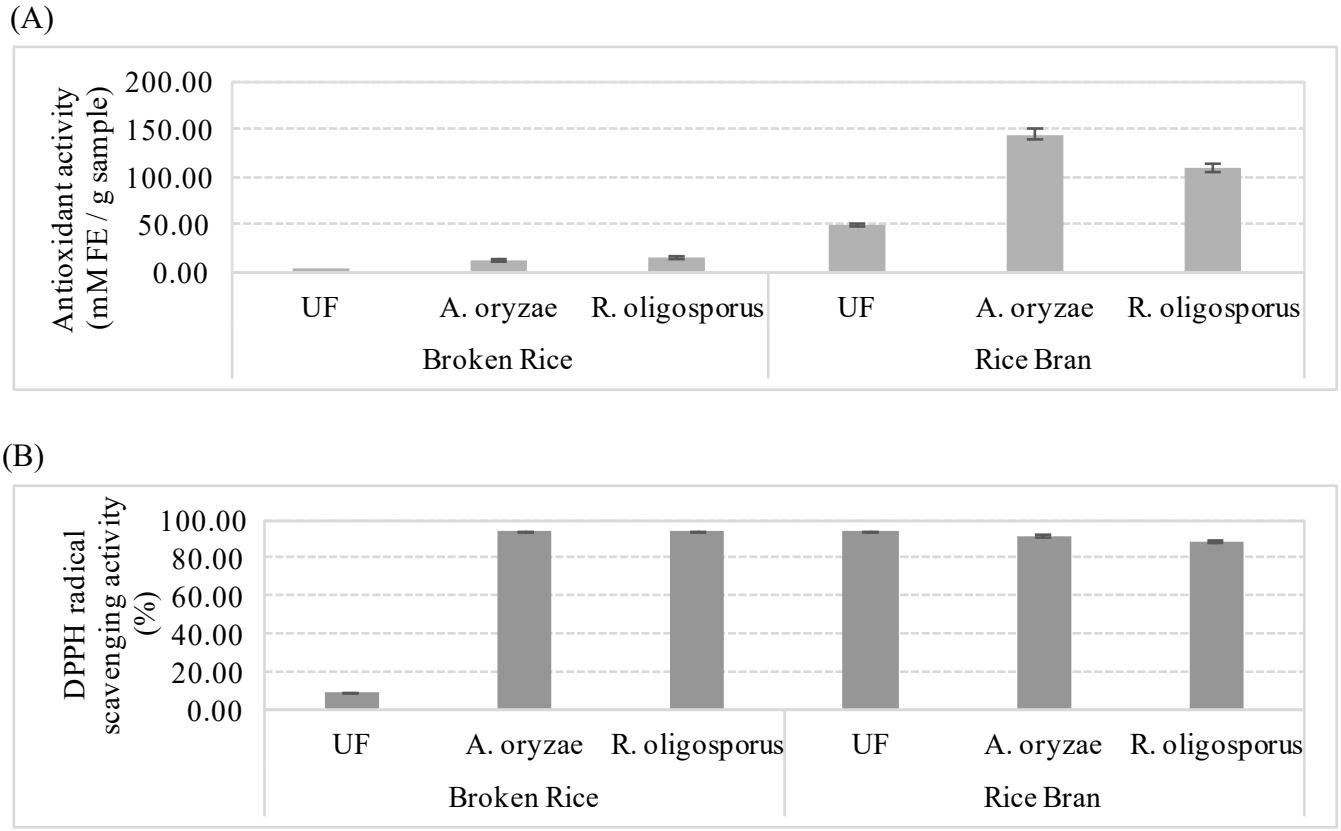

Each value is expressed as mean ± standard deviation (SD)

Figure 1
Antioxidant activities of broken rice and rice bran extracts as measured by different antioxidant assays; (A) ferric reducing antioxidant activity and (B) DPPH radical scavenging activity.

FRAP and DPPH are two different assays to measure the antioxidant activity or potential in studied samples. FRAP test measures the formed ferrous ions by increased absorbance, while DPPH test analyses the ability of sample to reduce radical cation by decreased absorbance (Schlesier et al., 2002). Every methods are selective for some antioxidant components and reactions, therefore the results of each assay are usually different.

The concentration of total phenolics in rice grains has been positively correlated with the antioxidant activity.[16] Our results suggested that the phenolic compounds were among the main responsible compounds for the antioxidant activity of fermented broken rice and rice bran. These results are consistent with a study[17] which reported that SSF with fungus increased the total phenolic content and intensified antioxidant properties of rice bran.

Cosmeceutical-related enzymatic inhibition of unfermented and fermented broken rice and rice bran
In the present study, the potential of fermented broken rice and rice bran extracts as skin whitening and anti-wrinkle agents was investigated by performing tyrosinase and elastase inhibition assays, respectively. Tyrosinase is a rate-limiting enzyme involved in the biosynthesis of melanin which, if over-produced, can cause hyper-pigmentation or darkening of the skin. Inhibitors of tyrosinase have become increasingly important in cosmeceutical products as depigmenting agents for hyperpigmentation disorders.[18] On the other hand, skin firmness and elasticity are mainly attributed to elastin, which can be degraded by the elastase enzyme.[19] Therefore, compounds that inhibit elastase are widely used in cosmeceutical products as anti-wrinkle or anti-aging agents.

Comparing rice bran to broken rice, fermentation with *A. oryzae* considerably increased tyrosinase inhibition activity of broken rice (Figure 2). Similar to radical scavenging activity, tyrosinase inhibition activity was

existed in rice bran prior to fermentation with fungi. Substrates fermented with *A. oryzae* exhibited strongest tyrosinase inhibition activity of the tested extracts, with a value of 69.4% for rice bran and 68.7% for broken rice. However, the inhibitory activity of these extracts was weaker than that of the reference inhibitor, kojic acid (96%).

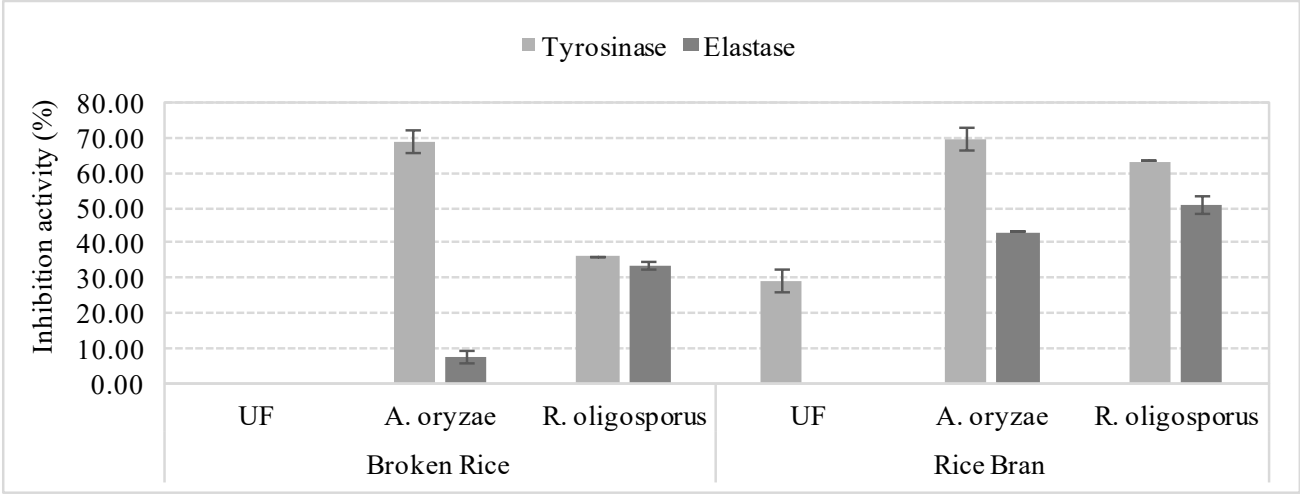

Each value is expressed as mean ± standard deviation (SD)

Figure 2

Tyrosinase and elastase inhibition activity of unfermented and fermented broken rice and rice bran.

Fermented extracts showed weak to moderate elastase inhibition activity, with the highest value exhibited by rice bran fermented with *R. oligosporus* (50.6%), but this was weaker than the reference inhibitor used in this study (n-methoxy, 98%). Unfermented extracts of broken rice and rice bran did not display any elastase inhibition activity, contrary to other research[20] which reported an IC_{50} value for elastase inhibition activity of rice extract of 107.51 µg/mL.

Bioactive compounds composition in unfermented and fermented broken rice and rice bran

Generally, *Aspergillus* spp. and *Rhizopus* spp. have different characteristics when growing on complex substrates and different ways of utilizing carbohydrates. Consequently they possess dissimilar potential for producing organic acids.[21] Our results (Table 2) showed that oxalic acid content displayed the most substantial increase in both substrates during fermentation with both fungi used in this study. Kojic acid, a strong antioxidant and a well-known skin-lightener [22], also stood out during the fermentation process with production in excess of 500 µg /mL (Table 2).

Table 2

Organic acid content of fermented broken rice and rice bran

Organic acid	Compound content (µg / mL)*					
	Broken Rice			Rice Bran		
	UF	*A. oryzae*	*R. oligosporus*	UF	*A. oryzae*	*R. oligosporus*
Oxalic	nd	69.60±4.5^{c}	829.18±14.9^{b}	59.30±0.1^{c}	2,236.11±11.48^{a}	827.16±56.89^{b}
Kojic	1.49±0.1^{e}	8.28±0.13^{d}	6.47±2.33^{d}	13.74±0.1^{c}	560.19±10.53^{a}	85.53±41.05^{b}
Ascorbic	nd	85.45±1.81^{a}	nd	nd	nd	96.44±7.1^{a}
Acetic	nd	638.16±38.61^{a}	nd	203.7±1.0^{b}	nd	nd

*Each value is expressed as mean ± SD. The values in the row with different letter are significantly different (p<0.05). nd= not detected; UF= unfermented

Phenolic acids are common secondary metabolites in rice grans with an extraction rate strongly affected by the extraction solvent and method.[13] Solid-state fermentation assisted in releasing the bound phenolic compounds due to the action of fungal enzymes in degradation of cell wall structure.[23] As reported in Table

3, fermentation of both substrates with *R. oligosporus* resulted in a greater increase in phenolic acid content during fermentation compared to unfermented substrates. *p*-coumaric and ferulic acids exhibited decreased content at the end of fermentation of rice bran with *R. oligosporus*, possibly due to oxidation processes that occur throughout the fermentation process. This result is consistent with a study[24] which also noted a reduced *p*-coumaric acid content after fermenting rice bran with *S. boulardii*. According to another sudy[15], ferulic acid was the main phenolic compound found in fermented and unfermented rice bran. Our results indicate otherwise. The type of fungus used in fermentation, as well as fermentation conditions, greatly affect the production of bioactive compounds. Consequently, it is difficult to compare our data with that of other studies due to different methods of extraction that were used. Moreover, compounds content and biological activities vary between species and varieties of grains.

Table 3
Phenolic acids content of fermented broken rice and rice bran

Phenolic acid	Compound content (µg / mL)*					
	Broken Rice			Rice Bran		
	UF	*A. oryzae*	*R. oligosporus*	UF	*A. oryzae*	*R. oligosporus*
Gallic	nd	3.11±0.83^{b}	22.54±1.44^{a}	nd	nd	nd
Protocatechuic	nd	nd	9.61±1.65^{a}	nd	nd	10.42±3.89^{a}
Hydroxybenzoic	nd	nd	6.63±0.81^{a}	nd	nd	5.15±1.71^{a}
Vanillic	nd	nd	12.78±1.06^{a}	2.78±0.06^{c}	nd	5.32±1.67^{b}
Caffeic	nd	nd	nd	nd	2.55±0.31^{a}	3.05±0.68^{a}
Syringic	nd	nd	nd	nd	nd	2.66±0.42
p-coumaric	nd	nd	nd	3.99±0.18^{a}	4.16±0.4^{a}	nd
Ferulic	nd	nd	nd	0.62±0.03^{b}	1.04±0.11^{a}	nd

*Each value is expressed as mean ± SD. The values in the row with different letter are significantly different (p<0.05). nd = not detected; UF= unfermented

Based on the content of kojic and ascorbic acids in fermented extracts, it is suggested that these two compounds contribute significantly to the tyrosinase inhibition activity of these extracts. As potent antioxidant compounds, ferulic and gallic acids were considered to be major contributors to the antioxidative activity of the fermented extracts. However, it is important to note that the biological activities exhibited by these extracts cannot be attributed directly to the type or the quantity of a single bioactive compound in the extract.[25] Different extracts contained diverse bioactive compounds in different quantities. Therefore, each extract possesses differing biological activities, which are also affected by the complex interactions – synergistic, additive or antagonistic - between the bioactive compounds. Previous research[26] has reported synergistic and antagonistic antioxidant effects of multiple combinations of some phenolic and flavonoid compounds. Also, other components, such as anthocyanins, tocopherols and gamma-oryzanol, may also contribute significantly to the biological activities of the tested extracts.

CONCLUSIONS:

The results of this study strongly suggest that both rice bran and broken rice can be successfully utilized to provide bio-ingredients with good cosmeceutical properties, through the application of fungal solid-state fermentation. Further investigations, for example on optimization of the fermentation process and *in vitro* studies, should be undertaken in order to fully achieve the maximum potential of these substrates in the cosmeceutical industry.

ACKNOWLEDGEMENTS:

This study was supported by the Malaysian Agricultural Research and Development Institute (MARDI) through the RMKe-11 Developmental Fund Research Grant (No. P-RBC-17).

REFERENCES:

1. Bird AR, Hayakawa T, Marsono Y, Gooden JM, Record IR, Correll RL, et al. Coarse brown rice increases fecal and large bowel short-chain fatty acids and starch but lowers calcium in the large bowel of pigs. J Nut. 2000 Jul;130(7):1780–7.
2. Grace R. Cosmeceuticals: Functional food for the skin. Nat Foods Merchandiser. 2002;23:92–9.
3. Truth In Aging. Cosmeceuticals-what are they? [Internet]. USA: Accord Media; 2012 [updated 2012 April 4; cited 2017 Oct 5]. Available from: https://www.truthinaging.com/review/cosmeceuticals-what-are-they
4. Yazid NA, Barrena R, Komilis D, Sanchez A. Solid-state fermentation as a novel paradigm for organic waste valorization: a review. Sustainability. 2017 Feb;9(2):224–252.
5. Chen HZ, He Q. Value-added bioconversion of biomass by solid-state fermentation. J Chem Technol Biotechnol. 2012 Dec;87(12):1619–25.
6. Raimbault M. General and microbiologial aspects of solid substrate fermentation. Electron J Biotechnol. 1998 Aug 15;1(3):0717–3458.
7. Chang C, Yang M, Wen H, Chern J. Estimation of total flavonoid content in propolis by two complementary colorimetric methods. J Food Drug Anal. 2002;10(3):178–82.
8. Benzie IF, Strain JJ. The ferric reducing ability of plasma as a measure of "antioxidant potential". Anal Biochem. 1996;239(1):70–6.
9. Thaipong K, Boonprakob U, Crosby K, Cisneros-Zevallos L, Byrne DH. Comparison of ABTS, DPPH, FRAP and ORAC assays for estimating antioxidant activity from guava fruit extracts. J Food Comp Anal. 2006 Nov;19(6):669–75.
10. Alam N, Ki NY, Kyung RL, Pyung GS, Jong CY, Ja MS, et al. Antioxidant activities and tyrosinase inhibitory effect of different extracts from *Pleurotus ostreatus* fruiting bodies. Mycobiol. 2011 Dec;38(4):295-301.
11. Robbins RJ, Bean SR. Development of a quantitative high-performance liquid chromatography-photodiode array detection measurement system for phenolic acids. J Chromatogr A. 2004 Jun;1038(1-2):97-105.
12. Nour V, Trandafir I, Ionica ME. HPLC organic acid analysis in different citrus juices under reversed phase conditions. Not Bot Hort Agrobot. 2010;38(1):44-48.
13. Shao Y, Bao J. Polyphenols in whole rice grain: Genetic diversity and health benefits. Food Chem. 2015 Aug 1;180:86-97.
14. Esa NM, Tan BL, Loh SP. By-products of rice processing: an overview of health benefits and applications. J Rice Res. 2013 Aug 15;1(1):1–11.
15. Schlesier K, Harwat M, Bohm V, Bitsch R. Assessment of antioxidant activity by using different in vitro methods. Free Radic Res. 2002 Feb;36(2):177 – 187.
16. Schmidt CG, Furlong EB. Effect of particle size and ammonium sulphate concentration on rice bran fermentation with the fungus *Rhizopus oryzae*. Bioresour Technol. 2012 Nov;123:36–41.
17. Zhang M, Guo B, Zhang R, Chi J, We Z, Xu Z, et al. Separation, purification and identification of antioxidant compositions in black rice. Agr Sci China. 2006 Jun;5(6):431-440.
18. Oliviera MS, Cipolatti EP, Furlong EB, Soares LS. Phenolic compounds and antioxidant activity in fermented rice (*Oryza sativa*) bran. Cienc Tecnol Aliment. 2012 Jul 10;32(3):531–7.
19. Petrillo AD, Gonzales-Paramas AM, Era B, Medda R, Pintus F, Santos-Buelga C, Fais A. Tyrosinase inhibition and antioxidant properties of *Asphodelus microcarpus* extracts. BMC Complement Altern Med. 2016 Nov;16:453–62.
20. Mathen C, Thergoankar R, Teredesai M, Soman G, Peter S. Evaluation of anti-elastase and antioxidant activity in anti-aging formulations containing Terminalia extracts. Int J Herb Med. 2014;2(2):95–9.

21. Widowati W, Fauziah N, Herdiman H, Afni M, Afifah E, Kusuma HSW, et al. Antioxidant and anti aging assays of *Oryza sativa* extracts, vanillin and coumaric acid. J Nat Remedies. 2016 Jul;16(3):88–99.
22. Magnuson JK, Lasure LL. Organic acid production by filamentous fungi. In: Lange J, Lange L, editors. Advances in fungal biotechnology for industry, agriculture and medicine. Boston, MA: Springer; 2004. p.307–40.
23. El-Kady IA, Zohri ANA, Hamed SR. Kojic acid production from agro-industrial by-products using fungi. Biotechnol Res Int. 2014 Mar;2014:1–10.
24. Sandhu K, Punia S, Kaur M. Fermentation of cereals: A tool to enhance bioactive compounds. In: Gahlawat SK, Salar RK, Siwach P, Duhan JG, Kumar S, Kaur P, editors. Plant biotechnology: recent advancement and developments. Singapore: Springer; 2017. p.157–70.
25. Ryan EP, Heuberger AL, Weir TL, Barnett B, Broeckling CD, Prenni JE. Rice bran fermented with *Saccharomyces boulardii* generates novel metabolite profiles with bioactivity. J Agric Food Chem. 2011 Mar 9;59(5):1862–70.
26. Sivakumar K, Mohandass S, Devika V. In vitro antioxidant and free radical scavenging activity of root extracts of Uraria lagopoides. Int J Pharma Bio Sci. 2012 Apr;3(2):1–8.
27. Hajimehdipoor H, Shahrestani R, Shekarchi M. Investigating the synergistic antioxidant effects of some flavonoid and phenolic compounds. Res J Pharmacogn. 2014;1(3):35– 40.

FP-06

OPTIMIZATION OF ENZYMATIC HYDROLYSIS PROCESS OF OIL PALM EMPTY FRUIT BUNCHES (EFBs) FOR GLUCOSE PRODUCTION

ERYATI DERMAN[1], RAHMATH ABDULLA[1,2]* AND RANISHA MARAPPAN[1]

[1]Faculty of Science and Natural Resources, Universiti Malaysia Sabah, 88400 Kota Kinabalu, Malaysia,
[2]Energy Research Unit, Universiti Malaysia Sabah, 88400 Kota Kinabalu, Malaysia

*Corresponding author: rahmahabdulla@gmail.com

ABSTRACT

Reducing the world's dependency on the non-renewable fossil fuel is the major aim of creating sustainable and renewable biofuels. Glucose production from oil palm empty fruit bunches (EFBs) is important for further fermentation steps for bioethanol production. This study sets out to establish the most optimal conditions for enzymatic hydrolysis of Oil palm empty fruit bunches (EFBs) using Response Surface Methodology approach to produce high yield of glucose. There were two major steps employed in the conversion of EFBs to glucose which were pretreatment and hydrolysis process. The screening of the best enzyme combination (Cellulase and β-glucosidase) was determined and it is observed that the ratio of 50:10 U/g of the enzymes gave the highest soluble glucose concentration up to 10.02 mg/mL. The effect of the independent variables (temperature, time, and pH) on the dependent variable (glucose concentration) was studied. The highest glucose production, 5.20 mg/mL was produced at 50°C, 48 hours, and pH 5. From the analysis, an optimized glucose concentration of 4.71 mg/mL was predicted at the operating condition of 54.88°C, 60.79 hours and pH 5.27 which is suggested by the model with desirability value 0.775.

KEYWORDS:
Oil palm empty fruit bunches, Pretreatment, Enzymatic hydrolysis, Optimization, Glucose

INTRODUCTION:

The 20th century has been an era of petroleum that has provided humanity with a wide range of fuels and chemicals that have influenced most aspects of human life. Finding new alternative and renewable energy resources were the main objectives to tackle the growing global demand for energy.[1] Biofuels are sustainable and non-polluting fuel produced from renewable bioresources that have gained prominence in recent years.[2] Bioethanol is the most common first generation biofuels produced from a biological conversion process.[3] Bioethanol is an attractive liquid biofuel which is widely used in automobile engines as fuel alone or by blending with gasoline.[4-5] Among the potential green energy resources, lignocellulosic biomass is chosen as an alternative raw material for bioethanol production and other value-added compounds.[6-7]

Empty fruit bunch (EFB) is a lignocellulosic biomass waste from oil palm industries which can be used as potential feedstock for bioethanol production. The high content of cellulose and hemicelluloses which are about 75 to 80% opens new approaches to convert EFB into bioethanol.[8] An efficient conversion process is needed in order for the potential feedstock EFBs to be converted into bioethanol.[9] Three prime steps; pretreatment, hydrolysis, and fermentation are the key factor in producing bioethanol.[10] However, EFBs conversion to glucose is one of the vital factors for the bioethanol production. Hence, optimization of hydrolysis process is focussed on this research for higher glucose yield. Hydrolysis had an essential and important role of yielding as many sugars as possible from EFBs before the fermentation process starts.[11] Response Surface Methodology (RSM) software is employed to create a series of experiments to find the desired parameters for the optimization process obtaining higher glucose yield using Central Composite

Design (CCD) as statistical design.[11-12] The objective of this research is to optimize the enzymatic hydrolysis process of oil palm empty fruit bunches (EFBs) to obtain high glucose yield using Response surface methodology (RSM). However, before it can be applied, it is very important to determine the best enzyme combination between cellulase and β- glucosidase in producing a higher yield of reducing sugar glucose.

MATERIALS AND METHODS:

EFB Collection and preparation

EFBs were collected from a local palm oil processing mill in Beaufort, Malaysia (Lumadan Palm Oil Mill). It was washed thoroughly with tap water to remove all the salts, dirt, oil and debris. Then, the EFBs were dried at 70°C for 3 days. It was then cut into smaller pieces so that it could be fed into a blender. The EFBs were blended by using laboratory blender (Waring Commercial), sieved and separated in fractions using a test sieve. The EFB samples then were stored in sealed plastic bags and in a dry place until further use in the pretreatment steps.

Chemical pretreatments of EFB

Dried EFB fibers were soaked in 2% (v/v) sulphuric acid (H_2SO_4) solution. Then, it was heated in an autoclave at 120°C, 15 psi for 20 minutes. Upon completion of the reaction, the solids were separated from the aqueous solution by filtration. The water-insoluble solids (WIS) fraction was collected, washed with distilled water until no traces of acid could be detected (until reached pH 7) and then dried in an oven at 70°C. This pretreated EFB was used as the substrate in the subsequent enzymatic hydrolysis experiments.

Determination of cellulase and β-glucosidase enzyme ratio

Enzymes Cellulase (Cellulase from *Trichoderma reesei* ATCC 26921, aqueous solution, 50 mL) and β-glucosidase (EC 3.2.1.21 from Almonds, 0.88 g solid, Crude, Lyophilized powder) used in this study were purchased from Sigma Aldrich. The pretreated EFB was enzymatically hydrolyzed in an Erlenmeyer flask using the commercial cellulolytic enzyme (Cellulase) and β-glucosidase with a ratio of 50:10 U/g.[13-14] Enzymatic hydrolysis was performed in 50 mL of 0.05 M sodium citrate buffer (pH 4.8) at 50°C and shaken at 150 rpm using the orbital shaker (Heidolph). First, 2% (v/v) pretreated EFB was added into the sodium citrate buffer solution and was preheated in the oven of 50 °C. After the temperature of the solution reached 50 °C, enzymes were added. Finally, the flasks were incubated at the shaker of 50 °C for the optimum time interval of 72 h.[15] The process was repeated with different enzyme ratios of Cellulase and β-glucosidase (10:50, 50:0 and 0:50 U/g). The sample was taken and put into the boiling water for 10 minutes to deactivate the enzyme activity prior to glucose concentration measurement.

Determination of glucose concentration by DNS assay

A 3,5- dinitrosalicyclic acid (DNS) assay is useful for the quantitative determination of reducing sugar. The analysis involves a set of glucose standard ranging from 0.0 to 1.0 mg/mL (total sample volume 1 mL). After that, 1.0 mL DNS reagent was added to each tube (include sample tube). All the tubes were heated in boiling water bath for 5 minutes to allow the reaction between glucose and DNS to occur. The tubes were left to cool down, the solution was mixed well and the absorbances of each solution were read at 540 nm by using Microplate reader (Thermo Scientific, Multiskan Go). The concentration of glucose was then determined through the standard curve.

Table 1
Experimental range and levels of independent process variables

Independent variable	Range and levels			
	Low actual	High actual	Mean	Standard. Deviation
Temperature (°C)	40.00	60.00	50.000	8.264
Reaction time (hour)	24.00	72.00	50.400	19.686
pH	4.00	6.00	5.000	0.826

Experimental design and RSM

For the experimental design, response surface methodology (RSM) was utilized to optimize the enzymatic hydrolysis process by adopting the central composite design (CCD). The design consisted of 20 sets of experiments. There were 3 factors selected for the enzymatic hydrolysis design which were temperature, reaction time and pH.[16]

Enzymatic hydrolysis of EFB

The pretreated EFB was enzymatically hydrolyzed in an Erlenmeyer flask using cellulase and β- glucosidase enzymes with the best ratio obtained from the previous enzyme screening. Effects of temperature (40 to 60°C), pH (4 to 6) and hydrolysis time (24 to 72 h) on the enzymatic hydrolysis process of EFBs were studied. The process was carried out with 2% (w/v) pretreated EFBs in 50 mL of 0.05 M sodium citrate buffer incubated in the orbital shaker at 150 rpm. Twenty sets of experiments with a different combination of parameters were done based on the design. At the end of the experiment, each sample was put into the boiling water for 10 minutes to deactivate the enzyme activity. The deactivated hydrolysate was then centrifuged at 10,000 rpm for 10 minutes to obtain a clear hydrolysate and later was stored at 4°C prior to glucose concentration analysis using High Performance Liquid Chromatography (HPLC).

Determination of glucose concentration by HPLC

The sugar contents of the hydrolyzed samples were determined using HPLC. Before the sample was brought for analysis, derivatization of monosaccharide using 1-phenyl-3-methyl-5-pyrazolone (PMP) was done. Firstly, 25 µl of sample/standard was added followed by addition of 25 µl of NaOH. Secondly, the mixture was added with 50 µl of PMP. The mixture was mixed thoroughly by vortex mixer and heated at 70°C for 100 min. Then, the mixture was cooled down at room temperature. Next, 50 µl of 0.3 HCl was added and further dried in fume hood. The residue was then added with 1.0 mL pure water (18.2 mΩ). Then, the mixture was added with 1.0 mL chloroform and the mixture was shaken vigorously. The upper layer was transferred into another microcentrifuge tube and added with 1.0 ml chloroform. The steps of removing the aqueous layer and adding centrifuge were repeated for four times. Finally, the aqueous layer that was taken after completing four steps was filtered using 0.45 µm PTFE membrane filters into vials. The required settings for HPLC were sodium phosphate buffer (83%) and acetonitrile (17%) as the mobile phase; run time of 20 min, wavelength of 245 nm, flow rate of 1.0 ml/min and injector volume of 20 µl. All samples were filtered through 0.45 µm PTFE membrane filters and injected into the column. The data are acquired and analyzed.[15]

RESULTS AND DISCUSSION:

Effect of acid pretreatment on EFB

After drying, the pretreated EFB showed more faded brown color and had soft texture as compared to the color as well as texture prior to pretreatment. Dilute acid treatment removes the silica component and impurities on the surface of EFB fiber. The silica component of cell walls acts as physical barrier whereby prevent the plant from being exposed to enzymatic hydrolysis.[17] Thus, to enhance the EFB digestibility, the removal of the silica during pretreatment is necessary. According to Astimar *et al*, H_2SO_4 acts as a swelling agent to increase the pretreatment process efficiency. The H_2SO_4 penetrates and swell both the accessible amorphous and crystalline region of cellulose.[18]

Screening of enzyme ratio combinations

The concentration for each combination was calculated from the equation obtained from the glucose standard curve. The result of the concentration of soluble glucose obtained from analysis using DNS is shown in Figure 1.

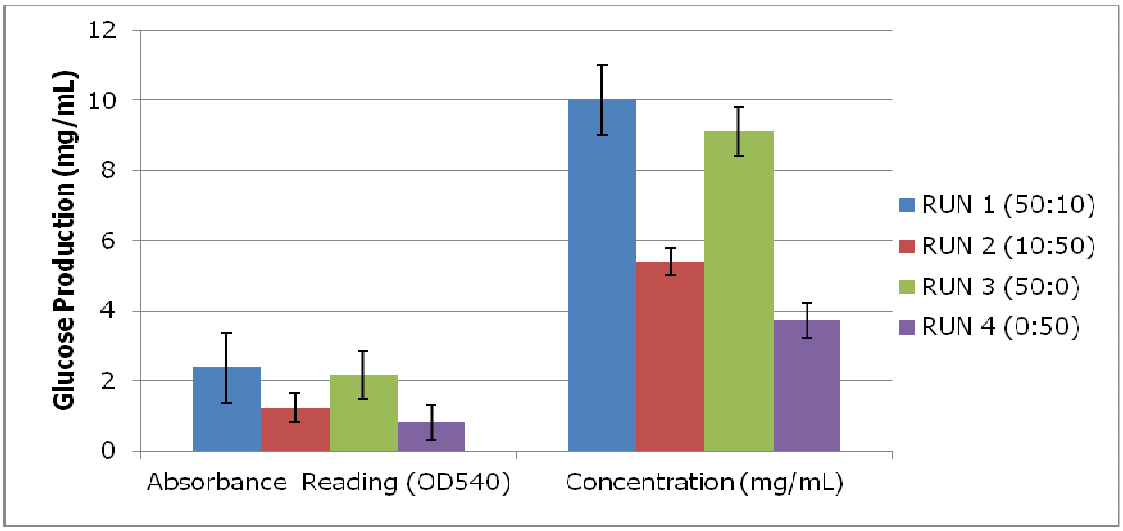

The values are Mean ± S.D. of triplicates (P<0.05)
* Ratio of the enzyme is in U/g

Figure 1
Production of soluble glucose using Cellulase and β,1-4 glucosidase.

Based on the results; it is revealed that the combinations of Cellulase and β-glucosidase were better in enhancing the glucose production than the single enzyme treatment. The ratio of 50:10 U/g of enzymes Cellulase: β-glucosidase hydrolyzed more cellulose from treated EFBs fiber and gave the highest soluble glucose concentration up to 10.02 mg/mL. Addition of β-glucosidase increases the glucose production due to further conversion of cellubiose into glucose. It also catalyzes the hydrolysis of cellodextrins, thus releasing glucose as the main product during the process.[20] However, only a limited amount of β-glucosidase is required in the process. This is to avoid enzyme inhibition because excess of cellubiose during the process inhibits the endoglucanases and cellobiohydrolase. [13, 21, 22] During the hydrolysis process, Cellulase enzyme which contains endoglucanase and cellubiohydrolase act directly on cellulose to yield glucose and cellubiose. Then, the β-glucosidase will further hydrolyzed the cellubiose formed in the process into glucose.[19] Rate of glucose formation from cellubiose is much slower than the rate of glucose formation from cellubiohydrolase and endoglucanase. Hence, more addition of β-glucosidase is unsuitable as it only increases the amount of the enzymes in the reaction mixture. [13]. Combination of both cellulase and β-glucosidase enzymes with ratio of 5:1 also hydrolyzed more cellulose from treated EFB fiber and gave highest soluble glucose concentration in studied by Barlianti *et al*., 2015 and Hamzah *et al*., 2011.[13-14]

Enzymatic hydrolysis process optimization by RSM
The experimental design and analysis were carried out using Design Expert Software Version 7.0.0 to study the effect of temperature, time and pH during enzymatic hydrolysis treatment for the conversion of EFB to glucose. A good correlation between the predicted and experimental glucose concentration was observed as it indicates high accuracy of a response surface model constructed in this study.

a) Fit summary for model
Further data analysis using RSM was conducted to determine the suitable model that best fit the experiment data. Table 1 shows the sum of squares of RSM sequential model. The highest order polynomial where the additional terms are a significant and not aliased model were selected. The quadratic model was suggested through the data analysis with the p-value of 0.0005 (<0.05). The corresponding statistical analysis for each model was also presented in Table 2 with more detailed statistical analysis on the models. The analysis focuses on the model maximizing the 'Adjusted R-Squared' and the 'Predicted R-Squared'. The quadratic model was found to have the large value of adjusted R-squared (0.7134) and the predicted R-squared (0.00349).

Table 1
Sequential model sum of squares

Source	Sum of squares	df	Mean square	F value	p-value Prob > F	
Mean vs Total	295.52	1	295.52			
Linear vs Mean	1.12	3	0.37	0.81	0.5075	
2 Factor Interaction vs Linear	0.42	3	0.14	0.26	0.8519	
Quadratic vs 2 Factor Interaction	**5.67**	**3**	**1.89**	**14.76**	**0.0005**	**Suggested**
Cubic vs Quadratic	0.63	4	0.16	1.46	0.3232	Aliased
Residual	0.65	6	0.11			
Total	304.01	20	15.20			

Table 2
Model summary statistics

Source	Std. Dev.	R-Squared	Adjusted R-Squared	Predicted R-Squared	PRESS	
Linear	0.68	0.1316	-0.0312	-0.2785	10.85	
2FI	0.73	0.1810	-0.1969	-2.3545	28.47	
Quadratic	**0.36**	**0.8492**	**0.7134**	**0.0349**	**8.19**	**Suggested**
Cubic	**0.33**	0.9235	0.7578		+	Aliased

b) ANOVA for Response Surface quadratic Model

From the ANOVA table, the Model F-value of 6.25 implies the model is significant. There is only a 0.42% chance that a "Model F-Value" this large could occur due to the noise. In this model, the p-value is 0.0042. In addition, the significance of each coefficient was determined using the p-value. The values less than 0.05 indicate model terms are significant. From Table 3, the A (Temperature), B (Time), A^2 (Temperature), B^2 (Time) and C^2 (pH) model terms are significant with a p-value of less than 0.05 (<0.05). However, for other terms the p-values are greater than 0.05, indicates insignificant effects. The "Lack of Fit F-value" of 1.46 implies the Lack of Fit is not significant relative to the pure error. There is only a 32.32% (p-value of 0.3232) chance that a "Lack of Fit F-value" this large could occur due to noise. Non-significant lack of fit is good as we want the model to fit. The value of the R^2 value in the quadratic model is 0.8492. The "Pred R-Squared" of 0.0349 is not as close to the "Adj R-Squared" of 0.7134. This may indicate a large block effect or a possible problem with the model or data. The Adeq Precision measures the signal to noise ratio. A ratio greater than 4 is desirable. The ratio of 6.906 indicates an adequate signal. The C.V. is the coefficient of variance. The value of C.V in this design is 9.31 %.

c) Diagnostic plot of quadratic model

Figure 2 shows the normal probability plot of the residuals of the data. The residuals roughly follow a straight line which indicates that the data of the experiment were normally distributed. Normal probability plot usually in the range 0 to 1. Since pH is not significant, it affects the normal probability plot

Table 3
Analysis of variance table (ANOVA)

Source	Sum of squares	df	Mean square	F value	p-value Prob > F	
Model	7.21	9	0.80	6.25	0.0042	**significant**
A-Temperature	0.76	1	0.76	5.91	0.0353	**significant**
B-Time	0.74	1	*0.74*	5.74	0.0375	**significant**
C-ph	0.11	1	*0.11*	0.85	0.3775	
AB	*9.382E-003*	1	*9.382E-003*	0.073	0.7921	
AC	*0.46*	1	*0.46*	3.59	0.0876	
BC	*0.11*	1	*0.11*	0.88	0.3692	

A^2	*1.40*	1	*1.40*	10.93	0.0079	**significant**
B^2	*0.90*	1	*0.90*	7.05	0.0241	**significant**
C^2	*4.42*	1	*4.42*	34.55	0.0002	**significant**
Residual	1.28	10	0.13			
Lack of fit	*0.63*	4	*0.16*	1.46	0.3232	**not significant**
Pure Error	*0.65*	6	*0.11*			
Cor Total	8.49	19				

Std. Dev.	0.36	R-Squared	0.8492
Mean	3.84	Adj R-Squared	0.7134
C.V. %	9.31	Pred R-Squared	0.0349
PRESS	8.19	Adeq Precision	6.906

The values are significant if P<0.05

d) Model graph of Quadratic for Contour and Surface plot

A surface plot (3D) displays a three-dimensional view that may provide a clear picture of the response surface. On the other hand, contour plot is viewed ad two-dimensional plane where all points that have the same response are connected to produce contour lines of constant responses.

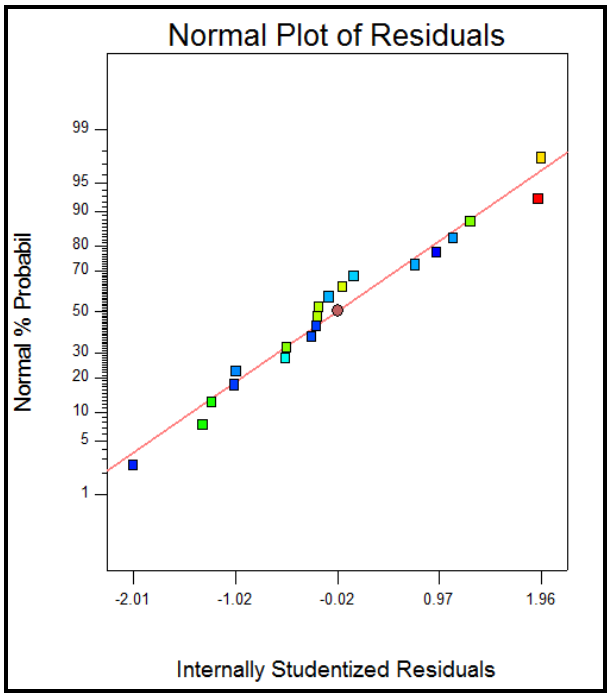

Figure 2
Normal probability plot of residuals

1. **Temperature versus Time**

The contour plot and 3D response surface show the result that as temperature increases to 50 °C and as the time increases to 72 h, the glucose concentration also increases. The maximum glucose concentration (4.48 mg/mL) was at temperature 50°C and time 48 h whereas the minimum glucose concentration (3.66 mg/mL) was at a temperature 40°C with time ranging from 24 to 36 h. According to theory, when the temperature increases, the kinetic energy of the molecules also increases. This means there are more random collisions between molecules per unit time in the buffer.[23] Since enzymes catalyze the reaction by randomly colliding with EFB molecules, the increase in temperature increases the rate of reaction whereby forming more products (glucose). According to Viikari *et al*., the conventional cellulases work within a range of temperature around 50°C and they are inactivated at temperatures above 60 to 70°C due to disorganization

of their three-dimensional structures followed by irreversible denaturation.[24] Aderemi *et al*. also reported an optimum yield at 50°C on the hydrolysis of rice straw.[25]

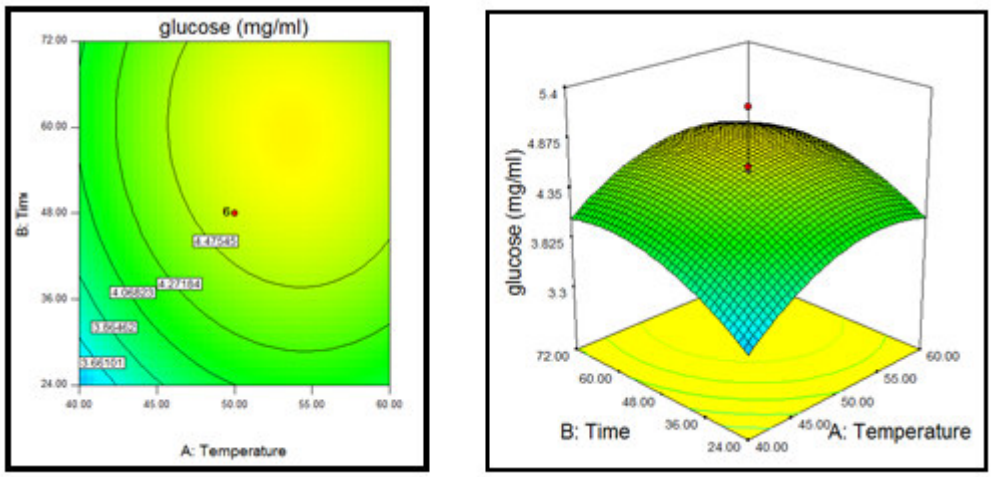

Figure 3
The response contour and surface plot of glucose concentration showing the interactive effect of temperature and time (hold value: pH, 5.00)

ii) Temperature versus pH

The contour plot and 3D response surface show the result that as temperature increases to 50°C and as the pH decreases to 4, the glucose concentration increases. The maximum glucose concentration (4.42 mg/mL) was at temperature 50°C and pH 5 whereas the minimum glucose concentration (3.73 mg/mL) was at a temperature of 40°C, pH 4/6 and 60°C with pH 4. A lower pH value is needed by the enzyme to maximize the glucose production. Lower pH values indicate high H^+ concentrations and low OH^- concentrations. The H^+ and OH^- are charged so hydrogen and ionic bonds that hold together an enzyme will interfere since they will be attracted or repelled by the charges created by the bonds. This interference causes a change in shape of the enzyme and also the active site.[26] Optimum pH is at which the bonds within them are influenced by H+ and OH- ions in such a way that the shape of their active site is the most complementary to the shape of EFB. Any change in pH above or below the optimum will quickly cause a decrease in the rate of reaction since more of the enzyme molecules will have an active site whose shapes are not complementary to the shape of EFB.[23] This is the reason the glucose concentration decreased dramatically after passing pH 5. The result on pH from this study is consistent with reports from Krishna and Chowdary, 2000. The research found out that pH has a significant effect on the hydrolytic behavior of the cellulases. Thus, the effect of pH on both adsorption and hydrolysis is similar that usually occur at around pH 4.8.[27] Furthermore, it was also reported that maximum hydrolysis of alkali-treated sugarcane bagasse was gain at pH 5.0.[28]

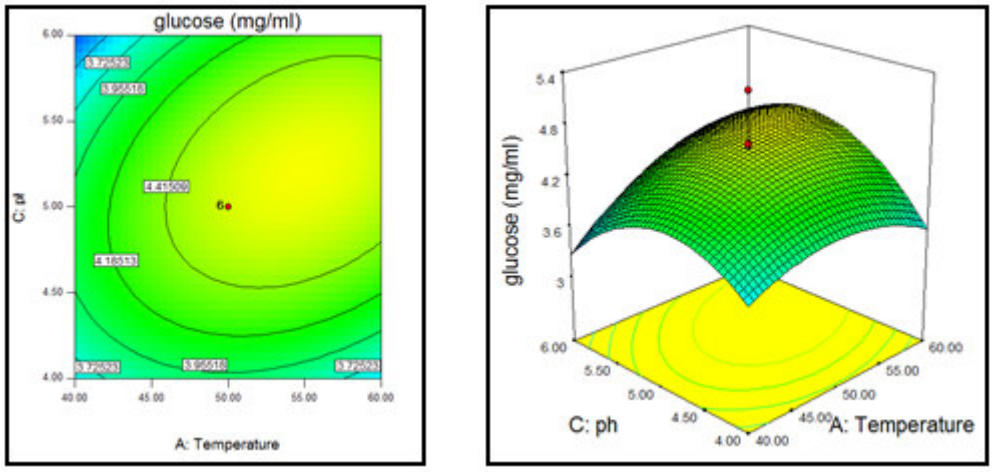

Figure 4

The response contour and surface plot of glucose concentration showing the interactive effect of temperature and pH (hold value: time, 48.00 hours)

iii) Time versus pH

The contour plot and 3D response surface show the result that as time increases to 48 h and as the pH increases to 5, the glucose concentration also increases. The maximum glucose concentration (4.45 mg/mL) was at time 48 h and pH 5 whereas the minimum glucose concentration (3.66 mg/mL) was at a time from 24 h with pH 4. When the reaction time increases, the interaction between enzymes and EFB also increases. This is because, as time increases, the EFB and enzyme molecules have a high chance of colliding with each other. Thus, enzyme can attach complementarily at a high rate at the active site of EFB molecule and convert it to glucose. However, as the reaction proceeds and EFB was consumed, the glucose production slowly reduced.[29] One of the research reported that the optimum conditions for hydrolysis of pretreated EFB were 50°C, 150 rpm, and incubation for 72 h.[30] The same parameters were also used by Nurul Adela *et al*., in her study which obtained the highest glucose yield of 567.2 mg/g.[15] In contrast, Nursyafiqah *et al*., which conducted an enzymatic hydrolysis of treated OPEFB produced 168.58 mg/mL glucose after 24 h only.[31]

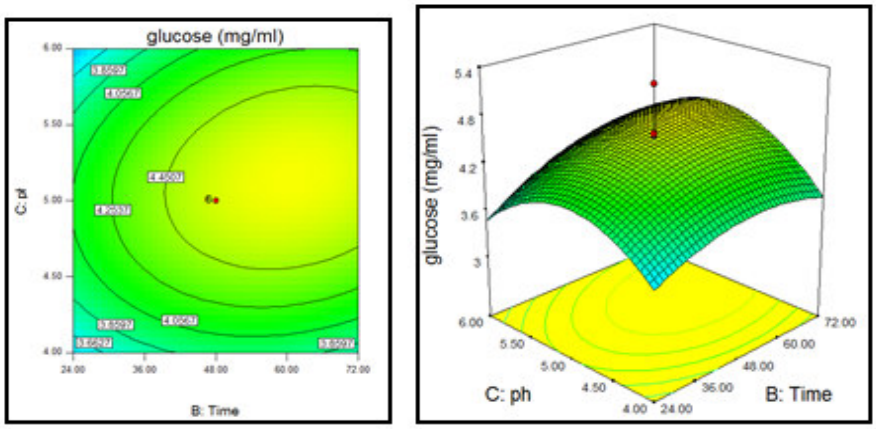

Figure 5

The response contour and surface plot of glucose concentration showing the interactive effect of time and pH (hold value: temperature, 50°C)

Optimization and validation of results

Based on the quadratic model from statistical design, numerical optimization was conducted. The factors were set "in range" and the glucose concentration was set to "maximize". The optimum conditions suggested are 54.88°C , 60.79 h, and pH 5.27 respectively. The highest predicted glucose concentration is 4.71 mg/mL. Figure 4.14 shows the experimental condition suggested by a model with desirability value 0.775. The value is quite near to 1 (maximum value) indicating that the factors optimized are quite desirable.

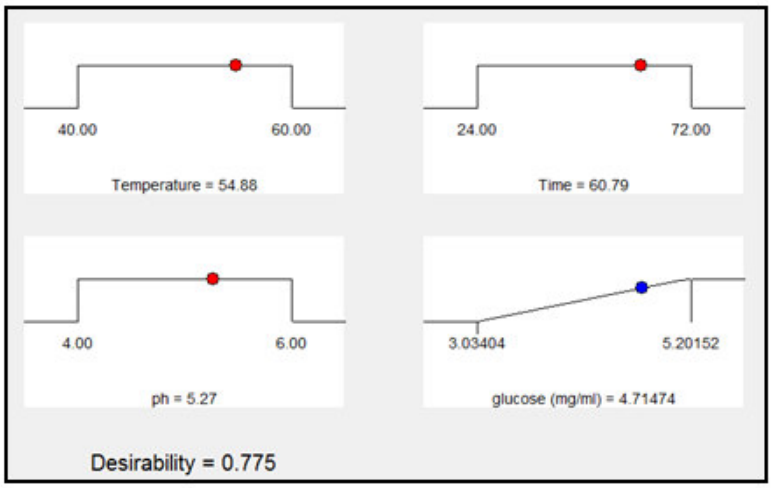

Figure 6
Optimum experimental condition suggested by the model

CONCLUSION:

In summary, a screening of enzyme combination ratio was carried out to enhance the glucose production in the enzymatic hydrolysis process of EFBs. From the studies, it was found out that the best combination of cellulase and β-glucosidase enzymes were at a ratio of 50:10 U/g as it produced the highest soluble glucose concentration of 10.02 mg/ml. After that, various runs were carried out under different combination of parameters as proposed by experimental design using RSM. It is concluded that an optimized glucose concentration of 4.71 mg/ml can be produced at the operating condition of 54.88 ˚C, 60.79 h and pH 5.27 as suggested by the model with desirability value 0.775.

REFERENCES:

1. Gaurav N, Sivasankari S, Kiran GS, Ninawe A, Selvin J. Utilization of bioresources for sustainable biofuels: A Review. Renew Sustain Energy Rev. 2017;73(November 2016):205–14.
2. Demirbas A. Biorefineries: For biomass upgrading facilities. London: Springer Science and Business Media; 2009. 58-75 p.
3. Luque R, Pinzi S, Campelo JM, Ruiz JJ, Lopes I, Luna D, et al. Chapter 8 Biofuels for transport: Prospects and challenges. In: Shah V, editor. Emerging environmental technologies. New York: Springer Science Business Media; 2009. p. 172–211.
4. Demirbas A. Biofuels sources, biofuel policy, biofuel economy and global biofuel projections. Energy Convers Manag. 2008;49(8):2106–16.
5. Özçelik a. E, Aydoğan H, Acaroğlu M. A Study of the Effects of Bioethanol-Gasoline Blends on Vehicle Emissions. J Clean Energy Technol. 2015;3(5):332–5.
6. Kricka W, Fitzpatrick J, Bond U. Metabolic engineering of yeasts by heterologous enzyme production for degradation of cellulose and hemicellulose from biomass: A perspective. Front Microbiol. 2014;5(APR):1–11.
7. Musatto SI, Dragone G, Fernandes M, Milagres AMF, Roberto IC. The effect of agitation speed , enzyme loading and substrate concentration on enzymatic hydrolysis of cellulose from brewer ' s spent grain. Sprimger Sci Media. 2008;15:711–21.
8. Tan HT, Lee KT, Mohamed AR. Second-generation bio-ethanol (SGB) from Malaysian palm empty fruit bunch: Energy and exergy analyses. Bioresour Technol. Elsevier Ltd; 2010;101(14):5719–27.
9. Bouza RJ, Gu Z, Evans JH. Screening conditions for acid pretreatment and enzymatic hydrolysis of empty fruit bunches. Ind Crops Prod. Elsevier B.V.; 2016;84:67–71.
10. Shamsudin S, Md Shah UK, Zainudin H, Abd-Aziz S, Mustapa Kamal SM, Shirai Y, et al. Effect of steam pretreatment on oil palm empty fruit bunch for the production of sugars. Biomass and Bioenergy. Elsevier Ltd; 2012;36:280–8.

11. Liong YY, Halis R, Lai OM, Mohamed R. Conversion Of Lignocellulosic Biomass From Grass To Bioethanol Using Materials Pretreated With Alkali And The White Rot Fungus, Phanerochaete Chrysosporium. Bioresources. 2012;7:5500–13.
12. Goh CS, Tan HT, Lee KT, Brosse N. Evaluation and optimization of organosolv pretreatment using combined severity factors and response surface methodology. Biomass and Bioenergy. Elsevier Ltd; 2011;35(9):4025–33.
13. Hamzah F, Idris A, Shuan TK. Preliminary study on enzymatic hydrolysis of treated oil palm (Elaeis) empty fruit bunches fibre (EFB) by using combination of cellulase and β 1-4 glucosidase. Biomass and Bioenergy. Elsevier Ltd; 2011;35(3):1055–9.
14. Barlianti V, Dahnum D, Hendarsyah H, Abimanyu H. Effect of Alkaline Pretreatment on Properties of Lignocellulosic Oil Palm Waste. Procedia Chem. 2015;16:195–201.
15. Nurul Adela B, Nasrin AB, Loh SK, Choo YM. Bioethanol production by fermentation of oil palm empty fruit bunches pretreated with combined chemicals. J Appl Environ Biol Sci. 2014;4(10):234–42.
16. Rahman SHA, Choudhury JP, Ahmad AL, Kamaruddin AH. Optimization studies on acid hydrolysis of oil palm empty fruit bunch fiber for production of xylose. Bioresour Technol. 2007;98(3):554–9.
17. Rezanka T, Sigler K. Biologically active compounds of semimetals. Chem Inf. 2008;39:585–606.
18. Aziz AA, Husin M, Anis M. Preparation of cellulose from oil palm empty fruit bunches via ethanol digestion: effect of acid and alkali catalysts. J Oil Palm Res. 2002;14:9–14.
19. Cao Y, Tan H. Effects of cellulase on the modification of cellulose. Carbohydr Res. 2002;337(14):1291–6.
20. 20. Garcia NFL, da Silva Santos FR, Gonçalves FA, da Paz MF, Fonseca GG, Leite RSR. Production of β-glucosidase on solid-state fermentation by Lichtheimia ramosa in agroindustrial residues: Characterization and catalytic properties of the enzymatic extract. Electron J Biotechnol. Elsevier B.V.; 2015;18(4):314–9.
21. Zhang Z, Wang M, Gao R, Yu X, Chen G. Synergistic effect of thermostable β-glucosidase TN0602 and cellulase on cellulose hydrolysis. Biotechnology. 2017;7(1):54.
22. Turan Y, Zheng M. Purification and characterization of an intracellular β- glucosidase from the methylotrophic yeast Pichia pastoris. Biochem. 2005;70(12):1363–8.
23. Zhang M, Su R, Qi W, He Z. Enhanced enzymatic hydrolysis of lignocellulose by optimizing enzyme complexes. Appl Biochem Biotechnol. 2010;160:1407–14.
24. Viikari L, Alapuranen M, Puranen T, Vehmaanpeera J, Siikka-aho M. Thermostable enzymes in lignocellulose hydrolysis. Adv Biochem Eng Biotechnol. 2007;108:121–45.
25. Aderemi BO, Abu E, Highina BK. The kinetics of glucose production from rice straw by Aspergillus niger. African J Biotechnol. 2008;7(11):1745–52.
26. Saravanakumar K, Kathiresan K. Bioconversion of lignocellulosic waste to bioethanol by Trichoderma and yeast fermentation. 3 Biotech. 2014;4(5):493–9.
27. Hari Krishna S, Chowdary G V. Optimization of simultaneous saccharification and fermentation for the production of ethanol from lignocellulosic biomass. J Agric Food Chem. 2000;48(5):1971–6.
28. Mahamud MR, Gomes DJ. Enzymatic Saccharification of Sugar Cane Bagasse by the Crude Enzyme from Indigenous Fungi. J Sci Res. 2011;4(1):227.
29. Karmakar M, Ray RR. Current Trends in Research and Application of Microbial Cellulases. Eff Br mindfulness Interv acute pain Exp An Exam Individ Differ. 2011;6(1):1689–99.
30. Kassim MA, Loh SK, Bakar NA, Aziz AA, Mat Som R. Bioethanol production from Enzymatically Saccharified Empty Fruit Bunches Hydrolysate using Saccharomyces cerevisiae. Reseach J Environ Sci (Academic Journals Inc). 2011;1–14.
31. Zulkiple N, Maskat MY, Hassan O. Pretreatment of Oil Palm Empty Fruit Fiber (OPEFB) with Aquaeous Ammonia for High Production of Sugar. Procedia Chem. Elsevier Ltd.; 2016;18(Mcls 2015):155–61.

FP-07

ULTRASOUND-ASSISTED EXTRACTION AS EFFICIENT METHOD FOR OBTAINING OPTIMUM ANTIOXIDANT FROM MANGROVE LEAVES OF *RHIZOPHORA MUCRONATA*

AUDAH KA[1]*, MANUELLA K[1], AMSYIR J[1], HAPSARI AM[1]‡, SUTANTO H[2]

[1]*Department of Biomedical Engineering,* [2]*Department of Chemical Engineering Swiss German University, Prominence Tower, West Sutera Road, South Tangerang 15143, Banten Province, Indonesia*

‡*Waterco Indonesia, Jl. Raya Boulevard Barat, Ruko Inkopal Blok B No. 31 – 32, DKI Jakarta 14240, Indonesia*

*Corresponding author: kholis.audah@sgu.ac.id

ABSTRACT

Extraction method plays a critical role in the study of medicinal plants. Nowadays, a wide range of technologies is available to promote different methods of extraction with the better extraction output. The aim of the study was conducted to compare two extraction method, maceration and ultrasound-assisted extraction (UAE), for obtaining optimum antioxidant. The mangrove leaves of *Rhizophora mucronata* was chosen as a natural source of antioxidant. The leaves were extracted by employing 24 hours maceration and UAE in five different extraction times (5, 15, 30, 45 and 60 minutes). The experiments were conducted using water and 70% ethanol as solvents. The total phenolic content was determined by Folin-Ciocalteau assay and flavonoid content by Aluminium chloride assay. While the antioxidant activity was determined by the DPPH method. As a result, the phenolic compounds yielded by UAE with ethanol was considerably higher and need shorter time than maceration. The IC_{50} value was obtained by UAE with ethanol is 52.86 ppm. All these data showed that UAE with ethanol was the efficient method and mangrove leaves *Rhizophora mucronata* is a very potent natural antioxidant source.

KEYWORDS:
antioxidant, phenolic compounds, Rhizophora mucronata, ultrasound-assisted extraction (UAE),

INTRODUCTION:

Free radicals are generated during metabolism and other biological system activities beyond the antioxidant capacity gave rise to oxidative stress which plays a role in heart diseases, neurodegenerative diseases, cancer and aging process (Huda-Faujan et al., 2009; Birben et al., 2012, Sies, 2015). As an answer, the dietary antioxidants can lower the risk of those diseases (Ghasemzadeh et al., 2010; Peng et al., 2014). Antioxidants are substances that at low concentration functioned to delay the oxidation of proteins, carbohydrates, lipids and DNA (Hamid *et al*., 2010; Sindhi *et al*., 2013).

Nowadays, most of the antioxidants used are manufactured synthetically. The synthetic antioxidants commonly used are Butylated hydroxyl anisole (BHA), Butylated hydroxyrotoluene (BHT), Propyl gallate (PG), Tertiary butyl hydroquinone (TBHQ) and Nordihydro guaretic acid (NDGA) (Hamid *et al*., 2010; Dolatabadi and Kashanian, 2010; Thorat *et al*., 2013). However, they have been under scrutiny since the potent hazardous effects to human health (Dolatabadi and Kashanian, 2010; Schilaci *et al*., 2014; Eskandani *et al*., 2014). Therefore, many of researchers have been interested more in exploring potent antioxidant from natural sources (Brewer, 2011, Celıkyurt, 2011; Shebis *et al*., 2013; Abourashed, 2013).

Indonesia as an archipelago country which possesses of an estimate of 95,181 km of coastline which bears the largest mangrove vegetated area in the world of about 3,244,018 ha (Bakosurtanal, 2009). Mangrove

forests have become the essential support of human lives along the coastlines for centuries, providing economic and environmental benefits (Mangkay et al., 2013; Duncan et al., 2016). In the past decade, extracts from mangroves and mangrove associates have been scientifically studied for their effectiveness against human, animals and plant pathogens, as well as for their antioxidant properties (Bandaranayake, 2002, Abeysinghe, 2010; Krishnaiah et al., 2011).

R. mucronata is a widespread species of mangrove in Indonesian coastline that has been described as a potent antioxidant agent (Banerjee et al., 2008; Rege and Chowdary, 2014; Wahyuni et al., 2015). The species is robust and even can survive harsh living condition in the contaminated water by producing their own antioxidant in the form of phenolic compounds (Michalak, 2006). Accordingly, the extraction of phenolic compounds from medicinal plants includes mangrove have become a hotspot.

Extraction method plays a critical role in the study of medicinal plants (Vagashiya et al., 2011; Azmir et al., 2013; Azwanida, 2015). The conventional extraction methods which have been employed for decades, maceration and soxhlet extraction, can be applied only at the small research setting and they are also time consuming (Dhayanithi et al., 2012; Yompakdee et al., 2012). Therefore, significant advances have been developed in the modern extraction methods. One of them is ultrasound-assisted extraction (UAE), in which this advance is aimed to the better extraction output (Azwanida, 2015; Sutanto et al., 2015). The purpose of this study was to compare two extraction methods, maceration and ultrasound- assisted extraction (UAE), for obtaining optimum antioxidant. So that antioxidant agents contained in the sample can be extracted better and the duration of extraction becomes shorter. So that an efficient extraction process can be obtained.

MATERIAL AND METHODS:

Plant material

The *R. mucronata* leaves *were* harvested from *Kawasan Ekowisata Mangrove*, Pantai Indah Kapuk, North Jakarta, Indonesia with the permission from *Dinas Kelautan, Pertanian, dan Ketahanan Pangan DKI Jakarta*. *R. mucronata* was identified by LIPI (Indonesian Institute of Sciences) taxonomist at Cibinong Science Center. Before use, the leaves were firstly cleaned with tap water to remove dirt and then rinsed with water. The leaves were cut into transverse sections of approximately 0.02 m width and dried using oven (Memmert, Germany) at the temperature of 45 ºC for 12 hours. The dried leaves were crushed using blender (Cucina Philips, Indonesia) and screened using mesh number 35 (CISA Cedaceria Industrial, Spain). The leaf powder was transferred into glass bottles with a rubber stopper, wrapped in aluminium foil and stored in the freezer -20 ºC prior to extraction.

Extraction

For the maceration method, five grams of leaf powder was transferred into erlenmeyer flask and immersed in the solvent (1:10) for 24 hours in a shaker set at 125 rpm, 25 ^{o}C. The erlenmeyer flask opening was sealed by using aluminium foil and parafilm, and the whole flask was covered by aluminium foil to protect the content from the light as described by Dhayanithi et al. (2012).

The UAE experiments were adapted from Molyneux (2004). The experiments were carried out with five different extraction times (5, 15, 30, 45 and 60 minutes) with using water and 70% ethanol as solvents. The ultrasonic device used was Bandelin SONOREX SUPER 10P ultrasonic bath (Germany). The frequency used was 35 kHz for 400 W ultrasonic devices and enabled transient cavitations with bubbles implosion effect. The ultrasonic probe was immersed in the mixture directly.

Five grams of leaf powder was transferred into erlenmeyer flask and 50 mL of solvent was added. A glass rod was used to evenly immerse the powder in the solvent. The opening of the flask was covered with aluminium foil and sealed with Parafilm. The erlenmeyer flask was then submerged inside a beaker glass filled with tap water, to ensure stability during extraction in the water bath shaker (Edmund Bühler SM 25 Shaker, Germany) and placed into the ultrasonic bath. The water level of the ultrasonic bath was adjusted so that it is the same or slightly higher than in the beaker glass and erlenmeyer flask. To prevent an excessive

increase in temperature, the power setting in the ultrasonic bath was adjusted to 50%. In the case of temperature increase, the water in the water bath was cycled with fresh cold water.

After extraction (maceration and UAE), the extracts were filtrated through cotton fine-meshed cloth (Triqtex, Indonesia) in order to remove most of the raw material and the filtrates were then centrifuged (Hettich Rotina 35R centrifuge, Germany) for 10 minutes at 10,000 rpm, 25 ºC. The supernatants were collected using a graduated pipette and used for determination of total phenols, flavonoids, antioxidant capacity spectrophotometrically. All treatments were carried out in quadruplicate.

Determination of total phenolic content (TPC)

The determination of TPC of extracts obtained was adapted from Banerjee et al. (2008) with slightly modification and calibrated against gallic acid as the reference standard. A 0.3 ml sample was mixed with 1.5 ml of Folin-Ciocalteu reagent and 1.2 ml of sodium carbonate (7.5%), consecutively. The mixture of each step should be mixed well by using vortex (Genie 2 mixer, Scientific Industries, USA) and allowed to stand for one hour in a dark chamber. Absorption was measured by using UV-Vis spectrophotometer (Genesys 10 UV-Vis spectrophotometer, Thermo Electron Corporation, USA) at 765 nm. The standard curve gallic acid was prepared by diluting the stock standard with the extraction solvents to yield 50 to 200 ppm TPC. The results were calculated according to the calibration curve for gallic acid and mass fraction of TPC, derives from quadruplicate analyses and expressed as gallic acid equivalents (GAE mg/ g) of dry material (DM).

Determination of flavonoid content (FC)

The determination of FC was adapted from Do et al. (2014) with slight modification and calibrated against quercetin as the reference standard. The Leaf powder was first diluted with its solvent to reach dilution factor of 25 for test the FC in the samples. A 1.5 ml of methanol was prepared in the test tube. A 0.5 ml sample was mixed with 0.1 ml of 10% aluminium chloride, 0.1 ml of 1 M potassium acetate and 2.8 ml distilled water, consecutively. The mixture of each step should be mixed well by using vortex. The mixtures were incubated in a dark chamber for 30 minutes and absorbance was measured by using a UV-Vis spectrophotometer at 415 nm. The standard curve quercetin was prepared by diluting the stock standard with the extraction solvents to yield 20 - 200 ppm of FC. The results were calculated according to the calibration curve for quercetin and mass fraction of FC, derives from quadruplicate analyses and expressed as quercetin equivalents (QE mg/ g) of dry material (DM).

Determination of antioxidant activity (AAT)

The higher the consumption of DPPH in a sample, the more the inhibitory concentration (IC_{50}) is reduced. A 500 µL of sample in a test tube covered with aluminium foil with various dilutions were prepared. A 500 µL of 250 µM DPPH solution was added into each of the samples in test tubes. A control was prepared by adding 500 µL of DPPH stock solution into 500 µL extraction solvent (water or 70% ethanol). The tubes were mixed and allowed to stand for 30 minutes in a dark chamber before transferred into a cuvette and subjected to the measurement of absorbance by using UV-Vis spectrophotometer at 517 nm according to the methodology adapted from Rege and Chowdary (2014). All determinations were performed in quadruplicate.

For each extract, at least four dilutions were made in order to be able to plot a graph of DPPH scavenging activity (%) versus concentration of sample (ppm). The IC value was defined as the concentration in mg of dry material per ml that inhibits the formation of DPPH radicals by 50%. Each value was determined by the following regression equation:

$$\mathbf{IC_{50}\ DM = IC_{50} \times (100\% - P_m)}$$

Equation 1. Calculation formula of IC_{50}

Where IC_{50} DM was the IC_{50} in dry mass base with the unit still in mg/L, IC_{50e} was the IC_{50} of extract in wet based raw material, while P_m was the percentage of moisture in *R. mucronata* powder measured using a moisture content analyser (MA35, Sartorius, Germany) for 30 minutes at 105ºC.

Statistical analysis

The statistical data analysis performed in this research was the simple linear regression analysis and ANOVA using Microsoft Excel. In addition, Tukey HSD post-hoc test and one sample t-test were performed in the OpenStat application. All analyses were conducted at 95% confidence level where $p<0.05$ show a significant difference. In regression analysis, the correlation coefficient r was range from -1 to 1. After the Tukey HSD post-hoc test, letters were assigned to the data. Data with the same letter were not significantly different from each other.

RESULTS AND DISCUSSION:

In this study, two methods (maceration and ultrasound-assisted extraction) were used to extract TPC or FC from *R. mucronata* leaves under previously described condition. Table 1 shows the comparison of extraction times, moisture content, TPC, FC, and IC_{50} in relation to extraction methods. Two variables influencing the extraction were investigated which are solvents (water and 70% ethanol) and time (5, 15, 30, 45 and 60 minutes, and 24 hours maceration).

The ultrasonic-assisted extraction has been widely used for obtaining phenolic compounds from plants using ethanol, water, a mixture of ethanol/water and acetone (Khan et al., 2010; Zlabur et al., 2015; Rosello-Soto et al., 2015). Based on the experiments, it was observed that TPC or FC obtained by ethanol considerably higher at any method and time of extraction. The choice of solvents depends on the chemical properties of the components which would be extracted from a matrix. Therefore, ethanol is possibly the most suitable solvent system for the extraction of *R. mucronata* leaves due to the different polarities of the active constituents (Boeing et al., 2014; Do et al., 2014; Iloki-Assanga et al., 2015).

In term of extraction times, the yield of TPC reached a maximum at 45 minutes UAE with ethanol, 156.20 ± 12.08 GAE mg/ g DM, as table 1 showed. It was indicated that long period of extraction time favors the TPC production. But further increased the extraction time (60 minutes) in UAE showed decreasing in the TPC. Accordingly, 45 minutes was chosen as the TPC extraction time in succeeding experiments. For the maceration, the longer extraction time exposed the extract to the more environmental factors such as oxygen, heat and UV radiation which may lead degradation of TPC (Murugesan et al., 2012; Xu et al., 2017). The UAE yield of FC slightly increased within 30 minutes (16.23 ± 0.28 QE mg/ g DM), but after 30 minutes, its yield lower. According to the Noyes-Whitney theory, the dissolution is fast at firstly and changed little when the active ingredient concentration between inner and outer diffusion layer reach equilibrium after a period of extraction (Wang et al., 2012). Therefore, 30 minutes was chosen as the FC extraction time.

Table 1
Comparison of extraction times, moisture content, TPC, FC, and IC_{50} in relation to extraction methods, UAE and maceration

Time	Moist (%)		Freq	TPC (GAE mg/ g DM)		FC (QE mg/ g DM)		IC_{50} (ppm) Eth	
	water	(KHz)	eth	water		eth	water	eth	Water
5 min	7.77	10.89	35	133.47	108.12	15.75	13.63	59.12	64.79
				135.71	111.25	15.53	13.07	55.51	65.60
				139.06	109.91	15.86	13.40	50.59	53.94
				142.52	108.57	15.41	13.74	46.20	58.35
			Avg	137.69	109.46	15.64	13.46	52.86	60.67
			SD	3.96	1.41	0.20	0.30	5.65	5.54
15 min	13.64	9.00	35	124.65	107.11	15.86	13.63	61.56	66.14
				124.76	104.88	15.97	12.84	65.42	75.22
				121.30	108.23	15.64	13.40	62.68	60.79
				122.31	107.56	14.97	12.84	61.69	59.79
			avg	123.26	106.95	15.61	13.18	62.84	65.49
			SD	1.72	1.45	0.45	0.40	1.79	7.06
30 min	10.71	7.48	35	140.40	108.79	16.53	13.63	57.00	74.58
				135.60	109.68	16.31	13.07	55.06	74.63
				142.19	106.89	16.20	14.74	55.28	71.84
				146.10	103.54	15.86	14.63	48.48	75.52
			avg	141.07	107.23	16.23	14.02	53.96	74.14
			SD	4.36	2.72	0.28	0.81	3.75	1.59
45 min	13.08	6.31	35	145.95	108.01	15.41	14.07	55.53	50.57
				145.54	104.88	15.30	14.07	60.14	62.13
				167.32	95.72	15.41	13.52	57.16	64.18
				165.98	97.84	16.08	13.52	52.70	57.14
			Avg	156.20	101.61	15.55	13.80	56.38	58.51
			SD	12.08	5.79	0.36	0.32	3.11	6.06
60 Min	13.73	11.43	35	111.25	96.84	15.86	15.86	61.12	68.63
				106.78	96.28	15.30	15.19	68.99	75.99
				119.07	101.53	15.75	15.53	60.79	69.53
				118.06	101.53	15.64	16.20	59.52	72.74
			avg	113.79	99.05	15.64	15.70	62.61	71.72
			SD	5.82	2.88	0.24	0.43	4.31	3.35
24 h	8.41	13.2		133.70	89.52	19.66	15.59	55.29	116.62
				136.61	88.80	19.77	14.58	58.41	104.84
				133.48	86.96	18.04	13.96	52.10	102.49
				130.18	87.96	18.93	14.41	41.15	102.19

*Moist (%): moisture content in %, Freq: frequency, eth: 70% ethanol, avg: average, SD: standard deviation.

When compared with maceration, UAE was produced a significantly higher TPC and FC. With only five minute extraction time, the TPC obtained by UAE with ethanol was comparable with the yield obtained by using 24 hours maceration (137.69 ± 3.96: 133.49 ± 2.63 GAE mg/ g DM). The FC obtained by 30 minutes UAE with ethanol was also efficient in terms of time compared with the yield obtained by using 24 hours maceration (16.23 ± 0.28: 19.10 ± 0.80 QE mg/ g DM). This indicated that this method was time efficient since it greatly reduced extraction time.

The mechanism of ultrasound in liquids relies on the mechanical effect caused by the implosion of cavitational bubbles. During implosion of micro-sized cavitational bubbles, strong shear forces are created, while both high pressures and temperatures generated as a consequence of the bursting bubbles, cause rapid plant tissue disruption or cell wall breakage allowing cellular material release and improved mass transfer as well that lead to mass transfer of phenolic compounds to the solvent (Saleh et al., 2016; Chemat et al., 2017). In addition, ultrasound-assisted extraction can provide the opportunity for enhanced extraction of

heat-sensitive bioactive components at lower processing temperatures and is a more effective technique than conventional thermal extraction with most of the plants extracted within 15 minutes (Vilkhu et al., 2008; Cares et al., 2010; Dent et al., 2015).

The AAT data showed that there was a significant difference in IC_{50} between the two different solvents (water and 70% ethanol). The lowest IC_{50} value was showed by five minutes UAE with ethanol and 24 hours maceration with ethanol, 52.86 and 51.74 ppm, respectively. Although IC_{50} of maceration is lower than UAE, UAE is more efficient in terms of time. The extracts produced by both UAE and maceration methods had considerably high antioxidant activity, indicated by the IC_{50} DM value lower than 200 ppm (Molyneux, 2004).

The IC_{50} analysis result was consistent with the proposed relation between TPC and AAT. Further analysis showed that there was no significant difference among the extracts with the same solvent regardless the difference in extraction times. There was a strong correlation between DPPH scavenging activity with TPC with R^2 value 0.911 which showed in Figure 1. It suggested that TPC contributed as much as 91.1% of AAT for each extract and 8.9% contribution came from other compounds. The results also showed that percentage of scavenging activity increased linearly to TPC of each extract. This result was consistent with the conclusion of a study on the correlation between TPC of several mangrove extracts and their AAT (Agati et al., 2013). Flavonoids have also been contributed to the AAT of the plants due to its role in protecting leaves against the UV radiation in sunlight (Agati et al., 2007). The higher phenolic compounds the lower IC_{50} value since the extract with higher phenolic compounds would be able to scavenge more of free radicals at a given extract concentration (Stanković, 2011; Gao et al., 2014; Pamulaparthi et al., 2016). The compounds that function as antioxidant determined by the presence of free -OH functional group, such as flavons, flavonons, squalens, β-carotene, tocopherol and vitamin C (Parwata et al., 2009).

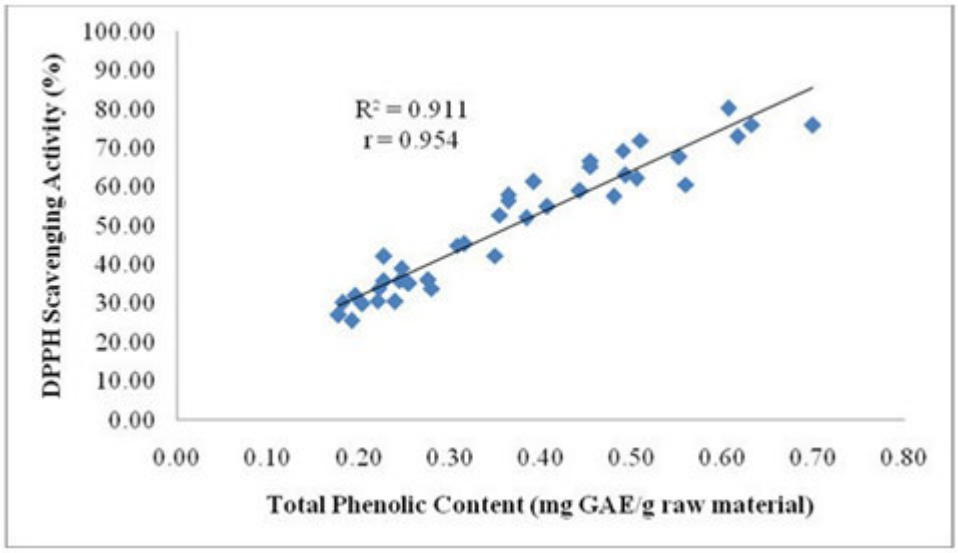

Figure 1
Correlation between phenolic content (mg GAE/g DM) with DPPH scavenging activity

Taken altogether, ultrasound-assisted extraction is an effective extraction technique that can offer high reproducibility in shorter time, higher yields of bioactive compounds, simplified manipulation, decreased temperature during processing, reduced solvent consumption, and lower energy input (Virot et al., 2010; Klen and Vodopivec, 2012; Dent et al., 2015).

CONCLUSION:

The results of this study showed that UAE with ethanol was a suitable and efficient method for the extraction of TPC and FC. Ethanol is possibly the most suitable solvent for the extraction of *R. mucronata* leaves due to the different polarities of the active constituents. The yield of TPC had reached a maximum at

45 minutes UAE with ethanol, 156.20 ± 12.08 GAE mg/ g DM. The UAE with ethanol yield of FC slightly increased within 30 minutes, 16.23 ± 0.28 QE mg/ g DM. The phenolic compound yielded by UAE with ethanol was considerably higher and need shorter time than maceration. The higher phenolic compounds obtained, the lower IC_{50} value since the extract with higher phenolic compounds would be able to scavenge more of free radicals. The IC_{50} value UAE with ethanol is 52.86 ppm. All this data showed that UAE with ethanol was the efficient method and *R. mucronata* is a very potent for the natural antioxidant source.

ACKNOWLEDGEMENTS:

The authors gratefully acknowledge that the present research is supported by the Central Research Fund of the Swiss German University with Contract Number A/REC/0073/IX/2015 and by Ministry of Research and Technology and the Higher Education Republic of Indonesia with Contract Number SP DIPA-042.06.1.401516/2017. We also thank Directorate of Marine, Agriculture and Food Security, DKI Jakarta Province for giving us permission to collect mangrove leaves at the Mangroves Sanctuary Region, Pantai Indah Kapuk, North Jakarta, Indonesia. We thank our research collaborators Dr. Irmanida Batubara and staffs at Biopharmaca Tropica Research Center, Bogor Agricultural University and Dr. Doddy Kustaryono and staffs at STKIP Surya, Tangerang. We also thank the Director and staffs of Academic Research and Community Services Swiss German University for their support throughout the project.

REFERENCES:

1. Abeysinghe PD (2010). Antibacterial activity of some medicinal mangroves against antibiotic-resistant pathogenic bacteria. Indian J Pharm Sci. 72(2): 167–172.
2. Abourashed EA (2013). Bioavailability of plant-derived antioxidants. Antioxidants. 2: 309-325.
3. Agati G, Brunetti C, Di Ferdinando M, Ferrini F, Pollastri S, Tattini M (2013). Functional roles of flavonoids in photoprotection: new evidence, lessons from the past. Plant Physiol Biochem. 72: 35-45.
4. Agati G, Matteini P, Goti A, Tattini M (2007). Chloroplast-located flavonoids can scavenge singlet oxygen. New Phytol. 174(1): 77-89.
5. Azmir J, Zaidul ISM, Rahman MM, Sharif KM, Mohamed A, Sahena F, Ghafoor K, Norulaini NAN, Omar AKM, Jahurul MHA (2013). Techniques for extraction of bioactive compounds from plant materials: A review. J Food Eng. 117: 426-436.
6. Azwanida NN (2015). A review on the extraction methods use in medicinal plants, principle, strength and limitation. Med Aromat Plants. 4(3): 1-6.
7. Bakosurtanal (2009). *Indonesian map of mangrove*. Cibinong: Survey Centre of Marine Resources, Coordination Bureau of Survey and National Mapping.
8. Bandaranayake, WM. (2002). Bioactivities, bioactive compounds and chemical constituents of mangrove plants. Wetlands Ecol Manag. 10(6), pp.421-452.
9. Banerjee D, Chakrabarti S, Hazra A, Banerjee S, Ray J, Mukherjee B (2008). Antioxidant activity and total phenolics of some mangroves in Sundarbans. Afr J Biotech. 2008; 7(6): 805-810.
10. Birben E, Sahiner UM, Sackesen C, Erzurum S, Kalayci O (2012). Oxidative stress and antioxidant defense. WAO Journal. 5: 9–19.
11. Boeing JS, Barizão EO, e Silva BC, Montanher PF, Almeida VC, Visentainer JV (2014). Evaluation of solvent effect on the extraction of phenolic compounds and antioxidant capacities from the berries: application of principal component analysis. Chem Cent J. 8: 48-56.
12. Cares MG, Vargasa Y, Gaetea L, Sainz J, Alarcón J (2010). Ultrasonically assisted Extraction of bioactive principles from *Quillaja saponaria* Molina. Phys Prosedia. 3: 169-178.
13. Brewer MS (2011). Natural Antioxidants: Sources, compounds, mechanisms of action, and potent applications. FoodSci FoodSaf. 10: 221-248.
14. Celıkyurt IK (2011). Thought-provoking molecules for drug discovery: antioxidants. Pharm Anal Acta. 1(3): 1-7.
15. Chemat F, Rombaut N, Sicaire A-G, Meullemiestre A, Fabiano-Tixier A-S, Abert-Vian M (2017). Ultrasound- assisted extraction of food and natural products. Mechanisms, techniques, combinations, protocols and applications. A review. Ultrason Sonochem. 34: 540–560
16. Dent M, Dragović-Uzelac V, Garofulić IE, Bosiljkov T, Ježek D, Brnčić M (2015). Comparison of

conventional and ultrasound-assisted extraction techniques on mass fraction of phenolic compounds from sage (S*alvia officinalis* L.). Chem Biochem Eng Q. 29(3): 475–484.
17. Dhayanithi N, Kumar T, Murthy R, Kathiresan K (2012). Isolation of antibacterials from the mangrove, *Avicennia marina* and their activity against multidrug resistant *Staphylococcus aureus*. Asian Pac J Trop Biomed. 2(3): 1892-1895.
18. Do Q, Angkawijaya A, Tran-Nguyen P, Huynh L, Soetaredjo F, Ismadji S, Ju Y (2014). Effect of extraction solvent on total phenol content, total FC, and antioxidant activity of *Limnophila aromatica*. J Food Drug Anal. 22(3): 296-302.
19. Dolatabadi JEN, Kashanian S (2010). A review on DNA interaction with synthetic phenolic food additives. Food Res Int. 43(5):1223-1230.
20. Duncan C, Primavera JH, Pettorellia N, Thompson JR, Loma RJA, Koldewey HJ (2016). Rehabilitating mangrove ecosystem services: A case study on the relative benefits of abandoned pond reversion from Panay Island, Philippines. Mar Poll Bullet. 109: 772-782
21. Eskandani M, Hamishehkar H, Dolatabadi JEN (2014). Cytotoxicity and DNA damage properties of tert- butylhydroquinone (TBHQ) food additive. Food Chem. 153: 315–320
22. Gao H, Cheng N, Zhou J, Wang BN, Deng JJ, Cao W (2014). Antioxidant activities and phenolic compounds of date plum persimmon (*Diospyros lotus* L.) fruits. J Food Sci Technol. 51(5): 950–956
23. Ghasemzadeh A, Jaafar HZE, Rahmat A (2010). Antioxidant activities, total phenolics and flavonoids content in two varieties of Malaysia young ginger (*Zingiber officinale* Roscoe). Molecules. 15: 4324-4333
24. Hamid AA, Aiyelaagbe OO, Usman LA, Ameen OM, Lawal A (2010). Antioxidants: Its medicinal and pharmacological applications. Afr J Pure Appl Chem. 4(8): 142-151.
25. Huda-Faujan N, Noriham A, Norrakiah AS, Babji AS (2009). Antioxidant activity of plants methanolic extracts containing phenolic compounds. Afr J Biotech. 8(3): 484-489
26. Iloki-Assanga SB, Fernandez-Angulo D, Lewis-Luján LM, Rubio-Pino JL, Lara-Espinoza CL, Haines DD (2015). Solvent effects on phytochemical constituent profiles and antioxidant activities, using four different extraction formulations for analysis of *Bucida buceras* L. and *Phoradendron californicum*. BMC Res Notes. 8: 396-409.
27. Khan MK, Albert-Vian M, Fabiano-Tixier AS, Dangles O, Chemat F (2010). Ultrasound- assisted extraction of phenolic compounds (flavanone glycosides) from orange (*Citrus sinensis L.*) peel. Food. Chem. 119: 851.
28. Klen TJ, Vodopivec BM (2012). Optimisation of olive oil phenol extraction conditions using a high-power probe ultrasonication. Food Chem. 134: 2481.
29. Krishnaiah D, Sarbatly R, Nithyanandam R (2011). A review of the antioxidant potent of medicinal plant species. Food Bioprod Process. 89: 217–33.
30. Mangkay SD, Harahab N, Polii B, Soemarno (2013). Economic valuation of mangrove forest ecosystem in Tatapaan, South Minahasa, Indonesia. J Envi Sci Toxicol Food Tech. 5(6): 51-57.
31. Michalak A (2006). Phenolic compounds and their in plants growing under heavy metal stress. Polish J Envi Stud. 15(4):.523-530.
32. Molyneux, P. (2004). The use of the stable free radical diphenylpicryl-hydrazyl (dpph) for estimating antioxidant activity. Songklanakarin J Sci Tech. 26(2): 211-219.
33. Murugesan R, Orsat V, Lefsrud M (2012). Effect of Pulsed Ultraviolet Light on the Total Phenol Content of Elderberry (*Sambucus nigra*) Fruit. Food Nutr Sci. 3: 774-783.
34. Pamulaparthi A, Prathap VR, Banala M, Nanna RS (2016). Total phenolic, flavonoid contents and antioxidant assays in leaf extracts of *Senna alata* (L.) Roxb. J Pharm Sci Res. 8(9): 981-985
35. Parwata IMOA, Rita WS, Yoga R (2009). Isolasi dan uji antiradikal bebas minyak atsiri pada daun sirih (*Piper betle* Linn) secara spektroskopi ultra violet-tampak. Jurnal Kimia. 3 (1): 7-13
36. Peng C, Zuo Y, Wang X, Liu Y, Chen J, Lei L, Jiao R, Ma KY, Wang L, Huang Y, Li YM, Chen Z-Y (2014). Biology of ageing and role of dietary antioxidants. hindawi publishing corporation. BioMed Res Int. Article ID 831841, 13 pages.
37. Rege A, Chowdhary A (2014). Evaluation of alpha-amylase and alpha-glucosidase inhibitory activities of *Rhizophora mucronata*. Int J Pharm Sci Res. 5(6): 2261-2265
38. Roselló-Soto E, Galanakis CM, Brnčić M, Orlien V, Trujillo FJ, Mawson R, Knoerzer K, Tiwari BK,

Barba FJ (2015). Clean recovery of antioxidant compounds from plant foods, by-products and algae assisted by ultrasounds processing: modelling approaches to optimize processing conditions. Trends Food Sci. Technol. *42*: 134.

39. Saleh IA, Vinatoru M, Mason TJ, Abdel-Azima NS, Aboutabl EA, Hammoudaa FM (2016). A possible general mechanism for ultrasound-assisted extraction (UAE) suggested from the results of UAE of chlorogenic acid from *Cynara scolymus* L. (artichoke) leaves. Ultrason Sonochem. 31: 330–336
40. Schillaci C, Nepravishta R, Bellomaria A (2013). Antioxidants in food and pharmaceutical research. Albanian J Pharm Sci. 1(1): 9-16.
41. Shebis Y, Iluz D. Kinel-Tahan Y, Dubinsky Z. Yehoshua Y (2013). Natural Antioxidants: Function and Sources. Food Nutr Sci. 4: 643-649.
42. Šic Žlabur J, Voća S, Dobričević N, Brnčić M, Dujmić F, Rimac Brnčić S (2015). Optimization of Ultrasound- assisted extraction of functional ingredients from *Stevia rebaudiana* Bertoni leaves. Int. Agrophys. 29: 231.
43. Sies H (2015). Oxidative stress: a concept in redox biology and medicine. Redox Biol. 4: 180–183
44. Stanković MS (2011). Total phenolic content, flavonoid concentration and antioxidant activity of *Marrubium peregrinum* l. extracts. Kragujevac J. Sci. 33: 63-72
45. Sutanto H, Himawan E, Kusumocahyo S (2015). Ultrasound-assisted Extraction of Bitter Gourd Fruit (*Momordica charantia*) and Vacuum Evaporation to Concentrate the Extract. Procedia Chem. 16: 251-257.
46. Thorat ID, Jagtap DD, Mohapatra D, Joshi DC, Sutar RF, Kapdi SS (2013). Antioxidants, their properties, uses in food products and their legal implications. Int J Food Stud. 2: 81-104.
47. Vaghasiya Y, Dave R, Chanda S (2011). Phytochemical analysis of some medicinal plants from western region of India. Res J Medicinal plant. ISSN 1819-3455. DOI: 10.3923/rjmp.2011.
48. Vilkhu K, Mawsona R, Simonsa L, Bates D (2008). Applications and opportunities for ultrasound assisted extraction in the food industry: A review. Inn Food Sci Emerging Technol. 9(2):161-169
49. Virot M, Tomao V, Le Bourvellec C, Renard CMCG, Chemat F (2010). Towards the industrial production of antioxidants from food processing by-products with ultrasound-assisted extraction. Ultrason. Sonochem. 17(6): 1066.
50. Wahyuni W, Darusman L, Surya N (2015). Potency of *Rhizophora spp.* Extracts as Antioxidant and Inhibitor of Acetylcholinesterase. Procedia Chem. 6: 681-686.
51. Wang J, Zhao Y-M, Guo C-Y, Zhang S-M, Liu C-L, Zhang D-S, Bai X-M (2012). Ultrasound-assisted extraction of total flavonoids from Inula helenium. Pharmacogn Mag. 8(30): 166–170.
52. Xu D-P, Li H-B, Li Y, Meng X, Zhou T, Zhou Y, Zheng J, Zhang J-J (2017). Natural Antioxidants in Foods and Medicinal Plants: Extraction, Assessment and Resources. Int J Mol Sci. 18: 96-137.
53. Yompakdee C, Thunyaharn S, Phaechamud T (2012). Bactericidal activity of methanol extracts of crabapple mangrove tree (*Sonneratia caseolaris Linn*.) against multi-drug resistant pathogens. Indian J Pharm Sci. 74(3): 230.

FP-08

THE ANTIMICROBIAL EFFECTIVENESS OF NOVEL NON-RESISTANT THESS FOR CARPET APPLICATION

AUDAH KA[1]*, MARSHA T[1], JULKIPLI[1], BARDANT TB[2]

[1]*Department of Biomedical Engineering, Swiss German University, The Prominence Tower, Jalan Jalur Sutera Barat Kav 15, Alam Sutera, Panunggangan Timur, Pinang, Kota Tangerang 15143, Banten, Indonesia*

[2]*Pusat Penelitian Kimia LIPI, Kawasan PUSPITEK, Muncul, Serpong, Kota Tangerang Selatan 15314, Banten, Indonesia*

*Corresponding author: kholis.audah@sgu.ac.id

ABSTRACT

Antimicrobial additives are used in numbers of products for their availability to prevent product degradation and to provide hygienic properties. These additives are also used for carpet application in controlling bio-contaminants in indoor environments. Bacteria contamination on the carpet has been recognized as one of the most common cause of diseases, such as Norovirus infection, Campylobacteriosis, Kawasaki Syndrome and many others. The aim of this study was to analyze two of the pertinent test methods to analyze the effectiveness of Tetra Hydroxyl Ethyl dibiSulphite-2-Sodium (THESS) for carpet application against *Escherichia coli* and *Staphylococcus aureus*. THESS is a novel class of antibacterial agent with a unique killing mechanism that works from outside of the bacterial cell. The unique feature of THESS as a sulphide chelating agent is the very strong bond formed with the target ligands. This bond is the main key of the bacterial peptidoglycan porosity enlargement which caused lysis and lead to bacterial cell death. The macrodilution technique was conducted for determining the minimal inhibitory concentration (MIC) of THESS. Antimicrobial effectiveness test was conducted by two methods, modified AATCC 174 test I and OECD guideline which was harmonized to ISO 22196. Both are well known standard methods for measuring the qualitative and quantitative inhibition of microbial growth on carpet. The effectiveness of the two methods was then analyzed. MIC of THESS was determined at 0.5% w/v solution against the two tested bacteria. In conclusions, the AATCC 174 test I did not show any inhibition zone in both THESS- carpet and untreated carpet, while the OECD guideline showed the effectiveness of THESS-carpet against *E. coli* and *S. aureus* with the reduction of colony numbers 95.86% and 95.07%, respectively. This result suggested that application of THESS as antimicrobial in carpet is considered effective according to the standard of minimum 90% reduction of bacterial colonies.

KEYWORDS:
Antimicrobial additives, THESS, carpet applications, *AATCC 174 test I, OECD guideline*

INTRODUCTION:

The term ''antimicrobial'' means the ability of a substance to kill bacteria, viruses, protozoa, algae, fungi, and other pathogens. Pathogens can exist in various surroundings for a long time without triggering any reactions. In the past two decades, much attention has been devoted to polymeric materials with antimicrobial properties (Huang et al., 2016, Alvarez-Paino et al., 2017). It was proven that addition of antimicrobial to polymer, even at low concentrations (from 0.1 to 3%), provides effective protection. In addition, their small amount will only slightly increase the cost of previously manufactured products as well as make it safe and innovative (Varesano et al., 2011).

The increased use of carpets in house, schools, hospitals, and other places demonstrates the need for an additional antimicrobial in carpeting (Tietjen et al., 2003; Rivero et al., 2015). Carpet is a famous textile that is commonly used indoors for comfort, place to sit on the floor, reducing sound from walking, thermal

properties, slip preventer and others. While bringing benefits to our life, carpet also can be a reservoir to many bacteria since fiber used in the carpet can trap dirt which is the nutrient for bacteria to grow (Moody & Needles, 2004). Bacteria contamination on the carpet has been recognized as one of the most common cause of diseases, such as Norovirus infection, Campylobacteriosis, Kawasaki Syndrome and many others (Siegel et al., 2007). If the carpet is not properly cleaned, it may cause a health problem to the one who is incontact with it. Many methods were being used to overcome these problems such vacuuming and shampooing the carpet routinely. However, it does not remove the bacteria that are already attached to the carpet. To control the spread of bacteria and minimize the possibility of people infected by pathogen bacteria attached on the carpet, antimicrobial-carpet are finally traded (Haldar, et al., 2007). Yet, the antimicrobial carpet that have been available in the market contained a lot of chemical additives such as formaldehyde and triclosans which are harmful for human body (Allsopp et al., 2001).

Various antimicrobial treatments are currently used in the carpet industry to impart antimicrobial properties to the manufactured carpet. The antimicrobial that is seeded in the carpet should have a broad spectrum of activity against numerous bacteria and also possess very low toxicity (Moody & Needles, 2004). Since Tetra Hydroxyl Ethyl dibiSulphite-2-Sodium (abbreviated as THESS) has been proven to have very low toxicity and capable to fight against numerous bacteria, THESS-carpet is now introduced for carpet application. In the manufacturing process, THESS is seeded on the carpet surface and it binds permanently to the pore of the carpet fibres (Wardoyo, unpublished data).

THESS is a novel antimicrobial agent with a unique killing mechanism that works from outside of the bacterial cell by binding with peptidoglycan cell wall. Before THESS-carpet enter the market, several tests including controls and parameters have to be performed. Methods used to substantiate claims of THESS for carpet application effectiveness include: quantitative assay by measuring zone of inhibition tests using a sample piece and qualitative assay by direct inoculation of the surface under evaluation. AATCC 174 test I and OECD guideline which harmonized to ISO 22196 were chosen for substantiate claims since both are well known for standard method for measuring the qualitative and quantitative inhibition of microbial growth on carpet (AATCC, 2008; OECD, 2012).

MATERIAL AND METHODS:

Reagent and Microorganism

The materials used in this research were 0.75% THESS-carpet based polystyrene butadiene latex and conventional carpet, distilled water, ethanol 70%, Mueller Hinton Broth (HIMEDIA, India), agar bacteriological (OXOID, England), $BaCl_2$ (Merck, Germany), H_2SO_4 (Merck, Germany), Tetra Hydroxyl Ethyl di Sulphate (THESS) liquid and powder (Novis Natura Navita, Indonesia). *Escherichia coli* and *Staphylococcus aureus* acquired from Chemistry and Microbiology Laboratory of Pusat Penelitian Kimia, LIPI (Study Center of Chemistry, Indonesian Institution of Science).

Culture bacteria

The effectiveness of THESS for carpet application was assessed against *E. coli* and *S. aureus.* Bacteria was inoculated by taking 2 colonies from bacteria stock using sterilized loop and transferred into the sterilized nutrient broth. The bacterial suspension was put in the 36ºC ± 1ºC incubator. Overnight cultures were kept for 16 hours and bacterial suspension was diluted with sterilized nutrient broth to a density of $6x10^5$ CFU/ml.

MIC determination

Inoculum was prepared as described previously, however, bacterial suspension was diluted with sterilized nutrient broth to a density of $1x10^6$ CFU/ml (turbidity = 0.5 McFarland standard with 100 times dilution). Further 1:2 serial dilutions were performed by addition of culture broth to reach concentrations ranging from 0.25% to 8% w/v of THESS solution. 1 ml of each dilution were distributed in test tubes and was inoculated

with 1 ml of bacterial suspension (10^6 CFU/ml), thus, forming a total volume of 2 ml. The positive control was made by replacing the sample with nutrient broth whereas the negative control was made by putting 2 ml of nutrient broth in the test tube. All experiments were performed in triplicate and the macrodilution tubes were incubated at 35 ± 1^0C for 24 hours. The bacterial growth was detected by the absorbance of each solution at 600nm after the incubation period was over. MIC values were defined as the lowest concentration of THESS to completely inhibited or reduced microbial growth.

Qualitative assay for effectiveness of antimicrobial for carpet application

The method was based on AATCC 174 test I with modification (AATCC, 2008). Solutions consist of 0.1, 0.5 and 1% of THESS were prepared in 5 ml distilled water. 6 mm filter paper discs were impregnated with each of different concentration. Paper discs impregnated with streptomycin were used as positive control. The carpet sample was cut and shaped to resemble the 6 mm filter paper. All paper discs and carpet samples were placed onto the agar surface that was impregnated with the bacterial culture. The approximation of cell density of bacterial inoculum should be around 1 x 10^8 CFU/ml in accordance to 0.5 McFarland standard. Test was performed in triplicate. Results were recorded after overnight incubation at 37°C.

Quantitative assay for effectiveness of antimicrobial for carpet application

The assay was adapted from OECD guideline harmonized with ISO 22196 with modification (OECD, 2012). The carpet sample was cut up to a size 1 cm x 1 cm that is fit for the vials used during the the inoculation, incubation, and neutralization process and placed inside each vials. Each samples were inoculated with 200 µl of cell suspensions. Later, incubation process at 37^0C for 24 hours was performed. After 24 hours incubation, the carpet sample that has been inoculated then transferred to another vials for neutralization. An aliquot 10ml of distilled water validated for the active substances employed in the treated material was added to each vials that contains the carpet sample. An aliquot from this vials then mixed with agar medium by pour method. Same as ISO 22196, untreated carpet were required as negative control. The amounts of bacterial growth on THESS-treated and untreated carpet was determined by colony count method and the obtained results were compared.

Data Analysis

Results were expressed as mean value ± standard error of the mean. Statistical differences between colonies found on treated and untreated carpet, and the MIC values obtained from 2 different bacteria were observed by T-test. Replication in all experiment was analyzed by Analysis of Variance (ANOVA) single factor. P values lower than 0.05 ($p < 0.05$) were considered significant. The data graphic was built using Microsoft Excel 2013. The inhibition percentage of concentrated solution in macrodilution method was analyzed using following formula:

$$\text{Inhibition percentage (\%)} = \frac{\text{Absorbancy of control} - \text{Absorbancy of sample}}{\text{Absorbancy of control}} \times 100$$

RESULTS AND DISCUSSION:

Based on the result shown in Figure 1, THESS solution was indicated strongly reduce the growth of all isolates at concentration 0.5% w/v. At this point, only approximate MIC value could be determined. In order to find more precise MIC value, the same procedure should be repeated in a smaller THESS concentration range. Also, an aliquot of solutions from the macrodilution testing tube that show inhibition (at and above the MIC) should be diluted 1:1000 in saline or broth and 0.1 ml of the final dilution should subcultured to an agar medium so that the number of colonies that grow on subculture can be compared with the actual number of organisms inoculated into the MIC tubes. If the number of colonies found on a subculture plate less than 0.1% indicating 99.9% of the initial inoculum has been killed, a bactericidal effect has been achieved (Mahon, et al., 2014).

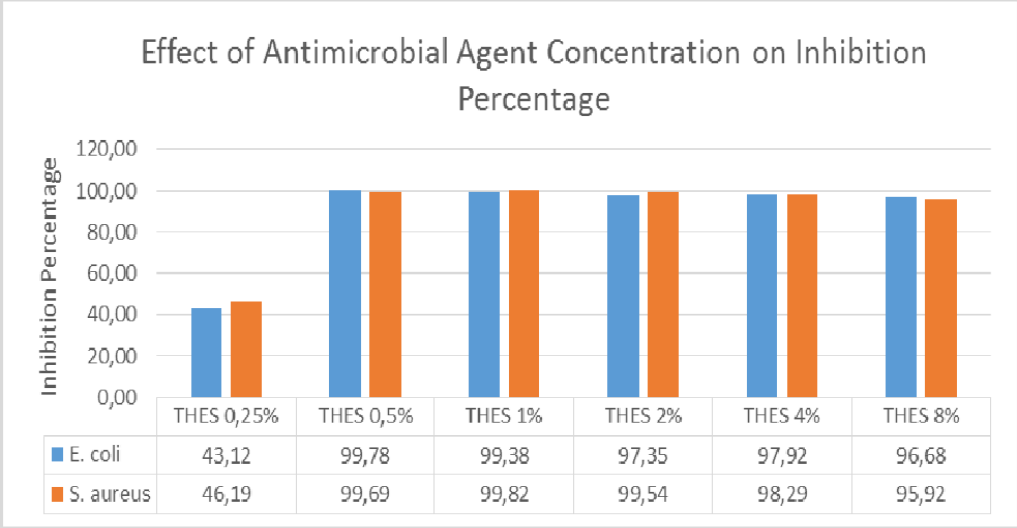

Figure 1
Effect of Antimicrobial Agent Concentration on Inhibition Percentage

In this study, 0.5 to 8% w/v solution of THESS were successfully reduced the growth of *Staphylococcus aureus* and *Escherichia coli* by about 96-99%, respectively, after 24 hours of treatment. At concentration 0.5%, THESS has attained its MIC and concentrations above 0.5% might cause diverse reaction. At first, when solutes dissolved, their particles were interacted with the solvent. Consequently, forming an unsaturated solution. However, when excessive amount of solutes were added into a solution, it became saturated. This described as a condition where the rate at which solute particles leave the surface of the solid equals the rate at which they return to the surface of the solid (National Science Foundation, 2016). At some environmental conditions, a saturated solution can be transformed into a supersaturated solution. Thereby, THESS solution at concentration above 0.5% was predicted to present similar or lower results to the 0.5% THESS solution due to the formation of saturated solution.

In conclusion, the addition of 0.5-8% w/v THESS solution had successfully reduce the growth of *Staphylococcus aureus* and *Escherichia coli.* Based on the obtained results, antimicrobial macrodilution method appear to be more reproducible since it provides sensitivity and MIC value even though macrodilution may produce in exact MIC data due to the performance of doubling dilutions (Patel, 2012). This study revealed that THESS is greatly effective as an antibacterial agent.
After the antibacterial propeties of THESS pure substance has been successfully confirmed, then test was perfomed for THESS-carpet. Methods used to substantiate claims of THESS for carpet application effectiveness include: Quantitative assay by measuring zone of inhibition tests using a test piece and qualitative assay by direct inoculation of the surface under evaluation. AATCC 174 test I and OECD guideline which harmonized to ISO 22196 were chosen for substantiate claims since both are well known for standard method for measuring the qualitative and quantitative inhibition of microbial growth on carpet (AATCC, 2008; OECD 2012).

In qualitative assay which is conducted with AATCC 174 test I method, THESS carpet was cut into a specific size and placed on the surface of agar plate that has been inoculated with a bacterial suspension of *S. aureus* and *E. coli.* After overnight incubation, the result shown that THESS carpet has no zone of inhibition against these two types of inoculum since the carpet sample only contain 0.75% of THESS. The zone of inhibition must be a minimum of 2 mm for Gram positive bacteria and a minimum of 1 mm for Gram negative bacteria (AATCC, 2008). This means, the higher the concentration, the wider zone of inhibition will be detected.

Taken altogether, it should be highlighted that the effectiveness of antibacterial agent is not only determined from the antibacterial agent or antibiotics producing the widest zone of inhibition. Careful consideration

should be taken in terms of the culture medium, diffusion rate, concentrations, sensitivity, and the interaction between drug and the medium (Poliak & Tsvetkova, 2007).

Based on OECD guideline, the bacterial colonies reduction on THESS-treated and untreated carpet was determined by colony count method and the results were compared. Figure 2 shown below expressed a mean value ± standard error of the mean of colony forming unit found on THESS-treated and untreated carpet after overnight incubation. By looking through the results, the ability of THESS-treated carpet to inhibit the growth of microorganisms can be verified.

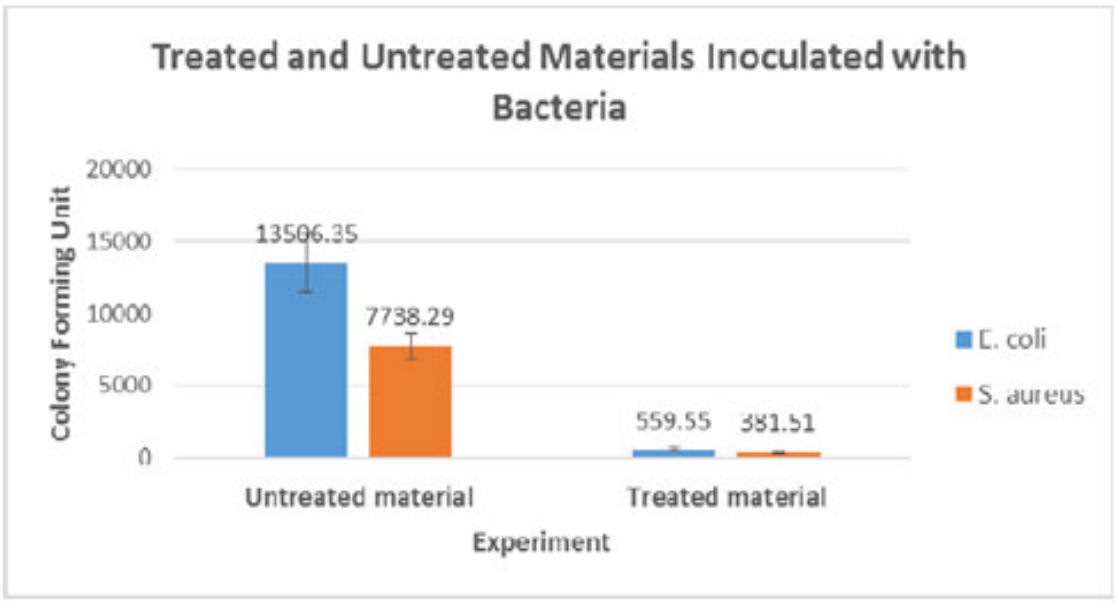

Figure 2
Colonies found on treated and untreated materials inoculated with bacteria

The result shown that the number of colonies found on untreated carpet is higher than THESS-treated carpet. It can be deduced that 0.75% THESS in carpet gives the opportunity to reduce the bacterial growth. A minimum of 90% reduction against each bacterium is required to be considered effective its application in the carpet product. Based on the figure above, THESS for carpet application reduced the number of *E. coli* and *S. aureus* colonies, 95.86% and 95.07%, respectively. Its mean, THESS for carpet application is considered effective since it can reduce more than standard of minimum bacterial colonies reduction which is 90% (AATCC, 2008). Figure 3 below respresented the colonies visible on agar plate for each test.

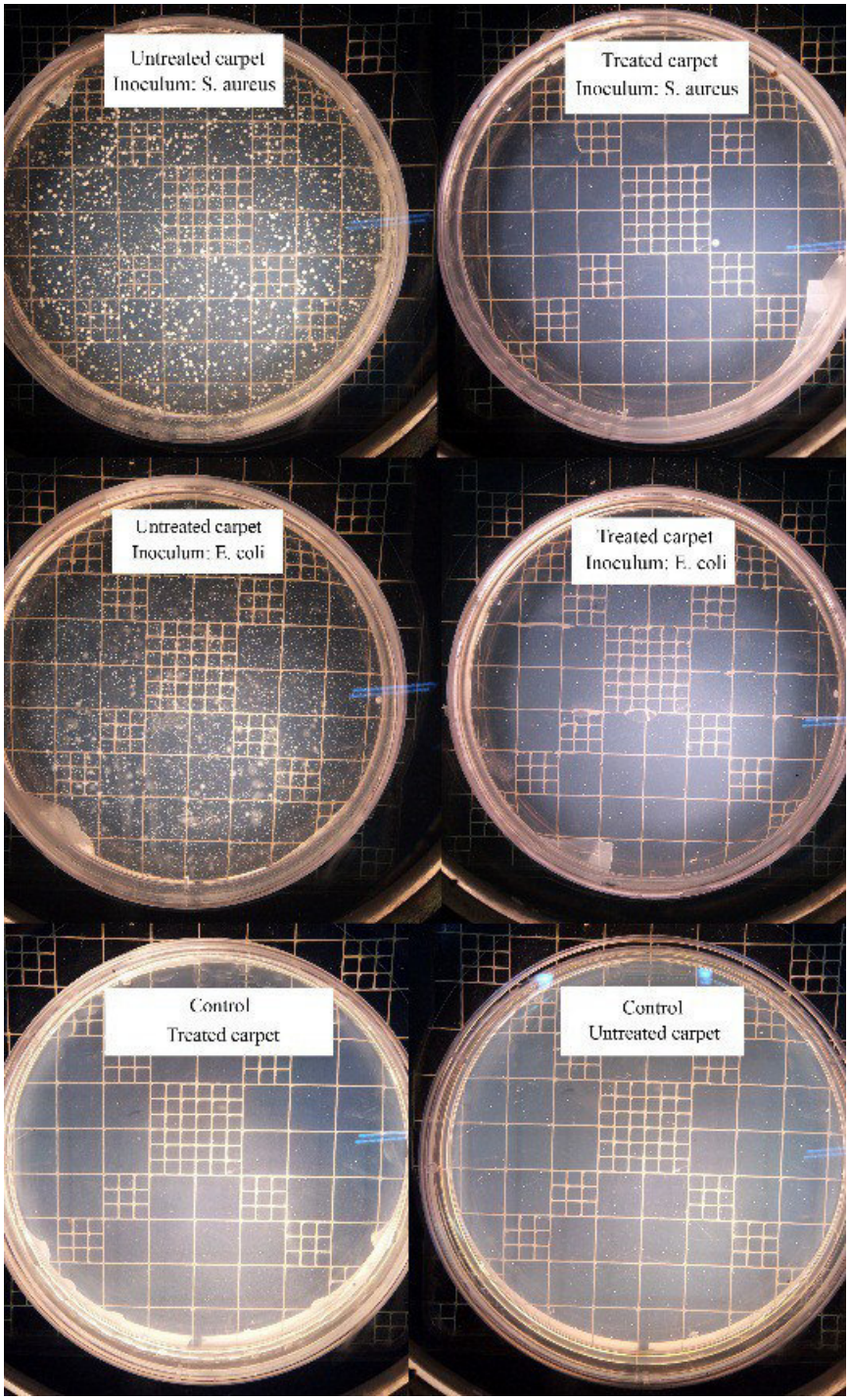

Figure 3.
Colonies found on agar plates

From this experiment, quantitative method established by OECD guideline were found to be excellent for evaluating the antimicrobial activity of treated materials and proving the quality of product THESS- treated and untreated carpet.

CONCLUSIONS:

This study suggested that THESS is potential as a novel non-resistant antimicrobial agent. The minimal inhibitory concentration of THESS in the macrodilution method found at 0.5% w/v solution (5mg/ml). Based on qualitative assay result which was conducted with AATCC 174 test I method shown that THESS carpet has no zone of inhibition against *E. coli* and *S. aureus*, while the OECD guideline showed the effectiveness of THESS-carpet against *E. coli* and *S. aureus* with the reduction of colony numbers 95.86%

and 95.07%, respectively. This result suggested that application of THESS as antimicrobial in carpet is considered effective according to the standard of minimum 90% reduction of bacterial colonies.

ACKNOWLEDGMENT:
The authors would like to express their gratitude to PT. N3 (Novis Natura Navita) who had provided research funding. The authors also wished to express their gratitude to Haryanto Wardoyo, Bobby Hadipraja and the late Dr. Doddy Kustaryono (STKIP Surya) and all those who had assisted the authors' research activities either directly or indirectly.

REFERENCES:

1. Huang KS, Yang CH, Huang SL, Chen CY, Lu YY, Lin YS. 2016. Recent Advances in Antimicrobial Polymers: A Mini-Review. Int. J. Mol. Sci. 2016, 17, 1578; doi:10.3390/ijms17091578.
2. Álvarez-Paino M, Muñoz-Bonilla A, Fernández-García M. 2017. Antimicrobial Polymers in the Nano-World. Antimicrobial Polymers in the Nano-World. Nanomaterials (Basel). 2017 Feb 22;7(2). pii: E48. doi: 10.3390/nano7020048.
3. Varesano A, Vineis C, Aluigi A, Rombaldoni F. *Antimicrobial polymers for textile products* in Mendez-Vilaz (Ed). Science against microbial pathogens: communicating current research and technological advances. 2011. Formatex Reseach Center. Spain.
4. Tietjen L, Bossemeyer D, McIntosh N. *Infection Prevention: Guidelines for Healthcare Facilities with Limited Resources*. 2003. JHPIEGO Corporation. Maryland. USA.
5. Rivero PJ, Urrutia A, Goicoechea J, FJ Arregui. 2015. Nanomaterials for Functional Textiles and Fibers. Nanoscale Research Letters (2015) 10:501. DOI 10.1186/s11671-015-1195-6.
6. Moody V, Needles HL. c*ufted Carpet: Textile Fibers, Dyes, Finishes and Processes.* 2004. William Andrew Inc. USA.
7. Siegel JD, Rhinehart E, Jackson M, Chiarello L, and the Healthcare Infection Control Practices Advisory Committee, 2007 *Guideline for Isolation Precautions: Preventing Transmission of Infectious Agents in Healthcare Settings.* Available at http://www.cdc.gov/ncidod/dhqp/pdf/isolation2007.pdf
8. Haldar J, Weight AK, Klibanov AM. 2007. Preparation, application and testing of permanent antibacterial and antiviral coatings. *Nature Protocols*, 2(10): 2412-2417.
9. Allsopp M, Santillo D, Johnston P. *Hazardous Chemicals in Carpets*. 2001. Greenpeace Research Laboratories. Exeter. UK.
10. American Association of Textile Chemists and Colorists. *AATCC TECHNICAL MANUAL*.Volume 83, 2008. Research Triangle Park, NC 27709, USA
11. Organisation for Economic Co-operation and Development. *Guidelines for the testing of chemicals: quantitative method for evaluating antibacterial activity of porous and non-porous antibacterial treated materials.* 2012. OECD Publishing. Paris. France
12. Mahon CR, Lehman DC, Manuselis G. Textbook of Diagnostic Microbiology (5th ed.). 2014. Elsevier Health Sciences. Kansas. USA.
13. National Science Foundation. 2016. *The LibreTexts libraries*. Available at https://chem.libretexts.org/Textbook_Maps/General_Chemistry_Textbook_Maps/Map%3A_Chemistry%3A_The_Central_Science_(Brown_et_al.)/13%3A_Properties_of_Solutions/13.2%3A_Saturated_Solutions_and_Solubility, Accessed on June 6,2017.
14. Patel, R. M. 2012. The guiding principles on antimicrobial susceptibility testing. *Bulletin of Pharmaceutical Research, 2*(3):146-153.
15. Poliak MS, Tsvetkova IA. 2007. Some factors inflluencing the efficiency of disk-diffusion test to determine the antibiotic sensitivity of microorganisms. *Klinicheskaia Laboratornaia Diagnostika,* 5:36-39.

FP-09

SINGLE STEP CROSS-FLOW ULTRAFILTRATION TECHNIQUE FOR RECOVERY AND PURIFICATION OF SURFACTIN PRODUCED BY *BACILLUS SUBTILIS* MSH1

MOHD HAFEZ MOHD ISA*[1], MUHAMMAD QADRI EFFENDY MUBARAK[1], NAJWA MOHAMED[1], SYAZRIN SYIMA SHARIFUDDIN[2] AND AIDIL ABDUL HAMID[3]

[1]Faculty of Science and Technology, Universiti Sains Islam Malaysia, Bandar Baru Nilai, 71800 Nilai, Negeri Sembilan, Malaysia.
[2]National Hydraulic Research Institute of Malaysia (NAHRIM), Jalan Putra Permai, 43300 Seri Kembangan, Selangor, Malaysia.
[3]Faculty of Science and Technology, Universiti Kebangsaan Malaysia, 43600 Bangi, Selangor, Malaysia.

*Corresponding author: m.hafez@usim.edu.my

ABSTRACT

Surfactin is a powerful biosurfactant and can be produced through fermentation of various strains of *Bacillus sp*. However, the extraction process is complicated due to the impurities present in the crude fermentation broth. In this study, benchtop cross-flow ultrafiltration (UF) unit equipped with hydrosart membrane (HT) and polyethersulfone membrane (PES) with 10 kDa and 30 kDa molecular weight cut-off (MWCO) were used to recover and purify surfactin from crude fermentation broth of *B. subtilis* MSH1 with transmembrane pressures (TMP) varying from 0.5 bar to 2.0 bar. Permeate flux, rejection coefficient of surfactin *(R)* and protein contents both in permeates and retentates were measured to evaluate the membranes performance for recovery and purification of surfactin in the final fraction. Surfactin was retained almost completely with an *R* close to 1 for all membranes used, with purity ranging from 82% to 88% and the four different TMPs applied during the filtration had no significant effect ($P < 0.05$) on *R*. In addition, surface tension measurements show high purity and fully functional purified surfactin and is comparable to the commercial surfactin standard.This study showed single step cross-flow ultrafiltration technique was successfully applied to achieve high recovery and purity of fully functional surfactin from crude fermentation broth of *B. subtilis* MSH1.

KEYWORDS:
Hydrosart membrane, Polyethersulfone membrane, Rejection coefficient, Surface tension, Transmembrane pressure.

INTRODUCTION:

Bacillus subtilis is a sporulating rod bacterium that thrives in the soil and is nonpathogenic to human beings,[1] making it one of the most studied Gram-positive bacteria.[2] The ability of *B. subtilis* strains to produce a series of lipopeptides (surfactin, iturin and fengycin) has been documented over 60 years[3] and it is a high-value bioproduct that offers advantageous application in various fields as an alternative to replace chemical surfactants. Surfactin is a heptapeptide linked to a β-hydroxy fatty acid chain of 13–16 carbon chains and always present in a series of isoforms. However, surfactin is an expensive lipopeptide, which makes it unable to compete effectively with chemical surfactants because the downstream process which contributes up to 60% of its total production cost.[4] Recovery and purification of surfactin is a complex processed due to the complexity of fermentation broth, which contains impurities such as proteins, sugar, lipid compounds and different types of amino acids.[5-6]

In recent years, various studies have been conducted with aims to reduce the downstream processing costs, including using foam fractionation[7], acid precipitation[8-9] and extraction using organic solvent, adsorption chromatography or a combination of these techniques. Unfortunately, all of these techniques give relatively low surfactin purity (<65%), and significant improvement to achieve higher performance on downstream processing is urgently needed. In addition, some of the approaches involving two-step treatment of fermentation broth make it impractical and less attractive for industrial purposes.[10-12] Furthermore, most of the conventional methods involve the use of toxic organic solvents such as chloroform and dichloromethane and these causes the final product to suffer from the loss of biosurfactant activity. Hence, there is a demand to develop more economic and environmentally friendly approaches to improve the current downstream processing technique.

Surfactin recovery and purification efficiency from fermentation broth is essential to increase cost efficiency of surfactin production. One of the alternative techniques for downstream processing is membrane filtration. Membrane filtration system was considered by various researchers[10-12] for the purpose of recovery and purification of biosurfactants as it is environmentally friendly and economical. Membrane filtration widely used in various chemical and biochemical processes. Most importantly, approach through membrane filtration involves no phase change,[6] which enables the molecular structure to be preserved. In much of the literature, membrane filtration meets downstream separation needs because the concentration and purification of the final product surpasses the limitations of traditional methods.[13-14]

The excellent characteristics of ultrafiltration (UF) membrane include the minimal physical damage of biomolecules from shear effects, minimal denaturation, high recovery yield, and the avoidance of resolubilization. In this study, cross-flow UF system equipped with hydrosart membrane (HT) and polyethersulfone membrane (PES) with a molecular weight cut-off (MWCO) of 10 kDa and 30 kDa was used for the filtration of crude fermentation broth of *B. subtilis* MSH1. The final surfactin and protein concentration both in permeates and retentates were analysed to evaluate the performance of UF. The aim of this work is to evaluate the type of membrane which can offer high recovery and purity of surfactin from crude fermentation broth operated under different transmembrane membrane pressure (TMP) ranging from 0.5-2.0 bar.

MATERIALS AND METHODS:

1. Preparation of culture media

A defined mineral salts medium (MSM) described by Cooper[15] was used as fermentation media throughout this study. The media consisted of NH_4NO_3, 0.05 M; Na_2HPO_4, 0.04 M; KH_2PO_4, 0.03 M; $CaCl_2$, 7.0×10^{-6} M; $FeSO_4\cdot7H_2O$, 4.0×10^{-6} M; EDTA, 4.0×10^{-6} M; $MgSO_4$, 8.0×10^{-6}M; and 4% (w/v) glucose.[7,12] All chemicals used were of analytical grade. Prepared medium was sterilized prior to fermentation.

2. Culture conditions and fermentation

Bacillus subtilis MSH1 was provided by Microbiology Laboratory, Faculty of Science and Technology, Universiti Sains Islam Malaysia (USIM). Stock culture was maintained on the nutrient agar. Two loopful of grown bacterial cells from the nutrient agar were transferred to 25 mL of nutrient broth containing 40 g/L of glucose, followed by the incubation of the culture broth at 200 rpm at 30°C for 24 h. A volume of 5 mL culture broth was then transferred to five conical flasks each containing 45 mL of Cooper's medium[9] incubated under the same conditions as previously described for 16 h.[12] An inoculum size of 5% (v/v) [11] were used to inoculate a 4750 mL Cooper's media with in submerged bioreactor (Sartorius Stedim, German) with a working volume of 5 L. The fermentation conditions were set at the temperature of 30°C, agitation speed of 100 rpm, air flow rate of 1 vvm^{-1} and at pH7 for 55 h. Culture broth samples were taken during the fermentation process at regular intervals for determination of bacterial growth and surfactin concentration.

3. Analytical methods

(i) Measurement of bacterial growth

Bacterial growth was measured by determining the biomass concentration (gram dry weight per litre of

culture medium) at different time intervals up to 55 h. Fixed volumes of the culture samples were withdrawn aseptically and transferred to centrifuge tubes for centrifugation at 10 000 rpm for 10 min. The supernatant was withdrawn and biomass left at the bottom of the tubes was dried using an oven. The dry weight was then measured using a balance until constant weight achieved.

(ii) Measurement of surfactin concentration

Culture samples were withdrawn aseptically at various time intervals and centrifuged at 10000 rpm for 10 min. Then the supernatant was filtered through a 0.2 µm nylon filter membrane. The surfactin concentration was measured using high-performance liquid chromatography (HPLC; Agilent Technologies, 1200 Series, USA) equipped with Chromolith® high performance RP-18 (100 mm × 4.6 mm, 5 µm) and detected at 205 nm with a variable wavelength detector according to method proposed by Mubarak *et al.,* 2015.[16] Mixtures of mobile phase consisted of acetonitrile (ACN) and 3.8 mM trifluoroacetic acid (TFA) solution at the ratio of 80:20 were pumped with an isocratic mode at a flow rate of 2.2 mL/min. The sample injection was set at 30 µL and the duration of each analysis was within 8 min. Surfactin standard with 98% purity (Sigma) was used as the standard.

(iii) Measurements of surface tension

Each sample, including surfactin standard was prepared in 5 mM of Tris buffer using deionized water. The surface tension of each sample was measured by ring method using a digital tensiometer (KRÜSS, Germany). A platinum ring was automatically submerged into each solution and then slowly pulled through the air/water interface. The ring was washed, flamed and cooled between each measurement. Each measurement was taken at room temperature.

(iv) Measurement of surfactin purity

Surfactin concentration was measured using HPLC as according to method proposed in section 3(ii). The purity of surfactin in the dried sample was calculated by Equation 1.[14]

$$\text{Purity}(\%) = \frac{\text{Concentration of surfactin determined by HPLC}}{\text{Weight of dried sample powder}} \times 98\% \qquad (1)$$

The purity of surfactin in the recovered product and in the treated broth were later used to calculate the total recovery of surfactin.

(v) Measurement of protein concentration

The total amount of protein present at each stage of the purification procedures was determined in order to assess the purity of recovered sample in each of the filtration step. Crude fermentation broth was centrifuged at 10 000 rpm to remove biomass impurities. The cell free supernatants which also contained macromolecules, mid-molecules, and small molecules was further treated by acid precipitation[8] by addition of 1M HCl to a pH 4 and was centrifuged at 10 000 rpm for 15 minutes. The obtained precipitate was oven-dried at 37 ˚C for 2 days and the weight of dried precipitate was recorded for measurement of protein concentration by using the following Equation 2.

Protein concentration (mg/L) = Weight of dried sample – weight of surfactin (HPLC)….. (2)

4. Recovery and purification of surfactin by UF

Figure 1 shows schematic diagram of UF procedure conducted in this study. Microfiltration was applied to completely remove biomass and small particle present in the fermentation broth and thus to prevent them from blocking the membrane pore at the UF stage. Small-scale crossflow UF procedures were carried out using a bench top crossflow filtration device (Sartorius Stedim, Germany) equipped with two sets of membranes which are polyethersulfone (PES) membrane and hydrosart (HT) membrane each with molecular weight cut-off (MWCO) of 10 kDa and 30 kDa with an effective area of 0.02 m^2. The driving force of the permeate flow was the pressure supplied by the external pump towards the system. In general, a feed volume of 250 mL was added to the reservoir and the volume was reduced to 25 mL. Later, retentates and permeates were recovered and analyzed for determination of surfactin concentration, protein

concentration, the rejection coefficient of surfactin by membrane (R) and the total recovery of surfactin in the final fraction. Recovery is defined as:

$$\text{Recovery}(\%)=\left(1-\left(\frac{C_p}{C_f}\right)\right)\times 100 \qquad (3)$$

Where C_p and C_f are the concentration of surfactin in permeate and feed respectively. The recoveries of surfactin were calculated according to surfactin concentration in the feed and permeate, respectively at the end of the experiments for all filtration fraction due to the filtration system was operated in concentration mode.

The concentration factors (R_F) as shown in Equation 4 (4) was used to assess the concentration increase of surfactin in the feed by referring to initial concentration in the feed (C_o):

$$R_F=\frac{C_f}{C_o} \qquad (4)$$

Throughout the UF procedure, the flow rate across the membrane was estimated by collecting permeates of interested volumes during a precisely controlled period of time. Permeate flux was calculated by using the following equation:

$$\text{Flux}\left(\text{LMH or}\frac{\text{L}}{\text{m}^2\text{h}}\right)=\frac{\text{flow rate (L/h)}}{\text{membrane area (m}^2\text{)}} \qquad (5)$$

The relative flux (RF) was defined as

$$RF(\%)=\frac{J_s}{J_w}\times 100 \qquad (6)$$

The Flux recovery (FR) was defined as

$$FR(\%)=\frac{J_f}{J_w}\times 100 \qquad (7)$$

Where J_w, J_s and J_f are the pure water flux of clean membrane, fermentation broth flux and pure water flux of fouled membrane, respectively.

The irreversible and reversible flux decline caused by fouling was calculated according the Equation 8 (8), while the reversible flux decline caused by either concentration polarization or reversible adsorption phenomena was calculated according Equation 9 (9):

$$\text{Fouling} = 100\text{-FR} \qquad (8)$$

$$\text{Reversible flux decline} = \text{FR-RF} \qquad (9)$$

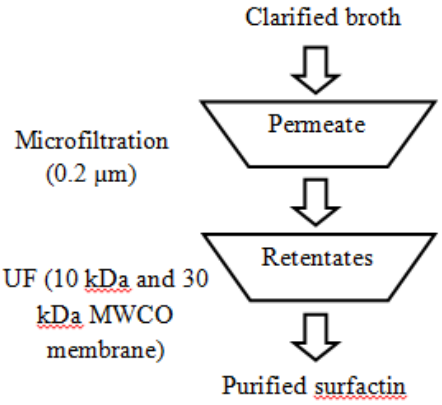

Figure 1

Schematic representation of filtration process carried out in this study.

The four different TMPs for this procedure ranged from 0.5 bar to 2.0 bar was controlled manually by adjusting the valve and pump controller. TMPs of filtration process were calculated following Equation 10 (10). The highest TMP applied was up to 2.0 bar.

$$TMP = \left(\frac{P_{in}-P_{out}}{2}\right) - P_{permeate} \qquad (10)$$

RESULTS AND DISCUSSION:

1. Production of surfactin by *B. subtilis* MSH1

Various authors have reported the ability of *B. subtilis* ATCC 21332 to produce surfactin[9,11] and Cooper's media with 4% (w/v) of glucose was chosen as the media because it has been designed to supply nutrients for bacterial cell growth and surfactin synthesis by *Bacillus* strains.[9,11,17] During the course of fermentation, the pH of the fermentation broth was maintained at pH 7 to avoid the acidification of the culture medium due to the change from aerobic to anaerobic respiration by the cell (Charcosset, 2006) where the cell grows in the absence of oxygen. Surfactin will lose its ability to solubilize if the pH drops to pH 5, causing surfactin to precipitate.[18]

B. subtilis MSH1 is a local isolated strains and was identified by Shannaq *et al.,*.[19] This *B. subtilis* strain is a surfactin-producer strain with the presence of 16s rDNA genes with accession number of JX080184.1 and CP002183.1), respectively as reported by.[19] Figure 2 shows bacterial cell growth and surfactin production during the course of fermentation of *B. subtilis* MSH1. Lag phase of *B. subtilis* MSH1 lasted for approximately 5 h shows almost no apparent cell growth due to adaptation of microorganism to the new environment in which cell growth was very low. Later bacterial grew exponentially and cell in a logarithmic pattern until 28 h and this indicates *B. subtilis* MSH1 had achieved the maximum cell growth before moving into stationary growth phase. It can be accepted that the production of surfactin is very closely related to the growth of the strains where the maximum production was obtained at the end of the exponential growth phase and this was in agreement with other previous studies.[9]

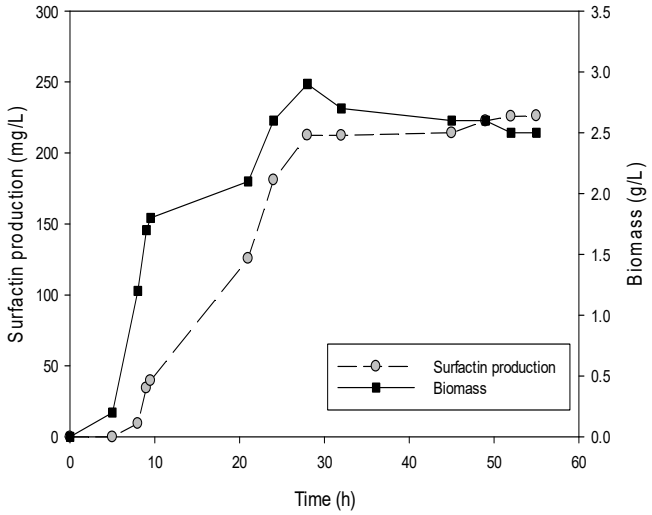

Figure 2
Production of surfactin by *B. subtilis* MSH1

2. Fermentation broth composition

The major content of raw fermentation broth of *B. subtilis* MSH1 is shown in Table 1. Other than the quantity bacterial biomass, surfactin concentration and total contents of protein as determined in this study, crude fermentation broth also consisted of other macromolecules, residual glucose and amino acids.[6,20] The harvested crude fermentation broth at the end of fermentation for production of surfactin was then subjected to the single-step cross-flow ultrafiltration (UF) process for recovery and purification of surfactin.

Table 1
Major composition of fermentation broth of *B. subtilis* MSH1 (means ± SD, n = 3)

Major composition of fermentation broth	Concentration
	***B. subtilis* MSH1**
Final concentration of biomass (g/l)	2.50 ± 0.03
Final concentration of surfactin (mg/l)	226.17 ± 1.83
Final concentration of protein (mg/l)	126.00 ± 2.28

3. Rejection coefficient, final recovery recovery and purity of UF retentate

The UF technique applied was able to achieve high degree of recovery and purity of surfactin in the retentate. The niche of UF compared to other downstream processing techniques is its ability to segregate the interested molecules based on molecular weight without phase changes. In this present study, surfactin was completely rejected by all tested membranes, and achieving high degree of recovery and purity in the range of 83% - 94% and 78% - 95%, respectively. The effect of increasing TMP on permeates flux, rejection coefficient (*R*) of surfactin by membrane, total recovery and purity of surfactin in the final fraction of all membranes (HT10, HT30, PES10 and PES30) were presented in Tables 2 and 3.

Insignificant differences ($P < 0.05$) were observed with increasing TMP towards *R* of surfactin by all applied membrane with almost complete rejection of surfactin by all membranes (R~1). Very limited differences in the rejection coefficient (*R*) on both membranes were observed. The possible explanation for this behaviour was due to the size of surfactin micelles was bigger than the MWCO of the applied membranes and this is in agreement with other previous studies.[12,21] Even though the molecular size of surfactin monomer varying from 994 Da to 1050 Da, at concentrations above 15 mg/L[22] surfactin able to form micelles structure with size varying from 30 kDa to 100 kDa.[10,20] At critical micelle concentrations (CMC), surfactin molecules readily associate to form supramolecular structures with nominal molecular diameters of up to two to three orders of magnitude larger than single unassociated molecules.[10] In this work, surfactin micelles were sufficiently retained by using membrane with MWCO of less than 100 kDa and this is in agreement with previously findings as previously discussed. The effectiveness of UF membrane applied in this study was due the fact that the surfactin micelles were big enough to be rejected by membrane of at least 30 kDa membrane. Given these facts, it was agreed that the size of the surfactin micelles was above 30 kDa, as reported in previous studies.[10,22]

According to Figure 4, all membranes were able to achieve high recovery and purity of surfactin from fermentation broth although the membrane material had an effect on the recovery and purity of surfactin. Through comparison of all membranes used in this study, the use of HT30 provided significantly higher ($P > 0.05$) recovery and purity of surfactin in the final fraction in comparison to PES10 and HT10 membranes. Approximately, 88% to 96% of surfactin were recovered under various applied TMPs. However, complete recovery of surfactin was not possible due to some loss of surfactin through membrane fouling. According to Mulder,[23] surfactin molecules able to form CMC and form a kind of dynamic membrane on top of membrane surface besides the possibility of surfactin monomers permeating through membranes pores,

although its concentration were too low and were undetectable by HPLC. On the other hand, results obtained suggest at least 13% of contaminants were able to pass through the membrane and this resulted to high purity of surfactin in the final fraction. This study indicated that HT membrane was more efficient in removing contaminants in comparison to PES membrane thus achieving better purity. Furthermore, the permeate flux with PES membrane decreased quite significantly over time (Figure 3 (a) - (d) and Table 4) in comparison to HT membrane which was due to the more severe concentration polarization caused by the hydrophobic interactions between PES and contaminants consisting of proteins and amino acids in feed solutions. The results obtained in this study was in agreement with other previous work, however with different mode of UF.[11] The gradual flux decline with HT 30 membrane implies weak adsorption of surfactin onto membrane surfaces, whereas pore radius was not significantly reduced although the membrane is comparatively hydrophobic in nature.[24-25]

Table 2
Total recovery and purity of fermentation broth of *B. subtilis* MSH1 after UF treatment

TMP	Type of membrane							
	PES10		HT10		PES30		HT30	
	Recovery (%)	Purity (%)	Recovery (%)	Purity (%)	Recovery (%)	Purity (%)	Recovery (%)	Purity (%)
0.5	92.9	78.0	95.8	84.0	92.8	92.2	94.1	94.5
1.0	93.1	80.4	96.2	85.4	90.6	91.8	92.6	94.7
1.5	93.2	87.8	96.0	88.7	89.5	90.4	91.3	93.4
2.0	92.8	88.2	96.5	91.5	88.9	88.0	90.8	93.0

Table 3
Rejection coefficient of fermentation broth of *B. subtilis* MSH1 after UF treatment

TMP	Type of membrane			
	PES10	HT10	PES30	HT30
	Rejection coefficient	Rejection coefficient	Rejection coefficient	Rejection coefficient
0.5	0.97	0.98	0.95	0.96
1.0	0.97	0.98	0.94	0.96
1.5	0.97	0.97	0.93	0.95
2.0	0.96	0.97	0.93	0.94

4. The flux of UF process

Cross flow UF mode was chosen in this study because the tangential flow of feed solution along the membrane will prolonged the time of the depositions on the membrane surface by sweeping effects, theoretically will result in less fouling and maintenance of high flux filtration process.[12] However, the permeate flux decay is affected by a number of factor such as TMP, temperature, feed concentration, membrane pore size, membrane material chemistry and the dynamics of the filtration process.[26] Figure 12 (a) - (d) to Figure 3 (a) - (d) show the permeate flux decay for crude fermentation broth of *B. subtilis* MSH1 under various processing condition (TMP, MWCO membrane materials) in order to obtain the most optimal conditions for high flux, high recovery and purity of surfactin from crude fermentation broth. As shown in Figure 12 (a) - (d) to Figure 13(a) - (d), flux were significantly decreased with increasing TMP in all the experiments even when the flux was high at initial stage. Long-term flux decline were observed on all membranes however with different profiles as a result of different surface interaction between membrane surfaces with solute. The expected possible interactions were concentration polarization, adsorption of surfactin molecules and other small impurities onto the membrane surface.[24] Interestingly, the flux of

permeate seems to be more stable at low TMP (0.5 bar and 1.0 bar) whereas at high TMP (1.5 bar and 2.0 bar), an obvious pattern of flux decline can be seen. Flux decline is an unavoidable deleterious phenomenon in the filtration process[27] even though we have high interest to maintain the highest possible flux value.

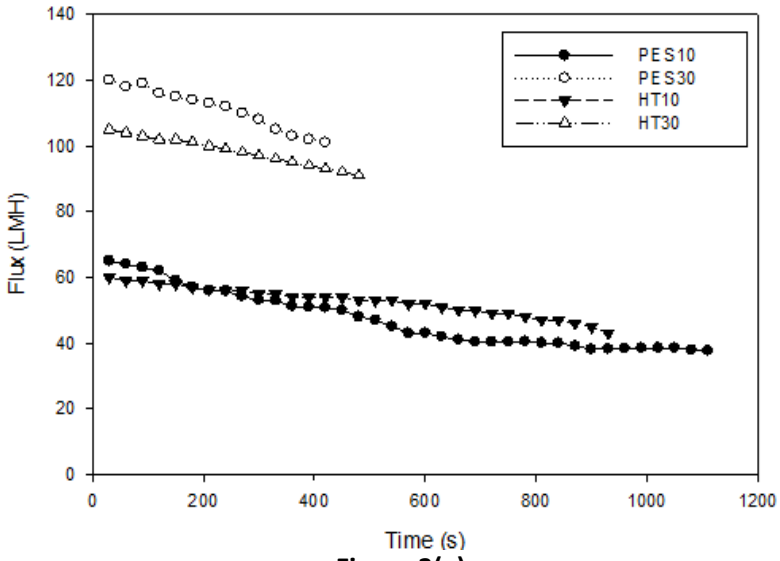

Figure 3(a)

Effect of TMP at 0.5 bar on the permeate flux on all membranes for *B. subtilis* MSH1

Table 4

The flux decline results and VRF values of all membranes for filtration of raw fermentation broth of *B. subtilis* MSH1 at various TMP

Type of membrane	TMP (bar)	Flux			Flux decline (%)					
		J_w	J_s	J_f	Total (100-RF)	Concentration polarisation (FR-RF)	Fouling (100-FR)	V_t (L)	V_c (L)	VRF (V_t/ V_c)
PES10	0.5	53.0	38.6	43.2	27.2	8.7	18.5	250.0	23.0	10.9
	1.0	69.2	41.0	46.3	40.8	7.7	33.1	250.0	23.0	10.9
	1.5	99.2	40.0	48.5	59.7	8.6	51.1	250.0	24.0	10.4
	2.0	147.6	89.0	119.0	39.7	20.3	39.4	250.0	23.0	10.9
PES30	0.5	91.0	71.2	77.6	21.8	7.0	14.7	250.0	23.0	10.9
	1.0	127.2	89.0	100.5	30.0	9.0	21.0	250.0	25.0	10.0
	1.5	180.2	101.2	108.5	43.8	4.1	39.8	250.0	25.0	10.0
	2.0	225.6	149.1	180.3	33.9	13.8	40.1	250.0	26.0	9.6
HT10	0.5	52.0	43.1	46.8	17.1	7.1	10.0	250.0	25.0	10.0
	1.0	77.2	57.9	64.3	25.0	8.3	16.7	250.0	24.0	10.4
	1.5	91.0	58.2	70.4	36.0	13.4	22.6	250.0	24.0	10.4
	2.0	140.2	110.0	135.4	21.5	18.1	33.4	250.0	23.0	10.9
HT30	0.5	98.1	79.8	86.0	18.7	6.3	12.3	250.0	24.0	10.4
	1.0	110.0	91.0	96.5	17.3	5.0	12.3	250.0	23.0	10.9
	1.5	134.5	102.0	112.6	24.2	7.9	16.3	250.0	22.0	11.4
	2.0	241.0	178.2	204.1	26.1	10.7	25.3	250.0	24.0	10.4

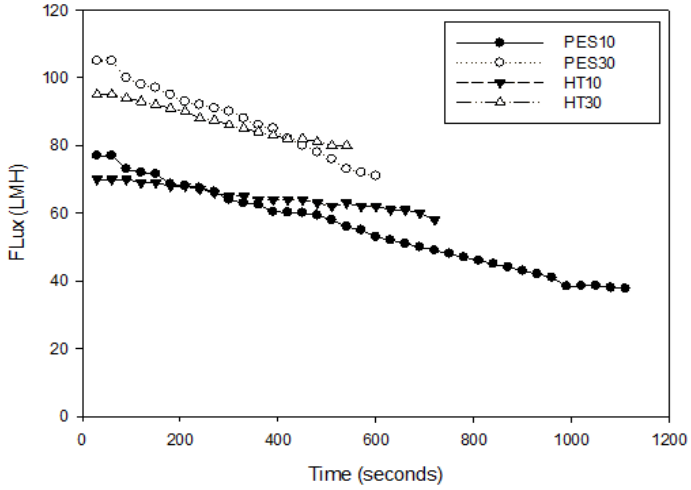

Figure 3(b)

Effect of TMP at 1.0 bar on the permeate flux on all membranes for *B. subtilis* MSH1

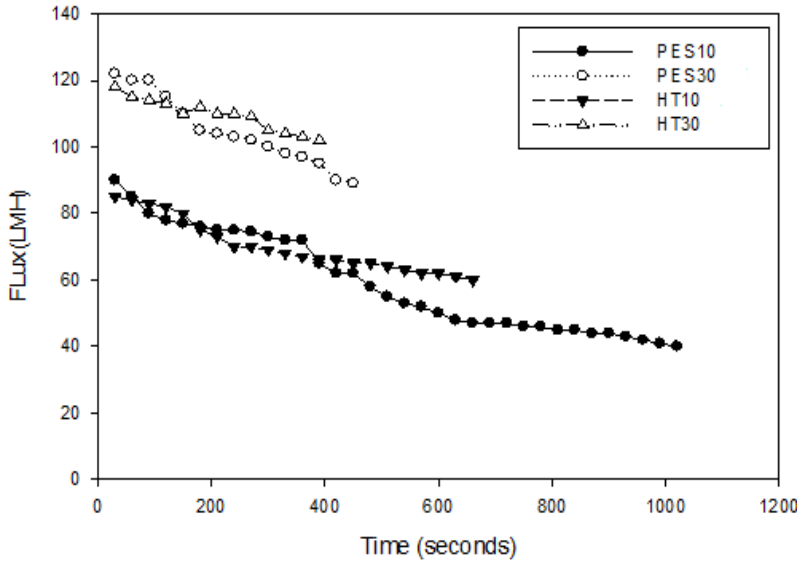

Figure 3(c)

Effect of TMP at 1.5 bar on the permeate flux on all membranes for *B. subtilis* MSH1

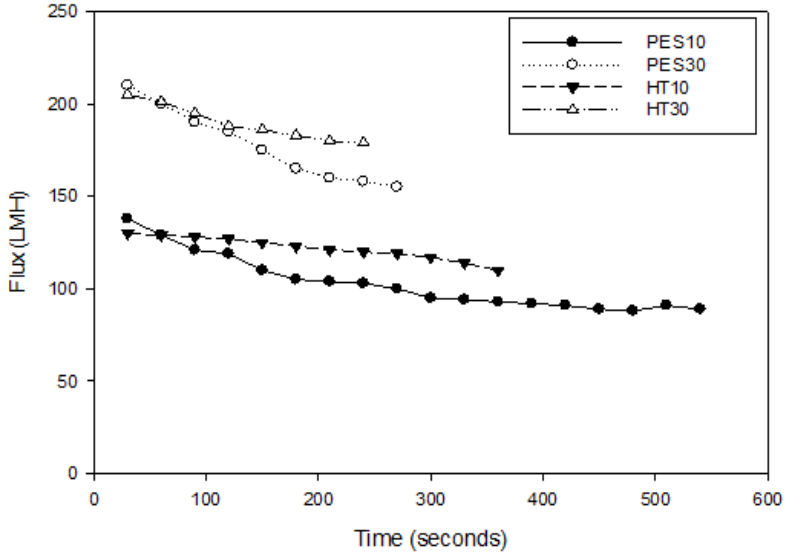

Figure 3(d)

Effect of TMP at 2.0 bar on permeate flux on all membranes for *B. subtilis* MSH1

5. Fouling behavior

According to Kaya *et al.*,[21] the flux decline occurs because of the accumulation of molecules in solutes on the membrane surface due to concentration polarization which later lead to membrane fouling. Gradual flux decline was clearly observed with increasing TMP over time although initially resulted to higher permeate flux. At a later stage of the filtration process, the higher TMP pulls more particles towards the membrane surface by providing faster permeate velocity thus contributes to the rapid generation of the deposited cake layer which causes a dramatic increase of resistance onto the membrane surface. Higher pressure will significantly compress the pre-built cake layer so it will become denser and contributed to the rapid flux decline.

When applying low TMP (0.5 bar and 1.0 bar), a gradual flux decline was observed for all membranes because of the slow formation of cake layer. At low TMP the permeate flux was maintained at its high value for a considerable time before decaying (Figure 4 (a)-(d)) due to the wettability of the membrane was only sufficient to minimize surfactin and impurities deposition on membrane surface. With times, the concentration of solute in feed solution was increasing with the decrease in volume of feed reservoir and hence speed up the rate of surfactin deposition which later resulted to decay of permeate. Concentration polarization layer starts to develop as a result of increased deposition of surfactin and impurities on top of membrane surface and forming a dynamic membrane layer which act as secondary layer.[23] These phenomena resulted to decrease of flux throughout the UF process. As the concentration of the surfactin on the membrane and within the pores increases over time, the permeate flux started to decay and effect of membrane material on permeate flux became less significant. The fouling occurs when substances in fermentation solutions coating the membrane surface which resulted to pore blockage and causes serious gradual permeate flux decline. In any membrane system, it is vital that concentration polarization is reduced as much as possible as it has a very significant impact on permeate flux decline and operating cost.

Flux decline and cake formation could be minimized through pre-treatment of crude fermentation broth via acid precipitation, salting out[18] or removal of large particle by centrifugation and microfiltration. In this study, pre-treatment of crude fermentation broth was conducted by removal of biomass with centrifugation and removal of any large particle using 0.2 mm membrane filtration. Howell and Velicangil[28] divided filtration with UF into three phases through evaluation of permeate flux pattern which are: (1) first few seconds (formation of a quasi-steady-state concentration polarization layer), (2) solute adsorption, (3) and long term (gel layer formation). Thus, occurrence of concentration polarization during the first few seconds of filtration process could explain the flux decline with PES 10 and PES 30 membrane at high TMP which primarily affects the flux behaviour throughout the filtration process. However, the time required for the filtration process to establish quasi-steady-state is very short which was less than 10 seconds and is therefore insignificant.[28] The gradual flux decline with HT 30 membrane is a result of concentration polarization as well as weak adsorption of surfactin micelles and other small impurities onto the membrane surface.[14] Permeate flux starts to decay only after the establishment of a slow decaying plateau region. Overall, permeate flux decreases with increasing solutes concentration in the feed solution which was due to rapid accumulation of molecules near membrane surfaces.

6. Hydrophilicities of membrane

HT and PES membranes were selected due to their high degree of hydrophilicities. The contact angles of water for PES membrane were greater than cellulose ester (similar material with HT membranes) with 62.9° and 56.4°, respectively.[18] This characteristic make HT membrane more hydrophilic than PES, resulting in earlier attachment of dissolved amino acids.[14] Thus, the steady-state flux of PES membrane is higher compared to HT membrane under identical conditions.

More severe flux decline was observed with PES membrane in comparison to HT membrane. The possible interactions between membrane surfaces and surfactin molecules can be in the form of severity of concentration polarization and deposition of surfactin molecules dependant of membranes degree of hydrophilicities which can lead to reduction of membranes pore radius and gradual decrease of permeate flux.[18,21] The net effect of flux decrease or increase, as well as severity of permeate flux decrease is highly

dependent on the hydrophobic interaction of surfactin molecules and other contaminants with membranes used in this study. Due to the highly hydrophilic nature of HT membrane with very low protein binding feature provided better permeate flux maintenance in comparison to the less hydrophilic PES membrane, although both membrane types provided high recovery and purity of surfactin in the final fraction.

Amongst different types of membranes used in this study, HT30 membrane provided better recovery and purity of final fraction of surfactin sample followed by HT10, PES30 and PES10. The understanding of molecular structure, shape and size, as well as the interaction between solute and membrane is important in order to optimize surfactin recovery and purification from crude fermentation broth. HT30 membrane is the more suitable membrane for single step UF for simple and highly cost effective downstream processing method which can offer high recovery and purity of surfactin from complex fermentation broth of *B. subtilis* MSH1.

7. Membrane cleaning

One of the major challenges in the application of membrane filtration technique applied in this study was the formation of concentration polarization on the membranes surfaces during the filtration process as what we had previously discussed. Concentration polarization is not desirable because it will reduce the flux of permeate and increasing filtration time. The cleaning protocols recommended by membrane manufactures consist of a series of acid-alkaline cleaning cycles, and dependant on the types of solutes in feed solution and types of membrane materials.[29-30] It was found that the increasing of TMP resulted to inefficient cleaning process. Thus, periodical chemical cleaning with *in situ* back-flushing is one possible way to restore and maintain the flux, preserve and prolong the membrane usage. Different types of cleaning solutions were tested, which were deionized water, NaOH solutions at pH 10, 12 and 14. The effects of flushing and back-flushing on the flux and surfactin rejection with PES 10, PES30 HT10 and HT30 are shown in Table 5. After 20 min flushing and back-flushing using deionized water, approximately 59% to 83% of the fluxes could be recovered on the basis of pure water flux. Furthermore, the use of deionized water alone was not sufficient to restore membrane initial flux especially for high concentrations of surfactin in complex mixture of crude fermentation broth.

Table 5
The efficiency of membrane cleaning using different cleaning solution on all membrane used in this study

Concentration of surfactin	Type of cleaning	Cleaning solution (flux recovery and cleaning time)			
		Deionized water	NaOH (pH10)	NaOH (pH12)	NaOH (pH14)
PES10	Flushing	20 min (61%)	20 min (67%)	10–15 min (100%)	10–15 min (100%)
PES10	Back-flushing	20 min (59%)	20 min (65%)	10–15 min (100%)	10–15 min (100%)
HT10	Flushing	20 min (74%)	20 min (82%)	15–20 min (100%)	15–20 min (100%)
HT10	Back-flushing	20 min (69%)	20 min (74%)	15–20 min (100%)	15–20 min (100%)
PES30	Flushing	20 min (75%)	20 min (86%)	10-15 min (100%)	10-15 min (100%)
PES30	Back-flushing	20 min (69%)	20 min (79%)	10-15 min (100%)	10-15 min (100%)
HT30	Flushing	20 min (83%)	15–20 min (89%)	5–10 min (100%)	5–10 min (100%)
HT30	Back-flushing	20 min (75%)	15–20 min (82%)	5–10 min (100%)	5–10 min (100%)

Previous studies have reported the effects of high-pH NaOH solution on flux recovery and cleaning time cycle for membranes fouled with proteins.[30] Results obtained as in Table 4 indicate membrane fluxes were able to be restored when the used membrane were cleaned using NaOH, by either flushing or back-flushing. Overall, more time needed to recover membranes initial flux using deionized water in comparison to NaOH solutions of pH 12 and pH 14. In terms of the different types of cleaning solutions used, the flux recovery performances decrease in the order of NaOH pH 14 > NaOH pH 12 > NaOH pH 10 > water. No significant difference (P> 0.05) was observed in the cleaning performance of NaOH solutions of pH 12 and pH 14; and these two NaOH solutions were the more effective solution to achieve high flux recoveries in this study. In addition, it was observed flux recovery by flushing was generally higher than that of back-flushing and shows membranes used in this study were mainly fouled by weak adsorption/gel layer formation, rather than pore blocking which can be observed by the gradual flux decline behaviour as shown in Figure 3(a)-(d) and as previously discussed. Considering the factors of cost reduction, NaOH at pH 12 appears to be the most suitable solution to clean used membranes in order to achieve practical and cost-effective initial flux recoveries of membranes used in this study.

8. Recovered and purified surfactin characterization

(i) Surface tension measurement

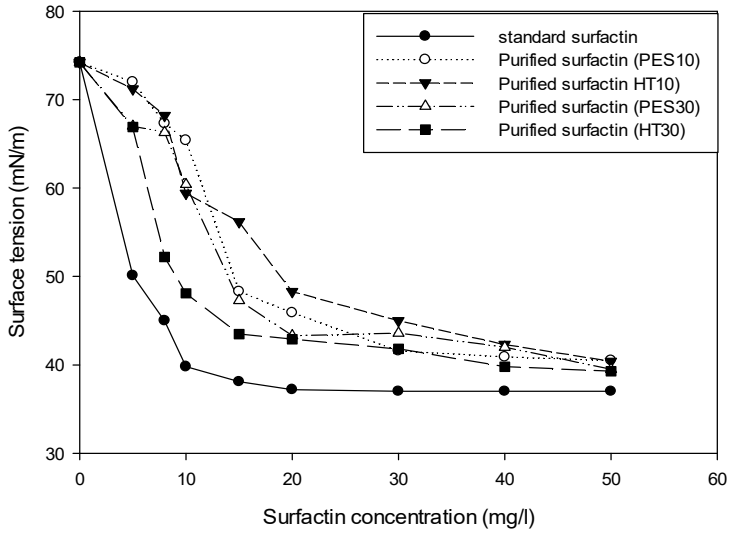

Figure 4

Surface tension of surfactin standard, purified surfactin (HT10), purified surfactin (HT30), purified surfactin (PES10), and purified surfactin (PES30) from fermentation broth of*B. subtilis* MSH1.

Surface tension measurements were used to evaluate the functionality and purity of the final fraction of surfactin samples using surfactin standard with 98% purity as reference sample under similar and controlled conditions.[12,22] Figure 4 shows the surface tension profiles of surfactin purified with different types of membranes in comparison to surfactin standard as reference. The results show close proximity in terms of the surface activity of purified surfactin in relation to surfactin standard, which indirectly shows high purity of final fraction of surfactin samples and this corresponds to the earlier results on purity measurements as shown in Table 2. In addition, Figure 4 shows the purified surfactin behaves as a highly surface active biosurfactant and the presence of some contaminants did not affect the original surfactin functionality.[31]

CONCLUSION:

Recovery and purification of surfactin from fermentation broth of *B. subtilis* MSH1 by a single-step cross flow UF technique using PES and HT membranes of 10 kDa and 30 kDa MWCO was evaluated through investigation of permeate flux, rejection coefficient(R) of surfactin and purity of surfactin at various TMP's. Surfactin was successfully retained by all membrane achieving R of almost 1 and this is due to the fact that surfactin micelles were unable to permeate by using at least 30 kDa MWCO membranes. All membranes

used in this study lead to high recovery and purity of surfactin from crude fermentation broth. Results obtained in this study can further assist in improving the cost-effectiveness of downstream processing of surfactin which in turn can promote surfactin commercialization. In addition, product characterization analysis was conducted to evaluate the functionality and purity of surfactin final fraction by using surface tension analysis with use of surfactin standard as reference under similar controlled conditions. Results showed close proximity of surface activity of purified surfactin in relation to surfactin standard which indirectly indicated the presence of small amount of impurities in the final fraction did not affect the original surfactin functionality. Among all of the membranes used, it was found that HT30 membrane is mostly suitable for the downstream processing of surfactin because it provides better purity of surfactin in the final fraction and provide higher flux rates with minimal concentration polarization and solutes deposition in comparison to the other membranes. It was found that the variation of TMP had no significant effect on recovery and purity of surfactin in the final fraction however it affects the permeate flux. The flux of filtration can be maintained by using lower TMPs which is an important characteristic in reducing operational cost in large scale downstream processing. It can be concluded highly selective recovery and purification of surfactin from fermentation broths could be achieved by a single step UF process at the laboratory scale and shows potential to be scaled-up for industrial application and improving the cost effectiveness of surfactin recovery and purification.

ACKNOWLEDGEMENT:

This research works was supported by the Fundamental Research Grants Scheme, Ministry of Higher Education of Malaysia (FRGS-FST-51716-50) and National Hydraulic Research Institute of Malaysia grant (NAHRIM-FST-40816 and USIM-NAHRIM-FST-41915).

REFERENCES:

1. Zweers JC, Barák I, Becher D, Driessen AJ, Hecker M, Kontinen VP, et al. Towards the development of Bacillus subtilis as a cell factory for membrane proteins and protein complexes, Microb. Cell Fact. 2008; 7:10 doi:10.1186/1475-2859-7-10.
2. Driks A. Overview: development in bacteria: spore formation in Bacillus subtilis, Cell. Mol. Life Sci. C. 2002; 59: 389–391doi:10.1007/s00018-002-8430-x.
3. Xiao X, Chen H, Wang J, Ren C, Wu L. Impact of Bacillus subtilis JA, a biocontrol strain of fungal plant pathogens, on arbuscular mycorrhiza formation in Zea mays, World J. Microbiol. Biotechnol. 2008; 24: 1133–1137 doi:10.1007/s11274-007-9584-3.
4. Satisfactory separation and MS-MS spectrometry of six surfactin isolated form Bacillus subtils natto, (n.d.).
5. Keller K, Friedmann T, Boxman A. The bioseparation needs for tomorrow, Trends Biotechnol. 2001; 19: 438–441 doi:10.1016/S0167-7799(01)01803-0.
6. Mulligan CN, Gibbs BF. Recovery of biosurfactants by ultrafiltration., J. Chem. Technol. Biotechnol. 1990; 47: 23–9 doi:10.1002/jctb.280470104.
7. Davis DA, Lynch HC, Varley J. The application of foaming for the recovery of Surfactin from B. subtilis ATCC 21332 cultures, Enzyme Microb. Technol. 2001; 28: 346–354 doi:10.1016/S0141-0229(00)00327-6.
8. Chen HL, Chen YS, Juang RS. Separation of surfactin from fermentation broths by acid precipitation and two-stage dead-end ultrafiltration processes, J. Memb. Sci. 2007; 299: 114–121 doi:10.1016/j.memsci.2007.04.031.
9. Reis Rv, Zydney A. Bioprocess membrane technology, J. Memb. Sci. 2007; 297: 16–50 doi:10.1016/j.memsci.2007.02.045.
10. Lin S, Jiang H. Recovery and purification of the lipopeptide biosurfactant of Bacillus subtilis by ultrafiltration, Biotechnol. Tech. 1997; 11: 413–416 doi:10.1023/A:1018468723132.
11. Isa MHM, Coraglia DE, Frazier Ra, Jauregi P. Recovery and purification of surfactin from fermentation broth by a two-step ultrafiltration process, J. Memb. Sci. 2007; 296: 51–57 doi:10.1016/j.memsci.2007.03.023.

12. Isa MHM, Frazier Ra, Jauregi P. A further study of the recovery and purification of surfactin from fermentation broth by membrane filtration, Sep. Purif. Technol. 2008; 64: 176–182 doi:10.1016/j.seppur.2008.09.008.
13. Sen R, Swaminathan T. Characterization of concentration and purification parameters and operating conditions for the small-scale recovery of surfactin, Process Biochem. 2005; 40: 2953–2958 doi:10.1016/j.procbio.2005.01.014.
14. Chen HL, Chen YS, Juang RS. Flux decline and membrane cleaning in cross-flow ultrafiltration of treated fermentation broths for surfactin recovery, Sep. Purif. Technol. 2008; 62: 47–55 doi:10.1016/j.seppur.2007.12.015.
15. Cooper DG, Macdonald CR, Duff SJB, Kosaric N. Enhanced production of surfactin from Bacillus subtilis by continuous product removal and metal cation additions, Appl. Environ. Microbiol. 1981; 42: 408–412 .
16. Isokratik K, Ringkas H. A Simple and Effective Isocratic HPLC Method for Fast Identification and Quantification of Surfactin 2015; 44: 115–120.
17. Charcosset C. Membrane processes in biotechnology: An overview, Biotechnol. Adv. 2006; 24: 482–492 doi:10.1016/j.biotechadv.2006.03.002.
18. Chen C, Baker SC, Darton RC. The application of a high throughput analysis method for the screening of potential biosurfactants from natural sources, Methods. 2007; 70: 503–510 doi:10.1016/j.mimet.2007.06.006.
19. Shannaq MA. Isolation and Molecular Identification of Surfactin-producing Bacillus Subtilis 2013; 1.
20. Yakimov MM, Amro MM, Bock M, Boseker K, Fredrickson HL, Kessel DG, et al. The potential of Bacillus licheniformis strains for in situ enhanced oil recovery, J. Pet. Sci. Eng. 1997; 18: 147–160 doi:http://dx.doi.org/10.1016/S0920-4105(97)00015-6.
21. Kaya Y, Barlas H, Arayici S. Evaluation of fouling mechanisms in the nanofiltration of solutions with high anionic and nonionic surfactant contents using a resistance-in-series model, J. Memb. Sci. 2011; 367: 45–54 doi:10.1016/j.memsci.2010.10.037.
22. Wei YH, Wang LF, Chang JS, Kung SS. Identification of induced acidification in iron-enriched cultures of Bacillus subtilis during biosurfactant fermentation, J. Biosci. Bioeng. 2003; 96: 174–178 doi:10.1016/S1389-1723(03)90121-6.
23. Mulder MHV. Polarization phenomena and membrane fouling, *Membrane Science and Technology* , 1995; 45-84.
24. Flux decline in crossflow microfiltration and ultrafiltration mechanisms and modeling of membrane fouling, (n.d.).
25. Cornelis G, Boussu K, Van der Bruggen B, Devreese I, Vandecasteele C. Nanofiltration of nonionic surfactants: Effect of the molecular weight cutoff and contact angle on flux behavior, Ind. Eng. Chem. Res. 2005; 44: 7652–7658 doi:10.1021/ie0501226.
26. Crossflow microfiltration behaviour of a double-chain cationic surfactant dispersion in water—I, (n.d.).
27. Chen H, Kim AS. Prediction of permeate flux decline in crossflow membrane filtration of colloidal suspension: a radial basis function neural network approach, Desalination. 2006; 192: 415–428 doi:10.1016/j.desal.2005.07.045.
28. Howell JA, Velicangil O. Theoretical considerations of membrane fouling and its treatment with immobilized enzymes for protein ultrafiltration, J. Appl. Polym. Sci. 1982; 27: 21–32. doi:10.1002/app.1982.070270103.
29. Li X, Li J, Fu X, Wickramasinghe R, Chen J. Chemical cleaning of PS ultrafilters fouled by the fermentation broth of glutamic acid, Sep. Purif. Technol. 2005; 42: 181–187. doi:10.1016/j.seppur.2004.07.005.
30. Cabero ML, Riera Fa, R. Álvarez. Rinsing of ultrafiltration ceramic membranes fouled with whey proteins: Effects on cleaning procedures, J. Memb. Sci. 1999; 154: 239–250. doi:10.1016/S0376-7388(98)00294-4.
31. Sheppard JD, Mulligan CN. The production of surfactin by Bacillus subtilis grown on peat hydrolysate, Appl. Microbiol. Biotechnol. 1987; 27: 110–116. doi:10.1007/BF00251931.

FP-10

THE POTENTIAL OF *ZINGIBER OFFICINALE* ROSCOE AQUEOUS EXTRACT AS NATURAL FOOD PRESERVATIVE

APANDI, SITI NOOR ALIZA[1], JASNIE, FARNIDAH*[1] AND LO CHOR WAI[1]

[1]Faculty of Applied Sciences, Universiti Teknologi MARA, Kota Kinabalu, Sabah, Malaysia

*Corresponding author: farni224@sabah.uitm.edu.my

ABSTRACT

Zingiber officinale Roscoe or commonly known as ginger is a common aromatic spice used in cooking. Its antibacterial and potential as natural food preservatives on raw chicken meat was investigated. The antibacterial activity was evaluated using Kirby-Bauer method against pathogenic bacteria of *Salmonella enterica* and *Escherichia coli*. The extract was then used to disinfect raw chicken meat that was exposed for 90 minutes at normal room temperature. The enumeration of bacteria using pour plate method was done every 30 minutes. The findings revealed that the average inhibition zone of fresh *Z. officinale* aqueous extract was 6.8 mm and 6.0 mm against *E. coli* and *S. enteric,* respectively, while the average inhibition zone of dried *Z. officinale* aqueous extract was 12.2 mm and 11.5 mm, respectively. The enumeration of bacteria on raw chicken meat after application of the extract at the 60th minute was 176 CFU/g (fresh extract) and 90 CFU/g (dried extract) compared to untreated raw chicken meat that was 2010 CFU/g. This showed that the highest antibacterial property and natural preservative potential was the dried *Z. officinale* aqueous extract.

KEY WORDS:
Zingiber officinale, Ginger, Antibacterial, Natural preservative

INTRODUCTION:

Spices and aromatic vegetables have been used as a preservative, medicinal and also in culinary for centuries and one of the most well-known aromatic vegetables is *Zingiber officinale* Roscoe. [(1)] *Zingiber officinale* belongs to the Zingiberaceae family [(2)] and has a natural medicinal property in its rhizomes, which is known as gingerol. [(3)] It has also been reported to have antioxidant, anti-inflammatory, antibacterial, antidiabetic and other therapeutic agents.[(4) (5) (6)]

Chicken meat is primarily referring to the carcass or boned out the meat of the *Gallus gallus* species.[(7)] Exposure of raw meat to the environment may cause contamination, especially in the market. Microorganisms are usually found on the skin, feathers or alimentary tract of animals. However, contamination by pathogenic microorganism may happen during the slaughtering process, storage or delivery, and also due to unhygienic handling.[(7) (8)] Contamination of pathogenic microorganisms in poultry may not only cause infection and disease in human but also cause malodour of meat that decreases marketable values. There are also reports on the prevalence of *Escherichia coli* on contaminated poultry [(8-10)] but one of the most prominent pathogenic bacterial infections in poultry is *Salmonella spp*.

Current preservation methods include chilling, freezing and using chemicals such as trisodium phosphate (TSP) as well as applying irradiation on raw, fresh or frozen packaged poultry [(8) (11).] TSP is an antimicrobial agent approved by FDA and 'generally recognised as safe'. [(11)] Whereas the change of temperature may affect the texture, quality and taste of the meat. Thus, without preservation, the raw meat will deteriorate in normal room temperature, which would shorten the shelf life, reduce profit and endanger consumers' health. The reported phytochemical screening and therapeutic claims of *Z. officinale* are tremendous. Therefore, it was suggested that the rhizome of *Z. officinale* would be used as an alternative natural preservative.

The objective of this study is to evaluate the potential of *Z. officinale* as a natural preservative. Antimicrobial property is generally associated with food preservation as inhibition of microbial growth will consequently prolong the shelf life of food. In this study, aqueous extract was utilised as its preparation is simple, safe and economical. The application of extract was also evaluated on fresh raw chicken meat. Hence, this study was expected to provide an alternative natural method of preservation on raw chicken meat.

MATERIALS AND METHODS:

Sample Collection & Preparation

The *Z. officinale* rhizome was initially bought from a local market and the rhizome was then planted where the rhizome was soaked overnight and cut according to bud protrusion. [12] It was planted approximately 5 cm deep with the growing buds facing upwards and harvested after three months.[13] The whole rhizome was cleaned and washed with water. The dried rhizome of *Z. officinale* was shaded sundried until a constant weight was achieved. Then, it was blended into a fine powder and kept in an airtight bottle until further analysis. [1] The fresh *Z. officinale* tuber was used directly for fresh extract preparation.

Sample Extraction

The fresh *Z. officinale* rhizome extract was prepared by blending 30g of fresh rhizome with 100ml of distilled water.[14] Then, it was filtered and centrifuged at 10 000 rpm to remove any residue, ensuring the final concentration of the crude extract as 300 mg/ml. In contrast, the aqueous extract of dried *Z. officinale* rhizome was prepared by macerating the dried rhizome in aqueous (1:10) in normal room temperature for 72 hours with constant shaking at 120 rpm. After evaporation, the crude extract was dissolved in sterile distilled water to a final concentration of 100 mg/ml and centrifuged at 10 000 rpm to remove any residue.

Microbiological analyses

(i) Kirby-Bauer disc diffusion assay [15]

The in-vitro antibacterial assay was performed by disc diffusion method using the fresh and dried extract of *Z. officinale* against *Escherichia coli* ATCC11229 and *Salmonella enterica* ATCC14028. Where the sterile paper discs of 6 mm diameter were impregnated with 5 µl of concentrated extract of *Z. officinale.* A 30mg disc of Nalidixic acid was used as positive control and a blank disc as the negative control. All assays were done in tri-replicates, and the inoculated agar plates were then incubated at 37˚C for 18 hours.

(ii) Determination of minimum inhibitory concentration (MIC)

The microdilution broth evaluation was done as described in [16]. Two-fold serial microdilution of 100 µl of antimicrobial agents with Mueller-Hinton broth was prepared in 10 batches. Then, each well was inoculated with 100 µl standardized suspension of *E. coli* and *S. enterica*. The final concentration of the antimicrobial agent was half of the initial concentration. The microtiter plate was incubated for 24 hours at 37°C. After incubation, the cloudy formation observed indicated the ineffective concentration to inhibit the bacterial growth. Hence, after the turbidity formation observed, the first clear well indicated the lowest dilution effective to inhibit the bacterial growth.

(iii) Determination of minimum bactericidal concentration (MBC)

The minimal bactericidal concentration was determined by transferring 100 µl of first two visible wells and the last two non-visible wells from the previous MIC evaluation on a sterile agar plate. The plates were then observed for any bacterial growth after being incubated at 37°C for 24 hours. Clear agar cultures indicated the lowermost concentration killed the bacteria. [16]

(iv) Evaluation of *Z. officinale* extracts as a disinfecting agent

The raw chicken meat was purchased from the local supermarket and divided equally into nine parts weighing 10 g each. The meat was then placed in a sterile petri dish and treated with the *Z. officinale* extracts. The concentration used was according to the MBC results and incubation time was 90 minutes at

normal room temperature. The enumeration of bacteria on the raw chicken meat was targeted on gram-negative bacteria only and was done using the pour plate method every 30 minutes. Serial dilution was performed from 1 g of the chicken meat for a 10^{-2} dilution. [17] The inoculation was done on MacConkey agar and incubated at 35°C for 24 hours. [18]

RESULTS AND DISCUSSION:

After the drying process, it was calculated that the moisture content of *Z. officinale* was 94.17%, in accordance with reports by other studies of approximate 90% moisture loss. [3] [19] Accordingly, the loss of distinctive ginger aroma was also detected as the rhizome was dehydrated.

The agar disc diffusion evaluation is a common method to test potential antimicrobial agents. By controlling the growth of bacteria, food spoilage could be slowed down, thus producing a natural preservative. Disc diffusion assay is common for antibacterial evaluation. The parameter used is the zone of inhibition by the impregnated disc that was placed on an agar bacterial culture. The susceptibility of microorganisms against antimicrobial agents is categorised into resistant for weak agents (inhibition zone ≤11mm), intermediate for stronger agents (inhibition zone between 12 to 14 mm) and susceptible for strongest antimicrobial agents (inhibition zone ≥15mm). [20]

Table 1 shows the average diameter of the inhibition zone of fresh and dried *Z. officinale* aqueous extracts against *S. enterica* and *E. coli*. In this investigation, both dried and fresh aqueous extracts showed antibacterial properties. However, the antibacterial activity of the fresh extract was categorised as resistant to both *S. enterica* and *E. coli*. Meanwhile, the dried aqueous extract was resistant towards *S. enterica* and intermediate against *E. coli*. This result suggested that the dried extract was more potent compared to the fresh extract. The drying process might contribute to the increased bioactivity as it was reported that dehydration could cause a significant increase in the total phenolic compound. [5] The extract might also have different effects on different organisms as investigators had also observed that sensitivity of microorganisms towards antimicrobial agents that differed based on the types of strain. [21]

Table 1
Antibacterial activity of fresh and dried aqueous extracts of *Z. officinale*

Extract	Diameter of inhibition Zone (mm)	
	Salmonella enterica ATCC 14028	*Escherichia coli* ATCC 11229
Fresh *Z. officinale*	6.0±1.50 (Resistant)	6.8±0.76 (Resistant)
Dried *Z. officinale*	11.5±0.50 (Resistant)	12.2±0.29 (Intermediate)
Nalidixic acid	24.7±0.58 (Susceptible)	25.0±1.00 (Susceptible)
Blank disc	0.0	0.0

The two-fold serial dilution of fresh and dried *Z. officinale* aqueous extract had resulted in eight different concentrations ranging from 300 mg/ml to 2.34 mg/ml for fresh extract and 150 mg/ml to 1.17 mg/ml for dried extract. By referring to Table 2, it is evident that the lowest concentration effective to inhibit both *E. coli* and *S. enterica* was 75 mg/ml for fresh extract and 12.50 mg/ml for dried extract. Therefore, it is evident that dried *Z. officinale* aqueous extract was more effective as smaller concentration was needed to suppress the growth of bacteria. This might be due to the oxidation of chemicals during the dehydration process which caused it to exhibit higher antibacterial activity. (6)

Table 2
MIC of fresh and dried aqueous extract of *Z. officinale*

	Minimal Inhibitory Concentration (mg/ml)	
Extract	*S. enterica*	*E. coli*
Fresh *Z. officinale*	75.0	75.0
Dried *Z. officinale*	12.5	12.5

The minimal bactericidal concentration (MBC) was determined by the minimum inhibition concentration results. The MBC was performed by culturing the last two invincible growth in the microtiter plate on McConkey agar. The absence of bacterial growth indicated that the particular concentration was sufficient as bactericidal agent and vice versa. The results showed that the MBC of the fresh extract was 150 mg/ml, where the concentration was higher than the MIC, while the MBC for the dried extract was 25 mg/ml which was also higher than the MIC. Therefore, the fresh and dried *Z. officinale* aqueous extract exhibited a bactericidal effect at concentration one dilution factor higher than the minimum inhibition concentration.

Table 3
MBC of fresh and dried aqueous extract of *Z. officinale*

	Minimal Bactericidal Concentration (mg/ml)	
Extract	*S. enterica*	*E. coli*
Fresh *Z. officinale*	150.0	150.0
Dried *Z. officinale*	25.0	25.0

The contamination of pathogenic microorganisms often happens during the production process, storage or poor hygiene management. (7) (22) The potential of fresh and dried aqueous extract of *Z. officinale* to control the growth of microorganisms on raw chicken meat was evaluated to determine their potential as a natural preservative. The number of gram-negative bacteria on raw chicken meat was determined using the MacConkey pour plate method. Disinfection using *Z. officinale* extract was static and the enumeration of gram-negative bacteria was done every 30 minutes for 90 minutes.

Table 3.4 shows that the prevalence gram-negative on raw chicken meat treated with fresh and dried *Z. officinale* aqueous extract and compared to untreated chicken meat which was used as the control. The classification of the quality of raw chicken meat was conducted. (23) The incubation of raw chicken meat was also done at normal room temperature at 28°C±1.

It could be seen that the initial number of bacteria was approximately similar and as soon as the raw chicken meat was treated with the extracts, the prevalence of bacteria decreased significantly. Compared to untreated chicken meat, the prevalence of bacteria increased with time of exposure and classified as borderline. In contrast, raw chicken meat treated with fresh *Z. officinale* extract showed a decrease of 87% in the bacterial prevalence, though the number increased after the 90th minute, indicating the reduction of antimicrobial activity. Although the number of bacterial prevalence increased after the 90th minute to 176 CFU/g, it remained low compared to untreated chicken meat (2470 CFU/g) which also considered as unsatisfactory for human consumption.

Table 4
Prevalence of gram negative bacteria on raw chicken meat

Extract	Time (minute)	Average colony counts (CFU/g)	Quality (Microbiological Guidelines for Food, 2014)
Treated with fresh *Z. officinale*	0	650	Borderline
	30	136	Borderline
	60	176	Borderline
	90	363	Borderline
Treated with dried *Z. officinale*	0	700	Borderline
	30	113	Borderline
	60	90	Borderline
	90	556	Borderline
Untreated raw chicken meat	0	700	Borderline
	30	1570	Unsatisfactory
	60	2010	Unsatisfactory
	90	2470	Unsatisfactory

The dried *Z. officinale* extract showed improved preservation activity as the prevalence of bacteria decrease 84% in the 30th minute and continued to decrease to 87% in the 60th minute. However, the prevalence of bacteria was increased to 556 CFU/g on the 90th minute, indicating the loss of antimicrobial and preservation capability. Similar to sample treated with fresh extract, the prevalence of bacteria remained low compared to untreated raw chicken meat. The concentration of extract might be affected by the moisture content in raw chicken meat. The changes of concentration might affect the effectiveness of the *Z. officinale* aqueous extract. [24]

The result has confirmed the ability of fresh and dried *Z. officinal* aqueous extract to preserve the freshness of raw chicken meat exhibited by controlling the growth of bacteria. It is suggested that the dried *Z. officinal* aqueous extract has the best preservation potential as it has the potential to lower the prevalence of bacteria in prolong time. This will also prolong the freshness of raw chicken meat in normal room temperature.

Table 5
Classification of microbiology quality

Classification	Definition
Satisfactory	Indicating good microbiological quality
Borderline	Indicating unsatisfactory but are also not satisfactory. This is the upper limit of acceptability and which indicate the potential for development of public health problems and of unacceptable risk.
Unsatisfactory	Indicate the food is potentially injurious to health and unfit for human consumption.

(Source: Microbiological Guidelines for Food, 2014)

CONCLUSION:

The fresh and dried aqueous extracts of *Zingiber officinale* are established to have antibacterial properties. However, the fresh extract is considered as weak agent and the dried *Z. officinale* aqueous extract is considered as an intermediate agent against *Salmonella enterica* and *Escherichia coli* respectively. The fresh *Z. officinale* aqueous extract has a bacteriostatic ability at 75 mg/ml and bactericidal ability at 150 mg/ml,

while the dried *Z. officinale* aqueous extract has a bacteriostatic ability at 12.5 mg/ml and a bactericidal capability at 50 mg/ml. Both fresh and dried extracts are still considered to have shown their potential as natural preservatives for raw chicken meat, even though the dried *Z. officinale* aqueous extract is suggested to have higher potential at 50 mg/ml. However, further studies are needed to evaluate its efficacy and to apply non-static treatment.

REFERENCES:

1. Sethi S, Ddutta A, Gupta LB, Gupta S. Antimicrobial Activity of Spices against Isolated Food Borne Pathogens: Determination of Minimal Inhibitory Concentration (MIC). International Journal of Pharmacy and Pharmaceutical Sciences. 2013;5(1).
2. System ITI. Zingiber officinale Roscoe 2015 [Available from http://www.itis.gov.
3. Azian MN, Ilia Anisa AN, Iwai Y. Mechanisms of ginger bioactive compounds extract using soxhlet and accelerated water extraction. International Journal of Chemical, Materials Science and Engineering. 2014;8(5):409-13.
4. Al-Nahain A, Jahan R, Rahmatullah M. Zingiber officinale: A Potential Plant against Rheumatoid Arthritis. Arthritis. 2014;2014:159089.
5. Kikuzaki H, Nakatani N. Antioxidant Effects of Some Ginger Constituents. Journal of Food Science. 1993;58(6):1407-10.
6. Puengphian C, Sirichote A. [6]-gingerol content and bioactive properties of ginger (Zingiber officinale Roscoe) extracts from supercritical CO2 extraction. Asian Journal of Food and Agro-Industry. 2008;1(1):29-36.
7. Bhaisare DB, Thyagarajan D, Churchil RR, Punniamurthy N. Bacterial Pathogens in Chicken Meat: Review. International Journal of Life Sciences Research 2014;2(3):1-7.
8. Mead GC. Microbiological quality of poultry meat: a review. Brazilian Journal of Poultry Science. 2004;6(3):135-42.
9. Moussa A, Saad A., Noureddine D, Aboud B, Meslem A, Baghdad K. The influence of starch ginger on the antibacterial activity of honey different types from Algeria against Escherichia coli and Staphylococcus aureus. International Journal of Microbiological Research. 2011;2(3):258-62.
10. Von V, Pichpol D. Experimental Reduction of Salmonella in Raw Chicken Breasts. Berlin: Freie Universität Berlin; 2009.
11. Agriculture USDo. Chicken from Farm to Table 2014 [cited 2016 8 November]. Available from: Retrieved from https://www.fsis.usda.gov.
12. Allen J. Garlic production. : Ontario Ministry of Agriculture, Food and Rural Affairs.; 2009 Available from http://www.omafra.gov.on.ca/english/crops/facts/09-011w.htm.
13. Bradtke B. Growing ginger root. 2010 [Available from: Retrieved from http://www.tropicalpermaculture.com/growing-ginger.html.
14. Ghalehkandi JG. Garlic (Allium sativum) juice protects from semen oxidative stress in male rates exposed to chromium chloride. Animal Reproduction. 2014;11(4):526-32.
15. Kirby-Bauer A. Antimicrobial sensitivity testing by agar diffusion method. Journal of Clinical Pathology. 1996;44(4):93.
16. Kowser MM, Fatema N. Determination of MIC and MBC of selected azithromycin capsule commercially available in Bangladesh. The ORION Medicinal Journal. 2009;32(1):619-20.
17. Frankhauser DB. Bacterial contamination of meat: pour plate assay. 2008.
18. Black J. Microbiology. 7 ed. Arlington, Virginia: John Wiley and Sons Inc.; 2008.
19. Goncagul G, Ayaz E. Antimicrobial effect of garlic (allium sativum) and traditional medicine: medical properties of garlic. Journal of Animal and Veterinary Advances. 2010;9(1):1-4.
20. Standards. NCfCL. Performance Standards for Antimicrobial Disk Susceptibility. 2012;32(1): M02-A11.
21. Voelz A, Muller A, Gillen J, Le C, Dresbach T, Engelhart S, et al. Outbreaks of Serratia marcescens in neonatal and pediatric intensive care units: clinical aspects, risk factors and management. Int J Hyg Environ Health. 2010;213(2):79-87.

22. Yusoff NH, Noor NF, Rukyadi Y. Effects of Cosmos caudatus Kunth. (ulam raja) extract on microflora in raw chicken meat. International Journal of Current Microbiology and Applied Sciences. 2015;4(2):426-35.
23. Food MGf. For ready-to-eat food in general and specific food items. 2014.
24. Ogbonna AI, Tanko JS, Falemara BC, Itelima JU, Makut MD, Onyimba I, et al. Studies on the effects of Zingiber officinale Roscoe (Ginger) aqueous and ethanolic extracts on some fungal and bacterial species. IOSR Journal of Pharmacy and Biological Sciences. 2014;9(5):16-23.

FP-11

BIODEGRADATION OF DIESEL OIL IN SHAKE FLASK SYSTEM USING FOOD WASTE AMENDMENTS

CHEAH JIN MIN[1], NORAZNAWATI ISMAIL[2], FAZILAH ARIFFIN[1*]

[1]School of Fundamental Science, Universiti Malaysia Terengganu, 21030 Kuala Nerus, Terengganu,
[2]Insitute of Marine Biotechnology, Universiti Malaysia Terengganu, 21030 Kuala Nerus, Terengganu

[*]Corresponding author: fazilah@umt.edu.my

ABSTRACT

Soil contamination by pollutants such as hydrocarbons has gained increasing public concern due to their hazardous nature to human health and the environment. Bioremediation is one of the alternative green technologies created to remediate this problem. The aims of this study were to determine the diesel oil degradation activity by soil bacteria amended with food wastes in the liquid system and to investigate the potential use of food wastes such as banana skin and chicken bone for enhanced biodegradation of diesel oil. Diesel oil that was amended with sterile banana skin or chicken bone was inoculated with hydrocarbon-contaminated soil and incubated for 5 weeks at 30°C, 150 rpm. Bacteria from the enrichment culture flasks were isolated and identified based on colony morphology and biochemical test using BBL Crystal Identification Kit. Hydrocarbon degradation was analyzed using gas chromatography - mass spectrometry (GC-MS). We found that the degradation rates of diesel oil compounds were higher in the flasks amended with food wastes as compared to the flask unamended with food wastes. A total of 4 diesel compounds which were decane, heptasiloxane hexadecamethyl, 3-cyclopetadiene, 1, 2, 3, 4-tetramethyl-5-methylene and cyclononasiloxane octadecamethyl showed the degradation rates of 13.7%, 22.34%, 74.27% and 61.98% respectively in the liquid system containing diesel oil and amended with banana skin. In comparison, these same 4 compounds were only degraded 24.67%, 30.18%, 50.52% and 65.29% in the liquid system containing diesel oil and amended with chicken bone after 5 weeks of incubation, respectively. A total of 5 hydrocarbon-degrading bacteria were successfully isolated and identified as *Acinetobacter baumannii, Pseudomonas aeruginosa, Stenotrophomonas maltophilia, Brevibacillus brevis* and *Bacillus cereus*. The results of this study demonstrated the potential use of food wastes for enhancing the bioremediation of diesel-contaminated soil.

KEYWORDS:
Diesel oil, Food waste, Degradation, Hydrocarbon-degrading bacteria

INTRODUCTION:

In recent decades, contamination of soil by polycyclic aromatic hydrocarbons (PAH) has become an important issue. PAHs are organic compounds containing only carbon and hydrogen atoms with a structure of two or more aromatic fused rings.[1] PAHs have widespread occurrence in various ecosystems which enable them to persist in the environment.[2] Due to its toxic, mutagenic and carcinogenic properties, prolonged exposure to high concentrations of PAHs can cause acute and chronic health problems.[3]

One of the techniques created to remediate PAH contamination is bioremediation. It is widely used to remove PAHs from the environment since it is cost effective and environmentally friendly as compared to other conventional methods. This technique involves the conversion of toxic chemical substances to less harmful substances by biological means such as through microbial activity.[4] Microorganisms such as bacteria and fungi are widely used in this approach due to their ability to degrade pollutants. However, the

degradation rate of microorganisms is influenced by various environmental factors such as temperature, pH and nutrient availability. Thus, bio stimulation which is defined as the addition of essential nutrients to enhance the bioremediation process by stimulating the bacterial growth can be used to improve the degradation rate.[5] The nutrients can be introduced in the form of organic nutrients such as food wastes and inorganic forms such as fertilizer.

The objectives of this study were to determine the PAH degradation activity by soil bacteria amended with food wastes in a liquid system. Furthermore, this study also aimed to investigate the potential of food wastes which were banana skin and chicken bone for enhanced biodegradation of PAH. Through this study, the function of food waste can be investigated so that they can be utilized and thus can reduce the impact of PAHs and food waste to the environment.

MATERIALS AND METHODS:

Sample collection

The soil sample was collected from a motorcycle service center at Jalan Pantai, 21300 Kuala Terengganu, Terengganu, Malaysia (N 5°24'48.732", E 103°6'9.7488"). One cm of the soil was first removed from the surface and discarded while the targeted soil was obtained by digging 10 cm into the soil. The temperature and pH of the soil were measured. Diesel oil was purchased from a Petron™ petrol station in Kuala Terengganu. Meanwhile, food wastes such as banana skins (BS) were collected from a banana fritters stall in Taman Bestari, Kuala Terengganu whereas the chicken bones (CB) were collected from the canteen of University Malaysia Terengganu (UMT). The food wastes were washed and dried at 90˚C for 6 hours. They were then finely ground with blender or mortar and pestle to become a powder and then autoclaved.

Enrichment Culture Set-up Description

For the enrichment culture (EC), two sets of Erlenmeyer flasks labelled A to C and A1 to C1 were prepared. Each flask was filled with 22.5 g of soil sample and 15 ml of diesel oil. Then, flasks C and C1 were filled with 112.5 ml of mineral salt medium (MSM) whereas the other flasks were filled with 105 ml of MSM. MSM consisted of the following composition: 0.2 g of $MgSO_4$, 0.02 g of $CaCl_2$, 1.0 g of KH_2PO_4, 1.0 g of K_2HPO_4, 1.0 g of NH_4NO_3 and 0.05 g $FeCl_3$.[6] The flasks were then left undisturbed for 2 days. After 2 days, 7.5 g of BS powder were added into flasks A and A1 while the same amount of CB powder was added into flasks B and B1. Flasks C and C1 served as control.

Sampling of the Biodegradation Activity

Periodic sampling from each flask of the EC was carried out at 7 day intervals for 42 days for the determination of total PAH in the liquid system. The PAH-degrading bacteria were also isolated, enumerated and identified.

PAH Extraction

The PAH in the liquid system was extracted by using a mechanical shaking method. Twenty g of EC in the liquid system was collected from each flask and transferred into 250 ml Erlenmeyer flasks. The EC was suspended with hexane in 1:1 ratio and sealed with aluminium foil to prevent the hexane from evaporating. The flasks were then shaken on the orbital shaker at room temperature for 1 hour.[6] The liquid mixtures were then centrifuged at 150 rpm for 5 minutes 7. Then, the resultant supernatants were transferred to the separation funnel and hexane was added in a 1:1 ratio.[7] The funnel was shaken gently to thoroughly mix the supernatant and hexane and left to stand for 10 minutes to allow the completion of the separation phase. The lower phase was then removed and the upper phase was evaporated to a final volume of 5 ml at 40° C by rotary evaporator. The extracts obtained were stored at 4°C until further analysis.

PAH degradation analysis using Gas Chromatography-Mass Spectrometry (GC-MS)

The extracted samples were diluted into 1 ppm by using the serial dilution method. The diluted samples were then filtered using 0.45µm PTFE membrane filter before being injected into the GC-MS (QP2010 ultra). The analysis conditions for the GC-MS are shown in Table 1.

Table 1

Analysis conditions of general hexane column

GC-MS	GCMS-QP2010 ultra
[GC]	
Column	Rtx-5MS 0.25 x 30 m df=0.25 µm
Inlet mode	Splitless
Column oven temperature	50℃ (1min) →300℃ (5min)
Carrier gas	Helium
Control mode	Constant linear velocity 35.5cm/sec
High pressure injection	150kPa (1.00min)
Purge flow rate	3.0 mL/min
Injection rate	1ul
[MS]	
Interface temperature	300℃
Ion source temperature	200℃
Data sampling time	1.00min
Measurement mode	Scan
Mass range	m/z 50-600
Event time	0.05sec

The concentration of compounds in the sample solution was calculate by using the formula.[8]

$$\text{Concentration of Cn in sample solution} = \frac{PA}{PA'} \; x \; \frac{Final\ volume\ of\ standard}{weight\ of\ analysed\ sample}$$

Where:

PA= Peak area of C_n in sample solution

PA'= Peak area of C_n in standard solution

Then, the degradation rate of the compound was calculated by using the modified formula.[8]

$$Rd = \frac{D1 - D5}{D1} \text{ x } 100\%$$

Where:

Rd= Diesel oil degradation rate

D1= Diesel-oil hydrocarbon concentration in Week 1

D5= Diesel-oil hydrocarbon concentration in Week 5

Enumeration of bacteria

EC was collected every 7 days for the enumeration of bacteria. The EC was serially diluted and 0.1 ml of diluted sample was transferred to nutrient agar (NA) plates using the spread plate method. The CFU/ml of sample was calculated by the formula below:

$$\text{Total number of bacteria} = \frac{\text{Number of Colonies}}{(\text{Dilution Factor}) \text{ X } (\text{Amount Volume Plated})}$$

Identification of bacteria

The diluted samples were transferred to oil agar (OA) using the spread plate method and incubated at 30˚C for 24 hours. The bacteria colonies with the clear clearing zones on OA were isolated and subculturled on the nutrient agar. Further sub-culturing of bacteria was conducted until pure isolates were obtained. The isolated bacterium was identified by using Gram staining technique and the cell morphology of bacterium were recorded. The bacteria species was further identified by using BBL Crystal Identification Kit (Fisher Scientific, USA) as per the manufacturer's instructions. The single pure bacteria colony was suspended in a BBL Crystal Inoculum Fluid Tube. The tube was shook shaken gently and the inoculum was poured into the target area of the base. The inoculum was rolled gently along the tracks until all of the wells were filled. The panel was closed with the lid and incubated at 37˚C for 24 hours. After the period of incubation, the panel was read using BBL Crystal Panel Viewer and identified using BBL Crystal MIND.

RESULTS AND DISCUSSION:

Sample collection

The soil sample was collected from a motorcycle service centre at Jalan Pantai, 21300 Kuala Terengganu, Terengganu, Malaysia (N 5°24'48.732", E 103°6'9.7488"). The temperature and pH value of the soil sample were recorded in Table 2.

Table 2

Temperature and pH value of the soil sample

Sample	Temperature	pH
Soil	29˚C	6.91

Effect of bacteria growth in the enrichment culture amended with food wastes

Figure 1 shows the bacterial cell count in the flask system containing banana skin (BS) and chicken bone (CB) after 5 weeks of cultivation. The results showed that the bacteria cell count in the flask amended with BS slightly increased from 1.18 x 10^{11} CFU/mL to 1.29 x 10^{11} CFU/mL at the first 3 weeks of cultivation. However, after week 5, it decreased to 6.46 x 10^{10} CFU/mL. Meanwhile, the bacteria cell count in flask containing CB after 5 weeks of cultivation slightly increased from 1.29 x 10^{11} CFU/mL to 1.41 x 10^{11} CFU/mL at the first 3 weeks of cultivation. Nonetheless, it dropped to 5.89 x 10^{10} CFU/mL after week 5. In comparison, the results showed that the bacteria cell count of the unamended flask was lower than the flasks amended with food wastes. The bacteria cell count in the unamended flask increased gradually from 1.10 x 10^{11} CFU/mL to 1.32 x 10^{11} CFU/mL at the first 3 weeks of cultivation but decreased to 2.04 x 10^{10} CFU/mL after week 5.

The results indicated that the nutrient enhancement provided by food wastes can stimulate and increases cell growth, which agrees with similar observation by previous researches.[9] The higher viable cell count in the flask amended with BS was due to the high nutrient content in banana skin such as nitrogen, potassium, calcium and phosphorus which are important nutrients that can enhance the bacterial growth.[9] Moreover, researches also proved that chicken bone contains high calcium and phosphorus content which can stimulate the growth of bacteria [11]. However, the viable cell count of all flasks amended with BS and CB decreased after week 3 which was due to the accumulation of toxic material and exhaustion of oxygen in the medium resulting in bacterial death [12]. In addition, similar results were also reported in previous studies where the depletion in nutrients towards the end of the experiment reduced the microbial activities and resulted in the reduction of the viable cell count.[13]

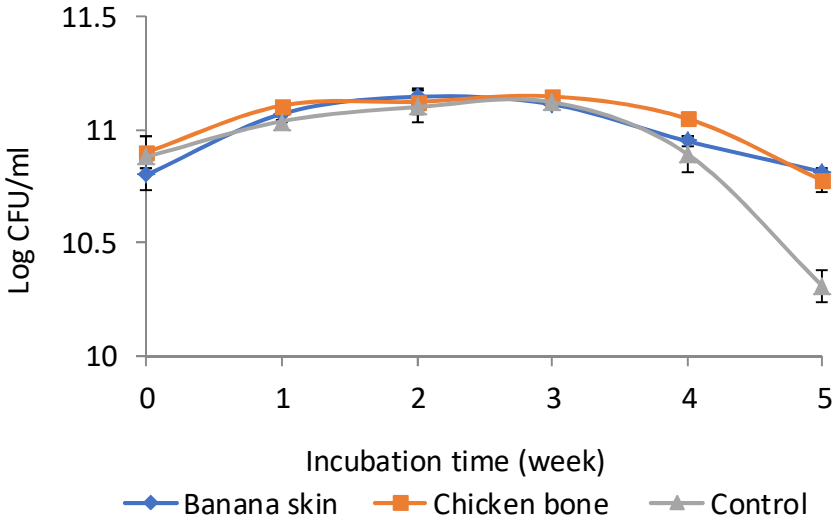

Figure 1

Profile of bacterial cell count (CFU/mL) in flask system containing banana skin and chicken bone after 5 weeks of cultivation

pH changes in the flasks system after 5 weeks of cultivation

Figure 2 shows that the pH of all flasks remained constant between pH 6.5 to 7.0 at the first 4 weeks of cultivation. However, all of the flasks became acidic after week 4 of cultivation as the pH dropped significantly from pH 7 to 4. The reduction of pH is due to the production of acidic by-products and metabolites such as organic acids, carbon dioxide, and ketones during the degradation of diesel by bacteria.14 In addition, the reduction of pH is also caused by cell lysis as cells became old and die at the end of the study. Furthermore, the accumulation of acidic by-products indicates that the bacteria in the soil samples were capable of degradation diesel-oil.

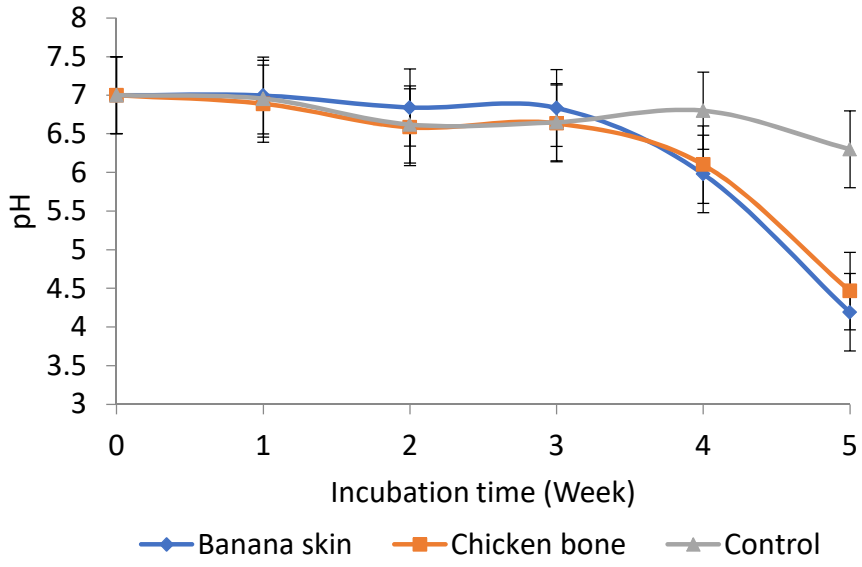

Figure 2

Profile of pH value in flask system containing banana skin and chicken bone after 5 weeks of cultivation

Identification of bacteria isolated from soil sample

A total of 5 isolates bacterial cultures were isolated from the soil sample flask system and identified using the BBL Crystal Identical System. The isolates bacteria were grown on nutrient agar and the physiological characteristics of the isolates were recorded in Table 2. It showed that 3Three isolates were Gram-negative

bacteria whereas 2 isolates were Gram-positive bacteria. Table 3 shows the identification of the 5 bacterial isolates based on BBL Crystal Identification System Kit. These identification kits system determined the reaction of the test strains to a total of 32 biochemical tests. All isolates were tested using the Enteric/ Non-fermenter test kits and Gram-positive ID kits. The five bacteria isolates tested were showed high confidence factors which were above 0.95 and identified as *Acinetobacter Baumannii, Pseudomonas aeruginosa, Stenotrophomonas maltophilia, Brevibacillus brevis* and *Bacillus cereus.*

Previous researches have proposed reported that these types of bacteria can be found in Malaysian soil and water and have been shown to be good oil decomposers which and exhibit excellent oil degradation properties.15 The physical characteristics showed by Isolate 1 was similar to the characteristic of *A. baumannii* which have been reported by previous researches.[16] *A. baumannii* are ubiquitously found in natural such as in the soil and a study showed that it was able to degrade 58.1% of diesel oil alkanes and being suggested as a hydrocarbon-degrading bacteria with the potential for bioremediation of oil-polluted marine environments.[16] Meanwhile, Isolate 2 was identified as *P. aeruginosa* as which it is commonly found in environment mainly in the soil and had exhibited similar characteristics such as pigmentation when grown on nutrient agar.[17]

Table 2
Physiological characteristics of isolated bacteria from enrichment culture

Characteristic	Isolate 1	Isolate 2	Isolate 3	Isolate 4	Isolate 5
Form	Circular	Circular	Circular	Circular	Circular
Pigmentation	White	Orange	White	White	White
Elevation	Raised	Raised	Convex	Raised	Flat
Margin	Entire	Undulate	Entire	Entire	Undulate
Gram Stain	-	-	-	+	+
Cell morphology	Coccus	Bacillus	Bacillus	Bacillus	Bacillus

A previous research also revealed found that *P. aeruginosa* carried out a high percentage of diesel degradation (66%) after 30 days of incubation in diesel- contaminated soil.[15] Moreover, Isolate 3 showed the same growth characteristics as *S. maltophilia* which had been proved by previous studies.[18] *S. maltophilia* has been proved with the had proven ability to degrade petroleum hydrocarbon-rich industrial wastewaters for hydrocarbons range n-alkanes with an efficiency rate of more than 70%.[19] In addition Isolate 4 was identified as, *B. brevis* which has also been characterized as a petroleum hydrocarbon- degrading microbe as reported by a study proved that it previous study where it showed high degradation of diesel of about 96.8%.20 Finally, Isolate 5 was identified as *B. cereus.* This bacterium is distributed widely in soil and is able to adapt in a wide range of environmental conditions. A previous research also showed that *B. cereus* is a good diesel degrader as it was able to degrade approximately 80% of diesel oil after 28 days of incubation in diesel contaminated medium.[21]

Table 3
Identification of bacterial isolates using BBL Crystal Identification Kit

Isolate	Bacteria species	Confidence Factor
1	*Acinetobacter baumannii*	0.9999
2	*Pseudomonas aeruginosa*	0.9625
3	*Stenotrophomonas maltophilia*	0.9999
4	*Brevibacillus brevis*	0.9999
5	*Bacillus cereus*	0.9999

Degradation analysis of diesel-oil compounds by soil bacteria in flask system amended with food wastes

Figure 3 shows the degradation rates of diesel-oil compounds by soil bacteria in all flasks. A total of 4 compounds were analyzed which were decane ($C_{10}H_{22}$), heptasiloxane, hexadecamethyl ($C_{16}H_{48}O_6Si_7$), 1,3-cyclopetadiene,1,2,3,4-tetramethyl-5-methylene ($C_{10}H_{14}$) and cyclononasiloxane,octadecamethyl

($C_{18}H_{54}O_9Si_9$). The results showed that the concentration of all of these compounds decreased and this indicates that the bacteria in the soil sample were able to degrade diesel oil. Moreover, Figure 3 shows that both the flasks amended with food wastes had higher diesel oil degradation rates as compared to the flask unamended with food waste after 5 weeks.

In this study, all bacteria isolated from the flask system are capable of degrading diesel as the results showed decreasing concentrations of diesel oil compounds. This is evidence of the bacteria utilizing the diesel oil as a source of carbon and energy for growth. Moreover, the degradation rates of diesel compounds in the control flask were lowest as shown in Figure 3 where only 44.4% of $C_{18}H_{54}O_9Si9$, 22.44% of $C_{10}H_{14}$, 10.29% $C_{16}H_{48}O_6Si_7$ and only 5.31% of $C_{10}H_{22}$ were degraded after 5 weeks of cultivation. This may due to the environmental factors such as insufficient of nutrients, pH, and temperature that limited the degradation process of diesel by bacteria.[9] Meanwhile, the flask amended with BS showed higher degradation rate of diesel oil compounds compared to the control flask. It showed the highest degradation of $C_{10}H_{14}$ (74.27%) followed by $C_{18}H_{54}O_9Si_9$ (61.98%), $C_{16}H_{48}O_6Si_7$ (22.34%) and $C_{10}H_{22}$ (13.70%). This result is in agreement with previous studies that reported the effectiveness of food wastes such as banana skin in stimulating the degradation of hydrocarbon by hydrocarbon degraders.[22] Furthermore, researches proved that banana skin can provide phosphorus and nitrogen to bacteria which stimulate their growth and eventually enhance the degradation process.[5] Figure 3 also showed that the flask amended with CB had higher degradation rates of diesel oil compunds as compared to the control flask. It degraded 65.29% of $C_{18}H_{54}O_9Si_9$, 50.52% of $C_{10}H_{14}$, 30.18% of $C_{16}H_{48}O_6Si_7$, and 24.67% of $C_{10}H_{22}$ after 5 weeks of cultivation. This is because chicken bone contains potassium and calcium which are vital nutrients for bacterial growth. From the result, the degradation rate of decane was the lowest as compared to other compounds. This result was in agreement with a previous study which showed that decane was less degraded (10%) by bacteria over 10 days of cultivation.[16] The low degradation of decane may due to the incomplete degradation of short-chain alkanes that was caused by limited dissolved oxygen and substrate toxicity.[15] However, the reduction of diesel oil compounds may not only be due to the degradation process induced by nutrient addition but also by other abiotic processes such as volatilization and adsorption to organic compounds.

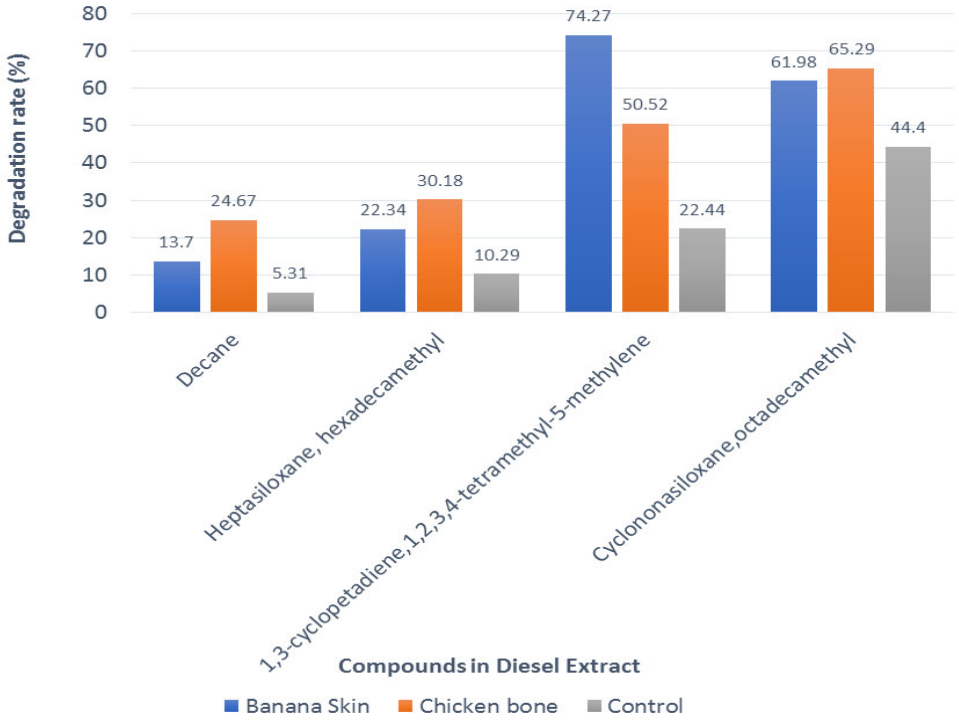

Figure 3

Degradation analysis of diesel-oil compounds by soil bacteria in the sample after 5 weeks cultivation at 30˚C

CONCLUSION:

In conclusion, a total of five bacterial species were isolated and preliminarily identified as *Acinetobacter baumanni, Pseudomonas aeruginosa, Strenotrophomonas maltophilia, Brevibacillus brevis*, and *Bacillus cereus.* These bacteria are proven to be capable of biodegrading the diesel oil in the flask system. Moreover, the viable cell count and the biodegradation rates of diesel-oil components for the flask amended with food wastes were higher as compared to the flask unamended with food waste. This indicated that the food wastes provided additional nutrients such as N, P, and Ca which are important components for bacterial growth and enhanced their degradation activity. In addition, the reduction of the diesel oil component as quantified by GC-MS adds more proof that these bacteria are hydrocarbon-degraders with the ability to degrade diesel oil as their source of carbon and energy. Furthermore, the degradation of diesel oil lead to the production of acidic metabolites such as organic acids which caused the pH value of the medium to drop significantly at the end of the study.

ACKNOWLEDGEMENT:

This study was supported by research grant Tabung Penyelidik Muda (TPM) from Universiti Malaysia Terengganu (UMT).

REFERENCES:

1. Rengarajan T, Rajendran P, Nandakumar N, Lokeshkumar B, Rajendran P, Nishigaki I. Asian Pacific Journal of Tropical Biomedicine. Asian Pac J Trop Biomed. 2015;5(3):182–9.
2. Abioye OP, Agamuthu P, Abdul Aziz AR. Biodegradation of used motor oil in soil using organic waste amendments. Biotechnol Res Int. 2012;2012:587041.
3. Abdel-shafy HI, Mansour MSM. REVIEW A review on polycyclic aromatic hydrocarbons : Source , environmental impact , effect on human health and remediation. Egypt J Pet. 2016;25(1):107–23.
4. Kumar A, Bisht BS, Joshi VD, Dhewa T. Review on Bioremediation of Polluted Environment : A Management Tool. 2011;1(6):1079–93.
5. Abioye PO, Abdul Aziz AR, Agamuthu P. Enhanced biodegradation of used engine oil in soil amended with organic wastes. Water Air Soil Pollut. 2010;209(1–4):173–9.
6. Prabhakaran P, Sureshbabu A, Rajakumar S, Ayyasamy PM. Bioremediation of Crude Oil in Synthetic Mineral Salts Medium Enriched With Aerobic Bacterial Consortium. Int Jounral Innov Res Sci Eng Technol. 2014;3(2):9236–42.
7. Oluseyi T, Olayinka K, Alo B, Smith R. Comparison of extraction and clean-up techniques for the determination of polycyclic aromatic hydrocarbons in contaminated soil samples. African J Environ Sci Technol. 2011;5(7):482–93.
8. Deng MC, Li J, Liang FR, Yi M, Xu XM, Yuan JP, et al. Isolation and characterization of a novel hydrocarbon-degrading bacterium *Achromobacter* sp. HZ01 from the crude oil-contaminated seawater at the Daya Bay, southern China. Mar Pollut Bull. 2014;83(1):79–86.
9. Victor TO, Celestine UA, Emmanuel OE, Oluwatayo M. Biostimulation of hydrocarbon utilizing bacteria in soil contaminated with spent engine oil using banana and plantain agro-wastes. J Soil Sci Environ Manag. 2015 Aug 1 [cited 2017 Apr 29];6(8):225–33.
10. Pawar RM. The Effect of Soil pH on Bioremediation of Polycyclic Aromatic Hydrocarbons (PAHS). J Bioremediation Biodegrad. 2015;6(3).
11. Suchý P, Straková E, Herzig I, Steinhauser L, Králik G, Zapletal D. Chemical composition of bone tissue in broiler chickens intended for slaughter. Orig Pap Czech J Anim Sci Czech J Anim Sci. 2009 [cited 2017 Apr 27];54(547):324–30.
12. Schaechter M, Engleberg C, DiRita VJ, Dermody T. Schaechter's mechanisms of microbial disease. Lippincott Williams & Wilkins; 2007 [cited 2017 Apr 27]. 762 p.
13. Nwogu TP, Azubuike CC, Ogugbue CJ. Enhanced Bioremediation of Soil Artificially Contaminated with Petroleum Hydrocarbons after Amendment with *Capra aegagrus hircus* (Goat) Manure. Biotechnol Res Int [Internet]. 2015 [cited 2017 Apr 29];2015:657349.
14. Bücker F, Santestevan NA, Roesch LF, Seminotti Jacques RJ, Peralba M do CR, Camargo FA de O, et

al. Impact of biodiesel on biodeterioration of stored Brazilian diesel oil. Int Biodeterior Biodegradation. 2011 [cited 2017 Apr 27];65(1):172–8.
15. Hamzah A, Phan C-W, Abu Bakar NF, Wong K-K. Biodegradation of Crude Oil by Constructed Bacterial Consortia and the Constituent Single Bacteria Isolated From Malaysia. Bioremediat J. 2013 Mar [cited 2017 May 6];17(1):1–10.
16. Nkem BM, Halimoon N, Yusoff FM, Johari WLW, Zakaria MP, Medipally SR, et al. Isolation, identification and diesel-oil biodegradation capacities of indigenous hydrocarbon-degrading strains of *Cellulosimicrobium cellulans* and *Acinetobacter baumannii* from tarball at Terengganu beach, Malaysia. Mar Pollut Bull. 2016 Jun 15 [cited 2017 Apr 28];107(1):261–8.
17. Mayz J, Manzi L, Lárez A. Isolation, characterization and identification of hydrocarbonoclastic Pseudomonas species inhabiting the rhizosphere of *Crotalaria micans* Link Pelagia Research Library. 2013;3(5):313–21.
18. Brooke JS. *Stenotrophomonas maltophilia*: an emerging global opportunistic pathogen. Clin Microbiol Rev. 2012 Jan [cited 2017 Apr 28];25(1):2–41.
19. Aris A., Tengku Ismail TH, Harun R, Abdullah AM, Ishak MY. From Sources to Solution: Proceedings of the International Conference on Environmental Forensics. Springer Science & Business Media; 2013 [cited 2017 Apr 26].
20. Ahamed F, Hasibullah M, Ferdouse J, Anwar MN. Microbial Degradation of Petroleum Hydrocarbon. Bangladesh J Microbiol. 2011 Dec 12 [cited 2017 Apr 26];27(1):10–3.
21. Borah D, Yadav RNS. Biodegradation of Complex Hydrocarbon by a Novel *Bacillus cereus* Strain. J Environ Sci Technol. 2014 Mar 1 [cited 2017 Apr 26];7(3):176–84.
22. Ekpo IA, Agbor RB, Okpako EC, Ekanem EB. Effect of crude oil polluted soil on germination and growth of soybean (Glycine max). Department of Genetics and Biotechnology , University of Calabar , Calabar , Cross River State , Department of Science Technology , Akwa Ibom State Polytechnic , Ikot-O. 2012;3(6):3049–54.

FP-12

EFFECTS OF INOCULUM SIZES OF PURPLE NON-SULFUR BACTERIUM, *AFFIFELLA MARIANA* STRAIN ME ON THE BIOCONVERSION OF LEAFY VEGETABLE WASTES

SUJJAT AL AZAD* AND MOHAMMAD TAMRIN BIN MOHAMMAD LAL

Borneo Marine Research Institute, University Malaysia Sabah, 88400, Kota Kinabalu, Sabah, Malaysia.

*Corresponding author: sujjat@ums.edu.my

ABSTRACT

Purple non-sulfur bacterium, *Afifella marina*, strain ME was cultured in 112 synthetic media together with vegetable waste powder under anaerobic light condition. Three different inoculum sizes, such as 10% (v/v), 20% (v/v) and 30% (v/v) were used to determine the optimum inoculum size for the bioconversion of leafy vegetable wastes through Liquid State Fermentation. The fermentation process lasted for eight days and culture condition was maintained at 2500 lux illumination of light intensity at a temperature of 30 ± 1°C under anaerobic condition. During bioconversion the changes in the nutritional values such as crude protein (%), crude lipid (%), crude fiber and crude ash (%) were determined. The highest crude protein of 18.95% was recorded with 30% inoculum size. The crude protein content increased significantly ($p<0.05$) for all three inoculum sizes and its highest value was reached at Day 4. , The crude lipid increased the highest value at 1.70%, 1.65% and 1.49% for 10%, 20%, and 30% inoculum respectively. The minimum value of of 8.22% and 15.01% and 23.02% crude fiber was obtained at Day 8 for 10%, 20% and 30% inoculum respectively The maximum crude ash yielded with inoculum size of 30% (32.50%) was significantly higher ($p<0.05$) than the crude ash obtained with 10% (29.57%) and 20% (30.60%) inoculum in Day 6. Nutritional values of vegetable wastes through fermentation with *Afifella marina* were observed better with 30% level of inoculum. *Afifella marina* strain ME, is one of the potential bacterium in the bioconversion process leafy vegetable wastes in the production of nutritionally enriched biomass and reduce wastes to the environment.

KEYWORDS:
Afifella marina, inoculum sizes, leafy vegetable wastes, bioconversion and nutritional values

INTRODUCTION:

Leafy vegetable wastes are produced during harvesting, marketing and processing of vegetables.[1] Since vegetables contain more than 90% water, it decomposes very fast and they will cause many unwanted consequences such as foul smell, pests, infections, and increase in leachates in dumping sites.[2] Vegetable wastes have high nutritional value, such as protein vitamins and minerals.[3] The dried vegetable powder consists of 4.04% of moisture, 18.26% of crude protein, 2.40% of crude fat and 19.97% of crude fibre. These wastes materials can be converted into commercially valuable products, especially single-cell protein through microbial fermentation.[4] It has also been proven that wastes from crops can be used in aquaculture feed ingredients as supplementary feeds or as pond fertilizers.[5] So, there is a high potential of using microbial fermentation to convert agricultural and industrial wastes to produce valuable by-products, at the same time reducing waste and pollution to the environment. Raw food materials such as cabbage, cauliflower, banana peel, potato, carrot, beet root, okra, peas, beans, and capsicum had been shown to increase in their protein content as a result of biomass yield from the fermentation by the fungus, *Aspergillus niger*.[3]

Purple non-sulphur bacteria (PNSB) are getting more and more attention nowadays from researchers due to its diverse pathway in the metabolic process and ability in converting agro-industrial waste into the value-added products. PNSB has high potential in biotechnology where they have extraordinary potential in

purification of agro and industrial waste to produce single cell protein (SCP).[6] *Rhodobacter sphaeroides, Rhodobacter capsulatus*, and *Rhodocyclus gelatinosus* were the PNSB that are widely used for the production of SCP.[7] Besides, these bacteria also contained numerous important proteins, lipids, enzymes, vitamins, carotenoids, and other co-factors which are important for many biotechnology application, especially in improving the value of feed supplement in aquaculture species,[8,9] improving water quality,[10] increase grazing ability,[11] reduces metamorphosis period in shrimp larvae.[10] *Rhodovulum sulfidophilum* produces amylase uses in food, pharmaceutical and fine chemical industry.[12] Some strain produces heat-stable protease and cellulase. These groups of bacteria have the ability to biologically convert agricultural and industrial waste into nutritionally value added product.[7] The inoculums size into the culture is one of the important factors in producing bacterial biomass. Inoculums size is responsible to decrease the lag phase in bacterial growth[13] and also reduce the organic load in wastewater.[6]

The amount of inoculum is important because generally, the bacterial population is strongly heterogeneous and it takes time for all sub-populations to adapt to the new conditions. Inoculum size of 10% (v/v) in 25% palm oil mill effluent (POME) media increase the nutritional value and production of bacterial biomass.[14] *Afifella marina* inoculum size of 20% (v/v) was used to observed the effects of light intensities and photoperiod of production of extracellular nucleic acids.[15] Growth characteristic *of Afifella marina* strain ME (KC205142), as well as production of exopolymeric substances like enzymes and nucleic acid has been documented.[16] However, there is lack of information about *Afifella marina* strain ME (KC205142) in the utilizations of leafy vegetable waste in the production bacterium biomass. In addition, no studies so far have been conducted on the effect of inoculum sizes of *Afifella marina* strain ME in the production of the nutritionally enriched biomass using vegetable waste during the fermentation process. This study was focused on the effect of inoculum sizes of purple non-sulfur bacterium, *Afifella marina* strain ME on bioconversion of leafy vegetable waste into nutritionally enriched bacterium biomass

MATERIALS AND METHODS:

(i) Preparation of leafy vegetable waste powder:

Leafy vegetable wastes were collected at Likas, Kota Kinabalu Sabah, Malaysia farmers market. Only discarded or thrown leafy vegetable wastes that no longer suitable for human consumption was collected. The vegetable wastes were washed with tap water, chopped and ground into small pieces with a food processor and dried in the oven at 65°C until constant weight was obtained. The dried vegetable wastes were ground into fine particles of powder (<400 mm) using a high speed blender. The vegetable waste powder was stored in air tight plastic bags until further use.

(ii) Preparation of *Afifella marina* strain ME inoculums:

Afifella marina bacterium strain ME (KC205142) was taken from BMRI culture collection. Synthetic media 112 was used to prepare the inoculum for A. marina. Five millilitre of liquid culture *A. marina* from the culture stock was added into each of 25ml previously sterilized bottle. These bottles were incubated anaerobically at 2500 lux light intensity at a temperature of 30 ± 1°C for 48 hours. After 48 hours, 5% (v/v) of culture was transfer into one litre of previously autoclaved 112 schots bottles and incubated anaerobically at 2500 lux light intensity at a temperature of 30 ± 1°C. After 48 hours, three different types of inoculum sizes which are 10% (v/v), 20% (v/v) and 30% (v/v) of *Afifella marina* were used in this experiment.

(iii) Culturing *A. marina* using synthetic media and vegetable waste as substrate:

One liter bottle containing 112 synthetic media were autoclaved. After autoclaved the media in 20 g of leafy vegetable waste powder were added and mixed properly. The mixing was done manually by inverting bottles 2-3 times every day. The bottles were incubated under 2500 lux illumination of light intensity at a temperature of 30 ± 1°C under anaerobic condition.

(iv) Sampling methods:

The nutritional values were determined before and after the fermentation of leafy vegetable wastes in 112 culture media. Fermentation was conducted for eight days and every 2-day interval, two bottles for each

inoculum and one bottle of control were taken to harvest the biomass by centrifugation (4.0 × 1000 rpm for 20 minutes). The biomasses were dried in the oven at 65°C overnight. The dry biomass were used to determine the crude protein, crude lipid, crude fiber and crude ash

(v) Analytical parameters:

The standard procedures were used to analyse the proximate composition analysis.[17] The analytical parameters were crude protein (%), crude fibre (%), crude ash (%) crude lipid (%) and carbohydrate (%). In addition to fermented product, initial proximate composition of the vegetable waste meal was also carried out. Kjeltec™ 2300, Fibertec™ 1020 and Soxtec™ 2043 Analyzer of Foss Tecator were used to estimate the crude protein (%), crude fibre (%), crude ash (%) and crude lipid (%) respectively. Nitrogen fee extract was calculated with the formula as NFE = % DM - (% CP + %CL+ % CF+% ash)

Where:NFE = nitrogen free extract, DM = dry matter, CP = crude protein, CL = crude lipid and CF = crude fiber

(vi) Statistical analysis:

One-way ANOVA test was used to test the significant difference between the nutritional value within the 8 days at $p<0.05$. Any significant difference in the one-way ANOVA test was subjected to post hoc test, Least Significance Difference (LSD) analysis. All statistical analyses were conducted using SPSS for windows (Statistical Package for Social Science, Windows version, Chicago IL, USA) and Microsoft Excel.

RESULTS:

1. Crude Protein (%):

The highest crude protein content for 10%, 20% and 30% inoculums were recorded at Day 2 and Day 4 with the value of 16.81%, 17.56%, 18.46% and 17.15%, 17.82%, 18.95% respectively (Table 1).

Table 1
The initial and maximum crude protein (%) content recorded in leafy vegetable waste biomass after fermentation with *Afifella marina*.

Inoculum Size	Before Fermentation	After Fermentation	Increment/decrease (%)
Control	16.59 ± 0.20^{b}	16.37 ± 0.08^{a}	- 1.75
10%	16.09 ± 0.30^{a}	17.15 ± 0.58^{b}	6.58
20%	16.74 ± 0.13^{a}	17.82 ± 0.41^{b}	6.45
30%	17.02 ± 0.84^{a}	18.95 ± 1.80^{b}	11.34

Different superscripts are significantly different ($p<0.05$)

Among the fermented samples with *Afifella marina*, the lowest of 15.33% crude protein was observed with 10% inoculum at 6th days of culture. Meanwhile, the highest crude protein of 18.95% was observed among fermented samples on Day 4 fermentation with 30% (v/v) inoculum size (Figure 1).

The increment of crude protein content from Day 0 until Day 4 for all samples in three inoculum size were highly significant ($p<0.01$).There were no observed significant differences ($p = 0.564$) in the crude protein content of fermented samples between Day 2 and Day 4. However, the crude protein content in 30% inoculum was significantly higher ($p<0.01$) than the control, 10% and 20% inoculum. Thus, the highest production of crude protein in the fermented product was achieved at Day 2 and 4 by using 30% inoculum.

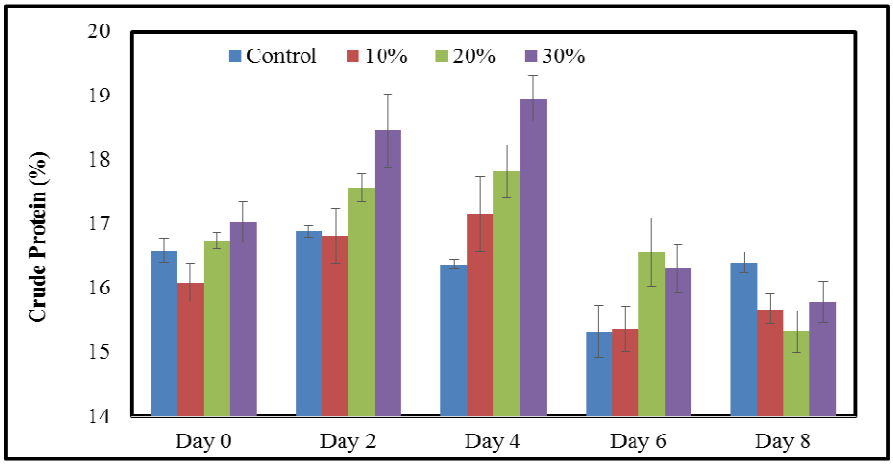

Figure 1

Comparison of crude protein (%) content in vegetable biomass derived from fermentation process with *Afifella marina* in three inoculum sizes and without *Afifella marina* (control) during the fermentation period.

2. Crude Lipid (%):

The crude lipid content of fermented vegetable waste was observed to fluctuate throughout the fermentation period (Figure 2). The highest crude lipid values were observed from the fermented products in all three inoculum size at Day 6, which were 1.70%, 1.74% and 1.60% for 10%, 20% and 30% inoculum size respectively. The maximum value of crude lipid obtained at Day 6 showed increment of 10.59% and 18.25% for 10% and 30% inoculum respectively.

Table 2

The initial and maximum crude lipid (%) content recorded in leafy vegetable waste biomass after fermentation with *Afifella marina*.

Inoculum	Before Fermentation	After Fermentation	% of increment/decrease
Control	1.52 ± 0.04^{b}	1.3 ± 0.05^{a}	5.34
10%	1.52 ± 0.06^{a}	1.72 ± 0.10^{b}	4.61
20%	1.78 ± 0.52^{a}	1.74 ± 0.07^{a}	14.60
30%	1.51 ± 0.06^{a}	1.63 ± 0.08^{b}	4.48

Different superscripts are significantly different ($p<0.05$)

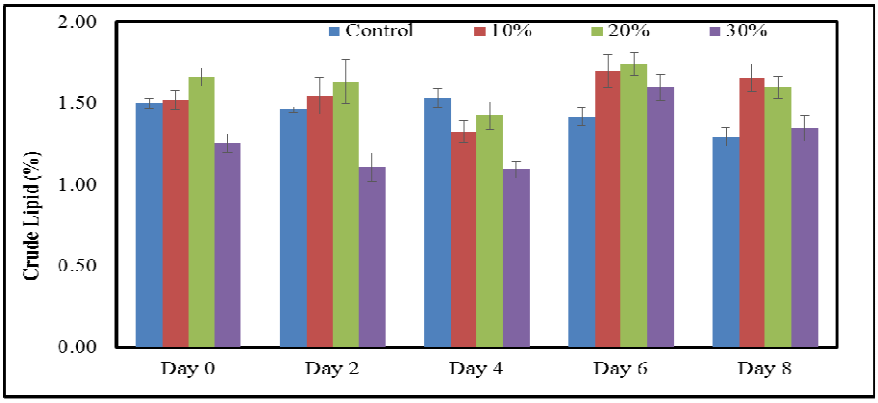

Figure 2

Comparison of crude lipid (%) content in vegetable biomass derived from fermentation process with *Afifella marina* in three inoculum sizes and without *Afifella marina* (control) during the fermentation period.

At Day 4, the crude lipid content for all three inoculum size were significantly lower (p = 0.001) compared to other days. The fermented product of 10% (p = 0.003) and 20% (p = 0.016). Inoculum at Day 6 was significantly higher than 30% but there were no significant difference (p = 0.384) between inoculum level of 10% and 20% at Day 6.

3. Crude fiber (%):

The crude fiber content of fermented vegetable waste was observed to decrease throughout the fermentation period. The lowest crude fiber values were observed from the fermented products in all three inoculum size at Day 8 (Figure 3). The minimum value of crude fiber obtained at Day8 showed decrease of 8.22% and 15.01% and 23.02% for 10%, 20% and 30% inoculum respectively.

Table 3.
The initial and maximum crude fiber (%) content recorded in leafy vegetable waste biomass after fermentation with *Afifella marina*.

Inoculum	Before Fermentation	After Fermentation	% of decrease
Control	15.0 ± 0.15^{a}	14.5 ± 0.50^{a}	0.34
10%	15.8 ± 0.16^{a}	14.5 ± 0.30^{b}	8.22
20%	$16 .0 \pm 0.42^{a}$	13.6 ± 0.57^{b}	15.00
30%	16.4 ± 0.06^{a}	12.6 ± 0.18^{b}	23.01

Different superscripts are significantly different ($p<0.05$)

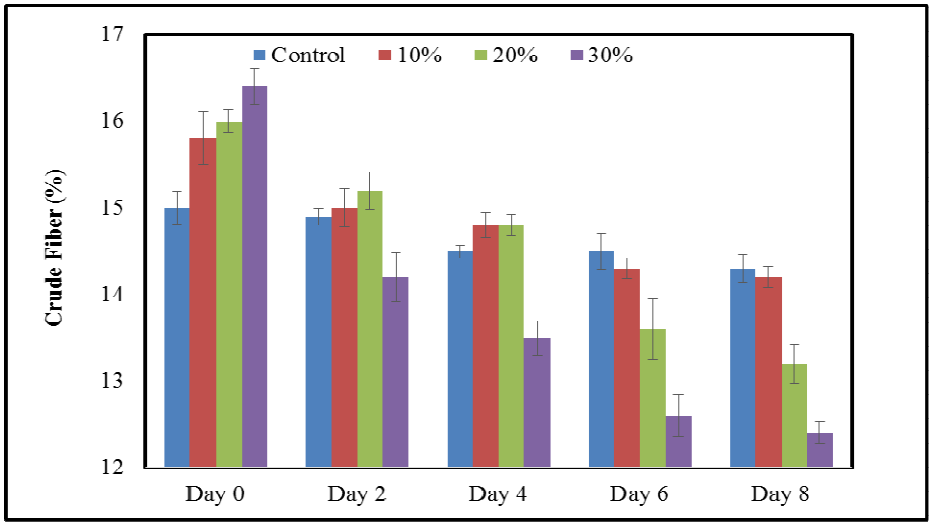

Figure 3
Comparison of crude fiber (%) content in vegetable biomass derived from fermentation process with *Afifella marina* in three inoculum sizes and without *Afifella marina* (control) during the fermentation period.

The fermented product of 20% (p = 0.01) and 30% (p = 0.001) inoculum at Day 8 was significantly higher than 10% but there were no significant difference (p = 0.458) between inoculum level of 10% and control at day 8.

4. Crude Ash (%):

Crude ash in fermented vegetable waste biomass with and without *Afifella marina* (control) had showed increase in trend until Day 6 of fermentation. The values in crude ash for 10%, 20% and 30% inoculum increased from Day 0 and reached the highest at Day 6. The highest values for 10%, 20% and 30% were recorded at Day 4 and Day 6, which were 29.33%, 29.09%, 32.12% and 29.57%, 30.60%, 32.50% respectively (Figure 4. The maximum value of crude ash was obtained at Day 6, which showed the increment of 6.91%, 17.83% and 11.07% for 10%, 20% and 30% inoculum respectively (Table 4).

Table 4
The initial and maximum crude ash (%) content recorded in leafy vegetable waste biomass after fermentation with *Afifella marina*.

Inoculum	Before Fermentation	After Fermentation	% of increment
Control	27.23 ± 0.19^{a}	30.19 ± 0.47^{b}	10.87
10%	27.66 ± 0.85^{a}	29.57 ± 0.88^{b}	6.91
20%	25.97 ± 1.14^{a}	30.60 ± 0.86^{b}	17.83
30%	29.26 ± 1.44^{a}	32.50 ± 0.19^{b}	11.07

a,b Means within same row with different superscripts are significantly different ($p<0.05$)

However, samples of 20% inoculum was significantly higher in fermented product of Day 6 ($p = 0.022$) compared to Day 4. The maximum crude ash yielded with 30% inoculum was significantly higher ($p<0.01$) compared to maximum crude ash yielded with 10% and 20% inoculum in both Day 4 and Day 6.

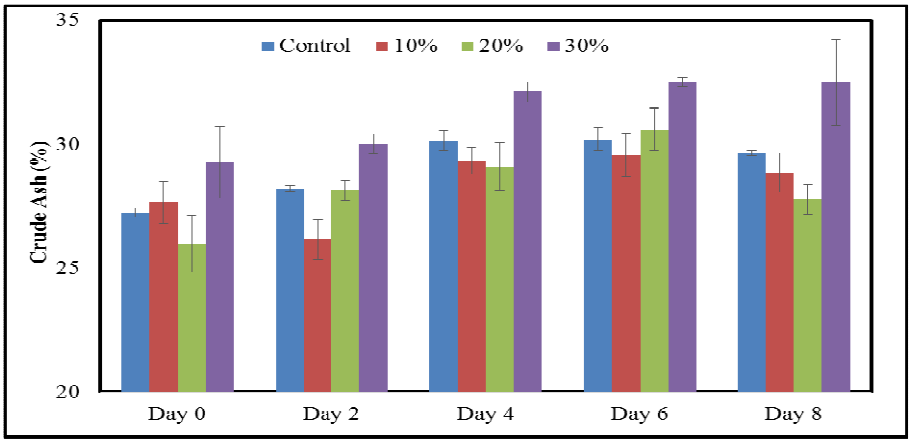

Figure 4
Comparison of crude ash (%) content in vegetable biomass derived from fermentation process with *Afifella marina* in three inoculum sizes and without *Afifella marina* (control) during the fermentation period.

Table 5
Summary of the proximate compositions of leafy vegetable waste before fermentation and after fermentation with *Afifella marina*

Inoculum	Crude protein (%)		Crude lipid (%)		Crude fiber (%)		Ash (%)		NFE (%)	
	Before	After	Before	After	Before	After	Before	After	Before	After
Control	16.6	16.4	1.5	1.3	15.0	14.5	27.3	30.2	39.6	37.6
10%	16.1	17.1	1.5	1.7	15.8	14.5	27.7	29.6	38.9	37.1
20%	16.7	17.8	1.8	1.7	16.0	13.6	25.9	30.6	39.6	36.3
30%	17.0	18.9	1.6	1.5	16.4	12.6	29.3	32.5	35.7	34.5

DISCUSSIONS:

The purple non-sulfur bacterium (PNSB), *Afifella marina* was grown in 112 synthetic media with the utilization of vegetable waste powder as its substrate has displayed an overall improvement in its nutritional values in terms of crude protein, crude lipid and crude ash. The crude protein content improved with 30% inoculum. The optimum period to obtain the highest crude protein from the fermented product was at Day 4. Compared to the study done by In the bioconversion of vegetable waste with fungi *Aspergillus niger* S14 and *Aspergillus niger* NCIM 616 through solid state fermentation showed that the highest level of crude protein was on Day 8 and 7 respectively which was delayed compared to using *Afifella marina* in this study.[3] The crude protein content in the fermented sample was an improved (from 40.02% to 43.07%) in the Thevetia cake after fermentation and comparable with present study.[18] On the other hand, crude protein

content of cassava peel increased from 5.4% to 16.9% after fermentation.[19] Microbial fermentation of some species of yeast (*Kluyveromyces marxianus*) was able to produce more protein (44 ± 0.38%) using cabbage wastes.[20] The difference between the crude protein content of all inoculated and fermented samples are due to the activities of microorganism.[21] It concluded that the suitability of vegetable wastes as a potential substrate for the production of microbial protein. The increased of crude protein can be related to the increased of cell mass generated by the organism due to conversion of the vegetable protein or other nitrogenous compounds into bacterial biomass protein, which might be in the form of single cell protein.[3,22] The increased in microbial biomass in the form of SCP can be one of the reasons for the increase in the protein content.[23,24] Many studies had showed that PNSB has high potential to produce SCP. *Rhodobacter sphaeroides, Rhodobacter capsulatus*, and *Rhodocyclus gelatinosus* were the PNSB that are widely used for the production of SCP.[7] *Rhodobacter sphaeroides* P47, another strain of PNSB is a strong candidate for SCP production from agricultural wastes due to its highly nutritious characteristic.[25] The production of SCP was obtained in anaerobic wastewater treatment process utilizing *Rhodopseudomonas palustris* in mix culture condition.[26] Hence, it can be postulated that *Afifella marina* might be a potential PNSB species in producing SCP. The increased in crude protein content could also be as a results of breakdown of fiber composition in the vegetable waste during fermentation. The subsequent substances are to be used by the bacteria as a carbon source to synthesis bacterial biomass rich in protein. The breakdown of fiber and bioconversion into protein may also due to secretion of enzymes, which are proteinous in nature, during fermentation. It has been reported that PNSB produces extracellular enzymes such as protease, lipases, esterase and alkaline phosphatase.[27] *Afifella marina* is capable to produce proteolytic enzymes among PNSB, which produces protease under anaerobic light conditions at temperature of 30 ± 2°C. The optimum proteolytic activity was recorded at 48h of incubation, which also explains the high level of crude protein at Day 2 and Day 4 in this study.[16] In addition, the extracellular proteases within the bacterium extracellular polymeric substances matrix play an important role in providing nutrients and alter extracellular polymeric substances composition.[16] The proteolytic activity of *Afifella marina* increases with dry cell weight, which the highest dry cell weight was of 4.97 g/l and proteolytic activity of 74.7 ± 2.31 U. It indicated that *Afifella marina* might secrete proteolytic enzyme to hydrolyze high molecular weight compound outside the cell, prior to the uptake of growth. Extracellular enzymes contributed to the nutrition of the bacterium by hydrolyzing large molecular organic compounds to smaller monomeric components which can readily absorbed by the bacterial cells.[28]

The crude lipid content in the fermented vegetable waste was low due to low lipid compositions and fatty acids in *Afifella marina* generally.[29] The crude lipid content in the fermented product gradually decreased from Day 0 to Day 4. The initial crude lipid content of 1.52%, 1.78% and 1.26% had decreased to the minimum of 1.33%, 1.43% and 1.09% on Day 4, for 10%, 20% and 30% inoculum size respectively. The values of crude lipid content in this study demonstrated a similar decreasing trend with other vegetable waste fermentation.[3] The reduction in crude lipid during the fermentation period maybe caused by assimilation of lipids from the substrate possibly for biomass production, which explains the results on the increased of value of crude protein in the fermented product from Day 0 to Day 4.[3] Loss of lipid in palm kernel meal during Solid State Fermentation with fungi was due to its conversion into fungal protein biomass.[30] Upon reaching Day 6, the value of crude lipid content increased. This could be due to the changed of metabolic pathway of the bacteria due to deprivation of nutrients on the 6th day of culture. Purple non-sulphur bacteria are a physiologically versatile group of purple bacteria and are able to adapt in many different conditions in order to grow in unfavourable pathway. The lipid composition under defined growth conditions is generally stable as bacterial cells grow and divide but is known to alter on bacteria response to changing environmental factors such as nutrient supplies.[31] The purple bacteria are able to synthesize phosphate-free lipid when the surrounding environment is lack of phosphate, which is an important component for membrane composition of the bacteria.[32] Fatty acid profile in purple non-sulphur bacteria is basically influenced by the cultivation medium.[29] Thus, it is important that bacteria used for aquaculture are cultured in appropriate substrate.

Crude fibre content had shown decreasing trends with 30% level of inoculums. Bacteria may be the utilization fiber and convert to protein in bioconversion process. However the enzymatic activity of such bacteria in the breakdown of fiber need to further investigation. On the other hand, NFE content showed a

decrease of 3.3% with 30% inoclulum level. The result show that the available carbohydrate in the substrate decreased with increase in protein and fat content during bioconversion of carbohydrate in to microbial protein and other compounds.[33] Unique of purple non-sulfur bacteria is to utilize wide range of carbon and also nitrogenous based substrate during growth phase.[29]

The highest crude ash of 32.50% was observed in 30% inoculum at Day 6. The results of current study is in agreement with the results obtained by researchers , which also showed an increasing trend in crude ash content by using fungi in solid state fermentation with vegetable wastes.[3] The initial ash content of their study was 9.83% ± 0.09 and continued to increase until it reached a maximum value of 12.73% ± 0.85. The ash content is a rough measure of the inorganic mineral elements in the samples. The increase in ash content in fermented product during the course of fermentation can be explained by the loss in organic matter obtained through fermentation process.[3] During fermentation, the organic matter will be broke down into simpler substances to be absorbed by the bacteria.[34] The unfermented samples are likely to have more mineral elements than the fermented samples and it is unlikely that microorganisms might have used some of the minerals for their metabolic activities.[24] All living organisms required some mineral elements to maintain some metabolic functions but there was no appreciable decrease in the mineral composition of fermented agro-industrial residues.[35]

It is observed in this study that the higher the inoculum size proportionally related to the higher the nutritional values of the fermented product. The maximum production crude protein, crude lipid and crude ash are achieved by using 30% (v/v) inoculum. Inoculum size of 30% (v/v) displayed the highest increment among the three inoculum sizes, which is up to 18.25% increment in protein and 11.07% increment in ash. The growth of PNSB in non-sterilised waste may be affected by the presence of other heterotrophic microbes. To suppress the growth of the heterotrophic microbes, the inoculum size of the bacteria must be have the good quality as well as sufficient quantity.[36] In the treatment of sardine processing waste 50% higher production of cell biomass was achieved when higher inoculum size of PNSB is used. They also stated that a 30% inoculum might provide high number of bacteria to utilize nutrients that were instantly available from substrate.[36] The inoculum size greatly affects the length of lag time. The lag time of *Pseudomonas ovalis* decreased from 14 hours to 5 hour and 30 minutes when the inoculum size increases from 10^3 to 10^6.[37] Bacterium, such as *Escherichia coli* also show similar results, which the lag time decreased from 20 hour 15 minutes to 9 hour when the inoculum size increases from 10^2 to 10^5. Using larger inoculum levels can results in shorter lag phase of *Penicullium expansum* from 173 hours to 106 hours when the inoculum size increased from 2 x 10^3 to of 2 x 10^6.[38] Thus, it can be speculate that higher inoculum size of *Afifella marina* can decrease the required lag time and enables the bacteria to reach exponential phase faster. Faster growth can cause the shelf life of bacteria to shorten and it is important to refer to the predictive growth models for quantitative microbiological risk assessment before attempting.[38] Thus microbial risk in *Afifella marina* with higher inoculums level needed to investigate the effect of inoculum size on the growth during fermentation process.

CONCLUSION:

Purple non-sulphur bacterium, *Afifella marina* strain ME has potentiality in improving nutritional values of leafy vegetable waste through fermentation. The optimal culturing period for liquid state fermentation (LSF) is between Day 2 to Day 6, depend on nutritional component of the fermented biomass. The fermentation of vegetable waste between the periods of four to six days with *Afifella marina* as inoculum at size of 10%, 20%, and 30% resulted in increased in nutritional values. The best inoculum for highest percentage of crude protein and crude ash yield was 30% inoculum. The highest percentage yield of crude lipid was 20% inoculum and the highest increment of crude lipid was 30% inoculum. Optimal crude protein and crude ash production recorded for vegetable waste fermented with 30% inoculum size was 18.95% (Day 4) and 32.50% (Day 6) respectively, whereas optimal crude lipid production was recorded with 20% inoculum size with the yield of 1.70% at Day 6. Maximum increment of 18.25% was recorded in 30% inoculum size, also at Day 6. The results of this study could play a significant role in future application for producing nutritionally enriched biomass for aquaculture feed production, which needs further investigations, at the same promoting an economical and eco-friendly approached by reducing wastes to the environment.

ACKNOWLEDGEMENT:
This study was supported by the grant of SBK0307.2017 from University Malaysia Sabah, Kota Kinabalu, Sabah, Malaysia and authors also appreciated the support from staff of Borneo Marine Research Institute, University Malaysia Sabah, Kota Kinabalu, Sabah, Malaysia.

REFERENCES:

1. Gangadhar MA, Rama Prasad J and Krishna N. Chemical composition and in-vitro digestibility of conventional and unconventional energy supplements. Indian Journal of Animal Science. 1993; 63: 1004–1005.
2. Magaji JY. Effects of waste dump on the quality of plants cultivated around Mpape dumpsite FCT Abuja, Nigeria. Ethiopian Journal of Environmental Studies and Management EJESM. 2012; 5(4): 567-573
3. Rajesh N, Joseph I and Raj RP. Value addition of vegetable wastes by solid-state fermentation using *Aspergillus niger* for use in aquafeed industry. Waste Management. 2010; 30:2223–2227.
4. Leman J, Bednarski W and Tomasik J. Influence of cultivation condition on the composition of oil produced by *Candida curvata*. Biological Waste. 1990; 31: 1-15.
5. Tacon A. Feed Ingredients for Carnivorous Fish Species: Alternatives to Fish Meal and Other Fishery Resources. FAO Fisheries Circular No. 881. 1994; Rome, Italy.
6. Azad S A and Shaleh SRM. Inoculum Sizes of Locally Isolated Phototrophic Bacterium on the Utilization of Palm Oil Mill Effluent. British Biotechnology Journal. 2015; 8(1): 1-11.
7. Sasikala C and Ramana VC. Biotechnological potentials of anoxygenic phototrophic bacteria. I. Production of single cell protein, vitamins, ubiquinones, hormones and enzymes and use in waste treatment. In: Neidlema, SL & Laskin AI. (Eds.) Advance in Applied Microbiology. 1995; 41, Academic Press, New York, pp. 173-226.
8. Azad SA, Vikineswary S, Chong CV and Ramachandran KB. Growth and Production of Biomass of *Rhodovulum sulfidophilum* in Sardine Processing Wastewater. Letters in Applied Microbiology.2001; 33: 264-268.
9. Shapawi R, Eee Ting T and Azad SA. Inclusion of Purple Non-Sulfur Bacterial Biomass in Formulated Feed to Promote Growth, Feed Conversion Ratio of Asian Seabass *Lates calcifier* juveniles. Journal of Fisheries and Aquatic Science. 2012; **7**(6): 475-480.
10. Azad SA, Chong CV and Vikineswary S. Phototrophic bacteria as feed supplement for rearing *Penaeus monodon* larvae. Journal of the World Aquaculture Society. 2002; 33 (2): 158-168.
11. He ZH, Wang Y, Cui,H, Guo LZ and Qian H. Studies on the mass culture of *Moina mongolica* in seawater. Journal of Fishery Sciences of China. 1998; 22: 17-23.
12. Sasaki K, Watanabe M, Tanaka T and Tanaka T. Biosynthesis, biotechnological production and application of 5-aminolevulinic acid. Applied Microbiology and Biotechnology. 2002; 58: 23-29.
13. Gongouli M, Kalantzi K, Beletsiotis E and Koutsoumanis KP. 2011. Development and application of predictive models for fungal growth as tools to improve quality control in yogurt production. Food Microbiology. 2011; 28: 1453-1462.
14. Loo PL, Vikineswary S and Chong VC. Nutritional value and production of three species of purple non-sulfur bacteria grown in palm oil mill effluent and their application in rotifer culture. Aquaculture Nutrition. 2013; 19: 895-907.
15. Tan KS, Azad SA and Ransangan J. Effects of light intensities and photoperiod on production of extracellular nucleic acids in purple non-sulfur marine bacterium *Afifella marina* strain ME (KC205142). International Journal of Research in Pure and Applied Microbiology. 2013; 3(3): 53-57.
16. Azad SA, Tan KS and Ransangan J. Effects of light intensities and photoperiods on growth and proteolytic activity in purple non-sulfur marine bacterium, *Afifella marina* strain ME (KC205142). Advances in Bioscience and Biotechnology. 2013; 4: 919-924.
17. AOAC. Official methods of analysis of the association of official's analytical chemists, 17th Ed. Association of official analytical chemists. 2003; Arlington, Virginia
18. Adeyemi OA and Adeleke AA. Replacement of soybean meal with fermented Thevitia cake in layers diet: Effect on the performance, egg quality and nutrient retention. Nigerian Journal of Animal Production. 2000; 27 (1): 24-28.

19. Ofuya CO and Obilor SN. The suitability of fermented cassava peel as poultry feedstuff. Bioresources Technology. 1993; 44:101-104.
20. Choi MH, Ji GE, Koh KH, Ryu YW, Jo DH and Park YH. Use of waste Chinese cabbage as a substrate for yeast biomass production. Bioresource Technology. 2002; 83: 251-253.
21. MacDonald P, Edwards RA, Greenhalg JFD and Morgan CA. Animal Nutrition (5th ed). London Longman GRP. Ltd. 1998. 607pp.
22. Akintomide MJ and Antai SP. Protein Enrichment of Irish potato (Solanium tuberosium) peels through Solid Substrate Fermentation by *Saccharomyces cerevisiae* and *Aspergillus Niger*. Journal of Environmental Science, Toxicology and Food Technology. 2012; 1 (5):15-19
23. Fasidi IO and Kadiri M. Use of agricultural wastes for the cultivation of *Lentinus subnudus* in Nigeria. Revista de Biologia Tropical. 1993; 41: 411-415.
24. Akinyele BJ, Olaniyi OO and Arotupin DJ. Bioconversion of Selected Agricultural Wastes and Associated Enzymes by *Volvariella volvacea*: An Edible Mushroom. Research Journal of Microbiology, 2011; 6: 63-70.
25. Kobayashi M and Kobayashi M. Roles of phototrophic bacteria and their utilization. In: Kojima H and Lee YK. (Eds.) Photosynthetic Microorganisms in Environmental Biotechnology. Springer-Verlag. Hong Kong. 2001; pp.11-26.
26. Honda R, Fukushi K and Yamamoto K. Optimization of wastewater feeding for single-cell protein production in an anaerobic wastewater treatment process utilizing purple non-sulfur bacteria in mixed culture condition. Journal of Biotechnology. 2006; 125: 565-573
27. Tielen P, Rosenau F, Wilhelm S, Jaeger KE, Flemming HC and Wingender J. Extracellular enzymes affect biofilm formation of mucoid *Pseudomonas aeruginosa*. Microbiology. 2010; 156: 2239-2252.
28. Prakash B, Veeregowda BM and Krishnappa G. Biofilms: A survival strategy of bacteria. Current Science. 2003; 85: 1299-1307.
29. Imhoff JF and Imhoff UB. Lipids, quinones and fatty acids of anoxygenic phototrophic bacteria. In: Blankenship RE, Madigan MT, Bauer CE (eds) Advances in Photosynthesis: Anoxygenic Photosynthetic Bacteria. Kluwer Academic Publisher. 1995; Dordrecht, The Netherlands.
30. Ng WK, Tee MC and Boey PL. Evaluation of crude palm oil and refined palm olein as dietary lipids in pelleted feeds for a tropical bagrid catfish, *Mystus nemurus* (Cuvier & Valenciennes). Aquaculture Research. 2000; 31: 337- 347.
31. Tamot B and Benning C. Membrane Lipid Biosynthesis in Purple Bacteria. In: Hunter CN, Dalda, F, Thurnauer MC, Beatty JT. (Eds.), The Purple Phototrophic Bacteria. Advances in Photosynthesis and Respiration, vol. 28. Springer, The Netherlands. 2009; pp. 119-132.
32. Van Mooy BA, Rocap G, Fredricks HF, Evans CT and Devol AH. Sulfolipids dramatically decrease phosphorus demand by picocyanobacteria in oligotrophic marine environments. Proceedings of the National Academy of Sciences USA. 2006; 103: 8607–8612.
33. Rama R and Srivastav SK. Effect of various carbon substrates on a-amylase production from *Bacillus* species. J. Microb. Biotechnol. 1995; 10 (2): 76–82.
34. Igbabul BD, Amove J and Twadue I. 2014. Effect of fermentation on the proximate composition, antinutritional factors and functional properties of cocoyam (*Colocasia esculenta*) flour. African Journal of Food Science and Technology. 2014; 5(3): 67-74.
35. Baert K, Devlieghere F, Li B, Debevere J and Meulenaer BD. The effect of inoculum size on the growth of *Penicullium expansum* in apples. Food Microbiology. 2008; 25: 212-217.
36. Azad SA, Vikineswary S, Chong CV and Ramachandran KB. *Rhodovulum sulfidophilum* in the treatment and utilization of Sardine Processing Wastewater. Letters in Applied Microbiology. 2003; 38 (1): 13-18.
37. Shida T, Komagata K and Mitsugi K. Reduction of lag time in bacterial growth: 1. Effect of inoculum size and nutrients. The Journal of General and Applied Microbiology. 1975a; 21: 75-86.
38. Bennet JW, Wunch KG and Faison BO. Use of Fungi in Bioremediation. In: Hurst CJ, Crawford RL, Garland JL, Lipson DA, Mills AL and Stetzenbach LD. (Eds.). Manual of Environmental Microbiology, 2nd Edition. ASM Press, Washington DC. 2002; pp. 960-971.

FP-13

EFFECTS OF LED LIGHTING SYSTEM ON THE GROWTH OF *STEVIA REBAUDIANA* BERTONI PLANT TISSUE CULTURES

NOORDIN NORAZLINA[1*], CHONG SAW PENG[1], LEONG YEE SHIEN[2], SEAH CHOON VOON[2]

[1]*Agrotechnology and Biosciences Division, Malaysian Nuclear Agency, Ministry of Science, Technology and Innovation Malaysia (MOSTI), Bangi, 43000 Kajang, Selangor,* [2]*Duta Nusajaya Plant Tissue Culture Facility, Kampung Minintod, Inanam, 88450, Sabah*

[*]*Corresponding author: azlina@nuclearmalaysia.gov.my*

ABSTRACT

Stevia rebaudiana Bertoni is a perennial herb that belongs to the family of Asteraceae. It is one of the 154 members of genus stevia which produce sweet steviol glycosides. The potential of stevia has been regarded worldwide and fast becoming the best alternative sweetener due to the health conscious of excessive sugar intake. LED lighting provides abundant opportunities to study various plant light responses. LED lights only deliver the colors of lights used by plants for efficient and healthy growth; therefore it offers many benefits for applications in plant studies and has promising potential in commercial cultivation of plants. A study was conducted in collaboration with a pre-commercial plant tissue culture facility as to apply the innovated LED lighting system incorporates with plant tissue culture technology for the enhancement of stevia tissue culture seedlings production. Having the highest formation of new shoots 3.24±0.846 and number of leaves formed 21.44±5.295 per sub-culture with LED lighting, this system will facilitate in the rapid and efficient large-scale production of stevia tissue culture seedlings for sustainable and continuous supply of planting materials for commercial plantation.

KEYWORDS:
Micropropagation, Pre-commercial plant tissue culture laboratory, Plant light responses, Dark red light, White light.

INTRODUCTION:

Stevia is a well-known herbaceous perennial shrub originated from the highlands of Paraguay and sections of Argentina and Brazil. Stevia was discovered by Antonio Bertoni, a South American Natural Scientist, in 1887. This plant is a natural sweetener and famously known as "Sweet Weed", "Sweet Leaf", "Sweet Herbs" and "Honey Leaf", which is estimated to be 300 times sweeter than cane sugar. *Stevia rebaudiana* Bert belongs to the family *Asteraceae*, one of 154 members of the genus Stevia, which produces sweet steviol glycosides (Robinson, 1930; Soejarto *et al*., 1982). The leaves of stevia are the source of diterpene glycosides, stevioside and rebaudioside (Yoshida, 1986). Stevioside is regarded as a valuable natural sweetening agent because of its relatively good taste and chemical stability (Yamada *et al*., 1985). Stevioside is of special interest to diabetic persons with hyperglycemia and the diet conscious (Arpita *et al*., 2011)). Stevia has been introduced as a crop in a number of countries including Brazil, Korea, Japan, Mexico, United States, Indonesia, Tanzania and Canada (Brandle and Rosa, 1992; Fors, 1995; Saxena and Ming, 1988; Shock, 1982) for food and pharmaceutical products. Currently *S. rebaudiana* production is centered in China with major market in Japan (Kinghorn and Soejarto, 1985). The product also can be added to tea and coffee, cooked or baked goods, processed foods, pickles, fruit juices, tobacco products, confectionary goods, jams and jellies, candies, yogurts, pastries, chewing gum and sherbets beverages (Arpita *et al*., 2011).

Recent advancements of LED lighting provide abundant opportunities to study various plant light responses. Solidity and longevity of LED lighting system enable easier installation and manipulation

compared to conventional lighting devices such as incandescent and fluorescent lamps, which have fragile glass sheaths. The main benefit of using LED lights is the lower running costs. The better ones on the market use up to 90% less electricity than comparable fluorescent lamp. The expected life of a LED lights is on average 100,000 hours. This is 5 to 10 times longer than a fluorescent lamp. Although initial purchase costs may be higher than comparable fluorescent lamp, unlike fluorescent lamp, LED lights do not need the electrical ballast. This eliminates a recurring cost from the grow room set-up. (Philips Technology, 2012)

Fluorescent Lamp emits all the spectrum of visible light and some sightless light but LED Lights only deliver the colors of light used by plants for efficient and healthy growth. Therefore, they provide better energy efficiency than conventional grow lights. The LED lighting system that is currently used in this project; Greenpower LED Dark red/White by Philips has the advantage of lowering the energy use and costs without sacrificing light levels or quality. These days most LED Lights only deliver the colors of lights used by plants for efficient and healthy growth. Therefore, they provide better energy efficiency than conventional grow lights.

Red and Blue light is essential for plant growth. It is well known that chlorophyll, which is contained in the green leaves of plant perform photosynthesis. Red and Blue are the wavelengths most essential for photosynthesis. The blue absorption region is 430-450 nm and red is 650-670 nm. Red Light is in the vicinity of the first peak of a plants light absorption spectrum (660nm) and it contributes to the plant photosynthesis. Red light, when combined with white light, has the ability to delay plants from early flowering (Cuenen, 2012). Red light also activates the phytochrome, a light-sensitive sensor pigment, resulting in a series of photomorphogenic responses that can encourage vegetative growth in crops (Cuenen, 2012).

A study was conducted in collaboration with a commercial plant tissue culture facility; Duta Nusajaya Sdn. Bhd. with the application of the LED lighting system incorporated with plant tissue culture technology for the enhancement of stevia tissue culture seedlings production. An advanced light-emitting diode (LED) lighting system is currently used as the source of lighting/photoperiod for the stevia tissue cultures. Although LED light has been widely used in many other fields, this new and innovative LED lighting system is currently being the pioneer to be used in a pre-commercial plant tissue culture laboratory in Malaysia. In this paper, a comparison study conducted in Duta Nusajaya Plant Tissue Culture Facility using different lighting systems incorporated with plant tissue culture technology for the stevia cultivation will be discussed.

MATERIALS AND METHODS:

Stevia variant S10A developed from mutation breeding using gamma irradiation was used in this study (Norazlina N. *et al*, 2014). Stevia single shoot tips (1 cm) were cultured onto semi-solid MS Medium (Murashige and Skoog, 1962) supplemented with 1.0 mg/l 6-furfurylaminopurine (kinetin). The shoot cultures were incubated in the incubation room at 22± 2°C with 12 hours photoperiod using different types of lighting systems. The lighting systems used in this study were Greenpower LED Dark Red/White (DR/W) light by Philips Technology, commercial LED seven (7) colors spectrum light and cool fluorescent light. Each treatment consisted of 5 replicates with 10 explants per replication. Observations and data collection were done weekly for 4 weeks interval. Data collected were survival rate (%), plant height (cm), number of new shoots formed (mean ± SD) and number of new leaves formed (mean ± SD).

RESULTS AND DISCUSSION:

Results from Table 1 showed significant differences on the effects of different lighting systems on stevia growth performance. For all lighting systems, stevia cultures showed 100% survival rate and there were increments in the plant height (cm), number of new shoots formed and also number of leaves formed after for weeks of culture.

However, in comparison with all the lighting systems used in this study, Greenpower LED DR/W light showed positive effects on the morphology and growth performance of the stevia *in vitro* plantlets.

Table 1
Effects of different types of lighting systems on *stevia rebaudiana* growth after 4 weeks of culture

Lighting system	Survival rate (%±SD)	Plant height (cm±SD)	No of new shoots formed (mean±SD)	No of leaves formed (mean±SD)
Greenpower LED Dark Red/White	100	5.284 ±1.124	3.24±0.846	21.44±5.295
Cool Fluorescent	100	4.762±1.348	1.20±1.049	14.46±4.175
Commercial LED 7 colours spectrum	100	4.806±1.357	1.64±1.289	18.26±5.386

After four weeks of culture, Greenpower LED DR/W light showed the highest plant height of 5.284 ±1.124 cm. It was also observed that with this lighting system, the internode distance was ±1.5cm apart and the stevia plantlets having more nodes formed (± 7nodes). Plantlets formed have more lateral branching (±5 branches) and this gave a bushier characteristic to the stevia plantlets. It is known that red light is responsible for shoot or stem elongation and responsible for the vegetative growth that will lead to healthier and bushier characteristics of plant and promotes regeneration and multiplication (Cuenen, 2012).

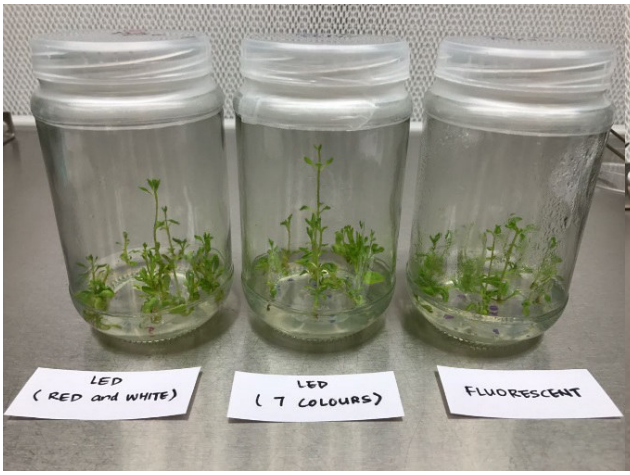

Fig. 1 One week of culture

Fig. 2 Four weeks of culture

Fig. 3
Stevia cultures under Greenpower LED lighting system

Meanwhile, Greenpower LED DR/W light also showed highest increment for number of new shoots formed and number of leaves formed, 3.24±0.846 and 21.44±5.295 respectively. From previous research and study conducted by Nuclear Malaysia and University of Ghent, Belgium, red light clearly sustained the vegetative growth in *Stevia rebaudiana*. With the advantages of the red light, it was observed that the formation of leaves was the highest as compared to other lighting systems that will lead to higher and steady accumulation of leaves biomass.

Fig 4
Stevia seedlings as planting materials for commercial plantation

CONCLUSION:

From this comparison study, it was clearly demonstrated that the Greenpower LED DR/W by Philips Technology that is currently being used as the lighting system in Duta Nusajaya Plant Tissue Culture Facility has the potential and promising advantages in the enhancement of stevia tissue culture seedlings production. Having the highest formation of new shoots **3.24±0.846** per sub-culture interval (30 days), 2-3 folds from other lighting systems, this will eventually facilitate in the rapid and efficient large-scale production of stevia tissue cultured seedlings in order to meet sustainable and continuous supply of planting materials for commercial plantation.

ACKNOWLEDGEMENTS:

The authors would like to thank the management of Malaysian Nuclear Agency for their continuous assistance and supports. Special thanks is also extended to the Ministry of Science, Technology and Innovation (MOSTI) for providing funds for the stevia Research and Development (R&D) projects under the Science Fund grant 02-03-01-SF0163, Techno Fund TF0614D122 and MOSTI Social Innovation Fund MSI 16009.

REFERENCES:

1. Arpita, D., Gantait, S. and Mandal, N. (2011). Micropropagation of an elite medicinal plant: *Stevia rebaudiana* Bert., *Int. J. Agric. Res*. 6(1):40-48.
2. Brandle, J.E., Rosa, N. (1992). Heritability for yield, leaf- stem ratio and stevioside content estimated from a landrace cultivar of *Stevia rebaudiana*, *Canad. J. Plant Sc*. 72: 1263-1266.
3. Cuenen Stijn (2012). Metabolism of Steviol Glycosides in Stevia Species. Doctoral dissertation. University of Leuven, Belgium.
4. Fors, A. (1995). A new character in the sweetener scenario, *Sugar J.* 58: 30-41.
5. Kinghorn, A.D. and Soejarto, D.D. (1985). Current status of stevioside as a sweetening agent for human use, *Econs and Meds Plant Res.* Academic Press, London. 263-268.
6. Murashige, T. and Skoog, F. (1962). A revised medium for rapid growth and bioassay with tobacco tissue culture, *Physiol. Plant*. 15: 473-497.
7. Norazlina, N., Rusli, I., Nurhidayah, MS., Salmah, M. and Sobri, H. (2014). *Effects of Acute and Chronic Gamma Irradiation on In Vitro Growth of Stevia rebaudiana Bertoni. Jurnal Sains Nuklear Malaysia (eJSNM). Vol 2, No. 2 (2014): Jurnal Sains Nuklear Malaysia*
8. Philips Green Power LED Research Team (2012).
9. Robinson, B.L. (1930). Contributions from the Grey Herbarium of Harvard University. *The Grey Herbarium of Harvard University, Cambridge.*
10. Saxena, N.C. and Ming, I.S. (1988). Preliminary harvesting characteristics of Stevia, *Phys. Prop. Agic. Mat. Prod*. 3: 299- 303.
11. Shock, C.C. (1982). Experimental cultivation of Rebaudia's stevia in California. Agronomy Progress Report, University of California, 122.
12. Soejarto, D.D., Kinghorn, A.D. and Fransworth, N.R. (1982). Potential sweetening agents of plant origin, *J. Nat. Prod*. 45: 590-599.
13. Yamada, A., Ohgaki, S., Noda, T. and Shimizu, M. (1985). Chronic toxicity study of dietary stevia extracts in F344 rats, *J. Food Hygn. Jap*. 26: 169-183.
14. Yoshida, S. (1986). Studies on the production of sweet substances in *Stevia rebaudiana*: I. Simple determination of sweet glucoside in Stevia plant by thin layer chromate-scanner and their accumulation patterns with plant growth, *Jap. J. Crop. Sci*. 55(2): 189-195.

FP-14

HYPOLIPIDEMIC AND ANTIDIABETIC ACTIVITY OF POLYPHENOL GLYCOSIDE CATALYZED BY TRANSGLYCOSYLATION REACTION OF CYCLODEXTRIN GLUCANOTRANSFERASE DERIVED FROM *TRICHODERMA VIRIDAE* IN DIABETIC RATS

SOHAIB NAZIR KAINTH[1], JOKO SULISTYO SOETIKNO[1]*, AI LING HO[1], AND MUHAMMAD DAWOOD SHAH[2]

[1]Faculty of Food Science and Nutrition, Universiti Malaysia Sabah, Jalan UMS 88400, Kota Kinabalu, Sabah, Malaysia, [2] Biotechnology Research Institute, Universiti Malaysia Sabah, Jalan UMS 88400, Kota Kinabalu, Sabah, Malaysia

[*]Corresponding author: jokosulistyo@ums.edu.my

ABSTRACT

The study aimed to synthesis polyphenol glycoside through enzymatic transglycosylation reaction using cyclodextrin glucanotransferase (CGTase) derived from culture of *Trichoderma viride* in the present of polyphenolic extract of *Moringa oleifera* to evaluate its antioxidant activities of the polyphenol glycoside as transglycosylation product. Chemical structures of the enzymatically synthesized product were identified using nuclear magnetic resonance (^{1}H NMR and ^{13}C NMR) spectroscopy as gallic acid-4-O-β-glucopyranoside (GAGP), ellagic acid-4-O-β-glucopyranoside (EAGP), and catechin-4'-O-glucopyranoside (CGP), respectively. The EAGP was furthermore applied to investigate its effect on hypolipidemic and antidiabetic activity in normal and alloxan-induced diabetic rats. Blood glucose levels were measured significantly ($p<0.05$) increasing in all diabetic rats as compared to normal control rats. Three different dosages of EAGP showed significantly decreasing ($p<0.05$) blood glucose levels of the diabetic rats as compared to untreated diabetic group. All diabetic groups presented significantly lower body weight as compared to normal rats as control. The diabetic groups administered with different dosages of EAGP showed improvement in weight gain as compared to untreated diabetic group. All the hyperglycemic groups which were treated with EAGP recorded lower biochemical parameters of blood serum as compared to untreated diabetic group.

KEY WORDS:
Transglycosylation, Polyphenol glycoside, Antidiabetic, Antioxidant activity

INTRODUCTION:

Diabetes mellitus is a metabolic syndrome of multiple etiologies described by chronic hyperglycemia with disorders of protein metabolism, fat and carbohydrate resulting from problems in insulin action, insulin secretion, or together. The level of hyperglycemia linked with diabetes escalates the danger of micro-vascular damage such as neuropathy, retinopathy and nephropathy. It is related by decreased lifetime expectancy, diminished quality of life, and increased risk of macro-vascular diseases for example peripheral vascular disease, stroke and ischemic heart disease. In 2000, according to the World Health Organization survey it was assessed that 171 million people around the world suffer in diabetes and this is expected to rise to 366 million in 2030.[1]

In conventional medication, side effects are reported in the present therapies of diabetes mellitus. The glucose level depressing medicines include α-glucosidase inhibitors, insulin sensitizers and insulin secretagogues.[2] Moreover the adverse effects connected with use of insulin includes dizziness, headache, digestive discomfort, permanent neurological deficit, idiosyncratic liver cell injury, lactic acidosis, severe

hypoglycemia at high doses and even death. Hence, due to the side effects allied with the existing hypoglycemic medicines, there is necessity to produce cheap, nontoxic and effective medicines for controlling diabetes. Such cheap, safe and effective drugs might be gained by utilizing curative plants which have been practiced by human beings to inhibit or control ailments comprising diabetes mellitus.[3] To the common people in the developed and developing world, these plant based herbal medicines are assumed to be inexpensive, safe and effective.

Moringa oleifera is well known for their pharmacological actions as well and are used for the traditional treatment of diabetes mellitus.[4] Its leaves, fruits and stem bark have been scientifically examined for their use in hypercholesterolaemia.[5-6] Fruits and stem bark have been reported to have anti-diabetic action.[7] It was found to contain many essential nutrients, for instance, vitamins, minerals, amino acids, beta-carotene, antioxidants, and anti-inflammatory nutrients.[8] Due to the presence of several sorts of phenolic compound, it was able to extend the period of food containing fats regarding with its antioxidant activity.[9-10] However, there are no reports on hypoglycaemic and anti-diabetic actions of its leaves.
Phenolic compounds are utilized as an antipruritic or antiseptic in cosmetic products, as a restrainer of melanogenesis, as an antioxidant, as a bacterial growth inhibitor, as a persuasive antimutagent, or as an antitoxic.[11] Nevertheless, polyphenols are of restricted use because they are easily spoiled in an aqueous solution following-on in rapid browning. It was described that a number of physical properties of the polyphenols were enhanced through enzymatic transglycosylation reaction.[12]

Polyphenols are of restricted use because they are easily degraded in an aqueous solution following-on in rapid browning. Nevertheless, although the constituents might have such beneficial properties, however, their use is restricted due to their low stability and solubility and is easily degraded in an aqueous solution following in rapid browning reaction.[13] For that reason, their antioxidant properties were influenced or reduced. It has been found that a number of physical properties of the polyphenols were enhanced through enzymatic transglycosylation reaction.[12] Glycosylation of polyphenols into glycosides have a number of advantages in contrast to chemical synthesis, for example low cost production and its enzyme which is derived from microbial culture as a source of enzyme with transglycosylation capacity can also be produced for the purpose of synthesis of several bioactive compounds due to its easyness and simplicity procedure.

Cyclodextrin glucanotransferase (CGTase, EC 2.4.1.19) is an enzyme which has transglycosylation ability in synthesizing a transfer product such kind of arbutin and alsocapable to convert starch into cyclodextrins and glycosides through intramolecular reactions and transferring glycosyl groups to an acceptor which has an OH-group.[14] On the other side, the chemical synthesis of glycosides is not only complex and complicated, but also expensive. Moreover it is not as simple as enzymatic reaction since it generates a complex mixture ofproducts with α- and β-configuration. Enzymatic transglycosylation permits insoluble and less stable organic bioactive compounds to be changed into the resultant soluble and more stable compounds during suitable single-step glycosylation.[15] The clinical importance of polyphenol glycosides is one of the pharmacological interests.[16]

The aim of the study was to investigate a purified and identified ellagic acid-4-O-β-D-glucopyranoside (EAGP) as enzymatically synthesized polyphenol glycoside that had been obtained by application of CGTase derived from *T. viride* in the present of polyphenolic extract of *Moringa oleifera* leaves, dealing with its capability as antioxidative, hypolipidemic and antidiabetic agents using animal model experiment.

MATERIAL AND METHODS:

Extraction of Polyphenols

Extraction of polyphenolic compounds was done by following the method of Charoensin[17] with slight modification. The leaves of *M. oleifera* (1.0 kg dried base weight) that had been purchased from a local market were dried in hot air oven at 50°C for 72 h and ground to powder (approximately 600 g) and preserved at 4°C until extraction. Fifteen grams of the powder was extracted with 350 ml of methanol and

the liquid extract was filtered through Whatman no. 1 filter paper. Solvent was removed by using rotary evaporator and extract was freeze dried to obtain crude polyphenol powder (approximately 30 g).

Isolation and Purification of Synthesized Glycosides

A reaction mixture (200 ml) containing polyphenolic constituents of *M. oleifera* used as substrate-acceptor and wheat flour as substrate-acceptor (2.5%, w/v) and a commercial wheat flour (5.0%, w/v) as substrate-donor were incubated with *T. viride* CGTase at 40ºCfor 24h as the same procedure mentioned above prior to extraction with diethyl ether to remove excess of polyphenolic residue, while the constituents of glycosides as transfer product might allegedly be remained in water phase was concentrated and furthermore charged onto column chromatography containing octa-dodecyl-silica (ODS). The column chromatography was then eluted with gradient solvent of methanol in 1% formic acid (v/v). Fraction solutions resulted by flushing the column that is exhibited single spots on TLC plate within their RF values were parallel to the spot of arbutin as an authentic reference of commercial polyphenol glycoside were then collected and concentrated.[18]

HPLC analysis and Structure Identification by NMR spectroscopy

The purified transfer products were also analyzed by using HPLC. The HPLC/UVVIS system was comprised of Agilent HPLC system provided with a pump, an automatic injector, a UV-VIS detector and a degasser. Separations were carried out using Apollo C18 reverse-phase column at a room temperature. Acetonitrile (A) and 0.1% aqueous H_3PO_4 (B) was used as a mobile phase with a gradient elution. The separation was monitored through absorbance at 254 nm at flow rate of 0.5 ml/min. [19] The ^{1}H-NMR, ^{13}C-NMR spectra were measured using a Varian XL-400spectrometer in DMSO solution as a polar solvent that dissolves both polar and nonpolar compounds and is miscible in a wide range of organic solvents as well as water.[20]

Animal model experiment

Male Sprague-Dawley rats weighing about 100 to 200g, obtained from Faculty of Food Science and Nutrition, Universiti Malaysia Sabah, were used. The animals were housed in colony plastic cages at ambient temperature of 25°C-27°C under a 12 h light/dark cycle and free admittance to standard rat diet and tap water. The rats were allowed to adapt to the laboratory environment for one week before starting the experiment. All the experimental procedures were performed according to the ethical guidelines for the use and care of laboratory animals.

Induction of diabetes

Diabetes mellitus was induced by a single intraperitoneal injection of alloxan monohydrate freshly prepared at a dose of 150 mg/kg, BW. After alloxan injection, tap water was changed with a 5% glucose solution in order to control severe hypoglycemia caused by alloxan as a result of β cells destruction and excessive release of insulin.[21] After injection, the blood glucose level of the overnight fasted animals was checked by the use of glucometer for evidence of a diabetic state. The animals that displayed glucose levels higher than 200 mg/dl were considered as diabetic rats and furthermore included in the study.[22]

Treatment protocol

Twenty five rats were randomly divided into five groups (5 rats in each group); Group-1, Normal untreated rats were given distilled water; Group-2, Diabetic untreated rats were given distilled water; Group-3, Diabetic rats were given EAGP at a dose of 100 mg/kg, BW. Group-4, Diabetic rats were given EAGP at a dose of 200 mg/kg, BW; Group-5, Diabetic rats were given EAGP at a dose of 400 mg/kg, BW. Distilled water and drug preparations were served orally by gastric intubation to the rats of respective groups using force feeding needle, once daily for four weeks.

Collection of blood samples

All five groups of rats were sacrificed on the last day of treatment after overnight fasting and the blood sample of each animal was collected from cardiac punctures after cervical dislocation before their heartbeats stop. The blood glucose levels were determined at different day intervals by using glucometer and blood was

collected from tail vein. The blood samples were collected in separated BD Vacutainer® Blood Collection Tubes. The blood samples were centrifuged at 1375 xg for 20 min and the serum was separated.

Determination of catalase activity

Catalase activity was determined by following the method of Pari and Latha[23]. The percent catalase inhibition was determined by monitoring decrease in absorbance at 620 nm. The pancreas was homogenized and centrifuged at 5000rpm in 0.01M phosphate buffer (pH 7.0). The reaction mixture comprised of 0.4 ml of H_2O_2 (0.2M), 1 ml of 0.01M phosphate buffer having pH 7.0 and 0.1ml of pancreas homogenate (10% w/v). The reaction was stopped by addition of 2 ml reagent (5% $K2Cr_2O_7$ prepared in glacial acetic acid). The changes in absorbance were observed at 620 nm. Percent catalase inhibition was analyzed as followed; [(normal activity – inhibited activity) / (normal activity)] × 100.

Determination of reduced glutathione activity (GSH)

Modified method of Oyedemi et al[24] was used to determine the reduced glutathione. One ml supernatant of pancreas homogenate was treated with 0.5 ml of Ellman's reagent (19.8 mg of 5, 5'-dithiobisnitro benzoic acid in 100 ml of 0.1 % sodium nitrate) and 3 ml of phosphate buffer (0.2 M, pH 8.0). The absorbance was recorded at 412 nm and percent inhibition of reduced glutathione was calculated as followed; % GSH inhibition = $(A_o - A_1)/A_o \times 100$, where; A_o is the absorbance of the control and A_1 is the absorbance of the sample extract.

Assessment of lipid peroxidation

Lipid peroxidation was determined colorimetrically by thiobarbituric acid reactive substances (TBARS). Briefly, 0.1 ml of pancreas homogenate (10% w/v) was treated with 2 ml of (1:1:1 ratio) TBATCA- HCl reagent (thiobarbituric acid 0.37%, 15% trichloroacetic acid and 0.25 N HCl). All the tubes were kept in water bath at 100 ^{0}C for half hour and cooled. The amount of malondialdehyde (MDA) produced in all samples was calculated by evaluating the absorbance of supernatant at 535nm against blank (Oyedemi et al., 2010). Percent inhibition was computed using the following equation; Percent inhibition = $\{A_o - A_1\}/Ao \times 100$, where; A_o is the absorbance of the control and A_1 is the absorbance of the sample extract

Determination of biochemical parameters

Biochemical parameters including total cholesterol, triglycerides, low-density lipoprotein, high-density lipoprotein, creatinine, urea and alkaline phosphatase levels in blood plasma were measured using special kits (Abbott Laboratories, USA) which utilized the colorimetric method in an auto-analyzer.[25] Twenty five rats were randomly divided into five groups (5 rats in each group); Group-1, Normal untreated rats were given distilled water; Group-2, Diabetic untreated rats were given distilled water; Group-3, Diabetic rats were given EAGP at a dose of 100 mg/kg, BW. Group-4, Diabetic rats were given EAGP at a dose of 200 mg/kg, BW; Group-5, Diabetic rats were given EAGP at a dose of 400 mg/kg, BW. Distilled water and drug preparations were served orally by gastric intubation to the rats of respective groups using force feeding needle, once daily for four weeks. All five groups of rats were sacrificed on the last day of treatment after overnight fasting and the blood sample of each animal was collected from cardiac punctures after cervical dislocation before their heartbeats stop. The blood glucose levels were determined at different day intervals by using glucometer and blood was collected from tail vein. The blood samples were collected in separated BD Vacutainer® Blood Collection Tubes. The blood samples were centrifuged at 1375 xg for 20 min and the serum was separated.

Statistical analysis

The values were expressed as mean± S.E.M. Data were analyzed using One-way ANOVA followed by Tukey B test. P value <0.05 was considered as significant.[26]

RESULTS AND DISCUSSION:

Purification and structural identification of transglycosylation products

Enzyme catalyzed synthesis of polyphenolic glycosides, as transglycosylation products of crude *M. oleifera* leaves extract, were purified using ODS column chromatography followed by structural identification on the

basis of spectroscopic techniques. According to the analysis using ^{13}C-NMR and ^{1}H-NMR spectra, the isolated compounds were identified as gallic acid-4-O-β-glucopyranoside (GAGP), ellagic acid-4-O-β-glucopyranoside (EAGP) and catechin-4'-O-glucopyranoside (CGP), respectively (Fig. 1). These chemical structures were corresponded to composition of *M. oleifera* leaves extract where it contains approximately 10-11% gallic acid, 5-6% ellagic acid and 2-3% catechin.[27] The ^{1}HNMR and ^{13}CNMR spectrum of compound GAGP revealed the presence of glycosidic bond in gallic acid glucopyranoside. The broad singlet at δ_H 7.03 corresponds to the two protons of the aromatic ring. The ^{13}CNMR showed one signal resonating at δc 114.96, which could be attributing to C-4. The shifting of this signal to the higher field confirms the glycosidic linkage at C-4. The presence of signal at δc 123.6 corresponds to C-2 and C-6 while the signal at 138.9 corresponds to C-3 and C-5 reveals that aromatic ring of GAGP have plane of symmetry. More signals are provided in Table 1. Gallic acid-4-O-β-glucopyranoside: IRKBr (ν_{max}/cm^{-1}):^{1}H-NMR (500 MHz; CD_3OD-d_4/ppm) δ: 7.03 (1H, bs, H-3), 7.03 (1H, bs, H-7), 4.35 (1H, d, J 7.8 Hz, H-1′), 4.26 (1H, dd, J 8.3, 7.8 Hz, H-2′), 3.26 (1H, dd, J 9.3, 8.3 Hz, H-3′), 4.33 (1H, dd, J 9.3, 9.3 Hz, H-4'), 3.37 (1H,m, H-5′), 4.06 (1H, dd, J 11.3, 5.6 Hz, H-6′α), 4.37 (1H, bd, J11.3 Hz, H-6′β).^{13}C-NMR spectrum (125MHz; DMSO-d_6/ppm): 166.2 (C-1),123.6 (C-2),108.8 (C-3),144.96 (C-4), 138.9 (C-5), 144.9 (C-6), 108.8 (C-7), 101.9 (C-1′), 73.8 (C-2′), 78.4 (C-3′), 71.1 (C-4′), 79.9 (C-5′), 63.9 (C-6′) (Fig. 1.A). Moreover, GAGP was furthermore used to apply for its functional properties including its effect as antioxidative, hypolipidemic and antidiabetic agents through *in vivo* and *in vitro* experiments.

Blood glucose levels

As shown in Table 1, diabetic control group rats which were induced with alloxan showed significant difference ($p<0.05$) in blood glucose levels throughout the study as compared to the normal control group rats probably due to the rapid action of alloxan since it results in rapid depletion of beta cells by DNA alkylation and accumulation of cytotoxic free radicals. In present study, three different dosages of EAGP at a concentration of 100 mg/kg, 200 mg/kg and 400 mg/kg of body weight showed significant difference ($p<0.05$) at day-8 of treatment in blood glucose levels in alloxan induced diabetic rats compared to diabetic control group. This may be due to the functional properties of EAGP as antidiabetic agent. However, there is also significant difference ($p<0.05$) between the blood glucose levels of the EAGP treated diabetic rats as compared to the diabetic control group from day-12 to end of study. In contrast, blood glucose levels of untreated diabetic rats remained elevated throughout the experiment.

Body weight

As shown in Fig. 2, this study demonstrated that all diabetes induced groups had significantly lower body weight as compared to the normal control group after alloxan injection on day-4. The decrease in BW is reported as a marker for the development of diabetes since the BW in diabetic animals' decreases due to the impairment in insulin action in transforming glucose into glycogen and catabolism of fats, beta cell destruction causes unavailability of lipolysis. However, there was significant difference ($p<0.05$) recorded in BW of treated diabetic groups at day-4 as compared to the diabetic control group. The diabetic groups treated with different concentrations of EAGP showed slight increment on BW throughout the experiment. The increase in BW of treated diabetic groups could be due to the preventive action of EAGP on the damage due to severe breakdown of muscle fats, tissues, and metabolism of protein in diabetic state.

Blood serum profile

As shown in Table 2, alloxan treatment will increase the chemical composition levels of serum such as alkaline phosphatase, urea, creatinine, LDL, cholesterol and decrease the HDL level. But, treatment with the EAGP reversed the alloxan induced changes. Serum of triglyceride, cholesterol, alkaline phosphatase, urea, HDL, LDL and creatinine levels were significantly decreased ($p<0.05$) as compared to the diabetic control group. Treatment with this EAGP improved the diabetes mellitus conditions as indicated by the parameters of serum profile.

Catalase activity

Catalase is one of an important enzyme in antioxidant system that plays crucial scavenger enzyme which can be found in peroxisomes. Furthermore, catalase is kind of hemoprotein which breaks down the harmful

H_2O_2 into O_2 and H_2O which guards the tissue from highly reactive hydroxyl radicals. In this investigation, catalase levels were found to decline as compared to diabetic control group, this might be due to inhibition of the enzyme. In contrast, treatment with EAGP demonstrated improved enzymatic activity towards the normal in various dosages. Therefore, result showed that EAGP has the ability to counter back the oxidative damage in alloxan induced hyperglycemic rats with increase in enzymatic activity, Additionally, there is significant difference ($p<0.05$) present among all the groups as compared to normal control as shown in Table 3.

Reduced glutathione (GSH)

Reduced glutathione or commonly known as GSH is the smallest intracellular molecules with low molecular thiol antioxidant that are ubiquitous in a living environment. GSH occurs naturally in all type of cells and plays important role in cell protection and act as a crucial defense against free radicals. In this research work, diabetic control group showed significantly reduced GSH level in pancreatic tissue compared to normal control group. On the other hand, administration of EAGP at various dosages to alloxan induced diabetic rats showed significant improvement in GSH levels near to normal as compared to normal control and diabetic control, Although, there is significant difference ($p<0.05$) among the groups as presented in Table 4.

Lipid peroxidation (LPO)

Lipid peroxidation can be defined as the oxidative deterioration of unsaturated fatty acids. Lipid peroxidation produces numerous products, which some of them are electrophiles.[24] One of the lipid peroxidation substance that is commonly used as a biomarker for tissue damage is the reactive aldehyde, malondialdehyde (MDA). MDA is a byproduct that generates naturally during the process of lipid peroxidation. As shown in Table 5, there was significant difference ($p<0.05$) between the diabetic groups as compared to the normal control group. Tissue lipid peroxidation in diabetic groups was increased as compared to control group because alloxan induces high level of MDA in diabetic animals which might be due to high glucose stress in diabetes which promoted production of reactive oxygen species that react with polyunsaturated fatty acids inside the cell membrane leading to increase in MDA level. In this study, significantly reduced lipid peroxidation was recorded in the groups administered with the different dosages of EAGP that almost attained to normal level as compared to untreated diabetic group.

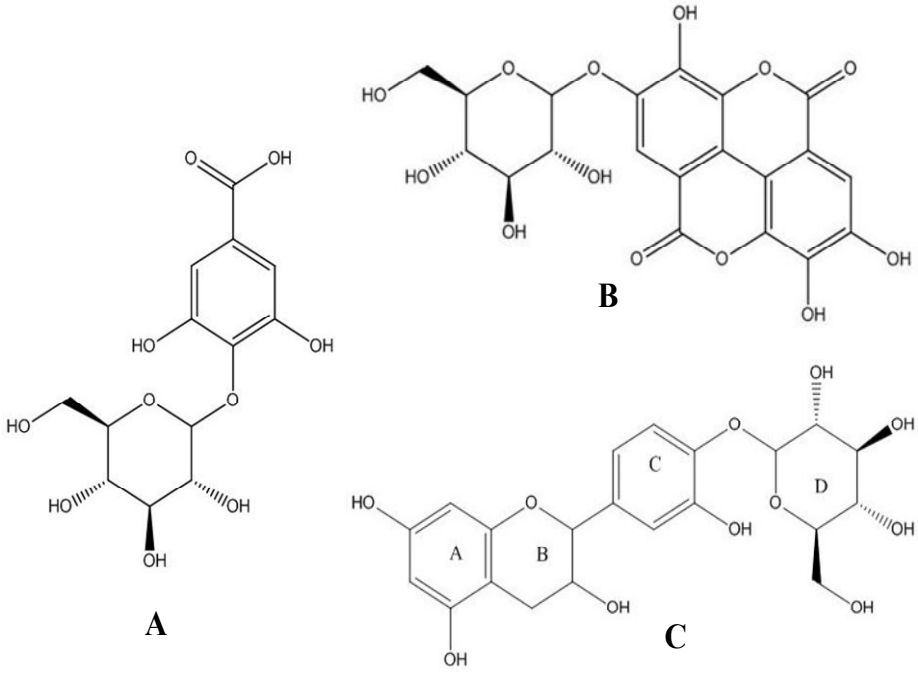

Figure 1
Chemical structure of gallic acid-4-O-β-D-glucopyranoside (A); ellagic acid-4-O-β-D-glucopyranoside (B); catechin-4'-O-β-D-glucopyranoside (C).

Table 1
Effect of administration of EAGP on blood glucose level

Group	Day-0 (mg/dl)	Day-4 (mg/dl)	Day-8 (mg/dl)	Day-12 (mg/dl)	Day-16 (mg/dl)	Day-20 (mg/dl)	Day-24 (mg/dl)	Day-28 (mg/dl)
Control (-) Rats	69.6±1.50[a]	70.8±1.42[a]	71.6±1.36[a]	72.2±1.46[a]	72.8±1.15[a]	73.4±0.92[a]	74.8±1.15[a]	75.6±1.07[a]
Control (+) Rats	208.6±2.73[b]	210.8±2.59[b]	234.0±5.76[c]	254.8±5.85[c]	276.0±3.86[c]	292.6±3.14[c]	315.0±5.30[c]	337.8±5.45[c]
+ EAGP (100mg)	211.0±3.24[b]	213.0±3.03[b]	214.6±2.71[b]	213.8±3.00[b]	212.0±2.93[b]	210.6±2.99[b]	209.4±2.98[b]	208.6±2.76[b]
+ EAGP (200mg)	217.8±3.20[b]	219.7±3.12[b]	221.2±3.32[bc]	219.7±3.21[b]	217.2±3.27[b]	215.7±3.20[b]	214.2±2.88[b]	212.8±3.02[b]
+ EAGP (400mg)	214.2±3.78[b]	215.8±3.78[b]	216.7±4.04[b]	214.6±3.86[b]	211.8±3.54[b]	209.5±3.14[b]	207.6±2.99[b]	205.7±3.23[b]

Values are expressed as mean ± SEM of n=5 (P< 0.05

Table 2
Effect of administration of EAGP on blood serum profile

Group	Triglyceride (mmol/L)	Cholesterol (mmol/L)	HDL (mmol/L)	LDL (mmol/L)	Creatinine (umol/L)	Urea (mmol/L)	Alkaline phosphate (u/L)
Control (-) Rats	1.23±0.06[a]	1.33±0.07[a]	0.79±0.03[b]	0.07±0.01[a]	21.8±1.66[a]	4.78±0.17[a]	341.6±21.20[a]
Control (+) Rats	1.68±0.20[b]	1.48±0.06[b]	0.58±0.04[a]	0.16±0.05[b]	30.0±1.14[b]	7.44±0.24[c]	473.8±58.30[b]
EAGP (100mg)	1.57±0.03[a]	1.47±0.08[a]	0.69±0.01[ab]	0.14±0.08[a]	28.26±1.09[ab]	6.92±0.15[bc]	441.8±24.41[a]
EAGP (200mg)	1.47±0.08[a]	1.42±0.05[a]	0.70±0.04[ab]	0.14±0.03[a]	27.36±2.33[ab]	6.78±0.44[bc]	439.4±37.26[a]
EAGP (400mg)	1.34±0.17[a]	1.39±0.04[a]	0.72±0.05[ab]	0.12±0.02[a]	26.66±1.47[ab]	6.32±0.14[b]	405.7±21.17[a]

Values are expressed as mean ± SEM of n=5 (P< 0.05)

Table 3
Effect of administration of EAGP on catalase activity

Group	µmoles H_2O_2/min/mg protein
Normal Control (Normal rats treat with distilled water)	32.70±0.62[d]
Diabetic Control (Diabetic rats treated with distilled water)	8.25±0.65[a]
Diabetic rats treated with EAGP (100mg/kg of BW)	12.56±0.27[b]
Diabetic rats treated with EAGP (200mg/kg of BW)	14.70±0.46[b]
Diabetic rats treated with EAGP (400mg/kg of BW)	18.85±0.82[c]

Values are expressed as mean ± SEM of n=5 (P< 0.05)

Table 4

Effect of administration of EAGP on reduced glutathione level (GSH)

Group	GSH (µmol reduced GSH/g tissue)
Normal Control (Normal rats treat with distilled water)	5.74±0.15^{c}
Diabetic Control (Diabetic rats treated with distilled water)	3.84±0.31^{a}
Diabetic rats treated with EAGP (100mg/kg of BW)	4.97±0.06^{b}
Diabetic rats treated with EAGP (200mg/kg of BW)	5.19±0.12^{bc}
Diabetic rats treated with EAGP (400mg/kg of BW)	5.64±0.05^{c}

Values are expressed as mean ± SEM of n=5 (P< 0.05)

Table 5

Effect of administration of EAGP on lipid peroxidation

Group	LPO (nmol MDA formed/g tissue)
Normal Control (Normal rats treat with distilled water)	39.90±0.35^{a}
Diabetic Control (Diabetic rats treated with distilled water)	58.96±0.50^{d}
Diabetic rats treated with EAGP (100mg/kg of BW)	46.26±0.92^{c}
Diabetic rats treated with EAGP (200mg/kg of BW)	43.25±0.12^{b}
Diabetic rats treated with EAGP (400mg/kg of BW)	41.81±0.16^{b}

Values are expressed as mean ± SEM of n=5 (P< 0.05)

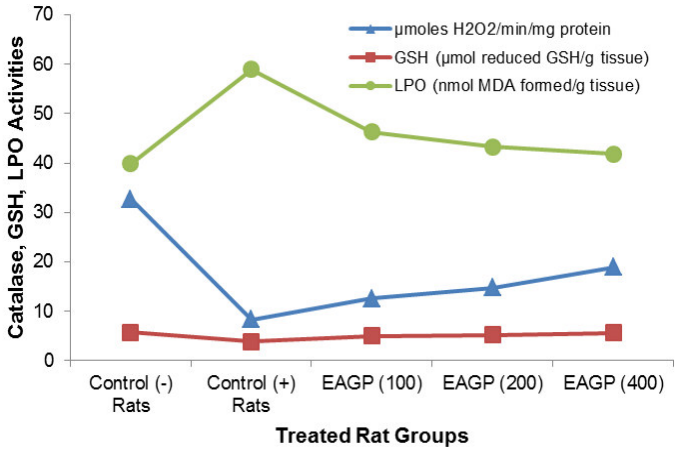

Graph 1

Effect of administration of EAGP on catalase, glutathione and lipid peroxidation activities

CONCLUSION:

Fungal culture *T. viride* has shown transglycosylation reaction through activity of CGTase on *M. oleifera* polyphenol constituents to synthesize polyphenol glycosides. Analysis of ^{1}H and ^{13}C NMR of the isolated polyphenol glycosides, established the chemical structures of gallic acid-4-O-β-glucopyranoside (GAGP), ellagic acid-4-O-β-glucopyranoside (EAGP) and catechin-4'-O-glucopyranoside (CGP). The EAGP was assayed for its anti-diabetic and antioxidant potential activities. The results show that *in vivo* treatment with EAGP reversed alloxan induced diabetes. Serum triglyceride, cholesterol, alkaline phosphatase, urea, HDL, LDL and creatinine levels were significantly decreased ($p<0.05$) as compared to the diabetic control group. Additionally, EAGP showed significant improvement in GSH levels near to normal and significantly reduced lipid peroxidation that is almost attained to normal level as compared to untreated diabetic group.

ACKNOWLEDGEMENT:

This work was financially supported by UMS Research Grant 2015, under the Universiti Malaysia Sabah. We are also thankful to Institute for tropical biology and conservation, Universiti Malaysia Sabah, Kota Kinabalu, Malaysia for NMR Spectroscopy analysis services.

REFERENCES:

1. Nicasio P, Aguilar-Santamarıa L, Aranda E, Ortiz S, Gonzalez M. Hypoglycemic effect and chlorogenic acid content in two Cecropia species. Phytother. Res. 2005. 19:661–664.
2. Suman BS, Afreena N, Krishna MP, Pothapragada SM. Antihyperglycemic effect of the fruit-pulp of Eugenia jambolana in experimental diabetes mellitus. J. Ethnopharmacol. 2006. 104:367–373.
3. Kameswara RB, Renuka SP Raja S. Antidiabetic activity of Terminalia pallida fruit in alloxan-induced diabetic rats. J. Ethnopharmacol. 2003. 85:169-172.
4. Babu R, Chaudhuri M. Homewater treatment by direct filtration with natural Coagulant. Journal of Water and Health. 2005. 3:27–30.
5. Ghasi S, Nwobodo E, Ofili JO. Hypocholesterolemic effects of crude extract of leaf of *Moringa oleifera* Lam. in high-fat diet fed wistar rats. J. Ethnopharmacol. 2000. 69:21–25.
6. Mehta K, Balaraman R, Amin AH, Bafna PA Gulati OD. Effect of fruits of *Moringa oleifera* on the lipid profile of normal and hypercholesterolemic rabbits. J. Ethnopharmacol. . 2003. 86:191–195.
7. Kar A, Choudhary BK Bandyopadhyay NG. Comparative evaluation of hypoglycemic activity of some Indian medicinal plants in alloxan diabetic rats. J. Ethnopharmacol. 2003. 84:105–108.
8. Kasolo JN, Bimenya GS, Ojok L. Phytochemicals and uses of *Moringa oleifera* leaves in Ugandan rural communities. J. Med. Plant Res. 2010. 4:753-757.
9. Dillard CJ, German JB. Review Phytochemicals: nutraceuticals and human health. J. Sci. Food Agric. 2000. 80:1744-1746.
10. Siddhuraju P, Becker K. Antioxidant properties of various solvent extracts of total phenolic constituents from three different agroclimatic origins of drumstick tree (*Moringa oleifera* Lam.) leaves. J. Agric. Food Chem. 2003. 51:2144-2155.
11. Sulistyo J, Yanuar Y, Suryanegara L. Antitoxic Activities of Enzymatically Synthesized Catechin Glucoside. BioSMART. 2002. 4:6-10.
12. Sulistyo J, Dinoto A, Handayani R. Inhibitory activity of enzymatically synthesized polyphenol glucosides against melanogenesis and mutagenesis. BioSMART. 2001. 3:1-6.
13. Sulistyo J, Handayani R, Rahayu RD. Assay for transglycosylation reaction of *Xanthomonas campestris* on carbohydrate sources. IJRAFS. 2014. 2:1-7.
14. Komentani T, Terada Y, Nishimura T, Nakae T, Takii H, Okada S. Acceptor specificity of cyclodextrin glucanotransferase from an alkalophilic Bacillus spesies and synthesis of glucosyl rhamnose. Biosci. Biotech. Biochem. 1996. 60:1176-1178.
15. Shimoda K, Kondo Y, Abe K, Hamada H, Hamada H. Formation of water soluble vitamin derivatives from lipophilic vitamins by cultured plant cells. Tetrahedron Lett. 2006. 47:2695–2698.

16. Satoh T, Miyataka H, Yamamoto K, Hirano T. Synthesis and Physiological Activity of Novel Tocopheryl Glycosides. Chem. Pharm. Bul. 2001. 49:948–953.
17. Charoensin S. Antioxidant and anticancer activities of *Moringa oleifera* leaves. J Med Plant Res. 2014. 8:318-325.
18. Hashmi MI, Nazir S, Sulistyo J. Antimelanogenesis activity of polyphenol glycoside synthesized by transglycosylation reaction of CGTase from *Xanthomonas campestris*. IJRAFS. 2014. 2:1-8.
19. Chiang HM, Lin YT, Hsiao PL, Su YH, Tsao HT, Wen KC. Determination of Marked Components-Aloin and Aloe-Emodin-In Aloe Vera before and After Hydrolysis. J Food Drug Anal. 2012. 20(3):646-652.
20. Shimoda K Hamada H, Enzymatic synthesis and anti-allergic activities of curcumin oligosaccharides. Biochem. Insights. 2010. 3:1–5.
21. Stanely M, Prince P, Kamalakkannan N, Menon PV. Antidiabetic and anti hyperlipidaemic effect of alcoholic Syzigiumcumini seeds in alloxan induced diabetic albino rats. J. Ethnopharmacol. 2004. 91: 209–213.
22. Manickam D, Periyasamy L. Antidiabetic effect of methanolic extract of *Decalepis hamiltonii* root in normal and alloxan-induced diabetic rats. J. Pharm. Res. 2013. 6:166–172.
23. *Pari L, Latha M. Protective role of Scopariadulcis plant extract on brain antioxidant status and lipid peroxidation in STZ diabetic male Wistar rats. BMC Complement. Altern. Med. 2004. 4:1-8.*
24. Oyedemi SO, Bradley G, Afolayan AJ. In vitro and vivo antioxidant activities of aqueous extract of *Strychnos henningsii* Gilg. AJPP. 2010. 4:070-078.
25. Cherbal A, Kebieche M, Yilmaz E, Aydoğmuş Z, Benzaouia L, Benguessoum M, Benkedidah M, Madani K. Antidiabetic and hypolipidemic activities of Algerian PistachialentiscusL. leaves extract in alloxan-induced diabetic rats. S. Afr. J. Bot. 2017. 108:157–162.
26. Bhargavi G, Josthna P, Naidu CV. Changes in serum biochemical parameters and lipid profile in normal and STZ induced diabetic rats with administration of ethanolic extract of *Polyalthia cerasoides* stem barks. IRJP. 2015. 6:153-156.
27. Nazir S, Sulistyo J, Hashmi MI, Ho AL, Khan MS. Enzymatic Synthesis of Polyphenol Glycosides Catalyzed by Transglycosylation Reaction of Cyclodextrin Glucanotransferase Derived from *Trichoderma viride*. J. Food Sci. Tech. 2018. 1-8. DOI:10.1111/jfbc.12499.).

FP-15

STUDY ON THE COSMECEUTICAL ACTIVITIES AND BIOACTIVE COMPOUNDS OF RICE BRAN FERMENTED WITH *Amylomyces rouxii*

AMSAL ABD GHANI*, ANISAH JAMALUDDIN, DANG LELAMURNI ABD RAZAK, NUR YUHASLIZA ABD RASHID, AZLINA MANSOR, MUSAALBAKRI ABDUL MANAN

Enzyme and Fermentation Technology Programme, Biotechnology and Nanotechnology Research Centre, MARDI, G.P.O Box 12301, 50440 Kuala Lumpur, Malaysia

*Corresponding author: amsal@mardi.gov.my

ABSTRACT

Demand for cosmeceutical products from natural ingredients has considerably increased worldwide and fermentation could be one tool that enhances the activity of the natural ingredient. Hence, this study was aimed to evaluate the cosmeceutical activities of rice bran fermented with *Amylomyces rouxii* (RBFAR). Solid state fermentation (SSF) of rice bran with *A. rouxii* was carried out for 20 days at 32°C with 50% initial moisture content. The results showed that water extract of RBFAR exhibited potent inhibitory effects on elastase (46.66%) and improved the inhibitory effects on tyrosinase (69.52%) in comparison with the unfermented substrate (8.57%) showing its potential as anti-aging and whitening agent, respectively. Besides, a three-fold increase of antioxidant activities of RBFAR has also been detected on day 20 of fermentation (152.7%). The total phenolic content was also improved upon the fermentation. Additionally, High-Performance Liquid Chromatography (HPLC) analysis showed gallic acid (50.65 µg/g) and kojic acid (79 µg/g) that are widely used for cosmeceutical purposes was identified after fermentation and increased almost to 2000-fold, respectively. This study validated the strong cosmeceutical potential of *A. rouxii* – fermented rice bran extract and it could be further exploited as natural and effective cosmetics ingredient.

KEY WORDS: Cosmeceutical, Elastase, Tyrosinase, Antioxidant, Phenolic acids, Solid state fermentation

INTRODUCTION:

Demand for cosmeceutical products from natural ingredients has considerably increased worldwide. Numerous cosmeceutical products nowadays have been incorporated with active ingredient derived from agricultural by-product as they are generally regarded as natural, safe, and rich in valuable compounds. Rice bran is one the most abundant agricultural by-product and currently its utility remains limited to the production of bran oil and animal feed. Rice bran contains high nutritive value and has been recognized as an excellent source of nutrients including 20% oil, 15% protein, 50% carbohydrate dietary fibers like beta-glucan[1], and bioactive compounds including oryzanol[2], ferulic acid[3], tocotrienols[4], and phytosterols.[5] These several unique properties could render its suitability for niche markets like cosmeceutical, nutraceutical and pharmaceutical industry.

Multiple scientific reports have confirmed that solid state fermentation (SSF) is a biotechnology tool that can enhance the biological activity and improve biological compounds of many plant substrates including rice bran. SSF of rice bran has led to the production of enzymes including amylase[6], protease[7] and beta-glucosidase[8], as well as secondary metabolites such as griseofulin[9]. Moreover, a study by Oliveira *et al.*,[10] also showed that SSF has increased the phenolic acids and antioxidative activity of rice bran.

Amylomyces is a monotypic genus, composed of the single species, *Amylomyces rouxii*.[11] For centuries, the species has been generally used as an important constituent of starter cultures to produce Asian fermented food such as "tapai" and rice wine.[12] However, the study on the potential of *A. rouxii* in cosmeceutical activities particularly using rice bran as the growth medium is not yet available. Thus, in this study,

cosmeceutical related activities including tyrosinase inhibition, elastase inhibition, antioxidant, and total phenolic content of rice bran during SSF at 32°C for 20 days with 50% moisture content were examined. Furthermore, their bioactive compound contents including phenolic acids and organic acids were also investigated.

MATERIALS AND METHODS:

Materials and chemicals

Rice bran was obtained from Padiberas Nasional Berhad (BERNAS, Selangor, Malaysia). *Amylomyces rouxii* (strain F0040) was obtained from Collection of Functional Food Culture (CFFC, MARDI, Serdang, Malaysia). The stock culture was grown on potato dextrose agar (PDA) and maintained at 32°C. Mushroom tyrosinase, porcine pancreatic elastase, L-3,4-dihydroxyphenylalanine (L-DOPA), dimethyl sulfoxide (DMSO), kojic acid, 2,2-diphenyl-1-picrylhydrazyl (DPPH), Folin–Ciocalteu phenol, standards for the five organic acids (oxalic, citric, kojic, succinic and acetic acids) and five phenolic acids (gallic, protocatechuic, p-hydroxybenzoic, vanillic and caffeic acid) were purchased from Sigma Chemical Co. (St. Louis, MO, USA). All other reagents were of the highest grade available unless otherwise indicated.

Solid state fermentation and sample extraction

Rice bran (30 g) was weighed in 250 ml Erlenmeyer flasks and autoclaved. Then, the moisture content of the rice bran was adjusted to 50% with sterilized distilled water. Next, 1% of fungal spores (10^6 spores/ml) was inoculated into the flask, mixed well and incubated at 32°C for 20 days. Each experiment was performed in triplicate. Non-fermented rice bran was used as a control. The subsamples were then harvested and dried at 50°C for 24 h before they were extracted with distilled water and filtered through Whatman No. 1 filter paper. The filtrates were kept at -20°C for further analysis.

Tyrosinase inhibition assay

Tyrosinase inhibition activity was performed using the dopachrome method with L- DOPA as the substrate, according to the method by Alam *et al*.,[13] with minor modifications. 40 µl of 10 mM L-DOPA solution, 40 µl of mushroom tyrosinase (31 U/ml), 80 µl of 0.1 M phosphate buffer (pH 6.8) and 40 µl of the test sample solution were mixed. Then, the mixture was incubated at 25°C for 5 min and absorbance was measured at 475 nm using the microplate reader (Versamax). Each sample was accompanied by a blank containing all components except L-DOPA. Kojic acid was used as positive controls. The results were compared with a control consisting of 50% DMSO. The percentage of tyrosinase inhibition was calculated as follow:

$$\text{Tyrosinase inhibition (\%)} = [(A_{control} - A_{sample}) / A_{control}] \times 100$$

Elastase inhibition activity

The elastase inhibition activity was measured with EnzChek Elastase Assay Kit (Invitrogen Life Technologies Inc., USA) according to the manufacturer's recommendations. 50 µl of sample or positive control was mixed with 100 µl of porcine pancreatic elastase (0.5 U/ml). The mixture was then incubated at room temperature away from light for 15 min. About 50 µl of 25 µg/ml DQ™ elastin working solution was added into the mixture, which served as a substrate. The mixture was then incubated for 30 min at room temperature in the dark and measured at 505/515 nm (Ex/Em) using a fluorescent microplate reader. Percent inhibition of elastase activity was calculated as follow:

$$\text{Elastase inhibition (\%)} = [(A_{control} - A_{sample}) / A_{control}] \times 100$$

1, 1-diphenyl-2-picrylhydrzyl (DPPH) radical scavenging assay

This assay was carried out according to Thaipong *et al*.,[14] with some modifications. A 150 µl aliquot of extract was allowed to react with 2850 µl of fresh DPPH working solution for 30 min in the dark. Percentage of scavenging activity was determined using the following equation:

$$\text{DPPH radical scavenging activity (\%)} = [(A_{blank} - A_{sample}) / A_{blank}] \times 100$$

Total phenolic content

The total phenolic content was determined according to The Folin–Ciocalteu methodology. A 1 ml aliquot of the samples was allowed to react with 5 ml of Folin–Ciocalteu phenol reagent and 4 ml of 7.5% sodium carbonate solution for 2 h at room temperature and in dark condition. Absorbance was measured at 765 nm using a spectrophotometer and the results were expressed as mg gallic acid equivalent (GAE) / gram sample.

Determination of bioactive compound content

The phenolic acids and organic acid in samples were determined using HPLC Alliance Separation Module (Waters 2695), equipped with a diode array detector (Waters, 2996). A 10 µl aliquot of sample solution was separated using a reverse–phase analytical column (150 mm x 4.6 mm XBridge C18, 3.5 µm, Waters) with the temperature controlled at 25°C. The mobile phase consisted of mobile phase A (0.1% formic acid) and mobile phase B (methanol) with a flow rate of 0.7 ml/min. The detector was set at λ=280 nm, and λ=306 nm. Meanwhile, for the determination of organic acid, a reversed phase (250 mm x 4, 6 mm, Extrasil ODS 5 µm) column was used, using the mobile phase of 50 mM phosphate solution. The flow rate of the mobile phase was set at 0.7 ml/min and the detector was set at λ=210 nm and λ=245 nm. Quantification was made using calibration curves obtained by injecting known amounts of pure compounds as external standards.

Statistical analysis

Mean values and standard deviations were calculated from the data obtained from triplicate experiments. All data were reported as mean ± standard deviation (sd).

RESULTS AND DISCUSSION:

Tyrosinase and elastase inhibition activity

Tyrosinase inhibition activity was measured to determine the ability of RBFAR to be utilized as whitening or lightening agent in cosmeceutical products. Tyrosinase is the rate-limiting essential enzyme in the biosynthesis of the skin pigment, melanin. As indicated in Table 1, tyrosinase inhibition activity of RBFAR increased by 5.1- 41.1 folds compared to the non-fermented sample (1.69%) and was found maximum on 14th day of fermentation (69.52%). On the other hand, in determining the anti-aging potential of RBFAR, elastase inhibition activity was measured. Elastase is a protease enzyme that works for elastin degradation, which can lead to skin aging. Interestingly, result showed that RBFAR exhibited potent inhibitory effect of elastase after the fermentation and greatly improved upon the fermentation with the highest activity was observed on day 20th of fermentation (46.66%). These results suggest that positive biochemical changes may occur during solid state fermentation by *A. rouxii*, leading to the bioactivity changes in the rice bran. These findings were comparable to the study by Razak *et al*.,[15] who found the 56.18% tyrosinase inhibition activity of extract of rice bran fermented with *A. oryzae* while elastase inhibition activity of the same extract was 60.52%.

Antioxidant activity and total phenolic content

As skin aging effect has been widely related to the free radicals, antioxidant effect was important to scavenge the free radicals. Thus, the antioxidant activity of RBFAR and non-fermented rice bran was measured by using the stable free radical, 1, 1-diphenyl-2-picrylhydrzyl (DPPH). Table 2 showed that the DPPH radical scavenging activity of RBFAR was increased than that of non-fermented rice bran (49.27%); the highest was on day 20th (152.74%). Upon the SSF by *A. rouxii,* the antioxidant activity of rice bran has been increased by two to three-folds. This result suggests that RBFAR, at a later stage of fermentation, can be a good source of antioxidant and may be incorporated as ingredient in cosmetic formulation.

Table 1
Tyrosinase and elastase inhibition activity of non-fermented and fermented rice bran extracts

Fermentation duration (days)	Tyrosinase inhibition activity (%)	Elastase inhibition activity (%)
Non-fermented	1.65 ±0.57	nd
0	8.57 ± 0.00	0.00 ± 0.35
2	15.24 ± 1.35	5.30 ± 2.65
4	17.14 ± 9.43	45.17 ± 12.09
6	16.19 ± 5.39	30.44 ± 6.44
8	16.19 ± 2.69	32.81 ± 9.79
10	17.14 ± 4.04	25.39 ± 5.12
12	16.19 ± 0.00	21.71 ± 3.62
14	69.52 ± 0.00	11.26 ± 0.13
16	17.14 ± 9.43	27.01 ± 0.71
18	18.10 ± 0.00	45.73 ± 2.82
20	9.52 ± 9.43	46.66 ± 11.91

Each figure represents the means of three duplicates ± standard deviation.
nd = not detected.

Antioxidant activity and total phenolic content

As skin aging effect has been widely related to the free radicals, antioxidant effect was important to scavenge the free radicals. Thus, the antioxidant activity of RBFAR and non-fermented rice bran was measured by using the stable free radical, 1, 1-diphenyl-2-picrylhydrzyl (DPPH). Table 2 showed that the DPPH radical scavenging activity of RBFAR was increased than that of non-fermented rice bran (49.27%); the highest was on day 20th (152.74%). Upon the SSF by *A. rouxii,* the antioxidant activity of rice bran has been increased by two to three-folds. This result suggests that RBFAR, at a later stage of fermentation, can be a good source of antioxidant and may be incorporated as ingredient in cosmetic formulation.

Table 2
Antioxidant activity and total phenolic content of non-fermented and fermented rice bran extracts

Fermentation duration (days)	DPPH radical scavenging activity (%)	Total phenolic content (mg GAE / g sample)
Non-fermented	49.27 ± 0.01	3.20 ± 0.00
0	51.49 ± 0.02	2.78 ± 0.13
2	46.33 ± 0.12	5.12 ± 1.35
4	62.66 ± 0.78	6.12 ± 1.07
6	58.87 ± 1.30	6.67 ± 1.80
8	106.34 ± 0.91	6.76 ± 1.71
10	72.28 ± 1.00	7.32 ± 2.68
12	103.23 ± 1.09	6.42 ± 0.37
14	88.44 ± 0.84	12.79 ± 0.25
16	129.12 ± 1.93	6.23 ± 0.53
18	118.11 ± 0.07	5.52 ± 0.26
20	152.74 ± 2.93	11.33 ± 1.85

Each figure represents the means of three duplicates ± standard deviation.

Results in Table 2 also showed that total phenolic content of RBFAR was increased than that of non-fermented rice bran (3.20 mg GAE/g), the highest was on day 14th (12.79 mg GAE/g). This study is correlated with other several studies that found that the higher antioxidant activity resulted in higher total phenolic content.[16,17] This is contributed by the ability of the phenolic compounds to destroy radicals as they

contain hydroxyl group. They give up hydrogen atoms from their hydroxyl groups and form stable phenoxyradicals.[18]

Bioactive compound contents

SSF by *A. rouxii* has also suggested the enhancement of bioactive compound contents in rice bran. There were four types of phenolic acids (gallic, protocatechuic, p-hydroxybenzoic, caffeic) which were not identified in non-fermented rice bran but were detected after the fermentation. As shown in Table 3, gallic acid was the major phenolic compound detected (50.65 µg/ml), followed by caffeic (9.60 µg/ml), protocatechuic (7.16 µg/ml) and p-hydrobenzoic (4.04 µg/ml). The presence of high amount of gallic acid in RBFAR showed that it has strong potential to be exploited as cosmeceutical agent. This is correlated with a study by Su *et al*.,[19] who has demonstrated the inhibitory effect of gallic acid against melanogenesis in their study and suggests the use of gallic acid as a therapeutic agent for use in reducing skin hyperpigmentation and component in lightening and whitening cosmetics.

Table 3
Bioactive compound contents of non-fermented and fermented rice bran extracts

Bioactive compound contents					
Phenolic acids (µg/ml)[a]			**Organic acids (µg/ml)[a]**		
	Non-fermented	**RBFAR**		**Non-fermented**	**RBFAR**
Gallic	nd	50.65 ± 0.0	Oxalic	2.73±0.07	1194.3±58
Protocatechuic acid	nd	7.16 ± 0.0	Citric	17.14±0.64	nd
p-hdroxybenzoic	nd	4.04 ± 0.00	Kojic	0.04±0.01	79±40
Vanillic	nd	nd	Succinic	1.21±0.02[a]	nd
Caffeic	nd	9.60±1.88	Acetic	2.37±0.06	nd

Each figure represents the means of three duplicates ± standard deviation.
nd = not detected.

On the other hand, there were two types of organic acids were detected in RBFAR, including oxalic acid and kojic acid. As indicated in Table 3, kojic acid content in RBFAR (79 µg/ml) was improved by almost 2000-fold compared to those non-fermented sample (0.04 µg/ml). Oxalic acid (1194.3 µg/ml) was also improved after the fermentation in comparison to the non-fermented rice bran (2.73 µg/ml). However, the other types of organic acids including citric, succinic, and acetic acid were only detected in non-fermented rice bran but were not detected after the SSF. The presence of high amount of kojic acid in RBFAR is interesting as kojic acid is known to inhibit the catecholase activity of tyrosinase, thus kojic acid is considered to be good skin whitening and may be used for cosmeceutical purposes.[20]

CONCLUSION:

SSF by *A. rouxii* enhanced the cosmeceutical activities of rice bran including tyrosinase and elastase inhibition, antioxidant, total phenolic, and also phenolic acid and organic acid contents. The results of this study suggested cosmeceutical potential of *A. rouxii* – fermented rice bran extract and it could be further exploited as natural and effective cosmetics ingredient.

ACKNOWLEDGEMENT:
This study was financially supported by development fund project under the 11th Malaysia Plan.

REFERENCES:

1. Nagendra Prasad MN, Sanjay KR, Shravya Khatokar M, Vismaya MN, Nanjunda Swamy S. Health benefits of rice bran-a review. J Nutr Food Sci. 2011;1(3):1-7.
2. Tilay A, Bule M, Kishenkumar J, Annapure U. Preparation of ferulic acid from agricultural wastes: its improved extraction and purification. Journal of Agricultural and Food Chemistry. 2008 Aug 16;56(17):7644-8.
3. Patel M, Naik SN. Gamma-oryzanol from rice bran oil–A review. Journal of Scientific and Industrial Research. 2004 July;63:569-578.
4. Rogers EJ, Rice SM, Nicolosi RJ, Carpenter DR, McClelland CA, Romanczyk LJ. Identification and quantitation of γ-oryzanol components and simultaneous assessment of tocols in rice bran oil. Journal of the American Oil Chemists' Society. 1993 Mar 1;70(3):301-7.
5. Jiang Y, Wang T. Phytosterols in cereal by-products. Journal of the American Oil Chemists' Society. 2005 Jun 1;82(6):439-44.
6. Kunamneni A, Permaul K, Singh S. Amylase production in solid state fermentation by the thermophilic fungus *Thermomyces lanuginosus*. Journal of Bioscience and Bioengineering. 2005 Aug 31;100(2):168-71.
7. Sandhya C, Sumantha A, Szakacs G, Pandey A. Comparative evaluation of neutral protease production by *Aspergillus oryzae* in submerged and solid-state fermentation. Process Biochemistry. 2005 Jul 31;40(8):2689-94.
8. Ng IS, Li CW, Chan SP, Chir JL, Chen PT, Tong CG, Yu SM, Ho TH. High-level production of a thermoacidophilic β-glucosidase from *Penicillium citrinum* YS40-5 by solid-state fermentation with rice bran. Bioresource Technology. 2010 Feb 28;101(4):1310-7.
9. Saykhedkar SS, Singhal RS. Solid-state fermentation for production of griseofulvin on rice bran using *Penicillium griseofulvum*. Biotechnology Progress. 2004 Jan 1;20(4):1280-4.
10. dos Santos Oliveira M, Feddern V, Kupski L, Cipolatti EP, Badiale-Furlong E, de Souza-Soares LA. Changes in lipid, fatty acids and phospholipids composition of whole rice bran after solid-state fungal fermentation. Bioresource Technology. 2011 Sep 30;102(17):8335-8.
11. Kito H, Abe A, Sujaya IN, Oda Y, Asano K, Sone T. Molecular characterization of the relationships among *Amylomyces rouxii*, *Rhizopus oryzae*, and *Rhizopus delemar*. Bioscience, Biotechnology, and Biochemistry. 2009 Apr 23;73(4):861-4.
12. Mienda BS, Idi A, Umar A. Microbiological features of solid state fermentation and its applications-An overview. Research in Biotechnology. 2011 Dec 24;2(6).
13. Alam N, Yoon KN, Lee KR, Shin PG, Cheong JC, Yoo YB, Shim JM, Lee MW, Lee UY, Lee TS. Antioxidant activities and tyrosinase inhibitory effects of different extracts from *Pleurotus ostreatus* fruiting bodies. Mycobiology. 2010 Dec 1;38(4):295-301.
14. Thaipong K, Boonprakob U, Crosby K, Cisneros-Zevallos L, Byrne DH. Comparison of ABTS, DPPH, FRAP, and ORAC assays for estimating antioxidant activity from guava fruit extracts. Journal of Food composition and Analysis. 2006 Nov 30;19(6):669-75.
15. Razak DL, Rashid NY, Jamaluddin A, Sharifudin SA, Kahar AA, Long K. Cosmeceutical potentials and bioactive compounds of rice bran fermented with single and mix culture of *Aspergillus oryzae* and *Rhizopus oryzae*. Journal of the Saudi Society of Agricultural Sciences. 2017 Apr 1;16(2):127-34.
16. Farasat M, Khavari-Nejad RA, Nabavi SM, Namjooyan F. Antioxidant activity, total phenolics and flavonoid contents of some edible green seaweeds from northern coasts of the Persian Gulf. Iranian Journal of Pharmaceutical Research: IJPR. 2014;13(1):163.
17. Sadh PK, Saharan P, Duhan JS. Bioaugmentation of phenolics and antioxidant activity of *Oryza sativa* by solid state fermentation using *Aspergillus* spp. International Food Research Journal. 2017 Jul 1;24(3).
18. Aksoy L, Kolay E, Ağılönü Y, Aslan Z, Kargıoğlu M. Free radical scavenging activity, total phenolic content, total antioxidant status, and total oxidant status of endemic *Thermopsis turcica*. Saudi journal of Biological Sciences. 2013 Jul 31;20(3):235-9.

19. Su TR, Lin JJ, Tsai CC, Huang TK, Yang ZY, Wu MO, Zheng YQ, Su CC, Wu YJ. Inhibition of melanogenesis by gallic acid: Possible involvement of the PI3K/Akt, MEK/ERK and Wnt/β-catenin signaling pathways in B16F10 cells. International Journal of Molecular Sciences. 2013 Oct 14;14(10):20443-58.
20. Cabanes J, Chazarra S, GARCIA-CARMONA FR. Kojic Acid, a Cosmetic Skin Whitening Agent, is a Slow-binding Inhibitor of Catecholase Activity of Tyrosinase. Journal of Pharmacy and Pharmacology. 1994 Dec 1;46(12):982-5.

FP-16

EFFECT OF WATER-FED STRATEGY TO THE XYLANASE AND CMCASE PRODUCTION IN SOLID STATE FERMENTATION OF OIL PALM FROND

NOOR AZRIMI UMOR[1], SYED ANUAR SYED MOHAMAD FAUAAD[2], NIK AZMI NIK MAHMOOD[2] AND NUR HAMIEZA HUZIR [2]

[1]Universiti Teknologi Mara Cawangan Negeri Sembilan, [2] Department of Bioprocess, Faculty of Chemical Engineering and Energy, UTM Johor Bahru

[*]Corresponding author: noorazrimi@ns.uitm.edu.my

ABSTRACT

Oil palm frond (OPF) is largely generated from oil palm plantation as a waste product of oil palm industry. If these waste are not properly managed it will created issues in storage and pollution to the environment. As an alternative these OPF can potentially used as a substrate for lignocellulolytic enzyme production. In this experiment, oil palm frond chips were used as a substrate in solid state fermentation using *Aspergillus fumigatus* to produce CMCase and Xylanase enzyme. The independent variables were the fermentation time and the water treatments apply. Experiment was run for 11days. Further investigation was continued to analyze the effect of water-fed strategy to the production of reducing sugar, Xylanase and CMCase activity. Maximum production of reducing sugar was 33.725µmole at day 5 in the presence of water. Both Xylanase and CMCase produced highest activity on the 11th day of experiment without water fed which were 1.13 and 0.497 U/ml respectively. Fermentation with water fed increased the moisture content and yielded more reducing sugar. Xylanase and CMCase were optimum in absence of water fed due to acidic condition of fermentation. Statistical analysis showed that water treatment does not have significant correlation towards reducing sugar production. Meanwhile, t test proved that water fed strategy do not affect the Xylanase but have an interaction towards CMCase.

KEYWORDS:
Xylanase, CMCase, Oil Paln Frond, *Aspergillus fumigatus*

INTRODUCTION:

Oil palm industry contributes to one of the highest agricultural waste in Malaysia. It was reported that approximately 51 million tons of oil palm frond (OPF) has generated in Malaysia (Goh *et al.,* 2010). This substance is considered as waste to the environment if not properly managed. Thus research has been carried out to alternatively utilize the OPF for producing value added product. OPF consists of polysaccharides and lignocellulosic components such as cellulases, hemicelluloses and lignin which an indication of high organic matter content. Various organisms have different potential for the synthesis of enzymes among them fungi are the most common source of hemicellulose like xylanase and glucanase One of the alternative methods to produce xylanase is through the solid state fermentation.

In solid state fermentation, wastes of agro-industrial have been used as substrate-support for enzyme production Solid state fermentation is differing from submerged fermentation because there is no free-flowing water is present (but must be enough moisture present to support cell growth) and it was found to be more favourable.

In this study, the substrate use for the solid state fermentation is oil palm frond. The fungi use in this study is local isolated fungi which is *Aspergillus fumigatus*. This study aimed to measure the production of reducing sugar, xylanase and cellulase activity by using oil palm frond through solid state fermentation.

MATERIALS AND METHODS:

Raw materials

The lignocellulosic materials used was Oil Palm Frond (OPF) which was obtained from Malaysian Palm Oil Board, Selangor. The OPF were grinded into 250µm particle size.

Microorganisms

Microorganisms used in this study were *Aspergillus fumigatus* which was previously isolated by the researchers from UiTM Kuala Pilah.

Inoculum preparation

The isolated culture was transferred to PDA agar plate and incubated at 37ºC for 7 days to allow the colony to grow. After 7 days of incubation, the spores were ready to be harvested by using 1% (v/v) sterile Tween-80 solution.

Solid state fermentation

Batch fermentation of OPF was conducted for 11 days. The first batch was run in absence of water while the latter in the presence of water in which 10 ml of distilled water was added at day 1 and day 2. Initial moisture content was 70%. Production medium used was the Mendel basal medium that served as a moisture agent. According to Ang *et al*. (2015), the modified Mendel basal medium contained, in grams per litre: 1.4 g/L of $(NH)_2SO_4$, 2.0 g/L of KH_2PO_4, 0.3 g/L of urea, 0.3 g/L of $CaCl_2$, 0.3 g/L of $MgSO_4$, 0.005 g/L of $FeSO_4$, 0.0016 g/L of $MnSO_4$. H_2O, 0.0014 g/L of $ZnSO_4.7H_2O$, 0.002 of $CoCl_2$, 0.75 g/L of peptone, 2ml of Tween-80.

Reducing sugar production

The reducing sugar produce was determined by using spectrophotometer at 540 nm and calculated through the standard curve of glucose.

Enzyme extraction and Enzyme assays

According to Norazlina *et al*. (2014), xylan ase activity was assayed by adding 0.5 ml of enzyme solution into 1 ml of solution of 1.0% (w/v) birchwoodxylan (Sigma) in 0.05 M sodium acetate buffer with pH 5.3. The mixtures then incubated for 30 minutes at 50°C in a water bath. The reaction was terminated by boiling the mixture at 100°C for 5 mins. The reducing sugar was determined at 540 nm by the dinitrosalycyclic (DNS) method. Absorbance of mixture was measured using UV visible spectrophotometer. One unit of xylanase was defined as the amount of enzyme that liberates 1µmol of xylose equivalents per minute under the assay conditions (Anthony *et al.,* 2003). A similar method was used to assay CMCase by using 1% (w/v) carboxymethylcellulose mixed with 1 ml of DNS, 1 ml of 0.05 M sodium acetate buffer and also 2 drops of 0.1 M NaOH. The reducing sugar was determined by using UV visible spectrophotometer at 540 nm. One unit of CMCase was defined as the amount of enzyme that released 1 µmol of glucose per minutes (Silva *et al.,* 2005)

Statistical analysis

Spearman's correlation coefficient test was used to determine the relationship between fermentation treatments with reducing sugar production and independent sample t-test was used to compare the effect of water treatment towards the enzyme activity. Both test was conducted by using SPSS.

RESULTS AND DISCUSSIONS:

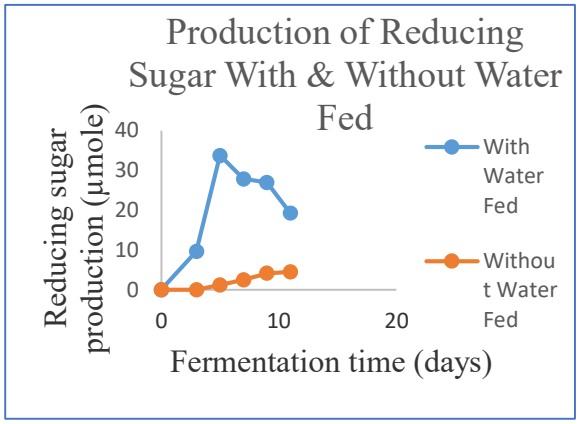

Figure 1
Production of reducing sugar (µmole) against fermentation time (days)

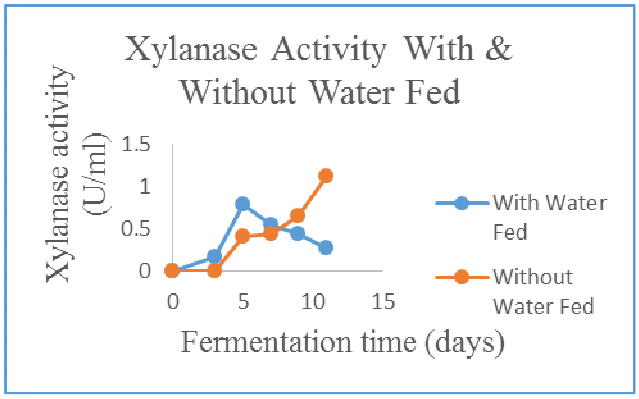

Figure 2
Xylanase activity (U/ml) against fermentation time (days)

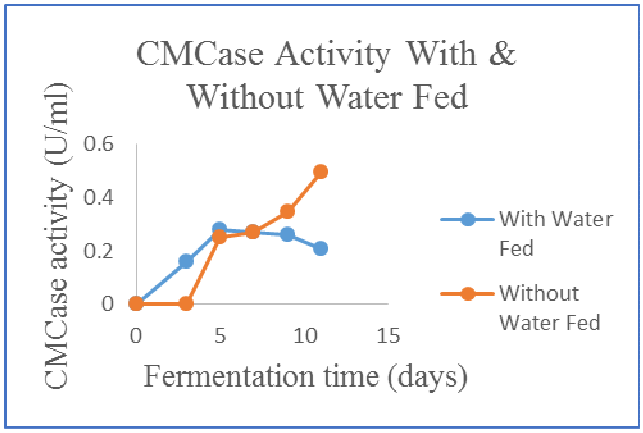

Figure 3
CMCase activity (U/ml) against fermentation time (days)

The production of reducing sugar without water fed shows little increment throughout 11 days of experiment. Meanwhile, when water was given, the reducing sugar produce increased from day 3 to the 5th day of cultivation time and after that decrease until the last day of experiment being conducted. The highest activity of xylanase was recorded at day 11 of fermentation time. In the presence of moisturity, the xylanase activities start to increased from day 3 and boost to the highest activity at day 5 of incubation time. After that, the enzyme activities start to declined until the end of experiment. CMCase activity in Figure 3 also shows a similar trend as xylanase activity.

Water activity related to the moisture content (Ibrahim, 2006). According to Gervais and Molin (2003), if the quantity of water insufficient, the cell metabolism will be slow or stop due to lack of substrates. In addition, water also cause swelling of substrate and facilitate effective absorption of nutrient from substrate for growth and metabolic activities. During fermentation time, the substrate continuously losing its moisture content. Depletion of moisture content caused the fungus to reduce its enzyme activity and thus production of reducing sugar also will declined. This trend can be seen in the second batch of fermentation whereby reducing sugar production decrease as the enzyme activity also decreased.

The highest production of reducing sugar in the presence of water was 33.725 µmole at the 5th day of fermentation time while in absence of water was only 4.522 µmole on the 11th days. This result was vary from the expected result which was when enzyme activity was high, the reducing sugar produced also will high. The graph of reducing sugar production in the presence of water boost to the 5th day of incubation due to higher amount of enzyme produced by fungi. Increasing in the amount of fungus lead to more enzymatic reaction to occur thus more yield of reducing sugar. Besides that, it was also due to variety of enzyme that degrade all components of lignocellulose consists of lignin, cellulose and hemicellulose. (Van Dyk and Pletschke, 2012).

From the result, both xylanase and CMCase achieving highest activity on the 5th day of incubation period with presence of water. The xylanase activity was 0.785 U/ml and CMCase activity was 0.280 U/ml on the 5th day. Thi was in accordance to the report by Park *et al*. (2002), the optimum cultivation time for production of xylanase was in day 5.

Meanwhile, when there was no water fed to the SSF, both xylanase and CMCase obtained the peaked activity on the 11th day where xylanase activity measured was 1.13 U/ml and CMCase activity was 0.497 U/ml. When compared the enzyme activity in condition of fermentation with and without water fed, the enzyme activity was higher when water was absence.

The decrease in the enzyme activity in the presence of water was due to the changes of pH value in the media. Optimum pH for both enzyme activities was in acidic condition. When water was added, the moisture content will increased but at the same time it will also increase the pH of fermented substrate. According to Shah and Madamwar (2005), maximum production of xylanase was found on the pH 5.0 and the activity decrease rapidly on the pH 6.0 and pH 7.0. These studies support the reason of decreasing activity of xylanase and CMCase.

Based on statistical results, the p value (0.000) was less than the α value of 0.05. Thus, there was significant correlation in fermentation time without water fed with reducing sugar production, and there was strong positive relationship since the correlation r_s was 0.972. Statistical analyses showed that water treatment do not have significant correlation towards reducing sugar production. Meanwhile, t test proved that water fed strategy do not affect the Xylanase but have an interaction towards CMCase.

CONCLUSION:

In conclusion, optimum fermentation time for the production of reducing sugar, xylanase and CMCase activity was in the 5th day of incubation in the presence of water. When water was absence, the reducing sugar and enzyme activity does not performed efficiently as the optimum time was in the 11th day of experiment. In this study, the xylanase activity recorded higher enzyme activity than CMCase in presence and absence of water. This indicate that xylanase yield more production of reducing sugar compared to CMCase.

ACKNOWLEDGEMENT:

The author wish to express gratitude to Ministry of High Education and IRMI UiTM Malaysia for funding the research through RAGS.

REFERENCES:

1. Ang, S. K., Adibah, Y., Abd-aziz, S. and Madihah, M. S. (2015). Potential Uses of Xylanase-Rich Lignocellulolytic Enzymes Cocktail for Oil Palm Trunk (OPT) Degradation and Lignocellulosic Ethanol Production. Energy & Fuels, 29(8), 5103-5116.
2. Anthony, T., Raj, K. C., Rajendran, A. and Gunasekaran, P. (2003). High molecular weight cellulase-free xylanase from alkali-tolerant Aspergillus fumigatus AR1. Enzyme and Microbial Technology, 32(6), 647-654.
3. Gervais, P., & Molin, P. (2003). The role of water in solid-state fermentation. Biochemical Engineering Journal, 13(2), 85-101.
4. Goh CS et al., (2010). Hot compressed water pretreatment of oil palm fronds to enhance glucose recovery for production of second generation bio-ethanol. Bioresource Technology 101, 19. 7362-7367.
5. Ibrahim, C. O. (2006). Xylanase production by a local isolate, Trichoderma spp. FETL c3-2 via solid state fermentation using agricultural wastes as substrates.
6. Silva, R. D., Lago, E. S., Merheb, C. W., Macchione, M. M., Park, Y. K., & Gomes, E. (2005). Production of xylanase and CMCase on solid state fermentation in different residues by Thermoascus aurantiacus miehe.Brazilian Journal of Microbiology, 36(3), 235-241.
7. Van Dyk, J. S., & Pletschke, B. I. (2012). A review of lignocellulose bioconversion using enzymatic hydrolysis and synergistic cooperation between enzymes—factors affecting enzymes, conversion and synergy.Biotechnology advances, 30(6), 1458-1480.

FP-17

PRELIMINARY INVESTIGATIONS FOR ANTIOXIDANT PROPERTIES OF FERNS SPECIES COLLECTED IN LONG BANGA, SARAWAK

NUR RAMZIAHRAZANAH JUMAT[1], MOHD. AMINUR FAIZ SUIS[2], NOR AMIRAH SHAMSUDIN[3], FADZILAH AWANG-KANAK[1], MAKDI MASNODDIN[1], JUALANG AZLAN GANSAU[3] AND AZLINAH MATAWALI[1*]

[1] Preparatory Centre for Science and Technology, Universiti Malaysia Sabah, Jalan UMS, 88400 Kota Kinabalu, Sabah, Malaysia
[2] Forest Research Centre, Sabah Forestry Department, P. O. Box 1407, 90715 Sandakan, Sabah, Malaysia
[3]Faculty of Science and Natural Resources, Universiti Malaysia Sabah, Jalan UMS, 88400 Kota Kinabalu, Sabah, Malaysia

*Corresponding author: azlinah@ums.edu.my

ABSTRACT

Ferns are traditionally consumed as vegetables and used to prevent or cure various ailments as they have a few medicinal properties including antioxidant activity. However, little is known on ferns in Long Banga, Sarawak such as *Calymmodon clavifer, Hymenophyllum acanthoides, and Oleandra pistillaris* especially on their medicinal properties.Thus, the study study is carried out to evaluate the antioxidant activity of crude extracts of *Calymmodon clavifer, Hymenophyllum acanthoides* and *Oleandra pistillaris* collected in Long Banga, Sarawak. All crude methanolic extracst were subjected to 1,1-diphenyl-2-picrylhydrazyl (DPPH) antioxidant assay. Total phenolic and total flavanoid content were also determined for phytochemical analysis. DPPH antioxidant test of all extracts showed that *H. acanthoides* gave the significant EC_{50} value 0.030 mg/ml in comparison to the EC_{50} value of the standard used, Trolox 0.035 mg/ml. Furthermore, phytochemical analysis showed higher total phenolic and total flavonoid content in the crude extract of *H. acanthoides* with the values of 304.81 ± 0.47 mg gallic acid equivalent (GAE)/g and 231.09 ± 0.91 mg catechin equivalents (CE)/g, respectively supporting the high antioxidant activity of *H. acanthoides* from DPPH test. Therefore, ferns collected in Long Banga, Sarawak shows promising potential as antioxidant agents to be used as alternative approach in therapeutic applications or preventions.

KEYWORDS:
Hymenophyllum acanthoides, DPPH, EC_{50}, flavonoid, phenolic, Long Banga

INTRODUCTION:

Ferns and lycophytes are a member of vascular plant groups and represented with at least 11,000 species [1]. Accroding to the latest unpublished record, Sarawak is home to at least 1,012 species of ferns and lycophytes (Meekiong Kalu, pers. comm), many of which have been utilized as traditional remedies for various ailments. Ferns are traditionally used to treat gastric and renal infections; they are also valued as antibacterial, diuretics, painkillers and even as anti-inflammatory agents [2]. Recently, various studies have been carried out to evaluate the medicinal properties of ferns and several studies reported on the antioxidant activities of some Malaysian ferns [3,4,5,6].

Calymmodon is a genus that belonged to family Polypodiaceae which is also treated as a grammitid fern. The distribution of this genus is ranging from Sri Lanka to Polynesia. In Borneo, this genus could be found until up to 3,400 m a.s.l. In state of Sabah, there were 12 species of *Calymmodon* recorded in Mount Kinabalu, with *Calymmodon innominatus* and *Calymmodon kinabaluensis* are endemics to Kinabalu [7,8]. Besides, Mount Kinabalu, there was also a record of *Calymmodon pallidivirens* could be collected from Mount Alab in Sabah [7]. Meanwhile, in Sarawak, there were seven species of this genus recorded in Mount

Mulu. A species that endemic to Borneo, *Calymmodon borneensis* was recorded for both mountains. *Calymmodon clavifer* that was used as a material in this study was previously recorded in Mount Jaya, Papua. This species distribution is ranging between Sumatra to New Guinea [8]. The previous record of *C. clavifer* in Borneo was from Mount Kinabalu and Tawau.

Oleandra is a genus of fern which name was derived from an angiosperm species of *Nerium oleander* from family Apocynaceae [9]. *Oleandra* is classified as a member of Oleandraceae family, the description of this genus by Smith *et al.* (2006) include blades simple; leaves articulate, abscising cleanly upon senescence from pronounced phyllopodia; sori indusiate, indusia round-reniform; spores reniform,monolete; $x = 41$ as characters [10]. The variability of *Oleandra* species can be found in the rhizome, although in herbarium collection rhizome part is seldom preserved. The distribution of this genus is pantropical however, some Malesian species could be found in Continental Asia to Australia or the Pacific [9]. There are nine *Oleandra* species described by Hovenkamp & Ho (2012), with only two species previously recorded from Borneo; *Oleandra coriacea* and *O. sibbaldi*. The former species is noted as endemic to Borneo, it previously found in Brunei, East Kalimantan (Indonesia), and Sarawak (Malaysia) [9]. There are at least three specimens of Oleandra kept in Sandakan Herbarium (SAN), they are; *O. cumingii*, *O. neriiformis*, *O. undulata*, and *O. pistillaris*.

Genus *Hymenophyllum* is noted as the largest genus of Hymenophyllaceae family, its distribution is throughout temperate region with about 250 species, and the habitat of this genus is mostly epiphytic and sometimes epillithic [7]. Other than *Hymenophyllum*, there are eight other genera classified under Hymenophyllaceae [7]. The members of this filmy fern family are identifed by their single cell thick laminae. Nurul Hafiza (2014), had collected specimen of Hymenophyllacaea from Mount Ulu Kali, Pahang [11]. Their sample that included three genera; *Cephalomanes*, *Hymenophyllum*, and *Trichomanes* were used to investigate leaf photosynthetic charecteristics. *Hymenophyllum acanthoides* was recently found in Trus Madi Range in Sabah [12]. Other than *Hymenophyllum*, there are eight other genera classified under Hymenophyllaceae [7].

However, information regarding benefits and bioactivity of most fern species which might have the potential to become sources of novel medicines is still limited and not clear [13]. Several ferns have been reported to have phenolic compounds and flavanoid components that exhibit antioxidant, antibacterial, anti-tumour and anti-inflammatory activities [2]. Little is known about the antioxidant activities of *Calymmodon clavifer* (Hook.) T. Moore, *Hymenophyllum acanthoides* (v. d. Bosch) Rosenst., and *Oleandra pistillaris* (Sw.) C. Chr. Hence, this study is carried out to evaluate the antioxidant activities of crude extrats of *Calymmodon clavifer* (Hook.) T. Moore, *Hymenophyllum acanthoides* (v. d. Bosch) Rosenst., and *Oleandra pistillaris* (Sw.) C. Chr. collected in Long Banga, Sarawak.

MATERIALS AND METHODS:

Collection and identification of plants

Wild plants of *Calymmodon clavifer* (Hook.) T. Moore, *Hymenophyllum acanthoides* (v. d. Bosch) Rosenst., and *Oleandra pistillaris* (Sw.) C. Chr. were collected during the Heart of Borneo (HoB) Scientific Expedition in Long Banga, Sarawak (Figure 1). The collection site represented a transition zone between upland mixed dipterocarp forest and lower montane forest. The altitude of collection site ranged from 1,173 to 1,203 m a.s.l.

The collected plants were cross-matched with the authentic voucher specimens in Herbarium of the Sabah Forestry Department (SAN). The identification process was also influenced by a reliable book (see Beaman & Edwards, 2007) [15]. Additionally, the identity of these plants was confirmed by fern para-taxonomist, Mr. Markus Gubilil of SAN.

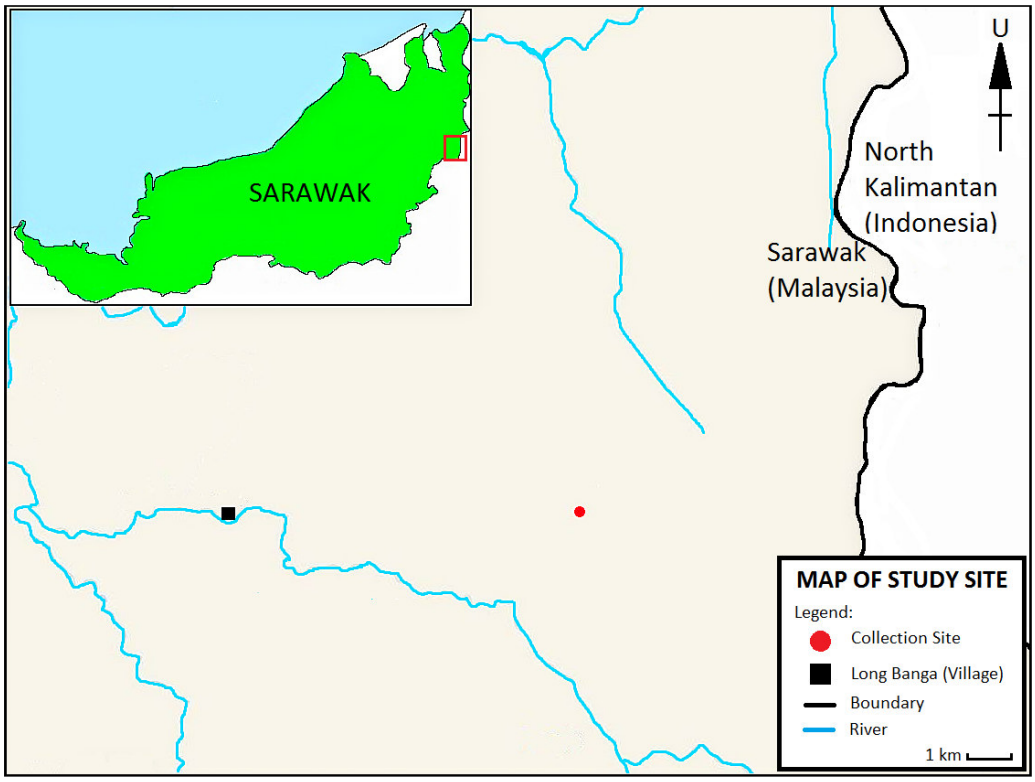

Figure 1
Map showing the location of Long Banga and collection site. Inset: Map of Sarawak (not drawn to scale) showing the study area. (Source: Mohd. Aminur Faiz Suis).

Taxonomic descriptions

Calymmodon clavifer (Hook.) T. Moore (Figure 2) is an epiphytic fern with ascending rhizomes and found among bryophytes on tree trunks. Fronds sessile, densly tufted and pinnatifid. Sori solitary and oblong on each pinna, and protected by a fold of the lobe. *Hymenophyllum acanthoides* (v. d. Bosch) Rosenst. (Figure 3) is a filmy epiphytic fern, and often forms mats on tree trunk and branches. Rhizomes long and thin. Fronds vary in size and margin sharply toothed and conspiciously crisped. Sori at apices of short acroscopic segments, often in apical part of fronds. *Oleandra pistillaris* (Sw.) C. Chr. (Figure 4) is a large terrestial fern with thick and long-creeping rhizomes. Fronds simple and oblanceolate. The margin sub-entire and a little wavy. Sori in one irregular row on each side of the midrib.

Figure 2
***Calymmodon clavifer.* (Source: Mohd. Aminur Faiz Suis).**

Figure 3
Hymenophyllum acanthoides. **(Source: Mohd. Aminur Faiz Suis)**

Figure 4
Oleandra pistillaris. **(Source: Mohd. Aminur Faiz Suis).**

Plant samples collection, preparation and extraction

Samples collected were cleaned up and divided into different parts (stem, leaves, root and flower). Samples were carefully examined to remove old, insect damaged, fungus-infested and twigs. Then, samples were cut into pieces and dried using air dried at control temperature. After they reach its constant weight, all of them were grinded into powdery form using blender. Samples were soaked three times with 100% (v/v) methanol (Fisher) solvents for overnight (24 hours) in ratio of (1:10); which is 1g samples to 10 ml of methanol. The combined methanolic extracts were filtered using Whatman paper no.1 and evaporated under vacuum using rotary evaporator. Extract powder were kept in 4^0C. Upon test, the extract will be dissolved back using methanol (Fisher) in 100 mg/ml concentration (Harborne, 1998).

DPPH (1,1-diphenyl-2-picryl hydrazyl) free radical scavenging assay

Free radical scavenging activity of extract samples were determined by measuring the radical scavenging ability using the stable radical DPPH reagent (Mensor *et al.,* 2001). Crude methanolic extracts ranging from 0.6 to 500 µg/mL were prepared with methanol or 10% DMSO-methanol (v/v). The reaction mixtures in the

96-well plates consisted of sample (100 µL) and DPPH radical (100 µL, 0.2 mM) dissolved in methanol. The mixture was stirred and left to stand for 15 min in dark. Then the absorbance was measured at 517 nm against a blank. All determinations were performed in triplicates.

The percentage scavenging effect was calculated as:

$$\text{Scavenging rate} = [1 - (A_1 - A_2) / A_0] \times 100\%$$

where A_0 is the absorbance of the control (without sample) and A_1 is the absorbance in the presence of the sample, A_2 is the absorbance of sample without DPPH radical. The scavenging ability of the samples was expressed as EC_{50} value, which is the effective concentration at which 50% of DPPH radicals were scavenged. The EC_{50} values were calculated from the relationship curve of scavenging activities (%) versus concentrations of respective sample. The lowest EC_{50} indicates the strongest ability of the extracts to act as DPPH scavengers.

Statistical Analysis

All anaysis were carried out in triplicates and the result was presented as mean ± standard deviation. The data was statistically analyzed by using one-way ANOVA with significance value of $p<0.05$ followed by least significance difference (LSD) test. All statistical analysis were performed using SPSS version 22.

RESULTS AND DISCUSSION:

Wild plants of *Calymmodon clavifer*, *Hymenophyllum acanthoides* and *Oleandra pistillaris* were collected in Long Banga, Sarawak and methanolic extracts of the plants were prepared based on the method by Harborne (1998). There were two samples of *Calymmodon clavifer* used in the experiment in which *Calymmodon clavifer* 1 was collected at 800 m a.s.l while *Calymmodon clavifer* 2 was collected at 1000-1200 m a.s.l. Based on the sample extraction, the highest percentage yield obtained based on the methanol extraction method was *Calymmodon clavifer* 2 with 27% while the lowest percentage yield was *Calymmodon clavifer* 1 with 3% as shown in Table 1.

Table 1
Extraction yield in percentage (w/w)

Sample	Weight (g)	Percentage yield (%)
Calymmodon clavifer 1	1.0	3.0
Calymmodon clavifer 2	3.1	27.0
Hymenophyllum acanthoides	2.4	24.8
Oleandra pistillaris	10.0	7.0

The potential antioxidant activities of the crude extracts of fern samples collected in Long Banga was tested by using DPPH scavenging assay and the result is expressed as EC_{50} value or defined as the total antioxidant needed to reduce the initial DPPH radical concentration by 50% [14]. Based on the DPPH scavenging assay in Table 2, the EC_{50} values obtained for the crude extracts of *Calymmodon clavifer* 1, *Calymmodon clavifer* 2, *Hymenophyllum acanthoides* and *Oleandra pistillaris,* and even for Trolox as the positive control were appeared to be less than 1 mg/ml. The EC_{50} value for Trolox was 0.035 mg/ml. Our results showed that the crude extract of *Hymenophyllum acanthoides* had the lowest EC_{50} value with 0.030 mg/ml while the crude extract of *Calymmodon clavifer* 1 had the highest EC_{50} value with 0.894 mg/ml. Hence, the results indicate that the crude extracts of *Hymenophyllum acanthoides* to have the highest antioxidant activity compared to the other crude extracts of ferns collected in Long Banga, Sarawak. The low EC_{50} value of the crude extract of *Hymenophyllum acanthoides* indicates high antioxidant activity similar to several ferns that have been reported to show not only high total phenolic content but are also potent antioxidants such as *C. latebrosa, C. barometz, D. quercifolia, B. orientale* and *D. linearis* [16].

Table 2
Scavenging activity of *Calymmodon clavifer* 1, *Calymmodon clavifer* 2, *Hymenophyllum acanthoides* and *Oleandra pistillaris* crude extracts on DPPH radicals

Sample	DPPH (mg/ml)[a]
Calymmodon clavifer 1	0.894
Calymmodon clavifer 2	0.497
Hymenophyllum acanthoides	0.030
Oleandra pistillaris	0.446
Trolox *	0.035

Notes: Data are mean ± standard deviation (n=3). *: Positive control
C. clavifer 1 was collected at 800 m a.s.l, *C. clavifer* 2 was collected at 1000-1200 m a.s.l.
[a] : DPPH free radical scavenging activity was expressed as EC_{50} (mg/ml)

Based on Table 3, crude extract of *Hymenophyllum acanthoides* showed the highest total phenolics (304.81 mg GAE/g) and total flavanoids (231.09 mg CE/g) when compared to the other crude extracts. The total phenolic content of the crude extract of *Hymenophyllum acanthoides* was found to be higher. Several medicinal ferns have been reported to have high phenolic content including *A. aureum*, *A. nidus, B. orientale, C. barometz* and *D. linearis* [17] while *S. palustris* was reported to have high flavanoid content [4]. The high total phenolics and total flavanoids content found in the crude extract of *Hymenophyllum acanthoides* suggests the possible contribution of the total phenolics and total flavanoids in the high antioxidant activity of *Hymenophyllum acanthoides.* Plants contain various free radical scavenging molecules including phenolics compounds and flavanoids which have antioxidant activity. Several studies have reported on significant correlation between total phenolic content with DPPH activities [18,19].

Table 3
Total phenolics and total lfavanoids of *Calymmodon clavifer* 1, *Calymmodon clavifer* 2, *Hymenophyllum acanthoides* and *Oleandra pistillaris* crude extracts

Sample	Total Phenolics [a]	Total Flavanoids [b]
Calymmodon clavifer 1	40.32 ± 0.82^{c}	22.76 ± 1.14^{c}
Calymmodon clavifer 2	49.08 ± 0.71^{d}	27.61 ± 1.6^{d}
Hymenophyllum acanthoides	304.81 ± 0.47^{e}	231.09 ± 0.91^{e}
Oleandra pistillaris	169.23 ± 0.23^{f}	9.42 ± 1.39^{f}

Notes: Data are mean ± standard deviation (n=3), different letters (within columns) are significantly different at $P < 0.05$.
C. clavifer 1 was collected at 800 m a.s.l, *C. clavifer* 2 was collected at 1000-1200 m a.s.l.
[a] :Total phenolic content was expressed as mg gallic acid equivalent in 1g of dried sample (mg GAE/g).
[b] :Total flavonoid content was expressed as mg catechin equivalent to 1g of dried sample (mg CE/g)

CONCLUSION:

The preliminary study on biological activities of fern and fern allies collected in Sarawak further revealed their importances as natural remedies. *Hymenophyllum acanthoides* was proven to have high antioxidant activity and high phytochemical content. As the sample are limited, further investigations on various biological assays and identifications of active compound(s) should be conducted in future studies on ferns collected in Long Banga especially on *Hymenophyllum acanthoides*. The ferns collected in Long Banga shows promising potential as antioxidant agents to be used as alternative approach in therapeutic applications or preventions

ACKNOWLEDGEMENT:

The authors feel gratitude to every opportunity given from Universiti Malaysia Sabah, Jabatan Perhutanan Sarawak, Jabatan Perhutanan Sabah and all members in Long Banga Scientific Expedition 2016.

REFERENCES:

1. Sharpe, JM, Mehltreter, K & Walker, LR. Ecological importance of ferns. In: Mehltreter, K, Walker, LR. & Sharpe, JM. (eds.). Fern Ecology. New York: Cambridge University Press, 2010.
2. Ho, R, Teai, T, Bianchini, JP, Lafont, R, & Raharivelomanana, P. Ferns: from traditional uses to pharmaceutical development, chemical identification of active principles. In Working with Ferns. Springer New York, 2010.p. 321-346.
3. Lai, HY, & Lim, YY. Antioxidant properties of some Malaysian ferns. In 3rd International Conference on Chemical, Biological and Environmental Engineering. IPCBEE (Vol. 20), 2011a.
4. Chai, TT, Panirchelvum, E, Ong, HC & Wong, F. Phenolic contents and antioxidant properties of Stenochlaena palustris, an edible medicinal fern. Botanical Studies. 2012; 53:439-446.
5. Chai, TT, Elamparuthi, S, Yong, AL, Quah, Y, Ong, HC & Wong, FC. Antibacterial, anti-glucosidase, and antioxidant activities of selected highlands ferns of Malaysia. Botanical Studies. 2013; 54 (55):1-7.
6. Shah, MD, Gnanaraj, C, Haque, AE, & Iqbal, M. Antioxidative and chemopreventive effects of Nephrolepis biserrata against carbon tetrachloride (CCl4)-induced oxidative stress and hepatic dysfunction in rats. Pharmaceutical biology. 2014;53 (1):31-39.
7. Ebihara, A, Fraser-Jenkins, CR, Parris, BS, Zhang, XC, Yang, YH, Chiou, WL, Chang, HM, Lindsay, S, Middleton, D, Kato, M, Praptosuwiryo, TN, Amoroso, VB, Barcelona, JF, Ranil, RHG., Park, CH, Murakami, N & Hoya, A. Rare and threatened pteridophytes of Asia 1. An enumeration of narrowly distributed taxa. Bulletin of the National Museum of Nature and Science, Series B. 2012; 38(3): 93.
8. Parris, BS. Grammitidaceae (Pteridophyta) of Mount Jaya, New Guinea and Other Montane Malesian Localities. Fern Gaz. 2005;17 (4): 183-2005.
9. Hovenkamp, P. H. & Ho, B. C. A revision of the fern genus Oleandra (Oleandraceae) in Asia. PhytoKeys, 2012; 11:1-37.
10. Smith, AR, Pryer, KM, Schuettpelz, E, Korall, P, Schneider, H, & Wolf, PG. A classification for extant ferns. Taxon. 2006; 55 (3): 705-731.
11. Nurul Hafiza, MR, Yong, KT, Osman, N, & Nasrulhaq-Boyce, A. Leaf photosynthetic characteristics in eight shaded Malaysian filmy ferns. Phyton (Buenos Aires). 2014; 83:353-361.
12. Suis, MAF, Anthony, F, Andi, MAM, & Suleiman, M. Additions to the Fern Flora of the Trus Madi Range, Sabah, Malaysia. Transactions on Science and Technology. 2016; 3 (2): 313-318.
13. Cao, J, Zheng, Y., Xia, X & Wang, Q. Total flavonoid contents, antioxidant potential and acetylcholinesterase inhibition activity of the extracts from 15 ferns in China. Industrial Crops and Products. 2015; 75:135-140.
14. Beaman, JH & Edwards, PJ. Fern of Kinabalu: An Introduction. Kota Kinabalu: Natural History Publications (Borneo), 2007.
15. Masalu, RJ, Hosea, KM & Malendeja, S. Free radical scavenging activity of some fungi indigenous to Tanzania. Tanzania Journal of Health Research. 2012; 14 (1): 1-8.
16. Lai, HY & Lim YY. Evaluation of Antioxidant Activities of the Methanolic Extracts of Selected Ferns in Malaysia. International Journal of Environmental Science and Development. 2011b; 2 (6): 442-447.
17. Lai, HY, Lim, YY, & Tan, SP. Antioxidative, tyrosinase inhibiting and antibacterial activities of leaf extracts from medicinal ferns. Bioscience, biotechnology, and biochemistry. 2009; 73 (6): 1362-1366.
18. Veglioglu, YS, Mazza, G, Gao, L & Oomah, BD. Antioxidant Activity and Total Phenolics in Selected Fruits, Vegetables and Grain Products. Journal of Agriculture and Food Chemistry. 1998; 46 (10): 4113-4117.
19. Cai, Y, Luo, Q, Sun, M & Corke, H. Antioxidant activity and phenolic compounds of 112 traditional medicinal plants associated with anticancer. Life Sciences. 2003; 74:2157-2184.

FP-18

PRODUCTION OF LUTEIN BY MICROALGAE, *Scenedesmus obliquus* GROWN IN STIRRED-TANK PHOTOBIOREACTOR

RAHA AHMAD RAUS[1*], AHMAD BADRUL AMIR MOHD ATAN[1], NOR JANNAH SALLEHUDIN[1], AND RASHIDI OTHMAN[2]

[1]*Department of Biotechnology Engineering, Kulliyyah of Engineering, International Islamic University Malaysia*
[2]*International Institute for Halal Research and Training, International Islamic University Malaysia*

**Corresponding author:* rahaar@iium.edu.my

ABSTRACT

Lutein is a photosynthetic pigment located inside the chloroplast of photosynthetic organisms. It has high market value due to its various benefits particularly act as a natural food colorant other than benefit to human health such as preventing age-related macular degeneration disease and cataract. Currently, lutein is extensively produced from marigold plant. In this study, microalgae were studied as alternative source for lutein due to high lutein content inside their bodies. The microalgae, *Scenedesmus obliquus* was grown in a photobioreactor (PBR) and the effects of temperature, light exposure and carbon dioxide flow rate on the production of lutein were investigated. One factor at a time (OFAT) method was adopted in this study in which one of the parameters was varied at a time instead of multiple factors simultaneously. Lower temperature and gas flow rate had a tendency to increase lutien content while balanced light-dark cycle improved lutien content. The best lutein production was obtained when the temperature, light exposure duration and flow rate were set at 25°C, 12 hours/day, and 0.5 lpm, respectively.

KEYWORDS:
Lutein, *Scenedesmus obliquus*, OFAT, photobioreactor, carbon dioxide

INTRODUCTION:

Lutein, a carotenoid found in most of the green plants, is one of the promising biotechnology products which have a great market value. This is due to its extensive medical benefits such as its ability to prevent macular degeneration disease[1] and cataract[2], plays a critical function in maintaining a normal visual function[3], hampering the progression of and atherosclerosis[4] as well as prevention of certain cancers[5]. It is widely used as a food dye especially as a feed additive in aquaculture and poultry farming; it is also used for the coloration of pharmaceutical products and cosmetics.[6] Statistics showed that about $150,000 sales of lutein-made food colorants sold in United States only.[1]

Currently, lutein is commercially produced from marigold plant (*Tagetes erecta* and *Tagetes patula*).[7] However, the ordinary way of harvesting lutein from the plant has many drawbacks such as expensive plantation costs, and influenced by seasonal and climatic changes. Marigold plant requires about 80 to 92 days producing the first flower since sowing8 and only containing 0.03% lutein composition inside the petals[1]. Like other terrestrial plants, marigolds also susceptible to pest attacks and diseases. Thus, microalgae are believed to be a better candidate to replace marigold due to its high content (0.5-1.2% dry weight) inside all microalgae naturally and better production yield compared to marigold plant.[1] Furthermore, the cultivation of the microalgae culture inside closed system such as photobioreactor (PBR) makes it unsusceptible to environmental influences.

In this study, micoalgae, *Scenedesmus obliquus* which is isolated from Tasik Layang-Layang, Kepong, Kuala Lumpur, was grown in suspension inside a stirred tank PBR. After three days of cultivation with

atmospheric air, 5% CO_2 were supplied for the remaining days of culture. De Morais and Costa (2007) demonstrated that biomass concentration of *S. obliquus* was at the highest when approximately 6% of CO_2 was introduced.[9] In this study, the relations between the lutein production and physical parameters of PBR including temperature, light exposure duration, and gas flow rate were investigated.

MATERIALS AND METHODS:

Growth profiling

Growth profiling of *S. obliquus* was conducted by culturing the microalgae for 8 days at 30°C, 12 hrs/day light exposure, and 0.5 lpm air flow rate. Daily sampling was aseptically conducted and cell count of the microalgae was recorded.

Preparation of inoculum

The microalgae inoculum stock was prepared approximately 1 week before 1.5 l microalgae cultivation in a 2.5 l PBR vessel was conducted. Firstly, a colony of microalga *S. obliquus* from a Tris acetate phosphate (TAP) agar plate was aseptically transferred into a sterilized 250 ml conical flask containing 125 ml TAP fresh media. Then, the microalgae were grown inside the flask until they attained exponential growth (6-7 days). The inoculum (300 ml) was later adjusted to $1x10^6$ cells/ml before transferred aseptically into the PBR vessel.

Photobioraector operation

To investigate the effect of temperature, light exposure duration, and gas flow rate on lutein prodution, one factor at a time (OFAT) method was adopted in which the microalgae were cultured at various growth conditions as shown in Table 1-3. Each batch of culture was conducted for 5 days in which the PBR was supplied with atmospheric air for the first 3 days and followed by 5% CO_2 for the remaining 2 days.

Table 1

Growth conditions of microalgae at various temperature but at fixed gas flow rate and light exposure

Run	Temperature (˚C)	Light exposure (hrs/day)	Air flow rate (lpm)
1	20	12	0.5
2	25	12	0.5
3	30	12	0.5
4	35	12	0.5

Table 2

Growth conditions of microalgae at various light exposure duration but at fixed gas flow rate and temperature

Run	Temperature (˚C)	Light exposure (hrs/day)	Air flow rate (lpm)
5	30	8	0.5
6	30	12	0.5
7	30	16	0.5
8	30	24	0.5

Harvesting and freeze drying

After five days of PBR operation, the culture was harvested by centrifugation at 9000*g* for 10 minutes at 10°C. The axenic status of the culture was checked by sample observation under a microscope. Then, the supernatants were discarded and the resulting pellets were freeze dried for three days.

Table 3
Growth conditions of microalgae at various air flow rate but at fixed light exposure duration and temperature

Run	Temperature (˚C)	Light exposure (hrs/day)	Air flow rate (lpm)
9	30	12	0.5
10	30	12	1.0
11	30	12	1.5
12	30	12	2.0

Extraction of lutein
The methods of extraction and saponification were conducted according to Othman method (2009).[10] The freeze dried sample from previous step was rehydrated with minimal amount of de-ionized water followed by addition of 40 ml of acetone and methanol mixture (7:3) which was previously mixed with calcium carbonate ($CaCO_3$). The mixture was mixed and left overnight. The overnight mixture was then centrifuged at 9000*g* at 10^{o}C for 5 minutes and result in two immiscible layers. The upper layer was collected and transferred into falcon tubes, while lower layer was re-extracted by using acetone and methanol mixture (7:3). The extraction process was repeated until the upper layer became colorless. The collected upper layers were then mixed with the same volume of hexane and de-ionized water mixture (1:1), and later centrifuged. Upon centrifugation, the upper layers were collected. Extraction process was repeated on the lower layer until the upper layer turned to colorless. The collected upper layers were dried with nitrogen N_2 gas.

Subsequently, the resulting dried extract was mixed with several components: 20 µl of ethyl acetate; 380 µl of acetonitrile and water mixture (9:1); and 400 µl of methanolic potassium hydroxide (10% w/v) and left overnight in the dark. On the following day, the mixture was combined with 4 ml mixture of hexane and butylated hydroxytoluene (0.1% w/v) and then added with 2 ml of 10% sodium chloride (NaCl). After centrifugation, the upper layer was collected. The remaining lower layer was re-added with the mixture of hexane and butylated hydroxytoluene (0.1% w/v), mixed, centrifuged and these steps were repeated until the upper layer turned to colorless. The collected upper layers were later washed with few milliliters of de-ionized water, centrifuged and dried with N_2 gas.

Purification of lutein
Purification of lutein from the microalgae extract was carried out using high performance liquid chromatography (HPLC, Agilent Technology 1200 series with UV-VIS DAD detector) by employing C 18 column (particle size 5 µm; 4.6 mm × 250 mm). To separate the carotenoids, a binary mobile phase consisted of acetonitrile and water (9:1); and ethyl acetate was utilized. The operating conditions were: i. 20^{o}C temperature of column, ii. gradient elution (0 – 20 min 60% A, 20 -25 min 40% A, 25 – 35 min 100% B, and 35 -35.1 min 100%A), iii. flow rate of 1 ml per minute. The carotenoids content was detected by measuring absorbance at the wavelength range of 350-550 nm and with lutein absorbance measured at 447 nm.

RESULTS AND DISCUSSION:

Growth Curve
After conducting growth profiling experiment for eight days, growth curve as in Figure 1 was obtained. Figure 1 indicates that the cell concentration slowly increased for the first two days, before exponentially increased for the next three days. The slow cell growth for the first two days was because the cells were in the transition phase, wherein they were still in the mode of adapting to the culture environment.[11] During lag phase, the cells are busy in transcripting and translating specific messenger RNA (mRNA) to synthesize specific protein to suit new culture environment.[11] Then, the culture reached exponential growth phase

where the cells experienced rapid increase in cell numbers. The calculated maximum specific growth rate (μ_{max}) during exponential growth is 0.9745 day^{-1} or 0.0406 hr^{-1}.

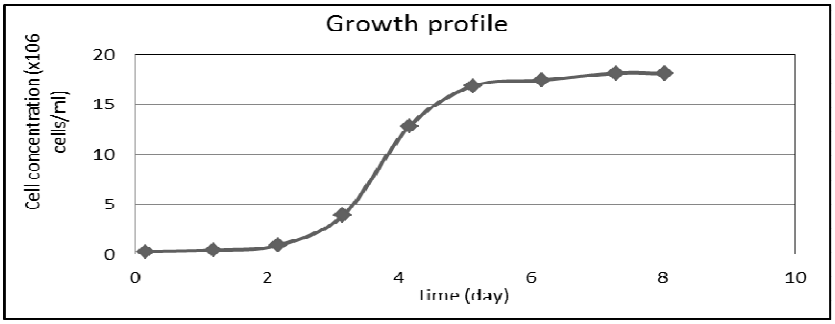

Figure 1
The growth profile of Scenedesmus obliquus

After exponential growth phase, the microalgae reached stationary phase approximately after surpassing the fifth day of the culture. One of the reasons the culture may reach stationary phase is the depletion of nutrients inside the culture media. Stationary phase reflects zero net growth because the growth or division of cells is balanced by the equal number of dying cells.[11] As a primary metabolite, lutein content should be at the maximum amount at the very end of log phase. Thus, it was decided to do each of PBR run for exactly five days in order to harvest the greatest amount of lutein.

Effect of temperature

To investigate the influence of temperature on the biomass and lutein productivity of *S. obliquus*, the temperature to cultivate the microalgae was varied (Table 1) and the flow rate and the duration of light exposure were fixed at 0.5 lpm and 12 hrs/day, respectively. The results showed that the microalgae lutein (64.28 mg/g) and biomass (719.4 mg/l) concentrations were at the maximum when *S. obliquus* was cultured at 25°C and 35°C, respectively (Figure 2). While both lutein (13.71 mg/g) and biomass (129.42 mg/l) were found at the lowest value when the culture was cultivated at 20°C. This indicated that *S. obliquus* cultivation at 20°C does not support the species's lutein production as well as the growth of the microalgae.

Figure 2 indicates that the biomass concentration steadily increased when the temperature of cultivation increased. Maximum biomass concentration was recorded at 35°C in this study and similar observation was observed by Christov et al. (2001)[12] and Cassidy (2011)[13] when *Scenedesmus* sp. was cultured at 35°C. In contrast, lutein concentration was decreased as cultivation temperature increased and maximum lutein concentration was observed at 25°C. This demonstrated that lutein was less produced at high temperture compared to a lower temperatue.

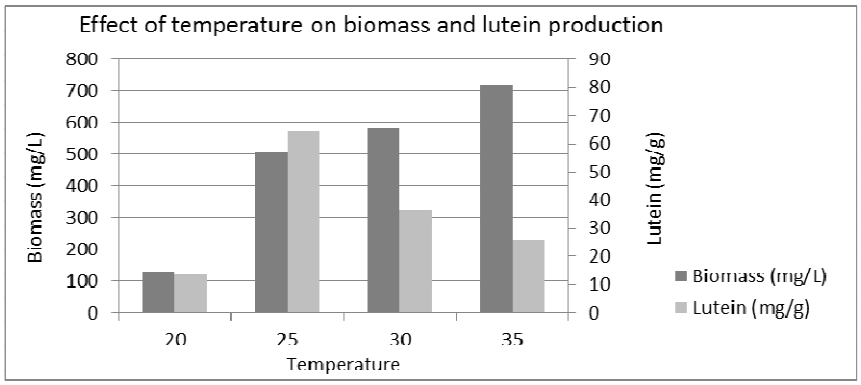

Figure 2
Concentration of biomass and lutein at day 5 of the culture when cultivated at varying temperature, while light exposure duration and air flow rate were fixed at 12 hrs/day and 0.5 lpm, respectively

Effect of light exposure duration

Effect of light exposure duration on lutein production by *S. obliquus* was studied by varying the duration of light exposure (Table 2) while fixing other parameters such as air flow rate at 0.5 lpm and temperature at 30°C. The specification of the lamp used in this study is shown in the following Table 4.

Table 4
Specification of the lamp used

Aspect	Specification
Brand, Type, Color	Designer, LED, white
Height x length x width	29cm x 3cm x 3cm
Rated voltage, power, frequency	AC220-240V, 8W, 50-60Hz
Illuminance, photon flux density	2,107.4 lux, 28.48 µmol m^{-2} s^{-1}

Based on the results in Figure 3, the maximum lutein (22.35 mg/g) obtained was when the light exposure duration was set at 12 hrs per day and lutein concentration reduced as the duration of light exposure increased. Although lutein is known as a secondary light-harvesting pigment in the photosynthetic organisms and its content should increased when microalgae was exposed to more light, previous study showed that the the pigments will be damaged if the light exposure period is too long.[14] Normally, photosynthetic organisms require balanced durations of light and dark periods to undergo light dependent reaction and dark cycle which are complementary to each other for photosynthesis.[15] Light period is to support the biochemical requirements, while the remained dark period was used to synthesize carbohydrates as well as to repair any damaged pigments. If the period of light exposure is too short, the pigments inside the chloroplast will be unable to absorb sufficient light energy to undergo photosynthesis while if the period of light exposure is too long, the microalgae lack of dark period to repair photo induced damage.[16]

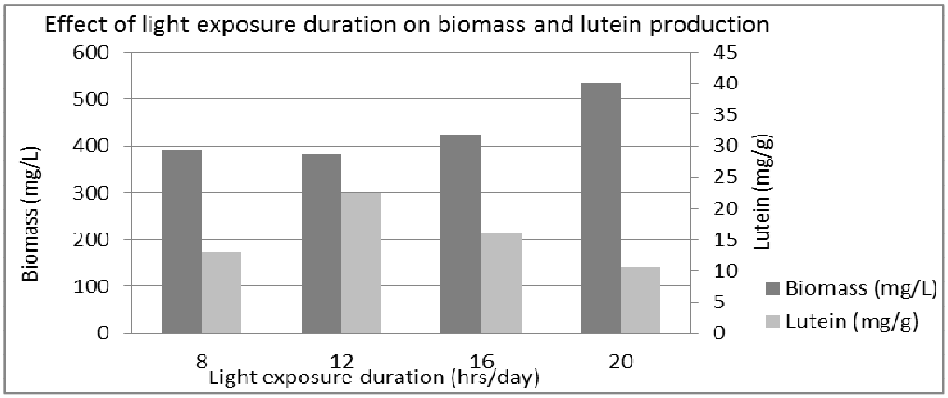

Figure 3
Concentration of biomass and lutein at day 5 of the culture when cultivated at varying light exposure duration, while temperature and air flow rate were fixed at 30°C and 0.5 lpm, respectively

Based on Figure 3 also, the trend of obtained lutein did not match the trend of obtained biomass when the duration of light exposure was varied. The biomasses tend to increase with longer light exposure while the lutien reduced. However, the difference between the biomass of microalgae at longer and shorter light exposure is small, hence most probably, the light expoure has no effect in improving the biomass of microalgae.

Effect of gas flow rate

The gas flow rate was set differently for each experiment (Table 3), while other parameters such as temperature and light exposure duration were set at 30°C and 12 hrs/day, respectively in order to investigate the influence of gas flow rate on lutein productivity.

The results from the experiments demonstrated that the maximum lutein and biomass concentrations were both obtained when the gas flow rate was set at 0.5 lpm (Figure 4). While increase in the gas flow rate has tendency to decrease both lutein and biomass concentrations. It has been showed that the increase of gas

flow rate does not necessarily increase microalgae growth rate due to shearing effect.[17] These 1.0 lpm, 1.5 lpm, and 2.0 lpm probably create shear stress as the size of the vessel is only 2.5L (volume). When the rate of fed air or gas into the vessel is too large compared to the rate of respiration by microalgae, congestion of air in the system will generate shear stress on the culture which will kill some of the microalgae.

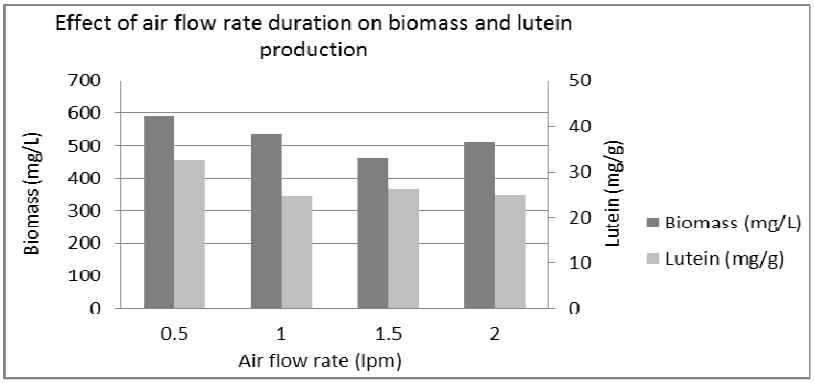

Figure 4

Concentration of biomass and lutein at day 5 of the culture when cultivated at varying air flow rate, while temperature and light exposure duration were fixed at 30°C and 12 hrs/day, respectively

CONCLUSION:

Tremendous demands on lutein highly favor this project in studying the consequences of varying temperature, light exposure, and gas flow rate on lutein production by *S. obliquus*. Based on the results of all experiments, the highest lutein and biomass concentration of *S. obliquus* were obtained when the PBR conditions were set at 25°C, 12 hours/day, 0.5 lpm; and 35°C, 12 hours/day, 0.5 lpm, respectively. Both of these maximum values were obtained when the temperature of the microalgae cultivation was varied and the duration of light exposure and the gas flow rate were fixed. This indicated that temperature greatly affected the lutein and biomass concentration of *S. obliquus*. It is interesting to observed that in spite of high biomass obtained when *S. obliquus* was cultured at 35°C, it does not necessarily result in high concentration of lutein. As the lutein and biomass concentration values of other experiments are lower compared to the two PBR growth conditions mentioned above, it is safe to conclude that these two growth conditions should be the basis for much larger scale of microalgae cutivation to obtain high lutein and biomass concentrations in the future.

ACKNOWLEDGEMENTS:

The authors would like to thank Malaysian Government for the research grant RACE14-005-0011 to support this study. The authors (s) declare that they have no competing interests.

REFERENCES:

1. Fernández-Sevilla JM, Fernández FA, Grima E. M. Biotechnological production of lutein and its applications. App. Microb.Biotech. 2010: 86(1):27-40.
2. Arnal E, Miranda M, Almansa I, Muriach M, Barcia JM, Romero FJ, Díaz-Llopis M, Bosch Moreer F. Lutein prevents cataract development and progression in diabetic rats. Graefes Arch. Clin. Exp. Ophthalmol. 2009:247:115–120.
3. Bosch Moreer F. Lutein prevents cataract development and progression in diabetic rats. Graefes. Arch. Clin. Exp. Ophthalmol. 2009:247:115–120.
4. Dwyer JH, Navab M, Dwyer KM, Hassan K, Sun P, Shircore A, Hama-Levy S, Hough G, Wang X, Drake T, Merz NB, Fogelman AM. Oxygenated carotenoid lutein and the progression of early atherosclerosis. Circulation. 2001:103:2922–2977.
5. Basu HN, Del Vecchio AJ, Flider F, Orthoefer FT. Nutritional and potential disease prevention properties of Carotenoids. J. Am. Oil Chem. Soc. 2001:78:665–675.

6. Johnson E.A, Schroeder WA. Advances in Biochemical Engineering, Biotechnology. In Microbial Carotenoids; Fiechter, A., Ed.; Springer: Berlin, Germany, 1995; Volume 53; pp. 119–178.
7. Del Campo JA, Garcia-Gonzalez M, Guerrero MG. Outdoor cultivation of microalgae for carotenoid production: Current state and perspectives. Appl. Microbiol. Biotechnol. 2007: 74:1163–1174.
8. Wien HC. Cut flower cultural practice studies and variety trials 2010. Dept. of Hort., Cornell Univ. Ithaca, NY. 2012.
9. De Morais MG, Costa JAV. Carbon dioxide fixation by *Chlorella kessleri*, *C. vulgaris, Scenedesmus obliquus and Spirulina sp.* cultivated in flasks and vertical tubular photobioreactors. Biotech. Lett. 2007: 29(9):1349-1352.
10. Othman R. Biochemistry and genetics of carotenoid composition in potato tubers. 2009. (Doctoral dissertation, Lincoln University).
11. Maier RM, Pepper IL, Gerba CP. Environmental microbiology (Vol. 397). Academic press; 2009.
12. Christov C, Pouneva I, Bozhkova M, Toncheva T, Fournadzieva S, Zafirova T. Influence of temperature and methyl jasmonate on Scenedesmus incrassulatus. Biologia plantarum 2001:44(3): 367-371.
13. Cassidy KO. Evaluating algal growth at different temperatures. John Wiley & Sons; 2011.
14. Ren T. Primary Factors Affecting Growth of Microalgae Optimal Light Exposure Duration and Frequency. 2014. (Doctoral dissertation, Iowa State University).
15. Lee C. Photosynthesis. In Michelle, H. (Ed.), Pre-U Text STPM Biology Volume 1 (pp. 166-190). Petaling Jaya: Pearson Malaysia Sdn Bhd; 2011.
16. Vasumathi KK, Premalatha M, Subramanian P. Parameters influencing the design of photobioreactor for the growth of microalgae. Renew. and Sust. Ener. Rev. 2012:16(7):5443-5450.
17. Rocha J M, Garcia JE, Henriques MH. Growth aspects of the marine microalga Nannochloropsis gaditana. Biomol. Eng. 2003:20(4):237-242.

FP-19

EFFECT OF LAPATINIB ON T84 COLONIC EPITHELIAL MONOLAYER INTEGRITY

W.N.I. WAN MOHAMAD ZAIN *[1], J. BOWEN [3], E. BATEMAN [2] AND D. KEEFE [2,4]

[1]Faculty of Medicine, Universiti Teknologi MARA, Sungai Buloh, Selangor, Malaysia. [2]School of Medicine, University of Adelaide Adelaide, South Australia, Australia. [3]School of Medical Sciences, University of Adelaide Adelaide, South Australia, Australia. [4]Cancer Centre, Royal Adelaide Hospital, Adelaide, South Australia, Australia

*Corresponding author: wnizzah@salam.uitm.edu.my

ABSTRACT

Lapatinib, an ErbB1/ErbB2 tyrosine kinase inhibitor is effective in breast cancer treatment but is associated with diarrhoea. ErbB1 is widely expressed in gastrointestinal mucosa. It maintains normal gut homeostasis by regulating chloride secretion. Thus, ErbB1 inhibition by lapatinib may interfere with chloride secretion in intestines, causing diarrhoea. This study aimed to determine the effect of lapatinib on T84 colonic cell permeability and on chloride secretion. T84 monolayers were treated with lapatinib at 10 and 100 µM. Then, cell permeability was measured via transepithelial resistance (TEER) at 0, 0.5, 24 and 48 hours incubation. Effect of lapatinib on chloride secretion was measured as changes in short circuit current (ΔI_{sc}) across lapatinib pre-treated T84 monolayers that were mounted in Ussing chambers. It was observed that lapatinib did not affect colonic cell permeability at different concentrations *($p>0.05$)* and different incubation hours *($p>0.05$)* suggesting that lapatinib does not damage cell-cell adhesion properties. Lapatinib also did not affect chloride secretion. No significant difference in ΔI_{sc} was observed between control untreated and lapatinib pre-treated monolayers *($p>0.05$)*. A link between ErbB1 and diarrhoea was not found by these studies. However, as lapatinib is an ErbB1 tyrosine kinase inhibitor which could interfere with chloride secretion, further investigations are required.

KEYWORDS:
ErbB1, Colon, Permeability, Chloride secretion, Diarrhoea

INTRODUCTION:

Lapatinib, an ErbB1/ErbB2 dual tyrosine kinase inhibitor, is known to be effective in treating ErbB2-positive advanced or metastatic breast cancer.[1] Although lapatinib has been recognised for its effectiveness, diarrhoea has been associated with the drug's administration[2, 3] and the mechanism leading to diarrhoea remains to be fully elucidated. Unlike diarrhoea associated with the use of conventional chemotherapeutic agents[4, 5], the diarrhoeal side effects of lapatinib are associated with no apparent damage to the intestinal epithelium.[6] It is well-established that treatment with conventional chemotherapy drugs causes atrophy of intestinal mucosa leading to mixed secretory/osmotic-type diarrhoea due to inability to control solute absorption and secretion through decreased surface area[7], however, it seems that lapatinib-induced diarrhoea occurs through a different mechanism.

Activated chloride secretion from the intestinal crypt plays a major role in secretory diarrhoea.[8] The generation of the electrochemical driving force required for chloride (Cl^-) secretion by crypt epithelial cells depends on their ability to accumulate intracellular Cl^- ions to concentrations greater than their electrochemical equilibrium.[9, 10] Chloride enters the cell across the basolateral membrane through the activity of sodium-potassium-chloride (Na^+-K^+-$2Cl^-$) cotransporters. The cotransporter is, in turn, driven by a strong inwardly-directed electrochemical Na^+ gradient established by the basolaterally-located sodium-

potassium-adenosine triphosphatase (Na^+-K^+-ATPase). In order to maintain the membrane potential at rest and during Cl^- secretion, both Na^+ and K^+ must be recycled out of the cell through the basolateral membrane. The Na^+-K^+-ATPase serves to recycle Na^+, while basolateral K^+ channels recycle K^+.[11] The basolateral K^+ conductance in intestinal epithelial cells is formed by at least two different types of K^+ channels; one is activated by calcium (Ca^{2+})-mobilizing secretagogues and the other by cyclic adenosine monophosphate (cAMP)-dependent agonists.[12]

Studies have revealed that ErbB1 is a critical regulator in intestinal ion transport.[13, 14] ErbB1 is widely expressed in the gastrointestinal mucosa in which it regulates Cl^- secretion in order to maintain normal gut homeostasis.[15] A study also found that during chronic inflammation, there is a potential effect of ErbB1 activation on epithelial electrogenic Na^+ that would be expected to ameliorate diarrhoeal symptoms associated with colitis (14). The process of Cl^- secretion is under tight control, and regulatory breakdown can lead to various complications, such as diarrhoea.[16] It has been suggested that inhibition of ErbB1 may cause dysregulation of the Cl^- secretory process, leading to diarrhoea; this has been suggested for lapatinib as well as with other ErbB1 tyrosine kinase inhibitors.[17, 18] However, studies by Bowen et al do not support that the inhibition of Cl^- leads to diarrhoea as blood biochemical analysis found that 240 mg/kg lapatinib had no significant effect on serum chloride.[6] However, it has to be noted that terminal blood collection occurred 24 hours after lapatinib treatment in which not all rats had diarrhoea at time of death. Furthermore, there was no effect on serum chloride only at this particular concentration (240 mg/kg).[6, 19] Thus, the role of chloride secretion in lapatinib-induced diarrhoea remains unclear.

In this study, both measurements of permeability via transepithelial electrical resistance (TEER), and paracellular ion movement using the Ussing chamber was carried out. TEER measured the movement of ions actively transported by epithelial cells from the passive movement of ions through paracellular or intercellular pathways, while Ussing chamber analysis is able to eliminate the passive transepithelial driving force created by the spontaneous electrical potential across the epithelium by clamping the potential to zero with an external current passed across the epithelium.[20] This current which is known as the short-circuit current (I_{sc}), is equivalent to the algebraic sum of electrogenic ion movement by active transport.[20] Previous study had shown that I_{sc} values in T84 monolayers are solely reflective of net chloride transport.[21] The T84 cell line was derived from a lung metastasis of human colon carcinoma. T84 cells are able to spontaneously differentiate into an enterocyte-like phenotype.[22] This cell type forms monolayers with well-developed tight junctions[22, 23] and has been proven to be a robust model for the study of molecular mechanisms of intestinal secretion since the early 1980s.[24, 25] As such, this study was carried out to determine the effect of lapatinib on T84 human colonic epithelial monolayer integrity.

MATERIALS AND METHODS:

Cell culture

The T84 (human colon carcinoma) cell line was obtained from the European Collection of Cell Cultures (ECACC), UK, and is derived from a lung metastasis of colon carcinoma in a 72 year old male. Experiments using the cell line were carried out between passages 2 and 10. T84 cells were grown in DMEM/ Nutrient F-12 Ham supplemented with 10% FBS, 1% penicillin-gentamicin with fungizone and 2mM L-glutamine. The cells were cultured using 75 cm^2 flasks in a 37°C incubator with 5% CO_2.

Chemicals

Chemicals were purchased from Sigma Chemical Co. (St Louis, MO, USA) unless otherwise stated. Lapatinib was supplied by Glaxo SmithKline (GSK, Australia). Lapatinib powder was dissolved in 100% DMSO to 10 mM.[26] The drug solution was then diluted with serum-free medium for cell culture assays.[27]

Ringer's solution used for Ussing chambers consisted of 4 stock solutions. Stock A solution was made up of 2.3 M sodium chloride (NaCl) while Stock B was 48 mM potassium hydrogen phosphate (K_2HPO_4) and Stock C was 0.5 M sodium hydrogen carbonate ($NaHCO_3$). Stock D was prepared by combining 24 mM magnesium chloride hexahydrate ($MgCl_2.6H_2O$) with 24 mM calcium chloride dihydrate ($CaCl_2.2H_2O$).

Prior to experiments using Ussing chambers, 300 ml of Milli-Q water (Milli-Q® Intergral Water Purification System, Merck Millipore, Australia) was added into a 500 ml volumetric flask. Then, 25 ml of each stock solution was added into the volumetric flask, followed by MilliQ water to make up 500 ml of Ringer's solution. Prior to usage, 5 ml of 1 M glucose was added to the 500 ml of Ringer's solution composition.

Effect of lapatinib on cell permeability

Four hundred microliters of T84 cell suspension, consisting of $4x10^5$ cells, was seeded in Millicell-HA culture plate inserts (0.6 cm^2 membrane area, 0.45 µm pore diameter and 12 mm diameter) (Millicell®, Millipore, USA) in a 48-well plate (Becton Dickinson, USA), to which was added with 600 µl medium. The cell density of T84 cells to form a monolayer was determined based on previous studies.[28, 29] The cells were then incubated at 37°C with 5% CO_2 for 48 hours to allow cell attachment prior to transepithelial electrical resistance (TEER) measurement. The culture plate insert in which the cells were seeded is termed as apical chamber while the 48-well plate in which the medium was added is termed as basolateral chamber.

After 48 hours incubation, the cell medium was refreshed prior to TEER measurement every 24 hours using a voltohmmeter (Millipore EVOM^2, World Precision Instruments, USA). The formation of a sealed monolayer was monitored by serial measurements of the TEER. Monolayer integrity was established once the TEER reached more than 800 ohms/cm^2. A higher TEER reflects stronger tight junctions between cells and decreased monolayer permeability.[30] To calculate the resistance measurement of the cell monolayer, the mean resistance measurements of inserts without cells were subtracted from the monolayer measurements and corrected for the area of the filter.[31]

Lapatinib 10 mM was diluted to 10 and 100 µM. Treatment with lapatinib began once the TEER of the seeded cells reached >800 ohms/cm^2. Experiments were carried out using medium (DMEM/ Nutrient F-12 Ham) supplemented with 10% serum. Optimal concentrations of the drugs were determined based on the results obtained from cell proliferation assay. As the main objective of this study is to determine the effect of lapatinib on cell permeability, lapatinib was added either to the apical, basolateral or both apical and basolateral chambers of the monolayer system. The apical chamber is considered as the luminal-side, while the basal chamber is analogous to the serosal side. Then, TEER measurement was taken prior to incubation (0 hour). The TEER measurements were carried out subsequently at 0.5, 24 and 48 hours without changing the medium. DMSO and triton x-100 (TX-100) were used as control treatments. The experiment was performed in duplicate and was repeated 3 times.

Effect of lapatinib on Cl^- secretion

T84 cell monolayers, prepared as described in the previous section, were pre-treated with lapatinib for 48 hours. Concentrations of lapatinib used in this experiment were determined based on the results obtained from the TEER experiment (effect of lapatinib on cell permeability).

Prior to each experiment, the Ussing chamber set up was calibrated according to manufacturer instructions (Physiologic instrument, USA). Salt bridges were adjusted for voltage, current and resistance using the manual (Physiologic instrument, USA). After the Ussing equipment had been set up, the Ringer's solution in the chamber was emptied in order to insert the monolayers which had been pre-treated with the drugs as mentioned in the first paragraph. Baseline TEER values of the pre-treated monolayers were measured according to the method described in previous section. Then, the pre-treated monolayers were rinsed gently with PBS prior to mounting into the sliders. Subsequently, the sliders were inserted into Ussing chambers while ensuring not to change the distance between the electrodes. The left side of the chambers indicates the luminal surface of T84 cells while the right chamber indicates the basolateral surface of the cells. Both sides of the monolayer were bathed with 5 ml of Ringer's solution supplemented with 1 mM glucose. The monolayers in the Ussing chambers were then left to equilibrate for 5 minutes. After that, short-circuit current (I_{sc}) was applied continuously by voltage clamp apparatus to maintain the transepithelial voltage at zero potential difference. Samples were allowed to equilibrate for 15 minutes before proceeding to stimulation with secretagogues. I_{sc} was recorded and analysed using a digital data acquisition system

(Acquire & Analyze version 2.3). Change in I_{sc} (ΔI_{sc}) demonstrated changes in net electrogenic ion movement across the monolayer, where a positive value indicated ion secretion in the apical direction.[32]

Baseline measurement of TEER, I_{sc} and conductance were recorded prior to stimulation with the first secretagogue. As mentioned above, I_{sc} is a measure of ion movement across the monolayer, while conductance (G) and its reciprocal, resistance or TEER, are a useful measure of the integrity of the monolayer preparation, in relation to the paracellular pathway across the monolayer.[33]

To assess secretion, the monolayers were first pre-incubated with 20 µM amiloride from the apical side for 15 minutes prior to stimulation of calcium (Ca^{2+})-dependent Cl^- secretion by the muscarinic agonist, carbachol (200 µM from the basolateral side), for 15 minutes. Lastly, cyclic adenosine monophosphate (cAMP)-dependent Cl^- secretion was induced by forskolin (10 µM from apical and basolateral sides), for 20 minutes. The secretagogue was induced once stable I_{sc} was attained and measurements were taken at baseline and peak secretion, respectively.

Statistical analysis

Results were statistically analysed using the Kruskal-Wallis test with Tukey's multiple comparisons test to compare means between all groups. Statistical significance was accepted as $p<0.05$.

RESULTS:

Effect of lapatinib on permeability

The T84 human colonic epithelial monolayers were exposed to lapatinib to investigate the effect of the drugs on permeability. The cell permeability was measured via TEER at 0, 0.5, 24 and 48 hours incubation. Results were expressed as change of resistance from baseline. DMSO was used as negative control while TX-100 was used as a positive control.

At 0.5, 24 and 48 hours, data show that the cell monolayers exhibited higher resistance associated with lapatinib 10 µM and 100 µM when treated on the apical (Figure 1A), basolateral (Figure 1B) and both apical and basolateral sides (Figure 1C) when compared to TX-100. The cell monolayer also showed a higher resistance against DMSO compared to TX-100. Results showed no significant differences in the cell resistance between lapatinib 10 µM and 100 µM at different incubation periods ($p>0.05$) (Figures 1A-C). Results also showed no significant differences between LAP 10 µM and LAP 100 µM treated apically, basolaterally or both apically and basolaterally ($p>0.05$) (Table 1).

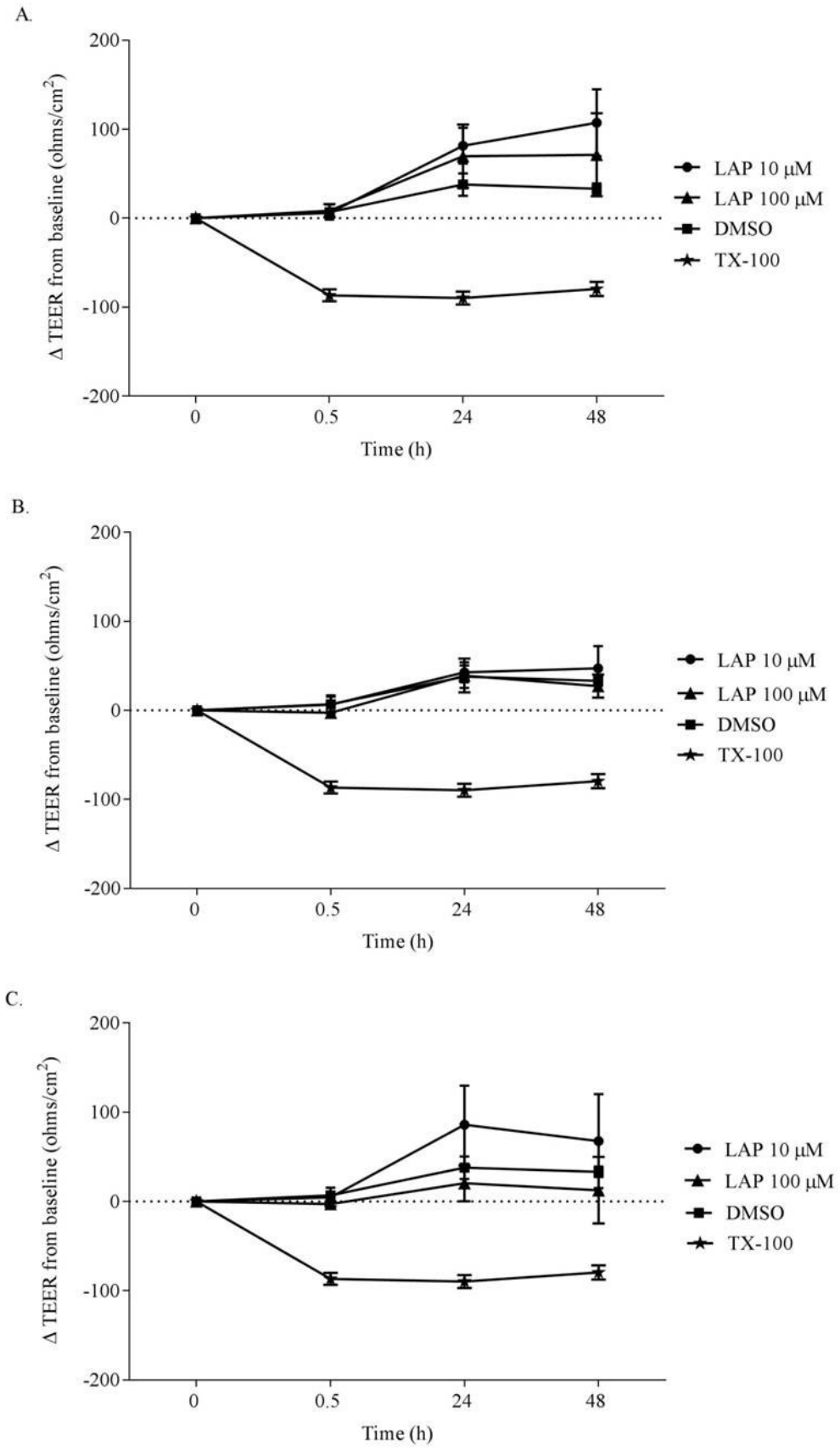

Figure 1

The effect of lapatinib at 10 and 100 µM on T84 colonic epithelial monolayer permeability as evaluated by TEER. A. Apical treatment. B. Basolateral treatment. C. Both apical and basolateral treatment. Data are presented as mean ± S.E.M (n=6). *LAP: lapatinib.*

Table 1
The effect of lapatinib (10 and 100 µM) on T84 colonic epithelial monolayer permeability as evaluated by TEER.

Sample	Δ TEER from baseline (ohms/cm^2)			
	0 h	0.5 h	24 h	48 h
LAP 10 µM A	0.00 ± 0.00	6.08 ± 3.01	81.53 ± 20.08	107.38 ± 37.62
LAP 100 µM A	0.00 ± 0.00	8.39 ± 7.55	69.65 ± 35.60	71.42 ± 46.57
LAP 10 µM B	0.00 ± 0.00	6.56 ± 10.28	42.84 ± 11.25	47.21 ± 25.00
LAP 100 µM B	0.00 ± 0.00	-2.69 ± 4.60	39.21 ± 19.03	27.25 ± 12.90
LAP 10 µM A + B	0.00 ± 0.00	4.66 ± 3.74	86.03 ± 43.88	67.68 ± 52.54
LAP 100 µM A + B	0.00 ± 0.00	-2.80 ± 2.86	20.45 ± 20.09	12.69 ± 37.23
DMSO	0.00 ± 0.00	6.92 ± 8.50	37.91 ± 12.53	33.27 ± 5.74
TX-100	0.00 ± 0.00	-86.64 ± 6.70	-89.58 ± 7.27	-79.48 ± 7.90

*Data presented as mean ± S.E.M (n=6). Results were compared between different concentration of lapatinib at different region of treatment. Results were significantly different at the level of $p<0.05$. *LAP: lapatinib, A: apical treatment, B: basolateral treatment, A + B: apical and basolateral treatments.*

Effect of lapatinib on Cl^- secretion

Monolayers of T84 colonic epithelial cells were pre-treated with lapatinib and incubated for 48 hours and mounted into Ussing chambers. Concentration of the drug used in this experiment was determined based on results obtained from TEER experiment. Concentrations of the drugs used were lapatinib 100 µM treated from apical side (LAP 100 A) or basolateral side (LAP 100 B) or both apical and basolateral sides (LAP 100 A+B). The concentration was also selected based on the assumption that they would be able to potentiate response to Cl^- secretion.

Experiments were conducted at established monolayer resistance and it was observed that pre-treatment of T84 cells with lapatinib did not affect baseline $I_{sc.}$ Baseline resistances of all samples were recorded. Baseline I_{sc} compared to the untreated monolayers were also noted. As shown in Figure 2A, all of the samples showed TEER >1000 ohms/cm^2 which demonstrated established monolayer integrity. There were no significant differences in resistance between any samples ($p>0.05$). Pre-treatment of monolayers with lapatinib for 48 hours also exhibited no significant differences in baseline I_{sc} between samples ($p>0.05$) (Figure 2B). Likewise, baseline conductance (G) were not significantly different between all samples ($p<0.05$) (Figure 2C).

After 15 minutes equilibrium the pre-treated monolayers were stimulated apically for 15 minutes with amiloride which stops the Na^{2+} current by preventing Na^{2+} absorption via the epithelium sodium channel. As such, any change in I_{sc} is not expected as Na^{2+} does not contribute to basal isogenic current in T84s.
The monolayers were then treated with the Ca^{2+}-dependent Cl^- secretagogue, carbachol, added to the basolateral sides. Readings were taken for 15 minutes following carbachol. There was a decreased response in Cl^- conductance in monolayers treated with lapatinib (Figure 3A). However, no significant differences were seen in ΔI_{sc} between all samples ($p>0.05$) (Figure 3B).

Next the cAMP-dependent Cl^- secretagogue, forskolin was added to the apical and basolateral chambers and changes in Cl^- conductance were measured for 20 minutes. All monolayers that were pre-treated with lapatinib (Figure 4A) had reduced response to forskolin compared to controls, but no significant differences in ΔI_{sc} were seen between any group ($p>0.05$) (Figure 4B).

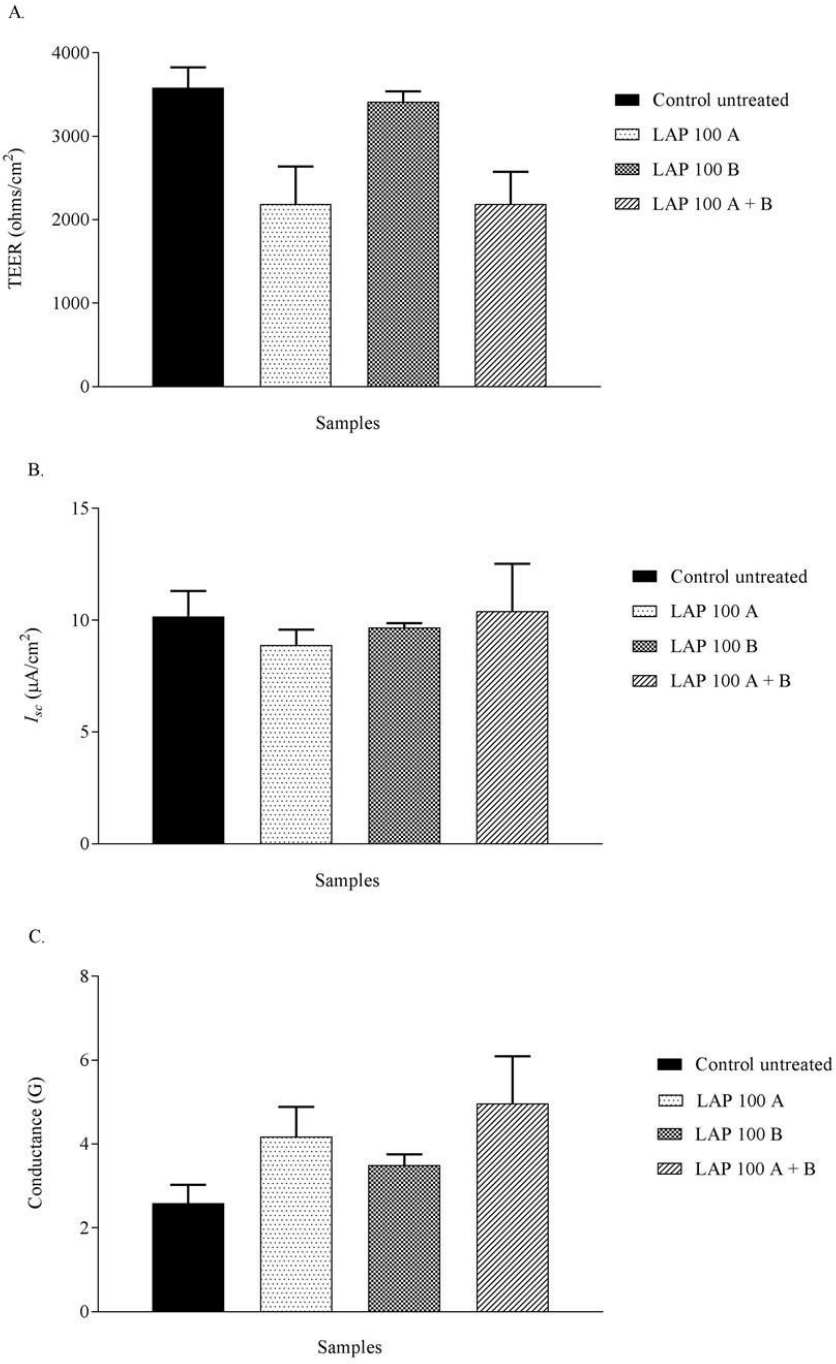

Figure 2

Baseline readings of T84 monolayer after 48 hours pre-treatment with lapatinib at 100 µM. A. TEER. B. I_{sc}. C. Conductance. Data are presented as mean ± S.E.M (n=6). ***LAP: lapatinib, A: apical treatment, B: basolateral treatment, A + B: apical and basolateral treatments.***

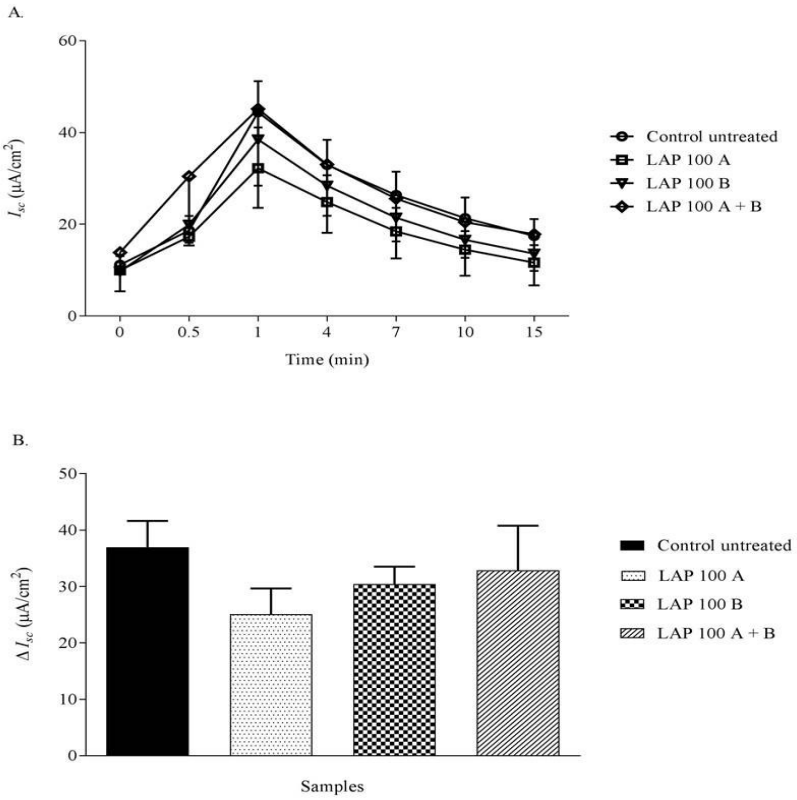

Figure 3

Effect of lapatinib at 100 µM after 48 hours pre-treatment on T84 cell monolayer on Cl^- secretion induced by carbachol as evaluated by I_{sc} measurement. A. I_{sc}. B. Changes in I_{sc}. Data are presented as mean ± S.E.M (n=6). *LAP: lapatinib, A: apical treatment, B: basolateral treatment, A + B: apical and basolateral treatments.*

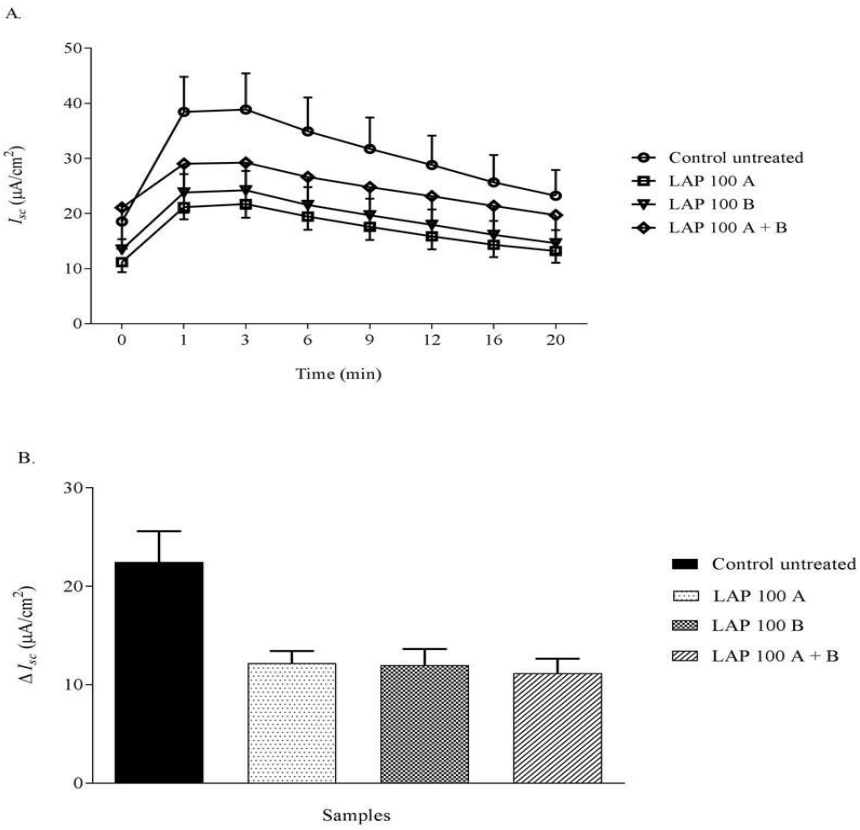

Figure 4

Effect of lapatinib at 100 µM after 48 hours pre-treatment on T84 cell monolayer on Cl^- secretion induced by forskolin as evaluated by I_{sc} measurement. A. I_{sc}. B. Changes in I_{sc}. Data are presented as mean ± S.E.M (n=6). *LAP: lapatinib, A: apical treatment, B: basolateral treatment, A + B: apical and basolateral treatments.*

DISCUSSIONS:

This is the first study to specifically investigate the effect of lapatinib treatment on chloride secretion in the T84 model of colonic epithelium. TEER experiments were conducted to determine the effect of the drug on cell permeability. Concentrations of lapatinib that were used in permeability studies were estimated from the cytotoxicity assay (results were not shown).

Based on the TEER results obtained, it was observed that lapatinib at both higher and lower concentrations, treated either from apical, basal or both apical and basal sides, as well as at different incubation hours does not affect colonic epithelial cell permeability. This suggests that lapatinib does not damage cell-cell adhesion properties and likely spares epithelial tight junctions. As such, the mechanism of diarrhoea is not related to overt changes in membrane barrier permeability.

In order to traverse the epithelium, two routes are available which are the transcellular and paracellular. Molecules with hydrophobic properties, or those able to interact with transport mechanisms, are absorbed primarily through the transcellular pathway. Passive diffusion of remaining molecules occurs through the paracellular pathway which is regulated by tight junctions.[34] The permeability of the intestinal epithelium depends on the regulation of intercellular tight junctions. Tight junctions were originally conceptualised as secreted extracellular cement forming an absolute and unregulated barrier within the paracellular space.[35] The present study evaluated that lapatinib does not alter T84 paracellular permeability which means not affecting the cells' tight junctions. However, investigations are needed to further clarify effects of lapatinib on the tight junctions.

Chloride secretion is the predominant driving force for fluid secretion in the intestine.[9] To examine the effect of lapatinib on intestinal chloride transport, T84 human colonic epithelial cell monolayers were mounted in Ussing chambers and the changes in short circuit current (I_{sc}) were measured. This experiment was conducted to examine the possibility that diarrhoeal side effects experienced by patients administered with lapatinib could be related to alterations in chloride secretion. In this experiment, the effect of lapatinib at suprapharmacological concentration was tested because it was shown in TEER results that lapatinib at lower concentrations did not affect cell permeability. Experiments were then conducted at established monolayer resistance and it was observed that pre-treatment of T84 cells with lapatinib did not affect baseline $I_{sc.}$ Chloride secretion was measured as I_{sc} across the T84 cell monolayers that were mounted in Ussing chambers,[21] thus the findings reflected that pre-treatment with both drugs does not alter baseline chloride secretion.

Besides baseline I_{sc} of pre-treated monolayers, baseline conductance was also measured. Conductance acts as an electrophysiological indicator of barrier function in which tissue conductance can also be used as an indication of passive ion transfer that reflects the permeability.[36] Baseline conductance of cell monolayers pre-treated with lapatinib were in parallel with the TEER results that reflected lower permeability, consequently higher barrier function/resistance which was not significantly different compared to control untreated monolayers.

Again, in opposition to our working hypothesis, lapatinib did not potentiate a significant response to known chloride secretagogues, such as carbachol or forskolin. As mentioned earlier, chloride secretion was measured as changes in I_{sc} in which decrease in I_{sc} indicates decrease in chloride secretion which could be related to the transactivation of ErbB1 and recruitment of downstream effectors such as the subsequent activation of extracellular signal-regulated kinase (ERK, also known as p 44/42 mitogen activated protein kinase or MAPK) activity.[37] Thus, indicating lapatinib-induced diarrhoea might be independent of ErbB1 transactivation.

CONCLUSION:

Lapatinib does not affect colonic epithelial monolayer permeability. Lapatinib also does not affect chloride secretion, however, due to lapatinib being an ErbB1 inhibitor which could interfere with chloride secretion,

further investigations are required. Effect of lapatinib on chloride secretion might occur via other mechanisms unrelated to calcium or cAMP regulated chloride secretion. The mechanism of lapatinib-induced diarrhoea may be mediated by other unknown mechanisms. Overall, further investigations are needed to clarify the possible mechanisms of lapatinib-induced diarrhoea.

REFERENCES:

1. Medina PJ, Goodin S. Lapatinib: a dual inhibitor of human epidermal growth factor receptor tyrosine kinases. Clin Ther. 2008;30(8):1426-47.
2. Crown JP, Burris HA, 3rd, Boyle F, Jones S, Koehler M, Newstat BO, et al. Pooled analysis of diarrhea events in patients with cancer treated with lapatinib. Breast Cancer Res Treat. 2008;112(2):317-25.
3. Burris HA, 3rd, Taylor CW, Jones SF, Koch KM, Versola MJ, Arya N, et al. A phase I and pharmacokinetic study of oral lapatinib administered once or twice daily in patients with solid malignancies. Clinical cancer research : an official journal of the American Association for Cancer Research. 2009;15(21):6702-8.
4. Gibson RJ, Bowen JM, Inglis MR, Cummins AG, Keefe DM. Irinotecan causes severe small intestinal damage, as well as colonic damage, in the rat with implanted breast cancer. J Gastroenterol Hepatol. 2003;18(9):1095-100.
5. Logan RM, Stringer AM, Bowen JM, Gibson RJ, Sonis ST, Keefe DM. Is the pathobiology of chemotherapy-induced alimentary tract mucositis influenced by the type of mucotoxic drug administered? Cancer Chemother Pharmacol. 2009;63(2):239-51.
6. Bowen JM, Mayo BJ, Plews E, Bateman E, Stringer AM, Boyle FM, et al. Development of a rat model of oral small molecule receptor tyrosine kinase inhibitor-induced diarrhea. Cancer Biol Ther. 2012;13(13):1269-75.
7. Gibson RJ, Keefe DM. Cancer chemotherapy-induced diarrhoea and constipation: mechanisms of damage and prevention strategies. Support Care Cancer. 2006;14(9):890-900.
8. Field M. Intestinal ion transport and the pathophysiology of diarrhea. J Clin Invest. 2003;111(7):931-43.
9. Barrett KE, Keely SJ. Chloride secretion by the intestinal epithelium: molecular basis and regulatory aspects. Annu Rev Physiol. 2000;62:535-72.
10. Kunzelmann K, Mall M. Electrolyte transport in the mammalian colon: mechanisms and implications for disease. Physiological reviews. 2002;82(1):245-89.
11. Schultheiss G, Diener M. K+ and Cl- conductances in the distal colon of the rat. General pharmacology. 1998;31(3):337-42.
12. Heitzmann D, Warth R. Physiology and pathophysiology of potassium channels in gastrointestinal epithelia. Physiological reviews. 2008;88(3):1119-82.
13. McCole DF, Truong A, Bunz M, Barrett KE. Consequences of direct versus indirect activation of epidermal growth factor receptor in intestinal epithelial cells are dictated by protein-tyrosine phosphatase 1B. J Biol Chem. 2007;282(18):13303-15.
14. McCole DF, Rogler G, Varki N, Barrett KE. Epidermal growth factor partially restores colonic ion transport responses in mouse models of chronic colitis. Gastroenterology. 2005;129(2):591-608.
15. McCole DF, Barrett KE. Decoding epithelial signals: critical role for the epidermal growth factor receptor in controlling intestinal transport function. Acta Physiol (Oxf). 2009;195(1):149-59.
16. Barrett KE. New insights into the pathogenesis of intestinal dysfunction: secretory diarrhea and cystic fibrosis. World J Gastroenterol. 2000;6(4):470-4.
17. Bowen JM. Development of the rat model of lapatinib-induced diarrhoea. Scientifica (Cairo). 2014;2014:194185.
18. Loriot Y, Perlemuter G, Malka D, Penault-Llorca F, Boige V, Deutsch E, et al. Drug insight: gastrointestinal and hepatic adverse effects of molecular-targeted agents in cancer therapy. Nat Clin Pract Oncol. 2008;5(5):268-78.

19. Bowen JM, Mayo BJ, Plews E, Bateman E, Wignall A, Stringer AM, et al. Determining the mechanisms of lapatinib-induced diarrhoea using a rat model. Cancer Chemother Pharmacol. 2014;74(3):617-27.
20. Clarke LL. A guide to Ussing chamber studies of mouse intestine. Am J Physiol Gastrointest Liver Physiol. 2009;296(6):G1151-66.
21. Dharmsathaphorn K, Pandol SJ. Mechanism of chloride secretion induced by carbachol in a colonic epithelial cell line. J Clin Invest. 1986;77(2):348-54.
22. Ou G, Baranov V, Lundmark E, Hammarström S, Hammarström ML. Contribution of intestinal epithelial cells to innate immunity of the human gut–studies on polarized monolayers of colon carcinoma cells. Scandinavian journal of immunology. 2009;69(2):150-61.
23. McRoberts J, Barrett K. Hormone-regulated ion transport in T84 colonic cells. Functional epithelial cells in culture: Alan R. Liss New York; 1989. p. 235-65.
24. Dharmsathaphorn K, McRoberts JA, Mandel KG, Tisdale LD, Masui H. A human colonic tumor cell line that maintains vectorial electrolyte transport. Am J Physiol. 1984;246(2 Pt 1):G204-8.
25. Barrett KE. Positive and negative regulation of chloride secretion in T84 cells. Am J Physiol. 1993;265(4 Pt 1):C859-68.
26. Rusnak DW, Alligood KJ, Mullin RJ, Spehar GM, Arenas-Elliott C, Martin AM, et al. Assessment of epidermal growth factor receptor (EGFR, ErbB1) and HER2 (ErbB2) protein expression levels and response to lapatinib (Tykerb, GW572016) in an expanded panel of human normal and tumour cell lines. Cell Prolif. 2007;40(4):580-94.
27. Zhou Y, Li S, Hu YP, Wang J, Hauser J, Conway AN, et al. Blockade of EGFR and ErbB2 by the novel dual EGFR and ErbB2 tyrosine kinase inhibitor GW572016 sensitizes human colon carcinoma GEO cells to apoptosis. Cancer Res. 2006;66(1):404-11.
28. Hoda MR, Scharl M, Keely SJ, McCole DF, Barrett KE. Apical leptin induces chloride secretion by intestinal epithelial cells and in a rat model of acute chemotherapy-induced colitis. Am J Physiol Gastrointest Liver Physiol. 2010;298(5):G714-21.
29. Paul G, Marchelletta RR, McCole DF, Barrett KE. Interferon-gamma alters downstream signaling originating from epidermal growth factor receptor in intestinal epithelial cells: functional consequences for ion transport. J Biol Chem. 2012;287(3):2144-55.
30. Forsythe RM, Xu DZ, Lu Q, Deitch EA. Lipopolysaccharide-induced enterocyte-derived nitric oxide induces intestinal monolayer permeability in an autocrine fashion. Shock (Augusta, Ga). 2002;17(3):180-4.
31. Xiao WD, Chen W, Sun LH, Wang WS, Zhou SW, Yang H. The protective effect of enteric glial cells on intestinal epithelial barrier function is enhanced by inhibiting inducible nitric oxide synthase activity under lipopolysaccharide stimulation. Molecular and cellular neurosciences. 2011;46(2):527-34.
32. Ohland CL, DeVinney R, MacNaughton WK. Escherichia coli-induced epithelial hyporesponsiveness to secretagogues is associated with altered CFTR localization. Cell Microbiol. 2012;14(4):447-59.
33. Clarke LL. A guide to Ussing chamber studies of mouse intestine. American Journal of Physiology-Gastrointestinal and Liver Physiology. 2009;296(6):G1151-G66.
34. Wardill HR, Bowen JM, Gibson RJ. Chemotherapy-induced gut toxicity: are alterations to intestinal tight junctions pivotal? Cancer chemotherapy and pharmacology. 2012;70(5):627-35.
35. Fasano A, Shea-Donohue T. Mechanisms of disease: the role of intestinal barrier function in the pathogenesis of gastrointestinal autoimmune diseases. Nature clinical practice Gastroenterology & hepatology. 2005;2(9):416-22.
36. Penner G, Aschenbach J, Wood K, Walpole M, Kanafany-Guzman R, Hendrick S, et al. Characterising barrier function among regions of the gastrointestinal tract in Holstein steers. Animal Production Science. 2014;54(9):1282-7.
37. Chow JY, Carlstrom K, Barrett KE. Growth hormone reduces chloride secretion in human colonic epithelial cells via EGF receptor and extracellular regulated kinase. Gastroenterology. 2003;125(4):1114-24.

FP-20

A STUDY OF LIGHT INTENSITY AND ENERGY CONSUMPTION OF DIFFERENT LIGHT SOURCES FOR PLANT TISSUE CULTURE

CHONG SAW PENG[1*], NORAZLINA NOORDIN[1], NORELLIA BAHARI[1]

[1]Agrotechnology and Bioscience Division, Malaysian Nuclear Agency (Nuclear Malaysia) Ministry of Science, Technology and Innovation (MOSTI), Bangi, 43000 Kajang, Selangor, Malaysia

[*]Corresponding author: sawpeng@nm.gov.my

ABSTRACT

Light plays an important role in influencing growth and development of the *in vitro* culture plants. Control of light spectrum and light cycle had been used in plant tissue culture to regulate growth and development, improve plant quality and increase rate of growth in plants leading to improved plant yields. In this study, light intensity and energy consumption experiments were carried out to determine 4 different light sources used commonly by the plant tissue culture industry. Measurements were made using lux light meter and energy meter for each light source. The results showed that although warm fluorescent lamp gave the highest intensity among the other light sources, the cool white fluorescent lamp and white/far red TLED Lamp were more suitable for plant tissue culture used. Moreover, the energy consumption study showed that despite the increased upfront costs of TLED lighting, the operation and maintenance was significantly lower (56%) than fluorescent fixtures, making TLED a cost effective option to use for plant tissue culture.

KEY WORDS:
Light intensity, Energy consumption, TLED lighting

INTRODUCTION:

Nowadays to satisfy commodity industries demand for seedling materials throughout the year, more and more plant tissue culture facilities had been established. Such seedling production facilities provide a grower the ability to produce more planting materials under precisely control for temperature, humidity and lighting. Light plays an important role in influencing growth and development of the *in vitro* culture plants. The control of light spectrum and light cycle can be used in plant tissue culture to regulate growth and development, improve plant quality and increase rate of growth in plants leading to improved plant yields (Economou and Read, 1987). Therefore artificial lighting is a key component of plant tissue culture facilities because it is crucial to healthy and rapid plant growth. Artificial light sources are used in plant tissue culture laboratory to provide all the light a plant needs. Thus the energy requirement and their cost are main expenditure of the laboratory as much as or more than the cost of manpower and others. In recent years, many kinds of artificial light sources have evolved and been available for vary utilization which are energy and cost effective.

Traditionally, artificial lighting has been supplied by tubular fluorescent lamp in plant tissue culture and transplant production, which was sufficiently economic and readily available. However, growers continue to search for ways to reduce operating costs while improving growth rates and yields of seedling because among these traditional light sources, no one type of lamp has satisfied the needs of growers. This is because plants use light to grow with the help of pigments and the most important pigments to plant growth is chlorophylls a and b. According to the McCree curve represents the average photosynthetic response of plants to light energy (Sager et al., 1982), the chlorophylls have two light absorption peaks, one in the red region (700 nm wavelength) of the light spectrum and the other in the blue region (400 nm wavelength). The range between these wavelengths is commonly referred to as the photosynthetically active radiation range.

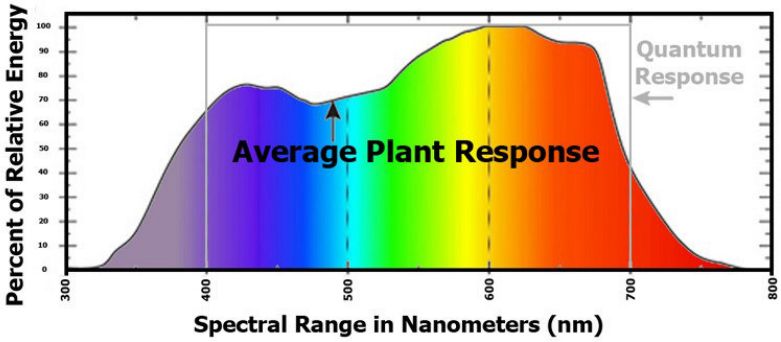

Figure 1
The McCree curve of light spectrum.

To overcome these limitations, a new light emitting diodes (LED) lighting technology has been developed by Philips and is gaining acceptance among commercial growers. The reason is that LED colors can be optimized for specific plant needs and due to the compact size of the individual diodes, single fixtures can mount diodes of different colors to provide light recipes. Besides, the energy reduction and maintenance requirements are other factors driving LED acceptance into the market. Since the early 1990s, LED technology has improved dramatically via focused research and manufacturing improvements. Modern LED provide several advantages over traditional fluorescent lighting, including the ability to control spectral composition, the ability to produce very high light levels with low radiant heat output and no long-wave radiation. They also maintain useful light output for years without replacement (Morrow, 2008). LEDs provide spectral composition control permitting lighting recipes whereby wavelengths can be matched to plant photoreceptors for optimal production, plant morphology, pathology and composition. Thus, narrow-band LED avoid the inefficient energy burden of broad wavelength light, as a result energy is further saved (Yeh & Chung, 2009). They are safer to operate because they do not have glass envelopes or high surface temperatures (Morrow, 2008).

In this study, tubular fluorescent lamps that produce series of white light include daylight, cool white and warm light and the LED lamp with combination of white/far-red were used to compare their light intensity and energy consumption in the experiments. As we know that the length and diameter of the tube enter into the calculation of how much power the lamp will consume and how much light it can generate, thus those lamps are alternative choice of light source for reducing cost of energy consumed in plant tissue culture industry.

METHODOLOGY:

Energy Consumption

Our study used a multi levels rack equipped with lighting for plant tissue culture incubation in the laboratory of Malaysian Nuclear Agency to compare the life cycle costs of LED fixtures to fluorescents. The location was selected to develop an accurate model of an actual plant tissue culture laboratory facility using Philips costs. The parameters of this study were the cost of the fixture and the electrical costs to operate the fixtures. This study assumed other costs of the fixtures for both technologies would be approximately equal. The fixtures included in the study were 4 fluorescent cool white lamps (Philips Lifemax Cool White), 4 fluorescent cool daylight lamps (Philips Lifemax Cool Daylight), 4 fluorescent warm lamps (Philips Lifemax Warm) and 4 LED lamps (Philips GreenPower TLED White/Far red). The lightings were operated at full lighting capacity in 16 hours photoperiod per day, which resulted in 30 days operating hourly total of 480 hours.

Light Intensity

The comparison study was conducted in one of the plant tissue culture laboratory in Malaysian Nuclear Agency. Four different light sources produced by Philips were used in this study to compare intensity between warm lamps, cool white lamps, cool daylight lamps and LED lamps. Approximately 6 detection points from A to F were measured under the light source with a distance of 30 cm in height (Fig. 2). The intensity was measured using a digital light meter. Measurement was read in lux unit. The intensity

was measured by placed the light meter at each of the detection points under different light sources. Background intensity was measured from each detection points before measuring the light intensity. The light meter was placed under the light source for 3 min before any reading was taken. Three reading were measured at each detection points.

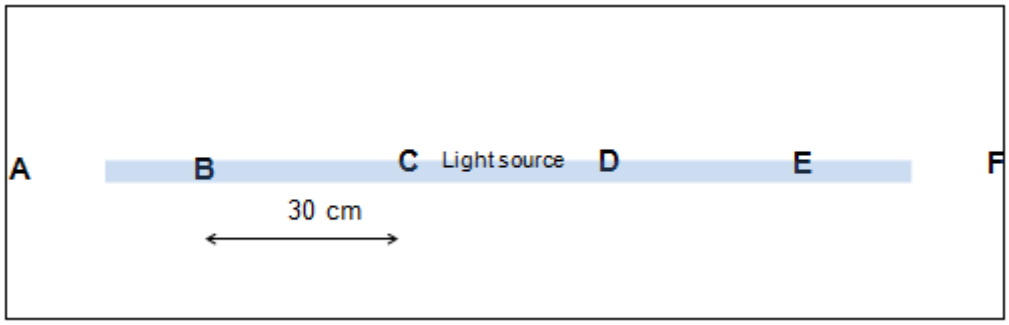

Figure 2
The view from top of detection points measured by flux meter under light source

RESULTS AND DISCUSSION:

For the energy consumption study, the cost for the LED and fluorescent fixtures differed dramatically. The LED and fluorescent fixtures extended out to RM 390 and RM 13 respectively. The difference between these costs was RM 377. The differences in energy usage for the fluorescent and LED lighting fixtures were calculated by subtracting the LED usage from the fluorescent. The monthly values were showed in Table 1. These differences resulted in additional monthly cost of RM 10.34 for the fluorescent fixtures (according to electrical cost RM 0.218 per unit in Malaysia). This additional cost indicated that the operational cost of the LED fixtures was 56% less than the fluorescent (Fig. 3).

For the light intensity study, the averages of measurements made at the different light sources of each detection point were showed in table 2. The figure 4 was the comparison graph showed the differential between each light source. The result showed that the warm fluorescent lamp gave the highest light intensity among the others, followed by the cool white fluorescent lamp and white/far red TLED lamp. The white/far red TLED lamp was made of combination of far red and white (1:2) LED bulbs in the lamp. The spectrum emission of a far red is at 735 nm. Although the warm fluorescent lamp gave the highest light intensity, it also created the highest heat among the others. This heat not only is ambient temperature raised, also the potential for leaf burn is increased. As a result, the warm fluorescent lamp is not suitable for plant tissue culture used.

Table 1
Energy consumption of different light sources between LED and fluorescent.

Light Sources	Total Time (hour)	Total Power (Kwh)
White/Far Red TLED lamp	480	38.88
Cool White lamp	480	86.27
Cool Daylight lamp	480	86.44
Warm lamp	480	86.24

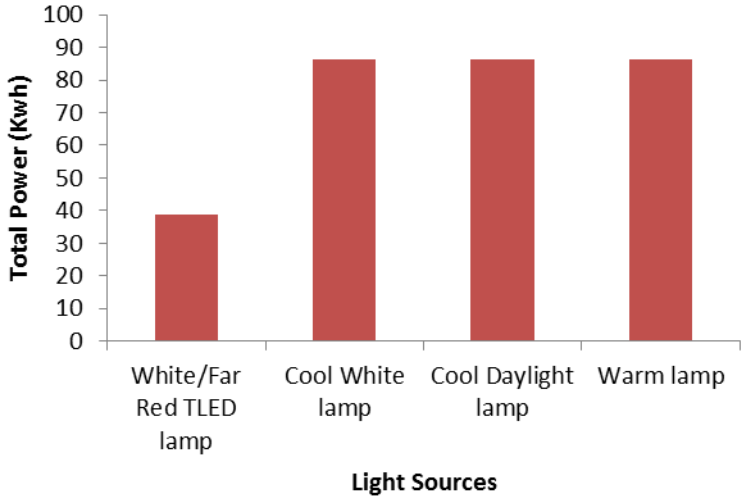

Figure 3
Comparison of energy consumption between LED and fluorescent light sources.

Table 2
Light intensity of different light sources between LED and fluorescent.

Light Sources	Total Intensity (Lux)
White/Far Red TLED lamp	898
Cool White lamp	904
Cool Daylight lamp	829
Warm lamp	984

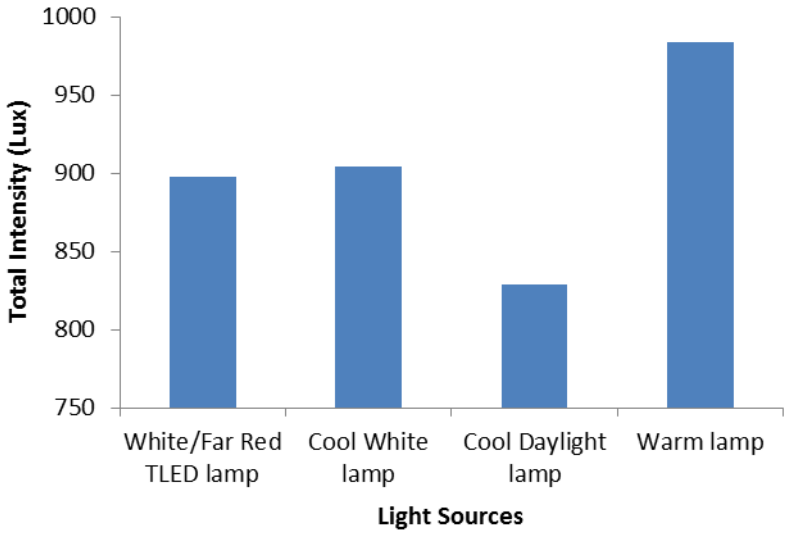

Figure 4
Comparison of light intensity between LED and fluorescent light sources.

The most optimum light intensity with a lower heat produced lamps were the white/far red TLED lamp and cool white fluorescent lamp. Both gave similar light intensity, the differential between them was the cool white fluorescent lamp emitted the full spectrum of equal intensity for all electromagnetic waves of different wavelengths from 400nm to 700nm. On the other hand, the white/far red TLED lamp not only emitted a spectrum of white light, a spectrum of far red (735 nm) was added in the LED light recipe to enhance the plant growth. This wavelength band is known to be important independently or complementarily for plant photosynthesis, pigment synthesis, growth, and development (Hoenecke et al.,

1992; Goins et al., 1997; Yorio et al., 2001; Nhut et al., 2003; Matsuda et al., 2004; Ohashi-Kaneko et al., 2006; Wu et al., 2007; Folta et al., 2008; Stutte et al., 2009; Hogewoning et al., 2010).

Light quality plays a major role in the appearance and productivity of plant. Far-red light, for example, is important for promoting internode elongation (Morgan and Smith, 1979). Blue light is important for phototropism (Blaauw and Blaauw-Jansen, 1970), for stomatal opening (Schwartz and Zeiger, 1984), and for inhibiting seedling growth on emergence of seedlings from a growth medium (Thomas and Dickinson, 1979). The blue light photoreceptor class of cryptochromes has been found to work in conjunction with the red/FR phytochrome photoreceptor class to control factors such as circadian rhythms and de-etiolation in plants (Devlin et al., 2007).

CONCLUSION:

The studies concluded that despite the increased upfront costs of LED lighting, the operation and maintenance is significantly lower than fluorescent fixtures, making LED a cost effective option to use for plant tissue culture. Moreover, LED is a more efficient lighting system for plant tissue culture than the normal fluorescent lighting due to its high intensity and light quality that enhances the plant growth. An important issue for LED in plant tissue culture concerns their economic viability. Like with any developing technology, as demand increases and research results accumulate, the cost of LED for plant growth lighting will decrease over time. With advancing technology developments, LED are poised to become the light source with the highest electrical energy conversion ratio.

REFERENCES:

15. Blaauw, O. & G. Blaauw-Jansen. 1970. The phototropic responses of Avena coleoptiles. *Acta Botan. Neer*. 19: 755–763.
16. Devlin, P.F., J.M. Christie, & M.J. Terry. 2007. Many hands make light work. *J. Expt. Bot.* 58: 3071–3077.
17. Economou A. S. & Read P. E. 1987. Light treatments to improve efficiency of *in vitro* propagation systems. *Hort Sci* 22: 751-754.
18. Folta K.M. & Childers K.S. 2008. Light as a growth regulator: controlling plant biology with narrow-bandwidth solid-state lighting systems. *Hort Sci* 43:1957–1964.
19. Goins G.D., Yorio N.C., Sanwo M.M., & Brown C.S. 1997. Photomorphogenesis, photosynthesis, and seed yield of wheat plants grown under red light-emitting diodes (LEDs) with and without supplemental blue lighting. *J Exp Bot* 48: 1407–1413.
20. Hoenecke M.E., Bula R.J., & Tibbitts T.W. 1992. Importance of 'blue' photon levels for lettuce seedlings grown under red-light-emitting diodes. *Hort Sci* 27: 427–430.
21. Hogewoning S.W., Trouwborst G., Maljaars H., Poorter H., Van Ieperen W., & Harbinson J. 2010. Blue light dose – responses of leaf photosynthesis, morphology, and chemical composition of Cucumis sativus grown under different combinations of red and blue light. *J Exp Bot* 61: 3107–3117.
22. Matsuda R., Ohashi-Kaneko K., Fujiwara K., Goto E., & Kurata K. 2004. Photosynthetic characteristics of rice leaves grown under red light with or without supplemental blue light. *Plant Cell Physiol* 45: 1870–1874.
23. Morrow R.C. 2008. LED lighting in horticulture. *Hort Sci* 43: 1947–1950.
24. Nhut D.T., Takamura T., Watanabe H., Okamoto K., & Tanaka M. 2003. Responses of strawberry plantlets cultured in vitro under superbright red and blue light-emitting diodes (LEDs). *Plant Cell Tissue Organ Cult* 73: 43–52.
25. Ohashi-Kaneko K., Matsuda R., Goto E., Fujiwara K., & Kurata K. 2006. Growth of rice plants under red light with or without supplemental blue light. *Soil Sci Plant Nutr* 52: 444–452.

26. Sager J., Edwards J., and Klein W. 1982. Light energy utilization efficiency for photosynthesis. Trans. ASAE 25: 1737–1746.
27. Schwartz, A. & E. Zeiger. 1984. Metabolic energy for stomatal opening: Roles of photophosphorylation and oxidative phosphorylation. *Planta* 161: 129–136.
28. Stutte G.W. & Edney S. 2009. Photoregulation of bioprotectant content of red leaf lettuce with light-emitting diodes. *Hort Sci* 44: 79–82.
29. Thomas, B. & H.G. Dickinson. 1979. Evidence for two photoreceptors controlling growth in de-etiolated seedlings. *Planta* 146: 545–550.
30. Wu M.C., Hou C.Y., Jiang C.M., Wang Y.T., Wang C.Y., Chen H.H., & Chang H.M. 2007. A novel approach of LED light radiation improves the antioxidant activity of pea seedlings. *Food Chem* 101: 1753–1758.
31. Yeh N. & Chung J.P. 2009. High-brightness LEDs – energy efficient lighting sources and their potential in indoor plant cultivation. *Renew Sust Energ Rev*. 13: 2175– 2180.
32. Yorio N.C., Goins G.D., Kagie H.R., Wheeler R.M., & Sager J.C. 2001. Improving spinach, radish, and lettuce growth under red light-emitting diodes (LEDs) with blue light supplementation. *Hort Sci* 36: 380–383.

FP-21

OPTIMAL PARAMETERS OF DEVELOPED ACETYLCHOLINESTERASE BASED BIOSENSOR FOR CARBAMATE PESTICIDE DETECTION

ANWAR SAMSIDAR[1], SHAFIQUZZAMAN SIDDIQUE[1*], SHARIFUDIN MD SHAARANI[2], LAILA NAHER[3,4], ZARINA AMIN[1], MD. AKHTER UZZAMAN[5]

[1]Biotechnology Research Institute, Universiti Malaysia Sabah, Jln UMS, 88400 Kota Kinabalu, Sabah, Malaysia
[2]Faculty of Food Science and Nutrition, Universiti Malaysia Sabah, Jln UMS, 88400 Kota Kinabalu, Sabah, Malaysia
[3]Department of Agricultural science, Faculty of Agro-Based Industry, Universiti Malaysia Kelantan Jeli Campus, 17600, Kelantan, Malaysia
[4]Institute of Food Security and Sustainable Agriculture, Universiti Malaysia Kelantan, Jeli Campus, 17600 Kelantan, Malaysia
[5]Planning and Development Division, Bangladesh Atomic Energy Commission, Dhaka, Bangladesh

Corresponding author: shafiqpab@ums.edu.my

ABSTRACT

Carbamate pesticides are commercially important in agriculture as it applied extensively for the crop protection and better quality. Carbamate has broader spectrum of activity, great insecticidal action as well as demonstrate low persistence in environment. Despite its effectiveness for protection against numerous pests organisms, pesticides overuse contribute to detrimental human health effects and environmental destruction. Carbamates are known as cholinesterase inhibitor with ability to inhibit activity of acetylcholinesterase enzyme that found in mammal nervous system. Herein, an electrochemical biosensor based on immobilized AChE is developed for carbamate detection. This work presents parameters optimization to find the best conditions for the developed AChE biosensor. The effect of pH buffer, reaction time, scan rate and inhibition time were studied. Results revealed that the conditions which favor the performance of developed biosensor found respectively pH 7.0 of buffer solution, 20 s of reaction time, 0.1 V/s of scan rate and 8 min of inhibition time. The value of optimized parameters was subsequently applied for further pesticide analysis.

KEYWORDS:
Carbamate, Electrochemical biosensor, Acetylcholinesterase

INTRODUCTION:

Pests present significant threats to worldwide agriculture especially during cultivation of crops. Pesticides are chemicals generally applied to kill various kinds of pests. Often sprayed onto the crops, carbamates are synthetic pesticides which usually used against insects. Upon its wide use, the agricultural productivity is increasing and the quality of yielded crop products is improved. However, overuse of pesticides results in accumulation of pesticides in foodstuffs and environment. The toxicity of carbamates is exhibited from its capability to inhibit acetylcholinesterase (AChE) activity, a main enzyme involve during signal transmission in human nervous system [1,2]. The conventional methods currently existed for pesticide detection includes high performance liquid chromatography (HPLC), gas chromatography mass spectrometry (GCMS), capillary electrophoresis and spectroscopy. Those pesticide detection methods are expensive, time-consuming and requires high skilled of personnel in order to handle the instruments. Biosensors offer rapid

detection, simple, sensitive and specific for pesticide analysis. The demand for this biosensor is highly increased as it allows 'on-site' sample analysis which is lack in conventional way.

Among them, AChE based electrochemical biosensors have appeared as a robust technique for the analysis of environmental contaminant such as pesticides. The detection of pesticide is based on enzyme inhibition. As carbamates are known by its ability to inhibit the AChE, the reduction of this enzyme activity correlated with the pesticide concentration. On the basis of this principle, AChE biosensors have been used to detect carbamate in environment. On the surface of electrode, the immobilized AChE displays its catalytic action by catalyzing the hydrolysis of acetylthiocholine chloride (ATCl), producing an electroactive species of thiocholine (TCh). However, the electrochemical reaction often associated with high potential voltage that leads to poor sensitivity. As for that, implementation of nanomaterials would be useful for improvement of the biosensor and lowering potential voltage.

Chitosan (CS), a polysaccharide derived from chitin that exists abundantly in nature. It possesses incredible features including biocompatibility, ability in formation of film, non- toxicity and susceptible to chemical modifications [3-4]. This will provide natural microenvironment for the immobilized enzyme on the electrode and permit accessibility of electron flow between enzyme and the electrode [5]. Besides, carbon based materials such as multi-walled carbon nanotubes (MWCNTs) have wide application for modification of biosensor interface because of their high electrical and mechanical conductivity [6]. It is well known that metal nanoparticles have received increasing interest for amperometric biosensor construction particularly gold nanoparticles (AuNPs). The unique properties of AuNPs consists of high stability of physical and chemical, catalytic role resulted by its nanosize [7-9]. This paper presents the conduction of parameters optimization based on glassy carbon electrode (GCE) modified with nanomaterials to identify the favorable conditions for the construction of biosensor in order to determine carbamate pesticide.

MATERIALS AND METHODS:

Materials

Acetylcholinesterase enzyme (AChE from Electric eel, 827units/mg), acetylthiocholine chloride (ATCl), glutaraldehyde (GA), chitosan (CS), carbaryl, multi-walled carbon nanotubes (MWCNTs) and gold powder were purchased from Sigma-Aldrich. Glacial Acetic acid (99%) was obtained from Systerm. All chemicals used in the experiments were analytical reagent grade. All solutions were prepared with double distilled water

Apparatus

Electrochemical measurements were carried out an electrochemical analyzer Nova Potentiostat Galvanostat Autolab machine (AUT85150). A conventional three-electrode system was employed with a Pt (platinum) wire as counter electrode and a silver/silver chloride (Ag/AgCl) as reference electrode and the modified GCE as working electrode. All experiments were performed in an electrochemical cell with 15 mL of 0.1 M Tris-HCl buffer containing 0.5 mM acetylthiocholine chloride (ATCl) at room temperature. A model of Ultrasonic Cleaner UC 1050 was used for sonicating and cleaning the electrode.

Preparation of nanomaterials

For the preparation of modification solution, MWCNTs was initially treated according to Han et al. [10] with some modifications. 500 mg of raw MWCNTs was weighed and dissolved in 250 mL mixture of concentrated sulfuric and nitric acid, H_2SO_4:HNO_3 (3:1, v/v ratio) with magnetic stirring at 26°C for 4 h in order to promote functionalization. The mixture was filtered through 50 mM Whatmann filter paper and continuously washed with double distilled water until pH of filtrate is neutral (pH 7.0). Then, it was followed by drying in oven at 60°C for 12 hr. In this step, the carboxylic acid groups were introduced on the nanotubes surface in order to improve its dispersibility in chitosan (CS) [9]. The resulted functionalized carbon nanotube referred to as MWCNTs-COOH [11] and was kept in a small beaker.

A 1% CS solution was prepared by dissolving CS flakes into acetic acid (1%) solution. Preparation of MWCNTs in CS solution was done according to the procedures described by Yang et al. [9] with some modifications. A mixture was stirred for 3 h at room temperature until complete dissolution. A 2.5 mg functionalized MWCNTs (f-MWCNTs) were dispersed in 4 mL of CS solution. The CS-MWCNTs mixture was stirred for 2 h prior to sonicated for 10 min to ensure complete dissolution and a homogeneous mixture. Then, a high-dispersed colloidal suspension was produced where linkages were formed between the amino groups of CS and carboxylic group of MWCNTs as described by Ghica et al. [12].

The gold nanoparticles (AuNPs) were prepared and functionalized based on procedures described by Grabar et al. [13] with modifications. 2.5 mL of chloroauric acid ($HAuCl_4$) aqueous solution was diluted into 250 mL with double distilled water and heated until boiled. Quickly, 4.4 mL of 1% trisodium citrate ($Na_3C_6H_5O_7$) solution was added to the boiling solution of 0.01% $HAuCl_4$.The solution was continued to boil for an additional 10 min under vigorous stirring at 100°C until the color changed from light yellow to dark red solution. Then, the solution was cooled down slowly at the room temperature. The prepared AuNPs was stored in a dark bottle at 4°C before use.

Preparation of the modified electrode

A glassy carbon electrode (GCE, diameter of 3 mm) was pre-treated initially before each experiment. The bare GCE was polished with 3 µm alumina slurry for 2 min to free the surface of electrode from any contaminants. Then, the GCE was rinsed thoroughly with double distilled water prior to sonicate for 2 min in distilled water and dried in air. Preparation of CS/MWCNTs solution was performed based on procedures described by Yang et al. [9] with slight modifications. 1.25 mg f-MWCNTs were dispersed into 2 mL of CS solution. The mixture was stirred for 7 to 8 hrs prior to sonicated for 15 min. An appropriate amount of AuNPs was added to the CS/MWCNTs composite in a ratio of 1:2 and stirred for 2 h. The mixture was then sonicated for 10 min to form homogeneous suspension of CS/MWCNTs/AuNPs.

A 5 µL of as prepared CS/MWCNTs/AuNPs solution was deposited on the surface of pre-treated GCE and dried at room temperature. Then, 5 µL of AChE was coated on the CS/MWCNTs/AuNPs/GCE. Finally, 3 µL of glutaraldehyde (GA) was added as a cross-linking agent on the modified GCE. The resulted enzyme biosensor was denoted as GA/AChE/CS/MWCNTs/AuNPs/GCE.

RESULTS AND DISCUSSION:

In this study, carbaryl, belongs to carbamate family was used as model of compound detected. Different experimental parameters were studied to optimize the electrochemical response of GA/AChE/CS/MWCNTs/AuNPs/GCE biosensor to carbaryl. These including pH of the buffer solution, reaction time, scan rate and inhibition time. The CV method was used to investigate the optimal parameters in order to determine the optimum working conditions of the AChE biosensor.

Effect of pH

The effect of the supporting electrolyte pH was the first parameter investigated. The enzyme tends to denature at extreme pH values due to conformational changes observed in a native tertiary structure of AChE enzyme [14]. Since the bioactivity of nearly all of intracellular enzymes including AChE, depended strongly on the pH of buffer solution, the biosensor response against various pH in 0.1M Tris-HCl (pH range 6.0 to 8.0) was measured. Highest response of biosensor was shown in a buffer solution of pH 7.0 (**Figure 1**). Thus, pH 7.0 was selected as optimum pH and used further in experiment. Murray et al. [15] reported that mostly enzymes exhibit optimal activity between pH 7 and 9. At high and low pH values may denature the enzyme. Moreover, according to Ganesana et al. [16], the optimum pH for the AChE enzyme is ranged of 7.0 to 8.0.

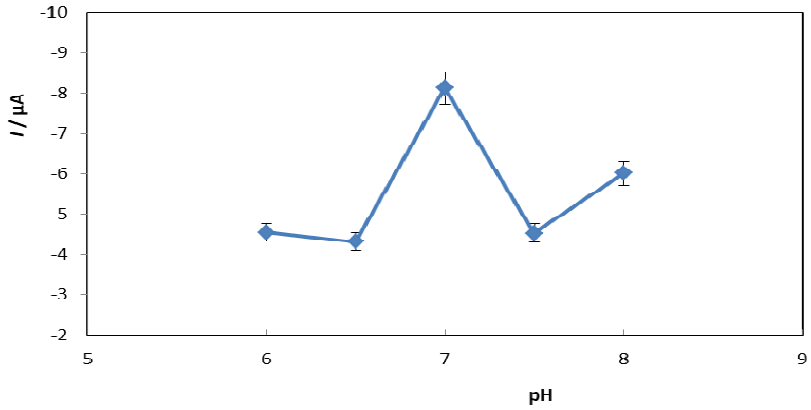

Figure 1.
Effect of different pH buffer (0.1M Tris-HCl).

Effect of reaction time

The response time was another important factor in the performance of biosensor. The amperometric response of prepared biosensor electrode was measured in a series of 10 to 60 seconds. As seen in Fig. 2, the response time of 20 s showed maximal value and was chosen in subsequent experiment.

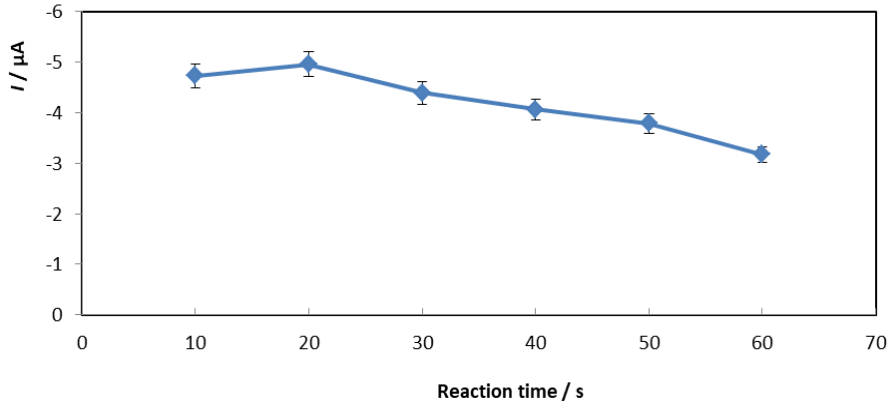

Figure 2.
The effect of different reaction time.

Effect of scan rate

The effect of scan rate was also explored ranging from 0.02 to 0.10 V/s like shown in Figure 3. The peak currents increasing with the scan rate values. A 0.1 V/s was therefore selected throughout the study.

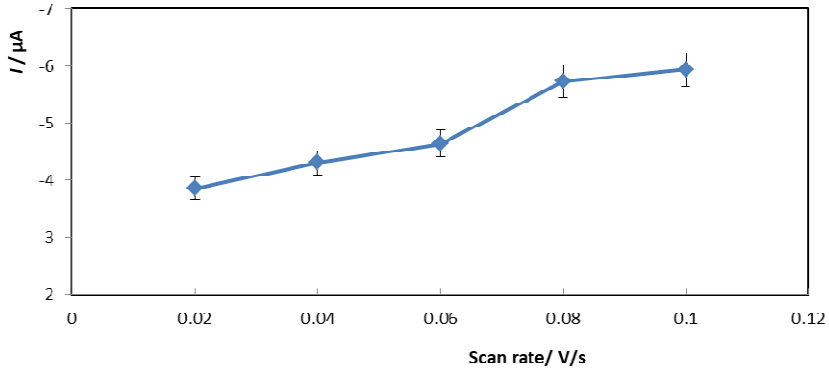

Figure 3.
The effect of different scan rates.

Effect of inhibition time

The inhibition of carbaryl pesticide on AChE activity were tested at different incubation times 2 to 12 min (with two-interval) in a fixed concentration of pesticide. As can be seen in Figure 4, it was observed that as the incubation time increased, the AChE inhibition also increased. The highest response obtained at 8 min incubation time. However, when the incubation time was exceeding 8 min, the curve trended to a stable value. This indicates the binding interaction with the enzyme active sites was saturated. Thus, 8 min incubation time of carbamate was used in the following experiment. However the maximum value of inhibition was not 100%, which was likely to attribute to the binding equilibrium between pesticide and binding sites in enzyme. Thus, the incubation time of 8 min was chosen for the pesticide determination. Such result was found similar with the previous research by Du et al [17].

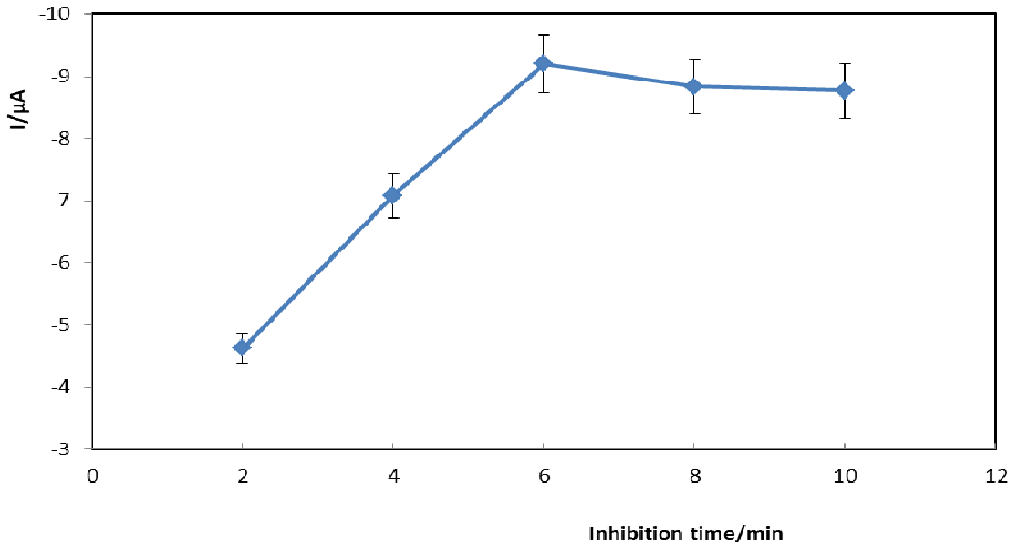

Figure 4.
The effect of different inhibition time.

ACKNOWLEDGEMENTS:

This work was supported by grants from the Ministry of Education Malaysia, Fundamental Research Grant Scheme (FRGS) (No. FRGS/1/2014/SG05/UMS/02/4).

CONCLUSION:

In conclusion, AChE biosensor based on CS/MWCNTs/AuNPs modified GCE with cross linking agent of glutaraldehyde has been applied for determination of carbamate pesticide. Parameters including pH buffer, reaction time, scan rate and inhibition time are successfully optimized and identified for a better performance of the developed AChE biosensor. The obtained optimum conditions are pH 7 for the buffer solution, 20 s of reaction time, 0.1 V/s of scan rate and 8 min for inhibition time. Further studies are in progress to evaluate the behaviours of the developed AChE biosensor towards detection of carbamate pesticide.

REFERENCES:

1. Abad JM, Pariente F, Hernández L, Abruna HD, Lorenzo E. Detemination of Organophosphorus and Carbamate Pesticides Using a Piezoelectric Biosensor. Anal. Chem. 1998 May 30; 70(14): 2848–2855.
2. Du D, Wang M, Cai J, Tao Y, Tu H, Zhang A. Immobilization of acetylcholinesterase based on the controllable adsorption of carbon nanotubes onto an alkanethiol monolayer for carbaryl sensing. Analyst 2008 Oct 17; 133: 1790–1795.

3. Wang XY, Gu HF, Yin F, Tu YF. A glucose biosensor based on Prussian blue/chitosan hybrid film 2009. Biosensors and Bioelectronics. 2009 Jan 1; 24(5): 1527-1530.
4. Salam MA, Makki MSI, Abdelaal MYA. Preparation and characterization of multi-walled carbon nanotubes/chitosan nanocomposite and its application for the removal of heavy metals from aqueous solution. Journal of Alloys and Compounds. 2011 Feb 3; 509(5): 2582-2587.
5. Sassolas A. Blum LJ, Leca-Bouvier BD. Immobilization strategies to develop enzymatic biosensors. Biotechnol. Adv. 2012 May-June; 30(3): 489–511.
6. Wang C, Wang G, Fang B. Electrocatalytic oxidation of bilirubin at ferrocenecarboxamide modified MWCNT-gold nanocomposite electrodes. Microchim. Acta. 2009 Jan; 164(1): 113- 118.
7. Wu BY, Hou SH, Yin F, Li J, Zhao ZX, Huang JD, Chen Q. Amperometric glucose biosensor based on layer-by-layer assembly of multilayer films composed of chitosan, gold nanoparticles and glucose oxidase modified Pt electrode. Biosens. Bioelectron. 2007 Jan 15; 22(6): 838–844.
8. Pavlov V, Xiao Y, Willner I. Inhibition of the acetycholine esterase-stimulated growth of Au nanoparticles: nanotechnology-based sensing of nerve gases. Nano Lett. 2005 Apr; 5(4): 649–53.
9. Yang Y, Yang G, Huang Y, Bai H, and Lu X. 2009 May 15 A new hydrogen peroxide biosensor based on gold nanoelectrode ensembles/multiwalled carbon nanotubes/chitosan film-modified electrode. Colloids and Surfaces A: Physicochem. Eng. Aspects. 2009 May 15; 340(1-3): 50-55.
10. Han Y, Zheng J, Dong S. A novel nonenzymatic hydrogen peroxide sensor based on Ag-MnO_2-MWCNTs nanocomposites. Electrochimica Acta. 2013; 90: 35–43.
11. Havens N, Trihn P, Kim D, Luna M, Wanekaya AK, Mugweru A. Redox polymer covalently modified multiwalled carbon nanotube based sensors for sensitive acetaminophen and ascorbic acid detection. Electrochimica Acta. 2010 Feb 15; 55(6): 2186–2190.
12. Ghica ME, Pauliukaite R, Fatibello-Filho O, Brett CMA. Application of functionalised carbon nanotubes immobilised into chitosan films in amperometric enzyme biosensors. Sens. Actuators B-Chem. 2009 Oct 12; 142(1): 308–315.
13. Grabar KC, Freeman RG, Hommer MB, Natan MJ. Preparation and Characterization of Au Colloid monolayers. Anal. Chem. 1995 Feb 15; 67(4): 735-743.
14. Raghu P, Madhusudana Reddy T, Reddaiah K, Kumara Swamy BE, Sreedhar M. Acetylcholinesterase based biosensor for monitoring of Malathion and Acephate in food samples: A voltammetric study. Food Chemistry. 2014 Jan 1; 142: 188–196.
15. Murray RK, Bender DA, Botham KM, Kennelly PJ, Rodwell VW, Weil PA. Harper's illustrated biochemistry, 29th ed, The McGraw-Hill Companies, Inc, USA, 2012.
16. Ganesana M, Istarnboulie G, Marty JL, Noguer T, Andreescu S. Site-specific immobilization of a (His)6-tagged acetylcholinesterase on nickel nanoparticles for highly sensitive toxicity biosensors. Biosensors and bioelectronics. 2011 Dec 15; 30(1): 43-48.
17. Du D, Wang MH, Cai J, Qin YH, Zhang AD. One-step synthesis of multiwalled carbon nanotubes-gold nanocomposites for fabricating amperometric acetylcholinesterase biosensor. Sensors and Actuators B: Chemical. 2010 Jan 7; 143(2): 524-29.

FP-22

THERMODYNAMIC STUDIES OF PROTEIN IMMOBILIZATION ON POLYMERIC MEMBRANE

IDERIS, NORHIDAYAH[1], MOHD RASHID, AMIRAH ASYIQIN[1] AND ABDUL RAHMAN, NADHRATUL NUR AIN[1]

[1]Faculty of Chemical Engineering, Universiti Teknologi MARA, 40450 Shah Alam, Selangor, Malaysia

*Corresponding author: norhidayah7229@salam.uitm.edu.my

ABSTRACT

Adsorptive membrane is considered as one type of membrane that mostly applied in biotechnology field such as in a case of antibody-antigen diagnostic kit and affinity membrane chromatography. The aim of this current study is to investigate the thermodynamic aspects for static adsorption of Bovine Serum Albumin (BSA) as a model protein of 50 kDa *Salmonella Typhi* antigen on different types of polymeric membranes; polyvinylidenefluoride (PVDF) and nitrocellulose (NC). The polymeric membranes were characterized to understand their morphology, polymorph and intrinsic characteristics. For thermodynamic study, the influence of temperature on the adsorption behavior of BSA was examined using van't Hoff plot in order to obtain the thermodynamics' constants which were the change in standard enthalpy ($\Delta_r H^\theta$) and standard entropy ($\Delta_r S^\theta$). The results obtained revealed that the process of protein adsorption on both polymeric membrane was endothermic and the distribution of BSA adsorbed on membrane was more chaotic than that in aqueous solution. However, according to the $\Delta_r H^\theta$ value, the membrane-protein interaction is promoted by physicosorption for PVDF membrane and chemisorption for NC membrane. By understanding the possible membrane-protein interaction for each type of membrane, improvement of membranes' surface characteristics can be further examined for the enhancement of the adsorptive properties.

KEY WORDS:
Polyvinylidenefluoride (PVDF), Nitrocellulose (NC), Bovine serum albumin (BSA), Temperature, Biosensor

INTRODUCTION:

Immobilization of protein molecules on a sorbent surface is an important phenomenon in many fields of technology, particularly in biomedical and pharmaceutical fields. Many studies have shown how this process is greatly influenced by the characteristics of the specific protein, sorbent surface, and physicochemical environment [1]. Several reviews on protein adsorption on artificial membrane surfaces have been published, by focusing either on protein-repellent [2, 3] or protein-adsorptive [4-6] membranes for applications such as ultrafiltration and anion-exchange chromatographic separation processes. One such application is the biochemical immunoassay, where a higher amount of protein immobilization with strong binding is necessary for achieving accurate results.

These assays are generally classified as homogeneous or heterogeneous. In the latter, one protein constituent is immobilized on an active layer of solid sorbent surface, while the other components are delivered via the solution phase [7, 8]. The output signal of this type of assay usually consists of an observable color change such as that observed in the widely used enzyme-linked immunosorbent assay (ELISA) [7]. A heterogeneous assay is an attractive choice for overcoming the limitation of very low concentrations of biological markers in bodily fluids. The concept of heterogeneous immunoagent assay or immunoassay is important in the development of the diagnostic tool kit, such as those used in the initial screens for HIV [9], tuberculosis [10], typhoid [11], and malaria . Another example would be the very

commonly available pregnancy test strip [12]. For this application, the immunoagents are immobilized on a polymer membrane matrix in a process known as protein immobilization.

A number of polymeric materials have been used to improve final assay performance, and membrane function may be controlled by manipulating the material behaviour during the fabrication process. Among the different types of polymers used, nitrocellulose (NC) and polyvinylidene fluoride (PVDF) have great potential to be used as an adsorptive membrane for their excellent characteristics such as high porosity, high pore connectivity, and high binding affinity [13]. An NC membrane is inherently hydrophilic, which makes it easy to use because a solution of protein can be immobilized directly on its surface without any pre-treatment [14]. Although NC is the most commonly documented membrane material in protein immobilization, its applications are limited because it has low resistance to harsh conditions such as those found in highly acidic and alkaline environments. Moreover, NC membranes become brittle and discolored through use [15].

To overcome the weak mechanical characteristics of NC, PVDF membrane is used as an alternative types of polymer membranes. PVDF displays excellent mechanical characteristics compared with NC. The intrinsic characteristic of PVDF such as high in hydrophobicity is advantageous because it promotes irreversible protein–membrane binding interactions. However, due to that, PVDF membranes require pre-wetting before protein immobilization, which can be time-consuming and can hinder protein immobilization.

Accordingly, in this study, adsorption characteristics of protein on membrane in terms of thermodynamic aspect is essential in understanding the possibility of the interaction involved, in consideration of different type of polymeric membrane. These observations are essential to analyze the membrane–protein immobilization behavior in regards to the two different physical properties of the membranes. The improved understanding of the polymeric membrane morphology and membrane-protein interaction acquired in this study can be used in the future modification and development of immunoassays with enhanced performance.

MATERIALS AND METHODS:

Materials

The NC and PVDF membranes were manufactured by Bio-Rad and Millipore Corporation respectively. Bovine serum albumin (BSA, A4378) was used as the model protein and was supplied by Sigma-Aldrich. Bicinchoninic acid-working reagent was used in protein static adsorption and purchased from Merck. All the reagents were used without further purification.

Membrane Characterization

The pore size distribution and membrane porosity, ε, were determined in accordance with a previous published work [16]. The membrane wettability is characterized by static contact angle using VCA-3000 (AST Inc., USA). A droplet of deionized water was dropped onto the dry membrane surface using a micro syringe at ambient temperature with the live video was used to capture the image immediately. The value was observed until there is no change in contact angle during the short measurements.

Static Protein Immobilization and Thermodynamic Studies

Static adsorption experiments of BSA solutions on membranes were carried out in test tubes at 298 K, 308 K and 318 K. Each of membrane samples, 12 mm in diameter were inserted in test tubes containing 3 mL of 0.5 mg/mL BSA protein solutions. The test tubes were placed in water bath for 3 hours at 298 K. Unbound BSA on the surface was washed (repeated two times) with the distilled water. Each membrane sample was transferred to a test tube. Subsequently, a 2 mL bicinchoninic acid working reagent was added, and the test tubes were incubated at 310 K for 30 min. The BSA concentration from the incubated test was detected at 562-nm wavelength using a spectrophotometer. The procedures were repeated at two different temperatures, 308 K and 318 K respectively. In the immobilization process, the change in thermodynamic

parameters, such as enthalpy change ($\Delta_r H^\theta$) and entropy change ($\Delta_r S^\theta$) were estimated using the equation as follows:

$$K = \frac{C_i - C_e}{C_e} \quad (1)$$

$$\ln(K) = \frac{\Delta_r S^\theta}{R} - \frac{\Delta_r H^\theta}{RT} \quad (2)$$

where K is equilibrium constant, R is universal gas constant (8.314 J/mol.K), T is temperature (K) and C_i is protein's initial concentration and C_e is protein's equilibrium concentration.

RESULTS AND DISCUSSION:

Prior to analyze the static protein immobilization and thermodynamic studies, the synthesized membranes were characterized with respect to morphology. Figure 1 shows the pore size distribution of NC and PVDF membranes. From the figure, it shows that both membrane samples consists of microporous structure with PSD value of 12.32±4.73 µm and 0.9±0.4 µm, while the porosity were 59.58 ± 0.89% and 81.93 ± 0.79% for NC and PVDF membrane respectively.

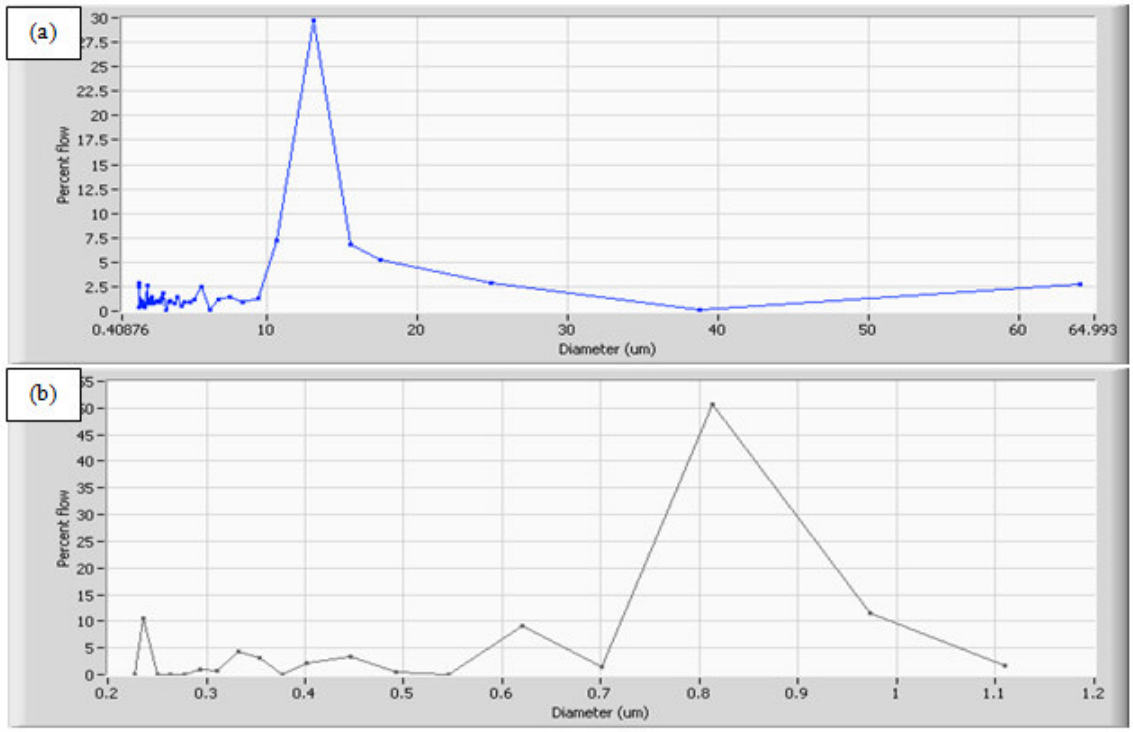

Figure 1
Pore Size Distribution of Membrane Samples; (a) NC membrane (b) PVDF membrane

In general, an appropriate combination of small pores and high porosity is required for obtaining microporous membranes with a high degree of interconnectivity. The membranes with smaller pore size at equal porosity will contribute to maximum internal surface area for protein interactions between the membrane surface and the protein [17]. Comparing between NC and PVDF membranes, PVDF membrane will have an advantage in providing higher internal capacity since it has higher porosity with small pore size. For the result of water contact angle, PVDF membrane is highly hydrophobic in nature (97.6°). The enhanced hydrophobicity of fluorinated surfaces arises because fluorocarbons pack less densely on surfaces than the hydrocarbons, leading to poorer van der Walls interactions with water [18].

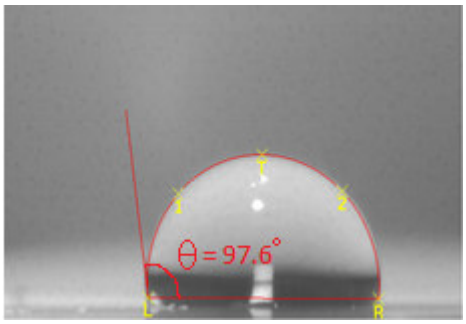

Figure 2
Water Contact Angle for PVDF Membrane

In contrary, NC shows a hydrophilic characteristic with detection of bands corresponding to the OH bonds stretching, detected in the 3500-3100 cm^{-1} [14]. It implies that the membrane preferentially absorbs water. For water contact angle, the NC membrane used is highly hydrophilic in such a way that it was unable to form a water droplet for angle measurement. The process of protein immobilization required pre-wetting for hydrophobic surface, which can be time-consuming and can cause inefficient membrane-protein binding interaction. For this particular characteristic, NC membranes are much preferable than the PVDF membrane.

In order to determine whether the adsorption process was endothermic or exothermic in nature, the adsorption studies of BSA were carried out at 298 K, 308 K and 318 K with constant initial protein solution of 0.5 mg/mL. Figure 3 shows the vant't Hoff plots of BSA adsorption onto membrane samples at three different temperatures.

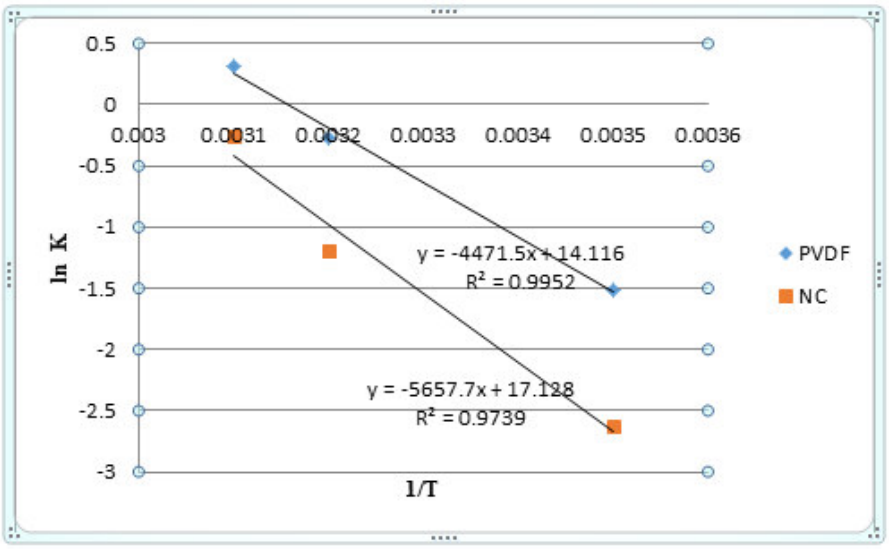

Figure 3
vant't Hoff plot for PVDF and NC membrane.

From the linear equation, the value of enthalpy change ($\Delta_r H^\theta$) and entropy change ($\Delta_r S^\theta$) for two different membrane samples tabulated in Table 1:

Table 1
Thermodynamic data of NC and PVDF membrane

Membrane Samples	Enthalpy Change ($\Delta_r H^\theta$) (kJ/mole)	Entropy Change ($\Delta_r S^\theta$) (J/mol.K)
Nitrocellulose, NC	47.04	117.36
Polyvinylidenefluoride. PVDF	37.18	142.40

The positive values of enthalpy change for both membrane samples indicated the adsorption process was endothermic. For the evaluation of type of adsorption, Alkan and co-workers stated that the adsorption is considered as chemical adsorption or chemisorption if the value of enthalpy change ($\Delta_r H^\theta$), is between 40 to 120 kJ/mol [19]. According to the $\Delta_r H^\theta$ value, the membrane-protein interaction is promoted by physicosorption for PVDF membrane and chemisorption for NC membrane. As stated before, both PVDF and NC membranes have drawbacks in certain characteristics due to their polymeric nature. Thus an improvement and modification of the membrane is necessary to overcome the limitations without scarifying the advantages of the membranes respectively. For PVDF, since the protein immobilization is promoted by the physical adsorption particularly hydrophobic interaction [20], an enhancement should be made to increase the level of hydrophobicity of the membrane to promote higher protein retention. In the same time, to overcome the issue of pre-wetting, surface modification of PVDF membrane through a process such coating is necessary with a hydrophilic material such as cellulose acetate. For NC membrane, a development of mixed-matrix membrane with other polymer was required for promoting the membrane-protein reaction and enhancing the membrane's physical strength as well. The value of entropy change was 117.36 J/mol.K and 142.40 J/mol.K for NC and PVDF membrane respectively. The positive value reflects that the distribution of BSA adsorbed on the membranes was more chaotic than that in the aqueous solution, which could be due to the protein immobilization.

CONCLUSIONS:

An evaluation of thermodynamic studies shows the membrane-protein interaction for NC and PVDF membrane is contributed by chemical adsorption and physical adsorption respectively. Improvement of membranes' surface characteristics can be further examined accordingly for the enhancement of the adsorptive properties.

ACKNOWLEDGMENTS:

The authors acknowledge Universiti Teknologi MARA (600-IRMI/MyRA5/3/LESTARI (0106/2016) for financial support.

REFERENCES:

1. Kingshott, P. & Hocker, H., Adsoprtion of proteins: Measurement methods, in: A.T. Hubbart (Ed.) Encyclopedia of Surface and Colloid Science, Boca Raton, Fla.: Taylor & Francis, 2006, pp. 669-694.
2. Chen, X., Bi, S., Shi, C., He, Y., Zhao, L. & Chen, L. (2013) Temperature-sensitive membranes prepared from blends of poly(vinylidene fluoride) and poly(N-isopropylacrylamides) microgels, *Colloid and Polymer Science*:1-10.
3. Zhou, J., Meng, S., Guo, Z., Du, Q. & Zhong, W. (2007) Phosphorylcholine-modified poly(ethylene-co-vinyl alcohol) microporous membranes with improved protein-adsorption-resistance property, *Journal of Membrane Science*. 305 (1-2):279-286.
4. Ghosh, R. (2003) Purification of lysozyme by microporous PVDF membrane-based chromatographic process, *Biochemical Engineering Journal*. 14 (2):109-116.
5. He, D. & Ulbricht, M. (2008) Preparation and characterization of porous anion-exchange membrane adsorbers with high protein-binding capacity, *Journal of Membrane Science*. 315 (1-2):155-163.
6. Kosior, A., Antosova, M., Faber, R., Villain, L. & Polakovic, M. (2013) Single-component adsorption of proteins on a cellulose membrane with the phenyl ligand for hydrophobic interaction chromatography, *Journal of Membrane Science*. 442 (0):216-224.
7. Debnath, M., Prasad, G.B.K.S. & Bisen, P.S., Immunoassay, in: Molecular Diagnostics: Promises and Possibilities, Springer Science+Business Media, 2010, pp. 171-180.
8. O'Sullivan, M.J., Immunoassays, in: F.P. Nijkamp, M.J. Parnham (Eds.) Principles of Immunopharmacology, Springer Science+Business Media, Basel, 2005.

9. Yuan, Z., Chen, W., Zhang, J., Xiang, T., Hu, J., Wu, Z., Du, X., Huang, A. & Zheng, J. (2012) Development of an immunoassay for differentiating human immunodeficiency virus infections - from vaccine-induced immune response in Tiantan vaccine trials in China, *Clinical Biochemistry*. 45 (15):1219-1224.
10. Attallah, A.M., Osman, S., Saad, A., Omran, M., Ismail, H., Ibrahim, G. & Abo-Naglla, A. (2005) Application of a circulating antigen detection immunoassay for laboratory diagnosis of extra-pulmonary and pulmonary tuberculosis, *Clinica Chimica Acta*. 356 (1-2):58-66.
11. Olsen, S.J., Pruckler, J., Bibb, W., Thanh, N.T.M., Trinh, T.M., Minh, N.T., Sivapalasingam, S., Gupta, A., Phuong, P.T., Chinh, N.T., Chau, N.V., Cam, P.D. & Mintz, E.D. (2004) Evaluation of Rapid Diagnostic Tests for Typhoid Fever, *Journal of Clinical Microbiology*. 42 (5):1885-1889.
12. Albertini, A., Ghielmi, S. & Belloli, S. (1982) Structure, immunochemical properties and immunoassay of human chorionic gonadotropin, *Ricerca in clinica e in laboratorio*. 12 (1):289-298.
13. Aizawa, K. & Gantt, E. (1998) Rapid method for assay of quantitative binding of soluble proteins and photosynthetic membrane proteins on poly(vinylidene difluoride) membranes, *Analytica Chimica Acta*. 365 (1-3):109-113.
14. Low, S.C., Ahmad, A.L., Ideris, N. & Ng, Q.H. (2011) Interaction of isothermal phase inversion and membrane formulation for pathogens detection in water, *Bioresource Technology*. 113 (0):219-224.
15. Ben Rejeb, S., Tatoulian, M., Arefi Khonsari, F., Fischer Durand, N., Martel, A., Lawrence, J.F., Amouroux, J. & Le Goffic, F. (1998) Functionalization of nitrocellulose membranes using ammonia plasma for the covalent attachment of antibodies for use in membrane-based immunoassays, *Analytica Chimica Acta*. 376:133-138.
16. Ahmad, A.L., Ideris, N., Ooi, B.S., Low, S.C. & Ismail, A. (2012) Synthesis of polyvinylidene fluoride (PVDF) membranes for protein binding: Effect of casting thickness, *Journal of Applied Polymer Science*. 128 (5):3438-3445.
17. Baker, R.W., Membrane technology, in: H.F. Mark (Ed.) Encyclopedia of Polymer Science and Technology, A John Wiley & Sons Publication, New Jersey, 2003, pp. 184-249.
18. Dalvi, V.H. & Rossky, P.J. (2010) Molecular origins of fluorocarbon hydrophobicity, *PNAS Early Edition*.
19. Alkan, M., Demirbas, O., Celikcapa, S. & Dogan, M. (2004) Sorption of acid red 57 from aqueous solution onto sepiolite, *Journal of Hazardous Materials*. 116 (1):135-145.
20. Norde, W., Proteins at Solid Surfaces, in: A. Baszkin, W. Norde (Eds.) Physical Chemistry of Biological Interfaces, Marcel Dekker Inc., New York, 1999, pp. 115-135.

FP-23

EFFECT OF NITROGEN SUPPLEMENTATION ON THE PRODUCTION OF B-GLUCOSIDASE IN SOLID STATE FERMENTATION OF BROKEN RICE AND RICE BRAN BY *Aspergillus oryzae*

AMSAL ABD GHANI[1*], ANISAH JAMALUDDIN[1], DANG LELAMURNI ABD RAZAK[1], NUR YUHASLIZA ABD RASHID[1], AZLINA MANSOR[1], MUSAALBAKRI ABDUL MANAN[1]

[1]Enzyme and Fermentation Technology Programme, Biotechnology and Nanotechnology Research Centre, MARDI, G.P.O Box 12301, 50440 Kuala Lumpur, Malaysia
[*]Corresponding author: amsal@mardi.gov.my

ABSTRACT

Rice by-products including rice bran (RB) and broken rice (BR) may be used as cheap substrate for production of b-glucosidase through solid state fermentation (SSF) while nitrogen supplementation could influence the enzyme activity during the process. Thus, in this study, the effect of utilizing RB and BR as the substrate for b-glucosidase production by *Aspergillus oryzae* in SSF was investigated. Then, the effect of nitrogen supplementation at different level of concentration (0, 1, 2, and 3%) on the production of b-glucosidase in both substrates by *A. oryzae* was also evaluated using soy bean waste (SBW) as the source of nitrogen. SSF was carried out for 18 days at 32°C with 52% moisture content (RB) and 37% (BR). The results indicated that the activity of b-glucosidase produced by *A. oryzae* was significantly higher ($p<0.05$) in RB (68.16 U/g) in comparison to BR (3.96 U/g). Results also showed that the activity of b-glucosidase in SSF of RB was improved at day 4, using 1% of SBW which was 2125.7 U/g. Besides, the activity of b-glucosidase in SSF of BR was also enhanced at day 16 by adding 2% of SBW (1500.5 U/g). These results demonstrated that nitrogen supplementation through SBW can considerably enhance the production of b-glucosidase in SSF of BR and RB by *A. oryzae*. These findings will contribute towards the development of an economical b-glucosidase production process using agro-industrial residues.

KEY WORDS:
Soy bean waste, broken rice, rice bran, beta-glucosidase, nitrogen supplementation, solid state fermentation

INTRODUCTION:

Rice by-products including rice bran and broken rice are produced in a large quantity by rice processing industry. Rice bran (RB) is the second layer underneath the husk of paddy while broken rice (BR) is pieces of rice kernels segregated during the milling process and they are mainly utilized as ingredient in animal feed and in rice noodle manufacturing, respectively. However, only a small portion of these by-products are fully utilized. In addition to being a great loss of valuable materials, they also raise serious management problems, both from the economic and environmental point of view. One alternative for the economic utilization of these by-products is to utilize them as substrate in solid state fermentation (SSF) processes for the production of enzyme like b-glucosidase.

B-glucosidase is very crucial as it has various applications mainly in cosmetics, textile, detergent, pharmaceutical, animal feed, and food industry[1]. In addition, it also can be used for biofuel production and de-inking of waste paper in paper and pulp industry.[1] B-glucosidase hydrolyzes b-1,4-glycosidic bonds of various compounds including alkyl-b-D-glucosides, aryl-b-D-glucosides, cyanogenic glucosides, and also liberates D-glucose from the non-reducing ends of cellobiose and short chain oligosaccharides.[2] B-glucosidase, in under certain circumstances, also catalyzes synthetic reaction through reverse hydrolysis and transglycosylation.[1] The ever-increasing demand for b-glucosidase mandates the exploration of strategies to improve the yield of the enzyme and to reduce the cost of production. These include the studies and the

investigation on the suitable selection of SSF substrates and the effect of nitrogen supplementation in the SSF substrate for the maximum production of enzymes.

Multiple reports have described the effects of nitrogen supplementation on the production of b-glucosidase in various agricultural by-products in SSF. For example, Elyas et al.,[3] found that *Aspergillus* strain SA 58 has produced high level of b-glucosidase when grown on wheat bran medium containing beef extract as nitrogen source while least production was noticed when ammonium salts were used. Furthermore, high level of extracellular b-glucosidase was also produced by *Penicillium citrinum* YS40-5 when cultivated on rice bran medium supplemented with urea as nitrogen source in SSF[4]. Besides, *Aspergillus protuberus* also produces optimum b-glucosidase when ammonium sulfate was used as nitrogen source in SSF of rice husk[5]. However, the performance of BR and RB as SSF substrate for b-glucosidase production by *A. oryzae* and the effect of supplementing soy bean waste (SBW) as nitrogen source on the production are yet to be studied. SBW is a by-product of soy milk and tofu manufacturing process. It contains high quality protein, especially essential amino acids and about 27% of its protein (dry basis) has good nutritional quality and a superior protein efficiency ratio[6]. Therefore, the aim of this study is to investigate and validated the performance of BR and RB as SSF substrate for b-glucosidase production by *A. oryzae* and also the effect of SBW as nitrogen source on the production of b-glucosidase.

MATERIALS AND METHODS:

Microorganism

Aspergillus oryzae (strain F0017) was obtained from Collection of Functional Food Culture (CFFC, MARDI, Serdang, Malaysia). The stock culture was grown on potato dextrose agar (PDA) and maintained at 32°C for 7 days. Subsequently, it was stored at 4°C for downstream application.

Materials

Rice bran and broken rice were obtained from Padiberas Nasional Berhad (BERNAS, Selangor, Malaysia). mM p – nitrophenol β – D glucopyranoside (pNPG), 4-nitrophenol and sodium acetate buffer, were purchased from Sigma Chemical C0. (St. Louis, MO, USA). All other chemicals used were of analytical grade.

Inoculum

The spore inoculum was prepared by growing the fungal strain on PDA for 7 days to ensure mature spores were obtained. The mature spores were harvested by adding 0.1% (v/v) sterile Tween 80 onto the plate surface and gently scraped using hockey stick under strict aseptic condition. Spores at the concentration of 1 x 10^6 spores/mL were used as inoculums.

Solid state fermentation

SSF was carried out in separate tray containing sterilized 30 g and 90 g of RB and BR, respectively. All experiments were done in triplicate. Then, the substrates were moistened to 52% (RB) and 37% (BR) with distilled water. The trays were then aseptically inoculated with 1% (10^6 spores/ml) of fungal spores. Following that, the trays were incubated at 32°C under static conditions for 18 days. The un-inoculated trays containing sterile RB and BR with 52% and 37% moisture content were also run in parallel as control, respectively.

Enzyme extraction

The crude enzymes were extracted by suspending the fermented substrates with 150 ml and 450 ml of distilled water for RB and BR, respectively, and thoroughly mixed on a rotary shaker at 150 rpm and room temperature for 2 hours. Following this, the residue of substrate and the biomass were separated by centrifugation at 4000 rpm for 15 minutes at 4°C. The clarified supernatant representing the crude enzyme was used for assaying b-glucosidase activities.

B-glucosidase assay

B-glucosidase activity was determined accoding to Hang and Woodams[7] with some modifications. 0.1 ml of crude enzyme extract was mixed with 0.1 ml of 9 mM p – nitrophenol β – D glucopyranoside (pNPG) and 0.8 ml of 200 mM sodium acetate buffer (pH 4.6). The mixture was incubated at 50°C for 15 minutes. Then, the reaction was stopped by adding 1 ml of 0.1M sodium carbonate. The absorbance was spectrophotometrically quantified at 400 nm using a 4-nitrophenol standard curve. One unit of b-glucosidase was defined as the amount of enzyme that releases 1 µmol of nitrophenol per minute of reaction.

Effect of nitrogen on b-glucosidase assay

To investigate the effect of nitrogen on b-glucosidase activity, soy bean waste was supplemented to the substrates at different level of concentrations (0-3%). Then, SSF was carried out at 32°C for 16 days and the b-glucosidase activity was measured after the SSF.

Statistical analysis

Mean values and standard deviations were calculated from the data obtained from triplicate experiments. One-way Analysis of Variance (ANOVA) test was used to determine significant differences between variables using Minitab (Version 18) Statistical Software. Differences with a probability value of <0.05 were considered significant. All data were reported as mean ± standard deviation (S.D).

RESULTS AND DISCUSSION:

B-glucosidase activity in SSF of BR and RB by *A. oryzae*:

The b-glucosidase activity in SSF of RB and BR by *A. oryzae* for 18 days was reported in Figure 1. Results showed that SSF of RB by *A. oryzae* produced maximum activity of 68.16 U/g on day 18 of fermentation while SSF of BR produced maximum activity of only 3.96 U/g also on day 18 of fermentation. The activity of b-glucosidase in SSF of RB is significantly higher ($p<0.05$) compared to the b-glucosidase activity in SSF of BR. These findings concluded that RB is considered as better substrate to produce b-glucosidase in comparison to BR. Selection of proper substrate is one of the key aspects in SSF. The right selection of the solid substrate is a great importance for an efficient and economical production of the compound of interest. Many agriculture by-products have been used as SSF substrate to produce b-glucosidase such as corn cob[8], rice straw[9], and wheat bran[10], however, higher b-glucosidase activity was recorded in this study. Previous work by Brijwani et al[11] who has used *A. oryzae* in SSF of soybean peel supplemented with wheat bran obtained a lower production of b-glucosidase activity (10.71 U/g). Lower b-glucosidase activity (11.1 U/g) was also reported in SSF of sugarcane bagasse by *Litcheimia ramosa*.[8] Mostly the production of enzymes can be improved with a suitable choice of substrate with appropriate nutrient supplementation. Next, the effect of adding nitrogen source on the both substrates will be identified.

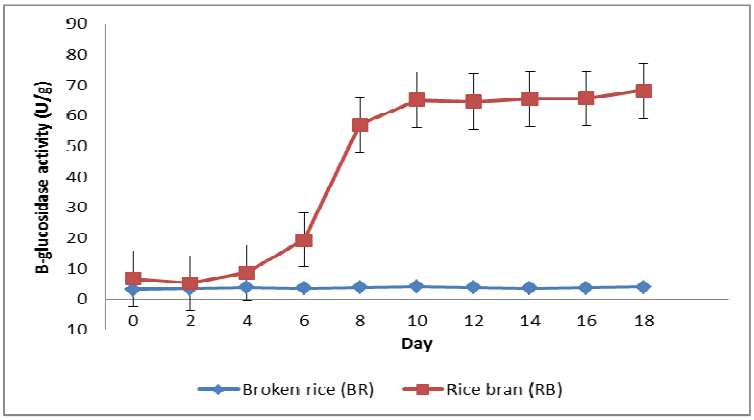

Figure 1
B-glucosidase activity in SSF of BR and RB by *A. oryzae*
The values are Mean ± S.D of triplicates (p<0.05)

Effect of SBW supplementation on the b-glucosidase production in SSF of rice bran

It is generally known that nitrogen supplementation could influence the enzyme production by fungi. Nitrogen source is required in the fermentation medium for the synthesis of amino acids, proteins, nitrogenous compounds, vitamins and bioactives.[1] In this study, the effect of supplementing the SBW as the nitrogen source on the production of b-glucosidase in BR and RB was investigated. SWB is cheap, rich in high quality proteins and also abundantly available as it is one of the by-products of tofu and soy-milk manufacturing. Thus, supplementing fermentation substrate with SBW in this study may suggest an enhancement of b-glucosidase production in SSF of BR and RB. Figure 2 showed the effect of nitrogen supplementation on the production of b-glucosidase in SSF of RB using SBW as the nitrogen source at different percentages (control, 1%, 2%, and 3%) of concentration. Results indicated that the highest activity of b-glucosidase in SSF of RB was obtained at day 4, using 1% of SBW which was 2125.7 U/g. Results also revealed that b-glucosidase activity has significantly increased ($p<0.05$) to 244-folds when supplementing the BR with 1% SBW in comparison to the control with no added SBW (8.7 U/g) at day 4. At 2% and 3%, the maximum production was 1639.9 U/g and 1629.1 U/g, respectively. However, the production of b-glucosidase was decreased after day 4 of fermentation for all level of SBW concentration, where the maximum production was achieved. The yield of b-glucosidase in this study was relatively higher than a study by Ng et al.,[4] who cultured *Penicillium citrinum* YS40-5 in SSF of rice bran and supplemented 0.5% urea as the nitrogen source (122.8 U/g). The result from this study also showed that the period of fermentation was also reduced when 1% SBW was supplemented in the fermentation medium. The reduced cultivation time, achieved in the present work, is a key improvement for fermentation techniques, since the cost of enzyme production is proportional to incubation time. Qian et al.,[10] obtained maximum b-glucosidase production by *Aspergillus niger* after 3 days of incubation in solid medium containing 100% wheat bran, 2% ammonium chloride, 0.5 % magnesium sulphate, and 1.5% monopotassium phosphate but the production of the b-glucosidase is comparatively lower (508 U/g) in comparison to this work.

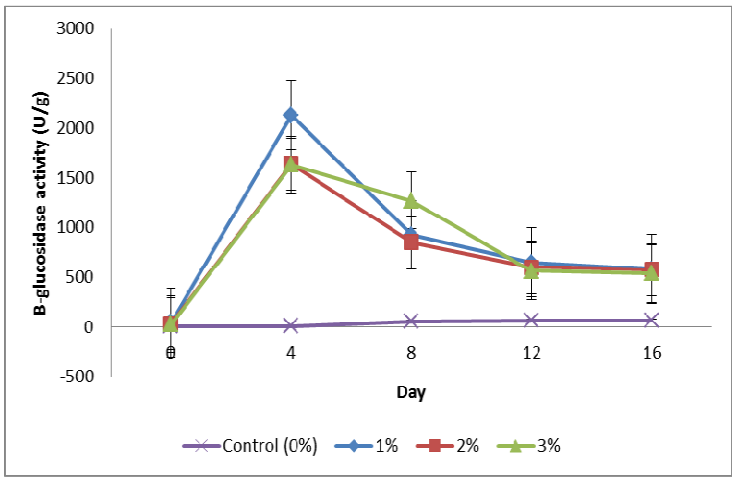

Figure 2
Effect of SBW supplementation on the b-glucosidase production in SSF of rice bran
The values are Mean ± S.D of triplicates (p<0.05)

Effect of SBW supplementation on the b-glucosidase production in SSF of broken rice

Figure 3 depicts the effect of nitrogen supplementation on the production of b-glucosidase in SSF of BR using SBW as the nitrogen source at different level (control, 1%, 2%, and 3%) of concentration. Interestingly, the results obtained showed a significant of b-glucosidase activity increase by adding 2% of SBW in the BR (1500.5 U/g) in comparison to control (3.7 U/g) at day 16 and this is relatively similar to 405-folds of increment. At 1% and 3%, the maximum production was 731.3 U/g and 938.3 U/g only, respectively. The production in all level of SBW concentration was increased till day 16, where they showed the maximum activity. This finding may suggest the importance of nitrogen supplementation in the production of b-glucosidase in SSF of BR by *A. oryzae*. The solid substrate medium composed of BR alone without the nitrogen supplement may not lead to the high biosynthesis of b-glucosidase in SSF. Variable

effects of nitrogen source have been reported on the b-glucosidase production, and each fungal species respond differently to different nitrogen sources. For example, *Flammulina velutipes* produced highest b-glucosidase activity when L-asparagine was used as nitrogen source (1.6 U/ml)[12] and *Stereum hirsutum* produced optimal b-glucosidase when tryptone was used as nitrogen source[13]. On the other hand, *F. velutipes* produced negligible to low activity b-glucosidase when ammonium salts was used as nitrogen source.[12]

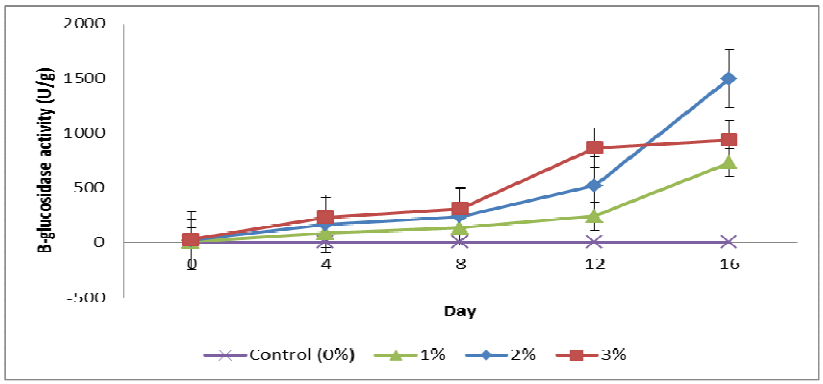

Figure 3

Effect of SBW supplementation on the b-glucosidase production in SSF of broken rice

The values are Mean ± S.D of triplicates (p<0.05)

CONCLUSION:

The present study was successfully revealed that rice bran is a better substrate in producing b-glucosidase in SSF by *A. oryzae* in comparison to broken rice. However, through the nitrogen supplementation by SBW in the fermentation medium, the b-glucosidase production in SSF of RB and BR by *A. oryzae* can be greatly enhanced. This research contributes towards the development of an economical b-glucosidase production process using agro-industrial residues. Future studies should be implemented to investigate the mechanism by which these nitrogen sources influence the expression of b-glucosidase. Besides, future studies on the effects of other fermentation parameters such as carbon source, temperature, and pH are also beneficial for maximum production of b-glucosidase in SSF of RB and BR by A. *oryzae*.

ACKNOWLEDGEMENT:

This study was financially supported by development fund project under the 11th Malaysia Plan (No: 21003004170001-C).

REFERENCES:

1. Ahmed A, Batool K, Bibi A. Microbial β-Glucosidase: Sources, Production and Applications. Journal of Applied & Environmental Microbiology. 2017 Mar 30;5(1):31-46.
2. Tiwari P, Misra BN, Sangwan NS. β-Glucosidases from the fungus *Trichoderma*: an efficient cellulase machinery in biotechnological applications. BioMed Research International. 2013 Aug 1;2013.
3. Elyas KK, Mathew A, Sukumaran RK, Ali PM, Sapna K, Kumar SR, Mol KR. Production optimization and properties of beta glucosidases from a marine fungus *Aspergillus*-SA 58. New Biotechnology. 2010 Sep 30;27(4):347-51.
4. Ng IS, Li CW, Chan SP, Chir JL, Chen PT, Tong CG, Yu SM, Ho TH. High-level production of a thermoacidophilic β-glucosidase from *Penicillium citrinum* YS40-5 by solid-state fermentation with rice bran. Bioresource technology. 2010 Feb 28;101(4):1310-7.

5. Yadav PS, Shruthi K, Prasad BS, Chandra MS. Enhanced Production of β-glucosidase by New Strain *Aspergillus protuberus* on Solid State Fermentation in Rice Husk. Int. J. Curr. Microbiol. App. Sci. 2016;5(12):551-64.
6. Li S, Zhu D, Li K, Yang Y, Lei Z, Zhang Z. Soybean curd residue: composition, utilization, and related limiting factors. ISRN Industrial Engineering. 2013 Sep 8;2013.
7. Hang YD, Woodams EE. Apple pomace: a potential substrate for production of β-glucosidase by *Aspergillus foetidus*. LWT-Food Science and Technology. 1994 Dec 1;27(6):587-9.
8. Garcia NF, Santos FR, Gonçalves FA, Paz MF, Fonseca GG, Leite RS. Production of β-glucosidase on solid-state fermentation by *Lichtheimia ramosa* in agroindustrial residues: Characterization and catalytic properties of the enzymatic extract. Electronic Journal of Biotechnology. 2015 Jul;18(4):314-9.
9. Raza FA, Raza NA, Hameed U, Haq I, Maryam I. Solid state fermentation for the production of β-glucosidase by co-culture of *Aspergillus niger* and *A. oryzae*. Pak J Bot. 2011;43:75-83.
10. Qian LC, Fu SJ, Zhou HM, Sun JY, Weng XY. Optimization of fermentation parameters for β-glucosidase production by *Aspergillus niger*. J Anim Vet Adv. 2012 Jan 1;11:583-91.
11. Brijwani K, Oberoi HS, Vadlani PV. Production of a cellulolytic enzyme system in mixed-culture solid-state fermentation of soybean hulls supplemented with wheat bran. Process Biochemistry. 2010 Jan 31;45(1):120-8.
12. Mallerman J, Papinutti L, Levin L. Characterization of β-glucosidase produced by the white rot fungus *Flammulina velutipes*. J Microbiol Biotechnol. 2015 Jan 1;25(1):57-65.
13. Jeya M, Lee JK. Optimization of β-glucosidase production by a strain of *Stereum hirsutum* and its application in enzymatic saccharification. J Microbiol Biotechnol. 2013;23(3):351-6.

FP-24

CHARACTERIZATION AND EVALUATION OF HUMAN WHARTON'S JELLY DERIVED MESENCHYMAL STEM CELL ON GRAPHENE OXIDE SUBSTRATES: *IN VITRO* APPROACH

YUSOFF UMUL HANIM[1], ABDUL AJAK WARDA[2], SIEW ENG HOW[1], VUN FEI CHEONG[1], PING CHIN LEE[1], PAK YAN MOH[1], PIEK LIN TEOH[2]

[1]*Faculty of Science and Natural Resources, University Malaysia Sabah,*
[2]*Biotechnology Research Institude, University Malaysia Sabah,*
Jalan UMS, 88400, Kota Kinabalu, Sabah, Malaysia

[*]Corresponding author: sehow@ums.edu.my

ABSTRACT

A nifty propagating of human Wharton's Jelly Mesenchymal Stem Cell (hWJMSCs) diligence has germinated all over the world by innovative investigators. However, the clinical and basic research applications of hWJMSC require novel finding biomaterials interfacial interaction especially in sustainable the morphology, physiology, multipotent and phenotypically in vitro cultivation. A prominent of biomaterials benefit to hWJMSCs culture has triggered the multitudinous field especially in regenerative medicine. In order to hinder the deprivation of MSCs stemness especially in purity and potency, the alternative cell-substrate materials of hWJMSCs culture are essential to be discovered due to it is highly recommended for an abundance biomedical waste. This study epitomizes the idea to explore the method of biomaterials in bio-adhesively, and sustainability to maintain the morphologically, physiologically, multipotent and phenotypically of organic biomaterial substrates coated coverslip. Multitude of Graphene Oxide (GO) biomaterial substrate parameters has been collected from co-researchers to conduct the initial of 20 myriad cell-material fabrications of substrates. Human Wharton's Jelly-derived Mesenchymal Stem Cells (hWJMSCs) has been seeded on each substrate. Top two leading substrates have been selected for further screening cultivation. Several variables such as cell attachment, cell viability, kinetic growth, cell-materials differentiation and cell phenotype have been analysed. Morphologically, GOy1-hWJMSC showed the significant result among others including gelatin and blank coverslip and has been chosen for further study ultimately. The percentage mean of GOy1-hWJMSC at passage five (P5) is m=375±4% significantly different against 0.1%gelatin as a positive control, m=100%. Kinetic growth calculated that GOy1-hWJMSC has been achieved the highest cell numbers. The manual cumulative growth curve of mean transparent substrates showed that GOy1-hWJMSC is m=63,217±42 cells which is contrary to positive control, 0.1% Gelatin (Ge) which is m=50,045±46 cells and mean of pristine glass coverslip (b) is m=62,056±58 cells at passage five (P5). Importantly, the phenotypic study has been depicted to express the cell membrane antigen-antibody binding in the sense of incubation with CD105, CD271 and the STRO-1 antibody which as to fulfil the minimal criteria of MSCs. GOy1-hWJMSC succinctly differentiated into osteogenic and adipogenic differentiation in the inductive media. This study aspires the platform to discover the outstanding distinguishable of libraries synthetic biomaterials interface hWJMSCs for instance interface to GO for long-term sustainability as a high durability device to elicit the desired of novel finding in regenerative medicine and basic research consumable.

KEYWORDS:
Graphene Oxide substrate, APTES functionalization, Piranha functionalization, Spin coatin g,Wharton's Jelly, Mesenchymal Stem Cell, Proliferation, Differentiation, Immunoflourescence, Screening biomaterial.

INTRODUCTION:

Mesenchymal Stem Cells (MSCs) are devoted a potentially useful platform for tissue regeneration, cell-based therapeutics, and disease in- a-dish models for screening that diligence huge delight in recent year

due to their high plasticity, great self-renew and wide-lineage potential with attractive immunosuppressive properties (Omar et al., 2014). There are various sources of MSCs including Wharton's jelly as a component of an umbilical cord, denuded amnion, commonly from bone marrow, fat, and also from the urinary membrane (Bharadwaj et al. 2013). Human Wharton's Jelly-derived Mesenchymal Stem Cells (hWJMSCs) conquered a feasible source basically in tissue engineering approach due to it is readily isolated, expanded, cell direct injection and transplanted either intra-peritoneum or intravenous (Neuss et al., 2008; Chaudhuri et al., 2015;Gu et al., 2014: Zhao et al., 2015). However, the current innovative investigation has prone to highly recommended hWJMSCs due to their rapid growing, abundance readily collective biological sample (Soraya et al. (2013) and additionally under free legal ethical due to consider as a waste medical product. To some extent, there is a major challenge in MSCs whenever attach in the culture tissue plastic will lose their potential of adipogenic and osteogenic differentiation which bring epitomized by ample of scientists regardless chemistry, biology engineering also physician successively construct the synthetic substrates to induce a desirable cell types differentiation (Choi et al., 2008; Omar et al., 2014). However, that strategy needs to be orchestrated to accomplish the feeble of cell culture maturation into distinct lineages as required weeks to months of cell culture in order to maintain their stability on the suitable substrate (Lee et al., 2011). There is a pressing indispensable to define synthetic substrates for further study on culture MSCs to overcome the loss of adipogenic and osteogenic differentiation. The use of animal-derived substrates such as gelatin, collagen or fibronectin is problematic regarding undefined factors, batch variation and pathogen transfer. At the present time to overcome the problem, this study will be employed a screening various of defined functionalization inorganic materials of graphene oxide (GO) and their bio-composites to optimize MSCs proliferation and differentiation in vitro as demonstrated by Duffy et al. (2014), studied the promising of copolymer and hydrogel permitted human embryonic derived Mesenchymal progenitors and adipose tissues derived MSCs maintained over 10 passages with retaining expression of MSCs markers. GO impressive biomaterial that has been ideally proven as a novel material notably interest in the field of biomedical as for in vivo implantation application especially in orthopedic therapy significantly (Alegria et al. 2016) in a position of its excellent amphiphilic compound properties specifically synthesis in a heavily oxidized by oxidation and exfoliation procedures of graphite (Lee et al. 2011; Liu et al. 2013; Gu et al., 2014; Park et al.2015; Rosa et al. 2016 ; Rahul et al. 2016), derived from the two-dimensional carbon from carboxyl group, epoxide and hydroxyl group, draw amazing effect to the physical, mechanical and biological properties of cell lines enable interaction by amphiphilic bonding (Shen et al. 2012:Li et al., 2015:Kim et al., 2013: Yang et al., 2009). Therefore, the next horizon in the fast-growing field which in biomaterial composites exceptionally remain crucial challenges in elucidating the complexity understanding in advance modification of new germinated biomaterial namely graphene oxide (GO) loaded with complete advantages package particularly will enumerated in this review with the meaning of synthetic materials applicability in the promoting the stem cell behavior for instances in multipotency of stem cell (Puah et al., 2018: Lee et al., 2011: Nakajima et al., 2007:Luo et al., 2015:Kim et al., 2013) precisely serve as a transferable and implantable application evenly giving high impact of benefit in the fields of biomedical, biotechnology, bioengineering, pharmacology, biosensors (Park et al. 2015), energy conversion and storage (Li et al., 2015). The package of these unique properties of GO recently has driven the cellular behaviors for instance cell adhesion, proliferation, differentiation, polarization, and biocompatibility in MSCs on GO substrates or scaffold with regard to remaining eliminated in severely declining stemness of adult and fetal derived human-MSCs during in vitro expansion of tissue culture polystyrene (TCPS) presently limits their therapeutic efficacy prior to cell transplantation (Kalbacova et al., 2010; Gu et al., 2014) by manipulation of natural and synthetic biomaterials innovation, therefore, various attempting in incorporating interface of GO-based biomaterials.

MATERIALS AND METHODS:

Isolation and cell culture preparation

This study elucidated precisely the multivariable of substrates ascribed from graphene oxide based on the proper process designed that generated many combinations for screening in order to perceptible the better effect to trigger the proliferation and differentiation of hMSC resource. The sample of hMSC resource which is human Wharton's Jelly from umbilical cord has been provided by the specific private hospital in Kota

Kinabalu, Sabah. Isolation part has been assisted by a co-researcher from Institute of Biotechnology Research (BRI), University Malaysia Sabah (UMS).
The primary cell line was cultured in a 5% (v/v) CO2 incubator at 37oC in standard tissue culture polystyrene (TCP). The cell culture was using a basic technique by growing in a media of Dulbecco's Modified Eagle's Medium (DMEM/F-12) supplemented with 10% FCS (FBS), 1% GlutaMax (100 units/ml), 1% of A-A (Antibiotic-Antimycotic), 1% of Vitamin C and 1% GlutaMax then incubated at 37 ºC with 5% CO2 as culture preparation from primary cell line of passage zero (P0) until passage two (P2) orderly envisioned to maintain the cell culture before continuing treated with GO substrates.

Substrate preparation
The pristine coverslip was functionalized with a treatment in two different cross-linker solutions. One treated group was immersed in piranha solution mixture of sulphuric acid (H2SO4) and hydrogen peroxide (H2O2). The second group was immersed in (3-Aminopropyl) triethosilane (APTES) solution (Khazaei et al., 2016; Chen et al., 2017) (Table 1 and Figure 1).
GO suspension was deposited onto the treated coverslip into another three groups of spin coating layer measured as thickness. For the purpose of sterility, GO-coated coverslips were put under UV-irradiation about 20min for both sides. Subsequently, GO-coated coverslip was placed into 48 well plate using sterilized forceps and immersed in Phosphate Base Saline (1xPBS) between 2-3min. For the purpose of storage, the sterilized plate can be used with parafilm before used the well plate and stored at the room temperature.

Cell seeding preparation
Seeding preparation onto 48 wellplate was taken part accordingly to the density of 1x104cells/cm2. Occasionally, 7,500 cells/well of 48 wellplate were seeding in 3 replicated wells. The morphology of cell attachment was illustrating in figure 2. A 0.1% Gelatin Solution (Type B, bovine skin gelatin) was purchased from Sigma Aldrich and followed the preparation protocol to coat onto the coverslip which managed to use as a positive control in every passaging procedure provided from ThermoFisher. The key concerned was purity whereas to avoid high purity of gelatin solution in cell culture compliant. The dilution made up in milli-Q to dissolve the 2% Gelatin solution stock. Coat one side of the cover-slip by standing on the end of coverslip to allow excess to run off and to dry starting from 2 hours until overnight either in room temperature or placed in the incubator (37^0C) as to ensure the thin homogenize coated was formed.

Cell viability
The measurement of cell viability is used to determine the number of active cells. In this study, we directly inserted based on the protocol of PrestoBlueTM (Thermo Fisher) viability reagent for the confluent day of every passage in 48 wellplate. The result has observed reader by using a spectrophotometer (Tecan). The graph showed in figure 4. The wavelength was 570 nm corrected with normalized of 600 nm.

Kinetics growth
Manual cell counting was detected using hemocytometer and Trypan Blue exclusion test, the growth curves were encountered according to the living cell values. The growth kinetics of GO-hWJMSC was observed from passage 1 (P1) to passage 3 (P3) for the specific day was shown as the growth curves in Figure 4. Basically, preparation of passaging the cell culture was taken about 6 days to ultimately become pre-confluent 80-90%. Subsequently, the cell culture was replenished every 2 days. The medium supplemented DMEM/F-12 was thawed and inserted into a new microcentrifuge. The cells culture were rinsed with 1x PBS for less than 2 min and discarded into a waste beaker. Subsequently, the cells were incubated in trypsin-buffer EDTA (TE) 10mM Trizma base pH 7.5, 1m M Na2 – Ethylene diamine tetraacetic acid (0.125% EDTA) using warm water-bath at 37^0C. Cells were detached after incubate with TE and media about 1:1 ratio. The wells were observed under an inverted microscope to ensure the complete detachment of cell occurred. The medium and cells were aspirated into the named microcentrifuge tube then washed and shake vigorously. In short time, every microcentrifuge tubes were centrifuged for 5 mins, 5000 rpm and 25^0C. The supernatant was discarded and the pellet was re-suspended in 400uL of fresh DMEM-F12 media.

The concentration of cell suspension was counted in a hemocytometer using the initial of 90uL cell suspension and 10 uL 5% trypan blue.

Osteogenic and adipogenic differentiation

GO-hWJMSCs were plated in duplicate at 2.76 x 10^4 cells per well, in 48 well-plate for osteogenic differentiation and 0.75 x 10^4 of adipogenic differentiation. After 24-72 hours attachment, the media was changed to induced osteogenic and adipogenic media respectively. Cells were cultured for 14-20 days with media changed every 2-3 days for osteogenic induction and 7-15days for adipogenic induction. Cells were fixed in 4% Paraformaldehyde (PFA). Osteo-induced cells were stained with Alizarin red S solution (Sigma Aldrich) and adipo-induced cells were stained with oil Red O staining (Sigma Aldrich). Qualification of the percentage differentiation was achieved by imaging stained wells using the Zeiss Observer microscope. In the meanwhile, the quantitative measurement by absorbance was immersed in Dimethyl sulfoxide (DMSO) for cell lysed in the osteogenic induction and Natrium Hydroxide (NaOH) for adipogenic induction and measured using spectrophotometer of 560 nm and 490 nm simultaneously (Zhao et al., 2015).

Immunocytochemistry

The cells culture were stained using standard immunocytochemistry according to the protocol by (Duffy et al., 2015). The cells culture at passage 5 of leading GO-hWJMSC were blocked for 1 h with 5% goat serum in PBS and incubated 1h with primary against the MSC markers STRO-1 (mouse anti-human, Invitrogen) at 1:200, CD105 (goat anti-human Invitrogen) at 1:200 and CD271 (rabbit anti-human, Invitrogen) at 1:200 dilution. Cells were incubated with the appropriate Alexa Fluor-conjugated secondary antibodies; STRO-1 (goat anti-mouse 488) at 1:200, CD105 (goat anti-rabbit 555 at 1:200) and CD271 (goat anti-mouse) at 1:100. Imaging has been performed with an Olympus Confocal fluorescent microscope (Duffy et al., 2014).

Table 1
List of GO coated coverslip substrates.

Nomenclature of GO substrates				
No.	**Substrate**	**Concentration of GO (mg/mL)**	**Number of cycles**	**Surface treatment**
1.	GOf1	1	1	Piranha
2.	GOf4	1	3	Piranha
3.	GOf7	1	5	Piranha
4.	GOh1	5	1	Piranha
5.	GOh4	5	3	Piranha
6.	GOh7	5	5	Piranha
7.	GOy1	1	1	Piranha + APTES
8.	GOy4	1	3	Piranha + APTES
9.	GOy7	1	5	Piranha + APTES
10.	GOk1	5	1	Piranha + APTES
11.	GOk4	5	3	Piranha + APTES

*GO:Graphene Oxide, Piranha solution: Sulphuric acid (H_2SO_4) and Hydrogen Peroxide (H_2O_2), Piranha + APTES: combination crosslinker (3-Aminopropyl) triethosilane.

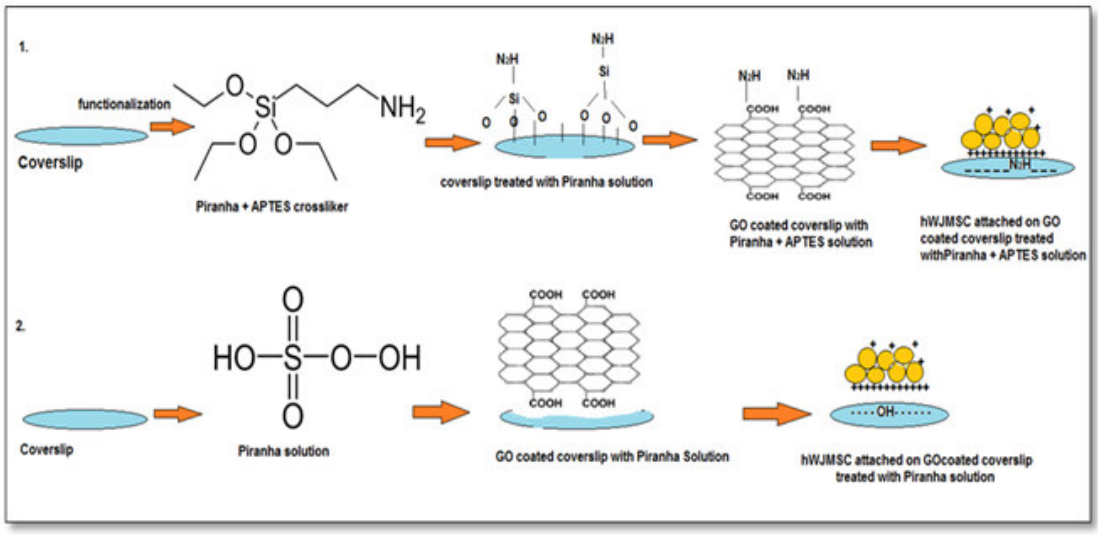

Figure 1
Synthematic diagram of GO group functionalization. GO coated coverslip functionalization with Piranha + APTES solution (1), and GO coated coverslip functionalization with Piranha solution alone (2).

RESULTS AND DISCUSSION:

Cell morphology

Human umbilical cords were collected caesarian cases of the delivery mother. The morphology of cell culture when grown on the GO substrates, was observed from passage one (P1). Human WJMSCs exhibited fibroblast-like shape or star-like shape on the standard tissue culture plate (TCP). Figure 2 showed the morphology of GO-hWJMSCs was observed under Olympus Research Inverted Microscope every passage to identify any changes in the morphology. The substrates with the concentration of 1mg/ml with 1 layer thickness that functionalized with Piranha + APTES observed clearer fibroblast-like morphology compared to 5mg/ml concentration and 5 layers of thickness functionalized either Piranha alone or Piranha + APTES solution. The highest GO concentration (f7, h7, k7 and y7) were not inhibiting the cell culture however it reduced the confluence of the cell when compared to 1mg/ml. The coverslips were functionalized with crosslinker agent for instance, Piranha solution and APTES solution were improved the GO flakes attachment during spin coating preparation. Demonstrated by Park and team was reported that the flakes of GO enable to attach by the Piranha and APTES crosslinker accordingly to covalent interaction (Park et al., 2015). The positive–negative charges have incorporated the cell-material attachment by functional oxygenated group (FOG). Studied by Yang et al. 2014 have reported the success of GO attachment by improving the FOG to interact with the carboxyl group (COO), hydroxyl group (OH) and epoxide group (C-C) (Figure 1)

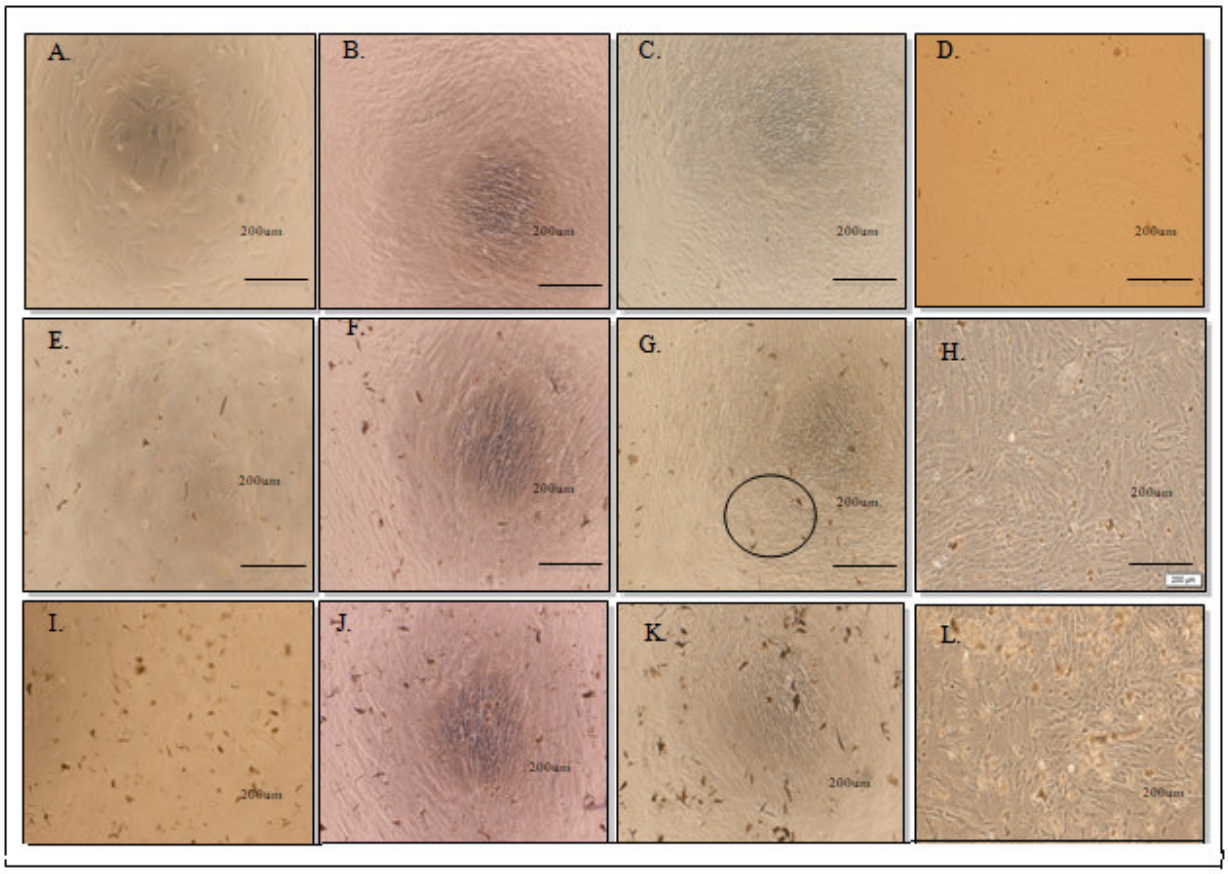

Figure 2
The morphology of hWJMSCs of day1, day6, passage 3 and passage 5. (A-D) showed the morphology of hWJMSCs on control. (E-H) GOy1-hWJMSCs is fibroblast-like shape. (I-L) exhibited the GOh7-hWJMSCs on the highest GO concentration substrate of day1, day6, passage3 and passage5. *Circle indicative the highest concentration of GO flakes.

The latency cell culture was projected the rhomboid-like shape or elongation fibroblast-like shape in control or standard TCP however it was not observed in GO-hWJMSCs. This indicates the GO-hWJMSC is a good potential substrate to maintain the shape of the cell. The report on the same line was demonstrated by Song et al. 2008 exhibit the morphology of bone marrow mesenchymal stem cells (BM-MSCs).

Cell viability

Cell-materials survival was determined by assessing the viability. We determined that GOy1-hWJMSCs was the good candidate that promote the growth and support cell viability compared to 0.1% Gelatin coated coverslip. Obviously, the graph indicated the higher GO concentration and the higher number of spin coating cycles was affected the viability of hWJMSC every expanded passage. The percentage mean of GOy1-hWJMSC at passage five (P5) is m=375±4% significantly different against 0.1%gelatin as a positive control, m=100%. The study supported by Baker, (2011) has responded the great fascinate biomaterial such as GO modified surface interaction has reflected the better stem cell biological respond meantime sustain the cell behaviour including cell morphology, cell adhesion, cell viability and phenotype. The pivotal of GO biomaterial enhanced the higher protein adsorption to the cell condition where has to prolong the cell culture lifespan (Wu et al., 2006; Ning et al., 2016). Moreover, GOy1-hWJMSC has potentially promoted the survival of hWJMSC and highly recommended to further study in future. To further confirm the cell number of GO-hWJMSCs, we continue identified the counting cell number manually.

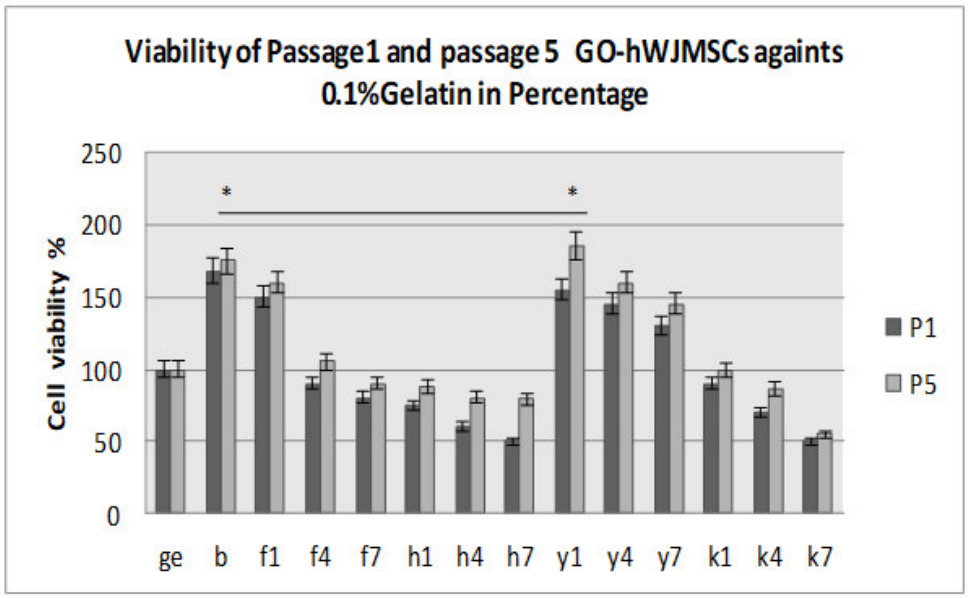

Figure 3
The viability percentage of targeted GO samples within P1GO-hWJMSC and P5GO-hWJMSC according to absorbance reading using PrestoBlue™. n=3.p>0.05 statically no significant different between control.

Kinetics growth

The cells of day 2 until day 22 were plated in 48 wellplate with a density of $1x10^4$/cm2. Ultimately, figure 4 showed GOy1-hWJMSC gave the highest cell counting after day 22 compared to positive control (0.1%Ge) and control coverslip (b). The curve of GO-hWJMSC in highest concentration enumerated by k1-3 and h7-9 were observed not supporting the growth of hWJMSC. The cell counting was decreasing significantly after day 2 and onwards indicative the lower biocompatibility of GO in highest concentration and thickness. In the sight of great graphene and its derivatives, Akhavan and the group have studied the fascinating effect of reduced graphene oxide nano-particles (rGONPs) elevate the viability of human umbilical cord MSC (hUCMSC) and maintained the genotype (Akhavan et al., 2012; Akhavan et al., 2013).

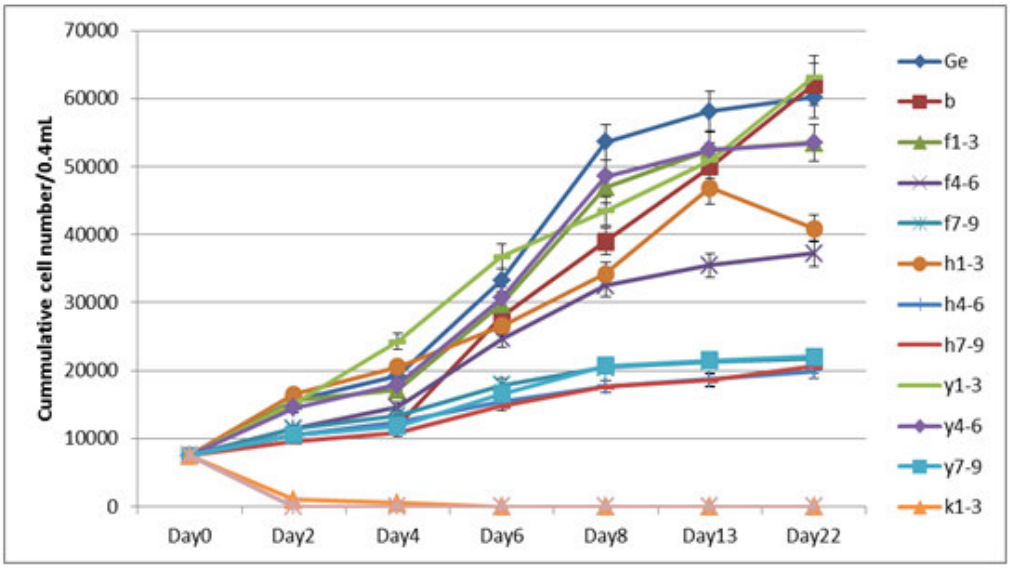

Figure 4
Initial data has been interpreted for every single GO coated coverslip substrates. The sigmoid shape was indicating the latency phase, logarithmic phase and plateau phase of cell-material yields (Sun *et al.*, 2014).

Osteogenic and adipogenic differentiation staining

Since GOy1-hWJMSC was the best candidate, we further evaluate this material in inducing media of osteogenic differentiation and adipogenic differentiation. We discovered that GO enable to influence hWJMSC to differentiate into calcium deposited formation by stained using Alizarin staining dye in Figure 5 within 14-20 days. GOy1-hWJMSC in an adipogenic inductive media identified easily to visualize the lipid droplet in the culture cell line within 7-13 days by staining by Oil Red O solution. Moreover, the optical density showed the higher potential of GOy1-hWJMSC to differentiate into osteocytes and adipocytes. The result demonstrates that GOy1 promoted to osteogenic and adipogenic differentiation. The report discovered by Elkhenany and colleagues encountered that GO coated plates succinctly support the caprine-MSC cell adherent, proliferation and spontaneously undergo osteogenic differentiation without specific induction or growth factor ultimately (Elkhenany et al., 2014).

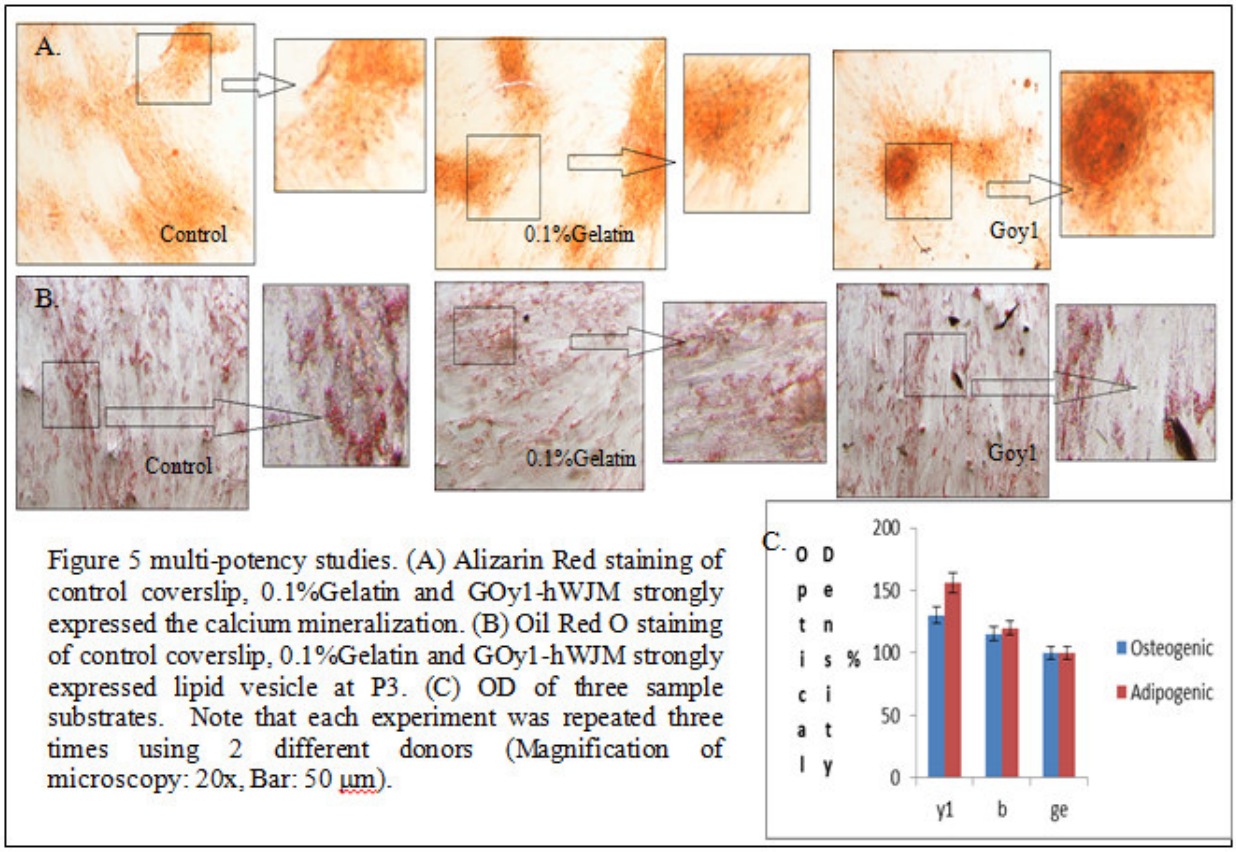

Figure 5 multi-potency studies. (A) Alizarin Red staining of control coverslip, 0.1%Gelatin and GOy1-hWJM strongly expressed the calcium mineralization. (B) Oil Red O staining of control coverslip, 0.1%Gelatin and GOy1-hWJM strongly expressed lipid vesicle at P3. (C) OD of three sample substrates. Note that each experiment was repeated three times using 2 different donors (Magnification of microscopy: 20x, Bar: 50 µm).

Immunocytochemistry

We also performed the analysis of immunocytochemistry to confirm that the cells are still MSC stemness. Markers for MSC were used such as STRO-1 (Cat.No.3f9-8401, Invitrogen), CD105 (cat. PA5-16895, Invitrogen) and CD271 (Cat. MA5-13314, Invitrogen) at 1:200 dilution with the appropriate Alexa Fluor-conjugated secondary antibodies; STRO-1 (goat anti-mouse 488) at 1:200, CD105 (goat anti-rabbit 555 at 1:200) and CD271 (goat anti-mouse) and nuclei were stained with DAPI (blue). The sample is mounted in ProLong diamond antifade reagent (ThermoFisher). All the three markers were detected as shown in figure 6. GOy1 gave positive expression of the STRO-1, CDl05 and CD271 indicating GOy1 substrate enable to maintain the MSC characterization. Results were interpreting using Olympus confocal fluorescent microscope using a 20x objective.

CONCLUSION:

In this study, we exposed the demonstration of GO coated coverslip entailed with two different coverslip functionalization enumerated by Piranha solution and Piranha + APTES solution influenced by covalent bonding between the GO and coverslip surface. Fascinating rules of GO coated coverslip elucidated protein

adsorption of hWJMSC culture enable to prolong the stem cell behavior until passage 5 and the potential candidate to further study in long-term cultivation. As to conclude according to the result analysis, we have succinctly grown the hWJMSCs on 2D GO coated coverslip substrates and maintained the spindle shape or fibroblast–like morphology until passage 5. Subsequently, GO coated coverslip strongly shown the GOy1-hWJMSC Piranha + APTES solution functionalization was identified with the highest proliferate number which is comparable to 0.1%gelatin as a positive control and blank coverslip. Multi-potency study depicted the differentiation of GOy1-hWJMSCs at passage 1 into adipocytes and osteocytes while using the inductive media. Phenotype result was studied by elucidating the targeted biomaterial which is GOy1-hWJMSC that positively expressed and retained the MSC surface marker of the STRO-1 (endothelial antigen), CD105 (endoglin type 1 membrane glycoprotein) and CD271 (Nerve growth factor receptor) at passage 5. Further study of future work on GO substrate is being conducted to achieve the long-term cultivation analysis.

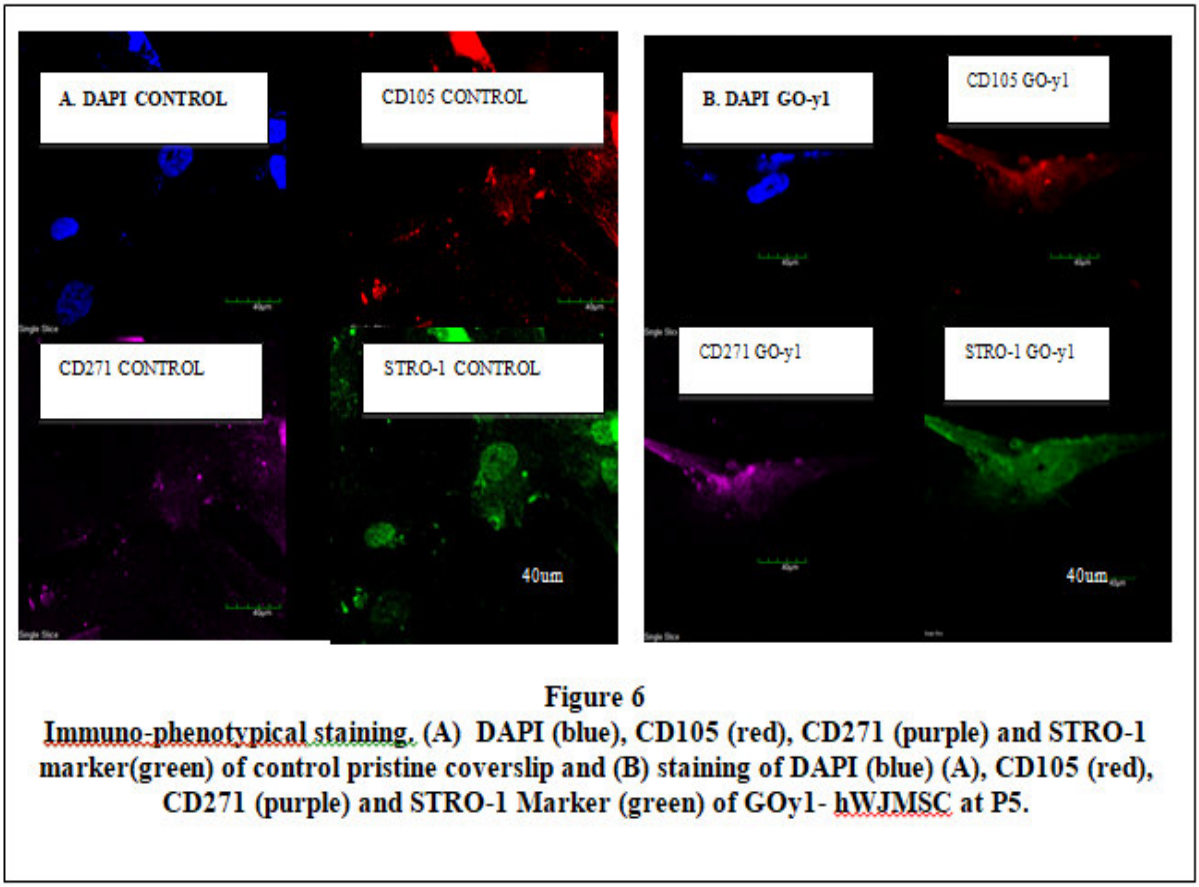

Figure 6
Immuno-phenotypical staining. (A) DAPI (blue), CD105 (red), CD271 (purple) and STRO-1 marker(green) of control pristine coverslip and (B) staining of DAPI (blue) (A), CD105 (red), CD271 (purple) and STRO-1 Marker (green) of GOy1- hWJMSC at P5.

ACKNOWLEDGEMENTS:

The author would like to acknowledge the financial support upon the research allocating to the Ministry of Higher Education from TRGS0002-SG2/2014 and to the members and institute for the contribution and kindness outstanding auxiliary especially Biotechnology Research Institute, University of Malaysia Sabah.

REFERENCES:

1. Akhavan,O., Ghaderi,E.,Akhavan,A. 2012. Size-dependent Genotoxicity of graphene nanoplatelets in human stem cells. Biomaterials, 33:8017-8025.
2. Akhavan,O.,Ghaderi,E.,Shahsavar,M. 2013. Graphene nanogrids for selective and fast osteogenic differentiation of human mesenchymal stem cells. Carbon, 59:200-211.
3. Alegria, G.E., Iluit, M., Stefanska, M., Silva, C., Heeg, S., Kimber, S.J., Kuoskoff, V., Lacaud, G., Vijayaraghavan, A., Batta, K. 2016. Graphene oxide promotes embryonic stem cell differentiation to haematopoietic lineage. Scientific Reports. Vol. 6:25917.

4. Baker,M. 2011. Stem cells in culture: defining the substrate. Nature Methods.Vol. 8:293-297.
5. Bharadwaj,S., Liu,G., Shi,R.W., Yang,B., He,T., Fan,Y., Lu,X., Zhou,X., Liu,H., Atala,A., Rohozinski,J., and Zhang,Y. 2013. Multipotential differentiation of human urine-derived stem cells: Potential for therapeutics applications in urology. Tissue-Specific Stem Cells, vol 31,9:1840-1856.
6. Chaudhuri,B., Bhadra,D., Moron,L., Pramanik,K. 2015. Myoblast differentiation of human mesenchymal stem cells on graphene oxide and electrospun graphene oxide –polymer composite fibrous meshes: importance of graphene oxide conductivity and dielectric constant on their biocompatibility. Biofabrication 7 ,015009.doi:10.1088/1758-5090/7/1/015009.
7. Choi, K.M., Seo, Y.K., Yoon, H.H., Song, K.Y., Kwon, S.Y., Lee, H.S., Park, J.K. 2008. Effect of ascorbic acid on bone marrow-derived mesenchymal stem cell proliferation and differentiation. *J Biosci Bioeng*.105(6):586-94.
8. Duffy,C.R.E., Zhang R. ,How S.E., Lilienkampf, A., De Sousa, P.A., Bradley, M. 2014. Long term mesenchymal stem cell culture on a defined synthetic substrate with enzyme free passaging, *Biomaterials* 35: 5998-6005.
9. Elkhenany,H., Amelse,L., Lafont,A., Bourdo,S., Caldwell,M., Neilsen,N., Dervishi,E., Derek,O., Biris,A.S., Anderson,D., Dhar,M. 2014. Graphene supports in vitro proliferation and osteogenic differentiation of goat adult mesenchymal stem cells: potential for bone tissue engineering. Applied Toxicology, 35:367-374.
10. Gu,M., Liu,Y., Chen, T.,Du,F.,Zhao,X.,Xiong,C.,Zhou,Y. 2014. Is graphene a promising nano-material for promoting surface modificationof implants or scaffold materials in bone tissue engineering? Tissue Eng., Part B, 20: 477-491.
11. Kalbacova,M., Broz,A., Kong,J., Kalbac,M. 2010. Graphene substrates promote adherence of human osteoblasts and mesenchymal stromal cells. Carbon, 48:4323-4329.
12. Khazaei,M., Nasseri,S., Ganjali,M.R., Khoobi,M., Nabizadeh,R., Mahvi,A.H., Nazmara,S., and Gholibegloo,E. 2016. Response surface modelling of lead (II) removal by graphene oxide-Fe3O4 nanocomposite using central composite design. Journal of Environment Health Science and Engineering, 14:2.
13. Kim, J., Kim, Y.R., Kim, Y., Lim, K.T., Seonwoo, H., Park, S., Cho, S.P., Hong, B.H., Choung, P.H., Chug, T.D., Choung, Y.H., Chung, J.H. 2013. Graphene-incorporated chitosan substrata for adhesion and differentiation of human mesenchymal stem cells. J.Mater Chem. B, 1: 933-938.
14. Lee, W.C., Lim, C.H.Y.X, Shi, H., Tang,L.A.L., Wang,Y., Lim,C.T., Loh,K.P. 2011. Origin of enhanced stem cell growth and differentiation on graphene and graphene oxide. American Chemical Society, vol. 15, No. 9:7334-7341.
15. Li, F., Jian, X., Zhao, J., Zhang, S. 2015. Graphene oxide: A promising nanomaterial for energy and environment applications. Nano Energy, 16: 488-515.
16. 16.Liu, J., Cui, L., Losic, D. 2013. Graphene and graphene oxide as new nanocarriers for drug delivery application. Acta Biomaterialia 9: 9243-9257.
17. Luo,Y., Shen, H., Fang, Y., Huang, J., Zhang,M., Dai,J., Shi,X., Zhang,Z. 2015. Enhanced proliferation and osteogenic differentiation of mesenchymal stem cells on graphene oxide-incorporated electrospun poly(lactic-co-glycolic acid) nanofibrous mats. ACS Appl. Mater. Interfaces. 7:6331-6339.
18. Nakajima, M., Ishimuro, T., Kato, K., Ko, I.K., Hirata, I., Arima, Y., Iwata, H. 2007. Combinatorial protein display for the cell-based screening of biomaterials that direct neural stem cell differentiation. Biomaterials, 1048-1060.
19. Neuss, S., Apel, C., Buttler, P., Denecke, B., Dhanasingh, A., Ding, X., Grafahrend, D., Groger, A., Hemmric, K., Herr, A., Dechent, W.J., Mastitskaya, S., Bouza, A.P., Rosewick, S., Salber, J., Wo\ltje, M., Zenke, M. 2008. Assessment of stem cell/biomaterial combination for stem cell-based tissue engineering. Biomaterials 29:302-313.
20. Ning,R., Wang,F., Lin,L. 2016. Biomaterial-based microfluidics for cell culture and analysis. Trends in Analytical Chemistry, 80:255-265.
21. Omar, E.R., Beroud, J., Stoltz, JF., Menu, P., Velot, E.,Decot, V. 2014. Umbilical cord mesenchymal stem cells: the new gold standard for mesenchymal stem cell-based therapies? Tissue Eng. Part B Rev., 20:523-544.

22. Park, J., Kim, B., Han, J., Oh, J., Park, S., Ryu, S., Jung, S., Shin, J.Y., Lee, B.S., Hong, B.H., Choi, D., Kim, B.S. 2015. Graphene oxide flakes as a cellular adhesive: Prevention of reactive oxygen species mediated death of implanted cells for cardiac repair. American Chemical Society. Vol. 9. No.5:4987-4999.
23. Perng Yang Puah, Pak Yan Moh, Ping Chin Lee & Siew Eng How (2018): Spincoated graphene oxide as a biomaterial for Wharton's Jelly derived mesenchymal stem cell growth: a preliminary study, Materials Technology. Doi.org/10.1080/10667857.2018.1515300.
24. Rahul, U., Sharmistha, N., Nitu, B., Suryasarathi, B., Bikramjit, B. 2016. Modulation of protein adsorption and cell proliferation on polyethylene immobilized graphene oxide reinforced HDPE bionanocomposites. ACS Appl. Mater Interfaces. Vol. 8:11954-11968.
25. Rosa,V., Xie,H., Dubey,N., Madanagopal,T.T, Rajan,S.S., Morin,J.L.P., Islam,I., Neto,A.H.C. 2016. Graphene oxide-based substrate: physical and characterization, cytocompatibility and differentiation potential of dental pulp stem cells. Dental materials 32:1019-1025.
26. Shen, H., Zhang, L., Liu, M., Zhang, Z. 2012. Biomedical applications of graphene. *Theranostics;*2(3):283-294.
27. Li, F., Jian, X., Zhao, J., Zhang, S. 2015. Graphene oxide: A promising nanomaterial for energy and environment applications. Nano Energy, 16: 488-515.
28. Song,G., Ju,Y., and Soyama,H. 2008. Growth and proliferation of bone marrow mesenchymal stem cells affected by type 1 collagen, fibronectin and bFGF. Materials Science and Engineering C, 28:1467-1471.
29. Soraya, R. G., Frances, J. H., Bahman , D., Stan, G., Nicola, Stan, H. V. 2013. Exploring the mesenchymal stem cell niche using high throughput screening. *Biomaterials **34***:7601-7615.
30. Sun,T., Yu,C., Gao,Y., Zhao,C., Hua,J., Cai,L., Guan,W., and Ma,Y. 2014. Establishment and biological characterization of a dermal mesenchymal stem cells line from bovine. Biosci. Rep. doi10.1042.
31. Wu,D., Zhao,B., Dai,Z., Qin,J., Lin,B. 2006. Grafting epoxy-modified hydrophilic polymers onto poly(dimethylsiloxane) microfluidic chip to resist nonspecific protein adsorption. Lab Chip, 6:942-947.
32. Yang,D., Velamakanni,A., Bozoklu,G. et al,. 2009. Chemical analysis of graphene oxide films after heat and chemical treatments by X-ray photoelectron and Micro-Raman spectroscopy. Carbon, 47:145–152.
33. Zhao, G., Liu, F., Lan, S., Li,P., Wang,L., Kou,J., Qi,X., Fan,R., Hao,D., Wu,C., Bai,T., Li,Y., and Liu,J.Y. 2015. Large-scale expansion of Wharton's jelly-derived mesenchymal stem cells on gelatin microbeads, with retention of self-renewal and multipotency characteristics and the capacity for enhancing skin wound healing. *Stem Cell Research & Therapy,* 6:38.

FP-25

EXPLORING THE POTENTIAL OF TANNASE-PRODUCING FUNGI FROM VARIOUS AGRI-INDUSTRIAL RESIDUES

MANSOR, AZLINA[1*], RAMLI, MOHAMMAD SHARIL[3], SAMAT, NORAINI[2], ABDUL RASHID, NUR YUHASLIZA[1], LANI, MOHD NIZAM[4], SHARIFUDDIN, SHAIFUL ADZNI[1], SIVA, RASEETHA [3]

[1]Enzyme and Fermentation Technology Programme, Biotechnology and Nanotechnology Research Centre, MARDI Headquarters, Serdang, Selangor, [2] Animal and Aquaculture Feed, Animal Sciences Research Centre, MARDI Headquarters, Serdang, Selangor, [3]Food Science &Technology Programme, Faculty of Applied Sciences, Universiti Teknologi MARA, Shah Alam, Selangor, [4] Centre of Knowledge Transfer and Industrial Networks, Universiti Malaysia Terengganu, Kuala Terengganu, Terengganu Darul Iman.

[*]Corresponding author: dikna@mardi.gov.my

ABSTRACT

Tannase or tannin acyl hydrolase (E.C 3.1.1.20) is an industrially important enzyme widely used in food, animal feed, pharmaceutical, leather and cosmetic industries. However, its application is still limited due to the high production cost. Several agri-industrial residues which reported containing tannin can be good sources for tannase producing fungi and served as fermentation substrate for tannase production. This study is aimed to explore the potent tannase producing fungal strains from the agri-industrial residues such as rice by-products, coffee ground, tea, desiccated coconut residues, fruits and tuber peels and cocoa by-products. These selected agri-industrial residues were subjected to natural fermentation prior to isolation and screening of tannase producer using the tannic acid agar (TAA) plate method. Addition of 2 % molasses was found to enhance the succession of naturally occurring fungal growth during the process of fermentation. A total of 53 tannase producing fungi were isolated from 12 different ranges of agri-industrial residues using TAA plate method. Most potent fungal strains which possess high tannase activity were isolated from substrates like cocoa by-products, coffee ground and banana peels which reported containing high tannin content, compared to other solid substrates.

KEYWORDS:
Isolation, Screening, agri-industrial residues, tannase, tannic acid

INTRODUCTION:

Tannase, also known as tannin acyl hydrolase (EC 3.1.1.20) is a hydrolase that catalyses the hydrolysis of ester and depside bonds in hydrolysable tannins and releases glucose and gallic acid as products. Tannase is an extracellular inducible enzyme that can obtain from various sources such as plants, animals and microbial sources such as fungi, yeast, bacteria [1].

Tannase has wide industrial applications in different food and feed, beverage, cosmetics, chemical and brewing industries, in preparation of gallic acid, instant tea, coffee flavoured soft drinks, clarification of beer and fruit juices, and detanification of food and increase the nutritive properties for animal feed and also in bioremediation of tannery effluents of leather industries[2]. Despite of the wide industrial application of tannase, it has not been fully exploited due the high production cost and involving pure tannic acid both as inducer and carbon sources. Pure tannic acid is very costly and not suitable to be used for large scale enzyme production[3].

In Malaysia, a large number of agricultural residues has been generated during harvesting and processing of the agri-based industries such as rice milling and the food processing industries and has caused environmental problem. Most of these substrates are rich in nutrients but often underutilized. Agro-industrial residues are generally considered as the best source of tannin-rich substrate to replace the use of pure tannic acid for tannase production[4]. Besides, it is known that tannin is the second largest group and most abundant

phenolic compound present in plants, therefore, these agro-industrial residues served as a good natural tannin resources and cost-effective substrate for tannase production.

Tannase produced by microbial sources is considered as the most reliable and important sources for production of commercial tannase due to the microbial tannase properties which are more stable than that obtained from other sources. Besides, microbial sources also produce tannase in high quantities, constantly and more readily subjected to genetic manipulation compared to plants and animals, resulting to an increase in tannase production[1]. Among the microorganisms, fungi have been the most studied and reported microorganisms for tannase production. Futhermore, most fungi are lignicellulosic enzyme producer that enable to degrade the liginicellulose and tannin that presents in plants, subsequently able to utilize the agri-industrial residues as substrate. Therefore, potential fungi as tannase producer could be exploited for tannase production using the agri-industrial residues via solid state fermentation.

This study is undertaken to explore potent tannase producing fungi that naturally occur in the the agri-industrial residues and subsequently can be used as producer for tannase production using the agri-industrial residues as potential substrate.

MATERIALS AND METHODS:

Sample collection

A total of 12 samples of agri-industrial by-products such fruit and tuber peels (banana, mango, sweet potato, tapioca), rice by-products, spent coffee ground, cocoa shell, pulp and seed spoiled chilli and onion and dessicated coconut residue were collected from various sources such as milling factory, wet market, restaurant and stalls and used for isolation of tannase-producing fungi. These samples were immediately subjected to natural fermentation process before continued with subsequent isolation work.

Natural Fermentation of Samples

Agri-industrial by-products collected were subjected to natural fermentation for enrichment and growth enhancement of the natural occurring microorganisms present in the samples. Some samples such as fruit and tuber peels were initially chopped into smaller pieces, placed in a beaker, added with 2% of molasses for enrichment of the substrate and to provide some moisture to the substrates before left for natural fermentation at room temperature (27-30°C under aerobic condition for 7-12 days, prior to isolation and screening of the tannase-producing fungi.

Isolation of Tannase-producing Fungi

Each naturally fermented sample was suspended in Ringer solution and serially diluted with sterile Ringer solution. Hundred microliters from an appropriate dilution were placed and spread plated onto the selective TAA medium. Incubation was carried out at 30□C for 96 hrs under aerobic conditions. Fungi capable to grow and form clearing zone around its colonies due to the hydrolysis of tannin were selected and purified. The cultures obtained were grown on PDA, then transferred to PDA slants and maintained at 4□C for storage.

Media

Tannic acid agar (TAA) was used for isolation of tannase-producing fungi and for the primary screening of fungal isolates. The composition of the TAA medium was as follows: $NaNO_3$ (3 g/L); K_2HPO_4 (1.0 g/L); $MgSO_4$.7H2O (0.5 g/L); KCl (0.5 g/L); $FeSO_4 \cdot 7H_2O$ (0.01 g/L); agar (30 g/L). The pH was adjusted to 5.0 prior to sterilization at 121°C for 15 min. The tannic acid solution was filter sterilized separately using 0.22µm pore size filter, then added to the medium and mixed well, before pouring into the plates. Potato dextrose agar (PDA) was used for maintaining fungal isolates.

Primary Screening and Selection of Tannase-producing Fungi

The positive fungal strains isolated from the naturally fermented agricultural residues were screened and determined for their strength in producing tannase based on the diameter of hydrolytic zone formed on

tannic acid agar, a defined medium containing tannic acid as the sole carbon source. Primary screening for the highest tannase producers was carried out on TAA plates using method described by Bradoo *et al.* (1996) with some modifications[5]. Fungal isolates obtained from the previous screening and isolation scheme were grown on PDA plates. Using a sterile pasteur tip, agar discs containing 3 days old fungal cultures (diameter ~6mm) were removed from PDA plates and placed onto the centre of TAA plates. The inoculated plates were incubated at 30°C for 96 h for observation on the diameter of hydrolytic zone and the growth of the microorganism as measured by the diameter of the colony. Tannase production was indicated by the appearance of a hydrolytic zone. This hydrolytic zone was measured for subsequent calculation of the enzymatic index (EI) using the expression:

$$EI = \frac{Diameter\ of\ hydrolysis\ zone}{Diameter\ of\ colony}$$

Microscopic and Morphological Characteristics

The morphology and microscopic of the fungal isolate on PDA agar plate were observed and recorded. The fungal spores and mycelium was placed on a slide using a loop and stained with lactophenol cotton blue and examined microscopically to determine their characteristics.

RESULTS AND DISCUSSION:

Natural Fermentation and Isolation of Tannase Producing Fungi

A total of 53 tannase-producing fungi have been isolated from 10 different agri-industrial residues using the spread plate method as indicated by the hydrolytic zone surrounding the colonies, which showed their utilization of tannic acid by producing tannase enzyme (Figure 1). The agri-industrial residues were initially enriched with molasses and moistened with distilled water before subjected to natural fermentation for 7-12 days, prior to isolation and screening of tannase-producing fungi. The objective of natural fermentation is to enhance fungal growth or allow the succession of naturally occurring microorganisms by the addition of molasses. The enrichment in natural fermentation step was found crucial to enhance fungal growth as isolation of tannase-producing microorganisms was not successful in the earlier isolation work, especially in samples containing less nutrients or carbon sources such as the spent coffee bean or spent tea (data not shown).

Selection of samples from agri-industrial residues for isolation were based on the abundantly available agri residues in which, consequently, they can be exploited and used as potential fermentation substrate for tannase production. Selection of sources was also based on the fact that the presence of tannase-producing fungi may exist in agri-industrial residues especially in those containing high tannin[7,8]. Most of the agri-industrial by-products available are rich in nutrients but often underutilized such as the rice by-products and desiccated coconut residues. Thus, these samples were used as sources for exploring potential tannase-producing fungi from these agriculture resources.

Highest number of tannase-producing isolates were obtained from cocoa shell, pulp and seeds with 18 isolates, followed by banana peels (13 isolates) and rice by-products (rice brans and brewer's rice) with 6 isolates. Four isolates were obtained from mango peels, tapioca peels, spent coffee beans and tea, while only 1 isolate was obtained from each of the rest substrates. The percentage on distribution and number of fungi isolated from different sources was as shown in pie chart as below (Figure 2)

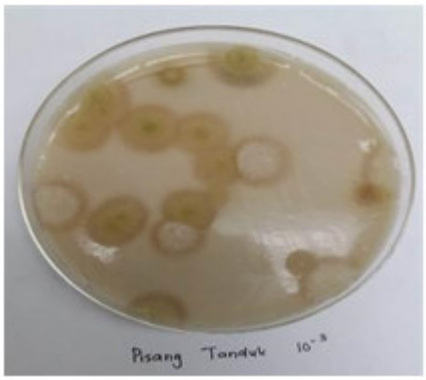

Figure 1
Tannase-producing fungi as indicated by the appearance of hydrolytic zone around the colonies on the TAA plate.

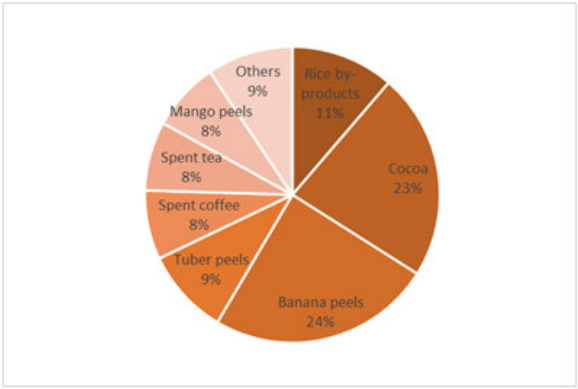

Figure 2
Distribution of tannase-producing fungi isolated from different agri-industrial residues.

Primary Screening of tannase producers

The diameter of hydrolytic zone produced and size of the colony was measured after 72 hrs and was varied among the fungi. Direct measurement of the colony diameter was a good indicator of the ability of tannic acid utilization as a carbon source due to the tannase activity in the medium [2]. The diameter of halo zone (including the colony) measured were ranging from 46 mm to 61.00 mm. Data presented in Table 1 showed the sum of colonies and diameter sizes of colony, hydrolytic zone and enzymatic index of among the strong tannase producer. The coded fungal strains were arranged in descending order according to the enzymatic index calculated each fungal strain. Pinto et al. (2001) reported that they preferred determination of colonies diameter instead of diameter of the clear zones because the observation of the clear zones was difficult[6]. However, in our cases, most of the hydrolytic clear zones were easily visualized.

Fungal cultures which exhibited high tannase activity in the primary screening, as indicated by the diameter size of the hydrolytic zone and enzymatic index, will be selected for further quantitative secondary screening for tannase production using submerged fermentation technique.

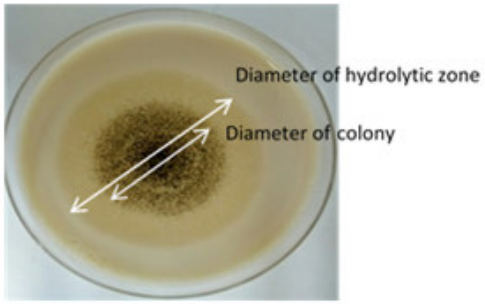

Figure 3
Measurement of diameter of hydrolytic zone and colony

Table 1
List of among the highest tannase activity as indicated by the bigger diameter zone of hydrolysis on TAA plate

No.	Code	Diameter of Hydrolytic zone, mm	Diameter of Colony, mm	Enzymatic index
1.	ON1	55.70	39.30	1.42
2.	C4	58.00	41.33	1.40
3.	KK2	58.30	42.3	1.38
4.	C2	57.70	42	1.37
5.	F0018	54.30	40.00	1.36
6.	KK1	51.70	38.00	1.36
7.	CN1	56.00	41.33	1.35
8.	KI2	55.30	41	1.35
9.	C1	58.30	43.6	1.34
10.	KI5	52.70	40	1.32
11.	MG2	46.30	35	1.32
12.	PN1	46.70	35.3	1.32
13.	UK1	55.30	42.33	1.31
14.	K14	53.00	41	1.29
15.	KI7	50.00	38.66	1.29
16.	MG3	46.00	35.70	1.29
17.	MG4	47.70	37.00	1.29
18.	PT6	45.00	35	1.29
19.	RB2	51.70	40.00	1.29
20.	UK2	61.30	47.667	1.29

Microscopic and morphology observation of the fungal isolates

Based on the microscopic and morphology observation of the fungal isolates has revealed that most potential isolates were identified as *Aspergillus niger*. The strains were identified owing to the sporulating structures under standard incubation conditions used. Fungal strains of the *Aspergillus* sp have been reported as important fungi that commonly used in tannase and other commercial enzyme production [9].

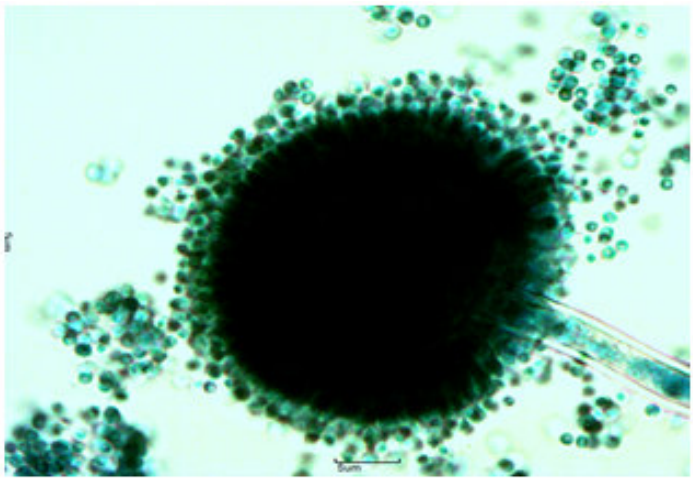

Figure 4
Microscopic observation the tannase-producing fungi (C1) under 100x magnification.

CONCLUSION:

A total 53 tannase-producing fungi have been successfully isolated from naturally fermented agri-industrial residues. Natural fermentation of enriched agri-industrial residue samples had enhanced fungal growth and assisted in isolation of potential fungal strains especially in substrates containing low nutrients or carbon sources. Isolation of tannase-producing fungi using the TAA plate method is a qualitative, simple and rapid screening procedure for tannase production. Most tannase-producing fungal isolates exhibiting high tannase activity were obtained from the banana peels, cocoa by-products, spent coffee and tea which probably due to the high tannin content in the substrates.

ACKNOWLEDGEMENT:

We would like to thank Dr. Tosiah Sadi for her support with the microscopic observation and identification of the fungal isolates. This work is supported by Fundamental Research Grants Scheme (FRGS) under Ministry of Higher Education (MOHE) Malaysia.

REFERENCES:

1. Abou-Bakr, HA, El-Sahn, MA., El- Banna, AA. Screening of tannase producing fungi isolated from tannin rich sources. Int. J. Agric. Food Res. 2013; 2(3): 1 12.
2. Aguilar CN, Augur C, Favela-Torres, E, Viniegra- Gonzalez G. Production of tannase by *Aspergillus niger* Aa-20 in submerged and solid-state fermentation: influence of glucose and tannic acid. Journal of Industrial Microbiology and Biotechnology. 2001; 26, pp: 296-302.
3. Lokeswari, N., Lenin Kumar, B. Tannase Production From Cashew Husk By Solid-State Fermentation. International Journal of Advanced Biological Research. 2013; V. 3(2): 295-299
4. Pandey A., Selvakumar P., Soccol C.R., Nigam, P. Solid-state fermentation for the production of industrial enzymes. Curr.Sci., 1999;77:149-162
5. Bradoo, S.; Gupta, R.; Saxena, R.K. Screening of extracellular tannase producing fungi: development of a rapid and simple plate assay. J. Gen. Appl. Microbiol. 1996; 42, pp: 325-329.
6. Pinto GAS., Leite SGF., Terzi SC., Couri S. Selection of tannase-*producing Aspergillus niger* strains. Braz. J. Microbiol. v. 32, n. 1, p. 24-26, pp.24-26.
7. Nandini KE, Gaur A and Sundari S. K. The Suitability of Natural Tannins from Food and Agricultural Residues (FAR) for Producing Industrially Important Tannase and Gallic Acid through Microbial Fermentation. International Journal of Agriculture and Food Science Technology. 2013; V. 4, Number 10, pp. 999-1010
8. Brahmbhatt D, Modi HA, Jain NK. Preliminary isolation and screening of tannase producing bacteria and fungi. Int. J. Curr. Microbiol. App. Sci. 2014; 3(11): 193-203
9. Mahdi ZS, Al-Tahan Shatha SS. Production of Tannase from Aspergillus niger under solid state fermentation. Iraqi Journal of Science. 2014; Vol 55, No.3B, pp:1188-1195.

FP-26

IDENTIFICATION OF *TRICHODERMA* SPECIES BY DNA BARCODE AND SCREENING FOR ITS LIGNOCELLULOLYTIC ACTIVITY

AZRIAH ASIS[1], SHAFIQUZZAMAN SIDDIQUEE[1]*, LAILA NAHER[2, 3], ZARINA AMIN[1], MD. AKHTER UZZAMAN[4]

[1]Biotechnology Research Institute, Universiti Malaysia Sabah, Jln UMS, 88400 Kota Kinabalu, Sabah, Malaysia
[2]Department of Agricultural science, Faculty of Agro-Based Industry, Universiti Malaysia Kelantan Jeli Campus, 17600, Kelantan, Malaysia
[3]Institute of Food Security and Sustainable Agriculture, Universiti Malaysia Kelantan, Jeli Campus, 17600 Kelantan, Malaysia
[4]Planning and Development Division, Bangladesh Atomic Energy Commission, Dhaka, Bangladesh

*Corresponding author: shafiqpab@ums.edu.my

ABSTRACT

Trichoderma is a cosmopolitan fungus that prevalent in the soil and other diverse habitats. It has gained vast economic importance such as in industrial enzymes production, antifungal, antibiotics, biocontrol agents and plant growth promoter. Apart from, *Trichoderma* species is widely used in the production of cellulolytic enzymes. Therefore, an accurate identification of *Trichoderma* isolates at the species level is highly desirable. The aim of this study was to analysis the genetic biodiversity of *Trichoderma* species collected from wet paddy field, Tuaran. Total of 53 isolates were identified at the species level by the combination of morphological characters and gene sequencing of internal transcribed spacer regions 1 and 2 (ITS 1 and 2) of the rDNA cluster. Among all the isolates, they were positively identified as *T. asperellum* (43 strains), *T. harzianum* (9 strains), and *T. reesei* (1 strain). The lignocellulolytic activities were assayed based on their ability to develop dark brown pigments, yellow halo zone, and clear white zone on tannic acid media (TAM), Jensen Media (JM) and modified Melin–Nokrans media (MMNM), respectively. The diameters of dark brown pigments and halo zones formation were measured as the indication for their ability to degrade lignin, cellulose, and starch. The different *Trichoderma* species isolates demonstrated variable lignocellulolytic activities where seven isolates [S1(9)10^{-1}(3), E3(6)10^{-1}(2), W2(2)10^{-1}(2), S3(1)10^{-1}(1), N2(4)10^{-2}(3), N2(2)10^{-1}(2) dan S3(6)10^{-1}(2)] were found as the best lignocellulolytic activities. Thus, the preliminary screening of these *Trichoderma* isolates for lignocellulolytic activities could apply for biocontrol along with rapid composting to enhance the soil fertility, increase the production of yield and controlling plant diseases.

KEYWORDS:
Trichoderma; Lignocellulolytic; Morphology; Internal Transcribed Spacer

INTRODUCTION:

The genus *Trichoderma* belongs to Ascomycetic (Ascomycota, Hypocreales) fungi found in various ecosystems such as agricultural field, forest, salt marshes and deserts, in almost all climatic zones (Roiger *et al*., 1991; Samuels, 2006; Kumar *et al*., 2010). Some *Trichoderma* species have economic importance because of its potential producers of enzymes, antibiotics and used as a biocontrol agent in the agricultural field (Harman and Björkman, 1998; Monte, 2001). An early approach for *Trichoderma* identification is on the morphological basis (Rifai 1969; Bissett, 1984; Dodd, Lieckfeldt and Samuels, 2000). Morphological descriptions were observed such as colony appearance and microscopic characteristics which including phialide and conidia sizes, conidiaphores and formation of chlamydospores. However, they are genetically diverse and characterized by variable morphology particularly between the closely related species, the morphological alone is insufficient to accurately identify *Trichoderma* at the species level (Chaverri and Samuels, 2003; Chaverri *et al.,* 2003; Druzhinina *et al.,* 2010). Alvindia and Hirooka (2015) claimed that the size of conidia and phialides overlapped between *T. catoptron* and *T. stramenium*, made identification more

complicated. Gams and Bissett (1998) also reported that variations among *Trichoderma* species could not be differentiated satisfactorily *via* morphological methods, thus making nomenclature placement uncertain.

An advent in the identification tools based on molecular data from DNA sequencing has led to satisfactory taxonomy identification. DNA barcoding are now routinely used in *Trichoderma* identification. It has done based on multilocus DNA sequence analysis of internal transcribed spacers (ITS 1 and 2) of the rDNA, gene cluster and fragments of the translational elongation factor 1-□ (*tef1*), RNA polymerase II subunit (*rpb2*), chitinase 18-5 (*chi18-5*), actin (*act*) or calmodulin (*cal*) (Kindermann *et al*., 1998; Dodd *et* al., 2000; Druzhinina *et al*., 2005; Gal-Hemed *et al*., 2011; Blaszczyk *et al*., 2011; Atanasova *et al*., 2013; Jaklitsch and Voglmayr, 2015). In addition, sequence data may useful for phylogeny study, providing valuable insights into their evolutionary relationships. Moreover, the correct identification served an efficient selection and use of such isolates for commercial applications.

Some *Trichoderma* species are a great hydrolytic enzyme producer and therefore important for the biotechnological industry, such as *T. reesei* and *T. viride* (Mandels *et al.,* 1971; Domigues *et al.*, 2000). The search of potential biomass degrading enzymes also led to the isolation of these fungi (Sallenave-Namont *et al*., 2000). Lignocellulolytic fungi have a potential to degrade a range of the lignocellulosic biomass. Many lignocellulosic materials such as wood, bagasse and wheat straw have been studied as potential substrates for the production of lignocellulolytic enzymes (Duff and Murray, 1996; Ogel *et al*., 2001; Kalogerist *et al*., 2003). The purified lignocellulolytic enzymes are used for commercial applications such as in coffee production where the hydrolysis of cellulose occurs during the drying of beans (Mussatto *et al*., 2011). Moreover, the application of lignocellulolytic fungi improves the composting process of biomass where the carbon to nitrogen ratio was not at the optimal rate (Hart *et al*., 2002). Therefore, the aim of this study was to analysis the sequences of ITS1 and ITS2 regions of *Trichoderma* isolates and to evaluate the potential of these fungi for the lignocellulolytic degradation.

MATERIALS AND METHODS:

Collections and isolation of Trichoderma isolates

The soil samples were collected from wet paddy field in Tuaran, Sabah, Malaysia and transported to the laboratory while stored in plastic bags at 4 ^{o}C. *Trichoderma* was isolated by using dilution plate technique (Aneja, 2003). Approximately 1 g of sample was aseptically added to 10 mL of sterile distilled water and incubated for 30 minutes at 25 ^{o}C while shaking at 210 rpm. The soil suspension was serially diluted by pipetting 1 mL of the solution to 9 mL of sterile distilled water for the first (10^{-1}) dilution and followed at 10^{-2} and 10^{-3} fold or appropriate concentration for the Colony Forming Unit (CFU) estimation. 1 mL aliquots from each dilution were transferred into Petri dish where approximately 15 mL of molten and cooled *Trichoderma* Selective Medium (TSM) agar poured into each Petridish. The inoculum was mixed by gentle rotation of the Petridish to get uniform distribution of soil suspension into the medium. Upon solidification, all the plates were incubated for 7-15 days at 28±2 ^{o}C. All isolated were maintained on Potato Dextrose Agar (PDA) slants after fungal purification.

Morphological characterization of Trichoderma isolates

The morphological characterization involves observation on Petridish and micro-morphological studies using slide culture following Riddell (1950) technique. The isolates were grown on PDA agar at 28 ^{o}C for 3-5 days. The colony appearance, conidiation color and coloration of the medium were examined. For slide culture preparation, the observations were focused on the sizes and shapes of conidia, the branching pattern of conidiaphores and phialides, as well as the presence of chlamydospores.

DNA extraction and PCR amplification

The extraction of genomic DNA was performed with minor modification as described by Cubero *et al*. (1999). The ITS region was amplified in an automated thermocycler using the primers ITS1 (TCTGTAGGTGAACCTGCGG) and ITS4 (TCCTCCGCTTATTGATATGC) (Kullnig-Gradinger *et al*., 2002). The PCR reactions were performed in a total of 60 □L, containing 1x PCR buffer, 0.5 □M of each primer, 200 □M of each of the dNTPs mixture, 1.25 U *Taq polymerase* and 50 ng of genomic DNA. The PCR condition of 95 ^{o}C for 1 min, annealing at 50 and 56 ^{o}C for 30 sec, and 90 sec elongation at 75 ^{o}C and

final extension of 7 min at 74 ^{o}C in 35 cycles were performed. A negative control with all the reaction mixtures except the DNA template was included with each set of the PCR amplification reactions. Finally, the PCR products were purified using QIAquick® PCR Purification Kit (Qiagen) according to the manufacturer's instruction and the products were visualized under UV light using gel imaging system. The purified PCR products were directly sent for sequencing at First Base Laboratories Sdn Bhd.

Phylogenetic analysis

The resulting sequencing data were analyzed using Bioedit Sequence Alignment Editor (BioEdit). All of the DNA sequences were compared to the deposited sequences at Basic Local Alignment Search Tool (BLAST) algorithm which available online at http://blast.ncbi.nlm.nih.gov to determine the identity each of the sequences.

Phylogenetic analyses were performed using Molecular Evolutionary Genetic Analysis 6 (MEGA 6) software package. The phylogenetic trees for all genes constructed by Unweighted Pair-Group Method Based on the Arithmetic Average (UPGMA) methods. Reliability and strength of the interior branches and the validity of the trees obtained were checked by using bootstrap tests with 10000 replications. Distance was defined as the probability of the nucleotide substitutions per site, based on the Kimura 2-parameter model (K2P). The phylogenetic tree were roots using *Fusarium solani* sequence as an outgroup (AM412643). Table 1 shows all the sequences obtained from the GenBank database used for the phylogenetic analysis.

A total number of 20 *Trichoderma* isolates exhibited with different ability to degrade lignin, cellulose and starch on tannic acid media (TAM), Jensen media (JM) and Modified Melin-Nokrans media (MMNM), respectively. These 20 isolates were chosen randomly among 53 *Trichoderma* isolates (11: *T. asperellum*, eight: *T. harzianum*, and one: *T. reesei)*. The data were calculated based on the average mean of three replicates.

Table 1
List of sequences from GenBank that used for the phylogenetic analysis of ITS gene.

***Trichoderma* species**	**GenBank accession number**
	ITS
T. asperellum	LC002586
	EU856298
	LC002589
	EU264001
	EU856297
	AF486006
	AF486023
	AF486024
	AF486025
	AF486028
H. lixii /*T. harzianum*	LC002580
	LC002571
	LC002568
	LC002577
	LC002583
H. jecorina / T. *reesei*	LC002607
	EU280094
T. atroviride	EU280107
T. koningiopsis	EU280131
T. evansii	EU856294
T. longibrachiatum	EU280090
T. brevicompactum	EU280087
H. virens	EU280090
Fusarium solani	AM412643

Lignocellulolytic analysis of Trichoderma species

1. Enzymatic degradation of lignin

Lignin degradation was tested on TAM. Approximately 15 mL of the sterilized tannic acid media was poured into each Petridish. A 5.0 mm diameter mycelia disc from four days old PDA culture was placed at the center of the plate. The plates were incubated in the entirely darkness at room temperature (28 ± 2 ^{o}C) for four days. The experiment was performed in triplicate for each isolate. Formation of a dark brown pigment surrounding the point of inoculation was used as indicator of polyphenol oxidase (PPO) activity on tannic acid media.

2. Enzymatic degradation of cellulose

Jensen media was used for the determination of cellulolytic activity. Approximately 20 mL of sterilized JM was poured into each Petridish. A 5.0 mm diameter mycelia disc from four days old PDA culture was placed at the center of the plate and incubated at room temperature (28 ± 2 ^{o}C) for seven days. The plates were flooded with an aqueous solution of Congo red (1 mg.mL^{-1}) for 15 min and were poured away. The media were further flooded with 1M NaCl solutions for 15 min and were poured away. Degradation of cellulose was visualized as a clear halo zone around the fungal colony. The diameters of the clear zone around colonies were immediately measured for the analysis of cellulose hydrolysis. The experiment was performed in triplicate for each isolates.

3. Enzymatic degradation of starch

Degradation of starch was examined through the appearance of halo zone on the MMNM. Approximately 20 mL of sterilized MMN media was poured into each Petridish. A 5.0 mm diameter mycelia disc from four days old PDA culture was placed at the center of the plate and incubated at room temperature (28 ± 2 ^{o}C) for three days. The plates were flooded with iodine solution [5.0 g of KI, 1.5 g of I, 100 ml of distilled water] for 5 min and decanted. A clear white zone indicated the hydrolysis of starch and exhibited amylase enzymatic activity. The experiments were performed in triplicates for each isolates.

RESULTS:

Isolations of fungal strains

Trichoderma isolates were cultured from 11 soil samples collected from Tuaran wet paddy field. Based on CFU counting, approximately 28% (142 CFU) of *Trichoderma* colonies were obtained on the *Trichoderma* selective medium (TSM) while 72% (369 CFU) non-*Trichoderma* isolates were not identified (unidentified genus and species). After that, the isolates were screened based on the similarity of the colony appearance and 53 *Trichoderma* isolates were selected for further studies.

Morphological characterization of Trichoderma isolates

Macroscopic characteristics of *Trichoderma* isolates were obtained using five-days old *Trichoderma* cultures grown on PDA that were incubated at 28 ^{o}C based on the colony color and appearance. Table 2 tabulated the macroscopic variation among 53 *Trichoderma* isolates. All *Trichoderma* isolates were grown well and formed conidia within three days. After one to three days of incubation, the colors of conidia were white to yellowish. Most of the isolates were produced green conidial masses while some of them were produced whitish to yellow colony. Some of the isolates also showed yellowish to green colony in mature culture. Furthermore, one or more concentric rings were formed, meanwhile, some of them showed no observable concentric rings. The microscopic characteristics of *Trichoderma* isolates were observed under a light microscope (Olympus CX31) with 400X magnification.

Table 2 Colony color variations among 53 *Trichoderma* isolates.

Colony color	Number of isolates
Green to dark green	20
Yellowish to greenish	15
Whitish to yellow	9
Total number of isolates	**53**

Molecular identification of Trichoderma *isolates*

Genomic DNA was successfully extracted from all 53 *Trichoderma* isolates. Each sample yielded a single DNA band. The purities (A_{260}/A_{280}) and concentration of all genomic DNA were ranged from 1.80 to 2.00 and 300 to 1000 µg/mL, respectively. The DNA extracts were subjected to 1.5% of agarose gel electrophoresis. PCR amplifications were performed using primer sets namely ITS1 and ITS2 with the expected product size of 600 bp.

All ITS sequences were compared to *Trich*OKEY database using *Trich*OKEY v 2.0 program which was available at http://www.isth.com. After that, all ITS sequences were compared to NCBI BLAST database which is available online at http://www.ncbi.nlm.nih.gov to verify the results given by *Trich*OKEY. BLAST results showed uncertainties of species identity for the few sequences. The BLAST identifications of the respective species were used the 'best hits' of 99-100% or a degree of sequence similarity. The first *Trichoderma* species listed in the BLAST results were taken as the most probable identity of the strains. *Trich*OKEY and BLAST search results are listed in Table 3. The *Trich*OKEY analyses for ITS sequences were showed more reliable result for species identity.

Trichoderma isolates were successfully identified using *Trich*OKEY search database. Based on analysis of *Trich*OKEY and BLAST, among 53 isolates were positively identified as *T. asperellum* (43 isolates), *T. harzianum* (9), *T. reesei* (1). In the case of E3(2)10^{-1}(2) strain, *Trich*OKEY search resulted as *Hypocrea* /*Trichoderma* belonging to XII Rufa clade. However, BLAST search suggested that sequences were most closely related to *T. asperellum*. The identification of isolate N3(3)10-1(1) showed disagreement between *Trich*OKEY and BLAST results. *Trich*OKEY result was *H. lixii*/*T. harzianum* but BLAST identify N3(3)10-1(1) as *T. virens* with 99% similarity. All these cases were given more priority to *Trich*OKEY search tool and its morphological characters which similar to *T. harzianum* species.

Phylogenetic analysis

The phylogenetic tree analysis of 53 isolates was constructed using MEGA6 software with UPGMA test with 10000 replicates. The phylogenetic tree was constructed using 77 ITS sequences which included 53 type strains. The rest of the sequences including 23 *Trichoderma* species as reference and one outgroup, *F. solani* (AM412643) that were downloaded from NCBI database.

The result of the phylogenetic analysis is shown in Figure 1. All the branches in this analysis were supported by high bootstrap values. The upper branch grouped the most dominant isolates that were identified as *T. asperellum* (clade *Pachybasium* 'A' or *Hamatum*) together with sequences from GenBank namely *T. atroviride* and *T. koningiopsis* (clade *Viride*). These two clades were felt into section "*Trichoderma*". There is strong bootstrap support (99%) for the grouping of these three species. The lower branch consists of two main branches which differentiate between section "*Longibrachiatum*" from section "*Pachybasium*". Isolate S1(9)10^{-1}(3) was placed into section "*Longibrachiatum*" together with *T. reesei*, *H. jecorina* and *T. longibrachiatum*, and were supported by bootstrap value of 99%. The second branch includes the section "*Pachybasium*" (*T. harzianum*) which formed a monophyletic grouping with a lack of bootstrap support (61%).

Note that N1(7)10^{-1}(3) which was identified previously as *T. asperellum* even though it was not located into any sections and formed an individual branch on the lower part of the tree. However, morphologically, this isolate was most similar to *T. asperellum* which was characterized by green colony color on PDA.

Table 3
BLAST and *Trich* OKEY comparison analysis of ITS1 and ITS2 regions and its accession number.

Isolate code	*Trich*OKEY results	BLAST		
		Species identified	Accession number	Percentage of homology (%)
E1 (4)10^{-2}(3)	-	*T. asperellum*	KU66400	100
E1 (4)10^{-1}(3)	*T. asperellum*	*T. asperellum*	KX538814	100
E1 (4)10^{-1}(1)	*T. asperellum*	*T. asperellum*	KX538814	100
E1 (7)10^{-1}(2)	*T. asperellum*	*T. asperellum*	KX538814	100
E1 (9)10^{-1}(2)	*T. asperellum*	*T. asperellum*	KX538814	100
E2 (1)10^{-2}(2)	*T. asperellum*	*T. harzianum*	KU66400	100
E2 (3)10^{-1}(1)	*T. asperellum*	*T. asperellum*	KX538814	100
E2 (4)10^{-1}(2)	*T. asperellum*	*T. asperellum*	KX538814	100
E2 (5)10^{-1}(1)	*T. asperellum*	*T. asperellum*	KX538814	100
E2 (6)10^{-1}(1)	*T. asperellum*	*T. asperellum*	KX538814	100
E3 (2)10^{-2}(1)	-	*T. asperellum*	KU66400	100
E3 (2)10^{-1}(2)	Unidentified species	*T. asperellum*	KX538814	99
E3 (3)10^{-1}(2)	-	*T. asperellum*	KU66400	100
E3 (3)10^{-2} (1)	*H. lixii/ T. harzianum*	*T. harzianum* Rifaii	NR137305	100
E3 (4)10^{-1}(3)	*T. asperellum*	*T. asperellum*	KX538814	100
E3 (6)10^{-1}(2)	*T. asperellum*	*T. asperellum*	KX538814	100
E3 (7)10^{-1}(2)	*T. asperellum*	*T. asperellum*	KX538814	100
E3 (8)10^{-1}(2)	*T. asperellum*	*T. asperellum*	KX538814	100
N1 (1)10^{-2}(2)	*T. asperellum*	*T. asperellum*	KX538814	100
N1 (2)10^{-2}(1)	*T. asperellum*	*T. asperellum*	KX538814	100
N1 (3)10^{-2}(1)	*T. asperellum*	*T. asperellum*	KX538814	100
N1 (4)10^{-1}(3)	*T. asperellum*	*T. asperellum*	KX538814	100
N1 (5)10^{-1}(3)	*T. asperellum*	*T. asperellum*	KX538814	100
N1 (7)10^{-1}(3)	-	*T. asperellum*	KC602356	100
N1 (8)10^{-1}(3)	*T. asperellum*	*T. asperellum*	KX538814	100
N2 (1)10^{-2}(3)	*T. asperellum*	*T. asperellum*	KX538814	100
N2 (2)10^{-1}(1)	-	*T. lixii*	KT588249	99
N2 (4)10^{-2}(3)	*T. asperellum*	*T. asperellum*	KX538814	100
N2 (6)10^{-1}(3)	*T. asperellum*	*T. asperellum*	KX538814	100
N2 (6)10^{-1}(2)	*T. asperellum*	*T. asperellum*	KX538814	100
N3 (1)10^{-2}(2)	*T. asperellum*	*T. asperellum*	KX538814	100
N3 (2)10^{-2}(1)	-		KU66400	100
N3 (3)10^{-2}(1)	-	*T. harzianum*	KC403947	99
N3 (3)10^{-1}(1)	*H. lixii/ T. harzianum*	*T. virens*	KT588282	99
N3 (3)10^{-2} (3)	*T. asperellum*	*T. asperellum*	KX538814	100
N3 (4)10^{-1}(2)	*T. asperellum*	*T. asperellum*	KX538814	100
W1 (3)10^{-1}(1)	*T. asperellum*	*T. asperellum*	KX538814	100
W1 (6)10^{-1}(3)	-	*T. asperellum*	KU534716	100
W2 (2)10^{-1}(2)	-	*T. harzianum*	KU215925	99
W2 (4)10^{-1}(2)	*H. lixii/ T. harzianum*	*T. harzianum*	KT277746	99
S1 (2)10^{-1}(3)	-	*T. asperellum*	KX538814	100
S1 (7)10^{-1}(3)	*T. asperellum*	*T. asperellum*	KX538814	100
S1 (9)10^{-1}(3)	*H. jecorina/T. reesei*	*T. parareesei*	NR138453	100
S2 (3)10^{-1}(1)	-	*T. harzianum* Rifaii	NR137305	100
S2 (3)10^{-1}(2)	*T. asperellum*	*T. asperellum*	KX538814	100
S3 (1)10^{-1}(1)	*H. lixii/ T. harzianum*	*T. harzianum*	KC403947	100
S3 (2)10^{-2}(2)	-	*T. asperellum*	KX538814	100
S3 (3)10^{-2}(3)	*H. lixii/ T. harzianum*	*T. harzianum*	KC403947	100
S3 (4)10^{-1}(1)	*T. asperellum*	*T. asperellum*	KX538814	100
S3 (4)10^{-1}(2)	*T. asperellum*	*T. asperellum*	KX538814	100
S3 (4)10^{-2}(3)	-	*T. asperellum*	KX538814	99
S3 (5)10^{-1}(1)	*T. asperellum*	*T. asperellum*	KX538814	100
S3 (6)10^{-1}(2)	-	*T. asperellum*	KX538814	100

Lignocellulolytic activities of Trichoderma isolates

Among 20 isolates tested, 11 isolates [W2(2)10^{-1}(2), W2(4)10^{-1}(2), E3(6)10^{-1}(2), S3(6)10^{-1}(2), N1(5)10^{-1}(3), N2(4)10^{-2}(3), E2(5)10^{-1}(2), S1(7)10^{-1}(3), W1(6)10^{-1}(3), N3(3)10^{-2}(3) and N3(1)10^{-1}(1)] were found to form a dark brown zone in the range of 10 – 16 mm on tannic acid-amended media. Isolates N2(4)10^{-2}(3) was produced significantly the biggest dark brown zone with the diameter of 15.43 mm followed by S3(6)10^{-1}(2) (14.73 mm) and E3(6)10^{-1}(2) (14.2 mm). Four isolates [S1(9)10^{-1}(3), N2(2)10^{-1}(2), N3(3)10^{-2}(1) and S2(3)10^{-1}(1)] were never produced any dark brown zone, which indicated that no degradation of lignin occurred.

The result for the enzymatic degradation of cellulose conducted by using CMC-amended media and showed eight isolates forming the biggest clearing zones between 10-15 mm after staining with Congo red. As shown in Figure 4.20, isolate S1(9)10^{-1}(3) was produced the highest clearing zone with the diameter of 14.42 mm. Two isolates [N3(3)10^{-2}(1) and S2(3)10^{-1}(1)] were produced no clearing zones.

All isolates were able to degrade the starch on MMNM media. Nine isolates [S1(9)10^{-1}(3), S3(3)10^{-2}(3), S3(1)10^{-1}(1), E3(6)10^{-1}(2), N2(1)10^{-2}(3), E2(5)10^{-1}(2), S1(2)10^{-1}(3), W1(6)10^{-1}(3) and N2(4)10^{-2}(3)] were found to form a clearing zone higher than 30 mm. Among the nine isolates, isolate S1(9)10^{-1}(3) was formed the highest clearing zone with the diameter of 45 mm. The smallest halo zone was produced isolate N1(5)10^{-1}(3) with a diameter of 10.93 mm.

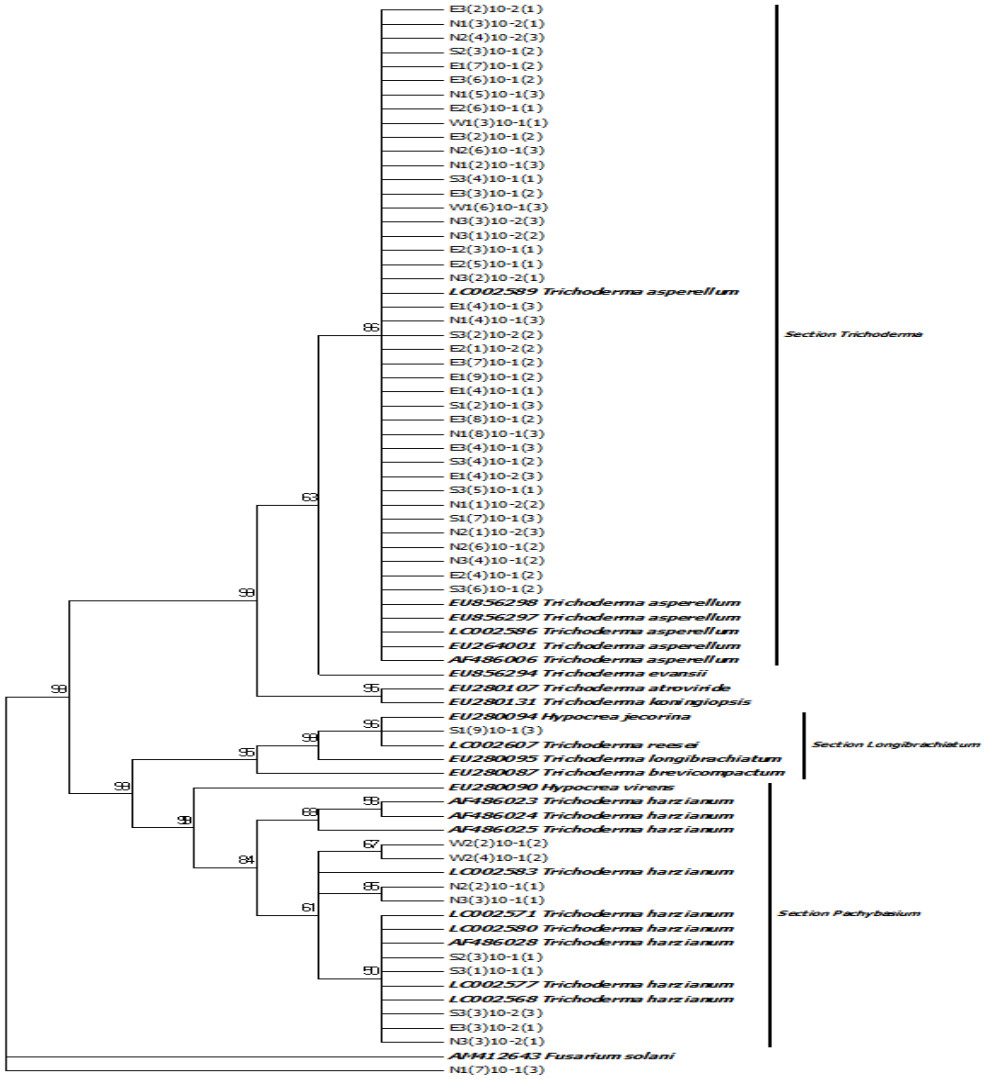

Figure 1

Phylogenetic relationship of 53 *Trichoderma* isolates inferred by UPGMA analysis of ITS1 and ITS2 regions. The numbers given above the selected branches indicate the bootstrap coefficients >50%. The bold letter indicates the respective sequences from GenBank, whereas all the isolates used in this study are given by the collection number without species identification. *F. solani* (AM412643) were used as an outgroup for this analysis.

DISCUSSION:

Morphological and molecular approaches are shown an important role in the identification of *Trichoderma* isolates. Morphological characterizations remain a potential approach for the identification of *Trichoderma* species. *Trichoderma* species has variation in colony color range from yellowish to dark green. Isolates of *T. asperellum* are shown to be dark green meanwhile *T. harzianum* isolates are observed to be yellowish to green colony. On the other hand, the conidiation of *T. reesei* showed to be yellow as observed by Atanasova *et al*. (2010). Saili (2016) stated that colony appearance commonly influenced by culture, pH (Suhr *et al*., 2002) and temperature (Singh *et al*., 2014). One of the morphological characteristics of *Trichoderma* colonies are the formation of concentric rings where the green color of the conidia are interleaved with the white of the mycelium as seen isolates of E3(3)10^{-1}(2) and S3(4)10^{-1}(1). The morphological observations are consistent with the characteristics previously described by several authors (Barnett and Hunter, 1998; Druzhinina *et al*., 2006; Samuels, 2006; Mendoza *et al*., 2015).

According to Tan (2013), the description of the shapes of conidia is not really useful in identifying most of the isolates due to different terms in different literatures in describing the shapes of conidia. In this study, *T. harzianum* is found to relatively small conidia (1.0 – 3.0 □m) as compared to *T. asperellum* (3.0 – 4.0 □m). The characteristics of small conidia are distinguished as *T. harzianum* from other *Trichoderma* species. A similar pattern has reported by Sriram *et al*. (2013) where the conidial size of *T. asperellum* is 3.5 – 4.5 □m with subglobose to ovoidal shape.

*Trich*OKEY is the first online program using oligonucleotides barcode (http://www.isth.info). The oligonucleotide barcode generated from a combination of various oligonucleotides of the ITS1 and 2 sequences of the rDNA gene on the basis of the *Trich*OKEY construction (Druzhinina *et al*., 2005). From our results obtained, *Trich*OKEY search is successfully used to identify *Trichoderma* species.

The most abundant species identified is *T. asperellum* which represents 81% of the total isolates. The results correspond with the previous studies which showed that *T. asperellum* found in diverse regions and habitat, including Iranian rice fields (Naeimi *et al*., 2011), tropical regions of American continent (Hoyos-Carvajal and Bissett, 2011), China (Sun *et* al., 2012), agricultural soil in Brazil (Cardoso-Lopes *et al*., 2012) and Sardinia island (Migheli *et al*., 2009). Strains belonging to *T. asperellum* have been reported to be the potential biological control agents against various plant pathogens. *T. asperellum* T8A reported to successfully overgrowth the mango pathogen, *Colletotrichum gleosporioides* both *in vitro* and *in vivo* (De los Santos-Villalobos *et al*., 2013). Moreover, *T. asperellum* showed highly antagonistic towards *Fusarium oxysporum* f. sp. *lycopersici* on tomato plants as well as effective against rice seed-borne pathogens (Watanabe *et al*., 2005; Segarra *et al*., 2010; El_Komy *et al*., 2015).

Previous studies have reported *T. harzianum* as the dominant species identified by Jiang *et al*. (2016) and Migheli *et al*. (2009), occurring in diverse ecosystems and ecological niche. However, only nine out of the 53 isolates belongs to *T. harzianum* were identified in this study. Migheli *et al.* (2009) found very little correlation between species distribution and soil abiotic parameters. Another factor that could affect the distribution of fungal species in soil is the cultivated plant (Anees *et al*., 2010). Until now, there is no data available to conclude whether the crop, especially paddy influence the diversity of *Trichoderma* species in soil.

T. reesei is originally collected on the Solomon Island during World War II, where it destroyed canvas and other cellulose-containing materials of the U.S. army. It first determined to be *T. viride* and later recognized as *T. reesei*. Finally, it has recognized to be identical to the pantropical Ascomycete *H. jecorina* (Atanasova *et al*., 2010). Kuhls *et al*. (1996) assumed that *T. reesei* is a clonally derived asexual form of *H. jecorina* based on small morphological differences between those species.

The phylogenetic tree revealed that the strains could be categorized into three different clades represent one species. The dominant isolates identified as *T. asperellum* grouped into clade *Pachybasium 'A' or Hamatum* (sect. *Trichoderma*), while *T. harzianum* isolates are clustered together into clade *Harzianum*. The only single isolate of *T. reesei* grouped into *Longibrachiatum* clade, together with all *T. reesei*/*H. jecorina* reference sequences. The phylogenetic tree was demonstrated that the *Trichoderma* isolates formed a monophyletic group. Kullnig-Gradinger *et al.* (2002) described the genus *Trichoderma* formed a monophyletic branch within *Hypocreaceae*.

As shown in Figures 1, *T. harzianum* isolates constituted many sub clusters. These results indicated that this exhibited a considerably higher variation in the ITS1 and ITS2 sequences and formed a paraphyletic phylogeny as previously reported by Kullnig-Gradinger *et al*. (2002) and Chaverri *et al*. (2003). Previous researches have been reported that sect. *Pachybasium* is a genetically variable complex which comprised by one morphological species and several phylogenies species (Druzhinina *et al.*, 2010; Gherbawy *et al*., 2014).

Lignocellulose is a key component of plant biomass, which is produced by photosynthesis. The abundance, renewability and sustainability of lignocellulose make it to be prospective in biocompost, hence become an intense subject of investigation now. The production of hydrolytic enzymes has frequently been emphasized as one of the major factors contributing to the biocontrol activity of *Hypocrea*/*Trichoderma* species (Migheli *et al*., 1998; Zeilinger *et* al., 2000; Howell, 2003; Roderick and Navajas, 2003). In this study, the color change on the tannic acid medium used as an indicator for the ability of soil microorganisms to decompose phenol-like compounds. Development of a dark brown zone on tannic acid medium confirmed the polyphenol oxidase (PPO) activity of the fungal isolate. PPO is a mixture of monophenol oxidase and catechol oxidase, which catalyzed the reaction between polyphenol and molecular oxygen to form dark brown complexes (Rodrigues *et al*., 2008; Zhang *et al*., 2005). Among 20 isolates tested, 18 isolates capable to produce dark brown zone which indicated lignin degradation and considered utilization of lignin as a carbon source.

The ability of *Trichoderma* isolates grown on both CMC and starch-amended media showed that they secreted cellulose and starch degrading enzymes. It is able to use these substrates as energy sources. The clearing zone on CMC media confirmed that all tested isolates degraded cellulose by producing endoglucanase and cellobiohydrolase enzymes. *Trichoderma* species have the ability to produce the complete cellulases, i.e. cellobiohydrolases, endoglucanases, and □-glucosidase enzymes (Shafique *et al*., 2009). In this study, *T. reesei* formed the biggest clearing zone for both CMC media and starch-amended media. Mandels and Reese (1959) predicted that cellobiose the repeating units of cellulose, could be the natural inducer of cellulase in *T. reesei.* In the presence of additives such as Tween 80 or sodium oleate has increased the production of cellulolytic enzymes in *T. viride* (Griffin *et al*., 1974). *T. reesei* is of industrial interest because of its high ability to produce cellulase (Montenecourt and Eveleigh, 1979; Kuhls *et al*., 1996; Moosavi-Nasab and Majdi-Nasab, 2007). *T. reesei* also has been employed for the production of its own enzymes as well for producing proteins because of its efficiency in producing cellulose- and hemicellulose-degrading enzymes (Häkkinen *et al*., 2014).

CONCLUSION:

In this study confirmed the usefulness of morphological and molecular identification of *Trichoderma* species. Morphological characterization involved in the identification includes colony appearance and conidiation, size of conidia and phialides, as well as the branching pattern of conidiaphores. Moreover, sequence analysis of ITS1 and ITS2 are deposited in *Trich*OKEY and GenBank database by using BLAST and *Trich*OKEY 2 program. From total of 53 isolates, 81% (43 isolates) is identified as *T. asperellum*, 17% (9 isolates) as *T. harzianum* and only 2% (one isolate) as *T. reesei*.

Enzymatic activities showed that *Trichoderma* exhibited good growth performance to tannic acid, cellulose and starch media, and it's have high ability to utilize different carbon sources. The results implied that these isolates could play an effective role for decomposing carbon substrate, owing high demand for industrial applications. From the total of 20 isolates tested, isolate $N2(4)10^{-2}(3)$ has the highest potential in degrading lignin. Meanwhile, isolate $S1(9)10^{-1}(3)$ found to degrade the both cellulose and starch at the high rate. This study indicated that *T. asperellum*, *T. harzianum* and *T. reesei* are successfully cultivated for the production of lignocellulolytic enzymes. The lignocellulolytic potential of selected these two strains of *Trichoderma* could apply for biocontrol along with rapid composting to enhance the soil fertility, increase the production of yield and controlling plant diseases.

ACKNOWLEDGEMENTS:

Financial support for this project has provided by Knowledge Transfer Programme (KTP)- I-GT6 (UMS-15-3), Ministry of Higher Education Malaysia for which the authors are most grateful.

REFERENCES:

1. Anees, M., Tronsmo, A., Edel-Hermann, V., Hjeljord, G. L., Hėraud, C., and Steinberg, C. 2010. Characterization of field isolates of *Trichoderma* antagonistic against *Rhizoctonia solani*. *Fungal Biology*. **114**(9): 691-701.
2. Aneja, K. R. 2003. Section XI: Cultivation techniques for isolation and enumeration of microorganisms. *In Experiment in Microbiology*, *Plant Pathology and Biotechnology*, 4th Edition, pp 157- 161. New Age International (P) Ltd.
3. Atanasova, L., Druzhinina, I. S. and Jaklitsch, W. M. 2013. Two hundreds *Trichoderma* species species recognized on the basis of molecular phylogeny. *In* Mukherjee, M., Schmoll, M. (eds.). *Trichoderma: biology and applications*, pp. 10-42. CABI. Wallingford, UK.
4. Atanasova, L., Jaklitsch, W. M., Komoń-Zelazowska, M., Kubicek, C. P. and Druzhinina, I. S. 2010. Clonal species *Trichoderma parareesei* sp. nov. likely resembles the ancestorof the cellulose producer *Hypocrea jecorina*/*T. reesei*. *Applied and Environmental Microbiology*. 7259-7267.
5. Barnett, H. L. and Hunter, B. B. 1998. Illustrated genera of imperfect fungi. 4ª ed. Aps Press.,
a. USA.
6. Bissett, 1984. A revision of the genus *Trichoderma*: I. Section *Longibrachiatum*, new section. *Can. J. Botany*. 62. 924-931.
7. Blaszczyk, L., Popiel, D., Chelkowski, J., Koczyk, G., Samuels, G. J., Sobieralski, K. and Siwulski,
a. M. 2011. Species diversity of *Trichoderma* in Poland. *J. Applied Genetics*. **52**: 233-243.
8. Cardoso-Lpose, F. A., Steindorff, A. S., Geraldine, A. M., Brandão, R. S., Monteiro, V. N., Lobo Junior, M., Caelho, A. S. G., Ulhoa, C. J. and Silva, R. N. 2012. Biochemical and metabolic profiles of *Trichoderma* strains isolated from common bean crops in the Brazilian Cerrado, and potential antagonism against *Sclerotinia sclerotiorum*. *Fungal Biol*. **116**: 815-824.
9. Chaverri, P., Castlebury, L. A., Samuels, G. J. and Geiser, D. M. 2003. Multilocus phylogenetic structure within the *Trichoderma harzianum*/ *Hypocrea lixii* complex. *Molecular Phylogenetics and Evolution*. **27**: 302-313.
10. Cubero, O. F., Crespo, A., Fatehi, J. and Bridge, P. D. 1999. DNA extraction and PCR amplification method suitable for fresh herbarium-stored, lichenized, and other fungi. *Plant Systematic Evolution.* 216. 243-249.
11. De los Santos-Villalobos, S., Guzmán-Ortiz, D. A., Gómez-Lim, M. A., Délano-Frier, J. P., De-Folter, S., Sánchez-Garcia, P. and Peña-Cabriales, J. J. 2013. Potential use of *Trichoderma asperellum* (Samuls, Liechfeldt et Nirenberg) T8a as a biological control agent against antrachnose in mango (*Mangifera indica* L.). *Biological Control*. 64(1): 37- 44.
12. Dodd, S. L., Lieckfeldt, E., and Samuels, G. J. 2000. *Hypocrea artroviridis* sp. nov., the teleomorph of *Trichoderma atroviride*. *Mycologia*. 95(1). 27-40.
13. Domigues, F. C., Queiroz, J. A., Cabral, J. M. and Fonseca, L. P. 2000. The influence of culture conditions on mycelial structure and cellulase production by *Trichoderma reesei* Rut C- 30. *Enzyme Microb. Technol*. **26**(5-6): 394-401.
14. Druzhinina, I. S., Kopchinskiy, A. G., Komoń-Źelaswoska, M., Bissett, J., Szakacs, G., and Kubicek, C. P. 2005. An oligonucleotide barcode for species identification in *Trichoderma* and *Hypocrea*. *Fungal Genetics and Biology*. 42(10). 813-828.
15. Druzhinina, I. S., Kopchinskiy, A. G. and Kubicek, C.P. 2006. The first 100 *Trichoderma* species
a. characterized by molecular data. *Mycoscience*. **47**: 55-64.
16. Druzhinina, I. S., Kubicek, C. P., Komoń-Źelazowska, M., Mulaw, T. B. and Bissett, J. 2010. The
a. *Trichoderma harzianum* demon: complex speciation history resulting in coexistence of hypothetical biological species, recent agamospecies and numerous relict lineages. *BMC Evolutionary Biology*. **10**: 10-94.
17. Duff, S. J. B. and Murray, W. D. 1996. Bioconversion of forest products industry waste cellulosics to fuel ethanol: a review. *Bioresources Technol.* **55**: 1-33.
18. El_Komy, M., Saleh, A. A., Eranthodi, A. and Molan, Y. Y. 2015. Characterization of novel *Trichoderma asperellum* isolates to select effective biocontrol agents against tomato fusarium wilt. *Plant Pathol*. *J.* **31**(1): 50-60.
19. Gal-Hemed, I., Atanasova, L., Komoń-Źelaswoska, M., Druzhinina, I. S., Viterbo, A. and Yarden, O. 2011. Marine isolates of Trichoderma spp. as potential halo-tolerant agents of biological control for arid-zone agriculture. *Applied and Environmental Microbiology*. 77(15). 5100-5109.

20. Gherbawy, Y. A., Hussein, N. A. and Al-Qurashi, A. A. 2014. Molecular characterization of *Trichoderma* populations isolated from soil of Taif city, Saudi Arabia. *Int. J. Current Microbiology and Applied Sciences.* **3**(9): 1059-1071.
21. Griffin, H. L., Sloneker, J. H., and Inglet, G. E. 1974. Cellulase production by *Trichoderma viride* on feedlot waste. *Applied Microbiol*. **27**(6): 1061-1066.
22. Häkkinen, M., Valkonen, M. J., Westerholm-Parvinen, A., Aro, N., Arvas, M., Vitikainen, M., Penttilä, M., Saloheimo, M. and Pakula, T. M. 2014. Screening of candidate regulators for cellulose and hemicellulose production in *Trichoderma reesei* and identification of a factor essential for cellulose production. *Biotecnology for Biofuels*. **7**(14): 2-21.
23. Harman, G. E. and Björkman, T. 1998. Potential and existing uses of *Trichoderma* and *Gliocladium* for plant disease control and plant growth enhancement. *In* Garman, G. E., Kubicek, C. P. (eds.). *Trichoderma and Gliocladium*, pp. 229-265. UK: Taylor and Francis Ltd. 2.
24. Hart, T. D., de Leij, F. A. A. M., Kinsey, G., Kelly, J. and Lynch, J. M. 2002. Strategies for the isolation of cellulolytic fungi for composting of wheat straw. World Journal of Microbiology and Biotechnology. **18**: 471-480.
25. Howell, 2003. Mechanisms employed by *Trichoderma* spp. in the biological control of plant diseases: the history and evolution of current concepts. *Plant Disease*. **87**: 4-10.
26. Hoyos-Carvajal, L. and Bissett, J. 2011. Biodiversity of Trichoderma in Neotropics, the dynamical processes of biodiversity-case studies of evolution and spatial distribution. *In* Grillo Oscar (ed.). *InTech*. China.
27. Jaklitsch, W. M. and Voglmayr, H. 2015. Biodiversity of *Trichoderma* (*Hypocreaceae*) in Southern Europe and Macaronesia. *Studies in Mycology*. **80**: 1-87.
28. Jiang, Y., Wang, J.-L., Chen, J., Mao, L.-J., Feng, X.-X., Zhang, C.-L., and Lin, F.-C. 2016. *Trichoderma* biodiversity of agricultural fields in East China reveals a gradient distribution of species. *PLoS One*. **11**(8): 1-14.
29. Kalogerist, E. P., Christakopoulos, P., Katapodis, A., Alexiou, S., Vlachou, D., Kekos and Macris, B. J. 2003. Production and characterization of cellulolytic enzymes from the thermophilic fungus *Thermoascus aurantiacus* under solid state cultivation of agricultural wastes. *Process Biochem*. **38**: 1099-1104.
30. Kindermann, J., El-Ayouti, Y., Samuels, G. J., and Kubicek, C. P. 1998. Phylogeny of the genus *Trichoderma* based on sequence analysis of the internal transcribed spacer region 1 of the rDNA cluster. **24**(3): 298-309.
31. Kuhls, K., Lieckfeldt, E., Samuels, G. J., Kovacs, W., Meyer, W., Petrini, O., Gams, W.,Borner, T.
a. and Kubicek, C. P. 1996. Molecular evidence that the asexual industrial fungus *Trichoderma reesei* is a clonal derivative of the ascomycete *Hypocrea jecorina*. *Proc. Natl. Acad. Sci.* **93**: 7755-7760.
32. Kullnig-Gradinger, C. M., Szakacs, G. and Kubicek, C. P. 2002. Phylogeny and evolution of the genus *Trichoderma*: a multigene approach. *Mycol. Res.* 106(7). 757-767.
33. Kumar, K., Amaresan, N., Bhagat, S., Madhuri, K. and Srivasta, R. C. 2010. Unreported species
a. of *Trichoderma* isolated from tropical regions of Andaman and Nicobar islands in India. *J. Mycol. Plant Pathology*. **40**(3). 314-321.
34. Mandels, M., and Reese, E. T. 1959. Induction of cellulose in fungi by cellobiose. *J. Bacteriol.* **79**: 816-826.
35. Mandels, M., Weber, J. and Parizek, R. 1971. Enhanced cellulase production by a mutant of *Trichoderma viride*. *Appl. Microbiol*. **21**(1): 152-154.
36. Mendoza, J. L. H., Pérez, M. I. S., Prieto, J. M. G., Velásquez, J. D. C.Q., Olivares, J. G. G. and Langarica, H. R. G. 2015. Antibiosis of *Trichoderma* spp strains native to northeastern Mexico against the pathogenic fungus *Macrophomina phaseolina. J. Microbiology*. **46**(4): 1093-1101.
37. Migheli, Q., Balmas, V., Komon-Zelazowska, M., Scherm, B., Fiori, S., Kopchinskiy, A. G., Kubicek, C. P. and Druzhinina, I. S. 2009. Soils of a Mediterranean hot spot of biodiversity and endemism (Sardinia, Thyrrhenian Islands) are inhabited by pan- European, invasive species of *Hypocrea/Trichoderma*. *Environmental Microbiology*. **11**(1): 35-46.
38. Migheli, Q., Gonzáles-Candelas, L., Dealessi, L., Camponogara, A. and Ramón- Vidal, D. 1998. Transformants of *Trichoderma longibrachiatum* overexpressing the beta-1,4- endoglucanas gene *egl1* show enhanced biocontrol of *Phytium ultimum* on cucumber. *Phytopathology*. **88**: 673-677.

39. Monte, E. 2001. Understanding *Trichoderma*: between biotechnology and microbial ecology. *Int. Microbiology*. **4**: 1-4.
40. Montenecourt, B. S. and Eveleigh, D. E. 1979. Selective screening methods for the isolation of high yielding cellulose mutants of *Trichoderma reesei*. *Adv. Chem. Ser.* **181**: 289-301.
41. Moosavi-Nasab, M. and Majdi-Nasab, M. 2007. Cellulase production by *Trichoderma reesei* using sugar beet pulp. *Iran Agricultural Res*. **25**(2): 107-116.
42. Mussatto, S. I., Carneiro, L. M., Silva, J. P., Roberto, I. C. and Teixeira, J. A. 2011. A study on chemical constituents and sugars extraction from spent coffee grounds. *Carbohydrate Polymers*. **83**(2): 368-374.
43. Naeimi, S., Khodaparast, S. A., Javan-Nikkhah, M. and Kredics, L. 2011. Species pattern and phylogenetic relationships of *Trichoderma* strains in rice fields of Southern Caspian Sea, Iran. *Cereal Res. Communications*. **39**(4): 560-568.
44. Ogel, Z. B., Yarangumeli, K. Dundar, H. and Ifrij, I. Submerged cultivation of *Scytalidium thermophilum* on complex lignocellulosic biomass for endoglucanase production. *Enzyme Microb. Technol*. **28**: 689-695.
45. Riddle, R. W. 1950. Permanent stained mycological preparation obtained by slide culture. *Mycologia*. 42. 265-270.
46. Rifai, M. A. 1969. A revision of the genus *Trichoderma*. *Mycol. Pap*. **116**: 1-56.
47. Rodrigues, S., Pinto, G. A. S. and Fernandes, F. A. N. 2008. Optimization of ultrasound extraction of phenolic compounds from coconut (*Cocos nucifera*) shell powder by response surface methodology. *Ultrasound Sonochem*. **15**: 95-100.
48. Roiger, D. J., Jeffers, S. N. and Caldwell, R. W. 1991. Occurrence of Trichoderma species in apple orchard and woodland soils. *Soil Biology & Biochemical*. **23**: 353-359.
49. Samuels, G. J. 2006. *Trichoderma*: systematics, the sexual state, and ecology. *Phytopathology*. **96**(2): 195-206.
50. Segarra, G., Casanova, E., Avilés, M. and Trillas, I. 2010. *Trichoderma asperellum* strain T34 controls Fusarium wilt disease in tomato plants in soilless culture through competition for iron. *Microb. Ecol.* **59**(1): 141-149.
51. Shafique, S., Bajwa, R., and Shafique, S. 2009. Cellulase biosynthesis by selected *Trichoderma* species. *Pak. J. Bot.* **41**(2): 907-916.
52. Singh, A., Shahid, M., Srivasta, M., Pandey, S., Sharma, A. and Kumar, V. 2014. Optimal physical parameters for growth of *Trichoderma* species at varying pH, temperature and agitation. *Virology and Mycology*. **3**(1): 1-7.
53. Sriram, S., Savitha, M. J., Rohini, H. S. and Jalali, S. K. 2013. The most widely used fungal antagonist for plant disease management in India, *Trichoderma viride* is *Trichoderma asperellum* as confirmed by oligonucleotide barcode and morphological characters. *Current Science*. **104**(10): 1332-1340.
54. Suhr, K. I., Haasum, I., Steenstrup, L. D. and Larsen, T. O. 2002. Factors affecting growth and pigmentation of *Penicillium caseifulvum*. *J. Dairy Sci*. **85**: 2786-2794.
55. Sun, R.-Y., Liu, Z.-C., Fu, K., Fan, L. and Chen, J. 2012. *Trichoderma* biodiversity in China. *J. Appl. Genetics*. **53**(3): 343-354.
56. Tan, S. H. 2013. *Morphological Characterization And Sequence Analysis of 5.8S–ITS Region Of Trichoderma Species.* Faculty of Science. Universiti Tunku Abdul Rahman.
57. Watanabe, S., Kumakura, K., Kato, H., Iyozumi, H., Togawa, M. and Nagayama, K. 2005. Identification of Trichoderma SKT-1, a biological control agent against seedborne pathogens of rice. *J. Gen. Plant Pathol.* **71**: 351-356.
58. Zeilinger, S., Haller, M., Mach, R. and Kubicek, C. P. 2000. Molecular characterization of a cellulose-negative mutant of *Hypocrea jecorina*. *Biochem. Biophys. Res. Commun*. **277**: 581- 588.
59. Zhang, Z., Pang, X., Xuewu, D., Ji, Z. and Jiang, Y. 2005. Role of peroxidase in anthocyanin degradation in litchi pericarp. *Food Chemistry*. **90**: 47-52.

FP-27

THE VALUE OF RED BLOOD CELLS PARAMETERS AS SCREENING MARKERS FOR EARLY ONSET NEONATAL SEPSIS

NIK MANSOR, NIK NOOR FADHILAH[1], HASSAN ROSLINE[*1], AHMED AL-SALIH, SUHAIR ABBAS[1], ABDULLAH, WAN ZAIDAH[1], WAN ROSLI, WAN ROSILAWATI,[2] IBRAHIM, NOR ROSIDAH[3]

[1]Hematology Department, Universiti Sains Malaysia, Kelantan, Malaysia, [2]Department of Obstetrics & Gynaecology, Universiti Sains Malaysia, Kelantan, Malaysia, [3]Department of Paediatrics School of Medical Sciences, Universiti Sains Malaysia, Kelantan, Malaysia.

*Corresponding author: roslin@usm.my

ABSTRACT

Early onset neonatal sepsis (EOS) is defined as an infection causing inflammation of neonates within 72 hours after birth. Signs of sepsis in neonates sometimes asymptomatic. Objective of the study was to evaluate red blood cells (RBC) parameters inclusive of absolute red blood cell (RBC), nucleated red blood cell (NRBC) and hemoglobin (Hb) as screening markers for EOS. The study involved 135 neonates within 72 hours of birth with high risk for sepsis and showing clinical signs of sepsis. Neonates with sepsis had positive blood culture and appearance of 16S rRNA PCR band. Meanwhile neonates without sepsis had negative blood culture and absent of 16S rRNA PCR band. RBC, NRBC and Hb were analysed by Sysmex XE-5000. Comparison between the groups showed absolute RBC and Hb was significantly lower in sepsis group compared to non-sepsis group ($p < 0.05$). Absolute NRBC was significantly higher in sepsis group compared to the non-sepsis group ($p < 0.005$). In this sepsis newborn, the low RBC count and Hb were the earliest markers indicating insult to the bone marrow hence dysregulate and impaired the erythropoiesis activity. While high NRBC could due to rapid release from stress bone marrow. The markers could be used as auxiliary markers for EOS screening.

KEYWORDS:
Erythropoiesis, NRBC, RBC, haemoglobin, 16S rRNA

INTRODUCTION:

Neonatal sepsis is defined as infection acquired during neonatal period which is within 28 days of life for term neonates. Meanwhile for preterm neonates, the timing of infection can be extended until 28 days from the expected date of delivery (Russell, 2015). Early onset neonatal sepsis (EOS) occurred within the first 72 hours of life. The neonates expose to pathogen through birth canal during delivery which ascends from the colonized vagina (Su *et al.*, 2014).

A study found that both NRBC and reticulocytes increased significantly regardless of gestational age and birth weight in EOS cases (Dulay et al., 2008; Abhishek and Sanjay, 2015). The previous findings suggest that NRBC and reticulocytes may have prognostic value in addition to current haematological markers.

There are evidences suggesting that some gram-negative bacteria such as G. vaginalis can directly bind to haemoglobin to extract iron. While *N. gonorrhoeae* may use either haemoglobin or lactoferrin for iron supply (Brabin *et al.*, 2013). S. *aureus* is also another pathogen utilizes iron from host proteins such as haemoglobin (Torres *et al.*, 2006). Furthermore, neonatal sepsis is associated with high free radical due to dysregulation in biochemical processes (Honda et al., 2016). Oxidation of haemoglobin in RBC by free radicals releases free iron which supports bacterial growth. Therefore, it is possible to utilize RBC and haemoglobin as screening markers for neonatal sepsis.

Diagnosing EOS solely on clinical assessments can be inaccurate (Avner and Baker, 2002). Normal procedures in Malaysia for presumed sepsis neonates within 72 hours of life is full blood count including differential count, C-reactive protein analysis, blood culture analysis and administration of intravenous antibiotics while waiting for blood culture result (Ismail *et al.*, 2005). Blood culture is used as the gold standard to rule out neonatal sepsis. However, blood culture has lengthy turnaround time. Blood culture result is also prone to technical problem such as insufficient inoculation of blood into the blood culture bottle (Ansari-Lari *et al.*, 2003). This study acknowledged reliability issues in blood culture thus provided an alternative gold standard by using molecular approach. Molecular approach utilized 16S rRNA gene to detect bacterial presence in the neonatal blood to produce highly sensitive and specific results with faster turnaround time (Yadav *et al.*, 2005; Reier-Nilsen *et al.*, 2009). 16S rRNA was used alongside with blood culture as alternative test to detect pathogen. 16SrRNA can be a great marker because the sequence is preserved throughout time, mostly presence in bacteria and fungi and has reasonable sizes for DNA or RNA PCR, DNA probing and sequencing (Chakravorty et al., 2007; Janda and Abbott, 2007). Mutation hardly occurs in the region because the gene exist in operon or a cluster of functional gene thus any changes to the function can be detrimental to the cell. Screening of neonatal sepsis can be done with clinical examination and supported by result of the laboratory parameters and molecular test. Early detection may decrease chances of morbidity and mortality of the neonates. Objective of the study was to evaluate red blood cells (RBC) parameters inclusive of absolute red blood cell (RBC), nucleated red blood cell (NRBC) and hemoglobin (Hb) as screening markers for EOS.

MATERIALS AND METHODS:

A cross sectional study was conducted in Hospital Universiti Sains Malaysia (HUSM) in Kelantan, Malaysia starting from January 2015 until August 2016. The sampling frame for neonate selection was neonates born in Hospital Universiti Sains Malaysia (HUSM), Kelantan. The study had been approved by HUSM Ethics Committee (Protocol code: USM/JEPEM/14120506). The study involved 135 neonates born within 72 hours of life with maternal risk factors and fetal risk factors. Maternal risk factors were mother with Group B *Streptococcus* (GBS) carrier, mother with GBS in her previous pregnancy, prolonged rupture of membrane (< 18 hours), maternal pyrexia and foul-smelling liquor. Fetal risk factor included APGAR score less than 5 or having tachycardia (>160/min) or bradycardia (<100/min), premature (<37 weeks) and low birth weight (<2500g). Clinical data from mothers and neonates were retrieved from record office, neonatal intensive care unit (NICU) and labour room. The data retrieved included mother condition, maternal risk of neonatal sepsis, gestational age and neonatal APGAR score. A total of 2 mL of neonatal blood was taken from neonate. One mL was sent for 16S rRNA analysis and full blood count by using Sysmex XE-5000 (SYSMEX Corporation, Kobe, Japan to find RBC count, NRBC count and haemoglobin level. Another 1mL was sent for blood culture in Bactec® Peds Plus Aerobic/F bottle. The bottles were incubated in BACTEC 9240 instrument (Becton Dickinson, Cockeysville, MD, USA). Positive bottles were proceeded for Gram staining processes and species identification by using Vitek 2 cards (bioMérieux, Marcy-l'Étoile, France). Neonates was classified as sepsis when had both positive blood culture and appearance of 16S rRNA PCR band. Meanwhile neonates were classified non-sepsis when had both negative blood culture and absent of 16S rRNA PCR band.

RESULTS:

A total of 135 neonates from NICU were presumed sepsis. The background of the neonates was represented in table 1.0. Sepsis was more common in male neonates but the difference between male and female neonates was not statistically significant (p-value < 0.05). The most frequent maternal risk factor related to neonatal sepsis was mother with prolonged rupture of membrane (more than 18 hours). More than 94% of EOS cases involved neonates with low APGAR score (APGAR score < 5). Majority of the neonates had low gestational age or preterm (< 37 weeks).

Table 1
Clinical demographic of newborn with presumed sepsis.

Risk factor for sepsis	Presumed sepsis, n = 135 (%)
Gender:	
Male	76 (56.30)
Female	59 (43.70)
Maternal risk factor:	
1. Foul-smelling liquor	14 (10.30)
2. Mother with GBS history	3 (2.22)
3. Prolonged rupture of membrane (> 18 hours)	35 (25.93)
Fetal risk factor	
4. APGAR score < 5	128 (94.81)
5. Gestational age:	
Preterm (< 37 weeks)	91 (67.41)
Term (≥ 37 weeks)	44 (32.59)
6. Birth weight	69 (51.11)
Low (< 2.5kg)	66 (48.89)
Normal (≥ 2.5kg)	

A total of 135 presumed sepsis neonates were tested with both blood culture and 16S rRNA. Twenty-five neonates (19%) were positive for both blood culture and 16S rRNA. Fifty-four (40%) were negative for both blood culture and 16S rRNA. Meanwhile 56 (41%) neonates had negative blood culture results but negative for 16S rRNA.

Table 2
Comparison between sepsis and non-sepsis for red blood RBC indices.

Predictors of EOS (unit)	Sepsis n = 25 Mean (SD)	Not sepsis n = 54 Mean (SD)	Mean score different (95% CI)	t-statistic (df)	p-value
RBC# (10^6/uL)	4.19 (0.85)	4.77 (0.86)	0.58 (0.17, 0.99)	2.79 (77)	0.007[a]
Hb# (g/dL)	14.51 (2.83)	16.52 (2.93)	2.01 (0.61, 3.41)	2.87 (77)	0.005[a]
RETIC# (10^6/uL	0.27 (0.16)	0.28 (0.12)	0.01 (-0.08, 0.09)	0.225 (53)	0.655[b]
NRBC# (10^3/uL)	1.35 (1.57)	0.42 (0.70)	-0.92 (-1.49, -0.36)	-3.28 (62)	0.009[b]

[a] Independent t-test
[b] Mann-Whitney U test

The significant red blood cell parameters were evaluated further by ROC curve to determine the sensitivity and specificity based on the cut-off point of the parameters.

Table 3
Area under the curve, sensitivity, specificity and cut-off point of red blood cell parameters.

Predictors of EOS (unit)	AUC	Sensitivity (%)	Specificity (%)	Cut-off point
RBC (10^6/uL)	0.647	72	60	4.40 10^6/uL
Hb (g/dL)	0.665	72	59	15.25 g/dL
NRBC# (10^3/uL)	0.644	70	51	1.25 x 10^3/uL

DISCUSSION:

Previous studies showed many factors which could influenced reduction RBC count and Hb level during sepsis occurrence such as oxidation of Hb in RBC by free radical resulted from redox imbalance of the body (Lang *et al.*, 2012). Redox imbalanced during sepsis was caused by oxidative stress in the blood system. It was suggested that free radicals and cytokines facilitated binding of toxic substances from bacteria to RBC thus reduce RBC deformability by altering the RBC membrane (Linderkamp *et al.*, 2006). Several studies suggested that impaired RBC caused by oxidative stress was trapped in several organs such as spleen and liver underwent erythrophagocytosis by monocytes (Piagnerelli *et al.*, 2007; Lang *et al.*, 2012). Sixty-seven percent of the neonates were premature. In addition, neonates unable to compensate for the loss of RBC and Hb through erythrophagocytosis due to low erythropoiesis activity in the first week specifically in preterm neonates which unable compensate the RBC loss (Cavaliere, 2004; Santos and Guinsburg, 2012). Another possible explanation was iron extraction from Hb and iron utilisation from bacteria (Torres *et al.*, 2006; Brabin *et al.*, 2013).

However, other studies showed different result from this study. The studies involved neonates aged from day 1-day 28 and neonates less than 4 days of life showed that RBC and Hb level was lower in sepsis cases compared to non-sepsis neonates but the difference was not statistically significant ($p > 0.05$) (Cosar *et al.*, 2017; Saleh *et al.*, 2017). Another study was conducted involving blood sample from neonatal cord blood yielded similar results which showed RBC was significantly lower in sepsis neonates ($p < 0.001$). The blood samples of sepsis neonates were taken within 1 hour of delivery from the cord blood (Dhananjay and Kumar, 2011).

Reticulocytes and NRBC were significantly higher in presumed sepsis neonates (p-value < 0.05). A significant increase was observed in sepsis group compared to non-sepsis group (p-value < 0.005). Plausible explanation for the higher values in presuned sepsis compared to healthy neonates was because during sepsis, cytokines stimulated release of reticulocytes and NRBC to blood circulation. The release of the immature RBC in EOS was not influenced by gestational age and birthweight (Dulay *et al.*, 2008). The result was in concordance with other study that showed NRBC was significantly higher among EOS neonates (Abhishek and Sanjay, 2015). . NRBC naturally present in healthy neonates but diminished rapidly by 50% after 12 hours of delivery and disappeared on the third or fourth day in normal neonates (Rolfo et al., 2007). Abnormally high NRBC at birth might be contributed by redox imbalanced caused by inflammation as suggested in a study (Dulay *et al.*, 2008). Redox imbalance caused oxidative stress which induced more NRBC production and released into blood. The condition explained significant increase in the NRBC count among sepsis neonates. NRBC was produced and stored in fetal bone marrow. The study found higher absolute NRBC in sepsis group compared to non-sepsis group. Concentration of NRBC was higher in sepsis group because sepsis triggered a rapid released from marrow and elevated NRBC in blood circulation. (Stachon *et al.*, 2005). Based on the ROC curve, RBC count, Hb level and NRBC count had moderate sensitivity and specificity values to be used in EOS screening. Studies regarding red blood cell indices in early onset neonatal sepsis particularly among neonates within 72 hours of life were scarce. Findings from this study were hoped to be useful for health care practitioners to screen neonatal sepsis as early as possible in addition to clinical manifestation and assessment of maternal and fetal risk factors for early onset neonatal sepsis without additional cost.

CONCLUSION:

Haemoglobin and red blood cell were among the earlier markers indicating insult to the bone marrow hence dysregulate and impaired the erythropoiesis activity. While high NRBC could be due to rapid release from stressed bone marrow. The markers could be used as auxiliary markers for EOS screening.

REFERENCES:

1. Abhishek, M. & Sanjay, M. (2015). Diagnostic efficacy of Nucleated Red blood cell count in the early diagnosis of neonatal sepsis. *Indian Journal of Pathology and Oncology,* **2(4),** 182-185.
2. Ansari-Lari, M. A., Kickler, T. S. & Borowitz, M. J. (2003). Immature granulocyte measurement using the Sysmex XE-2100. *American journal of clinical pathology,* **120(5),** 795-799.
3. Avner, J. R. & Baker, M. D. (2002). Management of fever in infants and children. *Emergency medicine clinics of North America,* **20(1),** 49-67.
4. Brabin, L., Brabin, B. J. & Gies, S. (2013). Influence of iron status on risk of maternal or neonatal infection and on neonatal mortality with an emphasis on developing countries. *Nutrition reviews,* **71(8),** 528-540.
5. Cavaliere, T. A. (2004). Red blood cell indices: Implications for practice. *Newborn and Infant Nursing Reviews,* **4(4),** 231-239.
6. Cosar, H., Yilmaz, O., Ozbay, P. O., Bulut, Y. & Karakulak, M. (2017). Relationship between Early-Onset Neonatal Sepsis and Red Blood Cell Distribution Width (RDW). *Journal of Hematology & Thromboembolic Diseases,* **5(2),** 1-5.
7. Dhananjay, B. & Kumar, N. S. (2011). Comparison of biochemical and pathological markers in neonates with sepsis and neonates without sepsis. *International Journal of Biological & Medical Research,* **2(4),** 1-4.
8. Dulay, A. T., Buhimschi, I. A., Zhao, G., Luo, G., Abdel-Razeq, S., Cackovic, M., Rosenberg, V. A., Pettker, C. M., Thung, S. F. & Bahtiyar, M. O. (2008). Nucleated red blood cells are a direct response to mediators of inflammation in newborns with early-onset neonatal sepsis. *American journal of obstetrics and gynecology,* **198(4),** 426. e1-426. e9.
9. Honda, T., Uehara, T., Matsumoto, G., Arai, S. & Sugano, M. (2016). Neutrophil left shift and white blood cell count as markers of bacterial infection. *Clinica Chimica Acta,* **457,** 46-53.
10. Ismail, H. I. H. M., Ng, H. P. & Thomas, T. (2005). Paediatric Protocols for Malaysian Hospitals. Ministry of Health.
11. Lang, E., Qadri, S. M. & Lang, F. (2012). Killing me softly–suicidal erythrocyte death. *The international journal of biochemistry & cell biology,* **44(8),** 1236-1243.
12. Linderkamp, O., Pöschl, J. & Ruef, P. (2006). Blood cell deformation in neonates who have sepsis. *NeoReviews,* **7(10),** e517-e523.
13. Piagnerelli, M., Boudjeltia, K. Z., Gulbis, B., Vanhaeverbeek, M. & VINCENT, J. L. (2007). Anemia in sepsis: the importance of red blood cell membrane changes. *Transfusion Alternatives in Transfusion Medicine,* **9(3),** 143-149.
14. Reier-Nilsen, T., Farstad, T., Nakstad, B., Lauvrak, V. & Steinbakk, M. (2009). Comparison of broad range 16S rDNA PCR and conventional blood culture for diagnosis of sepsis in the newborn: a case control study. *BMC pediatrics,* **9(1),** 5.
15. Rolfo, A., Maconi, M., Cardaropoli, S., Biolcati, M., Danise, P. & Todros, T. (2007). Nucleated red blood cells in term fetuses: reference values using an automated analyzer. *Neonatology,* **92(3),** 205-208.
16. Russell, A. R. B. (2015). Neonatal sepsis. *Paediatrics and Child Health,* **25(6),** 271-275.
17. Saleh, M. A., Kasem, Y. T. & Amin, H. H. (2017). Evaluation of neonatal sepsis and assessment of its severity by Red Cell Distribution Width indicator. *The Egyptian Journal of Community Medicine,* **35(3),** 1-12.
18. Santos, A. M. N. d. & Guinsburg, R. (2012). Why is it important to assess indications for red blood cell transfusion in premature infants? *Revista Brasileira de terapia intensiva,* **24(3),** 216-218.

19. Stachon, A., Bolulu, O., Holland-Letz, T. & Krieg, M. (2005). Association between nucleated red blood cells in blood and the levels of erythropoietin, interleukin 3, interleukin 6, and interleukin 12p70. *Shock,* **24(1),** 34-39.
20. Su, H., Chang, S., Han, C., Wu, K., Li, M., Huang, C., Lee, C., Wu, J. & Lee, C. (2014). Inflammatory markers in cord blood or maternal serum for early detection of neonatal sepsis—a systemic review and meta-analysis. *Journal of Perinatology,* **34(4),** 268-274.
21. Torres, V. J., Pishchany, G., Humayun, M., Schneewind, O. & Skaar, E. P. (2006). Staphylococcus aureus IsdB is a hemoglobin receptor required for heme iron utilization. *Journal of bacteriology,* **188(24),** 8421-8429.
22. Yadav, A. K., Wilson, C., Prasad, P. & Menon, P. (2005). Polymerase chain reaction in rapid diagnosis of neonatal sepsis. *Indian pediatrics,* **42(7),** 681.

FP-28

ISOLATION AND SCREENING OF LIGNOLYTIC FUNGI FROM SABAH BIODIVERSITY

INTAN NAZIRAH MOHAMMAD[1], CLARENCE M ONGKUDON[1]*, MAILIN MISSON[1]

[1]Bioprocess Engineering Research Group, Biotechnology Research Institute, Universiti Malaysia Sabah, Jln UMS, 88400, Kota Kinabalu Sabah

*Corresponding author: clarence@ums.edu.my

ABSTRACT

Lignocellulose biomass has a great potential as an alternative source for bio-ethanol production through enzymatic hydrolysis. However, the presence of high lignin content in biomass reduces the accessibility of enzyme to avail important chemicals from cellulose and hemicellulose compounds. Lignocellulose pretreatment appears as a prominent solution to degrade the lignin structure. In comparison with other methods, biological pretreament is more environmentally friendly and economically viable. In this study, samples were collected from various sources including oil palm plantation soil, decaying oil palm frond and decaying woods from mango and cempedak trees. Lignolytic fungal were screened on minimal salt media (MSM) containing kraft lignin as a carbon source. The characterization of fungal isolates was carried out using lactophenol cotton blue method. Meanwhile, a qualitative assay by observing the decolorization of remazol brilliant blue anthraquione R (RBBR) dye was employed to determine the lignolytic activity. Six fungal isolates were successfully isolated from the soil and decaying mango and cempedak trees. All isolates showed positive results on RBBR assay indicating the presence of lignolytic properties. Outcomes of this study offer a useful guideline in screening potential lignin degraders from environment.

KEY WORDS:
Lignolytic fungal, Lignin, Remazol brilliant blue anthraquinone R, Biological pretreatment

INTRODUCTION:

The fossil fuel energy crisis has led to a growing concern over searching for new alternative sources for clean energy. The biomass utilization for second generation biofuel production, such as rice husk, wheat straw, oil palm fruit bunch, woodchips, cotton stalks, and rubber wood has attracted many research attentions. In addition, their abundance and fair distribution around the world has put these materials as the cheapest carbohydrates sources (Ravindran & Jaiswal, 2016). Their conversion would be beneficial to solving waste management and energy issues.

In general, lignocellulosic biomass compost of cellulose (30%-50%), hemicellulose (15%-35%) and lignin (10%-20%) (Bhutto *et al*., 2017). These three components function as the main backbone for rigid plant cell wall to prevent any chemical and microbial attack (Ravindran & Jaiswal, 2016). Nevertheless, both cellulose and hemicellulose are strongly interconnected by lignin, which contributes to recalcitrant properties against enzymatic reaction and low enzymes accessibility (Sun *et al.,* 2016). Therefore, lignocellulosic pretreatment has become a biotechnological interest as prominent solution to degrade or/and modify lignin structures.

In contrast with physico-chemical pretreatment methods, biological pretreatment appears as an economically-friendly and cost-effective approach. Microorganisms such as white rot fungi, brown rot fungi, yeast and bacteria have been reported as lignin degraders (Zhu *et al.,* 2017). These microorganisms, isolated from soils, decaying woods, termite nest, warehouse of rice straw, cow dung, decayed coir and so forth, have the ability to degrade or modify lignin structure through secretion of lignolytic enzymes such as peroxidases, oxidases, and dehydrogenases, thus, allowing cellulose and hemicellulose to be accessible for

enzymatic hydrolysis (Masalu, 2016; Placcido & Capareda, 2015) To date, white rot fungi such as *Trametes* sp. and *Pleurotus* sp. are known as primary lignin degraders that secreted lignolytic enzymes. White-rot fungi have been recognized to degrade lignin faster than other organisms (Madi & Abbas, 2017).

The objective of this study was to screen fungi microorganisms with lignolytic properties from soil and decaying woods from Sabah Malaysia agricultural resources. Minimal salt media (MSM) containing lignin was used to screen lignin degraders after seven days incubation period. Pure fungal isolates were characterized through morphological and microscopic observations. Their lignolytic activity was later tested using remazol brilliant blue R (RBBR) assay (Narkhede *et al.,* 2013) which indicated lignin degradation thorough dye decolorization (Falade *et al.,* 2017).

MATERIALS AND METHODS:

Materials

Kraft lignin and remazol brilliant blue R anthraquinone (RBBR) were supplied by Sigma-Aldrich. Calcium chloride, magnesium sulphate, potassium hydrogen phosphate, potassium dihydrogen phosphate, ammonium nitrate, potato dextrose agar (PDA) and 99.9% of glycerol stock were purchased from Systerm-ChemAr. Agar powder was obtained from Fisher BioScientific while lactophenol cotton blue was purchased from by Merck Company.

Sample collection

Samples were collected from oil palm plantation soil, decaying oil palm frond and decaying woods from mango and cempedak trees located at northern part of Sabah, Langkon, Sikuati and Kota Belud. All samples were collected in sterile falcon tubes and stored at -20°C until further use. Minimal salt media (K_2HPO_4, 4.55 g ; KH_2P0_4, 0.53 g ; $CaCl_2$, 0.5 g ; $MgSO_4$, 0.5 g; NH_4NO_3, 5 g) containing 0.5 g lignin were used to grow fungal cultures at pH 7 (Sasikumar *et al.,* 2014).

Cultivation of isolates on MSM containing lignin media

Serial dilutions were prepared in each sample up to 10^{-5} dilutions. Approximately 1 µl of sample was poured into a MSM containing lignin and incubated at 30°C for 7 days. Pure cultures were obtained by sub-culturing onto a fresh PDA.

Morphological characterization of culture

Pure culture was stained by using lactophenol cotton blue (LPCB) staining protocol and microscopically observed under compound microscope (Olympus BX53) at 10X and 40X maginifications. Sample was taken from young colony at the outer part of the fungal plug in the agar plate.

Determination of lignolytic activity

Remazol brilliant blue R anthraquinone (RBBR) assay was employed on plate agar containing K_2HPO_4, 4.55 g; KH_2P0_4, 0.53 g ; $MgSO_4$, 0.5 g; NH_4NO_3, 5 g, yeast extract, 0.1 g; RBBR, 0.05% (w/v); glycerol, 40 mM and agar, 15 g (Falade *et al.* 2017). Approximately 1 cm×1 cm of fungal cultures, known as plug sample, were inoculated onto the RBBR plate and incubated at 30°C for seven days. The growth of cultures on the plates as well as the decolorization of the RBBR was observed daily.

RESULTS AND DISCUSSIONS:

Isolation and screening of lignolytic fungal

A total of six isolates with lignolytic properties were successfully isolated as tabulated in Table 1. The pure culture of all fungal isolates was shown in Figure 1. An isolate from oil-palm plantation soil (decoded as PSL2), two from decaying mango wood (decoded as PWM2, PWM3) and three from decaying cempedak wood (decoded as PWC1, PWC2 and PWC3) grew on minimal salt media containing lignin as sole carbon demonstrated having a lignolytic properties after seven days incubation at 30°C.

Table 1
Number and codes of isolates

Samples	Number of Isolates	Isolates Code
Oil palm plantation soil	1	PSL2
Decaying oil palm frond	-	-
Decaying mango wood	2	PWM2, PWM3
Decaying *cempedak* wood	3	PWC1, PWC2, PWC3

All isolates were subsequently transferred and grown on PDA agar plate. The pure cultures of all fungal isolates were shown in Figure 1. The finding indicates that the isolates were able to utilize lignin as carbon source supplemented in the media. According to Bi *et al.* (2012), microorganisms capable of utilizing supplemented lignin compounds would be able to grow susceptibly. Apparently, it could be a preliminary assessment approach in screening lignolytic microorganisms. The findings of study imply lignolytic fungi can be isolated from sources such as soil and decaying wood. It is in agreement with the previous studies that reported fungi such as *Ceriporiopsis subvermispora* (Liu *et al.*, 2017) *Trametes versicolor* (Nazarpour *et al*., 2013), *Phoma herabnum, Hypocrea pachybasiodes, Cylindrocarpon didymum, Cryptococcus podzolicus* and *Sphaerulina polyspora* (Bi *et al*., 2012) could be isolated from soil , sugarcane baggase, barley straw, decaying wood branches and rubberwood.

As shown in Figure 1, PWM3 isolate exhibited different morphological features compared with other isolated cultures. The isolate was found to grow randomly and did not spread evenly from the fungal plug at the middle of PDA plate. Instead, the purplish-like cultures formed a number of individual clusters around the plate. Meanwhile, isolate PWC3 shows the presence of mycelia around the plate. The fungus growth also was found spreading homogenously. It seems that the morphology of PWC3 shows similarity with *Trichoderma* species, a common lignin degrader in soil and rooting wood in most climatic areas (Lidia Blaszczyk *et al*., 2014).

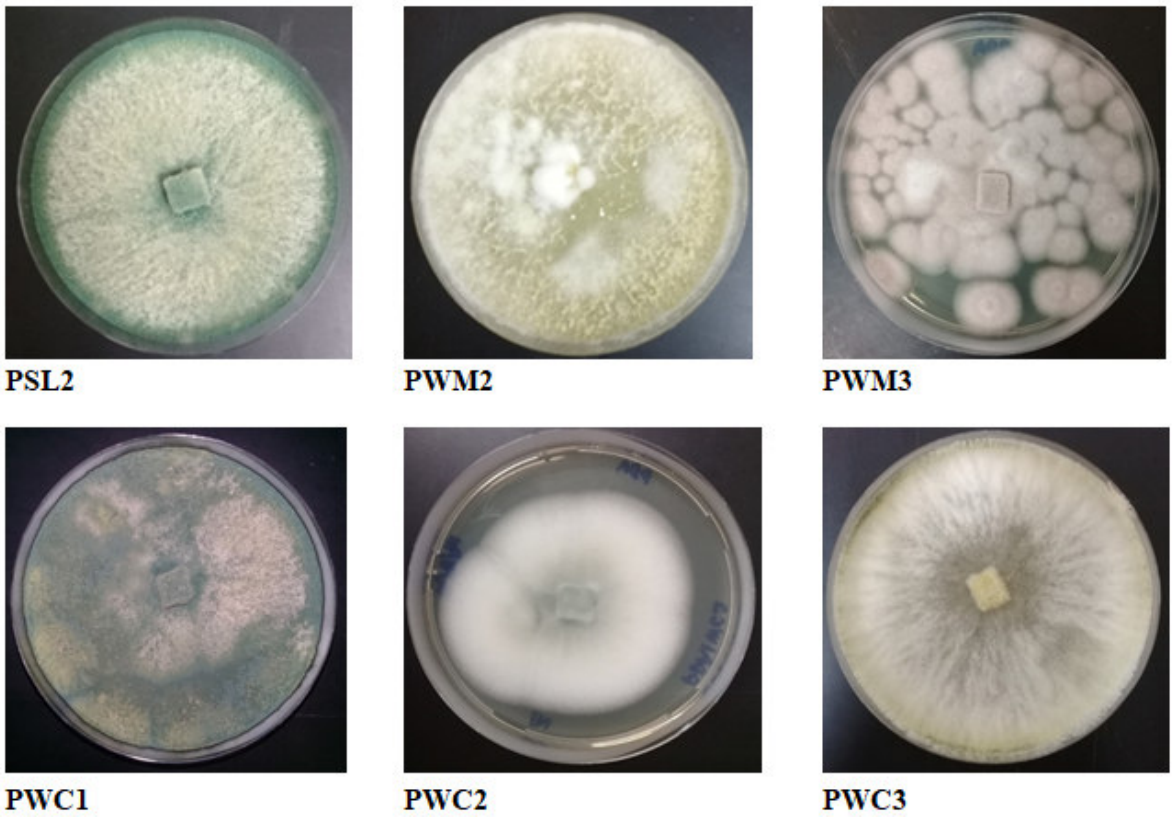

Figure 1
Pure isolates of fungi grown on potato dextrose agar (PDA) media after seven days of incubation at 30°C

Morphological observations

The isolated cultures were further characterized through morphological and microscopic observations. Morphological characterization is one of the preliminarily identifications of unknown microorganisms based on their physical appearance and morphology. The morphological observation was done by assessing the colony morphology and physical appearance including the color on PDA media, fungal structure, forms, elevation, and margin as well as the spore formation feature, as summarized in Table 2. The microscopic observation, on the other hand, was employed following the lactophenol cotton blue (LPCB) protocol and visualized using a microscope. The observation includes studying the mycelia, hyphae, conidia and sclerotia of each fungal colony as shown in Figure 2.

The color of the colonies differed from each other as shown in Table 2 and Figure 1. All isolates except for PWM2 and PWC3 (identified as yellow cultures) appeared as purple, green and white or combination of greenish-white. The morphological structures also varied showing rough surface like PSL1, cottony-rich (PWM2), curled-like ring (PWM3), dry and powdery (PWC1), and smooth shiny and heavy white for PWC2 and PWC3, respectively. All cultures isolated from the oil palm plantation soil and decaying mango wood demonstrated circular forms while the cultures from the decaying cempedak wood were either filamentous or in irregular forms. With regards to the morphological elevation, most of the cultures indicated a flat feature. The colonies' margin were characterized as entire, filiform and curled. There was no sporulation observed from PWM2, PWM3 and PWC2 colonies.

Colony characterization through microscopic observation is essential to recognize several characteristics of microorganisms which are invisible through naked eyes. Based on the microscopic images illustrated in Figure 2, isolate PSL2 was rich in spores. There was no mycelium or hyphae detected. Isolate PWM2 showed a very distinctive morphology attributed to the presence of mycelia and septate hyphae. Hyphae branching were observed at 45° and were evenly separated in width. PWM3 and PWC3 isolate potrayed irregular coenocytic hyphae and formation of pseudohyphae on their mycelia. Meanwhile, PWC1 isolate portrayed mycelia made up of irregular coenocytic hyphae branching. The presence of sclerotia structure and conidiophores were also noted. PWC2 showed shorter hyphae with irregular branching and a conidiophores-like structure. According to the morphological and microscopic observations, PWC2 indicated similar morphological characteristics with *Aspergillus* sp as reported by Yuri (2012). Future study can be conducted to further identify the species of the isolates up to genus level.

Table 2
Colony morphology and characterization

Isolates	Colony Morphology on PDA Media					
	Color	**Structure**	**Forms**	**Elevation**	**Margin**	**Spore formation**
PSL2	Greenish-white	Rough surface	Circular	Flat	Entire	Ring of spore
PWM2	Yellow	White cottony	Circular	Flat	Filiform	No sporulation
PWM3	Purple	Curled like-ring	Circular	Umbonate	Curled	No sporulation
PWC1	Green	Dry, powdery	Filamentous	Flat	Entire	Scattered green spores
PWC2	White	Smooth shiny	Irregular	Raised	Entire	No sporulation
PWC3	Yellow	Heavy white	Filamentous	Flat	Filiform	White spores

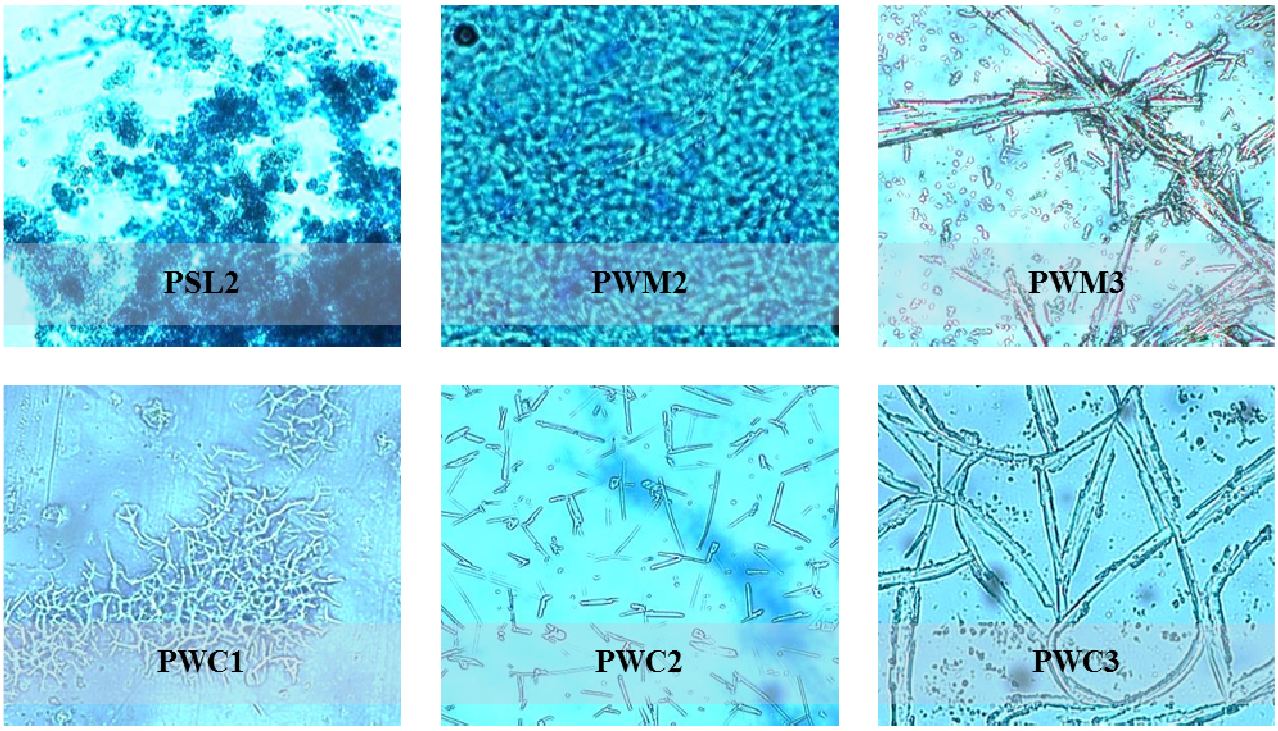

Figure 2
Microscopic images of each isolates stained using lactophenol cotton blue after seven days of incubation at 40X magnification.

Lignolytic activity using RBBR

The application of polymeric dye such as remazol brilliant blue, Congo red, azure B and methylene blue is a common detection method for lignin degradation (Narkhede *et al.*, 2013). Remazol brilliant blue anthraquinone R (RBBR) is a synthetic lignin compound used to detect the lignolytic activity of lignin degraders through decolorization of dye caused by the depolymerization of lignin due to enzymatic activity (Narkhede *et al*., 2013). According to Falade *et al.* (2017), the structural composition of RBBR is similar to lignin and their complexity leads to the recalcitrant properties of lignin.

In this study, the lignolytic activity of each fungal isolates was assessed with 0.05% of RBBR. Figure 3 presents the RBBR plate after seven days incubation at 30^{o}C. The isolates PSL2, PWM2, PWC1 and PWC2 grew susceptibly forming mycelia on RBBR media. Meanwhile, PWM3 and PWC3 exhibited a remarkable inhibition of fungal growth. It could be due to the toxicity level of dye suppressing secretion of enzymes, thus, inhibited the growth of the fungal cultures.

According to Przystas & Zablocka-Godlewska (2017), clear zones observed on plates containing dye inoculated with fungi indicate the presence of lignolytic enzymes. Isolates PSL2, PWM2, PWC1 and PWC2 demonstrated visible clear zones on the agar plates as well as the formation of mycelia. Meanwhile, only a slight decolorization was observed for PWM3 and PWC3. Halo zone formation is caused by the oxidation of polymeric dyes due to catalytic process of lignolytic enzymes such as peroxidases and oxidases (Masalu, 2016). Singh (2017) stated that the decolorization of dye is influenced by the efficiency of each isolate to secrete its enzymes. A study done by Kornittowicz-Kowalska & Rybcznska (2012) also indicated that RBBR media could support the lignolytic fungi isolated from soil with a cottony-colony and colorless mycelia.

In summary, all six isolates were found decolorize RBBR dye within seven days. The findings indicate that all isolates possess a lignolytic capability and hence are lignin degraders. The lignolytic activity of lignin peroxidase, manganese peroxidase and laccase secreted by the isolates, as well as their capabilities to degrade natural lignin-biomass can be futher studied.

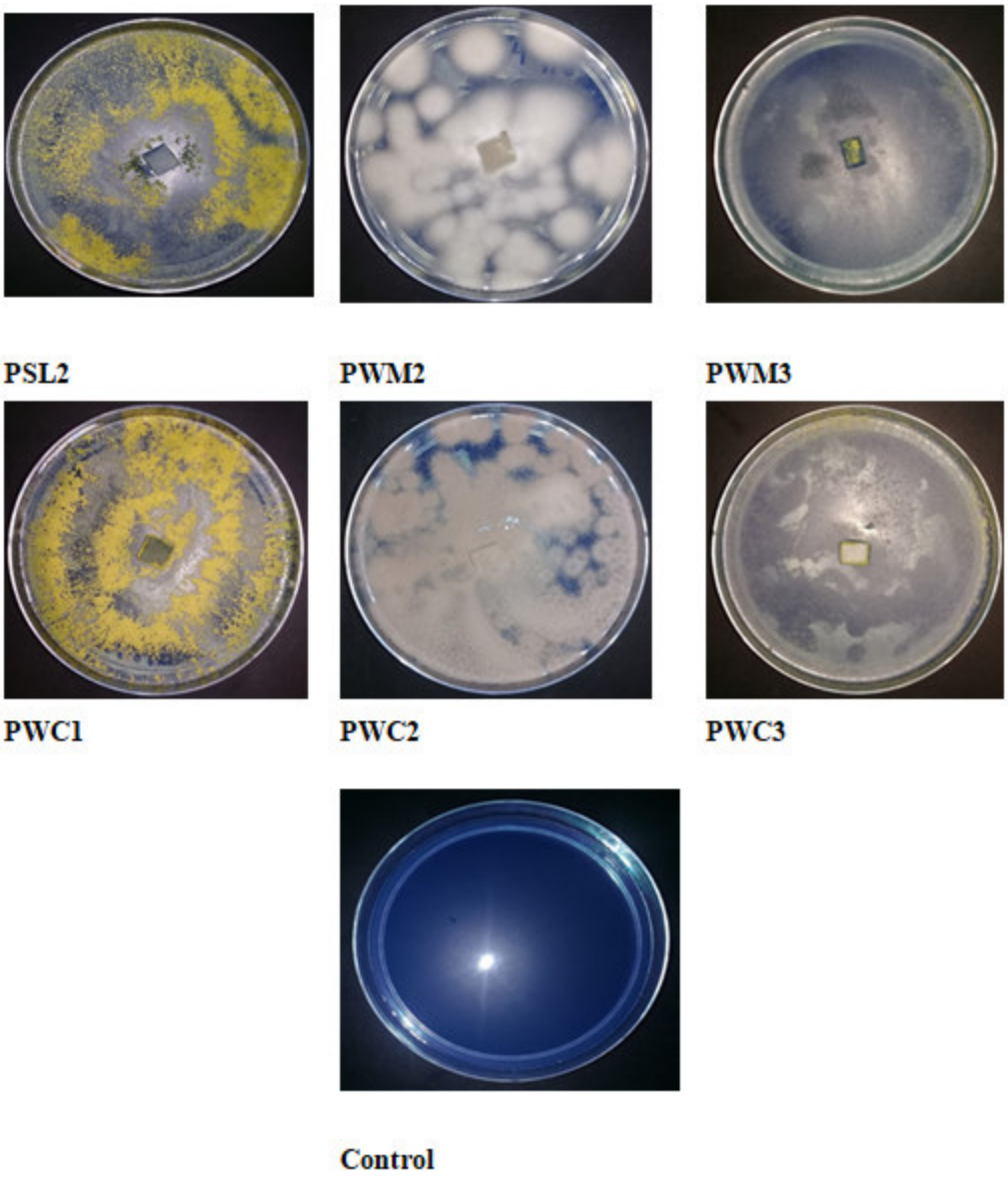

Figure 3
RBBR assays of each isolates after seven days incubated at 30°C

CONCLUSION:

Agricultural wastes, such as oil palm plantation soil and decaying woods, are vital sources of fungi microorganisms with lignolytic properties. The screening was done on minimal salt medium containing lignin to eliminate non-lignin degraders. Six isolates, one from oil palm plantation soil, two from decaying mango wood and three from decaying cempedak wood, were successfully isolated, screened and morphologically characterized. All isolates were found to grow successfully on the RBBR media after seven days of incubation. In addition, they exhibited a remarkable RBBR dye decolorization indicating lignin degradation activity. This work has provided a useful guideline in isolating and screening potential lignin degraders from the environment.

ACKNOWLEDGEMENT:

This research was funded by Universiti Malaysia Sabah under the collaborative research grant scheme GKP0003-SG-2016: Screening, characterization and optimization of lignin-degrading microorganisms from Sabah mega biodiversity for optimum bioconversion of oil palm waste.

REFERENCES:

1. Bhutto, A. W., Qureshi, K., Harijan, K., Abro, R., Abbas, T., Bazmi, A. A., Karim, S., & Yu, G. (2017). Insight into progress in pretreatment of lignocellulosic biomass, *Energy*. doi: 10.1016/j.energy.2017.01.005
2. Bi, R., Spadiut, O., Lawoko, M., Brumer, H., & Henriksson, G. (2012). Isolation and identification of microorganisms from soil able to live on lignin as a carbon source to produce enzymes which cleave the β-O-4 bond in a lignin model compound. *Cellulose Chemical Technology, 46* (3-4), 227-242.
3. Falade, A.O., Eyisi, O. A. L., Mabinya, L. V., Uchechukwu U. Nwodo, U.U., &. Okoh, A. I. (2017). *Biotechnology Report, 16*, 12-27.
4. Kornittowicz-Kowalska, T. & Rybcznska, K. (2012). Decolorization of Remazol Brilliant Blue R (RBBR) and Poly-R-478 dyes by Bjerkandera adusta CCBAS 930. *Central European Journal of Biology, 7*(5), 948-958.
5. Lidia Błaszczyk, Marek Siwulski, Krzysztof Sobieralski, Jolanta Lisiecka & Małgorzata Jędryczka (2014). *Trichoderma spp*. – application and prospects for use in organic farming and industry. *Journal of Plant Protection Research, 54*(4), 309-317.
6. Liu, X., Hiligsmann, S., Gourdon, R., & Bayard, R. (2017). Anaerobic digestion of lignocellulosic biomasses pretreated with *Ceriporiopsis subvermispora* . *Journal of Environmental Management, 193,* 154-162.
7. Masalu, R. J. (2016). Lignolytic enzymes of the fungus isolated from soil contaminated with cow dung. *Tanzania Journal Science*, 42, 85-93.
8. Narkhede, M., Mahajan, R. & Narkhede, K. (2013). Lignolytic enzyme production and remazol brilliant blue R (RBBR) decolorization by newly isolated white-rot fungus: Basidiomycota spp L-168. *International Journal of Phama and Bio Sciences.*
9. Nazarpour, F., 1, Abdullah, D. K., Abdullah, N., & Zamiri, R. (2013). Evaluation of biological pretreatment of rubberwood with white rot fungi for enzymatic hydrolysis. *Materials, 6*, 2059-2073; doi:10.3390/ma6052059
10. Przystas, W. & Zablocka-Godlewska, E. (2017). The possibility of using of Hypholoma fasciculare mycelium in decolorization of anthraquinone dye RBBR. *Architure Civil Engineering Environment, 1,* 137-146.
11. Ravindran, R. & Jaiwal, A. K. (2016). Comprehensive review on pre-treatment strategy for lignocellulosic food industry waste: Challenges and opportunities. *Bioresource Technology, 199,* 92-102.
12. Sasikumar, V., Priya, V., Shiv Shankar, C., & Sathish Sekar, D. (2014). Isolation and Screening of Lignin Degrading Microbes. Journal of Academia and Industrial Research, 3(6), 291-294.
13. Singh, L. (2017). Biodegradation of Synthetic Dyes: A Mycoremediation Approach for Degradation/ Decolourization of Textile Dyes and Effluents. *Journal of Applied Biotechnology & Bioengineering,* 3 (5).
14. Sun, S., Sun, S., Cao, X. & Sun, R. (2016). The role of pretreatment in improving the enzymatic hydrolysis of lignocellulosic materials. *Bioresource Technology, 199,* 49-58.
15. Yuri (2012, January 20). *Aspergillus fumigatus.* Retrived on 2018, March 2 from http://thunderhouse4-yuri.blogspot.my/2012/01/aspergillus-fumigatus.html
16. Zhu, D., Zhang, P., Xie,C., Zhang, W., Sun, J., Qian, W., & Yang, B. (2017). Biodegradation of alkaline lignin by *Bacillus ligniniphilus* L1. *Biotechnology for Biofuels, 10* (44), 1-14.

FP-29

A PRELIMINARY STUDY OF PESTICIDE ON MICROBIAL DIVERSITY IN AGRICULTURAL SOILS BY DGGE ANALYSIS AND PHYSIOLOGICAL PROFILES

LEONG WAN VUN[1], PEIK LIN TEOH[2]

[1]Environmental Science Programme, Faculty of Science and Natural Resources, Universiti Malaysia Sabah, 88400 Kota Kinabalu, Sabah, Malaysia, [2]Biotechnology Research Institute, Universiti Malaysia Sabah, Jalan UMS, 88400 Kota Kinabalu, Sabah, Malaysia

*Corresponding author: bvun@ums.edu.my

ABSTRACT

Agricultural practices have been known to alter the soil microbial community profiles. This study is to examine the effect of pesticide on microbial diversity in Kundasang agricultural soils. Denaturing gradient gel electrophoresis (DGGE) was used for the analysis of 16S ribosomal DNA (rDNA) and the substrate utilisation patterns of the soil microbial communities was determined using BIOLOG GN2 microplates. Results showed that a rich diversity of soil microbial communities existed in all soil types. Through DGGE fingerprints, it seemed that certain species were stimulated by the application of pesticide. The demise of certain functions was also observed in the case of GN2 profiles. The findings could be used in supporting sustainable agricultural practice.

KEYWORDS:
Pesticide, Agricultural soil, Microbial diversity

INTRODUCTION:

Unsustainable agricultural practices, especially in the case of high input of fertilizers and pesticides not only habitat-damaging, they can also cause changes to the soil microbial densities and community structure; these changes in long-term will contribute to a loss of density/function within the soil microbial communities and indirectly may affect the soil, ecological and human health.[1,2]

Soil health refers to the biological, chemical, and physical features of soil that are essential to long-term, sustainable agriculture productivity with minimal environmental impacts.[3,4] Thus, soil health, in part, depends upon the functional processes of soil microbial communities[1,4], however some agricultural malpractices may threaten the integrity of these communities.

In Sabah, the Kundasang agricultural area at Mount Kinabalu has been reported to be contaminated by excessive pesticides and fertilizers and thus posed as a potential threat to ecological and human health.[5] Monitoring on the usage of such compounds has been carried out periodically by the local governmental and research institutions[6]; however to date, there is still no studies that look into the effects of such compounds on the soil microbial communities in the area.

Therefore, the effect of pesticide on the soil microbial diversity was described in this project, so as to provide a meaningful data for the decision makers to promote sustainable agricultural practices. Understanding of the changes in the composition of a microbial community would assist in characterizing its response to environmental stresses. In long-term, such studies would help to develop a suite of microbial molecular biomarkers that would be able to indicate the threats of contaminants on soil health. Furthermore, these biomarkers can be used as monitoring tools in evaluating agricultural policies for sustainability.

MATERIALS AND METHODS:

Sample collection

Soils were collected from the 5-10 cm surface of the investigated areas in a Kundasang farm. Three types of soil samples were collected and labelled as shown in Table 1. A and B were soil samples from plots cultivated with different vegetables. A1 and A2 were collected from soils planted with common cabbage, *Brassica oleracea* var. capitata. B1 and B2 were collected from soils planted with mustard cabbage/Kai Choi, *Brassica juncea* (L.). Ac and Bc were controlled soils taken from plots with the different vegetables. On these plots, soil samples were collected at different locations (identified as a, b and c in the results and discussion). Soil samples without pesticide and vegetables were also taken from the respectively plots as control. The pesticide used in this study was an insecticide branded as Nucleus-V 505, with a concentration of chlorpyrifos and cypermethrin at 45.9 and 4.6 % w/w respectively. This pesticide has been registered with the Department of Agriculture, Malaysia since 2004.

Table 1
Collection of soil samples on site at Kundasang area.

Sample soil types	Label	
without both vegetable and pesticide	Ac	Bc
with vegetables and pesticide	A1	B1
without vegetables but with pesticide	A2	B2

Extraction and amplification of nucleic acids

Genomic DNA was extracted from 0.5 g of soil using method described in Zhou et al.[7] and purified by QIAEX II gel extraction kit (Qiagen, Germany) according to manufacturer's protocol. To analyse the microbial composition, 16S rDNA amplification was carried out in a total reaction volume of 20 µl containing 1 µl of DNA sample, 300 µM of dNTPs, 1.5 mM $MgCl_2$, 25 pmol of GC-968F (5'-CGC CCG GGG CGC GCC CCG GGC GGG GCG GGG GCA CGG GGG GAA CGC GAA GAA CCT TAC-3') and 1401R (5'-CGG TGT GTA CAA GGC CCG GGA ACG-3') primers and 2.5 U of Taq polymerase (Promega) in a 1X PCR buffer. The PCR was initiated with 5 min at 94°C, followed by 35 cycles of 1 min at 94°C, 1 min at 54°C, 1 min at 72°C and 10 cycles consisting of 0.5 min at 54°C and 1 min at 72°C.

Denaturing gradient gel electrophoresis (DGGE) analysis

DGGE was performed using the DCode System from Bio-Rad. Purified PCR products were loaded onto polyacrylamide gels with a denaturing gradient of 40 to 60%. Electrophoresis was done at a constant 40 mA and a temperature of 60°C for 17 hrs. After electrophoresis, the ethidium bromide stained gel was documented by a digital imaging system.

Community-level physiological profile (CLPP) analysis

A CLPP analysis was carried out to determine the functional changes of microbial communities in different soil types. BIOLOG GN2 microplates were directly incubated with the soil microbial communities at 30°C for 4, 24, 48 and 72 hrs. After incubation, the assays were read at 595 nm using a Tecan Microplate Reader and were analysed using MagellanCE software. Data analysis was carried out by determining the net OD after subtracting the control OD from the OD obtained for each of the 95 carbon sources. The physiological versatility of the microbial community was evaluated based on the number of carbon sources with OD595 of > 0.4.

RESULTS AND DISCUSSION:

To study the effect of pesticide on the microbial community present in soil, the total DNA of the soil microorganisms was isolated directly without culturing. Therefore the nucleic acids obtained are the mixture

of cultured and non-cultured microorganisms. This is particularly important for the community study because only small fraction (~1%) of microbes can be recovered by using standard culturing methods.[8,9] The total soil DNA was successfully extracted from all the samples and purified prior to PCR amplification (Figure 1). DNA purification is necessary as the presence of inhibitors such as humic and fulvic acids would inhibit the PCR reaction.[10,11] This would jeopardise the actual view of microbial community in soil due to selective amplification of DNA from mixed communities.

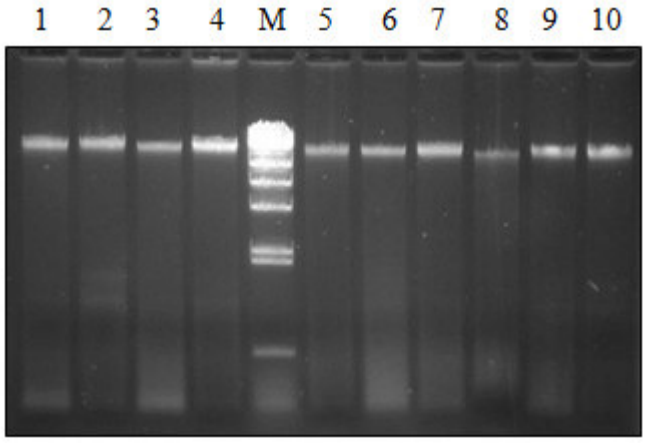

Figure 1

Genomic DNA extracted from soil samples. The gel electrophoresis was performed in 0.8% agarose gel, at 80V for 60 min. Lane M: λHindIII DNA marker (Promega, USA); Lane 1 to Lane 10: DNA (2 µl each) from the ten soil samples, from left to right, A1a, A1b, A2, Ac, B1a, B1b, B1c, B2a, B2b, and Bc respectively.

In our study, we were able to amplify the purified DNA by using 16S rDNA primers as a band with the size of ~1.5 kb could be detected in all soil samples (Figure 2). Although only a single band was observed in the agarose gel, it represents the mixture of various 16S rDNA fragments amplified from the whole microbial community. 16S rDNA has been widely used for bacterial identification and microbial community studies in environmental and clinical samples.[12] Amplification of 16S rDNA from complex microbial community is possible and feasible without prior cultivation as the PCR primers targeting the highly conserved regions are being applied. In addition, it allows comparative studies of temporal and spatial variation occurred in microbial diversity when multiple samples are analysed simultaneously.[13,14]

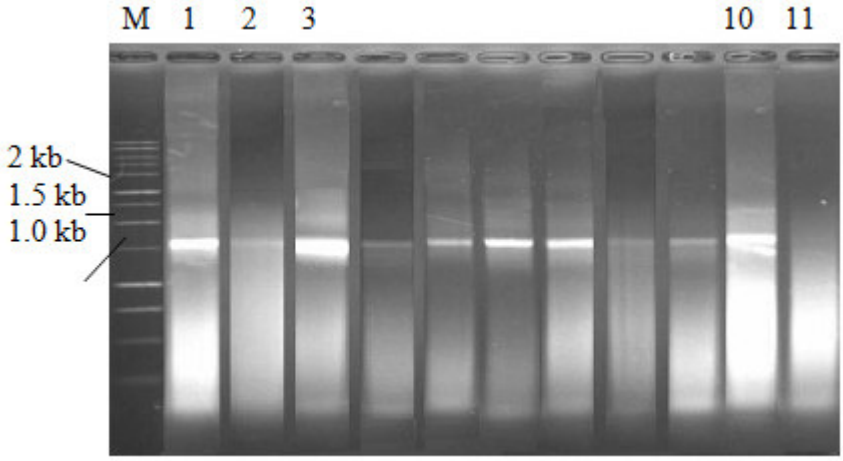

Figure 2

16S rDNA amplification of microbial community. M: 1 kb DNA ladder (Promega, USA); Lane 1 to Lane 10: 5µl samples of A1a, A1b, A2, Ac, B1a, B1b, B1c, B2a, B2b, and Bc respectively. Lane 11: the negative control in the absence of DNA template.

DGGE was done after PCR amplification of the 16S rDNA genes from the total soil DNA. The single bands observed in Figure 2 was separated as multiple bands as depicted in Figure 3. This is because the DGGE

separates the mixed amplified PCR product based on the variation of the 16S rDNA sequences found in different types of microbes. The preponderant bands seen on the gel can be considered as the more abundant bacterial species in each of the soil types. From the result, 16S rDNA fingerprinting from the soil samples for all soil types resulted in approximately similar, but not identical, DGGE profiles.

The different intensity of bands suggested that there was a high diversity of microbes existed in all three soil samples. At closer examination, there were more evident bands in soil with pesticide (Figure 3, Lane 1-3 and Lane 5-9) than the one without pesticide (Figure 3, Lane 4 and 10). This might suggest that the dominant species were more abundant in the pesticide-soil than in the control, which was without pesticide; this could be the effect of the pesticide on the microbial communities as certain species capable of adapting to the agricultural practice will take the advantage of the situation and establish a new microbial community.[15,16]

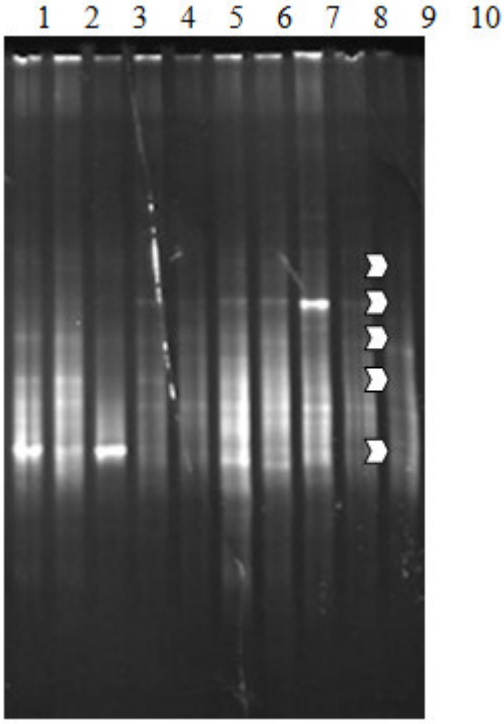

Figure 3

DGGE profiles of PCR amplified 16S rDNA. Lane 1 and 2: soil samples with both vegetables (common cabbage) and pesticide (A1a and A1b); Lane 3: soil samples with pesticide only (A2); Lane 4: soil sample without both pesticides and vegetables (Ac); Lane 5, 6 and 7: soil samples with vegetables (mustard cabbage) and pesticide (B1a, B1b and B1c); Lane 8 and 9: soil samples with pesticide only (B2a and B2b); Lane 10: soil sample without both pesticides and vegetables (Bc).

Soil samples taken from the same plots at different locations also showed markedly distinct DGGE profiles. This can clearly be seen with the samples taken from the plots planted with mustard cabbage (samples B, Fig. 3, Lane 5-7 and 8-9). From the three samples in B1 and the two samples in B2, it suggested that the microbial communities are spatially and not evenly distributed as the bands intensity varies. Since soil is a complex microhabitat for various microbes, no doubt that the microbial population will be very diverse. It was estimated the presence of 6000 different bacterial genomes per gram of soil or 4,000 to 10,000,000 genome equivalents per 10 or 30 g of soil based on DNA reassociation experiments.[17,18] On top of these diversities, soil is also considered as a structured, heterogeneous and discontinuous system, therefore the chemical, physical and biological characteristics of these microhabitats differ in both time and space, thus this would cause the microorganisms to live in discrete microhabitats having the right set of life support conditions.[13,19]

Likewise, soil samples taken from different vegetable plots also yielded different DGGE profiles as seen in Fig. 3 (between samples A and B). The different patterns as shown in the gradient gel would suggest that

environmental factors can affect the ecology and population dynamics of microbes in soil. The changes in the environmental factors (such as the availability of nutrients, water, temperature, surface, pH and etc) alter the microhabitats and thus lead to the changes in the microbial composition.[13]

For the study on community level physiological profiles (CLPP), only samples A were used. Our results indicate that the soil microbial community in the three soil types has the capacity to utilize a diverse array of carbon substrates and the rate of use differs for different carbon substrates (Table 2). The average level of C-substrate usage was higher for microbial community in soils without pesticide compared to the ones with pesticides; however this trend was only seen with some C-substrates (Figure 4).

Table 2
Utilisation profiles of the three soil types based on carbon sources on Biolog GN2 microplates.

Carbon sources (GN2)		Soil Microbes from
1.	Formic acid (4D)	Not utilised by any of the soil types
2.	L-alaninamide (4F)	
3.	2,3-butanediol (8H)	
4.	α-keto butyric acid (3E)	Ac only
5.	α-hydroxybutyric acid (10D)	
6.	glycyl-L-glutamic acid (12F)	
7.	Succinic acid mono-methyl ester (12C)	Ac and A2 only
8.	α-keto valeric acid (5E)	A2 only
9.	The other 87 sources	Utilised in all soil types with various rate

The pattern showed that the microbial communities in the agricultural soils are very diverse as they are able to utilise a vast array of carbon sources. It is found that there were three types of sources (α-keto butyric acid (3E), α-hydroxybutyric acid (10D) and glycyl-L-glutamic acid (12F)) that were not utilised at all in soil with pesticide, however only one type of carbon source (α-keto valeric acid (5E)) was utilised by microbes in soil with pesticide. This clearly showed that the functional abilities of the soil microbes were altered by the application of the pesticide. The demise of certain biochemical functions would directly and indirectly influence the soil health.

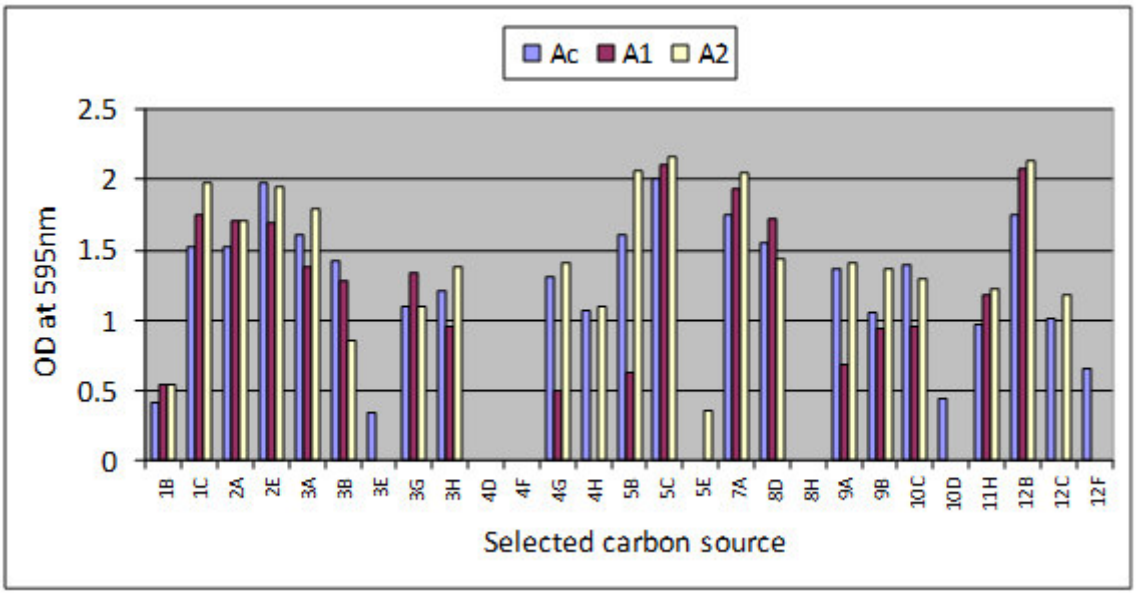

Figure 4
Diversity of soil microbial communities of the three soil types as measured using C-substrate utilization profiles on the Biolog GN2 microplates (Only 27 carbon sources are depicted here as these showed significant variations whereas the other 68 are not shown).

Table 3
Results of the comparison of Ac, A1 and A2 concerning substrate utilization patterns based on Figure 4 using matched t-test

Soil	Test value of t	Critical value of t* (p = 0.05, one-tailed), df = 26	Significance mean difference
Ac – A1	2.62		Yes as t > t*
Ac – A2	-0.93	1.71	No as t < t*
A1 – A2	-3.01		No as t < t*

This result was supported by the statistical analysis (Table 3). The comparison of substrate utilization profiles by soil microbial from the three soil types (Ac, A1 and A2) showed differences between the soil without pesticide and the soils with both pesticide and vegetables. However, no statistically significant differences were found between Ac-A2 and A1-A2. The statistical insignificance difference A1 and A2 was foreseen as they were soils with pesticides treatment, but the result for Ac and A2 was not as predicted. This could be due to the reason that only 27 carbon substrates utilisation profiles were used in the statistical analysis, most probably when more substrates profiles were included in the analysis, the result might be otherwise. Nevertheless, as seen in the DGGE profiles (Figure 3), there was a distinct difference of dominant microbial composition between samples of Ac and A2.

The rich diversity shown in the carbon source utilisation was parallel to the results from DGGE analysis as bacteria do not specialize on a single substrate, but their diversity is the ability to use combinations of substrates under different physico-chemical conditions.[15] Besides that, our results also suggest that the presence of vegetable also influenced the soil microbial communities and the usage of carbon source. As seen in Figure 4, there is a distinct difference between these two soils in term of carbon source selection such as 4G, 5B, 9A and 10C. Plant is the major source of available carbon for biological activity, hence soil biodiversity and biological activity is dependant on the quality and quantity of carbon inputs from plants through root exudation and above- and below ground residues.[13]

CONCLUSIONS:

In conclusion, this study clearly showed that the application of pesticides exert effects on the microbial communities in the soil. It is interesting to note that through DGGE fingerprints, it seemed that certain species were stimulated by the application of pesticide and the demise of certain functions was also observed in the case of GN2 profiles. The use of field samples however could not demonstrate the effect of different concentration of pesticide on the soil microbial community structure after treatment, a laboratory microcosm experiment can be used to shed more light on this matter. Further study by carrying out sequence analysis of predominant bands excised from DGGE gels would further verify the effect of pesticide on soil microbial communities.

ACKNOWLEDGEMENT:

The authors thank Universiti Malaysia Sabah and International Environmental Research Centre (IERC) of Gwangju Institute of Science and Technology (GIST) and also UNU and GIST Joint Program for Science and Technology for Sustainability for the gracious support.

REFERENCES:

1. Girvan MS, Bullimore J, Ball AS, Pretty JN, Osborn AM. 2004. Responses of active bacterial and fungal communities in soil under winter wheat to different fertilizer and pesticide regimens. Applied and Environmental Microbiology. 2004; 70(5): 2692-2701.

2. Jacobsen CS, Hjelmsø MH. Agricultural soils, pesticides and microbial diversity. Current Opinion in Biotechnology. 2014; 27: 15-20.
3. Arias ME, Gonzalez-Perez JA, Gonzalez-Vila FJ, Ball AS. Soil health-a new challenge for microbiologists and chemists. International Microbiology. 2005; 8: 13-21.
4. Cardoso EJBN, Vasconcellos, RLF, Bini D, Miyauchi MYH, dos Santos CA, Alves PRL, de Paula AM, Nakatani AS, Pereira JM, Nogueira MA. Soil health: looking for suitable indicators. What should be considered to assess the effects of use and management on soil health? Sci. Agric. (Piracicaba, Braz.). 2013; 70(4): 274-289.
5. Zakaria Z, Lee YH, Abdullah P, Osman R, Din L. The Environmental Contamination by Organochlorine Insecticides of Some Agricultural Areas in Malaysia. Malaysian Journal of Chemistry. 2003; 5(1): 78-85.
6. Jipanin J, Rahman AA, Jaimi JR, Phua PK. Management of Pesticide Use on Vegetable Production: Role of Department of Agriculture Sabah. 6th SITE Research Seminar, Kota Kinabalu, Sabah. 13-14 September 2001.
7. Zhou J, Bruns MA, Tiedje JM. DNA recovery from soils of diverse composition. Applied and Environmental Microbiology. 1996; 62: 316-322.
8. Torsvik V, Øvreås L. Microbial diversity and function in soil: from genes to ecosystems. Curr Opin Microbiol. 2002; 5(3): 240-245.
9. Stewart EJ. Growing unculturable bacteria. J Bacteriol. 2012; 194(16): 4151-4160.
10. Watson RJ, Blackwell B. Purification and characterization of a common soil component which inhibits the polymerase chain reaction. Can J Microbiol. 2000; 46(7): 633-642.
11. Matheson CD, Gurney C, Esau N, Lehto R. Assessing PCR inhibition from humic substances. The Open Enzyme Inhibition Journal. 2010; 3: 38-45.
12. Ward DV, Gevers D, Giannoukos G, Earl AM, Methé BA, Sodergren E, et al. Evaluation of 16S rDNA-based community profiling for human microbiome research. PLoS One. 2012; 7: e39315.
13. Nannipieri P, Ascher J, Ceccherini MT, Landi L, Pietramellara G, Renella G. Microbial diversity and soil functions. European Journal of Soil Science. 2003; 54: 655–670.
14. O'Sullivana DJ, Cottera PD, O'Sullivana O, Giblina L, McSweeney PLH, Sheehana JJ. Temporal and spatial differences in microbial composition during the manufacture of a continental-type cheese. Appl Environ Microbiol. 2015; 81(7): 2525–2533.
15. Øvreås L, Torsvik V. Microbial Diversity and Community Structure in Two Different Agricultural Soil Communities. Microbial Ecolology. 1998; 36: 303–315.
16. Umesha S, Singh PK, Singh RP. Biotechnology for Sustainable Agriculture: Emerging Approaches and Strategies. In Singh RL, Mondal S, editors. Microbial Biotechnology and Sustainable Agriculture. United Kingdom: Woodhead Publishing; 2018. p.185-205.
17. Torsvik V, Sorheim R, Goksoyr J. Total bacterial diversity in soil and sediment communities – a review. Journal of Industrial Microbiology. 1996; 17: 170-178.
18. Schloss PD, Handelsman J. Toward a census of bacteria in soil. PLoS Comp Biol. 2006; 2(7): e92.
19. Stotzky, G. Soil as an environment for microbial life. In van Elsas JD, Trevors JT, Wellington EMH (eds). Modern Soil Microbiology. New York: Marcel Dekker; 1997. p. 1-20.

FP-30

ENCAPSULATION OF TWO ALKALOIDS IN CHITOSAN-TRIPOLYPHOSPHATE MATRIX

BAMBANG CAHYONO[1], ANFA'UN NISA'[1], TRI YULIYANTI[1], AGUSTINA L. N. AMININ, MEINY SUZERY[1]

[1]*Organic Chemistry Laboratory, Department of Chemistry, Faculty of Science and Mathematics, Diponegoro University, Prof Soedarto SH street, Tembalang, Semarang 50275*

Corresponding author: meiny_suzery@live.undip.ac.id

ABSTRACT

The objective of this research is to study the performance of two encapsulated alkaloids for several indicators. Two pure alkaloid that used in this study are neutral alkaloid (caffein/CAF) and base alkaloid (allopurinol/ALP). Both are encapsulated in chitosan-tripolyphosphate and evaluated using UV-Vis spectrofotometry, Fourier transform infra-red (FT-IR) spectroscopy, and Scanning electron microscopy (SEM). The encapsulation efficiency of CAF was 9.62% (at 0.125 mM) to 40.61% (at 11.25 mM) and for ALP were 12.45 (at 0.125 mM) toward 65.90% (at 11.25 mM). The loading capacities were around 0.07%-1.29% for CAF and 0.37-10.54% for ALP. The result shows that the efficiency of encapsulation decreased by the decreasing of CAF concentration, but the increase was observed for ALP. In the other hand, the loading capacity has linear correlation with active compounds concentration. SEM images showed that the microparticles of CAF are rough surface with high porosity, while ALP is not uniform. The shifted of wave numbers in FTIR spectra indicated an interaction between chitosan particles with the encapsulated active compounds. The release of CAF and ALP from the microparticles in simulated gastric fluid and intestinal fluid showed an initial burst release afterward followed by subsequent slower release. Based on the results of the controlled release test, both alkaloids were released faster in the simulated gastric fluid (acid medium) than in simulated intestinal fluid (base medium).

KEYWORDS:
Allopurinol, caffeine, chitosan, encapsulation, sodium-tripolyphosphate

INTRODUCTION:

Some organic compounds are generally formulated in the form of encapsulated product accordingly that their organoleptic properties can be improved whilst preserve stability of the bioactive compounds from external environmental.[1,2] The success of encapsulation process influenced by several factors, such as encapsulation method, coating materials (type, molecular weights, etc) and crosslinkers. The properties of the active compound are also very influential on product quality. Several encapsulation methods have been reported, such as coacervation, spray cooling, lyophilization and extrusion.[3,4] Coacervation is a simple method and without using heating.[5] This method is one of the method that use macromolecules characteristic containing cation/anion charge to interact electrostatically to form a matrix.[6] Many wall material have been applied for encapsulation processes, such as chitosan, gelatine, sodium alginate, albumine, etc.[7] The nature of the low toxicity and biodegradable properties of chitosan, reasons this material often used as a matrix for drug delivery systems.[8] In some cases, the use of porous polymers is also expected to be suitable for the release of bioactive compounds over a period of time.[9] Sodium tripolyphosphate is an excellent crosslinking agent considering that high negative charge density.[10]

In our previous studies[11,12] encapsulation has been carried out using chitosan-NaTPP matrix towards the essential oils (eugenol) and flavonoid (rutin) compounds. Both of these compounds are acidic since they have phenolic groups. In this study, the encapsulation with the same system was carried out on alkaloid compounds. Free electrons of these nitrogen atoms have the ability to donate pair of its electrons to other

atoms so, they are generally base. The alkalinity of alkaloids compound may be reduced by the presence of an electron-withdrawing group, such as amide or when both free electrons are donated to the ring so that the molecule is aromatic.[13] Allopurinol (ALP) is a base alkaloid (pKa 10.2)[14,15], while caffeine (CAF) is a neutral alkaloid with pH 6.9.[16] ALP is purine base, and also used to inhibits xanthine oxidase enzyme,[17,18] while CAF has bioactivity as antibacterial dan anti-inflammation.[19,20] Theoretically, the two nitrogen atoms in the caffeine ring are amide groups whereas in allopurinol have one nitrogen in the form of alkaline amines, which allows interaction with the matrix. In addition, the ion pair of two nitrogen atoms of allopurinol is a free electron, while in caffeine one of the ion pairs of nitrogen is donated to aromaticity in the limestone ring system. Based on this, more molecular interactions between ion pairs of nitrogen atoms in allopurinol are possible than caffeine. Moreover, two hydrogen atoms attached to a nitrogen atom in allopurinol can make hydrogen bonds with electronegative atoms in the matrix. Thus, it is expected that the percentage of encapsulation of allopurinol is higher than caffeine (Figure 1).

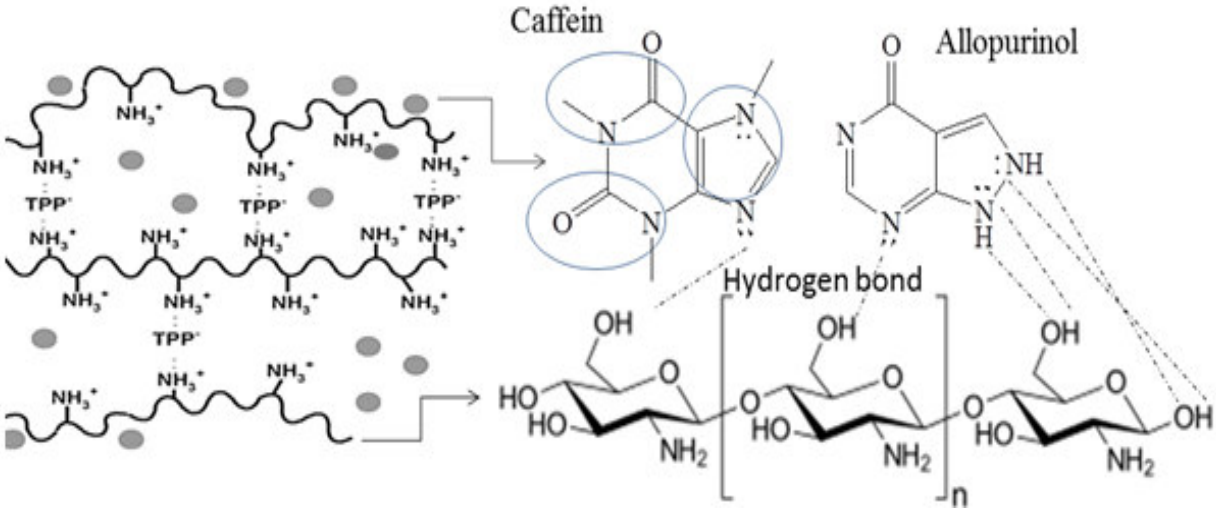

Figure 1
The hypothetical molecular interaction between CAF and ALP compounds with the chitosan-NaTPP matrix

MATERIALS AND METHODS:

Chitosan (molecular weight = 624.739 kDa, deacetilation degree = 64.2%).[11,12] Caffeine (isolated from green tea leaves by PT. Rumpunsari Medini, Kendal), allopurinol (PT. Indofarma Tbk. Jakarta). Chitosan solution (2%, w/v), sodium tripolyphosphate, solution buffer pH 7.4, and solution buffer pH 1.2 prepared based on previous study.[9,10]

Preparation of encapsulation products

Encapsulation process were prepared by coacervation method.[21] Tween-20 (0.3 g) was added to 40 mL chitosan solution (2%, w/v), and the mixture was stirrer for 30 min. CAF and ALP were separately added into the chitosan solution and stirred for 20 min according to the following concentrations: 0.125, 0.3125, 0.625, 1.25, 3.75, 6.25, 8.75, 11.25 mM for CAF and 3.75, 6.25, 8.75, 11.25, 13.75, 16.25, 18.75 for ALP.

Encapsulation efficiency and loading capacity

The freeze-dried sample of CAF-loaded chitosan particles were taken into aquadest, while ALP-loaded chitosan particles were taken into methanol and stirrer for 1 h, respectively. The supernatant was collected and the content of two alkaloids measured using UV-vis spectrophotometer[22] at 273.5 nm for CAF and 250.5 nm for ALP. The encapsulation efficiency (EE) and loading capacity (LC) were calculated.[9,10]

Instrumental analyses

Pure chitosan, chitosan-TPP, pure caffeine, pure allopurinol and encapsulation product were recorded by FTIR. Scanning electron microscopy (SEM) was used to analysis of morphology, was studied by 1000x magnification.[11,12]

In vitro release study

In vitro release was conducted by dissolving 20 mg freeze-dried particles separately in 20 mL simulated gastric fluid (SGF) and simulated intestinal fluid (SIF).[23] To calculate the total cumulative amount of CAF and ALP released, concentration (ppm) of the two alkaloids in the release medium were measured at sampling time intervals by a UV-Vis spectrophotometer at 273.5 nm for CAF and 250.5 nm for ALP.[11,12]

RESULTS:

The Efficiency of encapsulation and loading capacity

The encapsulated products formation of CAF and ALP in chitosan particles were varied from concentration of 0.125-18.75 mM. Graphic 1 showed percent encapsulation efficiency (% EE) and percent loading capacity (% LC) of caffeine and allopurinol, respectively. The amount of caffeine and allopurinol loaded was determined using UV-visible spectrophotometry at the absorbance of 273.5 nm and 250.5 nm respectively.

Morphology

Unallocated chitosan particles (control) and filled with CAF or ALP (loaded) can be distinguished visually using Scanning Electron Microscopy (SEM). SEM analysis serves to identify the morphology of the surface and shape of particles of chitosan that is displayed through an image. Based on the characterization by SEM at 1000x magnification showed that the particles of chitosan unallocated and treatment CAF or CAF loaded chitosan particles has a surface and a different shape that can be seen in Figure 2.

FT-IR Spectra

The FTIR spectra of pure CAF, pure ALP, chitosan, chitosan-TPP, and encapsulated products (CAF-loaded chitosan particles and ALP-loaded chitosan particles) were showed in Figure 3.

In Vitro Release Study

The cumulative release behavior of CAF and ALP from different concentration were performed in simulated gastric fluid/SGF (pH 1,2) and simulated intestinal fluid/SIF (pH 7,4) shows in graphic 2 and graphic. The amount of CAF and ALP released at different times was measured by UV-Vis spectrophotometric at 273.5 and 250.5 nm, respectively.

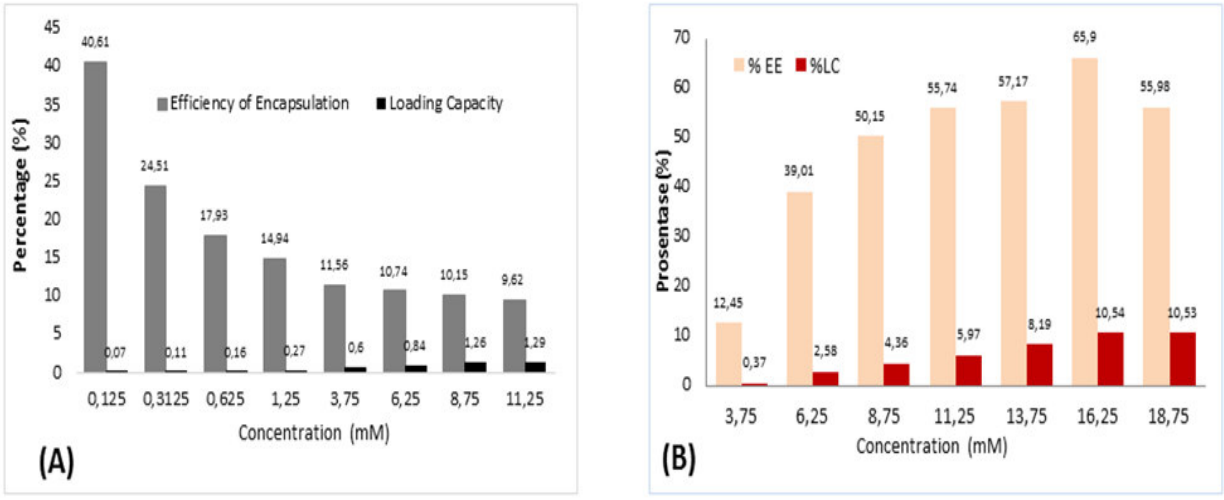

Graph 1
Encapsulation efficiency and loading capacity of (A) caffeine, (B) allopurinol loaded chitosan particles.

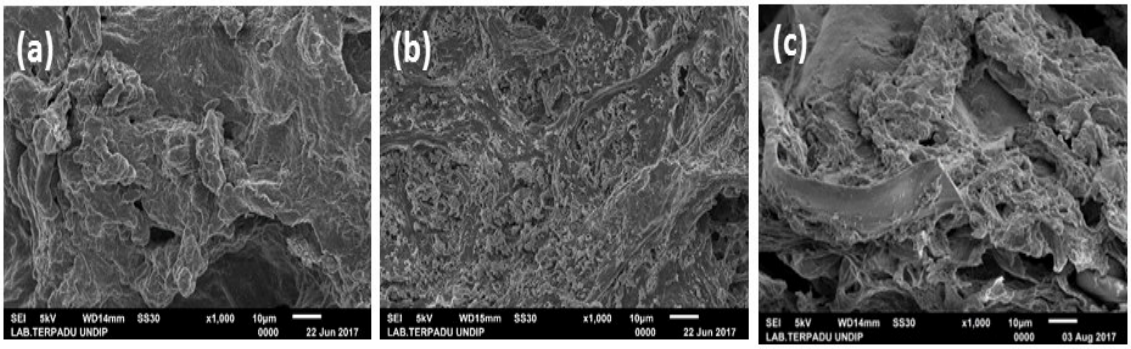

Figure 2
SEM analyses from (a) unallocated chitosan particles, (b) CAF-loaded chitosan particles, (c) ALP-loaded chitosan particles

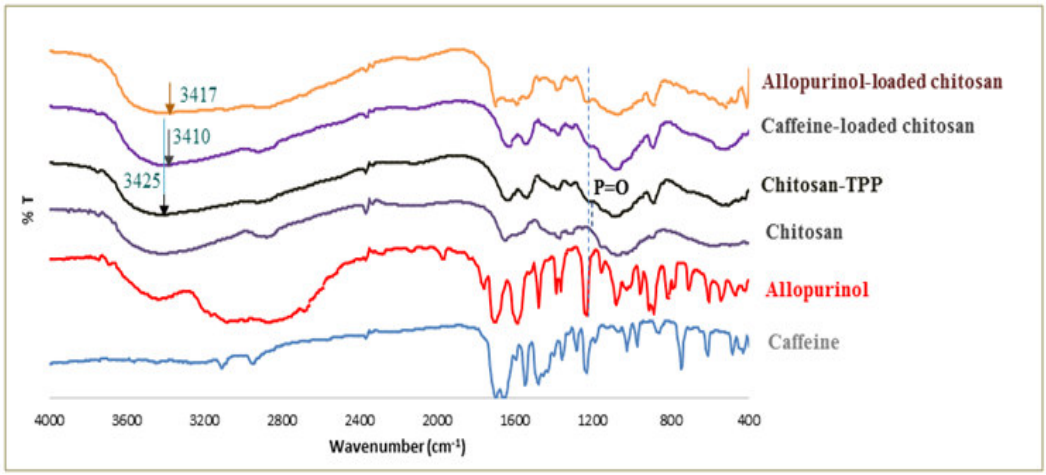

Figure 3
FTIR spectra of alkaloids, chitosan, chitosan-TPP and encapsulated product

The percentage of encapsulation efficiency of CAF and ALP were around 9.62% 40.61% and 12.45 65.90 %, respectively while the loading capacity were about 0.07% 1.29% and 0.37-10.54%. The result of encapsulation efficiency from these two compounds showed the contrary results. The efficiency of encapsulation was decreased by reducing the concentration of CAF[23-25], while the increase was observed for ALP. In other hand, loading capacity has linear positive correlation with active compounds concentration.[26]

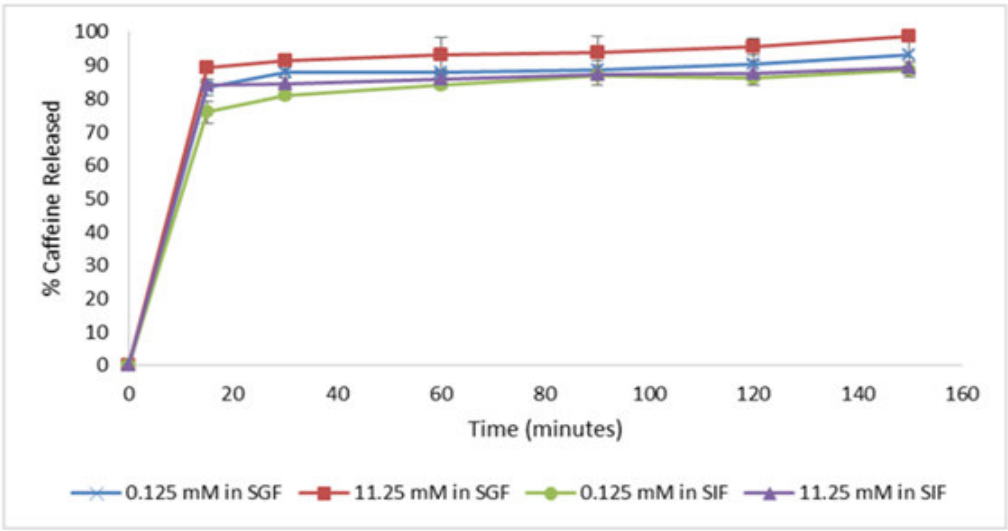

Graph 2
In vitro release profiles of caffeine from chitosan particles prepared by different concentration of caffeine 0.125 mM (LC minimum) and 11.25 mM (LC optimum) in SGF (acid medium) and SIF (base medium). Values were expressed as mean (n = 2)

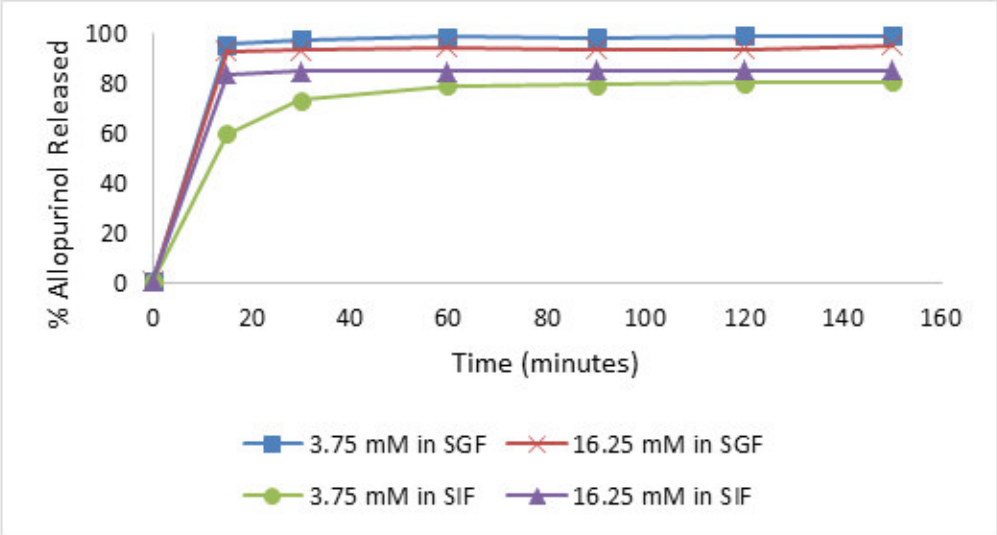

Graph 3

In vitro release profiles of allopurinol from chitosan particles using different concentration of allopurinol 3.75 mM (LC minimum) and 16.25 mM (LC optimum) in SGF (acid medium) and SIF (base medium). Values were expressed as mean (n = 2)

DISCUSSION:

The result shows that encapsulation efficiency ALP is higher than CAF (Figure 2A). Which can prove the hypothesis in this study? Base on Figure 1, there are three ion pairs in nitrogen can be uses for hydrogen bond and two hydrogen atoms can receive ion pairs from oxygen of the matrix. Compare with CAF which only have one possible hydrogen bond from the matrix. ALP may attach more to the matrix compare to CAF. Therefore, encapsulation efficiency of ALP is higher than CAF. The ALP loading capacity also higher than CAF (figure 1b), but the encapsulation efficiency and loading capacity tend to be in contrary. The efficiency of encapsulation was decreased by decreasing the concentration of CAF while the increase was observed for ALP. In the other hand, loading capacity has linear correlation with both bioactive compounds concentration. Previous studies also did not show the correlation between %EE and %LC.[20-24]

The morphology of the chitosan particles as shown in Fig. 2a has a coarse, coagulated and rough surface whereas, the CAF-loaded chitosan particles Fig.2b and ALP-loaded chitosan particle in Fig. 2c have rough surface morphology and shows higher porosity when compared to the chitosan particle which is not yet filled with CAF. This result is similar to the previous study.[24] The comparison of FTIR spectra of CAF, ALP, chitosan, chitosan-TPP, and encapsulated products (CAF-loaded chitosan particles and ALP-loaded chitosan particles) were showed in Fig. 2. In general, chitosan flake show characteristic peaks at 3382 cm^{-1} (overlapping of –OH and $–NH_2$ stretching vibration)[25], 2886–2854 cm^{-1} (-CH stretching), 1634 cm^{-1} (C=O stretching), 1565 cm^{-1} (-NH bending), 1062 cm^{-1} (C–O–C) and 887 cm^{-1} (pyranose ring).[21] For chitosan particles, the peak of C=O stretching 1651 cm^{-1} and -NH bending 1597 cm^{-1} shifted to 1635,64 cm^{-1} and 1543,05 cm^{-1} respectively, and new peak appeared at 1219 cm^{-1} (P=O) implying the complex formation via electrostatic interaction between phosphoric groups and ammonium ions.[26] The spectrum of CAF in KBr, the band at 3093 cm^{-1} corresponds to C–H stretching of heterocyclic compounds, while the strong bands at 1699 and 1659 cm^{-1} are attributed to the carbonyl group of amide (C=O).[27] Peak at 1234 cm^{-1} correspond to amine group (C-N) and at 748 cm^{-1} showed strong band of alkyl group.[28] The FTIR spectrum of CAF-loaded chitosan showing the possible interaction between CAF with chitosan-TPP. The spectrum of this product shows the shifted wavenumber in the –OH stretching from 3425 cm^{-1} to 3410 cm^{-1}, showing the possible interaction of CAF with chitosan-TPP. FTIR spectrum of pure ALP characterized by the absorption bands at 3441 cm^{-1} (N-H stretching band of secondary amine group), 3047 cm^{-1} (C-H stretching vibration of pyrimidine ring), 1705 cm^{-1} (C=O stretching vibration of the keto form of 4-hydroxy tautomer). The bands at (1589-1481) cm^{-1} are attributed predominantly to C-N stretching and C-C ring stretching respectively.

Bands at 1232-702 cm^{-1} denote CH in plane deformation.[29] The FTIR spectrum of ALP loaded chitosan show the shifted wavenumber of –OH stretching from 3425 cm^{-1} to 3417 cm^{-1} and peaks ALP appeared in 1705 cm^{-1} and 1234 cm^{-1}, showing the possible interaction of ALP with chitosan-TPP.

Graphs 2 and 3 showed the release outline of CAF and ALP. The cumulative release profile (in percent) for CAF and ALP is principally similar. The initial burst release of CAF occurred in 15 minutes reaching 70-80% in SIF (base medium) and 80-90% in SGF (acid medium), while for ALP happened in 59-83% in SIF and 92-95% in SGF. Profile releases are then followed by slow releases before reaching the plateau stage within 150 minutes. The slow release that occurs at the latter stage is probably due to the limited capacity of simulated gastric acid and intestinal to break down chitosan particles. This reasons the absence of the release of additional active compounds at this stage. The initial burst release of the two alkaloids is probably affected by the location of the active compound that adsorbed on the surface of the encapsulation matrix. The degradation rate of chitosan near the surface is high, consequently the amount of alkaloid released will similarly be high.[21,30] Release occurs faster in acid simulation fluid than neutral liquid. In the acidic environment, the swelling of the polymer matrix occurs due to protonation of the amine group in chitosan.[30] Protonation in this matrix triggers a weakening of the electrostatic interaction between ammonium ions in the chitosan chain and phosphorus groups of TPP molecules, subsequently the CAF and ALP are released very quickly.

CONCLUSION:

We can conclude that the maximum encapsulation efficiency of ALP is higher than CAF. The efficiency of encapsulation is decreased by reducing the concentration of CAF, while the increase was observed for ALP. In other hand, loading capacity has positive linear correlation with active compounds concentration. SEM images of the optimum efficiency of encapsulation product showed that the of CAF-loaded chitosan particles is rough surface with high porosity, while ALP is not uniform. The FTIR data showed the interaction between chitosan particles and CAF/ALP. Based on the controlled release test, both of these alkaloids released in the simulated gastric fluid (acid medium) is greater than in simulated intestinal fluid (base medium).

ACKNOWLEDGEMENTS:

We would like to acknowledge to the financial support from Universitas Diponegoro (RPP Research Programe, 2016/2017).

REFERENCES:

1. Suzery, M., Hadiyanto, Sutanto, H., Soetrisnanto, D., Majid, D., Setyawan, D., and Azizah, N., 2015, The improvement of phycocyanin stability extracted from Spirulina sp using extrusion encapsulation technique, AIP Conference Proceedings, 1699
2. Madene, Atmane, Muriel Jacquot, Joël Scher, and Stéphane Desobry, 2006, Flavour Encapsulation and Controlled Release - A Review, International Journal of Food Science and Technology, 41, 1–21.
3. Ezhilarasi, P. N., Karthik, P., Chhanwal, N., and Anandharamakrishnan, C., 2013, Nanoencapsulation Techniques for Food Bioactive Components: A Review, Food and Bioprocess Technology, 6, 628–647
4. Silva, P. T. da, Fries, L. L. M., Menezes, C. R. de, Holkem, A. T., Schwan, C. L., Wigmann, É. F., Silva, C. de B. da. , 2014, Microencapsulation: concepts, mechanisms, methods and some applications in food technology, *Ciência Rural*, *44*, 1304–1311
5. Chan, E., Yim, Z., Phan, S., Mansa, R. F., dan Ravindra, P., 2009, Food and Bioproducts Processing Encapsulation of herbal aqueous extract through absorption with ca-alginate hydrogel beads, Food and Bioproducts Processing, 88, 195–201
6. Park, K, and Yeo, Y., 2007, Microencapsulation Technology, In Swabrick, J. Encyclopedia of Pharmaceutical Technology, 3 rd ed, volume 4. New York: Informa Healthcare USA, 2317-2327.
7. Nagavarma, B.V.N., Hemant K.S.Y., Ayaz A, Vasudha, L.S, and Shivakumar, H.G., 2012, Different

Techniques For Preparation Of Polymeric Nanoparticles-A Review, Asian J Pharm Clin Res, 5, 16-23
8. Zhang, L., and Kosaraju, S. L. (2007). Biopolymeric delivery system for controlled release of polyphenolic antioxidants. *European Polymer Journal*, *43*, 2956–2966.
9. Natalia, I., Arruda, Q. De, Aniceto, V., Jr, P., and Stefani, R. (2017). Application of chitosan matrix for delivery of rutin. *Journal of the Iranian Chemical Society*, *14*, 561–566.
10. Zeng, R., Tu, M., Liu, H., Zhao, J., Zha, Z., and Zhou, C. (2009). Preparation , structure , drug release and bioinspired mineralization of chitosan-based nanocomplexes for bone tissue engineering. *Carbohydrate Polymers*, *78*, 107–111.
11. Cahyono, B., Suzery, M., Hadiyanto, H. and Pratiwi, S.B., Encapsulation Rutin with Chitosan-NATPP Using Coaservation Method, Reaktor.17(4), 215-220
12. Cahyono, B. A'yun, Q., Suzery, M., and Hadiyanto, H., Characteristics of eugenol loaded chitosan-tripolyphosphate particles as affected by initial content of eugenol and their in-vitro release characteristic, IOP Conference Series: Materials Science and Engineering 349 (1), 012010
13. Manske, RHF. The alkaloids. Chemistry and physiologi, Akademic Press Inc. Publisher, New York, 1960. vol 1. p. 17 and 133,
14. O'Neil MJ (ed), The Merk Index-anEncyclopedia of Chemical Drugs and Biologicals Whitenhouse Station, NJ: Merk and Co, Inc, 2006, p. 50
15. Day, R. O., Graham, G. G., Hicks, M., Mclachlan, A. J., Stocker, S. L., and Williams, K. M., 2007, Clinical Pharmacokinetics and Pharmacodynamics of Allopurinol and Oxypurinol, Clin Pharmacokinet, 46, 623–644
16. Agyemang-yeboah, Francis, and Sylvester Yaw Oppong, 2013, Caffeine : The Wonder Compound, Chemistry and Properties, Topical Series in Health Science 1, 661, 27–37.
17. Robert, A. M. and L. Robert, 2014, Xanthine Oxido-Reductase, Free Radicals and Cardiovascular Disease. A Critical Review, Pathology & Oncology Research, 20, 1-10
18. Fleeman, N., Pilkington, G., Dundar, Y., Dwan, K., Boland, A., Dickson, R., Anijeet, H., Kennedy, T., and Pyatt, J., 2014, Allopurinol for the treatment of chronic kidney disease: a systematic review, Health Technology Assessment, No. 18.40
19. Sledz, W., Los, E., Paczek, A., Rischka, J., Motyka, A., Zoledowska, S., and Lojkowska, E., 2015, Antibacterial activity of caffeine against plant pathogenic bacteria, 62, 605-612.
20. Lv, X., 2010, Caffeine protects against alcoholic liver injury by attenuating inflammatory response and oxidative stress. Inflammation Research, 59, 635- 645.
21. Woranuch, Sarekha, and Rangrong Yoksan, 2013, Eugenol-Loaded Chitosan Nanoparticles: I. Thermal Stability Improvement of Eugenol through Encapsulation, Carbohydrate Polymers, 96, 578–85
22. Jose, S., Prema, M. T., Chackoa, A. J., Thomas, A. C., dan Souto, E. B., 2011, Colon specific chitosan microspheres for chronotherapy of chronic stable angina, Colloids and Surfaces B: Biointerfaces, 83, 277–283.
23. Hosseini, Seyed Fakhreddin, Mojgan Zandi, Masoud Rezaei, and Farhid Farahmandghavi, 2013, Two-Step Method for Encapsulation of Oregano Essential Oil in Chitosan Nanoparticles: Preparation, Characterization and in Vitro Release Study, Carbohydrate Polymers, 95, 50–56.
24. Ajun, Wan, Sun Yan, Gao Li, and Li Huili, 2009, Preparation of Aspirin and Probucol in Combination Loaded Chitosan Nanoparticles and in Vitro Release Study, Carbohydrate Polymers, 75, 566–74.
25. Yoksan, Rangrong, Jatesuda Jirawutthiwongchai, and Kridsada Arpo, 2010, Encapsulation of Ascorbyl Palmitate in Chitosan Nanoparticles by Oil-in-Water Emulsion and Ionic Gelation Processes, Colloids and Surfaces B: Biointerfaces, 76, 292–97.
26. Wu, Y., Yang, W., Wang, C., Hu, J., and Fu, S., 2005, Chitosan nanoparticles as a novel delivery system for ammonium glycyrrhizinate, International Journal of Pharmaceutics, 295, 235–245.
27. Bhumkar, Devika R, and Varsha B Pokharkar, 2006, Studies on Effect of pH on Cross-Linking of Chitosan with Sodium Tripolyphosphate: A Technical Note, AAPS PharmSciTech, 7, E50.
28. Zou, X., Zhao, X., Ye, L., Wang, Q., and Li, H., 2015, Preparation and drug release behavior of pH-responsive bovine serum albumin-loaded chitosan microspheres, Journal of Industrial and Engineering Chemistry, 21, 1389–1397.
29. Xu, Yongmei, and Yumin Du,(2003, Effect of Molecular Structure of Chitosan on Protein Delivery

Properties of Chitosan Nanoparticles, International Journal of Pharmaceutics 250, 215–26.
30. Belscak-Cvitanovic, A., Komes, D., Karlović, S., Djaković, S., Špoljarić, I., Mršić, G., and Ježek, D., 2015, Improving the controlled delivery formulations of caffeine in alginate hydrogel beads combined with pectin, carrageenan, chitosan and psyllium, Food Chemistry, 167, 378–386.
31. Saputro, C. K. H., Suptijah, P., Djajadisastra, J., Kirana, C., Saputro, H., and Hidayat, T., 2015, The Characterization and Effectiveness Penetrasion of Caffeine Trapped and Coated Chitosan Nanoparticles as Anti-Cellulite, Journal of Nanoscience and Nanoengineering, 1, 198–205.
32. Ammar, A. A., Samy, A. M., Marzouk, M. A., and Ahmed, M. k., 2011, Formulation, Characterization And Biopharmaceutical Evaluation Of Allopurinol Tablets, International Journal of Biopharmaceutics, 80–88.
33. Anitha, A., Deepagan, V. G., Divya Rani, V. V., Menon, D., Nair, S. V., and Jayakumar, R., 2011, Preparation, characterization, in vitro drug release and biological studies of curcumin loaded dextran sulphate-chitosan nanoparticles, Carbohydrate Polymers, 84, 1158–1164.

FP-31

A FUNCTIONAL HYBRID PLASMID DERIVED FROM COMMERCIAL VECTORS PCAMBIA1303 AND PRI201-ON FOR HETEROLOGOUS GENE EXPRESSION IN MD2 PINEAPPLE

NOOR HYDAYATY MD YUSUF[1]; MARIAM ABD LATIP[2]; VIJAY S. KUMAR[1*]

[1]Biotechnology Research Institute; [2]Faculty of Science and Natural Resources, Universiti Malaysia Sabah, Kota Kinabalu, Sabah, Malaysia

*Corresponding author: vijay@ums.edu.my

ABSTRACT

Gene manipulation has become a routine procedure in many types of fundamental and applied research on plant transformation and tissue culture. Although various genetic transformation approaches are available, it generally shares a common component i.e., a plasmid vector equipped with various selection markers and a suitable expression cassette (promoter, enhancer, and terminator) to promote gene expression in specific plants. However, many commercially available vectors lack these components, including for pineapple. In addition to that, no expression vector available for the expression of artificial microRNA (amiRNA) in pineapple. To overcome this problem, we developed a functional hybrid plasmid using two commercial plasmid, pCambia1303 and pRI201-ON, using a simple two step protocols to examine the expression of amiRNA in MD2 pineapple. This new hybrid plasmid is equipped with markers for a selection of transformants, and an independent expression cassette for gene expression in monocotyledon crop. More importantly, it was able to express amiRNA in MD2 pineapple successfully. This protocol may also be applicable for the construction of similar hybrid plasmid for other monocotyledons and dicotyledons.

KEYWORDS:
MD2 Pineapple, artificial microRNA, pCambia Plasmid, pRI201 Plasmid, Expression Vector, Heterologous Expression

INTRODUCTION:

Genetic transformation is one of a major activity in plant-based research. It is generally used to discover novel genes and to profile its function leading towards the development of new varieties (Cantó-Pastor *et al*., 2015; Gordon-Kamm *et al*., 1990; Kasuga *et al*., 1999; Rakoczy-Trojanowska, 2002). The three commonly used techniques to horizontally transfer genes into plants are *Agrobacterium*-mediated transformation, particle bombardment, and gene gun. Although the mechanism of these techniques varies, they all share a common goal i.e. to deliver plasmids containing gene(s) of interest (GOI) into the host cells. To ensure the expression of the GOI, the transgene construct is fused with a set of regulatory genes, which includes a promoter, enhancer and terminator regions, resulting what is known as an expression cassette. In addition, to ensure efficient screening of transformants, the plasmid vector is equipped with a set of selection markers, which includes antibiotic resistance genes (for plant and bacteria), reporter genes for β-glucuronidase (GUS) staining, and a reporter gene for Green Fluorescent Protein (GFP) screening.

The pCambia plasmid series is one of the most utilised plasmid vector for studies on gene expression in plants (Costa *et al*., 2002; Hiei and Komari, 2006; Ma *et al*., 2012). It has at least 30 derivatives with various combinations of genes for the selection of transformants. These include genes for plant selection (hygromycin, kanamycin, or phosphinothricin resistance gene), bacterial selection (spectinomycin/streptomycin, chloramphenicol, kanamycin, and spectinomycin/streptomycin and kanamycin resistance gene), polylinker (pUC18, pUC8, and pUC9), and reporter genes for GUS and GFP screening (*gusA, mgfp*5, *gusA:mgfp*5 fusion, *mgfp5:gusA* fusion, and *Staphylococcus* sp. *gusA*) (www.cambia.org). However, the Multiple Cloning Site (MCS) region of pCambia (where the GOI is to be

inserted), lacks an expression cassette to ensure the expression of the transgene. In contrast, the pRI201 plasmid series offers a unique expression cassette, with specific enhancers for GOI expression in monocotyledons and dicotyledons. However, this plasmid lacks the selection markers that are present in pCambia, offering only kanamycin resistance and GUS reporter gene.

We, therefore, decided to combine the unique features of these two commercial plasmids to produce a functional hybrid plasmid that is able to negate each other's disadvantages. We then tested to see if this new hybrid plasmid, which is equipped with at least three selection markers and an expression cassette, is able to express the GOI in pineapple after performing *Agrobacterium* mediated transformation. For the purpose of this experiment, the GOI insert contained a region known as artificial microRNA (amiRNA). MicroRNAs (miRNA) are short sequences of RNA that are involved in gene silencing of mRNA transcripts, preventing the expression of proteins during translation (Ambros *et al*., 2003; Bartel *et al*., 2004). On the other hand, amiRNA is a genetic-based technology developed to mimic gene silencing by miRNA. Its difference, however, also represents an advantage over the use of miRNA, whereby it can be custom-designed to silence a specific target gene within an organism (Ossowski *et al*., 2008; Schwab *et al*., 2006). We have designed amiRNA named amiR535 aiming to silence *MIR535* gene in MD2 pineapple. We then performed qPCR to verify the expression of amiR535, which is indicative of a successful construction of the hybrid plasmid. *MIR535* is one of the many miRNAs found in pineapple and reported to be differentially expressed during fruit ripening (Yusuf *et al*., 2011; Yusuf *et al*., 2015). The function of MR535 is still unknown and yet to be profiled. The establishment of amiRNA expression vector targeting for this *MIR535* family may open a room for the development of knock-down mutant for functional profiling.

MATERIAL AND METHODS:

Construction of a hybrid plasmid

The hybrid plasmid for expression of amiR535 (amiR535-EC-pCambia1303) was constructed through a two-step approach (See Figure 1.A and 1.B). Firstly, the amiR535 was inserted into the pRI201-ON plasmid. The region with the expression cassette and amiR535 in pRI201-ON is referred to as the amiR535 expression cassette (amiR535-EC). Secondly, the amiR535-EC region was then digested and ligated into pCambia1303 to produce a hybrid plasmid for the expression of amiR535. This is referred to as the amiR535-EC-pCambia1303 plasmid, and it has a size of 13,712 bp. The hybrid plasmid without the amiR535 is referred to as EC-pCambia1303 (See Figure 1.C), and it has a size of 13,636 bp. This newly designed plasmid has a combination of the unique features found in the two commercial plasmids (See Figure 1.D). Details on the methodology for both steps as described below:

Step 1: Ligation of amiR535 in pRI201-ON plasmid (Figure 1.A)

The GOI (amiR535 gene) was flanked with an *Nde*I and *Sal*I RE site at the 5' and 3' end, respectively. The whole region was then custom-synthesised by Integrated DNA Technology (IDT, Singapore). Next, the pRI201-ON plasmid (Takara) was digested with *Nde*I and *Sal*I restriction enzymes (New England Biolabs) prior to ligation with the newly synthesized amiR535 using T4 DNA Ligase (New England Biolabs). Both digestion and ligation reactions were performed according to the protocol suggested by the manufacturer. The pRI201-ON plasmid ligated with amiR535 was then cloned into *E. coli* Top 10 (Invitrogen) and cultured in an LB broth. The plasmid was subsequently isolated using the Wizard® Plus VS Minipreps (Promega), and its DNA sequence was verified through Sanger sequencing using the BigDye Terminator V3.1 (Applied Biosystems). The protocols used were as suggested by the respective manufacturers.

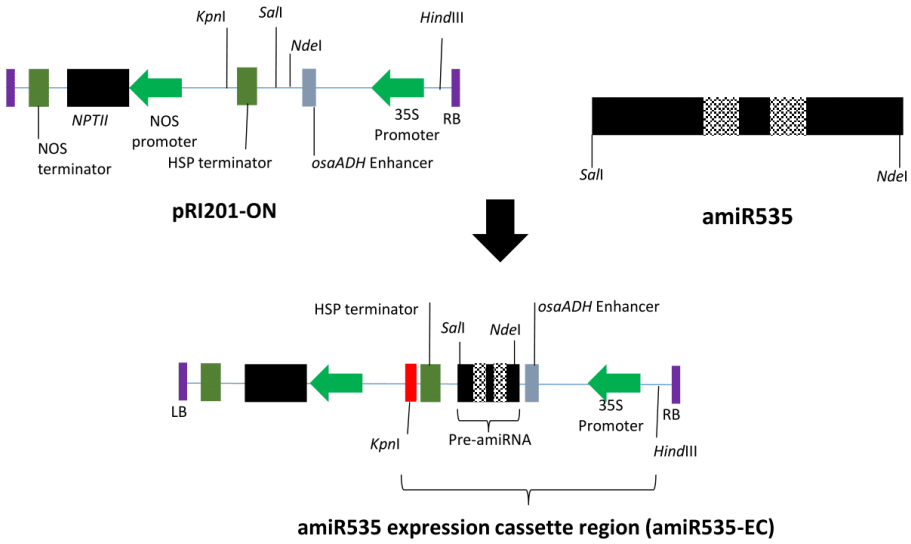

Figure 1 (A)

Figure shows the synthetic amiR535 with *Sal*I and *Nde*I was ligated inside complement restriction site region of pRI201-ON, at a position between OsADH 5'-UTR Enhancer and the HSP terminator. After ligation, the region between *Kpn*I and *Hind*III representing the amiR535 expression cassette region (amiR535-EC), which consists of the CaMV 35S promoter, OsADH 5'-UTR Enhancer, pre-amiRNA and HSP terminator. Note: The size does not represent the size of each element.

Step 2: Ligation of amiR535-EC in pCambia1303 (Figure 1.B)

The plasmid retrieved from step 1 (which is referred to as the amiR535 expression cassette or amiR535-EC and containing the 35S promoter, OsADH 5'-UTR enhancer, amiR5353, and HSP terminator) was digested with *Hind*III and *Kpn*I (NEB). The plasmid pCambia1303 was also digested, with the same enzymes, to ensure successful ligation with the amiR535-EC using T4 DNA Ligase (NEB). The newly formed hybrid plasmid, called amiR535-EC-pCambia1303, was then cloned into *E. coli* Top 10, cultured in LB broth, had its plasmid extracted and verified through Sanger sequencing as described in Step 1.

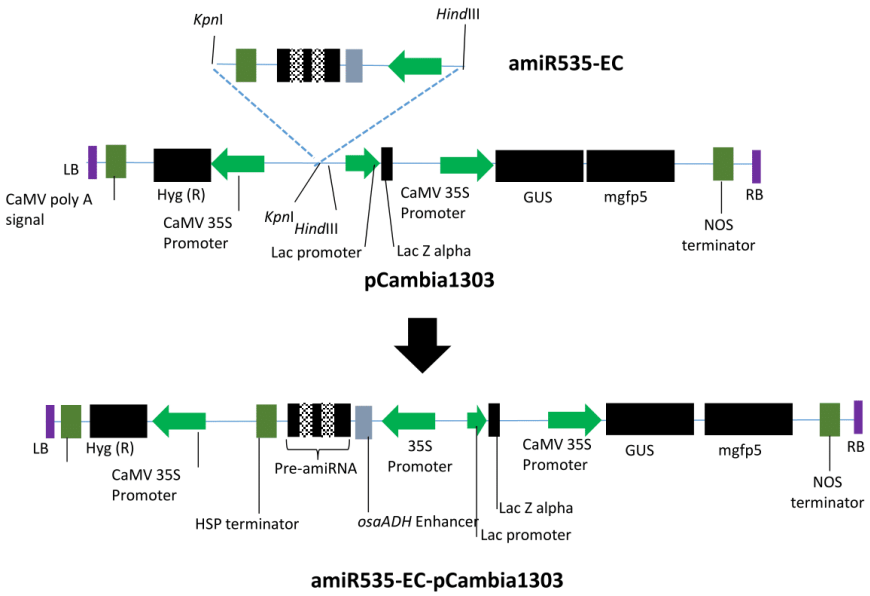

Figure 1 (B)

The ligation of amiR535-EC located between *Kpn*I and *Hind*III region of the pRI201-ON vector into the pCambia1303 vector. After ligation, the pCambia1303 with amiR535-EC representing the hybrid plasmid containing GOI (amiR535) called amiR535-EC-pCambia1303. Note: The size does not represent size of each element.

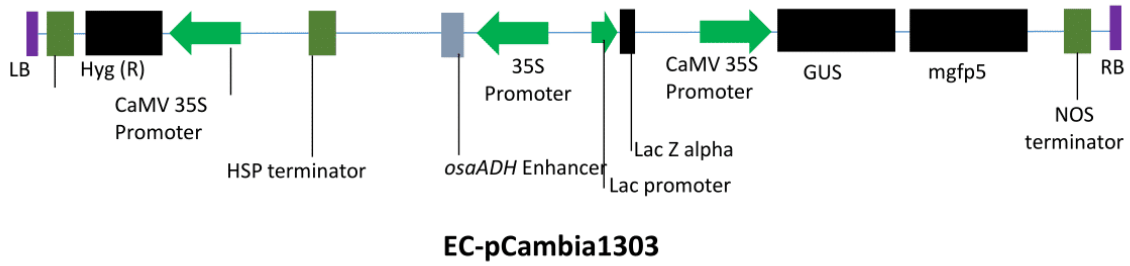

Figure 1 (C)
Figure shows the hybrid plasmid without GOI, called EC-pCambia1303. Note: The size does not represent size of each element.

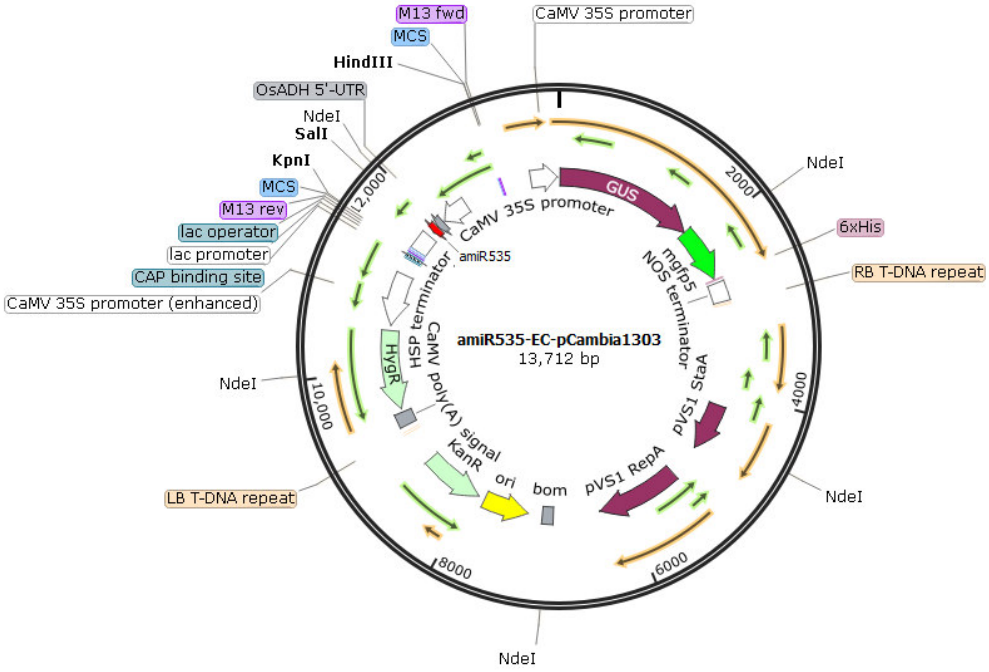

Figure 1 (D)
Overview of the map of the hybrid plasmid with GOI (amiR535), the amiR535-EC-pCambia1303 expression vector. The amiR535-EC is located in between *Kpn*I and *Hind*III region. The pCambia1303, which is the backbone of this hybrid plasmid contained all three selection markers (GUS, GFP, and hygromycin resistance gene), while the independent expression cassette (CaMV 35S promoter, OsADH 5'-UTR enhancer, and HSP terminator) for the gene expression in monocotyledons was from pRI201-ON.

Transformation of plasmids into pineapple and hygromycin selection

The newly designed plasmids were transformed into *Agrobacterium tumefaciens* strain LBA4404 (Invitrogen) using the cold shock transformation procedure as recommended by the manufacturer. The *Agrobacterium* strain was then used to transform the calli of MD2 pineapple. Prior to this, the calli were induced from shoot meristem obtained from the pineapple crown using optimum Calli Induction (CI) medium (Yusuf *et al*., 2016). It was then inoculated with *A. tumefaciens* and co-cultivated for three days, and then transferred into a medium containing hygromycin and carbenicillin for the selection of transformants (Yusuf *et al*., 2016).

GUS Histochemical Analysis

GUS histochemical analysis was performed by incubating the transformed calli in a GUS solution (100 mM of Na_3PO4 (pH 7.0), 10 mM of EDTA, 0.5 mM of $K_3Fe(CN)_6$, 0.5 mM of $K_4Fe(CN)_6$, 1 mg/ml of x-gluc powder, and 0.1% Triton X-100) for 48 hours at 37°C. Next, the calli was transferred into 75% ethanol and

incubated for 24 hours (Jefferson, 1987; Subramanian and Rathinam, 2010). The surface of the calli was then visually inspected for traces of blue, an indication of cell transformation. Non-transformed cells remained white in colour.

Gene expression profiling

RNA was then extracted from the transformed calli using Trizol (Invitrogen) according to the protocol recommended by the manufacturer. The quality and quantity of RNA extracted was examined with a Bioanalyzer using the RNA 6000 Nano Kit (Agilent). The RNA was then converted into cDNA through stem-loop reverse transcription reaction (stem-loop RT) according to the protocol of Li *et al*. (2009). The reaction was performed using the SuperScript® III First-Strand Synthesis System (Invitrogen) and the protocol used was as recommended by the manufacturer. The stem-loop RT product were then used for qPCR amplification and quantification of the *β-actin* gene using the iTaq Universal SYBR Green Supermix (Bio-Rad). The qPCR amplification began with pre-denaturation at 95^{O}C for 5 minutes followed by 35 cycles of incubation at 95^{O}C for 1 minute, 58^{O}C for 1 minute, and 72^{O}C for 1 minute, with a final elongation step at 72^{O}C for 5 minute (Li *et al*., 2009). Gene expression data were analysed according to the formula by Livak and Schmittgen (2001).

RESULTS AND DISCUSSION:

A new hybrid plasmid was developed using a combination of pRI201-ON and pCambia1303 genes. As such, the expression cassette (EC) encompassed a 35S promoter, OsADH 5'-UTR enhancer and a HSP terminator region of the pRI201-ON was inserted into pCambia1303. The hybrid plasmid is referred to as EC-pCambia1303. In addition to this, a hybrid plasmid for the expression of amiR535 is referred to as amiR535-EC-pCambia1303.

We performed *Agrobacterium* mediated transformation of pineapple callus. Putative transgenic calli of MD2 pineapple transformed with the hybrid plasmid EC-pCambia1303 tested positive when stained with GUS. The transformed calli was also found resistant towards hygromycin as it survived and regenerated when cultured on media supplemented with the antibiotic. The results also showed no significant changes of the *β-actin* gene between transgenic lines expressing empty pCambia1303 and EC-pCambia1303 when normalised with non-transformed pineapples (See Figure 1.E). Therefore, this hybrid plasmid is suitable for expressing genes in pineapples, as it does not interfere with differential expression or morphological changes. Then, we observe the efficacy of this hybrid plasmid to express the GOI (amiR535-EC-pCambia1303) in MD2 pineapple. High level expression of amiR535 (minimum C_Q value of 18) was noted hence, it marks the suitability of the expression cassette from pRI201-ON vector in expressing a gene in pineapples. We therefore, confirm the functionality and the expression stability of this hybrid plasmid.

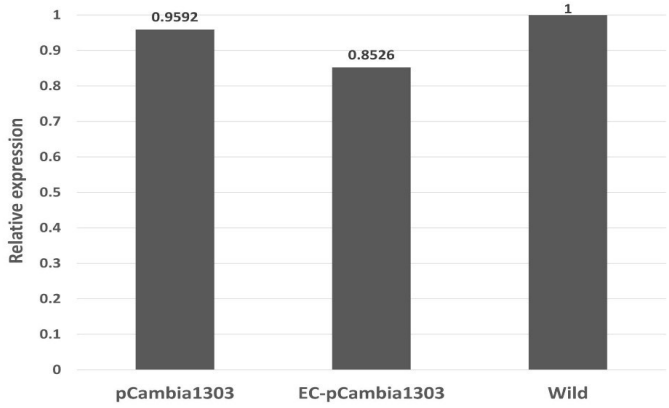

Figure 1 (E)
Overview of the relative expression of *β-actin* expressed by hybrid plasmid (EC-pCambia1303) and empty pCambia1303 (Control) in relation to the *β-actin* in wild (non-transformed) MD2 pineapple (control). There are no significant changes in the expression between all samples.

This simple two step protocol involves routine RE digestion and ligation procedure, which can potentially ease the difficulties faced in the lengthy conventional procedure on plasmid construction. The use of an expression cassette from pRI201-ON with OsADH 5'-UTR enhancer may help enhancing the gene expression in monocotyledon plants. As for dicotyledons, a similar hybrid plasmid can be constructed by utilising this protocol and replacing the pRI201-ON plasmid with any other plasmids in the pRI201 series for example, pRI201-AN, which contains a AtADH 5'- UTR enhancer for gene expression in dicotyledons. The OsADH 5' UTR and AtADH 5' UTR enhancer in this plasmid has been utilised for efficient transient expression and mutagenesis in plants (Blażejewska *et al*., 2017; Carvalho *et al*., 2016; Kaya *et al*., 2016). The components of this hybrid plasmid may also be customised to have different plant selection markers, bacterial selection markers, polylinkers, and reporter genes by utilising different derivatives of pCambia vectors. Therefore, this simple protocol can be used to construct a functional hybrid plasmid to fit different research objectives in monocotyledons or dicotyledons by utilising the pRI201 (pRI201-ON and pRI201-AN) and most plasmids in pCambia series.

The compatibility of these plasmids (pCambia1303 and pRI201-ON, and some of its derivatives) rely on the location of the selected RE site (*Nde*I, *Sal*I, *Kpn*I, and *Hind*III), which promotes direct insertion of DNA fragment into the specific region. Due to this, this two -step protocol may not work in other series of plasmid with differing RE sites.

ACKNOWLEDGEMENT:

This research was partly supported by the Ministry of Science, Technology and Innovation, Malaysia via the ScienceFund research grant scheme (SCF0087-BIO-2013), and from the Ministry of Higher Education, Malaysia via the Fundamental Research Grant Scheme (FRG0319-SG-2013).

ETHICS STATEMENT:

The transgenic activity was approved by the National Biosafety Committee, Ministry of Natural Resources and Environment, Malaysia (Reference number: JBK(S) 602-1/2/77(19).

REFERENCES:

1. Ambros, V., Bartel, B., Bartel, D.P., Burge, C.B., Carrington, J.C., Chen, X., Dreyfuss, G., Eddy, S.R., Griffithf-Jones, S., Marshall, M., Matzke, M., Ruvkun, G. & Tuschl, T. 2003. A uniform system for microRNA annotation. *RNA*. 9:277-279.
2. Bartel, D.P. 2004. MicroRNAs: Genomics, biogenesis, mechanism, and function. *Cell*. 116: 281–297.
3. Blażejewska, K., Kapusta, M., Zielińska, E., Tukaj, Z. and Chincinska, I. 2017. Mature Luffa leaves (*Luffa cylindrica* L.) as a tool for gene expression analysis by agroinfiltration. *Frontiers in plant Science*. 8:1-10.
4. Cantó-Pastor, A., Mollά-Morales, A., Ernst E., Dahl, W., Zhai, J., Yan, Y., Meyers, B., Shanklin, J. and Martienssen, R. 2015. Efficient transformation and artificial miRNA gene silencing in *Lemna minor*. *Plant Biology*. 17:59-65.
5. Carvalho, R. F., Carvalho, S. D., O'Grady, K. and Folta K. M. 2016. Agroinfiltration of strawberry fruit – A powerful transient expression system for gene validation. *Current Plant Biology*. 6: 19-37.
6. Costa, M. G. C., Otani, W. C. and Moore, G. A. 2002. An evaluation of factors affecting the efficiency of *Agrobacterium* mediated transformation of *Citrus paradisi* (Macf.) and production of transgenic plants containing carotenoid biosynthetic genes. *Plant Cell Reports*. 21:365-373.
7. Gordon-Kamm, W. J., Spencer, T. M., Mangano, M. L., Adams, T. R., Daines, R. J., Start, W. G., O'Brien, J. V., Chambers, S. A., Adams, W. R., Willetts, N. G., Rice, T. B., Mackey, C. J., Krueger, R. W., Kausch, A. P. and Lemaux, P. G. 1990. Transformation of maize cells and regeneration of fertile transgenic Plants. *The Plant Cell*. 2:603-618.
8. Hiei, Y. and Komari, T. 2006. Improved protocols for transformation of indica rice mediated by *Agrobacterium tumefaciens*. *Plant Cell, Tissue and Organ Culture*. 85:271-283.

9. Jefferson, R.A. (1987). Assaying chimeric gene in plants: the GUS gene fusion system. *Plant Molecular Biology Reporter*. 5:387-405.
10. Kasuga, M., Liu, Q., Miura, S., Yamaguchi-Shiozaki, K. and Shinozaki, K. 1999. Improving plant drought, salt, and freezing tolerance by gene transfer of a single stress-inducible transcription factor. *Nature Biotechnology*. 17:287–291.
11. Kaya, H., Mikami, M., Endo, A., Endo, M. and Toki, S. 2016. Highly specific targeted mutagenesis in plants using *Staphylococcus aureus* Cas9. *Scientific Reports*. 6: 1-9.
12. Li, H., Zhang, Z., Huang, F., Chang, L. & Ma, Y. 2009. MicroRNA expression profiles in conventional and micropopagated strawberry (*Fragaria X ananassa*Duch.). *Plant Cell Reports*. 10.
13. Livak, K.J. and Schmittgen, T.D. 2001. Analysis of relative gene expression data using real-time quantitative PCR and the $2^{-\Delta\Delta CT}$ Method. *Methods*. 5:402-408.
14. Ma, J., He, Y.H., Wu, C.H., Liu, H.P., Hu, Z.Y. and Sun, G.M. 2012. Effective Agrobacterium-mediated transformation of pineapple with *CYP1A1* by kanamycin selection technique. *African Journal of Biotechnology*. 11:2555-2562.
15. Ossowski, S., Schwab, R. and Weigel, D. 2008. Gene silencing in plants using artificial microRNAs and other small RNAs. *The Plant Journal*. 53: 674-690.
16. Schwab, R., Ossowski, S., Riester, M., Warthmann, N and Weigel, D. 2006 Highly Specific Gene Silencing by Artificial MicroRNAs in Arabidopsis. *The Plant Cell*. 18:1121–1133.
17. Subramaniam, S. and Rathinam, X. 2010. Emerging factor that influence efficiency of T-DNA gene transfer into *Phalaenopsis violacea* orchid via *Agrobacterium tumefaciens* –mediated transformation system. *International Journal of Biology*. 2:64-73.
18. Yusuf, N.H.M. & Kumar, S.V. 2011. Identification and characterization of differentially expressed microRNAs during fruit ripening in Pineapple (*Ananascomosus* var. *comosus*). *Acta horticulturae*. 902:123-131.
19. Yusuf, N.H.M., Ong, W.D., Redwan, R.M., Latip, M.A. & Kumar, S.V. 2015. Discovery or precursor and mature microRNAs and their putative gane targets using high-throughput sequencing in pineapple (*Ananas comosus* var. *comosus*). *Gene*. 571:71-80.
20. Yusuf, N. H. M., Latip, M. A. and Kumar, S. V. 2016. Efficient protocol for plant regeneration and from callus cultures and *Agrobacterium* transformation of MD2 pineapple. *Transactions of Persatuan Genetik Malaysia.* 3:137-141.

FP-32

IN SILICO STUDY: THE ANTICANCER POTENCY OF HYPTOLIDE AND ANALOGUE COMPOUNDS THROUGH MECHANISM OF α-TUBULIN INHIBITION

UMMI LAILI ROCHMAWATI[1], MUKHAMMAD ASY'ARI[1] AND MEINY SUZERY[2*]

[1]Biochemistry Research Group, Faculty of Science and Mathematics, Diponegoro University, Jl. Prof. H. Sudharto, SH., Semarang, Indonesia [2]Organic Chemistry Research Group, Faculty of Science and Mathematics, Diponegoro University, Jl. Prof. H. Sudharto, SH., Semarang, Indonesia

Corresponding author : meiny_suzery@yahoo.com

ABSTRACT

Cancer is abnormal cells that growth continuously and spread throughout the body. Cancer can be treatment by chemotherapy. The pironetin compound is a chemotherapy drug which works by inhibiting microtubule formation. Hyptolide is an analogue compound of pironetin which it has lactone ring. Based on in vitro results showed that hyptolide has anticancer activity. However, the current mechanism of hyptolide interaction against cancer cell components is still unknown. The purpose of this study was to predict the anticancer potency of hyptolide and analogue compounds as well as their interaction with tubulin. This research was performed by blind and direct molecular docking methods using autodock vina program as plugin PyRx 0.8 software. Based on the experiment results were indicated that blind docking results in single chain shows tendency to form clusters patterns on the part of body chain, while dimer and multi chains on the part of inter chain. The interactions pattern of ligands that occupy in area around the tubulin binding sites tends to increase base on docking result from single, dimer until multi chains. Based on direct docking results indicate the best position and orientation of ligands in the binding site tubulin that are synrotolide (38%), hyptolide (9%), pectinolide B (6%) and pironetin (4%). The best binding affinity values are for synrotolide (-6.9 kcal/mol), pectinolide B (-6.5 kcal/mol) and standard pironetin (-7.0 kcal/mol). Based on the most negative of binding affinity values (-7.5 kcal/mol) were caused the hyptolide is predicted to have the strongest potency of anticancer agent.

KEYWORDS:
Hyptolide, synrotolide, pectinolide B, pironetin, alpha-tubulin, anticancer, in silico, autodock vina

INTRODUCTION

Currently, cancer is the leading cause of death in the world. In 2012 there were 14.1 million cases of cancer and 8.2 million deaths worldwide. By 2017 there are projected 1.6 million cases of cancer and 600 thousand cancer deaths occur in the United States. The number will increase to 21.7 million cases of cancer and 13 million deaths by 2030.[1-2] Several ways can be used to treat cancer, ie. surgery, chemotherapy, hormonal therapy, radiation therapy, adjuvant therapy and immunotherapy.[3] Chemotherapy is a way of treatment by using chemical compounds that work directly on cancer cells. Several kinds of chemotherapy drugs are alkylating agents, antimetabolites, topoisomerase inhibitors, mitotic inhibitors and corticosteroids.[4] Drugs acting through the mechanism of mitotic inhibitors such as vinblastin and pironetin may inhibit microtubule formation. The drug inhibitory mechanism occurs by direct binding with the tubulin subunit so as to interfere with the formation of microtubules.[5] Microtubules are a key component of the cytoskeleton that plays a role in cell division and consists of α- and β-tubulin heterodimers.[6] Pironetin is a natural compound proven to be an anticancer by inhibiting the interaction of tubulin heterodimer through covalent bonding with cysteine-316 in α-tubulin.[5,7] The pironetin compound is similar to hyptolide which has a cyclic lactone ring in its molecular structure. The hyptolide compounds were isolated from the plant *Hyptis pectinata* Poit which has been experimentally proven to have cytotoxic properties of shrimp larvae *Artemia salina* leach and breast cancer cells MCF-7.[8] Hyptolide is analogous to synrotolide and pectinolide B because it has three

main functional groups, ie cyclic lactone ring, double bond C = C unconjugated and acetate group.[9] The verification of cytotoxic properties of hyptolide compounds has been performed but the mechanism of interaction with tubulin is still unknown. The protein-ligand interaction can be predicted by in silico method ie molecular docking. The molecular docking simulation objective to find the best position and orientation of ligand on target protein binding site.[10-11] Hence, the purpose of this research is to obtain in silico predictions the potency of hyptolide and analogue compounds as anticancer agents through the mechanism of inhibition of microtubule formation.

MATERIALS AND METHODS:

This research was carried out using hardware with Intel (R) Pentium (R) CPU processor N3540 @ 2.1GHz, RAM 2 GB, Windows 8.1 Pro 64-bit. The programs used are VMD 1.9.2,[12] Chimera 1.11.2,[13] autodock vina plugin PyRx 0.8 software,[11] Open Babel GUI 2.3.1,[14] and LigPlot + 1.4.5.[15] The 3-dimensional structure of hyptolide and analogue compounds is obtained from the website https://pubchem.ncbi.nlm.nih.gov. The 3-dimensional structure of tubulin and pironetin is obtained from protein databank (PDB) code: 5LA6 and 4I55 [7,16] accessible via http://www.rcsb.org.

Preparation of 3-dimensional structure of proteins and ligands

The 3-dimensional structure preparation was performed on all proteins and ligands using the Visual Molecular Dynamics program (VMD 1.9.2) and Chimera 1.11.2. Some formatting coordinate structures in dot pdb files were performed using the Open Babel GUI program. Improvements to missing loops on single chain tubulin (5LA6) were performed by modeling the refinement loop using the Chimera 1.11.2 plugin program Model/Refine Loop. The refinement model was selected based on the most negative value of ZDOPE. The complete 3-dimensional structures of the protein were carried out to minimization stage of the Chimera 1.11.2 plugin program called Minimize Structure with default settings.

Structural validation of proteins and ligands

The ligands structure was validated via website http://davapc1.bioch.dundee.ac.uk/cg i-bin/prodrg. On the validation of protein structures linked via site http://molprobity.biochem.duke.edu, by including the tubulin chain protein c code of 5LA6 PDB that has been separated through the VMD program.

Molecular docking

The molecular docking process was performed by two methods i.e., blind and direct docking using autodock vina program plugin PyRx 0.8. The direct docking was performed by adjusting the ligand position on the tubulin binding site (pdb code: 5LA6). The grid box settings are performed on coordinates (13, 37, 3) and 33.2 Å x 26 Å x 27.4 Å dimensions. The blind docking process was performed on two tubulin proteins i.e., pdb code: 5LA6 and 4I55, including single, dimer and multi chains. Coordinate settings were performed using the maximum scale grid box in the Pyrx 0.8 software. The data used in the docking analysis were resulted from 10 repetitions and has been selected based on position, clusters number and affinity binding values.

RESULTS:

Ligand-protein interaction patterns on tubulin surface

Based on results of blind docking of single and dimer chains showed a tendency to form clusters on the body chain while multi chains tend to the inter chain. Based on cluster pattern analysis showed that ligands from blind docking in multi chains have similarities with dimer chains that tend to occupy inter chain clusters between B and C chain (Figure 1).

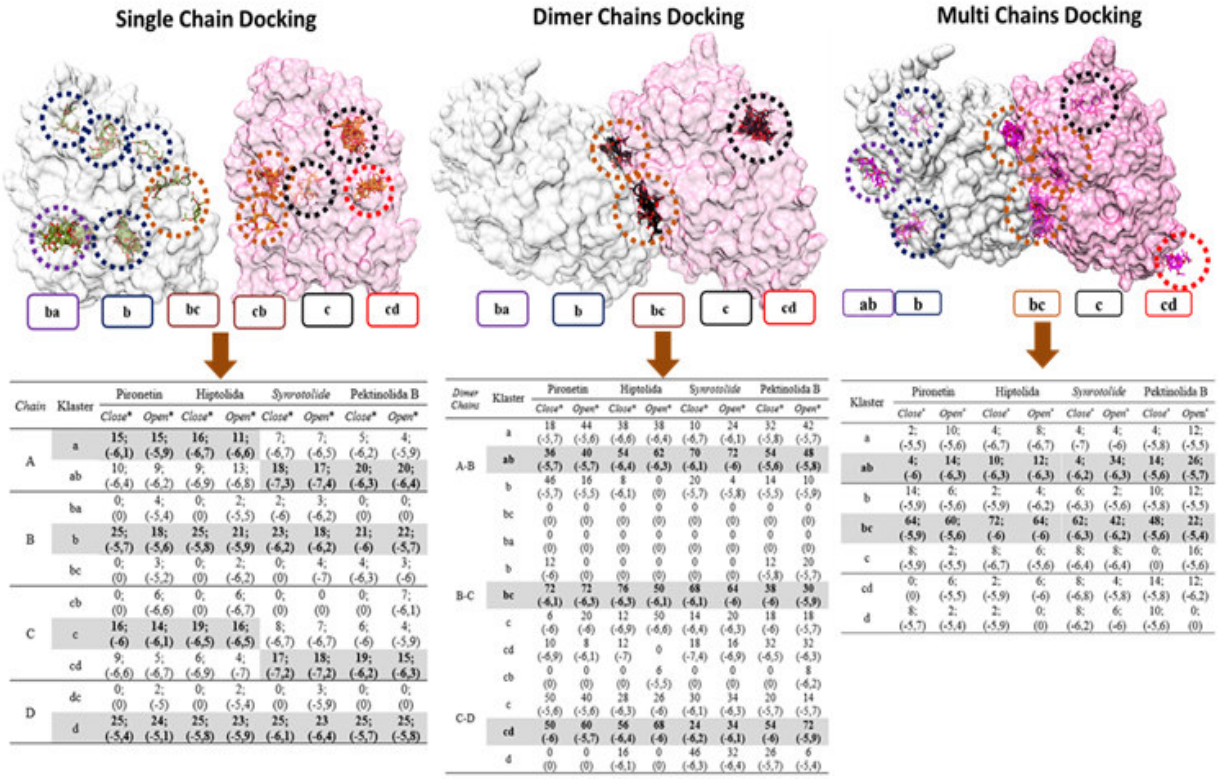

Chain	Klaster	Pironetin		Hiptolida		Synrotolide		Pektinolida B	
		Close*	Open*	Close*	Open*	Close*	Open*	Close*	Open*
A	a	15; (-6,1)	15; (-5,9)	16; (-6,7)	11; (-6,6)	7; (-6,7)	7; (-6,5)	5; (-6,2)	4; (-5,9)
	ab	10; (-6,4)	9; (-6,2)	9; (-6,9)	13; (-6,8)	18; (-7,3)	17; (-7,4)	20; (-6,3)	20; (-6,4)
B	ba	0; (0)	4; (-5,4)	0; (0)	2; (-5,5)	2; (-6)	3; (-6,2)	0; (0)	0; (0)
	b	25; (-5,7)	18; (-5,6)	25; (-5,8)	21; (-5,9)	23; (-6,2)	18; (-6,2)	21; (-6)	22; (-5,7)
	bc	0; (0)	3; (-5,2)	0; (0)	2; (-6,2)	0; (0)	4; (-7)	4; (-6,3)	3; (-6)
C	cb	0; (0)	6; (-6,6)	0; (0)	6; (-6,7)	0; (0)	0 (0)	0; (0)	7; (-6,1)
	c	16; (-6)	14; (-6,1)	19; (-6,5)	16; (-6,5)	8; (-6,7)	7; (-6,7)	6; (-6)	4; (-5,9)
	cd	9; (-6,6)	5; (-6,7)	6; (-6,9)	4; (-7)	17; (-7,2)	18; (-7,2)	19; (-6,2)	15; (-6,3)
D	dc	0; (0)	2; (-5)	0; (0)	2; (-5,4)	0; (0)	3; (-5,9)	0; (0)	0; (0)
	d	25; (-5,4)	24; (-5,1)	25; (-5,8)	23; (-5,9)	25; (-6,1)	23 (-6,4)	25; (-5,7)	25; (-5,8)

Dimer Chains	Klaster	Pironetin		Hiptolida		Synrotolide		Pektinolida B	
		Close*	Open*	Close*	Open*	Close*	Open*	Close*	Open*
A-B	a	18 (-5,7)	44 (-5,6)	38 (-6,6)	38 (-6,4)	10 (-6,7)	24 (-6,1)	32 (-5,8)	42 (-5,7)
	ab	36 (-5,7)	40 (-5,7)	54 (-6,4)	62 (-6,3)	70 (-6,1)	72 (-6)	54 (-5,6)	48 (-5,8)
	b	46 (-5,7)	16 (-5,5)	8 (-6,1)	0 (0)	20 (-5,7)	4 (-5,8)	14 (-5,5)	10 (-5,9)
	bc	0 (0)	0 (0)	0 (0)	0 (0)	0 (0)	0 (0)	0 (0)	0 (0)
	ba	0 (0)	0 (0)	0 (0)	0 (0)	0 (0)	0 (0)	0 (0)	0 (0)
	b	12 (-6)	0 (0)	0 (0)	0 (0)	0 (0)	0 (0)	12 (-5,8)	20 (-5,7)
B-C	bc	72 (-6,1)	72 (-6,3)	76 (-6,3)	50 (-6,1)	68 (-6,1)	64 (-6)	38 (-6)	50 (-5,9)
	c	6 (-6)	20 (-6)	12 (-6,9)	50 (-6,6)	14 (-6,4)	20 (-6,3)	18 (-6)	18 (-5,7)
	cd	10 (-6,9)	8 (-6,1)	12 (-7)	0	18 (-7,4)	16 (-6,9)	32 (-6,5)	32 (-6,3)
	cb	0 (0)	0 (0)	0 (0)	6 (-5,5)	0 (0)	0 (0)	0 (0)	8 (-6,2)
C-D	c	50 (-5,6)	40 (-5,6)	28 (-6,3)	26 (-6)	30 (-6,1)	34 (-6,3)	20 (-5,7)	14 (-5,7)
	cd	50 (-6)	60 (-5,7)	56 (-6,4)	68 (-6)	24 (-6,2)	34 (-6,1)	54 (-6)	72 (-5,9)
	d	0 (0)	0 (0)	16 (-6,1)	0 (0)	46 (-6,3)	32 (-6,4)	26 (-5,7)	6 (-5,4)

Klaster	Pironetin		Hiptolida		Synrotolide		Pektinolida B	
	Close'	Open'	Close'	Open'	Close'	Open'	Close'	Open'
a	2; (-5,5)	10; (-5,6)	4; (-6,7)	8; (-6,7)	4; (-7)	4; (-6)	4; (-5,8)	12; (-5,5)
ab	4; (-6)	14; (-6,3)	10; (-6,3)	12; (-6,3)	4; (-6,2)	34; (-6,3)	14; (-5,6)	26; (-5,7)
b	14; (-5,9)	6; (-5,6)	2; (-5,9)	4; (-6,2)	6; (-6,3)	2; (-5,6)	10; (-5,8)	12; (-5,5)
bc	64; (-5,9)	60; (-5,6)	72; (-6)	64; (-6)	62; (-6,3)	42; (-6,2)	48; (-5,6)	22; (-5,4)
c	8; (-5,9)	2; (-5,5)	8; (-6,7)	6; (-5,6)	8; (-6,4)	8; (-6,4)	0; (0)	16; (-5,6)
cd	0; (0)	6; (-5,5)	2; (-5,9)	6; (-6)	8; (-6,8)	4; (-5,8)	14; (-5,8)	12; (-6,2)
d	8; (-5,7)	2; (-5,4)	2; (-5,9)	0; (0)	8; (-6,2)	6; (-6)	10; (-5,6)	0; (0)

Figure 1
Percentage and binding affinity ligands from results blind docking on single, dimer and multi chains tubulin

Predictions of ligand-protein interaction on pathway to tubulin binding sites

The results of blind docking in open tubulin showed that ligands occupy four areas ie. 1, 2, 3, and 4. These four areas are predicted to be the ligands entry pathway to the binding sites. Whereas, in tubulin close, the ligands occupy only one area so that predicted ligands will enter to binding sites through only one pathway (Figure 2).

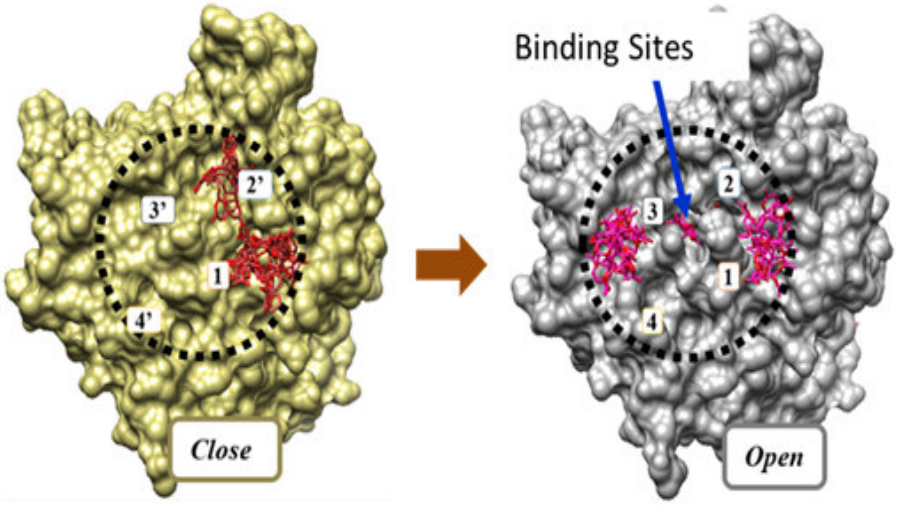

Figure 2
Prediction of ligands pathways to close and open tubulin binding sites.

The pattern of ligands interactions that occupy in area around the tubulin binding sites tends to increase base on docking result from single, dimer and multi chains (Table 1).

Table 1

Percentage and binding affinity ligands from results of direct docking on single, dimer and multi chains tubulin

Single chain

Position	Pironetin		Hiptolida		*Synrotolide*		Pektinolida B	
	*Close**	*Open**	*Close**	*Open**	*Close**	*Open**	*Close**	*Open**
Overlap	0 (0)	6 (-6,6)	0 (0)	4 (-7,1)	0 (0)	0 (0)	0 (0)	7 (-6,1)
Near	0 (0)	0 (0)	0 (0)	2 (-5,7)	0 (0)	0 (0)	0 (0)	0 (0)
	0 (0)	6 (0)	0 (0)	6 (-6,7)	0 (0)	0 (0)	0 (0)	7 (-6,1)

Dimer chains

Position	Pironetin		Hiptolida		*Synrotolide*		Pektinolida B	
	*Close**	*Open**	*Close**	*Open**	*Close**	*Open**	*Close**	*Open**
Overlap	0 (0)	10 (-6,7)	0 (0)	0 (0)	0 (0)	6 (-6,5)	0 (0)	20 (-5,4)
Near	0 (0)	30 (-6)	14 (-6,3)	50 (-6,1)	20 (-6,2)	52 (-6)	4 (-5,7)	4 (-6,2)
	0 (0)	40 (-6,2)	14 (-6,3)	50 (-6,1)	20 (-6,2)	58 (-6)	4 (-5,7)	24 (-6)

Multi chains

Position	Pironetin		Hiptolida		*Synrotolide*		Pektinolida B	
	*Close**	*Open**	*Close**	*Open**	*Close**	*Open**	*Close**	*Open**
Overlap	0 (0)	0 (0)	0 (0)	8 (-6,9)	0 (0)	0 0	0 (0)	0 (0)
Near	6 (-5,9)	42 (-5,5)	36 (-6)	40 (-6)	32 (-6,3)	40 (-6,2)	24 (-5,6)	12 (-5,4)
	6 (-5,9)	42 (-5,5)	36 (-6)	48 (-6,1)	32 (-6,3)	40 (-6,2)	24 (-5,6)	12 (-5,4)

The best position, orientation and binding affinity of ligands on tubulin binding sites

Observation of position and orientation ligands were performed based on the results of the direct docking on tubulin chain c "open" on it's binding site. Direct docking objective obtain the best position, orientation and binding affinity values of all ligand-protein interactions. Based on direct docking results indicate the number of the best position and orientation of ligands that are synrotolide (38%), hyptolide (9%), pectinolide B (6%) and pironetin (4%). The best binding affinity values for hyptolide (-7,5 kcal/mol), standard pironetin (-7.0 kcal/mol), synrotolide (-6.9 kcal/mol) and pectinolide B (-6.5 kcal/mol) respectively (Table 2).

Table 2

The number of Interactions and binding affinity values of ligands with amino acid residues on tubulin binding sites

	Pironetin	Hiptolida	*Synrotolide*	Pektinolida B
Binding Affinity (kkal/mol)	-7 (kkal/mol)	-7,5 (kkal/mol)	-6,9 (kkal/mol)	-6,5 (kkal/mol)
Hydrogen interaction	Ser241		Ile238, Ser241, Gln256,	Ile238, Ser241,
Hydrophobic interaction	Leu136, Leu167, Phe202, Ser237, Ile238, Thr239, Leu242, Phe255, Gln256, Cys316, Leu318, Cys376, Leu378,	Leu136, Leu167, Phe202, Ser237, Ile238, Thr239, Leu242, Ser241, Phe255, Gln256, Leu259 Cys316, Leu317 Leu318, Gln354 Leu378,	Gln133, Leu136, Leu167, Ser237, Leu242, Phe255, Leu 318, Leu378,	Leu136, Leu167, Phe169, Phe202, Thr239, Leu242, Phe255, Leu259 Cys316, Leu318, Leu378,
Number of residues	14	16	11	13

DISCUSSION:

The result of single chain docking was showed non-polar ligands such as pironetin and hyptolide tend to form clusters in the "body" of protein chain because that is non polar areas. In contrast, docking results in dimers and multi chains of ligands tend to lie in the inter-chain protein part because of the formation of new cavities shaped like "coconut shells" in the inter-chains encounter area to form strong ligand binding sites.[18] The bc cluster is the most potency place to bind ligand[5,7] because it has the largest percentage of ligand number and the most negative affinity binding value. In this study was also predicted ligands interaction pattern on the pathway of tubulin binding site. In tubulin "open" there are four areas that predicted to be ligands entry path to the binding site, whereas only one pathway in tubulin "close". These interactions were provided an overview of how ligands move toward to tubulin binding site. The depiction of initial and final conditions in the ligand-protein interaction were provided by two tubulin in closed and open state.[7,16] The results of previous analysis show that cluster bc in tubulin "close" is the starting point of ligand-protein interaction mechanism. The next stage, the ligand will enter to binding site by induction effect that tubulin will further conformational changes become "open" state condition.[5] The results of docking dimer chains results: the large sized ligands such as hyptolide and synrotolide tend to enter binding sites about 50-58%. In contrast, the results of multi chains docking are mostly small sized ligands such as pironetin and pectinolide B. This is due the surface area of tubulin dimer chains is narrow and clamping so that it will direct large sized of ligands to the binding sites area.[5] In addition to surface area and molecular weight of the ligand, polarity properties (based on log P values)[17] may also affect the ligand chances to occupying the binding sites. Based on direct docking results were provided the best binding affinity values were caused by hydrogen and hydrophobic interactions.[11] Whereas, hyptolide has the best negative binding affinity value (-7.5 kcal/mol), it showed the strongest anticancer agent than analogue compounds and pironetin as standard. The strength of hyptolide binding affinity was caused by hydrophobic interaction from 16 surrounding residues.

CONCLUSION:

The results of all blind docking were showed a different tendency to form clusters patterns. The pattern of ligands interactions on the pathway to tubulin binding site tend to increase from single, dimer until multi chains. Based on direct docking results indicate that only a small number of the best position and orientation of ligands. The best binding affinity values of all ligands were caused by hydrogen and hydrophobic interactions. Based on the most strength of hyptolide binding affinity (-7.5 kcal/mol) were caused the hyptolide is predicted to have the strongest potency of anticancer agent. The strength of hyptolide binding affinity was caused by hydrophobic interaction from 16 surrounding residues.

REFERENCES:

1. Siegel, R. L., Miller, K. D., and Jemal, A., Cancer statistics, CA: A Cancer Journal for Clinicians. 2017:67:7–30
2. Torre, L. A., Bray, F., Siegel, R. L., Ferlay, J., Lortet-Tieulent, J., and Jemal, A., Global cancer statistics 2012. CA: A Cancer Journal for Clinicians. 2015:20:1-22
3. Sudhakar, A., History of cancer, ancient and modern treatment methods, J. Cancer Sci Thai. 2010: 1(2): 1–7
4. Meschino, J. P., How chemotherapy drugs work, Dynamic Chiropractic Canada. 2010:3:1–6
5. Yang, J., Wang, Y., Wang, T., Jiang, J., Botting, C. H., Liu, H., Chen, Q., Yang, J., Naismith, J. H., Zhu, X., and Chen, L., Pironetin reacts covalently with cysteine-316 of α-tubulin to destabilize microtubule, Nature Communications. 2016:7:1–9
6. Jordan, M. A., and Wilson, L., Microtubules as a target for anticancer drugs, Nature Reviews. Cancer. 2004:4:253–265
7. Prota, A. E., Setter, J., Waight, A. B., Bargsten, K., Murga, J., Diaz, J. F., and Steinmetz, M. O., Pironetin binds covalently to cys316 and perturbs a major loop and helix of α-tubulin to inhibit microtubule formation. Journal of Molecular Biology. 2016: 428: 2981–2988

8. Suzery, M., and Cahyono, B., Evaluation of cytotoxicity effect of Hyptis pectinata Poit (Lamiaceae) extracts using BSLT and MTT methods. Jurnal Sains dan Matematika. 2014:22:84–88
9. Achmad, S., Hoyer, T., Kjaer, A., Makmur, L., and Norrestam, R., Molecular and crystal structure of hyptolide. a naturally occurring α,β-unsaturated δ-lactone. Acta Chem. Scand. 1987:B41:599-609
10. Leach, A. R., Molecular modelling principles and aplications. Second edition. 2001: Prentice Hall, Essex
11. Trott, O., and Olson, A. J., Software news and update autodock vina: improving the speed and accuracy of docking with a new scoring function, efficient optimization, and multi threading. Journal of Computational Chemistry. 2009:31:455–461
12. Humphrey, W., Dalke, A., and Schulten, K., VMD: visual molecular dynamics, Journal of Molecular Graphics. 1996:14:33–38
13. Pettersen, E. F., Goddard, T. D., Huang, C. C., Couch, G. S., Greenblatt, D. M., Meng, E. C., and Ferrin, T. E., UCSF Chimera - a visualization system for exploratory research and analysis. Journal of Computational Chemistry. 2004:25:1605–1612
14. O'Boyle, N. M., Banck, M., James, C. A., Morley, C., Vandermeersch, T., and Hutchison, G. R., Open babel : an open chemical toolbox. Journal of Cheminformatics. 2011:3:1-14
15. Laskowski, R. A., and Swindells, M. B., LigPlot+: multiple ligand-protein interaction diagrams for drug discovery. Journal of Chemical Information and Modeling. 2011:51:2778–2786
16. Prota, A. E., Bargsten, K., Zurwerra, D., Field, J. J., Díaz, J. F., Altmann, K.-H., and Steinmetz, M. O., Molecular mechanism of action of microtubule-stabilizing anticancer agents. Science. 2013:212:1–6
17. Lipinski, C. A., Lombardo, F., Dominy, B. W., and Feeney, P. J., Experimental and computational approaches to estimate solubility and permeability in drug discovery and development settings. Advanced Drug Delivery Reviews. 2001:46:3–26
18. Nogales, E., Wolf, S. G., and Downing, K. H., Structure of the αβ tubulin dimer by electron crystallography, Nature. 1998:391:199–204.

FP-33

STRUCTURAL HOMOLOGY MODELLING AND MOLECULAR DOCKING SIMULATION OF A PUTATIVE SWEET PROTEIN 2S ALBUMIN FROM *Theobroma cacao*

NORZULAIHA ABD KARIM[1], CAHYO BUDIMAN[*1], DIDIK HUSWO UTOMO[2], KENNETH FRANCIS RODRIGUES[1], AZWAN AWANG[3]

[1]Biotechnology Research Institute, Universiti Malaysia Sabah, Sabah, Malaysia, [2]Faculty of Mathematics and Natural Sciences, Brawijaya University, Malang Indonesia, [3]Faculty of Sustainable Agriculture, Universiti Malaysia Sabah, Sabah, Malaysia.

Corresponding author: cahyo@ums.edu.my

ABSTRACT

Mabinlin is a sweet protein which was first isolated from *Capparis masaikai* with uniqueness in its thermal stability and promising to be used as a safe sugar replacer. However, the scarcity of *C. masakai* with impractical and expensive extraction-purification method limits the availability of mabinlin. Recently, a proteomic study revealed that a mabinlin-like protein with 32.2% sequence identity, which was further identified as 2S albumin storage protein (Tc-2S) expressed in *Theobroma cacao* suggesting that Tc-2S might serve as an alternative source for mabinlin. Interestingly, Tc-2S (geneID: EOY12555.1) reported to undergo self-maturation yielding a 9kDa mature region (Tc-9M) that might specifically bind to human sweet taste receptors, hT1R2-T1R3. Yet, no study has been conducted on Tc-2S and Tc-9M as mabinlin-like protein. This study aims to predict possible sweetness of Tc-2S and Tc-9M using bioinformatics approach. The 3D structure of Tc-2S and Tc-9M were built by SWISS-MODEL while, the hT1R2-T1R3 receptor was built by SWISS-MODEL Beta server for modelling hetero-oligomers. The result showed that the 3D models of Tc-2S and Tc-9M are acceptable according to statistic evaluation parameters. To explore the possible interaction between Tc-2S and Tc-9M with the hT1R2-T1R3 receptor, 3D-Docking computational was performed using GRAMM-X v.1.2.0, Vakser Lab. Docking analysis showed that Tc-2S bind to the receptors at around the same sites of other sweet proteins do. However, Tc-9M apparently has better the fitting orientation towards the receptor as compared to Tc-2S. Nevertheless, these demonstrated the possibility of these proteins to exhibit a sweet response, yet had remained to be experimentally evidenced. Altogether, this study will provide platforms for further investigation on the sweetness of Tc-2S and Tc-9M as a mabinlin-like protein from *T. cacao* and applications as sugar replacers.

KEY WORDS:

Sweet protein, 2S albumin, Structural homology modelling, Docking, *Theobroma cacao*

INTRODUCTION:

The old hypothesis suggested that excessive sugar intake leads to cardiorenal diseases such as obesity, hypertension, metabolic syndrome, type 2 diabetes and kidney disease[1]. Besides, studies on artificial sweeteners showed that it may cause weight gain, brain tumors, bladder cancer, and many other health hazards[2]. Where, the discoveries of artificial sweeteners not only open the world for low calorie sweeteners and potential sugar replacer, but also started debated on its safety issues. Thus, the demand by consumers for sugar substitutes with high value products and health benefits has been increasing.

Most proteins are tasteless, but there are a limited number of proteins that able to exhibit sweet taste. Up to now, eight sweet proteins named thaumatin, monellin, brazzein, mabinlin, pentadin and egg white lysozyme including two taste modifying proteins, curculin and miraculin that has been identified. Among them, mabinlin II that isolated from *C. masaikai* was found to be 375 times sweeter than sucrose and extremely heat stable where its sweetness is not lost after 48 hours of incubation at 80°C[3,4,5]. However, the used of mabinlin II as natural sweet protein in industry limited by the scarcity of this plant. In addition, the extraction-purification process of mabinlin II from the plant is also complicated and expensive[6].

Recently, a proteomic study revealed that a mabinlin-like protein, which were further identified as 2S albumin storage protein (Tc-2S) expressed in *T. cacao* seed suggesting that *T. cacao* might serve as alternative sources for mabinlin[7,8]. Interestingly, the Tc-2S has been reported to undergo self-maturation yield 9kDa mature region (Tc-9M), which essential for protein packaging that stabilized the folding and subunit interaction[9,10]. The sequence identity with mabinlin II leading to an assumption that Tc-2S and Tc-9M may exhibit similar sweetness and heat stable properties.

The hT1R2 and hT1R3 are G protein coupled receptors that works in heterodimeric as human sweet taste receptor and able recognizes all classes of sweeteners[11,12]. The discovery of hT1R2-hT1R3 receptor allows identification of possible sweetness of Tc-2S and Tc-9M as a mabinlin-like protein and potential natural sugar replacer. However, the hT1R2-hT1R3 receptor having more than 800 residues for each subunit and it's difficult to identify the accurate complete structure experimentally[13]. In this study, the complete structure prediction of the hT1R2-T1R3 receptor was done by the computational study.

MATERIALS AND METHODS:

The Tc-2S sequence was retrieved from GenBank with accession code (gene ID) of EOY12555.1. While, Tc-9M sequence was identified according to a previous report[10]. The hT1R2 and hT1R3 receptors sequence were retrieved from GenBank with accession code (gene ID) of 80834 and 80834, respectively. Then, the Tc-2S and Tc-9M protein sequence were subjected for comparative homology modelling via SWISS-MODEL server[14,15,16]. The structure prediction of complete hT1R2-T1R3 receptor was done through SWISS-MODEL Beta Server for modelling of hetero-oligomers.

The generated 3D models of the hT1R2-T1R3 receptor, Tc-2S, and Tc-9M were structurally evaluated and stereo-chemically analyzed by different evaluation and validation tools. Based on its QMEAN Z-score[17], Ramachandran Plot Analysis by RAMPAGE[18], and compatibility of atomic models by VERIFY3D program[19]. Besides, the Atomic Non-Local Environment Assessment (ANOLEA)[20] and Groningen Molecular Simulation (GROMOS)[21] were determine using SWISS-MODEL server for Protein Structure & Model Assessment Tools.

The 3D protein docking computational was performed to explore the possible interaction between Tc-2S and Tc-9M with the hT1R2-T1R3 receptor. Where, the docking was performed using GRAMM-X Protein-Protein Docking Web Server v.1.2.0 from Vakser Lab server[22,23]. Then, Tc-2S and Tc-9M with hT1R2-T1R3 receptor docking model was view and further analysed by BIOVIA Discovery Studio (Accelrys, United States).

RESULTS AND DISCUSSION:

Homology Modelling and Structural Evaluation

Structure determination involved the arduous process such as expression, purification, finding appropriate crystallization condition, and performing structural analysis by X-ray crystallography or nuclear magnetic resonance (NMR) spectroscopy[24]. Today, informatics and computational biology allow high accuracy protein structure prediction based on template homology modelling that involves the detection of homolog's of known three-dimensional (3D) structure. The protein 3D structure is very important in understanding protein functions, interactions, and localizations[25,26]. Thus, understanding the structure of hT1R2-T1R3

receptor will allow us to identify the mechanisms behind sweet response and also help in designing more effective sweeteners.

The hT1R2-T1R3 receptor has more than 800 residues for each subunit, so finding its accurate structure is difficult either by experimental or computer modelling[13]. The complete structure prediction of both subunits of the hT1R2-TIR3 receptor was built by SWISS-MODEL Beta server for modelling hetero-oligomers that allows submission of multiple target sequences for a single modelling job. The crystal structure of the medaka fish taste receptor T1r2a-T1r3 ligand binding domains in complex with L-glutamine (PBD ID: 5x2m.1) with 33.81% sequence identity used as a template from 76 templates found, as show in figure 1[14,15,16].

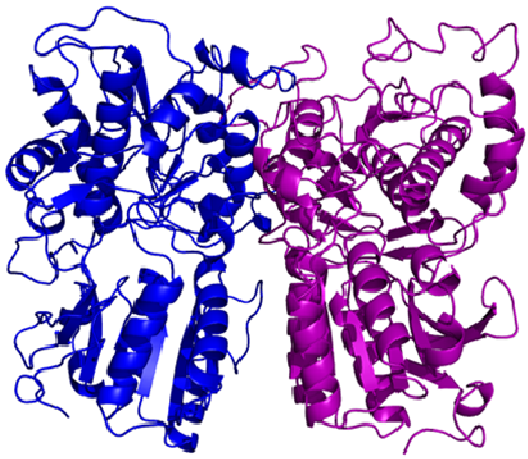

Figure 1
The predicted model of human sweet taste receptor (hT1R2-T1R3 receptor). The hT1R2 and hT1R3 receptor are represent as blue and purple color, respectively. The predicted models were visualized by PyMOL software in the cartoon view and lines removed mode.

The Tc-2S and Tc-9M models as shown in figure 2 were built by homology modeller SWISS-MODEL server based on target-template alignment. The Blast and HHBlits for evolutionary related structures matching the target sequence showed that 25 templates were found for Tc-2S while, 27 templates were found for Tc-9M[27,28]. However, only the solution structure of Brazil Nut 2S albumin Ber e 1 (PDB ID: 2lvf.1.A) with the highest quality compared to the other templates with 30.77% sequence identity to Tc-2S and 31.43 sequence identity to Tc-9M was selected to build both models.

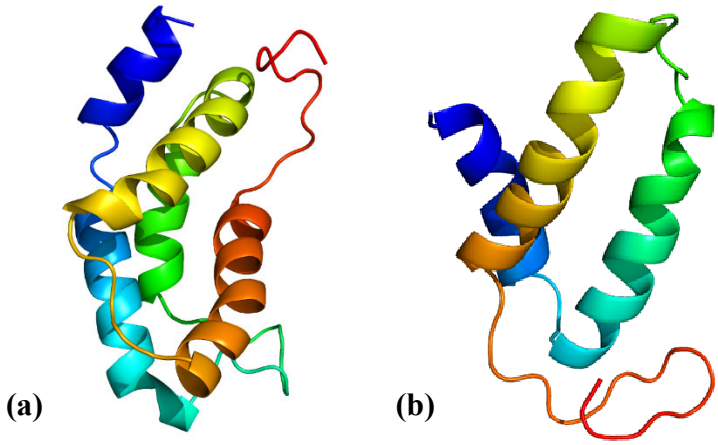

Figure 2
The predicted models of (a) 2S albumin seed storage protein, Tc-2S and (b) its 9kDa mature region, Tc-9M. The predicted models were visualized by PyMOL software in the cartoon view and lines removed mode.

Additional testing for verification and validation model was required to obtain the best predicted protein models with high geometry and conformational score. The predicted models of hT1R2-T1R3, Tc-2S, and Tc-9M were validated using several tools before proceed for the identification of possible interaction and exhibiting of sweet taste. In this study, the validation was done based on QMEAN Z-score, Ramachandran Plot Analysis, 3D-1D profile, ANOLEA, and GROMOS. Where, the model verification analysis using several tools proved that hT1R2-T1R3 receptor, Tc-2S, and Tc-9M models are acceptable.

The global model quality has been assessed using the QMEAN scoring function[17] where, the QMEAN Z-score provides an estimate of the degree of nativeness of the structural features observed in the model and indicates whether the model is of comparable quality to experimental structures. Higher QMEAN Z-scores indicates better agreement between the model structure and experimental structures of similar size. Where scores are more than -4.0 indicates high quality model. The QMEAN Z-score of the hT1R2-T1R3 receptor (-3.31), Tc-2S (-3.61), and Tc-9M (-3.03) indicated high quality models and acceptable quality for experimental.

Ramachandran Plot Analysis by RAMPAGE program was done to validate the backbone conformation with approximation of ideal covalent geometry and trans peptides, the phi (Φ) and psi (Ψ) plot[18]. Ramachandran plot analysis of hT1R2-T1R3 receptor, Tc-2S, and Tc-9M predicted structures as shown in table 1, indicated that all models are in acceptable quality with less than 5% residues in the outlier region.

Table 1
Ramachandran plot analysis of hT1R2-T1R3 receptor, Tc-2S, and Tc-9M predicted structures

Number of residues in:	hT1R2-T1R3 receptor	Tc-2S	Tc-9M
Favoured region (~98.0%)	862 (92.8%)	93 (87.7%)	57 (83.8%)
Allowed region (~2.0%)	49 (5.3%)	11 (10.4%)	9 (13.2%)
Outlier region (<5.0%	18 (1.9%)	2 (1.9%)	2 (2.9%)

Ramachandran plot of hT1R2-T1R3 receptor, Tc-2S, and Tc-9M models

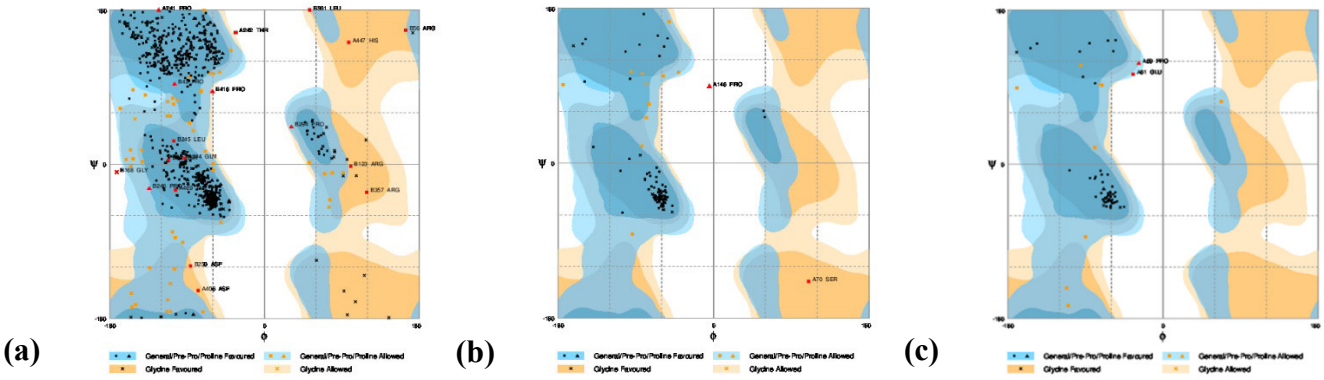

Figure 3
The Ramachandran plot analysis of (a) hT1R2-T1R3 receptor, (b) Tc-2S, and (c) Tc-9M models.

The compatibility of the models with its amino acid sequence were done by VERIFY3D program based on its location and environment such as alpha, beta, loop, polar, and nonpolar. Where, 3D profiles used to evaluate the undetermined protein models, based on low-resolution electron-density maps on NMR spectra with inadequate distance constraints or on computational procedures[19]. The Verify 3D plot indicated that all predicted models are pass with at least 80% of the amino acids have scored more than 0.2 in the 3D-1D profile as shown in table 2.

Table 2
The 3D-1D profile of hT1R2-T1R3 receptor, Tc-2S, and Tc-9M predicted structures

	hT1R2-T1R3 receptor	Tc-2S	Tc-9M
3D-1D score (%)	90.25	85.19	82.86

Local quality of the predicted structure can be estimated using graphical plots of ANOLEA mean force potential and GROMOS empirical force field energy. The atomic empirical mean force potential ANOLEA is used to assess the packing quality of the models. The program performs energy calculations on a protein chain, evaluating the "Non- Local Environment" (NLE) of each heavy atom in the molecule[20]. The y-axis of the plot represents the energy for each amino acid of the protein chain. Negative energy values (green) represent favourable energy environment while, positive values (red) unfavourable energy environment for a given amino acid. The hT1R2-T1R3 receptor (89.80%), Tc-2S (85.98%), and Tc-9M (97.10%) having high amino acid in favourable energy environment as shown on table 3.

Table 3
The favourable energy environment of hT1R2-T1R3 receptor, Tc-2S, and Tc-9M predicted structures

Favourable energy environment (%)	hT1R2-T1R3 receptor	Tc-2S	Tc-9M
ANOLEA	89.80	85.98	97.10
GROMOS	77.89	72.89	65.21

GROMOS is a general-purpose molecular dynamics computer simulation package to study the biomolecular systems and applied to the analysis of conformations obtained by experiment or by computer simulation. The y-axis of the plot represents the energy for each amino acid of the protein chain. Negative energy values (green) represent favourable energy environment whereas positive values (red) unfavourable energy environment for a given amino acid. The hT1R2-T1R3 receptor (77.89%), Tc-2S (72.89%), and Tc-9M (65.21%) having acceptable amino acid in favourable energy environment as shown on table 3.

3D-Docking with hT1R2-T1R3 receptor

Protein and receptor interaction are determined by the structure of each component and also physicochemical properties of the environment. Studies on the structure are important for better understanding of protein functions and interaction[29]. Recent progress in docking algorithms and computer hardware makes it possible to understand the protein interaction. Besides, computer server also allows docking methodologies conducted with unbiased by expert human intervention[23].

The hT1R2 subunit combines with hT1R3 subunit to form sweet taste receptor that responds to all classes of sweet molecules that able to bind with this receptor. This includes sucrose the common table sugar, artificial sweeteners, D-amino acids and intensely sweet protein[12,30]. Until today, the hT1R2-T1R3 receptor key groups or "sweet fingers" that responsible for the exhibition of sweet respond have not yet certainly identify. However, the widely accepted idea is that proper surface charge distribution and three-dimensional shape have to be maintained in order to trigger the sweet sensation.

In this study, 3D-docking computational was performed to explore the possible interaction between Tc-2S and Tc-9M with the hT1R2-T1R3 receptor. Where study on binding interaction with hT1R2-T1R3 receptor identify and prove the ability of Tc-2S and Tc-9M molecules to exhibits sweet taste. Docking was performed using GRAMMX, where the docking method has been optimized to circumvent the multiple minima problems and is best suited to cases in which there is no hint of likely binding sites[31]. Figure 4

shows that the Tc-2S and Tc-9M bind with the hT1R2-T1R3 receptor at the same sites as other sweet proteins do. The docking of other sweet protein as brazzein, mabinlin, neoculin, and thaumatin with the hT1R2-T1R3 receptor, shows that they bind in cleave between the hT1R2 receptor and the T1R3 receptor of the complex (*data is not shown). However, Tc-9M apparently has better the fitting orientation towards the receptor as compared to Tc-2S.

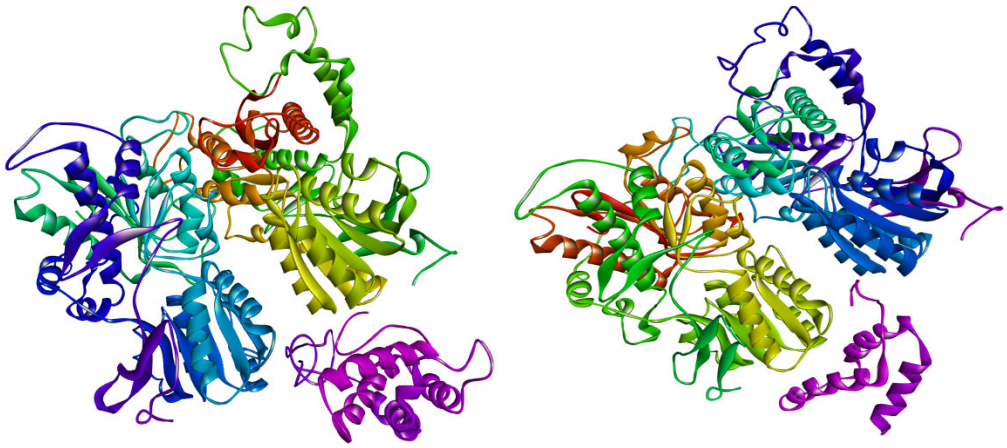

Figure 4
The 3D-docking analysis of (a) Tc-2S and (b) Tc-9M with hT1R2-T1R3 receptor. The predicted models were visualized by BIOVIA Discovery Studio in publication mode.

The further analysis by BIOVIA Discovery Studio showed the surface interaction of the hT1R2-T1R3 receptor with Tc-2S and Tc-9M. In this study, the receptor surface interaction was analysed based on aromatic, hydrogen bonds, interpolated charge, hydrophobicity, ionizability, and SAS. The other factor that most significantly correlates with sweetness is the surface charge. The surface of the hT1R2-T1R3 receptor complex that is described to bind sweet protein is characterized by the presence of a large number of acidic amino acids.

This study demonstrated the possibility of Tc-2S and Tc-9M to exhibit a sweet response. However, computational docking studies can only provide limited indications based on the structure of the receptor and also allow only resolutions predictions. Thus, the sweetness properties of Tc-2S and Tc-9M yet had remained to be experimentally evidenced using triangle tasted by trained panels. Altogether, this study proved that sequence identity and the ability of Tc-2S and Tc-9M to binds with the hT1R2-T1R3 receptor. This could be exploited for the development of potential safe natural low calories sugar replacer.

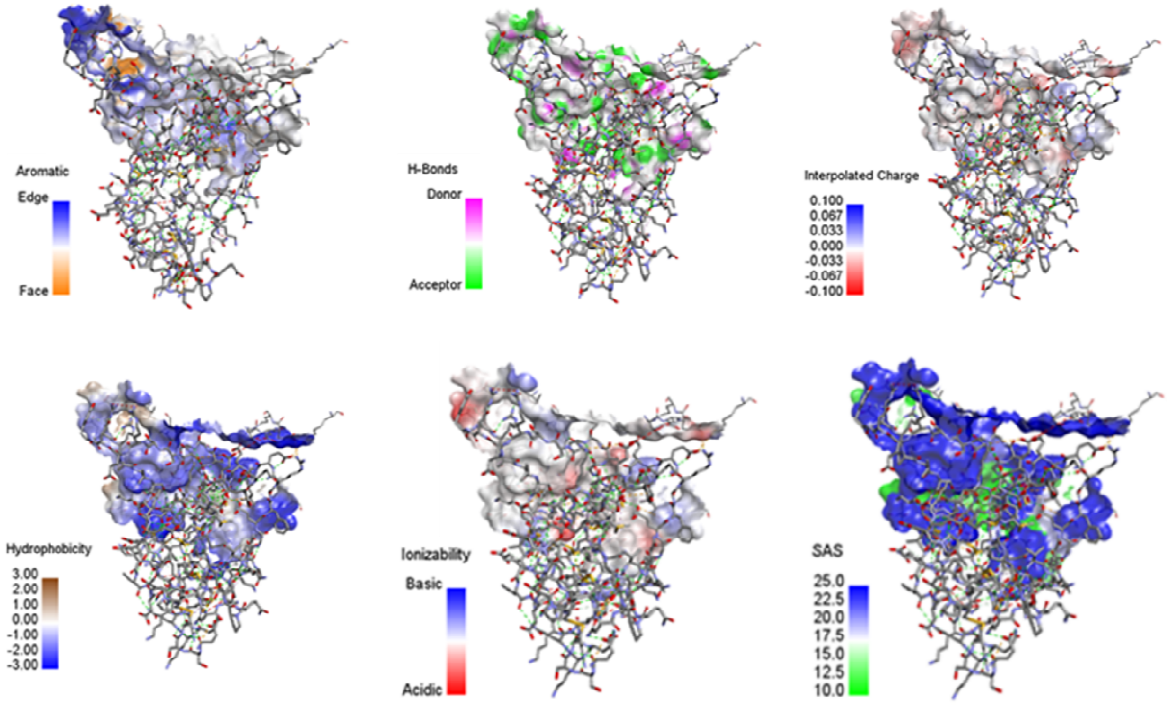

Figure 5
The hT1R2-T1R3 surface receptor interaction with Tc-2S

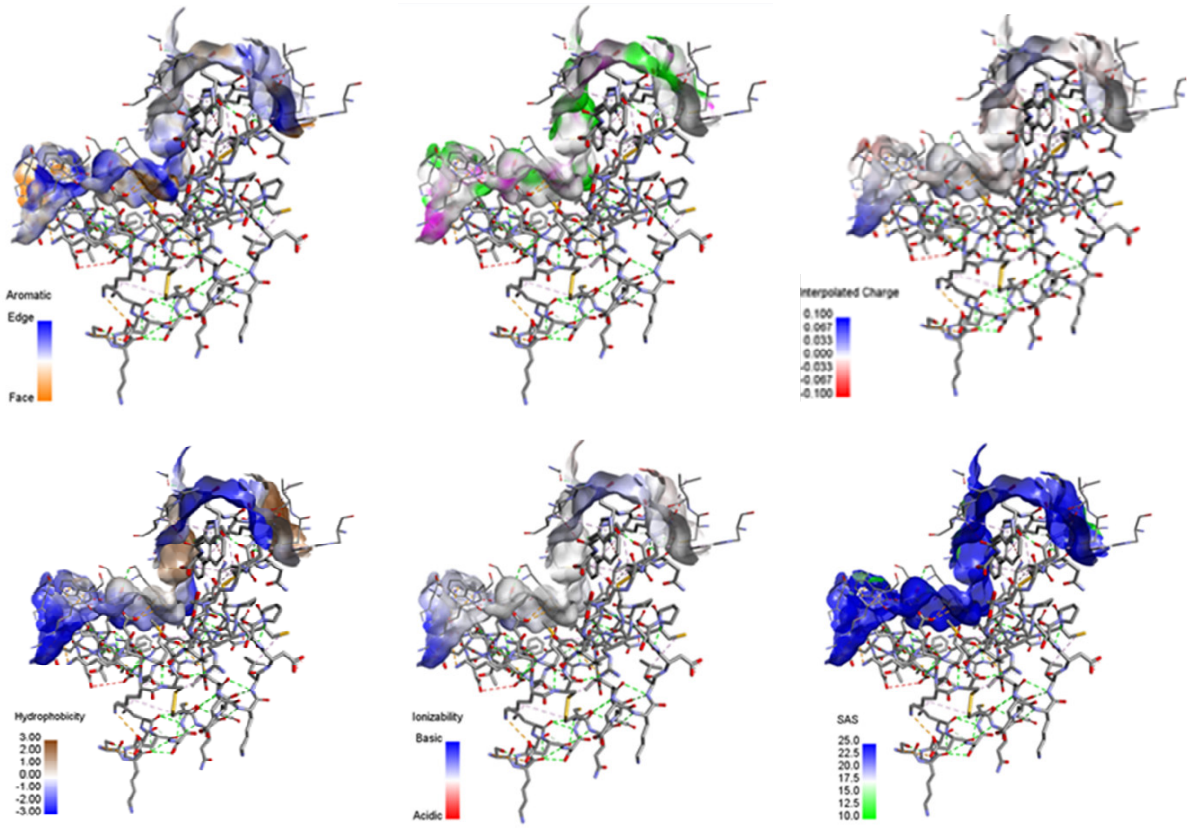

Figure 6
The hT1R2-T1R3 surface receptor interaction with Tc-9M

REFERENCES:

1. Johnson RJ, Segal MS, Sautin Y, Nakagawa T, Feig DI, Kang DH, Gersch MS, Benner S, Sánchez-Lozada LG. Potential role of sugar (fructose) in the epidemic of hypertension, obesity and the metabolic syndrome, diabetes, kidney disease, and cardiovascular disease–. The American journal of clinical nutrition. 2007 Oct 1;86(4):899-906.
2. Tandel KR. Sugar substitutes: Health controversy over perceived benefits. Journal of pharmacology & pharmacotherapeutics. 2011 Oct;2(4):236.
3. Li DF, Jiang P, Zhu DY, Hu Y, Max M, Wang DC. Crystal structure of Mabinlin II: a novel structural type of sweet proteins and the main structural basis for its sweetness. Journal of Structural Biology. 2008 Apr 1;162(1):50-62.
4. Nirasawa S, Liu X, Nishino T, Kurihara Y. Disulfide bridge structure of the heat-stable sweet protein mabinlin II. Biochimica et Biophysica Acta (BBA)-Protein Structure and Molecular Enzymology. 1993 Oct 6;1202(2):277-80.
5. Nirasawa S, Nishino T, Katahira M, Uesugi S, Hu Z, Kurihara Y. Structures of heat-stable and unstable homologues of the sweet protein mabinlin. The difference in the heat stability is due to replacement of a single amino acid residue. European journal of biochemistry. 1994 Aug;223(3):989-95.
6. Gu W, Xia Q, Yao J, Fu S, Guo J, Hu X. Recombinant expressions of sweet plant protein mabinlin II in Escherichia coli and food-grade Lactococcus lactis. World Journal of Microbiology and Biotechnology. 2015 Apr 1;31(4):557-67.
7. Kochhar S, Gartenmann K, Juillerat MA. Primary structure of the abundant seed albumin of Theobroma cacao by mass spectrometry. Journal of agricultural and food chemistry. 2000 Nov 20;48(11):5593-9.
8. Niemenak N, Kaiser E, Maximova SN, Laremore T, Guiltinan MJ. Proteome analysis during pod, zygotic and somatic embryo maturation of Theobroma cacao. Journal of plant physiology. 2015 May 15;180:49-60.
9. Higgins TJ. Synthesis and regulation of major proteins in seeds. Annual Review of Plant Physiology. 1984 Jun;35(1):191-221.
10. Kochhar S, Gartenmann K, Guilloteau M, McCarthy J. Isolation and characterization of 2S cocoa seed albumin storage polypeptide and the corresponding cDNA. Journal of agricultural and food chemistry. 2001 Sep 17;49(9):4470-7.
11. Li X, Staszewski L, Xu H, Durick K, Zoller M, Adler E. Human receptors for sweet and umami taste. Proceedings of the National Academy of Sciences. 2002 Apr 2;99(7):4692-6.
12. Nelson G, Hoon MA, Chandrashekar J, Zhang Y, Ryba NJ, Zuker CS. Mammalian sweet taste receptors. Cell. 2001 Aug 10;106(3):381-90.
13. Shrivastav A, Srivastava S. Human sweet taste receptor: Complete structure prediction and evaluation. International Journal of Chemical and Analytical Science. 2013 Mar 1;4(1):24-32.
14. Arnold K, Bordoli L, Kopp J, Schwede T. The SWISS-MODEL workspace: a web-based environment for protein structure homology modelling. Bioinformatics. 2006 Jan 15;22(2):195-201.
15. Benkert P, Biasini M, Schwede T. Toward the estimation of the absolute quality of individual protein structure models. Bioinformatics. 2010 Dec 5;27(3):343-50.
16. Biasini M, Bienert S, Waterhouse A, Arnold K, Studer G, Schmidt T, Kiefer F, Cassarino TG, Bertoni M, Bordoli L, Schwede T. SWISS-MODEL: modelling protein tertiary and quaternary structure using evolutionary information. Nucleic acids research. 2014 Apr 29;42(W1):W252-8.
17. Benkert P, Schwede T, Tosatto SC. QMEANclust: estimation of protein model quality by combining a composite scoring function with structural density information. BMC structural biology. 2009 Dec;9(1):35.
18. Lovell SC, Davis IW, Arendall III WB, De Bakker PI, Word JM, Prisant MG, Richardson JS, Richardson DC. Structure validation by Cα geometry: ϕ, ψ and Cβ deviation. Proteins: Structure, Function, and Bioinformatics. 2003 Feb 15;50(3):437-50.

19. Eisenberg D, Lüthy R, Bowie JU. [20] VERIFY3D: assessment of protein models with three-dimensional profiles. InMethods in enzymology 1997 Jan 1 (Vol. 277, pp. 396-404). Academic Press.
20. Melo F, Feytmans E. Assessing protein structures with a non-local atomic interaction energy1. Journal of molecular biology. 1998 Apr 17;277(5):1141-52.
21. van Gunsteren WF, Billeter SR, Eising AA, Hünenberger PH, Krüger PK, Mark AE, Scott WR, Tironi IG. Biomolecular simulation: the {GROMOS96} manual and user guide.
22. Tovchigrechko A, Vakser IA. GRAMM-X public web server for protein–protein docking. Nucleic acids research. 2006 Jul 1;34(suppl_2):W310-4.
23. Tovchigrechko A, Vakser IA. Development and testing of an automated approach to protein docking. Proteins: Structure, Function, and Bioinformatics. 2005 Aug 1;60(2):296-301.
24. Chen D. Structural genomics: exploring the 3D protein landscape. Simbios, the NIH National Center for Physics-Based Simulation of Biological Structures. 2009:11-8.
25. Alberts B, Johnson A, Lewis J, Raff M, Roberts K, Walter P. The shape and structure of proteins.
26. Cemanovic A. Comparative structural analysis of HAC1 in Arabidopsis thaliana. Network Biology. 2014 Jun 1;4(2):67.
27. Altschul SF, Madden TL, Schäffer AA, Zhang J, Zhang Z, Miller W, Lipman DJ. Gapped BLAST and PSI-BLAST: a new generation of protein database search programs. Nucleic acids research. 1997 Sep 1;25(17):3389-402.
28. Remmert M, Biegert A, Hauser A, Söding J. HHblits: lightning-fast iterative protein sequence searching by HMM-HMM alignment. Nature methods. 2012 Feb;9(2):173.
29. Vakser IA, Matar OG, Lam CF. A systematic study of low-resolution recognition in protein–protein complexes. Proceedings of the National Academy of Sciences. 1999 Jul 20;96(15):8477-82.
30. Li X, Staszewski L, Xu H, Durick K, Zoller M, Adler E. Human receptors for sweet and umami taste. Proceedings of the National Academy of Sciences. 2002 Apr 2;99(7):4692-6.
31. Temussi PA. Why are sweet proteins sweet? Interaction of brazzein, monellin and thaumatin with the T1R2-T1R3 receptor. FEBS letters. 2002 Aug 28;526(1-3):1-4.

FP-34

UTILISATION OF RESPONSE SURFACE METHODOLOGY IN THE ENZYMATIC PRODUCTION OF BIODIESEL FROM *Cerbera odollum*

M. RAJIN*[1], J. SARIAU[1], A.S. JUKA[1], J. JAIBET[1] AND A. ZULKIFLI[1]

[1]Chemical Engineering Programme, Universiti Malaysia Sabah, 88999, Kota Kinabalu, Sabah, Malaysia

*Corresponding author: mariani@ums.edu.my

ABSTRACT

Biodiesel production is one of the alternatives available to reduce our dependence on the fossil fuel. This is important because fossil fuels are being depleted day by day and hence it is necessary to produce more sustainable and renewable types of energy. Various feedstocks can be used to produce biodiesel, including edible and non-edible oils. Sea mango or *Cerbera odollum* is a non-edible oil that is suitable for biodiesel production due to the high content of free fatty acid. In this work, biodiesel is produced from Sea mango oil through enzymatic transesterification mediated by *Candida antartica* lipase B. The variables include the reaction temperature (30 to 70 ^{o}C), enzyme loading (2 to 15 wt%) and a methanol to oil ratio (1:1 to 7:1) were investigated and optimised using response surface methodology with central composite rotatable design. The highest yield of 30.8 % was obtained with optimum conditions of temperature 40 ^{o}C, 12.40 wt% enzyme loading, and a methanol to oil molar ratio of 5:1.

KEYWORDS:
Biodiesel, Transesterification, Sea mango oil, Lipase, Response Surface Methodology

INTRODUCTION:

Interest in the production and use of methyl esters of plant oils as biodiesel has vastly increased since the mid- to late 1990s, and standards have been explored largely with regard to these methyl esters.[1] Biodiesel is one of the sustainable alternative fuels and renewable energy sources that has attracted great attention from researchers. As environmentally friendly fuels and the use of enzymes along with eco-friendly catalysts have been prioritised instead of toxic chemicals, investigation of the reaction of triglyceride(s) transesterification has become necessary because they reduce the emission of various hazardous particles in the environment.[2] Therefore the deployment of biomass to substitute for petroleum fuel is highly attractive.

Biodiesel is produced by the transesterification of fatty acids or oils and fats with a short-chain alcohol. Oils and fats are converted into long-chain mono alkyl esters or also referred to as fatty acid methyl esters (FAME), which form biodiesel.[4] The synthesis of biodiesel can be chemically achieved using sodium hydroxide or potassium hydroxide, or by using enzymatic production according to the catalysts used in the reaction. A chemical transesterification process using acid or alkali-catalysts will produce high yields in a short time. However, this requires high energy and exhibits difficulty in the recovery of the catalyst and glycerol.[5] The disadvantages of using food-grade plants such as corn for the production of biodiesel are that it can lead to food shortages and possibly increased food prices.[6]

Various feedstocks have been used to produce biodiesel, including edible and non-edible oils. Since controversies have occurred regarding the use of edible feedstock for the production of biodiesel as such feedstock is in demand in other industries, a second generation of biodiesel has been developed comprising of non-edible oils which have demonstrated the capability to be a reliable feedstock for biodiesel. Among

these non-edible oils is *Cerbera odollum* or sea mango.[7] The Sea Mango, which also goes by the name Pong Pong Tree or Indian Suicide Tree, is normally found growing in coastal salt swamps and creeks. In Malaysia, sea mango grows on the roadside as ornamental trees. From research that has been conducted to date, it has been discovered that sea mango seeds contain up to 60 % oil, which makes it feasible as a feedstock for biodiesel production. This discovery has created a potential substitute for palm oil, especially in Malaysia due to the abundant unutilised sources of sea mango.[8]

Various techniques have been applied to produce biodiesel from the plants, for example using a chemical catalyst. However, the main problem is soap formation when the raw material contains a high amount of water or free fatty acids. A more conventional method uses an enzyme and has become another alternative to the catalyst. In this research, the production of biodiesel from sea mango oil is optimised using response surface methodology. Based on previous research, the optimisation of lipase-catalysed biodiesel has been carried out using different types of feedstock such as soybean oil, vegetable oil and rapeseed oil.[9,10,11] Sea mango has been used in various studies to produce biodiesel.[12,1,2] However, there are limited reports available on the production of biodiesel using this feedstock via enzymatic transesterification.[12] Therefore, in this research, sea mango oil is used as a feedstock to produce biodiesel via enzymatic transesterification, using Lipozyme *candida antartica* lipase B (CALB) as a catalyst. The effects of reaction temperature, enzyme loading, and the methanol to oil ratio on the biodiesel yield are studied. The operating parameters are further optimised using response surface methodology (RSM).

MATERIALS AND METHODS:

The lipase used for the biodiesel production was Lipozyme CALB L purchased from Novozymes. Sea mango was obtained locally from Sabah Tea, Ranau. Chromatographically pure palmitic acid methyl ester, myristic acid methyl ester, stearic acid methyl ester, oleic acid methyl ester, linoleic acid methyl ester, and heptadecanoic methyl ester were obtained from Sigma-Aldrich to be used in Gas Chromatography. The solvent used in the extraction of sea mango oil was n-hexane, while methanol was used in the reaction for biodiesel production.

Experimental Design

In this research, the central composite rotatable design (CCRD) of the response surface methodology (RSM) was utilised for optimisation and data analysis. The implementation of CCRD began with the design of the experimental run, followed by data analysis, and optimisation of parameters. Three-level experiments employing three factors were devised. The factors or the independent variables studied in this research were temperature, enzyme loading, and the methanol to oil molar ratio. The range of each variable was determined from the result of the preliminary study. There were 20 sets in the experimental run.

Enzymatic Transesterification

In the enzymatic transesterification, the reaction was carried out in a heated water bath at various temperatures (30 to 70 ^{o}C). The oil and methanol in the ratio of 1:1 to 7:1 were added to a stoppered flask followed by Lipozyme CALB (2 to 15 wt%). Then the flask was placed in the water bath for a reaction time of 6 hours. The sample was removed from the bath and then analysed for fatty acid methyl ester (FAME) content using Gas Chromatography.

Determination of biodiesel yield using Gas Chromatography

The FAME content in the sample was analysed using Agilent Gas Chromatography equipped with a flame ionisation detector. The run was conducted under optimised temperatures programmed as follows: initial column temperature 100 ^{o}C, programmed to increase at a rate of 30 ^{o}C min^{-1} up to 160 ^{o}C and then at 20 ^{o}C min^{-1} up to 220 ^{o}C. This temperature was maintained for two minutes, then at 25 ^{o}C min^{-1} up to a final temperature of 260 ^{o}C and held for two minutes. The injector and detector temperatures were at 260 ^{o}C and 280 ^{o}C, respectively. Helium was used as the carrier gas at a flow rate of 1 mL min^{-1} with a split ratio of 30:1.

Data analysis

Analysis of variance (ANOVA) and regression of the model was assisted by using Design Expert 7.0 software. Response surface plots were used to investigate the effects of the reaction parameters and to establish the conditions for optimum reaction yield.

RESULTS AND DISCUSSION:

Analysis of Biodiesel Production Using Response Surface Methodology (RSM)

From 20 experimental runs, it was found that the content of the FAME obtained was in the range of 5.51 % to 30.86 %, which was slightly lower as compared to the data reported by Sandip (2015) at 15 % to 66 % due to the better optimisation resulting from the analysis of the experiment.[12] The experimental data gained from central composite rotatable design (CCRD) are shown in Table 1.

The quadratic model was chosen in this study with a significant F-value of 3.29 and Prob>F of 0.0454 (<0.0500) and R^2 of 0.8, indicating a high significance for the regression model. The nearer the value of R^2 is to 1.00, the closer is the accuracy of the generated model.[12] As shown in ANOVA results in Table 2, from the statistical analysis, there is only one factor considered significant, which is the enzyme loading. However, the interaction between the other factors had a significant effect on the response. Equation 1 shows the quadratic equation (coded factors) for this reaction.

$$\text{Yield} = 21.19 - 2.61A + 5.47B + 2.05C + 0.65AB - 2.09AC - 1.48BC - 1.43A^2 - 1.50B^2 - 1.92C^2 \quad \textbf{(Equation 1)}$$

where A, B, and C are represent the temperature, enzyme loading, and the methanol to oil ratio, respectively.

Table 1

The experimental data for the production of biodiesel through enzymatic transesterification

Run	Factors			Response
	A: Temperature (^{0}C)	B: Enzyme Loading (wt%)	C: Methanol:Oil	Yield (%)
1	50.00	8.50	4.00	28.81
2	38.11	4.64	5.78	23.48
3	61.89	4.64	2.22	12.57
4	50.00	8.50	4.00	21.23
5	38.11	4.64	2.22	10.36
6	38.11	12.36	2.22	22.27
7	61.89	12.36	5.78	18.07
8	50.00	8.50	4.00	20.77
9	50.00	8.50	4.00	18.61
10	38.11	12.36	5.78	21.63
11	61.89	4.64	5.78	9.47
12	61.89	12.36	2.22	19.25
13	50.00	2.00	4.00	1.52
14	50.00	8.50	7.00	20.9
15	70.00	8.50	4.00	11.25
16	50.00	8.50	1.00	9.13
17	50.00	15.00	4.00	30.86
18	50.00	8.50	4.00	20.25
19	50.00	8.50	4.00	19.26
20	30.00	8.50	4.00	21.53

Table 2
ANOVA for regression model equation

Source	F-value	Prob>F	Remark
Model	3.29	0.0454	Significant
A-Temperature	3.88	0.0804	Not significant
B-Enzyme Loading	17.00	0.0026	Significant
C-Methanol:Oil	2.39	0.1566	Not significant
AB	0.14	0.7152	Not significant
AC	1.46	0.2575	Not significant
BC	0.73	0.4152	Not significant
A^2	1.23	0.2962	Not significant
B^2	1.35	0.2745	Not significant
C^2	2.21	0.1716	Not significant

The Interaction Effect of Two Factors on the Biodiesel Yield

(i) The effect of interaction between temperature and enzyme loading

Figure 1 shows the surface plot for the changes in yield of biodiesel with varying temperature and amount of enzyme loading. The third variable, the methanol to oil molar ratio, was kept constant at 4.00:1. From the plot, the highest conversion was obtained at a temperature of 38.1 ^{o}C to 50 ^{o}C and an enzyme loading of 7.95 wt% to 12.36 wt%.

It has been found in prior research that at low temperatures up to 50 ^{o}C an increase in the amount of enzyme increased the yield of the biodiesel because of the greater amount of active sites of the enzyme available in the reaction, corresponding to the data obtained, when sodium methoxide is used as a catalyst to produce fatty acid methyl ester from Kusum oil.[13] It was found that at low temperatures, an increase in enzyme amount led to higher FAME content. However there is a disagreement when Sulfated Zirconia is used as the catalyst for transesterification of oil from Sea mango where at lower temperatures, a larger amount of catalyst seems to produce a lower conversion rate compared to that of a lesser amount of catalyst.[14] Further, at an optimum temperature of the enzyme (30 ^{o}C to 60 ^{o}C), the enzyme becomes active and is not denatured by high temperatures. The increase of enzyme loading will accelerate the reaction rate. However, an excess amount of enzyme will cause an aggregation of enzyme molecules and reduce its activity. At lower temperatures, a small quantity of energy may be sufficient to activate a smaller quantity of catalyst but not sufficient to activate a larger amount of catalyst because of the difference in the available energy to the catalyst ratio.[14]

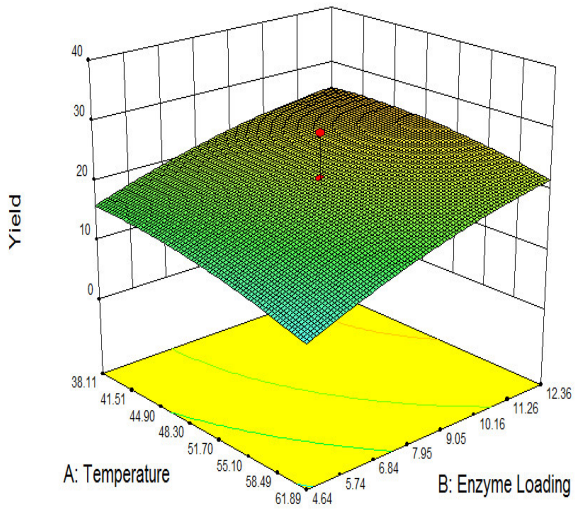

Figure 1
Response surface plot for the interaction between temperature and enzyme loading on biodiesel yield

(ii) The effect of interaction between the methanol to oil ratio and temperature

The effect of interaction between the methanol to oil ratio and temperature on the biodiesel yield is represented by Figure 2. It is shown that by keeping the enzyme loading constant, an increase in the amount of methanol will increase the biodiesel production up to optimum temperature (50 ^{o}C). The same result was obtained by Hamze, Akia and Yazdani (2015).[15] At a low methanol to oil molar ratio, a higher reaction temperature does not improve the FAME content. On the other hand, at a high molar ratio (50:1 mol/mol), an increase in the reaction temperature enhanced the reaction rate and led to higher FAME content. At low methanol values, the biodiesel yield change is in opposite direction. A higher yield was obtained at temperatures of 38.11 ^{o}C to 50 ^{o}C and a methanol to oil molar ratio of 2.22:1 to 3.80:1, which is a similar trend to the investigation by Ang et al. (2015).[16] Most of the past researchers reported that the conversion of oil to fatty acid methyl ester is high at the highest methanol to oil molar ratio tested.[16] A further rise in temperature, however, did not increase the conversion process because of the greater methanol loss from the system.[17]

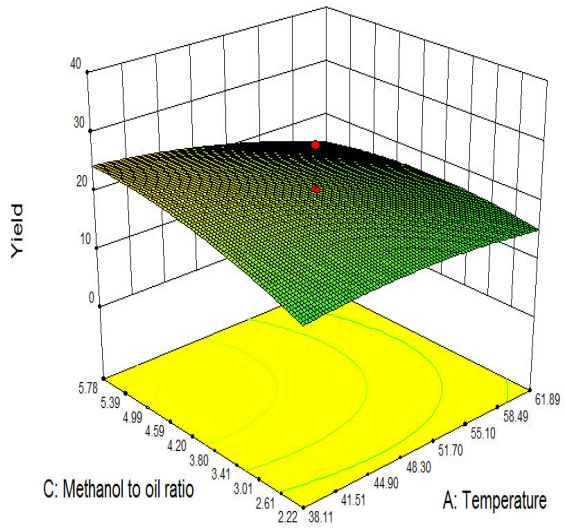

Figure 2

Response surface plot for the interaction between the methanol to oil ratio and temperature on biodiesel yield

(iii) The effect of interaction between enzyme loading and the methanol to oil ratio

The interaction effects of the enzyme loading and methanol to oil ratio can be seen in Figure 3.

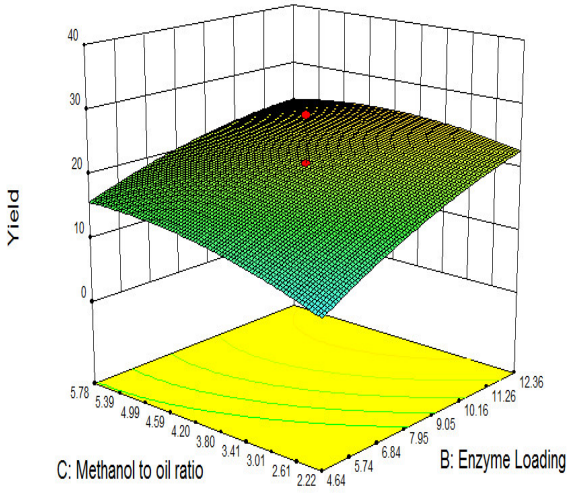

Figure 3

Response surface plot for the interaction between enzyme loading and the methanol to oil ratio on biodiesel yield

It is shown that the biodiesel yield increases as the enzyme loading and methanol increase, in line with the findings obtained in previous research.[12] The surface plot of the BC parameters as the value of the third parameter (A) is kept constant, indicated that increasing the B value will increase the reaction yield.

A higher yield can be achieved at an enzyme loading of 4.64 wt% to 9.05 wt% and a methanol to oil ratio of 2.22:1 to 3.80:1. At the higher ratio, a greater substrate concentration with more active sites of the enzyme will increase the yield. The available substrate will be utilised by the enzyme. According to Kansedo and Lee (2013), the molar ratio of oil to methanol shows an insignificant effect because it has the lowest F-test value.[14] A higher yield of methyl ester resulted from an increase in the amount of one of the reactants. For a complete conversion of oil to biodiesel, at least three molar equivalents of methanol are required.[18]

Optimisation of reaction parameters

In the numerical optimisation function in the Design Expert 7.0 software, the right combinations of the variables contributing to the yield of biodiesel were performed to obtain the optimum conditions. The objective of the optimisation was to determine the values of the reaction variables in order to obtain the highest yield. From the results, it was predicted that the highest yield of 31 % was obtained with a temperature of 40 ^{o}C, 12.36 wt% enzymes loading, and a methanol to oil molar ratio of 5:1.

CONCLUSION:

In conclusion, biodiesel production by the transesterification of sea mango oil was successfully carried out using Lipozyme CALB L as a catalyst. The statistical analysis showed that the reaction parameters have a significant effect on the biodiesel yield. Additionally, an attempt to use Response Surface Methodology (RSM) in the optimisation of biodiesel production from sea mango oil has been successfully completed. The small difference between the predicted and experimental results shows the great accuracy and consistency of RSM in predicting the value of the responses.

REFERENCES:

1. Gerhard Knothe, Luis F Razon. Biodiesel fuels. Progress in Energy and Combustion Science. 2017;58: 36-59.
2. Stojkovic N, Vasic M, Ljupkovic R and Zarubica A. The influence of selected process parameters on the reactions of n-hexane isomerization and transesterification catalyzed by Sulfated Zirconia. Advanced Technologies. 2017;6(1): 27-32.
3. Jonathan M Harris, Brian Roach. Environmental and natural resource economics: A contemporary approach. ME Sharpe. 2013.
4. Verma D, Raj J, Pal A and Jain M. A critical review on the production of biodiesel from various feedstocks. Journal of Scientific and Innovative Research. 2016;5(2): 51-8.
5. Math MC, Chandrashekhara KN. Optimization of alkali-catalyzed transesterification of safflower oil for production of biodiesel. Journal of Engineering. 2016.
6. Popp J, Harangi-Rakos M, Gabnai Z, Balogh P, Antal G and Bai A. Biofuels and their co-products as livestock feed: global economic and environmental implications. Molecules. 2016;21(3): 285.
7. Bhuiya MMK, Rasul MG, Khan MMK, Ashwath N and Azad AK. Prospects of 2nd generation biodiesel as a sustainable fuel—Part: 1 selection of feedstocks, oil extraction techniques, and conversion technologies. Renewable and Sustainable Energy Reviews. 2016;55: 1109-1128.
8. Nurhayati Abdullah, Fauziah Sulaiman. The oil palm wastes in Malaysia. In Biomass Now-Sustainable Growth and Use. InTech. 2013.
9. Su F, Li G, Fan Y and Yan Y. Enhanced performance of lipase via microcapsulation and its application in biodiesel preparation. Scientific Reports. 2016;6: 29670.
10. El-Batal AI, Farrag AA, Elsayed MA and El-Khawaga AM. Biodiesel production by Aspergillus niger lipase immobilized on barium ferrite magnetic nanoparticles. Bioengineering. 2016;3(2): 14.

11. Kia-Kojouri M, Darzi GN, Rupani B and Mohammadpour M. Production of biodiesel from rapeseed oil by porcine pancreatic mediated transesterification reaction in organic solvent. Indian Journal of Chemical Technology. 2016;23(3): 216-220.
12. Sandip S. Optimization of Biodiesel Production via Reflux Condenser Methyl Acetate Reaction from Cerbera Odollam (Sea Mango)(Doctoral dissertation, UTAR). 2015.
13. Sarve A, Varma MN and Sonawane SS. Optimization and Kinetic Studies on Biodiesel Production from Kusum (Schleichera triguga) Oil Using Response Surface Methodology. Journal of Oleo Science. 2015;64(9): 987-997.
14. Kansedo Jibrail, and Keat Teong Lee. Process optimization and kinetic study for biodiesel production from non-edible sea mango (Cerbera odollam) oil using response surface methodology. Chemical Engineering Journal. 2013;214: 157-164.
15. Hamze H, Akia M and Yazdani, F. Optimization of biodiesel production from the waste cooking oil using response surface methodology. Process Safety and Environmental Protection. 2015;94: 1-10.
16. Ang GT, Tan KT, Lee KT and Mohamed AR. Optimization and kinetic studies of sea mango (Cerbera odollam) oil for biodiesel production via supercritical reaction. Energy Conversion and Management. 2015;99: 242-251.
17. Kundu A, Mukherjee A, Halder G and Datta D. A kinetic study on acid catalyzed esterification of free fatty acids in Ricinus Communis oil for the production of biodiesel. International Journal of Research in Engineering and Technology. 2016;5(1): 31-44.
18. Talib NB, Triwahyono S, Jalil AA, Mamat CR, Salamun N, Fatah NA, Sidik SM and Teh LP. Utilization of a cost effective Lapindo mud catalyst derived from eruption waste for transesterification of waste oils. Energy Conversion and Management. 2016;108: 411-421.

FP-35

ELECTROCHEMICAL METHODS FOR DETECTION OF ZINC ION IN DRINKING WATER

RINGGIT GILBERT[1], SHAFIQUZZAMAN SIDDIQUEE[1*], MOHAMMAD TAMRIN MOHAMAD LAL[2], SURYANI SAALLAH[1], NOR HYDAYATY MD. YUSUF[1], ZARINA AMIN[1]

[1]Biotechnology Research Institute, University Malaysia Sabah, Jalan UMS, 88400 Kota Kinabalu, Sabah, Malaysia
[2]Borneo Research Marine Institute, University Malaysia Sabah, Jalan UMS, 88400 Kota Kinabalu, Sabah, Malaysia

*Corresponding author: shafiqpab@ums.edu.my

ABSTRACT

Recent years have witnessed the growing interest in the utilization of electrochemical methods for detection of heavy metal ions in comparison with the conventional techniques such as conventional methods such as atomic absorption spectroscopy (AAS), inductively coupled plasma mass spectrometry (ICP-MS), and inductively coupled plasma atomic emission spectroscopy (ICP-AES). This is mainly attributed to the less expensive instruments, simple preparation procedure, less time consuming, on-spot detection, and high sensitivity and selectivity of the electrochemical methods. In the present study, electrochemical detection of zinc ion using bare gold electrode was studied under various types of buffer, redox indicator, pH, scan rate and accumulation time. It was found that the optimal parameters for the detection of zinc ion were phosphate buffer saline (0.1 M, pH 2) supported by 5 mM Prussian blue under electrochemical measurements; scan rate = 250 mVs-1; stop/start potential = 0.8 V; accumulation time = 5 s within potential range of 0.0 V to 1.7 V. The linear of range (LOR) was 1 – 10 ppm, and the sensitivity was 19.25 µA. These parameters were applied under potential range of 0.55 V to 0.75 V. These basic parameters need to be considered and optimized using bare gold electrode before further modification to improve the electrode's sensitivity and selectivity, allowing fast analyses and lowest detection limits.

KEYWORDS:
Zinc ion, Safety level, Electrochemical methods, Prussian blue

INTRODUCTION:

Heavy metals are naturally occurring elements produced through biogeochemical processes. However, overpopulation, industrial development, poor sewage treatment, usage of heavy metal in manufacture and gas emission from transport caused heavy metals accumulation and release to the environment, thus increasing the heavy metal concentration in the biosphere (Oves et al. 2012). Recently, overexposure to heavy metals has become a global concern due to their potential negative effects to human being and nature due to their toxicity even at lower level (Duffus, 2002; Sathawara et al., 2004).

Zinc is one the essential heavy metals that plays an important role in various chemical and biological pathways. Since zinc ion is the cofactor for glycoprotein component, lack of enzymatic reaction by zinc ion resulting in various health problems such as Gaucher's disease, Tay-sachs disease, Fabry disease, Hurler syndrome, Galactosemia, among others (Burgit and Schmid, 1960; Humpath, 2017). However, long term exposure and excessive intake of zinc have negative impact to human health which resulted in epilepsy, Alzheimer's diseases (Weiss et al., 2000) and spasmolytic effects (Schnied and Small, 1971). In soil, the contamination of zinc happened through irrigation of zinc from mining or sewage and showed the

phytotoxic effects (Voegelin et al., 2005; Mertens et al., 2007) and deteriorating the plant quality (Chibuike and Obiora, 2014).

The potential hazardous effects of overexposure to zinc ion have called for efficient monitoring of zinc ion in food chain, especially drinking water sources. Conventional analytical techniques such as inductively atomic absorption and emission spectroscopy, X-ray fluorescence spectrometry, inductively coupled plasma mass spectrometry and capillary electrophoresis have been used to determine concentration of zinc and other heavy metals ions. Although these techniques are established, reliable and have high accuracy, they require expensive instruments, skilled operators, and time-consuming procedures. Electrochemical methods on the other hand offer low cost, easy operation, good specificity, excellent stability, high sensitivity and low limit of detection (Nagles et al., 2012; Güell et al., 2008). The other great advantages of electrochemical analysis are the possibility of electrode surface modification and on-site monitoring of pollutants.

Nevertheless, the detection of heavy metal ions especially zinc ion using electrochemical method is still new and it toxicity effects especially on biochemical process is still unknown. This is because the zinc ion is nontoxic element as compare to the other elements. Zinc ion becomes harmful to environment and organisms if the zinc ion undergoes bioaccumulation and bio-magnification. Detection of zinc ion using electrochemical method with different modifications has been studied by several researchers to increase the sensitivity and selectivity of electrode until reaching the detection limit. For example, Gunawardena et al. (2013) have used nafion/ionic liquid/graphene composite modified screen-printed carbon electrode with detection limit of 0.09 ng L^{-1} while Sindern et al. (2016) able to detect 0.11 µg L^{-1} zinc ion concentration by using ironoxide/graphene electrode.

In electrochemical methods, three different electrodes are used to connect the full circuit and it applying the external currents into the system. The three electrodes are working, counter and reference electrodes. Each of these electrodes has different function. The working electrode roles as selection on the target ion. In this research, the working electrode was bare gold electrode (AuE) while inert platinum is used as the counter electrode and reference electrode contains silver chloride to measure the current transferred in the electrolytic solution containing the target ion. Here, we analyse the presence of the zinc ion in the electrolysis solution using cyclic voltammetry (CV) method while the different concentrations of zinc ion were measure using differential pulse voltammetry (DPV) method. Our goal is to optimize the parameters such as buffer, redox indicator, pH, scan rate and accumulation time for determination of zinc ion in electrolytic solution using CV method and to analyse the different concentrations of zinc with current response using differential DPV method.

MATERIAL AND METHODS:

Pre-treatment of bare gold electrode (AuE)

Electrode is important in electrochemical method because it contacts with analyte on the surface of the electrode. Therefore, this research considered about any contamination from unwanted substances onto the AuE. The pre-treatment of AuE was using methods according to (Siddiquee et al., 2010). The surface of the electrode was polished with 0.3-0.5 µm aluminium slurry for about two minutes . After that, the gold electrode was dried using nitrogen gas. The analysis was using the redox indicator by adding 5 µL onto the surface of the gold electrode and left for 2 minutes. After 2 minutes, the redox indicator was cleaned from the surface of the gold electrode using the same buffer. Then, AuE was connected to the working electrode. Submerged it into the buffer solution with presence of analyte and it was ready for analysis. Counter and reference electrodes were submerged together with working electrode before running the cyclic voltammetry method.

Buffer Electrolyte Optimization of Zn/AuE Electrochemical Sensor

The effect of various types of buffer was tested for acetate buffer, phosphate buffer saline, ammonium buffer, citrate buffer and Tris-HCl buffer. Three types of buffer solution were used as an electrolytic solution to detect the presence of zinc ion such as acetate buffer, phosphate buffer saline and Tris-HCl buffer. A part

of that, two buffers were tested in this research because it was widely used in detection of heavy metal ions such as ammonium buffer and citrate buffer. All of the buffers were standardised with same concentration which is 0.1 M.

pH optimisation of Zn/AuE using electrochemical sensor

The pH optimisation was done by submersing the AuE with different pH (pH 2.0, pH 3.0, pH 4.0, pH 5.0, pH 6.0, pH 7.0, pH 8.0 and pH 9.0) in 0.1 M phosphate buffer saline containing zinc ion as an analyte with an applied potential range between 0.0 to 1.7 V versus Ag/AgCl for 5 s.

Scan rate optimisation of Zn/AuE using electrochemical sensor

Scan rate optimisation was done by submersing the AuE with different scan rate range from 50 mVs-1 to 450 mvs-1 versus Ag/AgCl in (0.1 M, pH 2) phosphate buffer saline containing zinc ion under 5 s.

Accumulation time optimization of Zn/AuE using electrochemical Sensor

Accumulation time optimization was done by submersing the AuE with different time that was 5 s, 10 s, 15 s, 20 s, 25 s, 30 s, 35 s, 40 s, 45 s and 50 s in (0.1 M, pH 2) phosphate buffer saline containing zinc ion with an applied potential range between 0.0 V to 1.7 V versus Ag/AgCl.

Optimisation of redox indicator

The optimisation of the redox indicator was performed by plusferocyanide ($K_3[Fe(CN)_6]/K_4[Fe(CN)_6]$), Prussian blue ($C_{18}Fe_7N_{18}$) and methylene blue ($C_{16}H_{18}C_lN_3S$) with same concentration which is 5 mM. Preparation of plusferocyanide was mixing the 5 mM potassium hexacyanoferrate (III) ($K_3[Fe(CN)_6]$ and 5 mM potassium ferrocyanide (II) trihydrate $K_4[Fe(CN)_6])•3H_2O$) into the solution. Besides that, the preparation of the 5 mM Prussian blue was mixing between 5 mM potassium hexacyanoferrate (III) ($K_3[Fe(CN)_6]$ and 5 mM iron (III) chloride ($FeCl_3$). Lastly, the 5 mM methylene blue powder was directly dissolved in the distilled water forming 5 mM methylene blue.

Preparation of zinc sulphate as a control in detection of zinc ion

Zinc sulphate is a model of the control for this research. The concentration of the zinc sulphate fixed as 3 ppm due to drinking water quality standard permitted by Ministry of Health, Malaysia. 3 ppm of zinc sulphate was mixed with 10 mL of electrolytic solution and ready to analysis. The mixture of the electrolytic solution buffer with 3 ppm zinc sulphate was stirred for 5 minutes before the analysis began. The analysis of the mixture using working electrode, counter electrode and reference electrode. After 5 s of accumulation time, the current started to flow and it forming cyclic voltammogram in cyclic voltammetry method. Analysis the different concentration of zinc sulphate with current responses was conducted using differential pulse voltammetry method. The linear of range (LOR) from 1 ppm to 10 ppm under range 0.55 V to 0.75 V of potential applied.

Electrochemical Measurements

The procedure of cyclic voltammetry measurement was set as waiting times = 5 s; stop and start potential = 0.8 V; scan rates = 250 mVs-1 and the potential range was from 0.0 V to 1.7 V in pH 2 buffer solution with the presence of the 3 ppm zinc sulphate. The differential pulse voltammetry measurement was using pulse amplitude: 50 mV; pulse period: 0.2 s; pulse width: 0.05 s; sampling width: 0.0167 s and waiting time: 5 s.

RESULTS AND DISCUSSION:

Determination of the buffer tolerant with redox indicator

Five buffers were tested with supported by redox indicator for potential range from 0.0 to 1.7 V as showed at Figure 1. The buffers such as citrate buffer, phosphate buffer saline, ammonium buffer, tris-HCl buffer and acetate buffer were compared based on formation of the reactions (oxidation and reduction reactions) with the presence of 3 ppm zinc sulphate. The redox indicators such as plusferocyanide, methylene blue and Prussian blue were used to support the bare gold electrode by increasing the current signal. Phosphate buffer saline supported by Prussian blue showed the highest current signals compared to other. The formation of

the both peaks for phosphate buffer saline with Prussian blue was compared at same figure. The comparison was based on the highest peak point for both reactions. In this case, the oxidation was showed the highest peak point was 1.70 mA at 1.30 V while reduction peak was 0.60 mA at 0.61 V. This information, however, we selected both current responses because in the electrochemical method, the selection of the parameter should be high with stable current response. Tris-HCl buffer with plusferocyanide was showed the oxidation peak almost the same compared to phosphate buffer saline with Prussian blue but it reduction peak was lower about 0.53 mA at 0.49 V. A part of that, the oxidation peak of Tris-HCl buffer with plusferocyanide was shifting more toward positive potential ranges due to high transfer of hydrogen ion (H+) in the oxidation process (Mazur and Krysinski, 2001). Therefore, phosphate buffer saline with Prussian blue was selected as the best buffer and redox indicator.

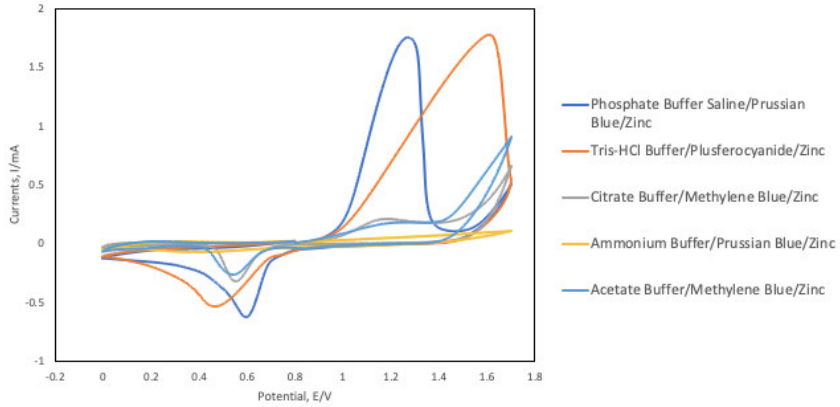

Figure 1

Cyclic voltammetry of optimisation of buffer and redox indicator. 0.1 M buffers while 5 mM redox indicator on surface of AuE. The buffers tested with 3 ppm of zinc ion such as phosphate buffer saline, tris-HCl buffer, citrate buffer, ammonium buffer and acetate buffer under 100 mVs-1 scan rate. This experiment was repeated at least three times (n > 3).

Optimization of parameters (pH value, scan rate and accumulation time)

After selection of buffer and redox indicator based on comparison among fire buffers with three redox indicators. (0.1 M, pH 5) phosphate buffer saline was selected for further optimisation step. The best redox indicator with good tolerant with bare gold electrode was 5 mM Prussian blue. These parameters were tested with different pH values. The range of pH values from pH 2 to pH 9 as showed at Figure 2A. Based on the same figure, the oxidation peaks increased as the pH value more acidic while pH 6 to pH 9 diminished. The zinc ion was showed the current responses with high signal as the pH was decreasing. The oxidation peaks also showed the shifting more to the right side of potential ranges. The relationship between the different pH correspond to the highest oxidation peaks was tested and it showed the pH 2 was the highest oxidation peak among the pH values about 0.86 mA at 1.32 V. The reduction peak was showed the signal of the current was 0.50 mA at 0.64 V. The comparison for both peak currents is shown in Figure 2B. Based on that result, the reduction peak showed highest at every reduction point until it reaching pH 7. In electrochemical method especially cyclic voltammetry method, both peaks are under consideration. The selection is not only focusing the highest peak response but it also involving the stability of the formation of the current. In this case, pH 2 was selected as a best pH because both peaks showed highest at both reactions. As the pH more basic, the formation of peak at oxidation site, it became lower and it diminished as it reaching pH 7 to pH 9 at. Reduction site showed the formation of the peak was shifted to negative potential as the pH value increasing from pH 2 to pH 9. This is showed that, the zinc ion very reactive in acidic condition and the reactivity less as it reaching basic condition. A part of that, this result proved that the zinc ion is highly tolerance with acid condition. Normally, the acid condition known as toxic condition if it translated into environmental condition. Therefore, the toxic substances such as zinc and other poisonous elements might be existed if that area has experienced unusual condition such as toxic condition.

(A)

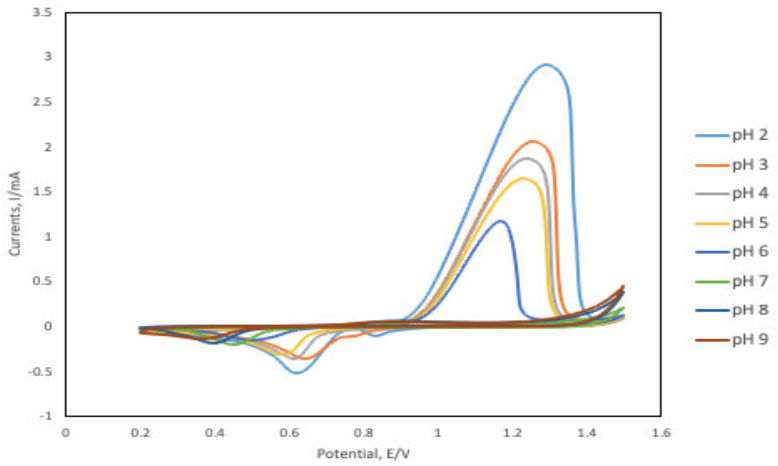

(B)

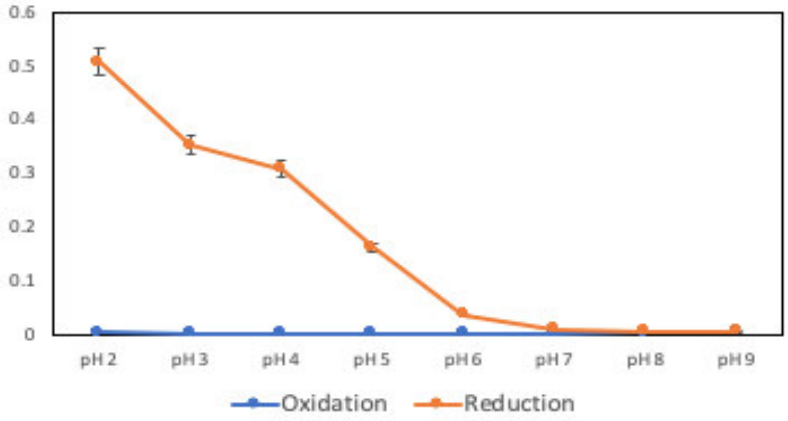

Figure 2
Cyclic voltammetry of pH optimisation. The range of pH from pH 2 to pH 9 for 0.1 M phosphate buffer saline supported by 5 mM Prussian blue for detection of 3 ppm zinc ion under 100 mVs^{-1} scan rate. The experiment was conducted more than three times (n > 3).

Then, pH 2 of the buffer was used to determine the good scan rate response to the formation of both peaks. The optimisation of scan rate was tested such as 50, 100, 150, 200, 250, 300, 350, 400, 450 and 500 mV^{-1} in Figure 3A. The increase the scan rates, the higher peak current responses until the scan rate 450 mV^{-1} showed the same at Figure 3B. This formation indicated that the diffusion controlled was happened in the electron transfer process. In addition, increase the scan rate applied, the oxidation current signals were shifting the positive potential. This limitation of this method known as kinetic limitation of the electrochemical reaction (Bard and Faulkner, 2001). The greater external force does not apply into the system if the formation of the current showed the 'noise' or unstable current travel through the voltammogram graph. In this case, the 250 mVs-1 was selected as optimum scan rate due to it stability. The 450 mV^{-1} was highest but it might be unstable formation of the current. As a result, the peak might be disappeared if it undergoes further optimisation stage. The other factors might be occurred due to ion transfer rate between solution and electrode surface. The charge of the ion with transfer resistance reaction (Gumpu et al., 2017). Zinc is a cation ion. The positive charges owned by zinc ion were transferred into surface electrode which is positively charge. The migration of the ions gave signals when scan rates run from 50 mV^{-1} to 200 mV^{-1}. When the voltage was applied above 200 mV^{-1}, the ion transfer was greater in their rate of flow than charge transfer resistance resulting the current response was rapid increasing until 450 mV^{-1} then it decreasing at 500 mV^{-1} due to hydrolysis of zinc ion. Therefore, the 250 mVs-1 was selected as a best scan rate due to complicated mechanism happens above 250 mVs-1. The strong evidence in this research proved that the formation of noise (unstable current) above 250 mVs-1. The mechanism electron transfer was highly influent the current response especially on the stability.

(A)

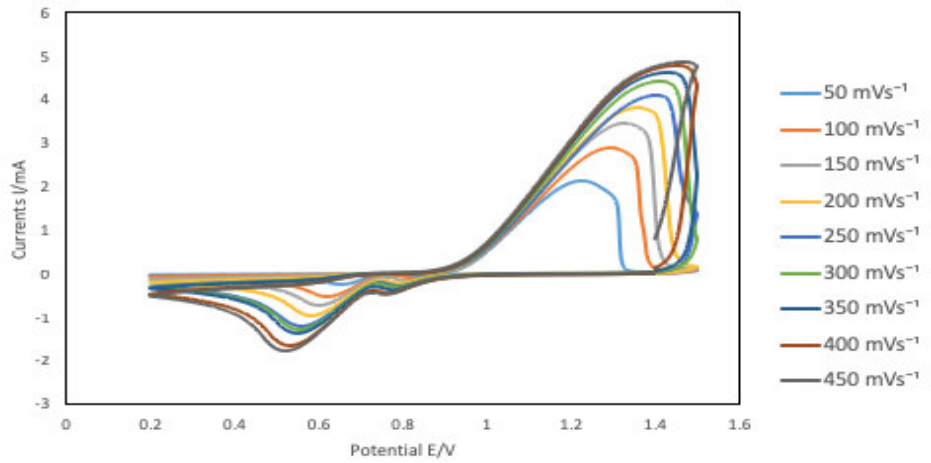

(B)

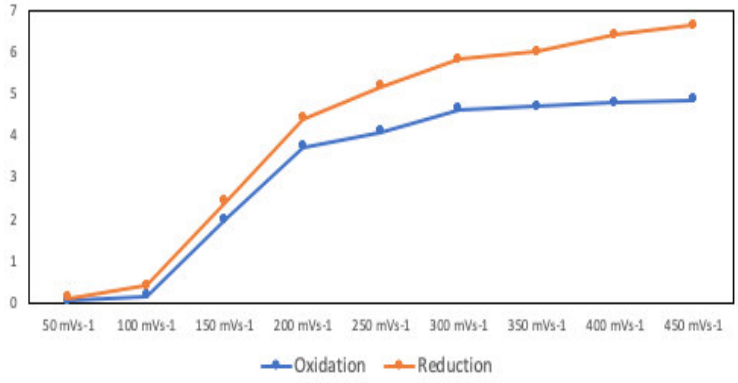

Figure 3
Cyclic voltammetry of optimisation scan rate. The range of scan rate from 50 to 450 mVs^{-1} for (0.1 M , pH 2) phosphate buffer saline with 5 mM Prussian blue for 3 ppm zinc ion detection. The number of repeating for this experiment more than three times (n > 3).

The last step optimisation is accumulation time. The accumulation time was selected from range 5 s to 50 s with 5 s interval time. The accumulation time allowed the mixture to react within the duration selected before the analysis of the zinc ion was conducted. The Figure 4A showed oxidation peaks were formed at same level of current response about 4.87 mV at 1.46 V while reduction peaks were clearly have significant response. The 5 s showed the highest reduction peak compared to other accumulation times at Figure 4B. The peak of 5 s approximately 2.25 mA. The reduction peak become slightly increase due to the capacity binding on the gold electrode itself according to the absorption capacity of target ion stated by (Xing et al., 2016). In other words, the times between 5 s to 10 s indicated that the zinc ion was actively binding on surface of the gold electrode at 5 s. Therefore, 5 s was selected as an accumulation time.

(A)

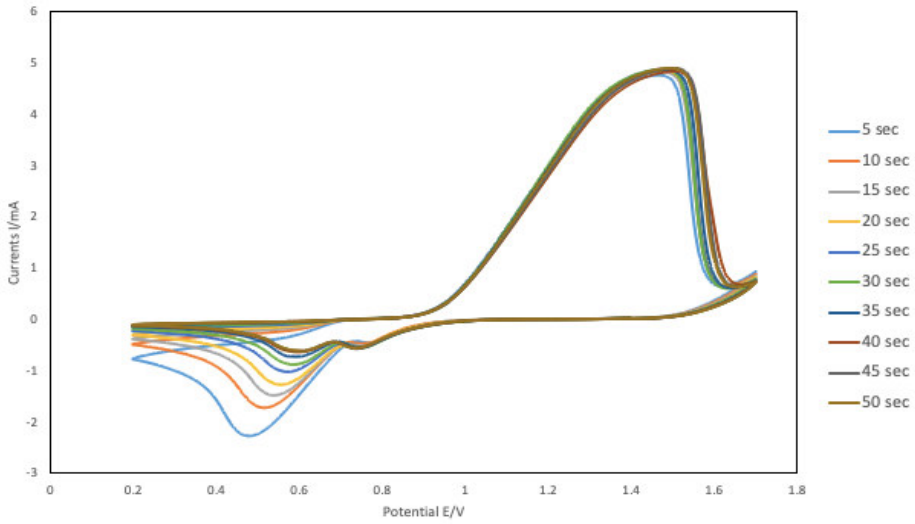

(B)

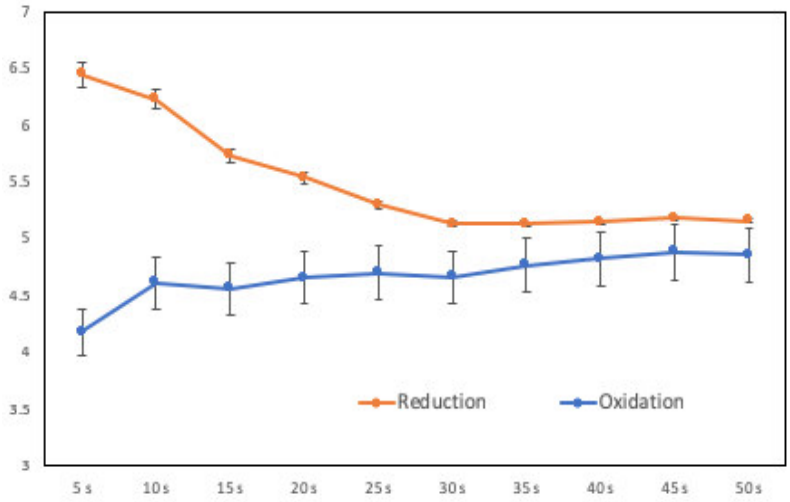

Figure 4
Cyclic voltammetry of optimisation accumulation time. The range of accumulation time from 5 to 50 s for (0.1 M, pH 2) phosphate buffer saline supported by 5 mM Prussian blue under 250 mVs^{-1} scan rate. The experiment was repeated at least for three times (n > 3).

Differential pulse voltammetry for analysis of different concentration of zinc ion

The linear range (LOR) of concentration of zinc ranged from 1 to 10 ppm. The selection of the range including the safety level provided. This method is to test the sensitivity of the bare gold electrode with different concentration of zinc ion. Differential pulse voltammetry is preferred because this method determines the absorption of the species (redox species) on the surface of the electrode. A part of that, the current response is not measuring by the distance from bulk to the surface of the electrode. As a result, it is increasing the sensitivity of the electrode by forming a sharp current signal. Based on the Figure 5, the formation of the peak was located at 0.65 V of potential applied. The limit of detection (LOD) of zinc ion for bare gold electrode was 2 ppm from 1 – 10 ppm under 0.55 V to 0.75 V of potential range. The sensitivity of the electrode was indicated from the control which is buffer without zinc concentration (0 ppm) about 19.25 µA. The current signal was increasing as the concentration of zinc ion added into the electrolytic solution. This showed that the zinc ion was attached onto the surface of AuE and it promoting the current signals.

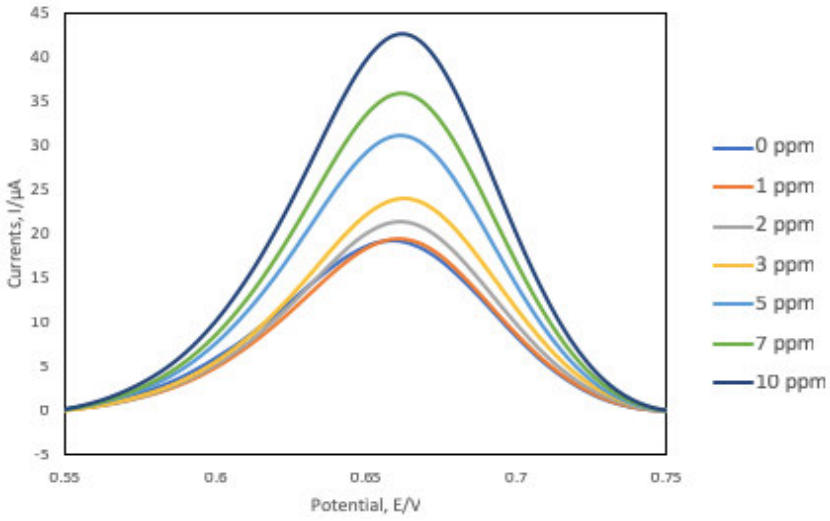

Figure 5.

Differential pulse voltammetry for different concentrations of zinc range from 1 to 10 ppm for (0.1 M, pH 2) phosphate buffer saline supported by 5 mM Prussian blue under 250 mVs-1 scan rate after 5 minutes accumulation time. The experiment was repeated at least three times (n > 3).

CONCLUSION:

Optimisation of parameters brings huge improvement especially in detection limit of zinc ion using AuE. The limit of detection was 2 ppm using differential pulse voltammetry with linear of range from 1 to 10 ppm. Unmodified AuE can detect the safety level of zinc marked as 3 ppm through optimisation step. The other huge improvement is the time needed for detection of zinc ion. It required 5 s for determine the presence of zinc ion with sensitivity of AuE was 19.25 µA. The proposed electrochemical sensor can be applied for monitoring the safety level of zinc in drinking water with rapid and on-spot detection.

ACKNOWLEDGEMENT:

This work was supported by Universiti Malaysia Sabah Research Priority Area Scheme (SBK0248-STWN-2015).

REFERENCES:

1. Bard, A. J., & Faulkner, L. R. (2001) Electrochemical Methods: Fundamentals and Applications. Wiley: New York, 2, 65–69.
2. Burgit, W., & Schmid, K. (1960) Preparation and Properties of Zn-alpha2-glycoprotein of Normal Human Plasma. The Journal of Biological Chemistry, 236.
3. Chibuike, G. U., & Obiora, S. C. (2014) Heavy Metal Polluted Soils: Effect on Plants and Bioremediation Methods. Applied and Environmental Soil Science, Volume 2014 Article ID 752708, 12 pages
4. Duffus, J. H. (2002) Heavy metals-a meaningless term? Pure and Applied Chemistry, 74(5), 793–807.
5. Güell, R., Aragay, G., Fontas, C., Antico, E., Merkoçi, A. (2008) Sensitive and stable monitoring of lead and cadmium in seawater using screen-printed electrode and electrochemical stripping analysis, Analytica Chimica Acta, 627, 219-224.

6. Gumpu, M. B., Veerapandian, M., Krishnan, U. M., Rayappan, J. B. B. (2017) Simultaneous electrochemical detection of Cd (II), Pb (II), As (III) and Hg (II) ions using ruthenium (II)- textured graphene oxide nanocomposite. Talanta, 162, 574-582.
7. Gunawardena, J., Egodawatta, P., Ayoko, G. A., & Goonetilleke, A. (2013) Atmospheric deposition as a source of heavy metals in urban stormwater. Atmospheric Environment, 68, 235-242.
8. Humpath, Enzymatic diseases 2017; At: www.humpath.com.
9. Mazur, M., & Krysinski, P. (2001) Bulk- and surface-initiated chemical in situ polymerisation of 2,5-dimethoxyaniline and 2-methoxyaniline on thiol-coated gold electrodes. Electrochimica Acta, 46, 26-27.
10. Mertens, J., Degryse, F., Springael, D., & Smolders, E. (2007) Zinc toxicity to 638 nitrification in soil and soiless culture can be predicted with the same biotic ligand model. Environmental Science of Technology, 41, 2992.
11. Nagles, E., Arancibia, V., Ríos, R., & Rojas, C. (2012) Simultaneous determination of lead and cadmium in the presence of Morin by adsorptive stripping voltammetry with a Nafioneionic liquidecoated mercury film electrode. International Journal Electrochemistry Science, 7, 5521-5533.
12. Oves, M., Saghir Khan, M., Huda Qari, A., Nadeen Felemban, M., & Almeelbi, T. (2012) Heavy Metals: Biological Importance and Detoxification Strategies. Journal of Bioremediation and Biodegradation, 7, 2.
13. Sathawara, N. G., Parikh, D. J., & Agarwal, Y. K. (2004) Essential heavy metals in environmental samples from western India. Bulletin of Environmental Contamination and Toxicology, 73, 756-761.
14. Schnied, H., & Small, R. C. (1971) Spasmolytic effects of cadmium and zinc ions upon the guine pig isolated ileum preparation. British Journal Pharmacology, 41, 488-499.
15. Siddiquee, S., Yusof, N. A., Salleh, A. B., Tan, S. G., Bakar, F. A. (2010) Electrochemical DNA biosensor for the detection of Trichoderma harzianum based on a gold electrode modified with a composite membrane made from an ionic liquid ZnO nanoparticles and chitosan, and by using acridine orange as a redox indicator. Microchimica Acta, 172, 357–363.
16. Sindern, S., Tremöhlen, M., Dsikowitzky, L., Gronen, L., Schwarzbauer, J., Siregar, T. H., Ariyani, F., Irianto, H. E. (2016) Heavy metals in river and coast sediments of the Jakarta Bay region (Indonesia) — Geogenic versus anthropogenic sources. Marine Pollution Bulletin, 110, 624–633.
17. Voegelin, A., Pfister, S., Scheinost, A. C., Marcus, M. A., & Kretzschmar, R. (2005) Environmental Science Technology, 39, 6616.
18. Weiss, J. H., Sensi, S. L., & Koh, J. Y. (2000) Zn (2+): a novel ionic mediator of neural injury in brain disease. Trends Pharmacological Science, 21, 395–401.
19. Xing, H., Xu, J., Zhu, X., Duan, X., Lu, L., Zuo, Y., Zhang, Y., & Wang, W. (2016) A new electrochemical sensor based on carboi